SLC11A1 PROMOTER POLYMORPHISMS, GENE EXPRESSION AND ASSOCIATION WITH AUTOIMMUNE AND INFECTIOUS DISEASES

A Thesis Submitted for the Degree

of

Doctor of Philosophy

by

Nicholas Steven Archer
B. Sc.(Hons1)

School of Medical and Molecular Biosciences, Faculty of Science,
University of Technology Sydney, Australia.

2012

CERTIFICATE OF AUTHORSHIP/ORIGINALITY

I certify that the work in this thesis has not previously been submitted for a degree nor has it been submitted as part of requirements for a degree except as fully acknowledged within the text.

I also certify that the thesis has been written by me. Any help that I have received in my research work and the preparation of the thesis itself has been acknowledged. In addition, I certify that all information sources and literature used are indicated in the thesis.

_____

Nicholas Steven Archer

2012

ACKNOWLEDGMENTS

I am grateful to many people who have supported and helped me throughout the completion of my postgraduate studies. In particular, my supervisors Dr Bronwyn O'Brien and Dr Najah Nassif, both of whom have provided immeasurable guidance, support and wisdom throughout the completion of my postgraduate work. I thank you for the effort and enthusiasm you have shown to my work.

I wish to extend a special thanks to Stephanie Dowdell for her friendship and support through the completion of my PhD and assistance with reverse-transcriptase real-time PCR. I also appreciate and acknowledge the support provided to me from the numerous postgraduate students, postdoctoral and support staff that I have had the privilege and honour to work alongside of and socialise with.

Futhermore, I would like to thank the following people for their technical guidance for the experimental work completed in this project. Paul Held and Sharon Guffogg for assistance with the Biotek fluorescent plate reader. Dr Lisa Sedger for assistance with flow cytometery and Dr Mike Johnson for confocal microscopy analysis. Narelle Woodland, Gilian Rozenberg and the Prince of Wales Hospital for assistance with staining of THP-1 cells and positive controls. Additionally, a big thankyou to David Hyatt and Lonza for the loan of the Nucleofector instrument.

I would like to also acknowledge Jenefer M. Blackwell, Anna Dubaniewicz, A Graham, Leonardo A Sechi, Lee E Sieswerda, Maria Gazouli, Margje Haverkamp, Linda Wicker, Jennie Yang, Eileen Hoal, Timothy Sterling and Alison Motsinger-Reif for supplying additional population data for the completion of meta-analyses.

Finally, I would like to thank the support of my family, my partner, Sarah, my parents, Lynette and Warwick and sister and brother-in law, Kerri and Daniel. While you never did understand exactly what I was doing, you still tried to show an interest!

ABSTRACT

Solute Carrier Family 11A Member 1 (SLC11A1) is a member of a highly conserved group of ion transporters and has restricted localisation to the phagosomal membrane of monocytes/macrophages. SLC11A1 plays an immunomodulatory role in influencing macrophage activation status and the T helper 1/T helper 2 bias. As such it modulates susceptibility to infectious/autoimmune diseases. A polymorphic $(GT)_n$ promoter microsatellite repeat is known to alter *SLC11A1* promoter activity. Of the nine $(GT)_n$ alleles identified, alleles 3 and 2, which account for a combined allele frequency of greater than 95%, drive high and low *SLC11A1* expression, respectively. The increased *SLC11A1* expression, driven by $(GT)_n$ allele 3 is hypothesised to result in a heightened activation status of classically activated macrophages, affording resistance to infectious disease, but conferring susceptibility to pro-inflammatory autoimmune diseases. Conversely, decreased *SLC11A1* expression in the presence of allele 2 would confer susceptibility to infectious disease, but resistance to autoimmune disease.

A large number of studies assessing the association between the presence of specific $(GT)_n$ promoter alleles with the incidence of infectious and autoimmune disease have produced inconsistent associations. Meta-analyses are powerful analytical tools which combine individual association studies to estimate the strength of an association, therefore, meta-analyses of case control association studies (from 1991-2006) analysing the association of *SLC11A1* promoter $(GT)_n$ alleles 2 and 3 with the incidence of autoimmune disease were performed. The meta-analyses found a weak predominance of disease in the absence of allele 2, with a fixed effects pooled OR of 0.80 (95% CI = 0.22), however, a random effects pooled odds ratio (OR) of 0.88 (95% CI = 0.66) for allele 3 suggested no association with the incidence of autoimmune disease.

The publication of additional case control studies between 2006 and the present allowed a more comprehensive meta-analysis to be completed. This analysis, which included additional *SLC11A1* polymorphisms, represents the largest study assessing the association of *SLC11A1* polymorphisms with disease occurrence to date. Allele 2 of the $(GT)_n$ microsatellite was associated with increased and reduced incidence of infectious [OR=1.32 (1.20-1.46)] and autoimmune diseases [OR=0.90 (0.81-1.00)], respectively. Allele 3 was significantly associated with reduced incidence of infectious disease

[OR=0.82 (0.76-0.88)], however, the association with susceptibility to autoimmune disease occurrence did not reach statistical significance [OR=1.11 (0.98-1.26)]. The findings of the meta-analysis challenges the hypothesis that allele 3 is the disease causing variant at the $(GT)_n$ microsatellite repeat.

The results of these meta-analyses highlight small sample sizes as a major limitation of case control association studies. Completion of large-scale studies has been impractical because conventional *SLC11A1* $(GT)_n$ genotyping methodologies are time consuming and cannot differentiate all $(GT)_n$ variants. A high resolution melt curve methodology has been designed and optimised to genotype two *SLC11A1* polymorphisms, the $(GT)_n$ and $(CAAA)_n$ microsatellite repeats. Assay validation yielded a 100% success rate for genotyping of the $(GT)_n$ and $(CAAA)_n$ microsatellites. The designed methodology is the first to enable accurate, sensitive and high-throughput genotyping of these microsatellites and will enable the completion of sufficiently large association studies required to determine the association between the *SLC11A1* $(GT)_n$ and $(CAAA)_n$ polymorphisms and disease occurrence.

In addition to the $(GT)_n$ microsatellite, the -237C/T polymorphism has also been shown to modulate *SLC11A1* expression, with the T variant driving low expression in the presence of $(GT)_n$ allele 3. Little is known about *SLC11A1* transcription or the mechanism by which the $(GT)_n$ and -237C/T promoter polymorphisms modulate *SLC11A1* expression. Bioinformatic studies were completed to identify putative regulatory elements involved in transcription and promoter constructs, containing different lengths of the *SLC11A1* promoter, were prepared and used to assess promoter function. A 581bp promoter region (-532 to +49) that controlled *SLC11A1* expression in monocytes was identified. Within this region was identified a 148bp minimal promoter region (-99 to +49) containing the core elements for the formation of the basal transcriptional complex. The greatest transcriptional enhancement was identified within a 170bp region (-532 to -362) containing a novel IRF-Ets composite sequence for the recruitment of transcription factors IRF-8 and PU.1. Additionally, the promoter constructs suggested that the *SLC11A1* promoter may mediate bidirectional transcription. It was further determined that, in monocytic cells, the ability of $(GT)_n$ alleles 2 and 3 to differentially modulate *SLC11A1* expression was not due to their differing abilities to form Z-DNA, but to monocyte-specific factor(s) binding to a 165bp

region (-362 to -197) of the *SLC11A1* promoter. Additional bioinformatic and functional assays suggested that the T variant of the -237C/T polymorphism reduced *SLC11A1* promoter activity independently of the $(GT)_n$ microsatellite repeat.

Infectious and autoimmune diseases are major contributors to morbidity and mortality. *SLC11A1* is instrumental in regulating macrophage function and hence susceptibility to infectious and autoimmune diseases. This study has provided insight into the association of *SLC11A1* with disease incidence, has developed a novel genotyping methodology to allow the completion of large association studies and has elucidated mechanisms of transcriptional regulation of *SLC11A1* and the influence of polymorphisms on *SLC11A1* expression.

PUBLICATIONS ARISING FROM THE WORK DESCRIBED IN THIS THESIS

(A) PUBLICATIONS IN PEER-REVIEWED JOURNALS

Nicholas S. Archer, Najah Nassif & Bronwyn A. O'Brien (2012) "The *SLC11A1* $(GT)_n$ promoter polymorphism modulates expression through monocyte specific factor(s) to alter susceptibility to infectious and autoimmune diseases", (Manuscript in preparation).

Nicholas S. Archer, Najah Nassif & Bronwyn A. O'Brien (2012) "Meta-analysis of *SLC11A1* polymorphisms: $(GT)_n$ allele 2 exerts selective pressure in infectious and autoimmune disease", (Manuscript in preparation).

Nicholas S. Archer, Melinda Sirmias, Stephanie Dowdell, Najah Nassif & Bronwyn A. O'Brien (2012) "Genotyping disease-associated *SLC11A1* microsatellite repeats by high resolution melt analysis", (Submitted).

Nicholas S. Archer, Najah Nassif & Bronwyn A. O'Brien (2010) "Discrimination of microsatellite repeat polymorphisms of the *SLC11A1* promoter by melting curve analysis using the Eppendorf Mastercycler ep *realplex*", Eppendorf Technical Application Note 206.

Bronwyn O'Brien, **Nicholas S. Archer**, Fraser Torpy & Najah Nassif (2008) "Association of *SLC11A1* Promoter Polymorphisms with the incidence of autoimmune and Inflammatory Diseases: A Meta-Analysis", *Journal of Autoimmunity*, 31(1): 42-51.

(B) CONFERENCE ABSTRACTS

Nicholas Archer, Najah Nassif & Bronwyn O'Brien (2011) Poster entitled: "Macrophage specific factors differentially regulate allele specific *SLC11A1* expression and consequent susceptibility to infectious and autoimmune disease", 32nd Lorne Genome Conference.

Nicholas Archer, Najah Nassif & Bronwyn O'Brien (2010) Presentation entitled: "The *SLC11A1* $(GT)_n$ promoter polymorphism modulates susceptibility to infectious and autoimmune disease", 27th Combined RNSH/UTS/USyd/KIMR Scientific Research Meeting – Winner of the John Hambly award for best UTS presentation.

Nicholas Archer, Najah Nassif & Bronwyn O'Brien (2010) Poster entitled: "Elucidation of the essential promoter region of *SLC11A1*", 31st Lorne Genome Conference.

Nicholas Archer, Melinda Sirmias, Stephanie Dowdell, Najah Nassif & Bronwyn O'Brien (2009) Poster entitled: "Genotyping of functional SLC11A1 polymorphisms associated with infectious and autoimmune diseases", 26th Combined RNSH/UTS/USyd/KIMR Scientific Research Meeting.

Nicholas Archer, Najah Nassif & Bronwyn O'Brien (2008) Presentation in the Young Investigator Category "Elucidation of the Essential Promoter Region of *SLC11A1*", 25th Combined RNSH/UTS/USyd/KIMR Scientific Research Meeting.

Nicholas Archer, Najah Nassif & Bronwyn O'Brien (2007) Presentation entitled: "Genotyping SLC11A1 promoter polymorphisms by high resolution melt (HRM) analysis", 24th Combined RNSH/UTS/USyd/KIMR Scientific Research Meeting.

(C) AWARDS

Awarded the John Hambly Award for the best UTS presentation at the Combined RNSH/UTS/USyd/KIMR Scientific Research Meeting 2010.

CONTENTS

LIST OF FIGURES

LIST OF TABLES

LIST OF APPENDICES

LIST OF ABBREVIATIONS

γ-IRE	interferon-γ response element
ALL	acute lymphocytic leukaemia
AML	acute myeloid leukaemia
AMML	acute myelomonocytic leukaemia
AP1	Activator protein 1
ARNT	aryl hydrocarbon receptor nuclear translocator
bp	base pairs
BRE	TFIIB-recognition element
BSA	bovine serum albumin
CCF2-AM	coumarin cephalosporin fluorescein
C/EBP	CCAAT/enhancer binding protein
CI	confidence interval
Ct	cycle threshold
DCE	downstream core element
DMEM	Dulbecco's modified eagle medium
DNA	deoxyribonucleic acid
DPE	downstream promoter element
EDTA	ethylenediaminetetraacetic acid
EMSA	electrophoretic mobility shift assays
FBS	fetal bovine serum
GM-CSF	granulocyte macrophage colony-stimulating factor
h	hours
HBSS	Hanks buffered salt solution
HIF-1	Hypoxia inducible factor 1
HIV	Human immunodeficiency virus
Idd	insulin dependant diabetes (murine)
IDDM	insulin dependant diabetes mellitus (human)
IECS	IRF-Ets composite sequence
IFN-γ	interferon-gamma
IL	interleukin
iNOS	inducible nitric oxide synthase
Inr	Initiator element
IRF	interferon regulatory factors
ISRE	IFN-stimulated response element
kb	kilobase
KLF	kruppel-like factor
l	litre
Lamp1	lysosome-associated membrane protein 1
LB	Luria Bertani
LD	linkage disequilibrium
LPS	lipopolysaccharide
MHC	major histocompatibility complex
min	minutes
MTE	motif ten element
NF-IL6	nuclear factor IL-6
NF-κB	nuclear factor kappa-light-chain-enhancer of activated B cells
NO	nitric oxide

Nramp	natural resistance-associated macrophage protein
NTC	no template control
Oct-1	octamer binding protein 1
OR	odds ratio
PAS	periodic acid-schiff
PBS	phosphate buffered saline
PCR	polymerase chain reaction
PMA	phorbol myristate acetate
PMN	polymorphonuclear
pol II	RNA polymerase II
PU.1	protein encoded by *SPI-1* gene
RES	reticuloendothelial system
RNA	ribonucleic acid
RNase	ribonuclease
RPMI	Roswell Park Memorial Institute
RT	room temperature
s	seconds
SBB	Sudan black B
SLC11A1	Solute carrier family 11A member 1 (Human protein)
SLC11A1	Solute carrier family 11A member 1 (Human gene)
Slc11a1	Solute carrier family 11A member 1 (non-human protein)
Slc11a1	Solute carrier family 11A member 1 (non-human gene)
SLC11A2	Solute carrier family 11A member 2 (Human protein)
SLC11A2	Solute carrier family 11A member 2 (Human gene)
SNP	single nucleotide polymorphism
Sp1	Specificity protein 1
SPI-1	spleen focus by forming virus proviral integration 1
TAF	TBP associated factor
TBP	TATA binding protein
TESS	Transcription Element Search Software
TFIID	transcription factor II D
TFBS	transcription factor binding site
Th1	T helper 1
Th2	T helper 2
T_m	melting temperature
TNF-α	tumour necrosis factor-alpha
TSS1	transcription start site 1
TSS2	transcription start site 2
UV	ultraviolet
XCPE1	X core promoter element 1
YY1	Ying-Yang 1
ZBP-1	Z-DNA binding protein 1

CHAPTER 1 – INTRODUCTION

1.1 STRUCTURE AND FUNCTION OF SLC11A1

1.1.1 Historical Background

SLC11A1 was first discovered by three independent research groups after observations of animal infection models. The first group designated the locus *Lsh* after the observation that inbred strains of mice exhibited differential growth of *Leishmania donovani* within macrophages (Bradley, 1977). A similar observation was made following infection of inbred mice with the macrophage trophic pathogen *Salmonella typhimurium*, where the resistance locus was named *Ity* (Plant and Glynn, 1974). The third group found that strains of inbred mice separated into susceptible and resistant groups when infected with *Mycobacterium bovis* (another macrophage trophic organism) and the disease locus was named *Bcg* (Skamene *et al.*, 1982). It was hypothesised that susceptibility, or resistance, to the three infectious organisms was controlled by a single locus, which encoded a protein that modulated macrophage function (Blackwell, 1989). It was further shown that the gene had restricted expression to reticuloendothelial organs; namely the spleen, liver and blood. Consequently, the gene was named natural resistance-associated macrophage protein 1 or *Nramp1* (Malo *et al.*, 1994, Vidal *et al.*, 1993).

Using positional cloning to determine the location of the *Bcg*/*Lsh*/*Ity* locus on mouse Chromosome 1, it was discovered that susceptibility to macrophage trophic pathogens was the result of a point mutation in the coding region of *Nramp1* (Vidal *et al.*, 1993). This mutation, leading to a single non-conservative amino acid substitution of a glycine for an aspartic acid residue at position 169 (G169D) in trans-membrane domain 4, produces a non-functional protein (Vidal *et al.*, 1996). Sequence analysis of *Nramp1* from 27 inbred mouse strains found concordance between the presence of the wild type G or mutant D amino acid at position 169 and resistance or susceptibility to infection, respectively (Malo *et al.*, 1994).

Verification that the susceptibility to infection associated with the *Bcg*/*Lsh*/*Ity* locus was due to the G169D mutation of *Nramp1* was provided by two *in vivo* studies. In the first, Vidal et al. (1995) took the normally resistant 129sv mouse strain and created a homozygous *Nramp1* knockout (*Nramp1*$^{-/-}$), which, when infected with *Mycobacterium*,

Leishmania or *Salmonella*, exhibited the same pathogenesis as that observed in mice carrying the G169D mutation. In the second study, Govoni et al. (1996) transfected embryonal mouse cells, homozygous for the G169D mutation (Nramp1$^{-/-}$), with the resistant *Nramp1* allele, along with a small region upstream and downstream of the gene, and produced a mouse strain in which macrophages were able to control infections comparable to the resistant (Nramp$^{+/+}$) mouse strains. Thus, the candidacy of *Nramp1* as the locus controlling resistance or susceptibility to these macrophage-trophic pathogens was established.

1.1.1.1 Discovery of the Human *SLC11A1* Gene

The region of mouse Chromosome 1 in which *Nramp1* is located is syntenic with human Chromosome 2 (Schurr *et al.*, 1990). The human *NRAMP1* gene has been isolated and sequenced (Cellier *et al.*, 1994, Kishi, 1994), however, in humans, analysis of the *NRAMP1* sequence has failed to identify any mutations that produce a non-functional protein, similar to the G169D mutation found in mice (Vidal *et al.*, 1996).

The human homologue, NRAMP1, is now known as Solute Carrier Family 11A Member 1 (SLC11A1) due to a standardised naming system used to describe a range of different transporters. The Solute Carrier Family 11 includes proteins that are involved in the transport of divalent cations, of which there are two members, SLC11A1 and SLC11A2. Solute Carrier Family 11A Member 2 (formerly NRAMP2) was discovered due to the high degree of sequence homology with SLC11A1. The SLC11A2 protein is ubiquitously expressed with localised expression to the plasma membrane of cells, where it functions to transport iron and other divalent cations (Mackenzie and Hediger, 2004). In mouse models, Slc11a2 has been shown to play a role in the transportation of dietary iron at the apical membrane from enterocytes lining the duodenal lumen and is also expressed in erythroid precursors, where it transports iron out of transferrin cycle endosomes. Substitution of a glycine to arginine at amino acid position 185 (G185R), in murine and rat models, results in a loss of Slc11a2 function, resulting in the development of microcytic anaemia, which is attributable to inefficient dietary iron uptake (Canonne-Hergaux *et al.*, 2000, Canonne-Hergaux *et al.*, 2001) and an inability to retain/utilise iron in erythroid precursors (Garrick *et al.*, 1999, Gruenheid *et al.*, 1999).

1.1.2 Structure of SLC11A1

The *SLC11A1* gene, located on chromosome 2q35, is approximately 14kb in length and contains 15 exons (Figure 1.1A) (Cellier *et al.*, 1994). The gene encodes a 550 amino acid protein containing 12 transmembrane domains, two N-linked glycosylation sites and a series of phosphorylation sites, resulting in a protein with a molecular weight between 90 and 100 kDa (53kDa unglycosylated) (Vidal *et al.*, 1996). The protein has a serine/proline rich Src Homology 3 (SH3) binding domain, located proximal to the amino terminus before the first transmembrane domain, which may interact with cytoskeletal proteins and/or play a role in signal transduction (Figure 1.1B) (Barton *et al.*, 1994, Blackwell, 1996). The G169D mutation identified in murine models, which results in a loss of Slc11a1 function, is located in the fourth transmembrane domain of Slc11a1 (Figure 1.1B).

SLC11A1 is part of a highly conserved group of ion transporters, known as the Nramp family, which are found in both eukaryotes and prokaryotes (Table 1.1). Proteins within this family are characterised by the presence of 10 trans-membrane domains, a series of highly conserved charged residues in thermodynamically unfavorable positions and the presence of a 20 amino acid consensus sequence motif (known as the 'binding protein-dependent transport system inner membrane component signature') located between trans-membrane domains 8 and 9 (Figure 1.1B) (Gruenheid *et al.*, 1995). There is a high level of amino acid sequence homology among Nramp family members and all members of the Nramp family play a role in the transport of divalent cations (Table 1.1). This sequence and functional conservation among evolutionarily diverse organisms suggests an important physiological role for the Nramp group of proteins.

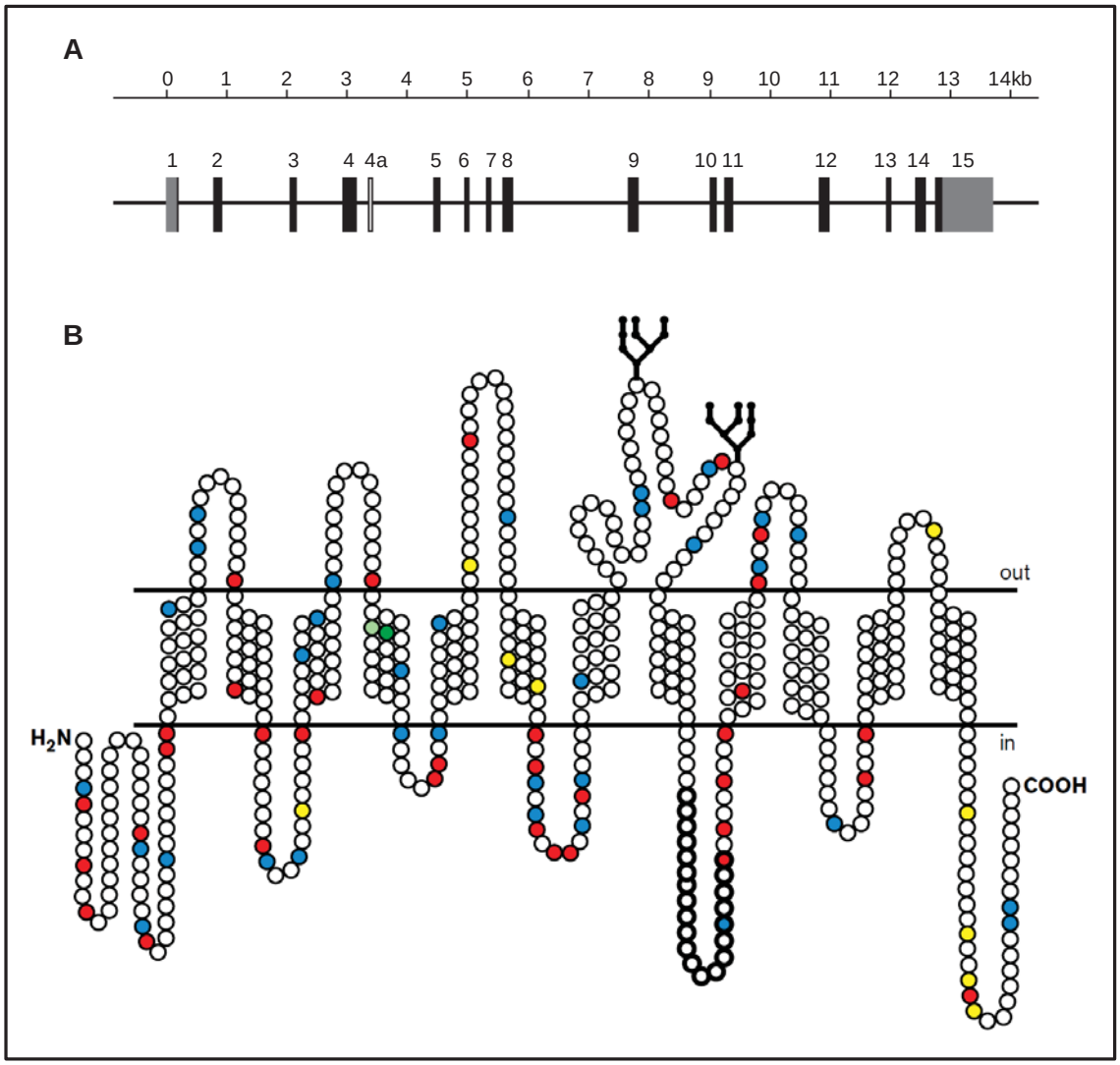

Figure 1.1 *SLC11A1* gene structure, protein conformation and membrane topology of Slc11a1. (A) The *SLC11A1* gene contains 15 exons and is approximately 14kb long. (B) Slc11a1 shares 93% amino acid sequence homology with human SLC11A1. The 12 transmembrane domains, the two N-linked glycosyl chains attached to the transmembrane loop between domains 7 and 8, and the 20 amino acid transport motif (residues in bold) are shown. The G169D mutation is indicated by the dark green residue in trans-membrane domain 4 (Gruenheid and Gros, 2000).

Table 1.1 Homology Among Selected Nramp Family Members

Organism	Protein	Homology[1]	Substrate(s)[2]	Reference
M.musculus	Slc11a1 (Nramp1)	100%	**Mn^{2+}**, Fe^{2+}, Zn^{2+}, Co^{2+}, Mg^{2+}	(Vidal *et al.*, 1993)
	Slc11a2 (Nramp2)	78%	**Fe^{2+}**, Mn^{2+}, Zn^{2+}, Co^{2+}, Cd^{2+}, Ni^{2+}, Pb^{2+}	(Gruenheid and Gros, 2000)
H.Sapien	SLC11A1	93%	NT[3]	(Cellier *et al.*, 1994)
	SLC11A2	79%	**Fe^{2+}**, Mn^{2+}, Zn^{2+}, Co^{2+}, Cd^{2+}, Ni^{2+}, Pb^{2+}	
C.familiaris	Nramp1	87%	NT	(Altet *et al.*, 2002)
G.gallus	Nramp1	83%	NT	(Hu *et al.*, 1996)
D.rerio	cdy/Nramp2	73%	**Fe^{2+}**	(Donovan *et al.*, 2002)
D.melanogaster	malvolio	79%	**Fe^{2+}**, **Mn^{2+}**	(Blackwell, 1996)
S.cerevisiae	Smf1	42%	**Mn^{2+}**, Co^{2+}, Cu^{2+}, Cd^{2+}	(Gruenheid *et al.*, 1997)
	Smf2	43%	**Mn^{2+}**, Co^{2+}, Cu^{2+}, Cd^{2+}	
C.elegens	Smf3	68%	NT	(Gruenheid *et al.*, 1997)
Mycobacterium spp	Mramp	40%	Mn^{2+}, Fe^{2+}, Zn^{2+}, Cu^{2+}	(Forbes and Gros, 2001)
Gram -ve bacteria	MntH	40-45%	**Mn^{2+}**, **Fe^{2+}**, Zn^{2+}, Cd^{2+}	(Forbes and Gros, 2001)
Plants	Class I, Class II	40-50%	Mn^{2+}, Fe^{2+}, Zn^{2+}, Cd^{2+}	(Curie *et al.*, 2000)

[1]Percentages are based on amino acid sequence comparison with mouse Slc11a1
[2]Substrate in bold is preferred substrate for transport
[3]NT - Not tested

1.1.3 Tissue and Cellular Expression of SLC11A1

In humans, expression of *SLC11A1* is restricted to the reticuloendothelial organs, with the highest level of expression in the blood, lungs and spleen (Cellier *et al.*, 1994, Nishimura and Naito, 2008). The restricted expression of other SLC11A1 homolog's to the reticuloendothelial system (RES) is also observed in murine (Cellier *et al.*, 1994), bovine (Feng *et al.*, 1996), ovine (Bussmann *et al.*, 1998), and gallus species. However, in gallus a high level of expression also occurs in the thymus (Hu *et al.*, 1996).

The cellular expression of *SLC11A1* is restricted to phagocytic cells. However, there appears to be species specific differences in the cellular expression of SLC11A1 between mice and humans. In mice, *Slc11a1* expression has been identified in the monocyte/macrophage lineage (Cellier *et al.*, 1994) and in dendritic cells (DC) (Stober *et al.*, 2007). In humans *SLC11A1* expression has been localised to monocytes/macrophages (Vidal *et al.*, 1996), polymorphonuclear (PMN) leukocytes (Canonne-Hergaux *et al.*, 2002, Cellier *et al.*, 1994) and DCs (Le Naour *et al.*, 2001, Lehtonen *et al.*, 2007). Putatively, expression of *SLC11A1* has also been identified in peripheral blood lymphocytes, however, this has only been reported in a single study (Kishi and Nobumoto, 1995).

1.1.3.1 SLC11A1 is Recruited to the Phagosomal Membrane in Macrophages/Monocytes

Studies of resting macrophages and DCs have shown that Slc11a1 colocalises with lysosome-associated membrane protein 1 (Lamp1) (Gruenheid *et al.*, 1997, Stober *et al.*, 2007) and cathepsin L (Searle *et al.*, 1998), both markers for the late endosomal and early lysosomal compartment of the trans-golgi network. Activation of macrophages, using inert spherical particles or pathogens (*Leishmania donovani* and *Mycobacterium avium*), results in their uptake into a plasma membrane derived phagosome. This phagosome is not bacteriocidal and requires a complex series of fusions with endosomes and lysosomes that possess the various bacteriocidal properties (Figure 1.2) (Niedergang and Chavrier, 2004).

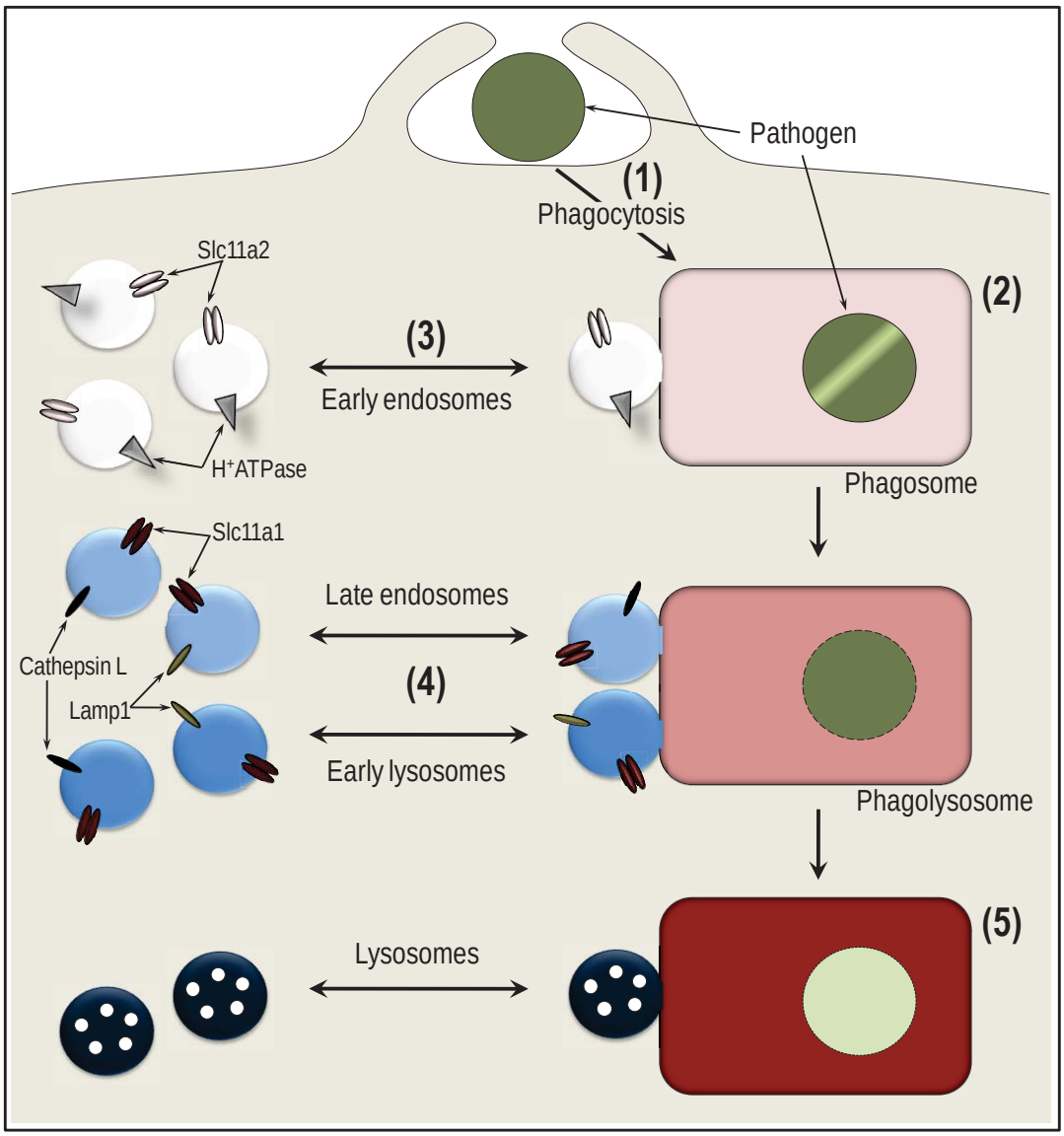

Figure 1.2 Phagosome maturation and Slc11a1 recruitment. When a pathogen is phagocytosed (1) it enters a plasma membrane derived phagosome (2). A complex series of fusions with endosomes and lysosomes then occurs. Early endosomes, containing H^+ ATPases and Slc11a2, are first recruited to the phagosomal membrane (3). Late endosome/early lysosome vesicles, where Slc11a1 is localised, as well as the markers Lamp1 and cathepsin L, join the early phagolysosomal membrane (4). Recruitment of endosomes and lysosomes containing bacteriocidal properties results in the destruction of the pathogen (5).

During the course of maturation, phagosomes migrate along microtubules from the periphery to a perinuclear location. The early endosomes are the first to fuse with the phagosome, introducing H^+ ATPases that transport hydrogen ions into the phagosome, thereby creating an acidic environment (Niedergang and Chavrier, 2004). SLC11A2 is also localised to the early endosomes where, after fusion with the phagosomal membrane, it transports a range of divalent cations out of the phagosome down a proton gradient (Gruenheid *et al.*, 1999).

Next, the late endosomes and early lysosomes, where Slc11a1 (along with Lamp1 and cathepsin L) is localised, fuse with the phagolysosomal membrane and Slc11a1 becomes concentrated around the phagosomal membrane where it is in close proximity to phagocytosed pathogens (Gruenheid *et al.*, 1997, Searle *et al.*, 1998), and phagosomal maturation is promoted (de Chastellier *et al.*, 1993, Frehel *et al.*, 2002, Hackam *et al.*, 1998) (Figure 1.2). Thus, Slc11a1 plays an important role in cells that possess phagocytic ability.

1.1.3.2 SLC11A1 Expression and Monocyte/Macrophage Development

SLC11A1 has restricted localisation to late endosomes/lysosomes of phagocytic cells where it is rapidly recruited to the phagosomal membrane after pathogen uptake. SLC11A1 expression varies according to the developmental stage of monocytes/macrophages (Figure 1.3). Gene expression profiling of bone marrow shows no (to extremely low) levels of *SLC11A1* expression (Nishimura and Naito, 2008), suggesting that monocytic precursors lack *SLC11A1* expression. As monocytes differentiate, *SLC11A1* expression increases. Realtime-PCR (RT-PCR) studies using cultured cell lines, which represent different stages of monocytic development, showed that the most immature monocytic cell lines (KG1 and HL-60) had no to low *SLC11A1* expression. The highest expression was observed in the more differentiated monocytic cell lines (U937 and THP-1 cells) (Cellier *et al.*, 1994). Furthermore, when monocytes migrate from the peripheral blood into tissues, *SLC11A1* expression increases consistent with monocyte to macrophage differentiation, which follows tissue residency (Cellier *et al.*, 1997).

SLC11A1 expression is further modulated by the activation status of macrophages. Activation of resting macrophages can occur in two ways. Firstly, classical activation of resting macrophages occurs in response to interferon (IFN)-γ and lipopolysaccharide (LPS), resulting in an M1 pro-inflammatory macrophage phenotype. Classically activated M1 macrophages have enhanced phagocytic ability, increased antigen presentation by major histocompatibility complex (MHC) class II molecules and the production of a range of cytokines, resulting in a Th1 mediated immune response (Gordon, 2003). During classical macrophage activation, *SLC11A1* expression is upregulated (Searle and Blackwell, 1999, Zaahl *et al.*, 2004). Secondly, alternative

activation of macrophages occurs through exposure to the cytokines, interleukin 4 (IL-4) and IL-13, to produce an anti-inflammatory M2 macrophage phenotype and a subsequent Th2 mediated immune response. This results in the down regulation of Th1 mediated macrophage function and the secretion of molecules associated with wound healing and resolution of inflammation (Gordon, 2003, Ma *et al.*, 2003). The expression of SLC11A1 in alternatively activated macrophages is yet to be elucidated, however, due to the pro-inflammatory effects of SLC11A1 (Section 1.1.5), it would be expected that alternative activation of macrophages would result in decreased SLC11A1 expression.

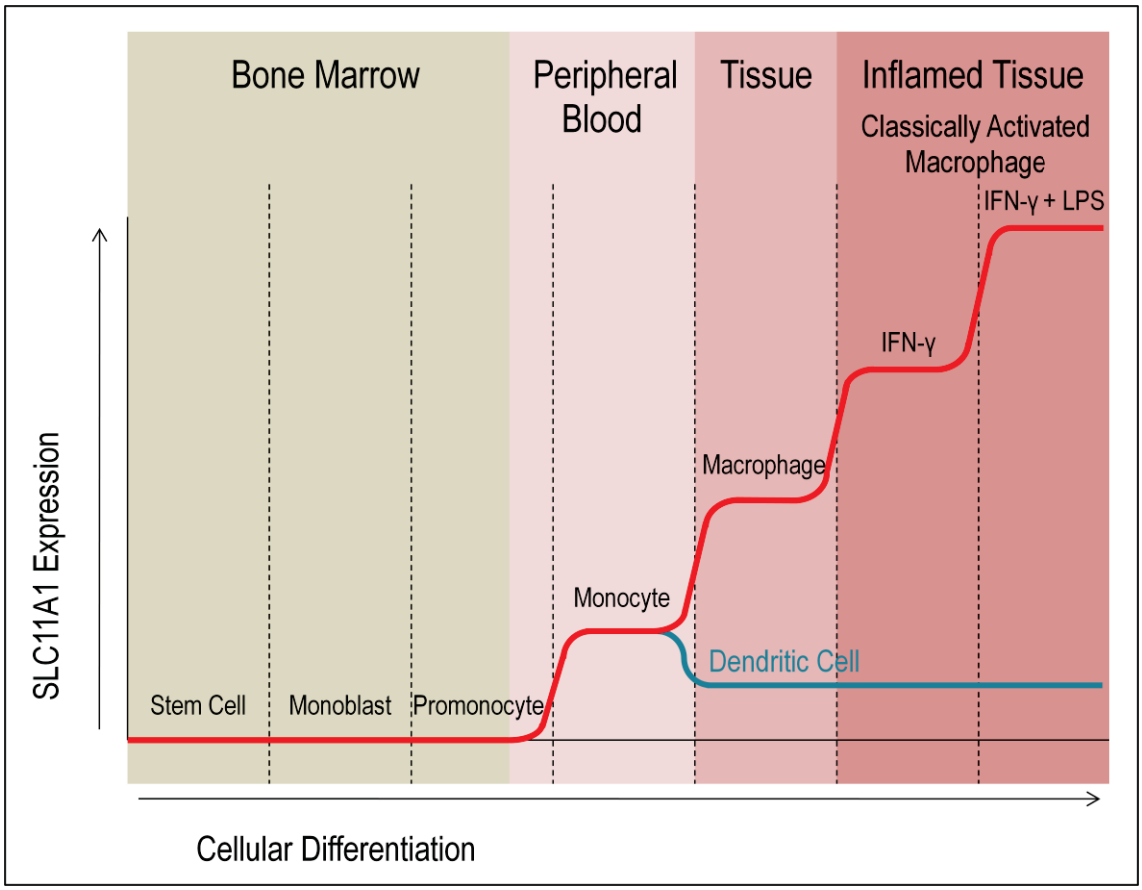

Figure 1.3 Relative SLC11A1 expression levels during macrophage differentiation and activation. The red and blue lines indicate the relative level of SLC11A1 expression in the macrophage lineage and dendritic cells, respectively. The dotted lines designate the different stages of maturation, while the background colours represent the different tissues in which the cells are located.

Microarray analysis of monocyte differentiated mature DCs (stimulated with granulocyte macrophage colony stimulating factor (GM-CSF), tumor necrosis factor (TNF)-α and IL-4) identified a two to seven fold decrease in *SLC11A1* expression in

DCs as compared to monocytes/macrophages (Le Naour *et al.*, 2001, Lehtonen *et al.*, 2007). The lower expression of *SLC11A1* in mature DCs is likely attributable to their reduced endocytic/phagocytic ability as compared to the immature phenotype.

Due to the restricted localisation of SLC11A1 to endosomes/phagosomes and the role of SLC11A1 in pathogen clearance, *SLC11A1* expression occurs when monocytes gain phagocytic or endocytic capabilities. Likewise, increasing *SLC11A1* expression appears to correlate with increased phagocytic ability, which is correlated with monocyte/macrophage differentiation and activation.

1.1.3.3 SLC11A1 Expression in PMN Leukocytes

From the analysis of peripheral blood, Cellier et al. (1997) identified that the highest level of *SLC11A1* expression was found in PMN leukocytes, followed by monocytes. Colocalisation studies have shown that SLC11A1 localised to gelatinase positive tertiary granules in PMN leukocytes, similar to its localisation pattern observed in macrophages (Canonne-Hergaux *et al.*, 2002).

1.1.3.4 Expression of SLC11A1 in Other Tissues

In mice, Slc11a1 expression has also been found in neurons (Evans *et al.*, 2001). Expression profiling of all SLC family members in humans has failed to find expression of *SLC11A1* in the brain, however, low expression levels were found in the spinal cord (Nishimura and Naito, 2008). This is consistent with findings presented in BioGPS that indicate a low level of expression in neurons associated with the spinal column (dorsal root ganglion, atrioventricular node and superior cervical ganglion) (Wu *et al.*, 2009). The role of SLC11A1 in neuronal activity is yet to be elucidated, however, it is thought that SLC11A1 may function in the stress response (Blackwell, 2001, Evans *et al.*, 2001). Expression of *SLC11A1* has also been found in endocrine tissues, including the anterior pituitary, adrenal medulla and pancreatic islets of Langerhans (White *et al.*, 2004). However, the expression of *SLC11A1* in these endocrine tissues may be due to the presence of resident phagocytic cells rather than expression by the local organ tissue. In summary, the majority of evidence indicates that SLC11A1 is principally expressed in phagocytic cells, namely macrophages and PMN leukocytes.

1.1.4 Function of SLC11A1

SLC11A1 functions as a divalent cation symporter with murine studies showing that Slc11a1 can mediate transportation of Fe^{2+}, Mn^{2+}, Zn^{2+}, Mg^{2+} and Co^{2+} ions (Table 1.1) (Forbes and Gros, 2003, Goswami *et al.*, 2001).When recruited to the phagosomal membrane, SLC11A1 transports ions out of the phagosome along the proton gradient (Forbes and Gros, 2001, Frehel *et al.*, 2002, Jabado *et al.*, 2000). SLC11A1 appears to have multiple functions, playing a role in both the resolution of infection and erythrophagocytosis (Sections 1.1.4.1 and 1.1.4.2). However, both activities are dependent upon, in part, transportation of divalent cations.

1.1.4.1 SLC11A1 Functions as a Symporter to Transport Cations Out of the Phagosome

SLC11A1 has been shown to function as a pH dependent cation symporter, removing ions from the phagosome into the cytosol in the direction of the proton gradient (Figure 1.4). This divalent cation transport is in direct competition with the pathogen's transporters (also members of the Nramp family displaying high homology with SLC11A1) (Table 1.1), where they play an essential role in the survival of the pathogen (Figure 1.4). Divalent cations are rate limiting for the metabolic activity of bacteria, for example, iron is an important co-factor for many enzymes and manganese is essential for the activity of the free radical scavenging enzyme, superoxide dismutase. Transport of ions out of the phagosome would limit the availability of these ions, thereby preventing the growth and replication of intraphagosomal pathogens, resulting in a bacteriostatic effect. Ion depletion might also enhance the bacteriocidal activity of macrophages by making the pathogen more susceptible to killing by oxygen radicals (McDermid and Prentice, 2006).

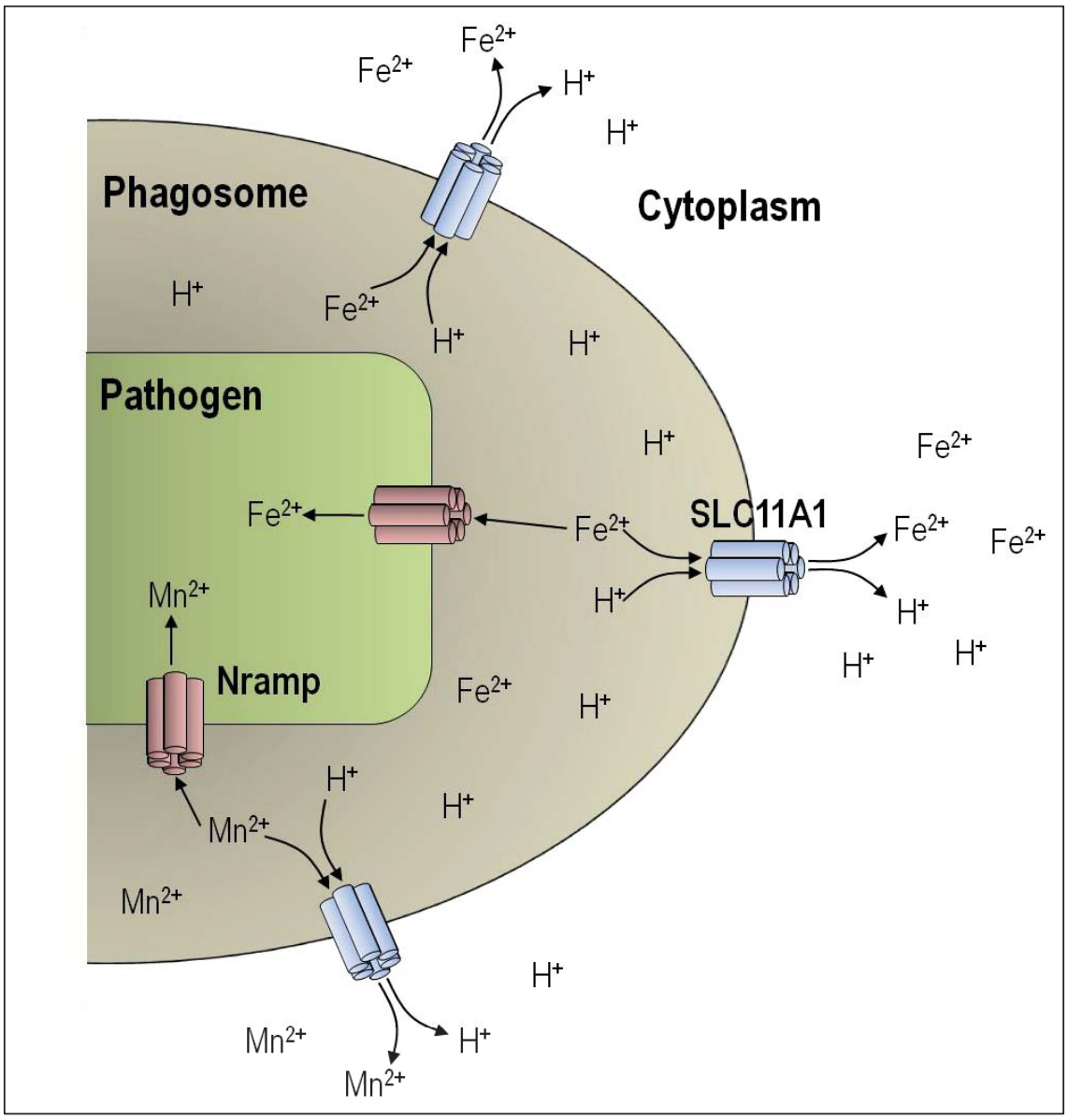

Figure 1.4 SLC11A1 functions as a divalent cation symporter. Pathogen phagocytosis results in the rapid recruitment of SLC11A1 to the phagosomal membrane where it transports a range of divalent cations out of the phagosome down the proton gradient. This transport of divalent cations is in direct competition with pathogen divalent cation transporters (Nramp), where sequestration of the cations is required for the normal metabolic activity of the pathogen.

1.1.4.2 Role of SLC11A1 in Resting Macrophages

Specialised macrophages, within the reticuloendothelial organs, phagocytose senescent erythrocytes, thereby facilitating their removal from the circulation (erythrophagocytosis) at a rate of ~ 2×10^6 cells/s into plasma membrane derived phagosomes. The breakdown of haemoglobin from these senescent erythrocytes represents the greatest daily turnover of iron in the body, recycling approximately 25mg of iron per day (Koay and Walmsley, 1996).

SLC11A1 may play a role in erythrophagocytosis by transporting ions out of the phagosome of macrophages. It has been suggested that SLC11A1, when localised to the phagosomal membrane, transports iron into the cytosol, thereby facilitating the export of iron from the cell (Atkinson and Barton, 1999, Biggs *et al.*, 2001, Knutson and Wessling-Resnick, 2003, Knutson *et al.*, 2003, Soe-Lin *et al.*, 2009, Soe-Lin *et al.*, 2010). A study using COS-1 cells expressing wild type Slc11a1 found a 40% cellular reduction in iron levels compared to Slc11a1 null cells suggesting that SLC11A1 plays a role in modulating total cellular iron levels (Atkinson and Barton, 1998, Barton *et al.*, 1999).

The hypothesis that SLC11A1 plays a role in erythrophagocytosis has been strengthened by a recent study showing that wild type RAW264.7 $Slc11a1^{+/+}$ macrophages (RAW+) are more efficient at recycling iron derived from haemoglobin than RAW264.7 $Slc11a1^{-/-}$ macrophages (RAW-). The study found that upon uptake of hemin or opsonised erythrocytes, Slc11a1 expression was significantly increased (Soe-Lin *et al.*, 2008), which is consistent with previous findings of a two-fold increase in Slc11a1 mRNA after erythrophagocytosis (Knutson *et al.*, 2003). RAW+ macrophages also had a significant increase in the labile iron pool ("iron in transport"), which constitutes the loosely bound cytosolic iron that is redox active and chelator sensitive, as compared with RAW- cells, suggesting that the increased removal of iron from the phagosome is due to the activity of Slc11a1 (Soe-Lin *et al.*, 2008). Furthermore, increased Slc11a1 expression was observed upon exposure of RAW+ cells to erythropoietin (EPO) (Soe-Lin *et al.*, 2008). The mechanism through which EPO modulates Slc11a1 expression is yet to be elucidated.

1.1.5 Pleiotropic Effects of SLC11A1

In classically activated macrophages, membrane fusion between SLC11A1 positive lysosomes and phagosomes, and consequent transport of divalent cations out of the phagosome results in a range of pleiotropic effects, which initiate and perpetuate a immune response that resolves infection (Figure 1.5). The studies used to define these pleiotropic effects have been completed using murine models. Mice, which lack functional Slc11a1, are susceptible to a range of macrophage-tropic pathogens (Section 1.1.1) due to the inadequate activation of a protective Th1 immune response.

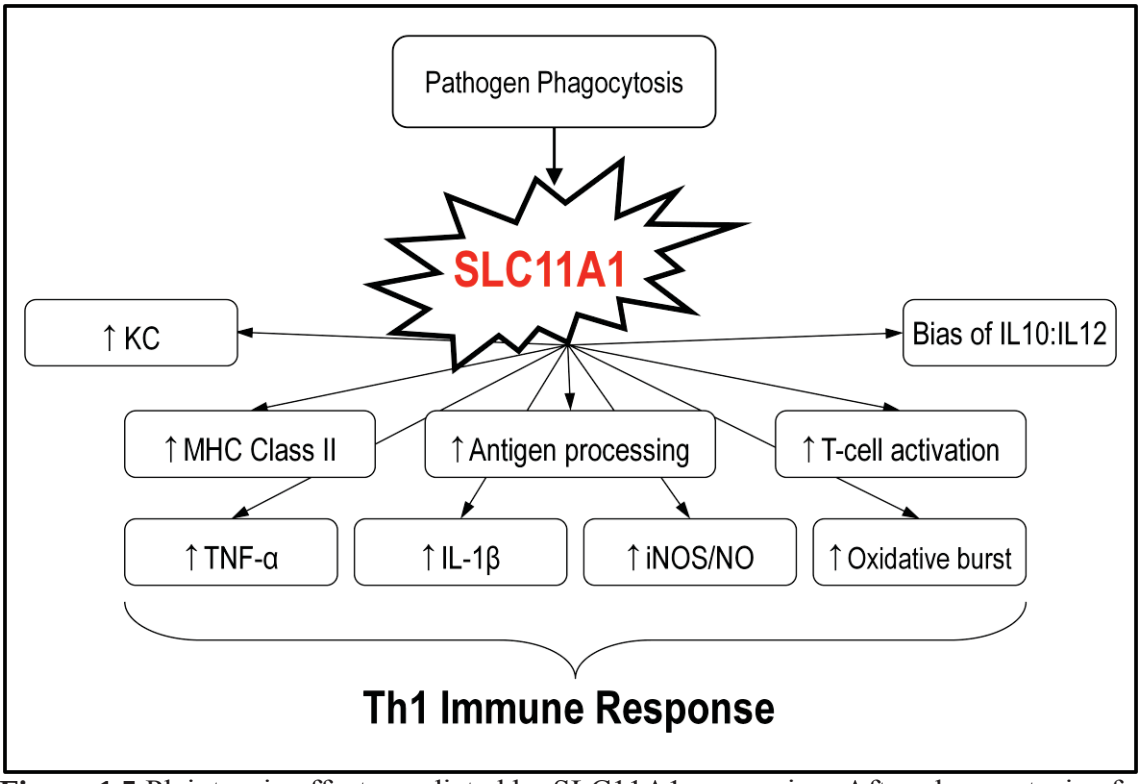

Figure 1.5 Pleiotropic effects mediated by SLC11A1 expression. After phagocytosis of the pathogen, SLC11A1 is recruited to the phagosomal membrane where it precipitates a multitude of effects that operate in concert to mount a pro-inflammatory (Th1) immune response, which facilitates clearance of the pathogen. TNF-α – tumour necrosis factor alpha, IL – interleukin, iNOS – inducible nitric oxide synthase, NO – nitric oxide.

1.1.5.1 SLC11A1 Modulates Adaptive Immune Responses

SLC11A1 functions to initiate and perpetuate a Th1 immune response. Macrophages and DCs from mice resistant to infection (i.e. express functional Slc11a1) express higher levels of MHC class II than susceptible mice, which do not contain functional Slc11a1 ($Slc11a1^{-/-}$) (Barrera *et al.*, 1997, Kaye and Blackwell, 1989, Kaye *et al.*, 1988, Lang *et al.*, 1997, Stober *et al.*, 2007, Wojciechowski *et al.*, 1999, Zwilling *et al.*, 1987). It has also been shown that protein processing for presentation to T-cells by MHC class II molecules is increased in both macrophages and DCs in resistant ($Slc11a1^{+/+}$) compared to susceptible ($Slc11a1^{-/-}$) mice (Lang *et al.*, 1997, Stober *et al.*, 2007). Additionally, the observed increase in antigen processing was independent of the increase in MHC class II expression. Furthermore, T-cell activation by macrophages of susceptible mice ($Slc11a1^{-/-}$) infected with *L.donovani* were significantly lower than in macrophages of resistant mice ($Slc11a1^{+/+}$) (Kaye *et al.*, 1988), with the decreased level of T-cell activation attributable to lower MCH class II expression. Therefore, through increased protein processing, up regulation of MHC class II molecules and increased T-cell activation, Slc11a1 plays an important role in the modulation of an adaptive immune response (Figure 1.5).

1.1.5.2 SLC11A1 Modulates Cytokine Levels

Slc11a1 modulates the expression levels of a range of cytokines/chemokines (Figure 1.5). Expression of TNF-α, IL-1β and KC were upregulated in macrophages from resistant mice ($Slc11a1^{+/+}$), as compared to macrophages of susceptible mice ($Slc11a1^{-/-}$) (Blackwell, 1996, Blackwell *et al.*, 1988, Formica *et al.*, 1994, Roach *et al.*, 1993, Roach *et al.*, 1994, Smit *et al.*, 2004). The expression of TNF-α and IL-1β facilitate the initiation/perpetuation of a Th1 immune response, while KC is a C-X-C chemokine belonging to the IL-8 family, which is a chemoattractant for PMN leukocytes.

Slc11a1 also influences the ratio of the cytokines IL-10 and IL-12 (Figure 1.5). No significant difference in the level of expression is found when IL-12 levels are compared at different time points post stimulation (using LPS and IFN-γ) between macrophages and DCs from susceptible and resistant mice (Jiang *et al.*, 2009, Stober *et al.*, 2007). However, a significant trend is observed for a higher ratio of IL-10:IL-12 produced by macrophages and DCs from susceptible mice compared to resistant mice

(Rojas *et al.*, 1999, Stober *et al.*, 2007). Increased IL-10 expression is associated with diminished pro-inflammatory immune responses. This cytokine also has stimulatory effects on B-cells, but an inhibitory effect on macrophages and Th1 cells (Couper *et al.*, 2008). Therefore the bias for IL-10 production in mice expressing non-functional Slc11a1 contributes to the inhibition of a Th1 pro-inflammatory response, and polarisation to a Th2 immune response, which is inadequate to clear infection.

1.1.5.3 SLC11A1 Modulates Expression of Pro-Inflammatory Effector Molecules

Slc11a1 mediates increased production of pro-inflammatory effector molecules, which exert bacteriocidal properties to resolve infection (Figure 1.5). An increase in inducible nitric oxide synthase (iNOS) expression, resulting in increased L-arginine flux, and subsequent production of nitric oxide (NO) was identified in macrophages of susceptible mice (Slc11a1$^{-/-}$) transfected with functional *Slc11a1*, as compared to non-transfected macrophages (Barton *et al.*, 1995). Slc11a1 also plays a role in the production of a respiratory burst (rapid release of reactive oxygen species), as splenic macrophages from resistant mice (Slc11a1$^{+/+}$) showed increased production of hydrogen peroxide (H_2O_2) and superoxide anion (O_2^-) as compared to macrophages of susceptible mice (Slc11a1$^{-/-}$) (Denis *et al.*, 1988).

The range of pleiotropic effects mediated by Slc11a1, some of which occur as early as thirty minutes post infection, suggests an important role for Slc11a1 in the early signaling pathways during infection leading to the production of a Th1 pro-inflammatory immune response which is important for the destruction of a range of intracellular pathogens (Dong and Flavell, 2000). In murine studies, macrophages with a non-functional Slc11a1 produce a Th2 response and are therefore unable to clear the infection (Lang *et al.*, 1997, Soo *et al.*, 1998). However, it is currently unclear as to how recruitment of Slc11a1 to the phagosomal membrane and consequent divalent cation transport out of the phagosome mediates the wide range of pleiotropic effects to elicit a Th1 pro-inflammatory immune response.

1.1.6 SLC11A1 and Autoimmune Disease

While the range of pleiotropic effects exerted by SLC11A1 modulate the elicitation of pro-inflammatory immune responses to clear infection, many of these effects are also involved in the induction and perpetuation of autoimmune/inflammatory diseases.

There is increasing evidence, from both human and mouse studies, to support a role for SLC11A1 in the development of Type 1 diabetes (T1D). The non obese diabetic (NOD) mouse is a spontaneous model of TID. The pathogenesis of disease development mimics, in many respects, that seen in humans, therefore the NOD mouse is the most widely used model by which to elucidate immune mechanisms of autoimmune diabetes in humans. The NOD mouse possesses a functional Slc11a1 protein ($Slc11a1^{+/+}$). A congenic mouse strain that is derived from the NOD strain, the NOD.B10, which has a low incidence of T1D, possesses a non-functional Slc11a1 protein ($Slc11a1^{-/-}$) (Wicker *et al.*, 2004). This observation corroborates the hypothesis that Slc11a1 may play a role in the pathogenesis of T1D.

The region of mouse chromosome 1 in which *Slc11a1* is located has been identified as an insulin dependent diabetes (Idd5.2) locus. Over 20 of these loci have been identified, which have been shown to be protective for disease development in NOD mice (Kissler *et al.*, 2006). Of the 42 genes located in the Idd5.2 locus, *Slc11a1* is the most likely candidate, due to its important immunomodulatory role, as well as the presence of the inactivating point mutation (G169D) in the coding region of *Slc11a1* (Hill *et al.*, 2000).

Kissler et al. (2006) has provided significant evidence to suggest Slc11a1 is responsible for the protection afforded at the Idd5.2 locus. Mice heterozygous for the *Slc11a1* G169D mutation ($Slc11a1^{+/-}$) were found to have a reduced frequency of disease compared to the homozygous NOD mice ($Slc11a1^{+/+}$). However, the reduced frequency of disease incidence was not as low as that observed with the NOD.B10 mice ($Slc11a1^{-/-}$), showing a dose dependant effect of *Slc11a1* on the initiation and perpetuation of autoimmunity, and T1D development.

Further evidence that *Slc11a1* is the candidate responsible at the Idd5.2 locus was provided by the production of a transgenic NOD mouse line expressing a short hairpin

RNA (shRNA) targeted against *Slc11a1*, resulting in the degradation of *Slc11a1* mRNA and generation of a phenotype analogous to that of Slc11a1$^{-/-}$ mice. When compared to their non-transgenic littermates, the transgenic mice exhibited a significant reduction in the incidence of T1D. This reduction in disease occurrence was comparable to the protective effect reported for congenic mice that carried the disease-protective Idd5.2 locus. Furthermore, silencing of *Slc11a1* resulted in a significant reduction in disease incidence in experimental autoimmune encephalomyelitis, a murine model of multiple sclerosis (Kissler *et al.*, 2006).

Additionally, using a murine model of colitis, resembling the human disease of ulcerative colitis, Jiang et al. (2009) observed that resistant mice (Slc11a1$^{+/+}$) had lower body weights, higher mortality rates and shorter colon lengths, as compared to susceptible mice (Slc11a1$^{-/-}$). These differences were attributable to differing cytokine profiles, where the resistant mice produced a pro-inflammatory immune response resulting in tissue destruction, in contrast to the anti-inflammatory immune response mounted by the susceptible mice (Jiang *et al.*, 2009). Thus *Slc11a1* modulated susceptibility to autoimmunity in three disease models (T1D, experimental autoimmune encephalomyelitis and colitis) providing further support for the premise *Slc11a1* is the gene responsible for the protective effect of the Idd5.2 locus, and the involvement of *Slc11a1* in the development of autoimmune disease *per se*.

The genetic region of mouse chromosome 1 containing *Slc11a1* and the protective Idd5.2 locus, is syntenic with human chromosome 2q35 (Schurr *et al.*, 1990), which has also been mapped as an insulin-dependent diabetes mellitus (IDDM) susceptibility locus, containing IDDM13, which has been shown to confer resistance to T1D (Esposito *et al.*, 1998, Fu *et al.*, 1998, Morahan *et al.*, 1996).

In addition to the pleiotropic effects of SLC11A1, the function of SLC11A1 as an iron transporter may contribute directly to the onset of autoimmune diseases. Increasing evidence suggests that dysregulation of iron metabolism occurs in many autoimmune diseases (Bowlus, 2003, Nielsen *et al.*, 1994, Weber *et al.*, 1988). For example, iron deposition and subsequent iron catalysed oxidative damage has been associated with tissue destruction in multiple sclerosis (Bakshi *et al.*, 2002, Bakshi *et al.*, 2001). Iron has also been shown to contribute to the pathogenesis of rheumatoid arthritis, whereby

patients have been shown to have significantly higher concentrations of iron deposited in their synovial membranes (Fritz *et al.*, 1996). Furthermore, SLC11A1 has been shown to be located within macrophages and neutrophils in the synovial membrane of individuals with rheumatoid arthritis (Bayele *et al.*, 2007, Rioja *et al.*, 2005). Due to the role of SLC11A1 in erythrophagocytosis (Section 1.1.4.2), SLC11A1 may orchestrate the deposition of iron to the synovium (Telfer and Brock, 2002). The presence of iron in the synovial membrane would then result in the generation of oxygen radicals leading to the tissue inflammation and destruction associated with rheumatoid arthritis.

Therefore, the use of murine models showing resistance ($Slc11a1^{+/+}$) and susceptibility ($Slc11a1^{-/-}$) to infection has established that Slc11a1 plays a significant role in the development of infectious and autoimmune/inflammatory disease, attributable to the role Slc11a1 plays in initiating and perpetuating Th1 pro-inflammatory immune responses.

1.2 *SLC11A1* POLYMORPHISMS

1.2.1 Genomic Organisation of the *SLC11A1* Locus

Located at chromosome 2q35, the *SLC11A1* gene is approximately 14kb in length, is composed of 15 exons (Figure 1.6) and produces an mRNA transcript of 3865 bases, with a coding sequence 1653 base pairs in length (NCBI NM_000578.3). An alternatively sized mRNA transcript of 2.0kb has also been identified in conjunction with the 3865bp transcript. The two transcripts differ at the 3'UTR and polyadenlyated tail. *SLC11A1* is located in a locus containing genes encoding proteins with immune functions (IL-8 receptors, IL8RA and IL8RB) (Figure 1.6).

The *SLC11A1* exon designated 4a, within the 4th intron, is an alternatively spliced variant produced by the replication of an Alu element (Figure 1.6). This splice variant has been shown to be transcribed *in vivo*, resulting in the introduction of a termination codon in exon 5 due to a frame-shift in the coding sequence. Due to the frame-shift, and early termination, this splice variant produces a truncated, functionally null protein. At the mRNA level, the ratio of truncated to functional transcripts in macrophages is relatively low (approximately 1:5) (Cellier *et al.*, 1994).

1.2.2 *SLC11A1* Polymorphisms

To date, 17 polymorphisms within *SLC11A1* have been extensively studied (Figure 1.6) (Table 1.2). Three polymorphisms have been identified in the *SLC11A1* promoter, which include two single nucleotide polymorphisms (SNP) and a polymorphic microsatellite $(GT)_n$ repeat polymorphism. Additionally, two deletion mutations have been identified in the 3' UTR of *SLC11A1* (Table 1.2). Within the *SLC11A1* gene, four SNPs exist in intronic areas along with a polymorphic $(ATA)_n$ repeat in intron 8. There are seven reported mutations in the coding region of *SLC11A1*, with three of these being silent mutations and 4 missense or insertion/deletion mutations, which alter the amino acid sequence. These include two SNPs that result in an amino acid substitution (1029C/T [A316V] and 1730G/A [D543N]) and two insertion/deletion polymorphisms located in exon 2 (136del9 and 157ins11) (Figure 1.6) (Table 1.2).

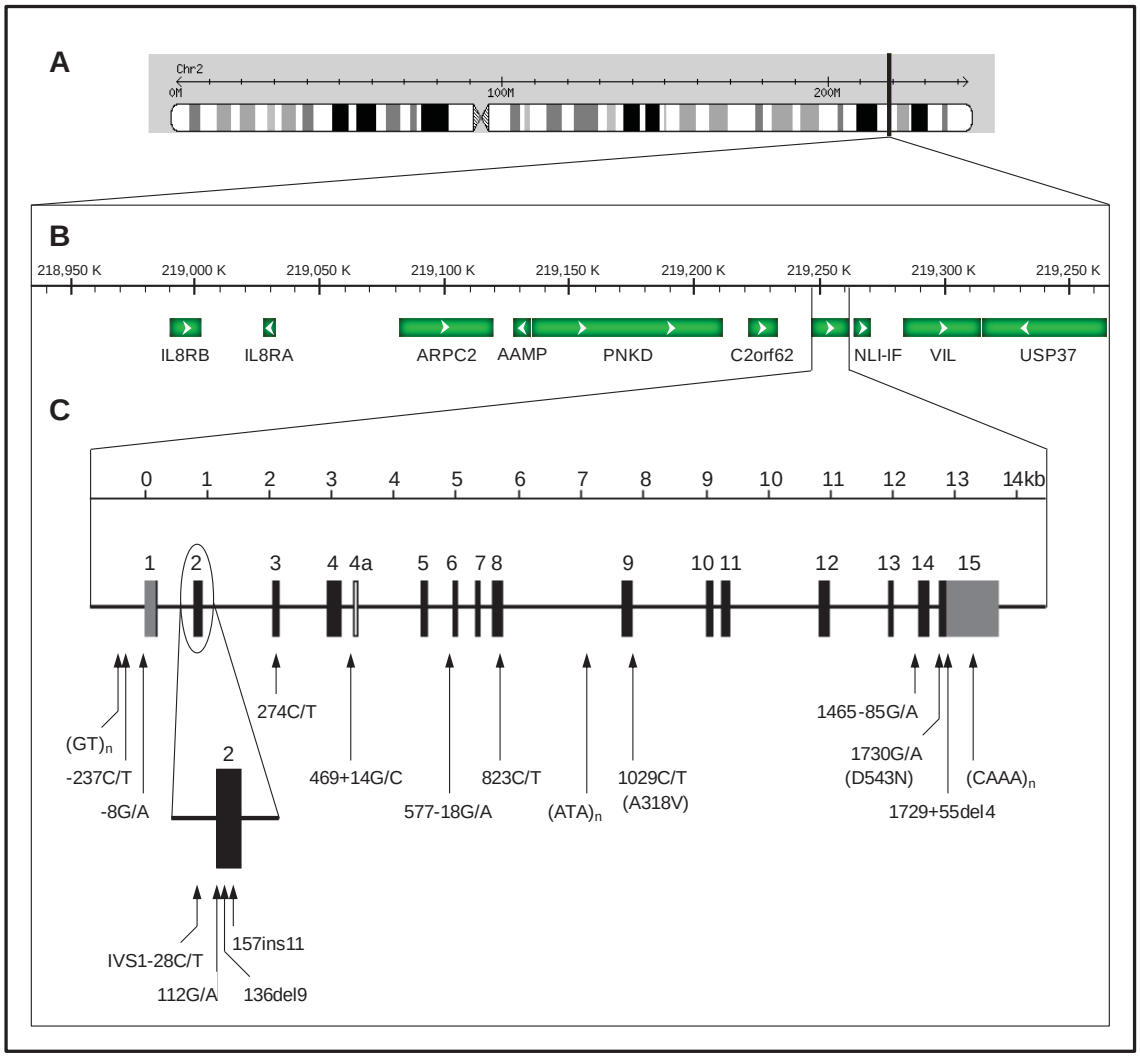

Figure 1.6 Location and genomic organisation of the *SLC11A1* locus. (A) The *SLC11A1* gene is located on Chromosome 2q35. (B) Genomic organisation around the *SLC11A1* gene showing the relative positions of immune (IL8RA and IL8RB) and non-immune related (PNKD and VIL) genes. 50kb separates each major marking on the scale bar at the top of the image. (C) Genomic organisation and location of studied sequence variants in *SLC11A1*. The 15 exons of the gene are shown as black boxes with their respective numbers and the corresponding scale above indicates the length (kb) of the gene. The grey boxes indicate the 3' and 5' untranslated regions and the introns and flanking regions are represented by a thin line. Arrows indicate the position of sequence variants where numbering is relative to the transcription start site.

Table 1.2 The Location of Analysed Polymorphisms within *SLC11A1*.

Polymorphism	Location of variant	Type	Reference
$(GT)_n$ microsatellite repeat	Promoter	Microsatellite	Liu *et al* ., 1995
-237C/T	Promoter	Base substitution	Lewis *et al* ., 1996
-8G/A	Promoter	Base substitution	Mohamed *et al* ., 2004
IVS1-28C/T	Intron 1	Base substitution	Zaahl *et al* ., 2005
112G/A	Coding	Base substitution (Silent)	Zaahl *et al* ., 2005
136del9	Coding	Missense - deletion of 9bp	White *et al* ., 1994
157ins11	Coding	Missense - insertion of 11bp	Zaahl *et al* ., 2005
274C/T	Coding	Base substitution (Silent)	Liu *et al* ., 1995
469+14G/C (INT4)	Intron 4	Base substitution	Liu *et al* ., 1995
577-18G/A	Intron 5	Base substitution	Liu *et al* ., 1995
823C/T	Coding	Base substitution (Silent)	Liu *et al* ., 1995
$(ATA)_n$	Intron 8	Microsatellite	Awomoyi *et al* ., 2006
1029C/T (A318V)	Coding	Base substitution (Missense)	Liu *et al* ., 1995
1465-85G/A	Intron 13	Base substitution	Liu *et al* ., 1995
1730G/A (D543N)	Coding	Base substitution (Missense)	Liu *et al* ., 1995
1729+55del4 (TGTG)	3'UTR	Deletion of 4bp	Liu *et al* ., 1995
1729+271del4 $(CAAA)_n$	3'UTR	Microsatellite	Buu *et al* .,1995

While 17 polymorphisms have been analysed extensively within the *SLC11A1* locus (Table 1.2), a large number of polymorphisms have been identified throughout the *SLC11A1* promoter and gene region which have not been studied (Figure 1.7). The majority of these polymorphisms are silent mutations in coding regions or are located in non-coding regions and therefore, are thought to exert no effect on the expression of the gene or the function of the protein.

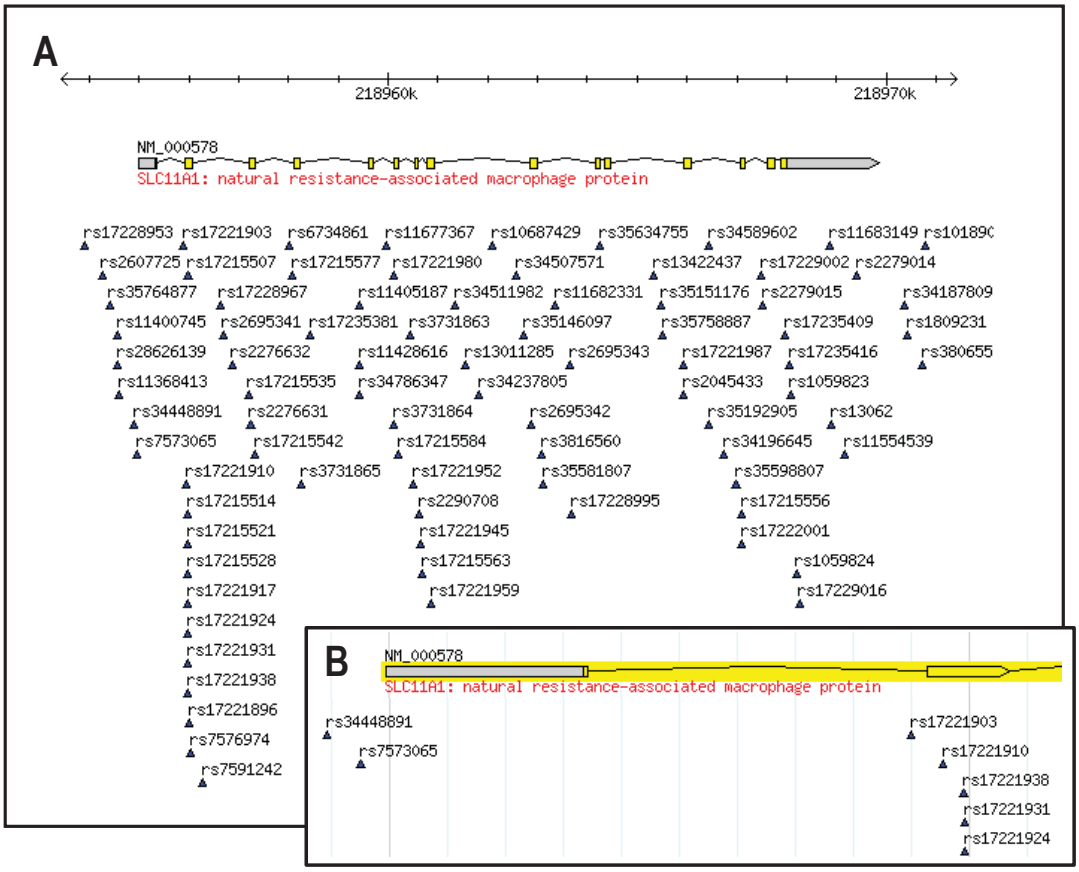

Figure 1.7 Location of all annotated sequence variants throughout the *SLC11A1* locus. (A) The bar at the top shows the location of the gene/variants respective to Chromosome 2. *SLC11A1* is shown below with the boxes and lines depicting the exon and intron structure, respectively. Each arrow represents a different sequence variant, with the respective accession number. (B) Close-up of the *SLC11A1* 5'UTR showing a lack of sequence variants. Annotated variants are from the NCBI SNP database (dbSNP) with the image from Hapmap (http://www.hapmap.org/).

1.2.3 *SLC11A1* Functional Polymorphisms

Of the *SLC11A1* polymorphisms identified to date, a single nucleotide polymorphism similar to that found in mice that produces a functionally null protein (G169D) has not been identified in humans (Vidal *et al.*, 1996). SLC11A1 appears to be essential to macrophage function, and therefore, directly influences innate immunity and, through modulation of antigen presentation and cytokine production, also impacts adaptive immunity (Section 1.1.7). Consequently, coding region mutations are predicted to be rare.

However, some coding region mutations, which result in a putative alteration of SLC11A1 function, have been identified. A putative functional coding region mutation

has been identified in exon 2 at nucleotide position 136 of the open reading frame of *SLC11A1* and consists of a deletion of 9 nucleotides (136del9) in a 3 × 9 nucleotide repeat in the region encoding the N-terminal proline/serine rich SH3 binding domain and is analogous to another reported polymorphism termed 148del9 (Figure 1.6) (Barton *et al.*, 1994, Blackwell *et al.*, 1995, White *et al.*, 1994, Zaahl *et al.*, 2005). However, this polymorphism only occurs at a frequency of 0-4% (Searle and Blackwell, 1999, White *et al.*, 1994), and has never been observed in the homozygous condition, further corroborating the important role played by SLC11A1.

The 157ins11 is another coding region mutation in exon 2, near the region encoding the SH3 binding domain, that results in the insertion of 11 bases (GACCAGCCCAG) (Figure 1.6). The insertion has only been observed in one individual in a heterozygous form (Zaahl *et al.*, 2005). The functional significance of this polymorphism is unknown, however insertion of 11bp would result in a shift in the reading frame, and therefore may result in a truncated, functionally null, protein. The low frequencies and the fact that the 136del9 and 157ins11 polymorphisms have only been found in a heterozygous state suggests that these polymorphisms would be fatal in the homozygous state.

Another mutation, occurring in exon 15, results in an amino acid substitution of a negatively charged aspartic acid residue for a neutral asparagine residue at position 543 (D543N) in the cytoplasmic carboxyl terminus of the SLC11A1 protein (Table 1.2). Due to the positioning of this polymorphism at the carboxy terminal end of the protein (and not the pore channel), the functional effects of this polymorphism are unknown (Figure 1.6). However, it is thought that this substitution may result in altered *SLC11A1* protein function, thereby altering the kinetics of transport of the divalent cations when localised to the phagosomal membrane (Liu *et al.*, 1995).

1.2.4 *SLC11A1* Polymorphisms Affecting Expression Levels

While coding region mutations like the 136del9 and D543N putatively affect the functionality of SLC11A1, polymorphisms located in the regulatory regions of the gene (5'UTR, 3'UTR and promoter region) may affect the level of expression of *SLC11A1* leading to different levels of functional SLC11A1 protein. Polymorphisms located in the promoter region may alter expression by increasing or decreasing the rate of

transcription, while polymorphisms located in the 3'UTR may alter protein levels at the translational level. These polymorphisms are therefore a more subtle way, as compared to coding region mutations, of altering the amount of functional protein expressed.

1.2.4.1 *SLC11A1* Promoter Polymorphisms

The *SLC11A1* promoter region contains several polymorphisms. The most studied of these are the $(GT)_n$ microsatellite repeat and -273C/T polymorphism, which have been shown to alter *SLC11A1* expression (Sections 1.3.2 and 1.3.3). Other promoter polymorphisms have been identified, however, these have not been shown to have an effect on *SLC11A1* expression in cells of monocytic origin (Donninger *et al.*, 2004, Mohamed *et al.*, 2004).

1.2.4.2 *SLC11A1* UTR Polymorphisms

No polymorphisms have been identified in the 5'UTR of *SLC11A1*. While there are a high number of polymorphisms located both before and after the 5'UTR, none have been identified within this region (Figure 1.7). The lack of polymorphisms in the 5'UTR compared to the large number of polymorphisms in the surrounding regions, suggests that this 5'UTR region plays an important role in *SLC11A1* expression as sequence conservation is well maintained.

Several microsatellite repeats have been identified within the 3'UTR of *SLC11A1*. The 1729+271del4, also known as the $(CAAA)_n$ polymorphism, is a polymorphic microsatellite repeat located in the 3'UTR. Two alleles of the polymorphism have been described, $(CAAA)_2$ [$CAAAAA(CAAA)_2CGAAAAA$] and $(CAAA)_3$ [$CAAAAA(CAAA)_3CAAAAAA$] (Buu *et al.*, 1995), which differ by a single 4bp CAAA repeat and a single C to G nucleotide polymorphism. The $(CAAA)_3$ variant is more common than the $(CAAA)_2$ variant with frequencies of approximately 63 and 37%, respectively. Another microsatellite repeat in the 3'UTR is the 1729+55del4 also known as the TGTG insertion/deletion (Liu *et al.*, 1995). Two variants of this polymorphic microsatellite repeat have been identified, which differ by a 4bp TGTG repeat. These 3'UTR polymorphisms may affect the stability of the mRNA transcript, therefore indirectly modulating *SLC11A1* expression. However, there are currently no published reports to support this hypothesis.

1.3 *SLC11A1* PROMOTER POLYMORPHISMS AND DISEASE OCCURRENCE

1.3.1 The *SLC11A1* $(GT)_n$ Microsatellite Promoter Polymorphism

The *SLC11A1* promoter contains a complex polymorphic $(GT)_n$ microsatellite repeat, which is located approximately 240bp upstream of the transcription start site (Figure 1.6). To date, nine different polymorphic variants of the $(GT)_n$ promoter, which vary in the number or composition of GT repeats, have been identified (Table 1.3) (Searle and Blackwell, 1999).

Table 1.3 $(GT)_n$ Repeat Polymorphisms of the *SLC11A1* Promoter.

Allele	Sequence	Length (bp)	Frequency (%)	Reference
Allele 1	$t(gt)_5ac(gt)_5ac(gt)_{11}ggcaga(g)_6$	59	>1	Blackwell *et al.* , 1995
Allele 2	$t(gt)_5ac(gt)_5ac(gt)_{10}ggcaga(g)_6$	57	15-30	Blackwell *et al.* , 1995
Allele 3	$t(gt)_5ac(gt)_5ac(gt)_9ggcaga(g)_6$	55	65-85	Blackwell *et al.* , 1995
Allele 4	$t(gt)_5ac(gt)_9ggcaga(g)_6$	43	>1	Blackwell *et al.* , 1995
Allele 5	$t(gt)_4ac(gt)_5ac(gt)_{10}ggcaga(g)_6$	55	2-5*,18#	Graham *et al.* , 2000
Allele 6	$t(gt)_5ac(gt)_5ac(gt)_4at(gt)_4ggcaga(g)_7$	56	>1	Graham *et al.* , 2000
Allele 7	$t(gt)_5ac(gt)_5at(gt)_{11}ggcaga(g)_6$	59	5†	Kojima *et al.* , 2001
Allele 8	$t(gt)_5ac(gt)_5ac(gt)_6ggcaga(g)_6$	49	>1	Zaahl *et al.* , 2006
Allele 9	$t(gt)_5ac(gt)_5ac(gt)_8ggcaga(g)_6$	53	>1	Zaahl *et al.* , 2006

* European population (Kotze *et al* ., 2001)
# Greek population (Gazouli *et al* ., 2007)
† Japanese population (Kojima *et al* ., 2001)

Originally, four promoter $(GT)_n$ alleles were identified and designated alleles 1-4 (Blackwell *et al.*, 1995). However, to date, the number of alleles identified has increased to nine (Table 1.3). Alleles 5 and 6 were discovered in a study of the inflammatory condition, primary biliary cirrhosis (Graham *et al.*, 2000). Allele 7 was found in an investigation of inflammatory bowel disease in a Japanese population (Kojima *et al.*, 2001). The most recently discovered alleles, 8 and 9, were identified during a study of inflammatory bowel disease within a South African population (Zaahl *et al.*, 2006). Several of the alleles have the same repeat length, with alleles 1 and 7 (both 59bp) differing by a single C to T base substitution between repetitive GT repeats while alleles 3 and 5 (both 55bp) differ in the composition of the GT repeats.

In all populations studied to date, *SLC11A1* $(GT)_n$ promoter allele 3 is the most commonly occurring variant, followed by allele 2, with frequencies of approximately 60-70% and 20-30%, respectively (Searle and Blackwell, 1999). In most populations, the combined $(GT)_n$ allele 2 and 3 frequencies account for greater than 95% of all alleles (Table 1.3). However, the frequencies of the *SLC11A1* promoter alleles vary with ethnicity (Awoymi, 2007). The incidence of allele 3 varies between different populations where it is found with lower frequencies (60%) in South American populations and higher frequencies (83%) in Asian populations. Likewise, the frequency of $(GT)_n$ allele 2 varies from 39% in South American populations to 12% in Asian populations.

$(GT)_n$ alleles 1 and 4-9 occur at very low frequencies, however, these less commonly occurring $(GT)_n$ promoter alleles also vary in frequencies depending on the population studied. Allele 7 has only been identified in Asian populations where it has a frequency of approximately 5% (Kojima *et al.*, 2001). Likewise, allele 5 has been found predominantly in Caucasian/European populations, while the highest frequency of allele 4 is found in South American populations (Table 1.3) (Calzada *et al.*, 2001, Ferreira *et al.*, 2004, Gazouli *et al.*, 2007, Kotze *et al.*, 2001).

1.3.2 The $(GT)_n$ Promoter Polymorphisms Modulate *SLC11A1* Expression

The $(GT)_n$ microsatellite repeat functions as an endogenous enhancer of *SLC11A1* expression (Searle and Blackwell, 1999). The nine known alleles of the $(GT)_n$ promoter polymorphism vary in the number and sequence composition of the GT repeats, and alteration of this important promoter motif alters the enhancement of *SLC11A1* promoter activity mediated by the $(GT)_n$ microsatellite repeat (Figure 1.8). Reporter assays have been used to determine the level of *SLC11A1* gene expression for the different $(GT)_n$ promoter alleles in monocytic cell lines (Searle and Blackwell, 1999, Zaahl *et al.*, 2004). Analysis of the basal level of expression in resting macrophages shows that alleles 1, 2 and 4 function as poor promoters, resulting in a low level of *SLC11A1* expression, while allele 3 drives high *SLC11A1* gene expression, showing endogenous enhancer activity (Blackwell *et al.*, 1995, Searle and Blackwell, 1999) (Figure 1.8). Alleles 5 and 8 also result in a decreased *SLC11A1* expression, as compared to allele 3 (Zaahl *et al.*, 2004). The mechanism surrounding differences in the basal level of *SLC11A1* expression between the different alleles of the $(GT)_n$ promoter polymorphism is unknown.

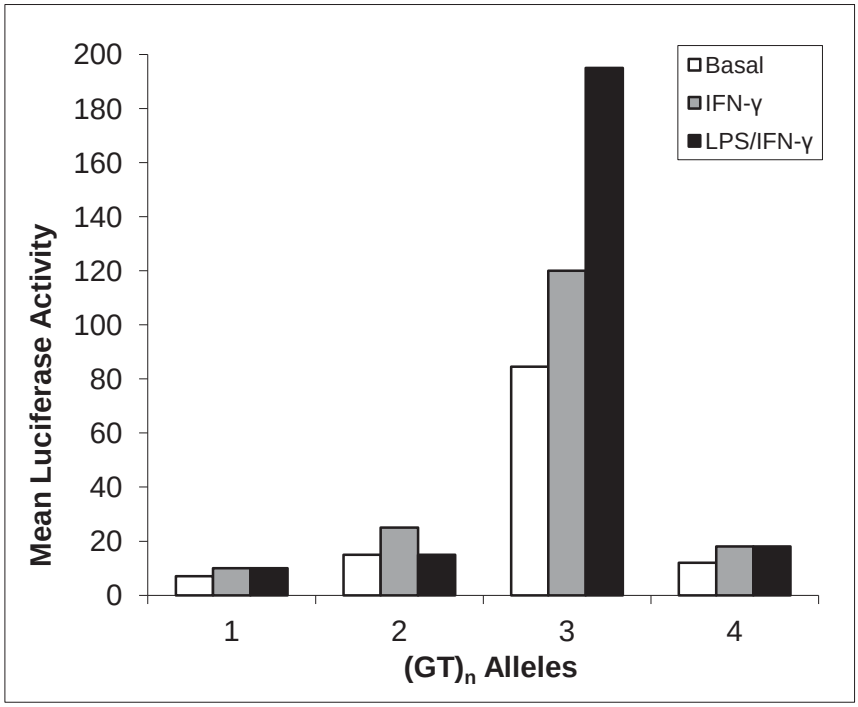

Figure 1.8 *SLC11A1* expression is differentially modulated by the different promoter $(GT)_n$ microsatellite alleles. Reporter constructs containing the different $(GT)_n$ alleles (x-axis) were transfected into the U937 cell line with or without the addition of the exogenous stimuli IFN-γ or LPS/IFN- γ (Adapted from Searle and Blackwell, 1999).

The addition of the exogenous stimulus, IFN-γ, in the luciferase reporter assays resulted in a similar percent increase in promoter activity of alleles 1 through to 4, compared to the basal level of expression observed without IFN- γ stimulation for each allele (Figure 1.8) (Searle and Blackwell, 1999). This finding is consistent with the presence of multiple putative IFN-γ response elements, located both upstream and downstream of the promoter (Blackwell, 1996). When LPS was added as a second exogenous stimulus in combination with IFN-γ, there was no significant difference in promoter activity of alleles 1 and 4 as compared with stimulation by IFN- γ alone. However, in the presence of both stimuli, there was a significant increase in *SLC11A1* expression in the presence of allele 3, while the presence of allele 2 resulted in a significant decrease in promoter activity (Figure 1.8) (Searle and Blackwell, 1999). The mechanism for the differential expression levels of SLC11A1, mediated by $(GT)_n$ alleles 2 and 3, in the presence or absence of exogenous stimuli, remains unknown.

1.3.3 The *SLC11A1* -237C/T Promoter Polymorphism

The -237C/T polymorphism, first discovered by Lewis et al. (1996) (Figure 1.6), is located 237 bases upstream of the transcription start site, and just downstream from the polymorphic $(GT)_n$ microsatellite repeat (Figure 1.6). This polymorphism consists of a single base substitution of a C to T, with the T variant frequency varying from 0-20% depending on the population analysed. Along with the *SLC11A1* $(GT)_n$ promoter polymorphism, the -237C/T polymorphism has also been shown to affect the level of expression of *SLC11A1* (Zaahl *et al.*, 2004). The less frequent -237 T variant is consistently detected in combination with allele 3 and has not been detected concurrently with allele 2. The more frequent -237 C variant has been shown to occur with all $(GT)_n$ alleles. It has been shown that the high basal level of *SLC11A1* expression driven by $(GT)_n$ allele 3 (Section 1.3.2, Figure 1.8), is significantly reduced to a level comparable to that of allele 2 when this allele is in *cis* with the less frequent -237 T variant (Zaahl *et al.*, 2004). Likewise, with the addition of the exogenous stimuli IFN-γ and LPS, expression levels of $(GT)_n$ allele 3 in association with the -237 T variant are reduced to levels comparable with those observed when these exogenous stimuli act in the presence of *SLC11A1* $(GT)_n$ allele 2. The reason for the decreased expression of *SLC11A1* by $(GT)_n$ allele 3 in association with the -237 T variant is unknown.

1.3.4 The Association of *SLC11A1* $(GT)_n$ Promoter Variants with Infectious and Autoimmune Diseases

From the aforementioned gene expression studies (Section 1.3.2), Blackwell, (1996) hypothesised that over-expression of *SLC11A1*, due to the presence of allele 3, would result in an enhanced Th1 pro-inflammatory immune response due to the pleiotropic effects of SLC11A1 leading to a chronic hyperactivation of macrophages. This hyperactivation would lead to an increased rate of pathogen clearance resulting in resistance to infection. However, this increase in activation of macrophages would lead to an enhanced Th1 pro-inflammatory immune response putatively causing an increased susceptibility to autoimmune diseases (Figure 1.9).

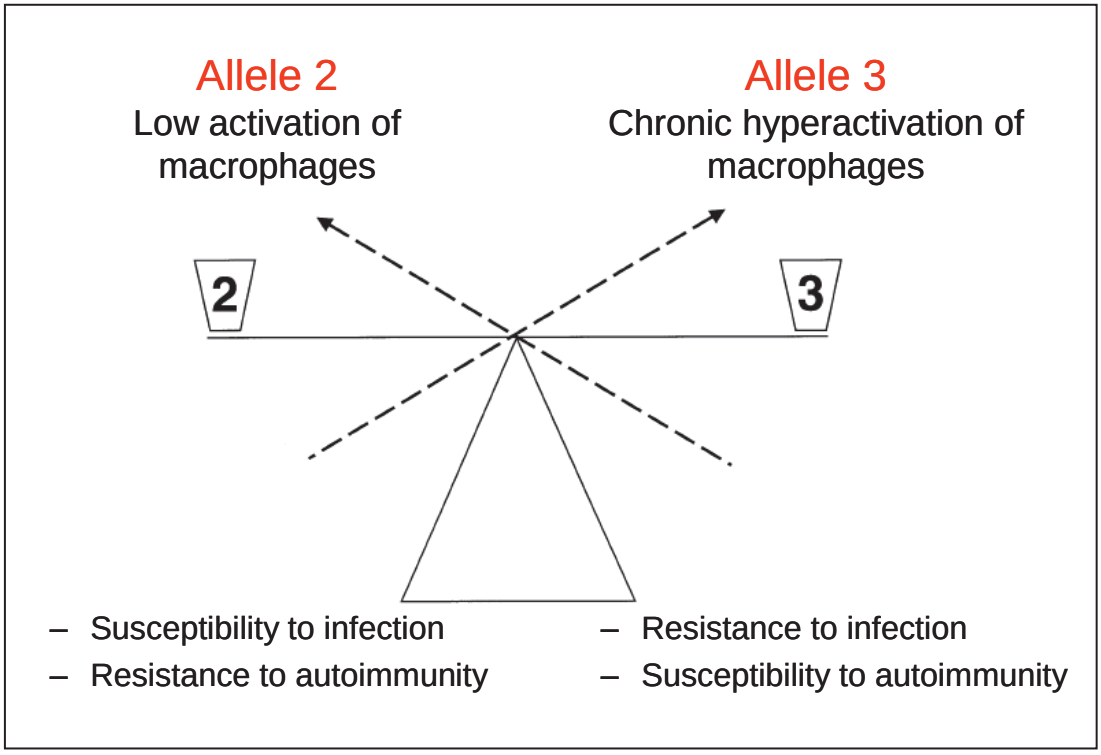

Figure 1.9 The influence of *SLC11A1* $(GT)_n$ allele 2 and allele 3 on macrophage activation. Allele 2 causes low activation of macrophages resulting in susceptibility to infection but resistance to autoimmune disease. Allele 3 results in over expression of *SLC11A1* causing chronic hyperactivation of macrophages. This leads to resistance to infection, but an increased susceptibility to autoimmune diseases (Modified from Blackwell *et al.*, 2003).

Likewise, low expression levels of *SLC11A1*, driven by allele 2, would result in a lower activation of macrophages, conferring resistance to autoimmune diseases. However, the

lower activation state of macrophages would result in an increased susceptibility to infection (Figure 1.9). Analogous to the wild type 169G ($Slc11a1^{+/+}$) mice, upon infection, $(GT)_n$ alleles 3 would elicit a range of pleiotropic effects, which collectively facilitate a Th1 mediated immune response to resolve infection. Alternatively, lower SLC11A1 expression driven by $(GT)_n$ allele 2 would elicit a low activation of macrophages and an inability to mount an effective Th1 mediated immune response to clear the infection, similar to the mice carrying the 169D mutation ($Slc11a1^{-/-}$). The *SLC11A1* alleles putatively conferring susceptibility to autoimmune disease may have been maintained in the population due to improved survival rates following infectious disease challenge (Smit *et al.*, 2004).

1.3.4.1 *SLC11A1* $(GT)_n$ Promoter Polymorphism and Infection

Due to the ability of the different alleles at the $(GT)_n$ promoter polymorphism to modulate differential expression of *SLC11A1*, numerous studies have investigated the association of specific $(GT)_n$ promoter alleles with the incidence of a range of infectious diseases to determine if specific alleles modulate disease susceptibility/resistance. These have included diseases caused by bacterial pathogens (*M. tuberculosis*, *M. leprae* and *S. typhi*), protozoan parasites (*Trypanosoma cruzi* and *Leishmania donovani*) and viruses (human immunodeficiency virus [HIV]). Table 1.4 summarises all familial and association studies completed to date that have assessed the association of the $(GT)_n$ promoter polymorphisms with the incidence of infectious disease. A common feature of all of the different diseases is the inconsistent associations between studies. While some studies show an association of a specific $(GT)_n$ allele with disease occurrence, other studies find no evidence of an association.

The majority of the studies which assess infectious disease susceptibility have examined the association of the *SLC11A1* $(GT)_n$ alleles with tuberculosis susceptibility and progression to clinical disease. A meta-analysis, compiled of association studies (from 1995-2004) assessing the association of variants of the $(GT)_n$ promoter polymorphism with pulmonary tuberculosis susceptibility, revealed that $(GT)_n$ allele 3 was

Table 1.4 Studies Assessing the Association of the *SLC11A1* $(GT)_n$ Promoter Polymorphism with the Incidence of Infectious Disease.

Study	Disease	Population	$(GT)_n$ allele associated[a]
Liu *et al* ., 1995	Tuberculosis	Combined Hong Kong & Canadian	No association
Newport *et al* ., 1995	Tuberculosis	Maltese	No association
Roger *et al* ., 1997	Leprosy	French Polynesian	No association
Shaw *et al* ., 1997b	Tuberculosis	Brazil	Allele 2[b]
Bellamy *et al* ., 1998	Tuberculosis	Gambian	3/other[b]
Huang *et al* ., 1998	MAI	American	No association
Marquet *et al* ., 1999	HIV	Columbian	Allele 2
Roy *et al* ., 1999	Leprosy	Indian	No association
Cervino *et al* ., 2000	Leprosy	Guinea-Conakry	No association
Gao *et al* ., 2000	Tuberculosis	Japanese	Allele 3
Greenwood *et al* ., 2000	Tuberculosis	Aboriginal Canadian	N/A[c]
Selvaraj *et al* ., 2000	Tuberculosis	Indian	No association
Calzada *et al* ., 2001	Chagas' disease (*T. Cruzi*)	Peru	No association
Dunstan *et al* ., 2001	Typhoid Fever	Vietnam	No association
Meisner *et al* ., 2001	Leprosy	Mali (West African)	No association
Awomoyi *et al* ., 2002	Tuberculosis	Gambia	Allele 3
Ma *et al* ., 2002	Tuberculosis	American	Allele 3
Selvaraj *et al* ., 2002	Tuberculosis	Indian	No association
Soborg *et al* ., 2002	Tuberculosis	Danish	No association
Blackwell *et al* ., 2003	Meningococcal meningitis	English	Allele 3
Bucheton *et al* ., 2003	Visceral leishmaniasis	Sudanese	No association[e]
El Baghdadi *et al* , 2003	Tuberculosis	Moroccan	No association
Ouchi *et al* ., 2003	Kawasaki	Japansese	Allele 1[d]
Donninger *et al* ., 2004	HIV	African/European	No association
Ferreria *et al* ., 2004	Leprosy & Mitsuda reaction	Brazil	Allele 2[b]
Fitness *et al* ., 2004a	Tuberculosis	Malawi	No association
Fitness *et al* ., 2004b	Leprosy	Malawi	No association
Hoal *et al* ., 2004	Tuberculosis	South African (SA coloured)	Allele 3
Mohamed *et al* ., 2004	Visceral leishmaniasis	Sudanese	Allele 3[e]
Dubaniewicz *et al* ., 2005	Tuberculosis	Polish	No association
Bravo *et al* ., 2006	Brucellosis	Spanish	No association
Hsu *et al* ., 2006	Tuberculosis	Taiwanese (aboriginals)	Allele 3
Hsu *et al* ., 2006	Tuberculosis	Han (Taiwan)	No association
Li *et al* ., 2006	Tuberculosis	Meta analysis	Allele 3
Leung *et al* ., 2007	Tuberculosis	Chinese	No association
Soborg *et al* ., 2007	Tuberculosis	Tanzanian	Allele 3
Takahashi *et al* ., 2008	MDR-TB	Japanese	Allele 3
Tanaka *et al* ., 2007	MAC	Japanese	No association
Ates *et al* ., 2009b	Tuberculosis	Dutch	No association
Chen *et al* ., 2009	Tuberculosis	Tibetan	Allele 3[f]
McDermid *et al* ., 2009	HIV	Gambia	No association
Velez *et al* ., 2009	Tuberculosis	Argentinian/American & African American	No association
de Wit *et al* ., 2010	Tuberculosis	South African (SA coloured)	Allele 3
Motsinger-Reif *et al* ., 2010	Tuberculosis	American	No association

[a] Unless otherwise stated, the specified allele is associated with disease resistance.

[b] Allele found to confer susceptibility.

[c] Minor allele frequency too low to determine an association.

[d] Allele 1 is most likely to represent allele 7 in this population.

[e] Additionally, significant linkage was obtained with $(GT)_n$ polymorphism and disease occurrence.

[f] Haplotype containing $(GT)_n$ polymorphism in association with other SLC11A1 polymorphisms.

MAI, *Mycobacterium avium intracellulare* ; MAC, *Mycobacterium avium* complex; MDR, Multi-drug resistant *Mycobacterium tuberculosis*

significantly associated with resistance to pulmonary tuberculosis infection (Li *et al.*, 2006). When the studies were stratified according to the origin of the population assessed, a significant association was identified in African and Asian populations, but not in European populations. The latter cohorts consisted of two sample sizes of 47 and 101 in which the incidence of allele 3 was associated with both susceptibility and resistance to pulmonary tuberculosis infection, thus highlighting the inconsistent associations between studies (Ma *et al.*, 2002, Soborg *et al.*, 2002).

1.3.4.2 *SLC11A1* $(GT)_n$ Promoter Polymorphisms and Autoimmune Disease

Increasing evidence suggests that *SLC11A1* may play a role in susceptibility/resistance to autoimmune disease (Section 1.1.6) due to the immunomodulatory role of *SLC11A1* in polarising a Th1 immune response. Thus, it has been hypothesised that increased *SLC11A1* expression by $(GT)_n$ allele 3, compared to the other $(GT)_n$ alleles, would predispose an individual to autoimmune disease (Section 1.3.4). Table 1.5 displays all of the association and familial studies which have assessed the presence of specific $(GT)_n$ alleles with the incidence of autoimmune diseases.

Numerous studies assessing the association of the $(GT)_n$ promoter alleles with rheumatoid arthritis (Rodriguez *et al.*, 2002, Sanjeevi *et al.*, 2000, Shaw *et al.*, 1996), T1D (Bassuny *et al.*, 2002, Esposito *et al.*, 1998, Nishino *et al.*, 2005, Takahashi *et al.*, 2004), inflammatory bowel disease/Crohns's disease (Gazouli *et al.*, 2008a, Zaahl *et al.*, 2006), sarcoidosis (Dubaniewicz *et al.*, 2005, Gazouli *et al.*, 2007) and multiple sclerosis (Gazouli *et al.*, 2008b) support the hypothesis that the presence of allele 3 predisposes to autoimmune disease (or conversely that the presence of allele 2 is protective against the occurrence of autoimmune disease). However, analogous to studies investigating the association of the $(GT)_n$ promoter alleles with the incidence of infectious diseases, other studies have failed to show the hypothesised association between the presence of allele 2 or 3 and resistance or susceptibility to autoimmune disease, respectively.

Table 1.5 Studies Assessing the Association of the *SLC11A1* $(GT)_n$ Promoter Polymorphism with the Incidence of Autoimmune Disease.

Study	Disease	Population	$(GT)_n$ Allele Associated[a]
Shaw *et al*., 1996	Rheumatoid arthritis	English	Allele 3[b]
John *et al*., 1997	Rheumatoid arthritis	English	No association
Esposito *et al*., 1998	Type 1 diabetes	English	Allele 3
Graham *et al*., 2000	Primary biliary cirrhosis	English	Allele 5
Maliarik *et al*., 2000	Sarcoidosis	African Americans	Allele 3 (allele 2 protective)
Sanjeevi *et al*., 2000	Juvenile rheumatoid arthritis	Latvian/Russian	Allele 3 (allele 2 protective)
Singal *et al*., 2000	Rheumatoid arthritis	Canadian	No association
Yang *et al*., 2000a	Rheumatoid arthritis	Korean	No association
Kojima *et al*., 2001	Inflammatory bowel disease	Japanese	Allele 7
Kotze *et al*., 2001	Multiple sclerosis	South African	Allele 5
Bassuny *et al*., 2002	Type 1 diabetes	Japanese	Allele 2 protective[c]
Rodriguez *et al*., 2002	Rheumatoid arthritis	Spanish	Allele 2 protective[d]
Comabella *et al*., 2004	Multiple sclerosis	Spanish	No association
Takahashi *et al*., 2004	Type 1 diabetes	Japanese	Allele 7 (allele 2 protective)[e]
Crawford *et al*., 2005	Inflammatory bowel disease	Caucasian	No association
Dubaniewicz *et al*., 2005	Sarcoidosis	Polish	Allele 3
Maier *et al*., 2005	Type 1 diabetes	English	No association
Nishino *et al*., 2005	Type 1 diabetes	Japanese	Allele 2 protective[f]
Runstadler *et al*., 2005	Juvenile rheumatoid arthritis	Finnish	No association
Kim *et al*., 2006	Behcet disease	Korean	Allele 3 protective
Sechi *et al*., 2006	Crohn's disease	Sardinians	No association
Zaahl *et al*., 2006	Inflammatory bowel disease	South African (mixed)	Allele 3[g]
Chermesh *et al*., 2007	Crohn's disease	Ashkenazi Jews	No association
Gazouli *et al*., 2007	Sarcoidosis	Greek	Allele 3
Ates *et al*., 2008	Systemic sclerosis	Turkish	Allele 2 (allele 3 protective)[h]
Gazouli *et al*., 2008a	Crohn's disease	Greek	Allele 3
Gazouli *et al*., 2008b	Multiple sclerosis	Sardinians	Allele 3
Kotlowski *et al*., 2008	Inflammatory bowel disease	Canadian	Allele 1 and 2[i], Allele 3[j]
Ates *et al*., 2009a	Behcet disease	Turkish	No association
Ates *et al*., 2009b	Rheumatoid arthritis	Dutch	No association
Paccagnini *et al*., 2009	Type 1 diabetes	Italian	No association
Ates *et al*., 2010	Multiple sclerosis	Turkish	No association

[a] Unless otherwise stated, the specified allele was positively associated with the incidence of disease.

[b] Allele 3 is transmitted in preference to allele 2 in affected sib-pairs.

[c] Frequency of allele 2 slightly lower, albeit not significantly, in the early onset (2-10 years) cohort than in controls.

[d] Only when patients and controls stratified according to MHC risk alleles.
An increase in 2/2 genotype frequency among patients carrying MHC risk alleles compared to controls.
Frequency of patients with allele 3 significantly decreased among patients without MHC risk alleles compared to controls also not carrying MHC risk.

[e] Allele 2 significantly lower when data analysed using c^2 test, but not after Bonferroni multiple adjustment.

[f] In all diabetic patients, allele 2 was less frequent and allele 3 was more frequent, albeit not significantly, than in controls.
Decreased frequency of allele 2 only among patients with early-onset (<11 years) compared to late onset (>11 years) patients and control subjects.

[g] No statistically significant differences when comparing $(GT)_n$ promoter alleles in patients and controls, except when data stratified according to the presence of the -237C/T polymorphism in association with allele 3.

[h] Evidence of a role of infection in the onset of systemic sclerosis.

[i] Associated with Crohn's disease.

[j] Associated with ulcerative colitis.

[k] Allele 2 shows a slight protective effect.

Nishino et al. (2005) completed a small meta-analysis that examined the association of the *SLC11A1* promoter polymorphisms with Type 1 diabetes as well as several other autoimmune diseases. These researchers did not find an association between allele 3 and the incidence of autoimmune diseases, but did find that allele 2 was negatively associated with the incidence of autoimmune diseases. However, this meta-analysis did not include all the available data that has examined an association of variants at the *SLC11A1* $(GT)_n$ promoter polymorphism with Th1 autoimmune/inflammatory diseases, as only seven studies were included in the analysis.

The development of autoimmune and infectious diseases are complex multifactorial processes, which depend upon a wide range of factors, including environmental influences, ethnicity and geographical variations, and the presence of predisposing alleles, especially those in the MHC loci (Azar *et al.*, 1999). Therefore, in populations lacking additional and/or environmental susceptibility factors *SLC11A1* may not play a major role in disease development and this may account for some of the inconsistent findings from the different studies.

1.3.5 Limitations of Association Studies Analysing the *SLC11A1* $(GT)_n$ Polymorphism and Disease Occurrence

Due to the inconsistent findings of studies assessing the association of the *SLC11A1* $(GT)_n$ alleles with infectious and autoimmune disease incidence (Section 1.3.4), no clear role for the $(GT)_n$ microsatellite in disease occurrence has been established. To date, a major limitation of the studies attempting to establish an association between different $(GT)_n$ promoter alleles and disease incidence has been the sample sizes of the individual studies. The majority of association studies completed to date have included less than 200 cases, and consequently, the power to detect authentic allelic associations is low. This means that these studies will not be able to establish significant associations, even if they exist. The issue of small sample sizes is further confounded when other environmental or genetic factors, which modulate the incidence of infectious and autoimmune diseases, are factored into a study. Such two-way interactions require sample sizes of 10^5 individuals if genuine associations are to be established (McDermid and Prentice, 2006). The use of small sample sizes also generates genetic bias, as such studies have a tendency to over-report the frequency of the minor allele, resulting in type I (false positive) or II (false negative) errors in the finding of an association study.

Therefore, there is a need for the completion of studies with larger sample sizes to determine the association between specific alleles of the $(GT)_n$ repeat with disease incidence. However, the ability to complete studies with large sample sizes is hindered by current genotyping methods. The methods used to genotype the *SLC11A1* $(GT)_n$ promoter polymorphism in previous studies have all followed a limited number of techniques. However, due to the complexity of the microsatellite repeat and the common microsatellite lengths of several alleles (Table 1.3), these methods, which include PCR amplicon size determination, restriction fragment length polymorphisms and sequencing, are unable to accurately discriminate all $(GT)_n$ alleles/genotypes (Kojima *et al.*, 2001). The inability to differentiate all alleles has resulted in the mis-reporting of allele frequencies. Likewise, cloning and sequencing, which is the only method that allows for accurate discrimination of all $(GT)_n$ genotypes, is laborious, time consuming and expensive. Therefore, there is a need for a specific, rapid and high-throughput methodology to genotype the *SLC11A1* $(GT)_n$ repeat to determine if specific alleles are associated with disease incidence.

1.4 BACKGROUND TO THE PROJECT AND AIMS

1.4.1 Background to Project

SLC11A1 has restricted expression to phagocytic cells, where it is localised to the late endosomal/early lysosomal compartment of the trans-golgi network. Upon pathogen phagocytosis, SLC11A1 is rapidly recruited to the phagosomal membrane where it transports divalent cations out of the phagosome. Recruitment of SLC11A1 to the phagosomal membrane results in the modulation of the adaptive immune system, increased expression of Th1 pro-inflammatory cytokines and effector molecules. These pleiotropic effects elicit a Th1 pro-inflammatory immune response to effectively clear an infection.

The *SLC11A1* promoter contains a polymorphic $(GT)_n$ microsatellite repeat, which modulates expression of the gene. Several alleles, differing in the number of $(GT)_n$ repeats, have been identified in the general population. A total of nine alleles have been characterised to date (designated alleles 1 to 9) of which alleles 2 and 3 are the most frequently occurring. Allele 3 drives high *SLC11A1* expression with a putative heightened Th1 pro-inflammatory immune response leading to a chronic hyperactivation of macrophages. While this is beneficial to the process of pathogen clearance, the increased levels of *SLC11A1* expression are thought to predispose individuals carrying allele 3 to autoimmune disease. In contrast, the presence of allele 2 drives decreased *SLC11A1* expression, as compared to allele 3, and thus a decreased pro-inflammatory immune response. Individuals carrying allele 2 would putatively exhibit increased susceptibility to infectious disease, but would be protected against autoimmune disease, as macrophages would be at a lower level of activation. The -237C/T polymorphism is another *SLC11A1* promoter variant which has been shown to modulate promoter activity. The mechanism for the differential expression levels of *SLC11A1* mediated by different variants at the $(GT)_n$ and -237C/T polymorphisms is currently unknown.

A large number of studies assessing the association between the presence of the specific $(GT)_n$ promoter alleles with the incidence of infectious and autoimmune disease have

produced inconsistent associations. These inconsistent associations are attributable to non-optimal genotyping methods that are time consuming or unable to detect all variants resulting in the completion of association studies with small sample sizes. In addition to the small sample sizes, these association studies try to determine whether an association exists between specific $(GT)_n$ alleles and disease incidence without knowledge of the mechanisms surrounding *SLC11A1* transcription. Currently there is a lack of functional knowledge about the mechanism of *SLC11A1* transcription initiation and transcription factors which regulate *SLC11A1* expression. A greater understanding of *SLC11A1* transcription will help to elucidate the mechanism by which different promoter variants at the $(GT)_n$ and -237C/T polymorphisms result in altered *SLC11A1* promoter activity to influence disease incidence.

1.4.2 Aims of the Project

The overall aim of this project was to characterise the *SLC11A1* promoter and the mechanisms by which variants at the $(GT)_n$ and -237C/T promoter polymorphisms regulate *SLC11A1* expression to influence the incidence of autoimmune and infectious disease.

This overall aim was addressed through the completion of the following specific aims.

Aim 1: To conduct meta-analyses to determine the strength of the association between the *SLC11A1* polymorphisms and the incidence of autoimmune and infectious diseases.
A large number of studies have assessed the association of specific $(GT)_n$ alleles with the incidence of autoimmune disease. A meta-analysis completed by Nishino et al. (2005), which found no association with allele 3, but a protective effect of allele 2, only analysed a small number of the association studies which had been completed. Since this report, a number of new studies have been published and therefore, a more robust meta-analysis of the association of the $(GT)_n$ promoter polymorphisms with Th1 mediated autoimmune/inflammatory disease was completed. The work presented in Chapter 3 analyses the association of specific $(GT)_n$ alleles with the incidence of autoimmune/inflammatory disease of studies published between 1991-2006.

Since the publication of the meta-analysis assessing the association of the *SLC11A1* polymorphisms with tuberculosis incidence (Li *et al.*, 2006), as well as the publication of the results presented in Chapter 3 assessing the association of specific $(GT)_n$ alleles with the incidence of autoimmune/inflammatory disease, a significant number of new studies had been completed. Therefore a more inclusive meta-analysis assessing the association of the *SLC11A1* polymorphisms with the occurrence of both infectious and autoimmune disease was completed (Chapter 7). In addition to the $(GT)_n$ promoter polymorphism, a large number of publications have analysed the association of other *SLC11A1* polymorphisms with the incidence of infectious and autoimmune diseases. Where a significant number of studies were completed, the association of the occurrence of these other *SLC11A1* polymorphisms with infectious and autoimmune disease incidence was assessed (Chapter 7).

Aim 2: To develop a specific, rapid and high-throughput methodology to genotype the *SLC11A1* $(GT)_n$ and $(CAAA)_n$ microsatellite repeats.

Current methods for genotyping the $(GT)_n$ promoter microsatellite repeat are time-consuming, inaccurate, and are not amenable to high throughput analysis, which is essential for conducting large association studies to determine if an association exists between the presence of specific *SLC11A1* promoter alleles and the incidence of infectious or autoimmune diseases. The difficulty in developing an accurate, high throughput methodology for the genotyping of the promoter alleles is due to the subtle sequence differences between the alleles. Therefore, a high-resolution melt curve analysis methodology was designed and optimised to enable accurate and high-throughput genotyping of *SLC11A1* microsatellite repeats. The design and optimisation of the high-resolution melt curve analysis methodology is presented in Chapter 4.

Aim 3: To determine the mechanisms by which *SLC11A1* is regulated at the level of transcription initiation.

Aim 4: To determine the mechanism mediating the variation in *SLC11A1* expression by the different *SLC11A1* promoter $(GT)_n$ microsatellite and -237C/T polymorphisms.

A large number of association and linkage studies have been completed to assess the association of the *SLC11A1* promoter $(GT)_n$ and -237C/T polymorphisms with the occurrence of infectious and autoimmune diseases. A major problem with these studies is that they try to determine what association exists between the presence of specific

functional promoter variants and disease incidence in a blinded fashion. These association and linkage studies lack fundamental information pertaining to the mechanisms which influence and regulate *SLC11A1* expression, and ultimately the mechanisms modulating differences in *SLC11A1* expression by promoter variants. Thus there is a basic lack of fundamental understanding regarding the functionality of the *SLC11A1* promoter region.

Using a range of *in silico* programs, bioinformatic analysis of the *SLC11A1* promoter was completed to define putative important regions involved in *SLC11A1* transcription. Different lengths of the *SLC11A1* promoter were then cloned into reporter vectors to functionally determine the importance of bioinformatically identified putative transcriptional regulatory regions. Additionally, multiple reporter constructs containing the same *SLC11A1* promoter region were prepared, which differed only by the functional variants at the $(GT)_n$ and -237C/T polymorphisms. The *in silico* analysis of the *SLC11A1* promoter and the design and preparation of the *SLC11A1* promoter constructs are presented in Chapter 5.

The promoter activity, driven by the different promoter lengths cloned into the reporter constructs, was determined by transfection into human cells lines, enabling the identification of important regulatory regions involved in transcription initiation and expression of *SLC11A1* (Aim 3). Furthermore, transfection of promoter constructs containing the different functional promoter variants enabled the elucidation of the mechanisms involved in the modulation of *SLC11A1* expression by different functional promoter variants (Aim 4). The important *SLC11A1* promoter regions identified were then further analysed bioinformatically to determine candidate transcription factors which may be involved in controlling *SLC11A1* expression. Analysis of the promoter activity of the different *SLC11A1* promoter constructs transfected into human cell lines is presented in Chapter 6.

CHAPTER 2 – GENERAL MATERIALS & METHODS

2.1 MATERIALS

2.1.1 General Materials and Reagents

Agarose, sodium chloride (NaCl) and Tris base were purchased from Amresco (Ohio, USA). 5-Bromo-4-Chloro-3-Indolyl B-D-galactopyranoside (X-gal) was obtained from Astral Scientific (Sydney, Australia). Bacto-tryptone was purchased from BD Bioscience (New Jersey, USA) and yeast extract was purchased from Fluka (Buchs, Switzerland). Glacial acetic acid was supplied by Merck (Darmstadt, Germany). Ammonium persulfate, ampicillin, bromophenol blue, ethidium bromide, ethylendiaminetetraacetic acid (EDTA), sodium dodecyl sulphate (SDS), spectinomycin and xylene cyanol were purchased from Sigma-Aldrich (Missouri, USA). The 2X PCR Master Mix was purchased from Promega (Wisconsin, USA). Purelink PCR Purification and Quick Plasmid Miniprep kits were purchased from Invitrogen (California, USA).

2.1.2 DNA Size Standards

DNA size standards used in agarose gel electrophoresis (Section 2.2.2.5) consisted of Hyperladder IV, Hyperladder V (Bioline, London, UK), 100bp and 1Kb ladders (New England Biolabs, Massachusetts, USA). The sizes of each of the size standards is shown below (all sizes are in base pairs).

Hyperladder IV	1000, 800, 700, 600, 500, 400, 300, 200, 100
Hyperladder V	500, 400, 300, 250, 200, 175, 150, 125, 100, 75, 50, 25
100bp Ladder	1517, 1200, 1000, 900, 800, 700, 600, 517, 500, 400, 300, 200, 100
1KB Ladder	10002, 8001, 6001, 5001, 4001, 3001, 2000, 1000, 517, 500

2.1.3 Oligonucletides

All oligonucleotides were purchased from Sigma Genosys or Invitrogen and obtained in the lyophilised state. Oligonucleotides were resuspended in TE Buffer (10mM Tris HCl pH 7.5, 0.1mM EDTA) to produce 200µM stock solutions. Unless otherwise stated, stock primer solutions were diluted to 20µM working solutions in sterile water. Primer stock and working solutions were stored at -20^{o}C.

Oligonucleotides, for the amplification of *SLC11A1* regions for high resolution melt curve analysis (Section 4.2.1.2) and the amplification of promoter regions for the generation of constructs for functional analyses (Section 5.2.1.2), or for the quantification of *SLC11A1* expression levels (Section 6.2.2.5.3), were designed using the sequence available in the Genbank database under the accession number AF229613. Primers specific for *SLC11A1* were designed using Oligo Version 4 (Molecular Biology Insights, Colorado, USA) or the Primer program of Lasergene (DNAStar, California, USA). Where possible, candidate primer sequences were designed to have a GC content of approximately 50%, no potential primer-primer interactions and no putative secondary structure. The specific oligonucleotide sequences are reported within the relevant chapters in which they are used.

2.2 METHODS

2.2.1 Sterility and Containment

To prevent contamination and nuclease digestion of genomic DNA (gDNA) and RNA, all surfaces were washed with 70% ethanol before and after use and all experimental work was completed wearing gloves. Separate areas were established for DNA extraction, reagent pipetting and general post-PCR work. A separate set of clean DNA-free pipettes were used for all work to prevent sample cross contamination. All PCRs were set up using filtered pipette tips to avoid aerosol contamination. All glassware, pipette tips, centrifuge tubes and solutions were autoclaved before use, or purchased as certified DNase/RNase free.

2.2.2 DNA Techniques

2.2.2.1 PCR 1 – General PCR

The general PCR amplification protocol was used to produce *SLC11A1* fragments containing the $(GT)_n$ and $(CAAA)_n$ alleles for cloning into plasmids used for high resolution melt analysis (Section 4.2.2.3), verification of designed HRM amplicons (Section 4.3.1.2), validation of gDNA collection methods (Section 4.3.4.2 and 4.3.4.3), and validation of the introduction of the mutant -237 T nucleotide after *in vitro* site-directed mutagenesis (Section 5.2.2.2.4). PCR amplification was carried out in a total volume of 50µl, which contained 1X PCR mix (1.25U *Taq* polymerase, 200µM dNTP and 1.5mM $MgCl_2$), 20µM of each of the forward and reverse primers, and 0.1ng plasmid DNA or a 2mm micropunch from an FTA card carrying immobilised gDNA. Each PCR experiment included a negative control in which sterile water or a micropunch from an unused FTA card replaced template DNA. The reactions were mixed well and briefly centrifuged. The PCR was carried out using an Eppendorf Mastercycler Gradient instrument (Eppendorf). The PCR was initiated by denaturation (95^oC, 5min), followed by 34 cycles of denaturation (95^oC, 30s), primer annealing (56^oC, 30s) and extension (72^oC, 40s), followed by a final extension step (72^oC, 10min). After the completion of the PCR, the efficiency and fidelity of amplification was assessed by agarose gel electrophoresis (Section 2.2.2.5) of an aliquot (10-15µl) of the PCR product in a 1.2% (w/v) agarose gel.

2.2.2.2 Purification of PCR Products

PCR products to be used for cloning (Sections 4.2.2.3, 5.2.2.2.1 and 5.2.2.2.6), restriction digestion (Section 5.2.2.2.8), or sequencing (Section 2.2.2.6) were purified using the Purelink PCR Purification kit, according to the manufacturer's instructions. DNA was eluted in 50µl of elution buffer. After purification, 5µl of the purified DNA was electrophoresed in 1.5% (w/v) agarose gels (Section 2.2.2.5). The concentration of DNA was determined using the NanoDrop 1000 (Thermo Scientific, Massachusetts, USA) (Section 2.2.2.7). Purified PCR products were stored at -20^{o}C, until required.

2.2.2.3 Restriction Enzyme Digestion

Restriction enzyme digestion was used to verify cloned plasmid inserts (Sections 4.2.2.3 and 5.2.2.2.8), verify base changes after *in vitro* site-directed mutagenesis (Section 5.2.2.2.4), and for the production of the plasmid emp-*bla*(M) (Section 5.2.2.2.9). Bioinformatic analyses of known restriction sites were conducted to select appropriate restriction enzymes (Section 2.2.4.1). Restriction enzyme digestions were carried out in a total volume of 20µl, which contained the appropriate restriction buffer and 1-5U of the relevant restriction enzyme, according to the manufacturer's instructions. Each digest contained either 15µl of PCR product, or 1µg of purified cloned plasmid DNA. Restriction digests were allowed to proceed at 37^{o}C for 3-5h. Restriction fragments were separated by agarose gels electrophoresis (Section 2.2.2.5).

2.2.2.4 Small-Scale Preparation of Plasmid DNA ('mini'-prep)

After overnight (O/N) growth (37^{o}C, with agitation [220rpm]) of isolated transformants containing recombinant plasmids (Sections 2.2.3.2 and 2.2.3.3), plasmid DNA was extracted from 3ml of the cell culture. Cells were collected by centrifugation (10000g, 2min) and plasmid DNA was isolated and purified from the cells using the Purelink Quick Plasmid Miniprep kit, following the manufacturer's instructions. The plasmid DNA was eluted from the spin column in 75µl of TE buffer. Plasmid yield and quality was determined by electrophoresis of the purified plasmid in 1.4% (w/v) agarose gels (Section 2.2.2.5) and NanoDrop quantitation (Section 2.2.2.7). Isolated recombinant plasmids were stored at -20^{o}C, until required.

2.2.2.5 Agarose Gel Electrophoresis

Horizontal agarose gel electrophoresis was carried out to determine the concentration and quality of purified PCR products (Section 2.2.2.2) and isolated gDNA (Section 4.2.2.1.3), to confirm the size of PCR products (Section 2.2.2.1) or cloned fragments (Section 2.2.2.4), and to resolve restriction enzyme digestion products (Section 2.2.2.3). Agarose gels varied from 0.8% (w/v) to 1.6% (w/v), depending on the expected size of the products to be separated. Gels were electrophoresed submerged in 1X Tris acetic acid EDTA (TAE) buffer (40mM Tris, 20mM glacial acetic acid, 1mM EDTA) and contained 0.5µg/ml ethidium bromide. Loading buffer (0.2-0.3 vol) (60% sucrose, 50mM Tris-HCl pH 8.0, 10mM EDTA and 0.01% (w/v) bromophenol blue) was added to all samples prior to electrophoresis. A molecular weight standard (Section 2.1.2) was electrophoresed with all samples to determine the sizes of fragments. Gels were electrophoresed at 70-80V for 30-60min and DNA fragments visualised by UV transillumination using a Uvitech UV transilluminator. Images were captured using a Kodak EDAS 290 digital camera.

2.2.2.6 DNA Sequencing

Sequencing was completed to verify PCR amplicons (Sections 4.3.1.2 and 5.3.2.1.1) and recombinant plasmid DNA (Sections 5.2.2.2.5 and 5.2.2.2.8), and for the determination of genotypes of the *SLC11A1* $(GT)_n$ and $(CAAA)_n$ microsatellite polymorphisms (Section 4.3.4.5). Purified PCR product (Sections 2.2.2.2 and 5.2.2.2.2) or plasmid DNA samples (Section 2.2.2.4) were sequenced at the Sydney University and Prince Alfred Molecular Analysis Centre (SUPAMAC, University of Sydney). All samples were completely sequenced on both strands. DNA and primer quantities were prepared for sequencing according to the instructions of SUPAMAC. Sequencing data was analysed using Chromas Version 2.13 and the Lasergene program Seqman (Section 2.2.4.2).

2.2.2.7 Determination of DNA Concentration

The concentration of PCR amplicons (Sections 2.2.2.1, 4.2.2.4.3 and 5.2.2.2.2), recombinant plasmids (Sections 2.2.2.4 and 5.2.2.3.1), gDNA (Section 4.2.2.1.3), and RNA (Section 6.2.2.5.1) was determined by spectrophotometry using the NanoDrop

1000 (Thermo Scientific, Massachusetts, USA). The concentration was determined from a 1µl aliquot, according to the manufacturer's protocol.

2.2.3 Microbiological Techniques

2.2.3.1 Luria Bertani Medium

Luria Bertani (LB) medium consisted of 5g/l yeast extract, 10g/l bacto-tryptone and 10g/l NaCl. Media for plates contained 15g/l agarose, which was added prior to autoclaving. Media for antibiotic selection plates contained 100µg/ml spectinomycin or ampicillin, which was added after the autoclaved media was cooled to less than 55^{o}C. Set media plates were stored at 4^{o}C, until required. Liquid cultures contained 70-100µg/ml spectinomycin or ampicillin.

2.2.3.2 Cloning of PCR Products

Purified PCR products (Sections 2.2.2.2 and 5.2.2.2.2) were cloned using the TOPO TA cloning system (Invitrogen) using the relevant plasmid (pCR8/GW/TOPO or pGeneBLAzer-TOPO), following the manufacturer's instructions. Purified PCR products were cloned into the appropriate TOPO vector. Topoisomerase-mediated ligation was carried out in a 5µl reaction volume, of which 3µl was subsequently transformed into *E.coli* TOP10 or MAX Efficiency DH5α-T1^{R} competent cells, according to the manufacturer's instructions. A pUC19 (10pg) transformation was always included as a control to determine viability of the competent cells. Transformed cells were plated on LB plates containing 100µg/ml spectinomycin or ampicillin and X-gal (1mg/plate). Cells were plated at 4 different volumes (10, 25, 50 and 100µl). Cells were grown by O/N incubation at 37^{o}C, after which positive colonies, containing recombinant plasmids, were selected for growth (Section 2.2.3.3) and plasmid DNA isolation (Section 2.2.2.4).

2.2.3.3 Isolation and Culture of Positive Colonies

After O/N growth of plated transformants (Section 2.2.3.2), 6-10 white (insert-containing) individual colonies were selected for each sample and grown in 5ml of LB medium (Section 2.2.3.1), containing 100µg/ml of spectinomycin or amplicillin. Cells

were grown O/N at 37^{o}C with agitation (220rpm). Recombinant plasmid DNA was then isolated from 3ml of cultured cells (Section 2.2.2.4).

2.2.4 Bioinformatics

2.2.4.1 Restriction Mapping

Restriction mapping was completed for the selection of appropriate restriction enzymes for the verification of recombinant plasmids produced (Sections 4.2.2.3 and 5.2.2.2.8), verification of base changes induced by *in vitro* site-directed mutagenesis (Section 5.2.2.2.4), and production of the emp-*bla*(M) plasmid (Section 5.2.2.2.9). Restriction maps of the *SLC11A1* nucleotide sequence (accession number AF229163) were generated using the SeqBuilder program (Lasergene, DNAStar) or *SLC11A1* SeqBuilder cloning file (Section 5.2.2.1.1). Appropriate restriction enzyme(s) were then selected for restriction enzyme digestion (Section 2.2.2.3).

2.2.4.2 Analysis of Sequence Data

Sequencing data (Section 2.2.2.6) was obtained in the form of raw sequence data and sequencing electrophoregrams. The electrophoregrams were analysed using the program Chromas Version 2.13. Both the forward and reverse sequences of PCR amplicons, or recombinant plasmid DNA, were imported into the Lasergene program SeqMan (DNAstar, Wisconsin, US), and aligned with a known sequence which was included for comparison (generated from AF229163). Any discrepancies in the alignments of the sample sequences with the known sequence were resolved by analysing the corresponding electrophoregrams.

CHAPTER 3 – ASSOCIATION OF *SLC11A1* PROMOTER POLYMORPHISMS WITH THE INCIDENCE OF AUTOIMMUNE AND INFLAMMATORY DISEASES: A META-ANALYSIS

3.1 PREFACE

The work completed in this chapter describes details of a published meta-analysis assessing the association of the $(GT)_n$ alleles with the incidence of autoimmune/inflammatory disease, of which I was a major contributor to the conception and completion of the study. The findings presented in this chapter were published in 2008 in the Journal Autoimmunity (issue 31 pgs 42-51) of which I was a co-author. This meta-analysis was conducted to indicate the effect of the *SLC11A1* $(GT)_n$ repeat on disease occurrence (using all available data at the time of completion), to determine whether it was worthwhile to conduct further functional analyses on how *SLC11A1* promoter variants may influence disease incidence.

3.2 INTRODUCTION

The solute carrier family 11a member 1 (SLC11A1) protein, formerly known as NRAMP1 (natural resistance associated macrophage protein 1), is localised within the acidic endosomal and lysosomal compartment of resting macrophages (Canonne-Hergaux *et al.*, 2002, Govoni *et al.*, 1999, Gruenheid *et al.*, 1997, Searle *et al.*, 1998). SLC11A1 functions as a divalent cation transporter, which regulates (Atkinson *et al.*, 1997), and is regulated by (Atkinson *et al.*, 1997), intracellular ion concentrations, notably iron. The pathogenicity of a broad range of intracellular parasites is dependent upon the availability of iron (Bullen, 1981, Payne, 1993), and phagosomal proteins that are associated with susceptibility or resistance to infections with intracellular pathogens, often function as iron transporters. SLC11A1 contributes to the antimicrobial functions of macrophages by extruding essential metal ions from the phagosome, through H^+/metal ion co-transport to directly influence the microenvironment of the phagosome, thereby depriving micro-organisms of essential growth factors (Atkinson and Barton, 1999, Biggs *et al.*, 2001, Forbes and Gros, 2001, Forbes and Gros, 2003, Gomes and Appelberg, 1998, Jabado *et al.*, 2000, Mulero *et al.*, 2002, Supek *et al.*, 1997, Wyllie *et al.*, 2002). The competition for divalent metal cations between host and pathogen may ultimately regulate host susceptibility to infection (Agranoff and Krishna, 1998).

SLC11A1 exerts pleiotropic effects on macrophage function, including increased expression of inducible nitric oxide synthase (iNOS) and subsequent generation of nitric oxide (NO), upregulation of MHC class II expression and enhanced antigen presentation

to T cells, increased production of pro-inflammatory cytokines (notably IL-1β and TNF-α), production of reactive species involved in oxidative burst, and upregulation of KC (a C-X-C chemokine, belonging to the IL-8 family, that is chemotactic for neutrophils) (Blackwell, 1996, Blackwell *et al.*, 1994, Karupiah *et al.*, 2000, Radzioch *et al.*, 1994, Roach *et al.*, 1994, Skamene, 1994, Zwilling *et al.*, 1987). Expression of *Slc11a1* in the late endosomal/lysosomal compartments of murine DCs has been recently reported (Stober *et al.*, 2007). Within DCs, *Slc11a1* modulates cytokine (IL-10 and IL-12) and MHC class II expression and antigen processing for presentation to T cells. Collectively, these pleiotropic effects generate a Th1 immune response bias, which is important for both resistance to infection as well as the induction and maintenance of autoimmunity and inflammation.

The *SLC11A1* gene, located on chromosome 2q35, is approximately 14 kb in length and contains 15 exons (Figure 1.6). In humans, a $(GT)_n$ microsatellite repeat polymorphism, with a high potential for Z-DNA formation (Bayele *et al.*, 2007), exists in the promoter region. The Z-DNA conformation is thought to modulate chromatin structure and, as a consequence, accessibility of transcription factors to gene sequences (Ha *et al.*, 2005, Liu *et al.*, 2006). A total of 9 *SLC11A1* $(GT)_n$ promoter alleles have been described (designated alleles 1-9) (Blackwell *et al.*, 1995, Graham *et al.*, 2000, Kojima *et al.*, 2001, Zaahl *et al.*, 2004) and expression of *SLC11A1* is modulated by the number of $(GT)_n$ repeats in the promoter. Of the 9 alleles identified, alleles 2 and 3 predominate and exert opposing effects on *SLC11A1* expression levels (Searle and Blackwell, 1999, Zaahl *et al.*, 2004). Allele 3, the most common promoter allele with a variable frequency of 0.65-0.85, depending upon geography and ethnicity (Awomoyi, 2007), has 9 GT repeats $[t(gt)_5ac(gt)_5ac(gt)_9g]$ and drives high *SLC11A1* expression [41, 42]. Allele 2, containing 10 repeats $[t(gt)_5ac(gt)_5ac(gt)_{10}g]$, occurs at a frequency of 0.10-0.30 (Awomoyi, 2007). This allele drives low expression of *SLC11A1*.

This sequence-dependent modulation of gene expression is further influenced by pro-inflammatory cytokine stimuli. In the presence of the pro-inflammatory stimulus LPS, a significant reduction in the expression driven by allele 2, and enhancement of expression driven by allele 3, is observed (Searle and Blackwell, 1999). This suggests that the juxtaposition of LPS response elements (nuclear factor kappa B, activator protein 1 like or NF-IL-6) may be differentially affected by the two most commonly

occurring alleles. Consistent with these functional effects and given the important role of macrophage function in the modulation of adaptive immune responses, alleles 2 and 3 have been inversely associated with susceptibility to autoimmune or infectious disease. It has been proposed that the presence of allele 3, which drives high *SLC11A1* expression with consequent classical (M1) activation of macrophages and pro-inflammatory responses, promotes efficient resolution of infection, but is associated with autoimmunity and inflammation (Dubaniewicz *et al.*, 2005, Kotze *et al.*, 2001, Maliarik *et al.*, 2000, Sanjeevi *et al.*, 2000, Zaahl *et al.*, 2005). In driving low expression levels of *SLC11A1*, allele 2 has been functionally linked to infectious disease susceptibility (Awomoyi *et al.*, 2002, Bellamy *et al.*, 1998, Gao *et al.*, 2000, Hoal *et al.*, 2004, Ma *et al.*, 2002), but putatively affords protection against autoimmunity and inflammation (Nishino *et al.*, 2005, Sanjeevi *et al.*, 2000, Takahashi *et al.*, 2004). Therefore, polymorphic variants of *SLC11A1* may provide an important link between gene expression, function and susceptibility to disease. In addition to its functional candidacy as a disease marker, *SLC11A1* is also a positional candidate for some autoimmune diseases, such as T1D, due to its location within a disease susceptibility locus (Esposito *et al.*, 1998, Todd *et al.*, 1996).

At the time of completion of this meta-analysis, studies of the association of *SLC11A1* polymorphisms and disease susceptibility showed inconsistent relationships between the presence of a given *SLC11A1* $(GT)_n$ promoter allele and the incidence of autoimmune or inflammatory diseases. The contradictions were determined to be attributable, in part, to limited statistical power (associated with small sample sizes), selection bias and/or population diversity. Meta-analyses are powerful and robust analytical tools for the estimation of genetic effects as they increase the effective sample size under investigation, thereby reducing the effects of some of the methodological limitations associated with individual studies (Lohmueller *et al.*, 2003). In this study, the literature was systematically reviewed to provide quantitative and summary estimates of the association between *SLC11A1* $(GT)_n$ promoter alleles 2 and 3 and the incidence of autoimmune and inflammatory diseases.

3.3 METHODS

3.3.1 Data Collection

Relevant publications were identified through a literature search using the keywords ("NRAMP1" or "SLC11A1") and ("autoimmune"or "autoimmunity" or "inflammation" or "inflammatory") in the Medline, Pubmed and Ovid literature databases. Additional literature was collected from cross-references within both original and review articles. Publication dates were restricted to the period from January 1991 to December 2006, inclusive. Criteria for the inclusion of papers were that publications analysed polymorphisms within the *SLC11A1* gene in patients diagnosed with specific autoimmune or inflammatory diseases according to clinical criteria, with non-familial subjects used as study controls. For each publication, total study numbers (individuals and alleles) and allelic frequencies (numbers and percentages) were tabulated according to case and control groups. Data regarding the geographical location, disease investigated, diagnostic criteria, sources of control subjects, *SLC11A1* polymorphisms analysed, genotyping methodology, and identified associations with specific *SLC11A1* polymorphisms and the incidence of disease were also extracted from each publication (Table 3.1).

If original genotype frequency data was unavailable in relevant articles, a request for additional data, to enable calculation of odds ratios (ORs), was sent to the corresponding author. The suitability of each publication for inclusion against the selection criteria was assessed and data was extracted. One study, investigating the association of polymorphic $(GT)_n$ promoter alleles with the incidence of rheumatoid arthritis in Canadian (Caucasoid) subjects (Singal *et al.*, 2000), was excluded as additional data to allow calculation of ORs was unavailable. This study analysed 88 cases and 92 controls and found no association between the frequency of any of the $(GT)_n$ promoter alleles and disease incidence. Data from one study investigating an association between the incidence of T1D and the presence of specific *SLC11A1* promoter alleles (Bassuny *et al.*, 2002) were only suitable for allele 2 analyses as insufficient data pertaining to the frequencies of allele 3 was provided and the necessary data was not forthcoming. However, Bassuny et al. (2002) reported that the frequency of $(GT)_n$ allele 3 was not significantly different between cases and controls.

Table 3.1 Details of Individual Association Studies of *SLC11A1* $(GT)_n$ Promoter Polymorphisms and Autoimmune/Inflammatory Disease.

Study	Disease	Population	(GT)n Allele Associated
Graham *et al*., 2000	Primary biliary cirrhosis	English	Allele 5
Maliarik *et al*., 2000	Sarcoidosis	African Americans	Allele 3 (allele 2 protective)
Sanjeevi *et al*., 2000	Juvenile rheumatoid arthritis	Latvian/Russian	Allele 3 (allele 2 protective)
Yang *et al*., 2000a	Rheumatoid arthritis	Korean	No association
Kojima *et al*., 2001	Inflammatory bowel disease	Japanese	Allele 7
Kotze *et al*., 2001	Multiple sclerosis	South African	Allele 5
Bassuny *et al*., 2002	Type 1 diabetes	Japanese	Allele 2 protective[b]
Rodriguez *et al*., 2002	Rheumatoid arthritis	Spanish	Allele 2 protective[c]
Comabella *et al*., 2004	Multiple sclerosis	Spanish	No association
Takahashi *et al*., 2004	Type 1 diabetes	Japanese	Allele 7 (allele 2 protective)[d]
Crawford *et al*., 2005	Inflammatory bowel disease	Caucasian	No association
Dubaniewicz *et al*., 2005	Sarcoidosis	Polish	Allele 3
Nishino *et al*., 2005	Type 1 diabetes	Japanese	Allele 2 protective[e]
Zaahl *et al*., 2006	Inflammatory bowel disease	South African (mixed)	Allele 3[f]

[a] Unless otherwise stated, the specified allele was positively associated with the incidence of disease.
[b] Frequency of allele 2 slightly lower, albeit not significantly, in the early onset (2-10 years) cohort than in controls.
[c] Only when patients and controls stratified according to MHC risk alleles.
An increase in 2/2 genotype frequency among patients carrying MHC risk alleles compared to controls.
Frequency of patients with allele 3 significantly decreased among patients without MHC risk alleles compared to controls also not carrying MHC risk.
[d] Allele 2 significantly lower when data analysed using χ^2 test, but not after Bonferroni multiple adjustment.
[e] In all diabetic patients, allele 2 was less frequent and allele 3 was more frequent, albeit not significantly, than in controls.
Decreased frequency of allele 2 only among patients with early-onset (<11 years) compared to late onset (>11 years) patients and control subjects.
[f] No statistically significant differences when comparing $(GT)_n$ promoter alleles in patients and controls,
except when data stratified according to the presence of the -237C/T polymorphism in association with allele 3.

3.3.2 Statistical Analyses

Using data for the $(GT)_n$ promoter polymorphisms extracted from the relevant publications (or obtained by personal communication with authors), the ORs and 95% confidence intervals (CIs) were calculated. Although nine different alleles of the $(GT)_n$ promoter polymorphism have been reported (Blackwell *et al*., 1995, Graham *et al*., 2000, Kojima *et al*., 2001, Zaahl *et al*., 2004), 7 of these alleles (alleles 1 and 4–9) occur at extremely low frequencies among all populations studied. Accordingly, studies have focused on the association of allele 2 or 3 with disease incidence. Therefore, frequency data for alleles 1, 2 and 4–9 were pooled and compared to frequencies for allele 3 among cases and controls. Similarly, data for the frequencies of alleles 1 and 3–9 were pooled and compared to frequencies for allele 2 among cases and controls.

Odds ratios were used as the measure of disease risk associated with the presence of particular alleles and all data were corrected for consistency in the direction of the ratios. For example, an OR > 1 indicated that an increased disease risk was associated with the presence of the particular $(GT)_n$ promoter repeat (allele 3 or allele 2). Conversely, an OR < 1 was indicative of reduced disease risk in the presence of the specific allele. Pooled OR values were first calculated by the fixed effects model

(inverse variance method) in which the estimated OR is a weighted average of the individual study values (Zhao *et al.*, 2006). The *Q* statistic was used to test for homogeneity in the data set (Zhao *et al.*, 2006). If the *Q* statistic was statistically significant ($p < 0.05$) for a data set, then the random effects pooled OR, which is more representative of the true biological effect, was calculated (Sterne *et al.*, 2001). Alternatively, if the data set was not significantly heterogeneous (*Q* statistic; $p > 0.05$), then the fixed effects pooled OR was used.

To test for publication, small-study and other biases in the data set (Egger *et al.*, 1997), a funnel plot was constructed using the log-base-10 of the ORs versus the reciprocal of their standard errors. Asymmetry in the resulting plot was confirmed by Egger's linear regression test of funnel plot asymmetry (Egger *et al.*, 1997). Whilst this test can have a high Type I error rate under certain circumstances (Deeks *et al.*, 2005), it is generally advised that a test of bias be routinely performed on meta-analyses, whilst treating the results of such tests with caution due to this tendency for false positive findings (Sterne *et al.*, 2001). Although the funnel plot-based test performed in the present study is commonly used to indicate literature bias in data sets, claims resulting from this analysis were only considered indicative of asymmetry rather than publication bias (Terrin *et al.*, 2005). The rank correlation method (Begg and Mazumdar, 1994) was not used due to its demonstrated low power to detect bias (Sterne *et al.*, 2001).

The trim-and-fill method was used to estimate the number of hypothetical studies that were not present in the data set, due to publication bias, and to estimate what the pooled ORs would be if these additional studies had been available (Duval and Tweedie, 2000a). The procedure used was based on an iterative procedure using a consensus of the three estimators of additional relevant studies presented by the authors. It is acknowledged that the use of this technique can lead to overestimation of 'missing' studies in some instances (Duval and Tweedie, 2000b), however its inclusion in the present study was valuable to provide an estimate of the ORs should symmetrical data sets have been available. Whilst no claims are made regarding the potential accuracy or otherwise of these estimates, they are presented as an indication of the magnitude of the change that occurs in the 'uncorrected' ORs when asymmetry is minimised in the datasets. Thus, either fixed or random effects pooled ORs, both before and after the trim-and-fill procedure are presented for comparison.

3.4 RESULTS

A total of 15 data sets were used in this meta-analysis to determine the likely association of the two predominant *SLC11A1* $(GT)_n$ promoter alleles with autoimmune or inflammatory disease (Table 3.1). An analysis of all the available allele 3 data produced an OR < 1.0 (pooled OR = 0.88, 95% = 0.65) (Table 3.2), suggesting that the presence of allele 3 is unlikely to be associated with an increased risk of autoimmune or inflammatory disease. Analysis of the allele 2 data also showed an OR < 1.0 (fixed effects pooled OR = 0.90, 95% CI = 0.24) (Table 3.3), indicating that the presence of allele 2 may exert a weak protective effect against the development of autoimmune or inflammatory disease. A protective effect of *SLC11A1* promoter allele 2 against autoimmune disease has been previously observed in a smaller meta-analysis incorporating 7 individual case-control studies (Nishino *et al.*, 2005). The findings of the present meta-analysis corroborate this study, which reported a fixed effects pooled OR of 0.71 (95% CI = 0.53-0.96) for allele 2. However, statistical estimates of publication bias were not included in this study and not all of the available data examining an association between *SLC11A1* $(GT)_n$ promoter polymorphisms and autoimmune disease were included (Nishino *et al.*, 2005).

Table 3.2 *SLC11A1* Allele 3 Frequencies (Case Versus Controls) of all the Individual Studies used in the Meta-Analysis.

	Population	Study Numbers				Allele Frequencies				Allele Frequencies				OR (95% CI)
		n (# people)		2n (# alleles)		Allele 3 +		Allele 3 -		Allele 3 +		Allele 3 -		
		Case	Control	Case	Control	Case	Control	Case	Control	Case	Control	Case	Control	
Inflammatory bowel disease														
Crawford *et al* ., 2005	Caucasian	277	90	554	180	423	136	131	44	76	76	24	24	0.96 (0.65-1.42)
Kojima *et al* ., 2001	Japanese	215	324	430	648	317	520	113	128	74	80	26	20	1.45 (1.08-1.93)
Zaahl *et al* ., 2006	European/African	77	110	154	220	118	176	36	44	77	80	23	20	1.22 (0.74-2.01)
Zaahl *et al* ., 2006	European	16	57	32	114	27	89	5	25	84	78	16	22	0.66 (0.23-1.89)
Zaahl *et al* ., 2006	African	9	25	18	50	16	42	2	8	89	84	11	16	0.66 (0.13-3.43)
Multiple sclerosis														
Comabella *et al* ., 2004	Spanish	195	125	390	250	260	178	130	72	67	71	33	29	1.24 (0.88-1.75)
Kotze *et al* ., 2001	African	104	329	208	658	160	434	48	224	77	66	23	34	0.58 (0.41-0.83)
Primary biliary cirrhosis														
Graham *et al* ., 2000	British	53	78	106	156	70	110	36	46	66	71	34	29	1.23 (0.72-2.09)
Rheumatoid Arthritis														
Rodriguez *et al* ., 2002	Spanish	141	194	282	388	189	277	93	111	67	71	33	29	1.23 (0.88-1.71)
Yang *et al* ., 2000a	Korean	74	50	148	100	115	80	33	20	78	80	22	20	1.15 (0.61-2.14)
Juvenile rhumatoid arthritis														
Sanjeevi *et al* ., 2000	Latvian/Russian	119	111	238	222	201	155	37	67	84	70	16	30	0.43 (0.27-0.67)
Sarcoidosis														
Dubaniewicz *et al* ., 2005	Polish	86	91	172	182	144	136	28	46	84	75	16	25	0.57 (0.34-0.97)
Maliarik *et al* ., 2000	African American	157	112	314	224	253	157	61	67	81	70	19	30	0.57 (0.38-0.84)
Type 1 diabetes														
Nishino *et al* ., 2005	Japanese	114	130	228	260	187	205	41	55	82	79	18	21	0.82 (0.52-1.28)
Takahashi *et al* ., 2004	Japanese	95	224	190	448	150	359	40	89	79	80	21	20	1.08 (0.71-1.64)

"+" and "-" indicate the presence of allele 3 or the absence of allele 3, respectively.

Table 3.3 *SLC11A1* Allele 2 Frequencies (Case Versus Controls) of all the Individual Studies used in the Meta-Analysis.

	Population	Study Numbers				Allele Frequencies				Allele Frequencies				OR (95% CI)
		n (# people)		2n (# alleles)		Allele 2 +		Allele 2 -		Allele 2 +		Allele 2 -		
		Case	Control	Case	Control	Case	Control	Case	Control	Case	Control	Case	Control	
Inflammatory bowel disease														
Crawford *et al* ., 2005	Caucasian	277	90	554	180	131	42	423	138	24	23	76	77	0.98 (0.66-1.46)
Kojima *et al* ., 2001	Japanese	215	324	430	648	65	96	365	552	15	15	85	85	0.98 (0.69-1.37)
Zaahl *et al* ., 2006	European/African	77	110	154	220	34	42	120	178	22	19	78	81	0.83 (0.50-1.38)
Zaahl *et al* ., 2006	European	16	57	32	114	5	23	27	91	16	20	84	80	1.36 (0.47-3.93)
Zaahl *et al* ., 2006	African	9	25	18	50	2	8	16	42	11	16	89	84	1.52 (0.29-7.96)
Multiple sclerosis														
Comabella *et al* ., 2004	Spanish	195	125	390	250	127	71	263	179	33	28	67	72	0.82 (0.58-1.16)
Kotze *et al* ., 2001	African	104	329	208	658	41	223	167	435	20	34	80	66	2.09 (1.43-3.05)
Primary biliary cirrhosis														
Graham *et al* ., 2000	British	53	78	106	156	28	42	78	114	26	27	74	73	1.03 (0.59-1.79)
Rheumatoid Arthritis														
Rodriguez *et al* ., 2002	Spanish	141	194	282	388	91	108	191	280	32	28	68	72	0.81 (0.58-1.13)
Yang *et al* ., 2000a	Korean	74	50	148	100	25	18	123	82	17	18	83	82	1.08 (0.55-2.10)
Juvenile rhumatoid arthritis														
Sanjeevi *et al* ., 2000	Latvian/Russian	119	111	238	222	37	65	201	157	16	29	84	71	2.25 (1.43-3.54)
Sarcoidosis														
Dubaniewicz *et al* ., 2005	Polish	86	91	172	182	28	46	144	136	16	25	84	75	1.74 (1.03-2.94)
Type 1 diabetes														
Bassuny *et al* ., 2002	Japanese	206	200	412	400	49	65	363	335	12	16	88	84	1.44 (0.96-2.14)
Nishino *et al* ., 2005	Japanese	114	130	228	260	21	36	207	224	9	14	91	86	1.58 (0.90-2.80)
Takahashi *et al* ., 2004	Japanese	95	224	190	448	22	69	168	379	12	15	88	85	1.39 (0.83-2.32)

"+" and "-" indicate the presence of allele 2 or the absence of allele 2, respectively.

Use of the *Q* statistic (Zhao *et al.*, 2006) indicated that the data available for allele 2 (Table 3.3) was not significantly heterogeneous ($p > 0.05$). Consequently, random effects analysis was not required and the fixed effects pooled OR was determined for the data set (Zhao *et al.*, 2006). However, unlike allele 2, the data for allele 3 was determined to be significantly heterogeneous (*Q* statistic; $p < 0.05$).

Asymmetry in the data set was determined by both the empirical assessment of the funnel plot of this data (Figure 3.1) and the application of Egger's linear regression test. Examination of the funnel plots generated revealed asymmetry in the allele 2 data set (Figure 3.1A). While a significant number of association studies have reported an OR > 1.0 (Table 3.3, Figure 3.1A), the fixed effects pooled OR determined here was < 1.0. This result is likely attributable to the weighting factor, which takes into account sample size. The trim-and-fill analysis indicated that there were 4 hypothetical studies 'missing' from the allele 2 data set. When these hypothetical studies were 'filled' into the data set, the resulting fixed effects pooled OR was still < 1 (0.80 with 95% CI = 0.22).

In the present meta-analysis, the random effects pooled OR for allele 3 (Table 3.2), before the trim-and-fill analysis was applied, was 1.04 (95% CI = 0.20). This suggested that the presence of *SLC11A1* $(GT)_n$ promoter allele 3 was weakly associated with a higher incidence of autoimmune and inflammatory disease, albeit with a 95% CI that included 1.0. However, the data for allele 3 was significantly heterogeneous (*Q* statistic;

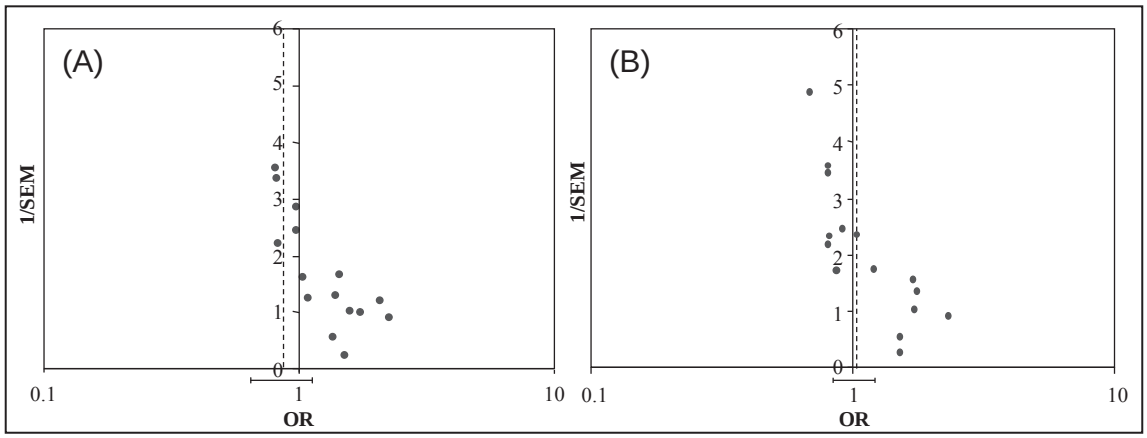

Figure 3.1 Funnel plots from the analysis of the association of $(GT)_n$ alleles with the occurrence of autoimmune disease. Funnel plots of allele 2 (A) and allele 3 (B), in which the odds ratio (OR) for each study was plotted against the reciprocal of its standard error (SEM). The dashed lines indicate the fixed (A) and random (B) effects pooled ORs, and the bars under the horizontal axis represent the 95% confidence intervals (CIs) of the ORs.

$p < 0.05$) and asymmetric (Figure 3.1B). It was further determined, using the trim-and-fill method, that the asymmetry in the data set for allele 3 was largely attributable to 6 of the 15 studies available. These 6 studies were then used in the trim-and-fill method to estimate the OR, in the absence of asymmetry in the data set, when the 'mirror images' of these studies were returned to the data set. When the hypothetical studies were 'filled' into the data set, this analysis resulted in a random effects pooled OR of 0.88 (95% CI = 0.66), thus substantially reversing the conclusion drawn from the unmodified data set. The results of the trim-and-fill procedure indicated the presence of substantial asymmetry in the available data related to the relationship between the presence of this allele and disease, which may lead to misinterpretation of any influence present. The existing data related to the association of *SLC11A1* promoter allele 3 with autoimmune and inflammatory diseases cannot conclusively support or refute the claim that this $(GT)_n$ microsatellite is associated with a higher risk of disease. It is unknown whether this asymmetry is related to publication bias, 'small study' bias or some other effect, and no speculation will be made in this regard. However, it can be concluded that if the allele 3 $(GT)_n$ microsatellite does exert an effect on the incidence of disease, then the magnitude of that effect will be small. Even if the assumption is made that there is no bias present in the data, which appears unlikely given the asymmetric funnel plot (Figure 3.1B), the 95% CI for the pooled OR includes 1, thus indicating that any effect present is of minor magnitude.

At the time this study was conducted, individual association studies investigating *SLC11A1* polymorphism frequencies other than the $(GT)_n$ promoter microsatellite were very few in number and there was insufficient power to yield statistically valid analyses. Whilst there was insufficient data for any of these polymorphisms to allow meaningful meta-analyses, it is worthwhile noting that a high degree of inconsistency was observed in the direction of the ORs in the different study populations for each of the polymorphisms analysed. What is explicit after examination of this data is that the knowledge base on the effects of these polymorphisms is far from at a stage where generalisations can be made with any degree of accuracy.

3.5 DISCUSSION

Due to their opposing effects on *SLC11A1* expression, promoter alleles 2 and 3 have been hypothesised to be associated with influencing the occurrence of autoimmune or infectious disease. The presence of allele 3, which drives high *SLC11A1* expression and consequent increased activation of macrophages, is thought to be associated with the development of autoimmunity and inflammation (Dubaniewicz *et al.*, 2005, Kotze *et al.*, 2001, Maliarik *et al.*, 2000, Sanjeevi *et al.*, 2000). Conversely, in driving low expression levels of *SLC11A1*, allele 2 has been linked to protection against autoimmunity/inflammatory disease (Nishino *et al.*, 2005, Sanjeevi *et al.*, 2000, Takahashi *et al.*, 2004). A number of association studies have been conducted to test this hypothesis, but the associations observed have been variable. Meta-analyses are a means of increasing the effective sample size under investigation through the pooling of data from individual association studies, thus enhancing the statistical power of the analysis for the estimation of genetic effects. At the time of completion, this meta-analysis represented the largest body of data analysed (15 data sets) analysing the association between variants at the $(GT)_n$ repeat and the incidence of autoimmune/inflammatory disease.

The results of the present meta-analysis suggest that, given the current published association studies, the presence of allele 3 is unlikely to be strongly associated with an increased incidence of autoimmune and inflammatory diseases. In fact, when the data was analysed to account for heterogeneity within the data set, the random effects pooled OR was reduced to a value that was less than 1.0 (0.88), indicating a decreased incidence of autoimmune and inflammatory diseases in the presence of allele 3. This substantially reverses the original hypothesis that the presence of *SLC11A1* promoter allele 3 would confer increased risk of autoimmunity and inflammation. It would appear that allele 3 may, under certain circumstances, possibly exert a protective effect against disease development. Interestingly, the allele 2 data indicated a predominance of disease in the absence of allele 2 among cases, suggesting that the presence of allele 2 may be associated, albeit weakly, with decreased susceptibility to autoimmune and inflammatory diseases. These findings corroborate those of a smaller meta-analysis in which no association between allele 3 and the incidence of autoimmune disease was reported (Nishino *et al.*, 2005).

While a pro-inflammatory milieu, generated by macrophages that become hyperactivated due to increased *SLC11A1* expression driven by promoter allele 3, will facilitate the efficient clearance of pathogens, it may increase susceptibility to chronic inflammation and autoimmune disease. Conversely, it has been argued that low levels of *SLC11A1* expression, driven by allele 2, may contribute to resistance to autoimmunity and inflammation by decreasing the level of macrophage activation. The hypothesised increased susceptibility to autoimmune and inflammatory diseases in the presence of allele 3 is not supported in this meta-analysis, and the results of a previous meta-analysis do not wholly support the hypothesis that the presence of allele 3 is associated with an increased incidence of autoimmune and inflammatory disease (Nishino *et al.*, 2005). The hypothesis is supported by empirical data from only 3 of the 13 studies used in the current analysis (Dubaniewicz *et al.*, 2005, Maliarik *et al.*, 2000, Sanjeevi *et al.*, 2000). Similarly, some individual association studies have found a negative association between the presence of allele 3 and the incidence of infectious diseases. However, an investigation of the association between $(GT)_n$ polymorphisms in the promoter region of *SLC11A1* and infectious diseases identified a predominance of allele 3 in the absence of infectious disease (tuberculosis) among cases (Li *et al.*, 2006). A significant negative association between the presence of allele 2 and the incidence of autoimmune disease was reported in only 3 of the 13 association studies (Maliarik *et al.*, 2000, Rodriguez *et al.*, 2002, Sanjeevi *et al.*, 2000) conducted to date, while an additional 3 individual studies reported that the frequency of allele 2 was lower, albeit not significantly, among cases (Bassuny *et al.*, 2002, Nishino *et al.*, 2005, Takahashi *et al.*, 2004). The present study and that of Nishino et al. (2005) suggest that the presence of the *SLC11A1* promoter allele 2 may exert a weak protective effect for the development of autoimmune disease.

The failure of this analysis, and the majority of individual association studies, to show an association of allele 3 with disease susceptibility may be attributable to a number of factors. Firstly, the presence of other functional *SLC11A1* promoter polymorphisms, which may also modulate the expression levels specified by promoter alleles 2 and 3, may further influence predisposition to autoimmunity and chronic inflammation. One likely candidate is the -237C/T promoter polymorphism, which is a single base pair substitution of a C for a T at position -237 (Zaahl *et al.*, 2004). Interestingly, the presence of a T at position -237 appears to further modify the expression of the

promoter microsatellite repeat when in the *cis* position with allele 3, resulting in lower levels of *SLC11A1* expression, comparable to levels observed in the presence of allele 2 (Zaahl *et al.*, 2004). Thus, the -237C/T polymorphism, through modulation of expression from the promoter alleles, may further modulate disease risk. An example of this is seen in the association of allele 3 with Crohn's disease only in the absence of -237 T variant (Zaahl *et al.*, 2006). The presence of the combination of allele 3 with a T at position -237 exerts a protective effect against chronic inflammation. Given the multitude of *SLC11A1* polymorphisms identified to date (Figure 1.6), the probability exists that *SLC11A1* expression may not be directly related to the presence of allele 3 or allele 2, due to the existence of additional modulators of gene expression. If multiple *SLC11A1* polymorphisms operate synergistically or antagonistically to modulate *SLC11A1* expression levels, then any potential association of *SLC11A1* with disease will be masked in association studies investigating only a single polymorphism.

Secondly, it is possible that alleles of another gene(s), in tight linkage disequilibrium (LD) with *SLC11A1*, could be the underlying cause of the non-random disease associations reported (White *et al.*, 1994, Yip *et al.*, 2003). The association of *SLC11A1* promoter allele 3 or 2 with protection against autoimmune and inflammatory disease may be attributable, in part, to LD of allele 3 or 2 with the authentic disease-causing variant(s). *SLC11A1* is located in a gene-rich region of chromosome 2 and complex LD occurs within and around the *SLC11A1* locus (2q35) (Shaw *et al.*, 1997a, Yip *et al.*, 2003). The IL-8Rα and IL-8Rβ genes are two such likely candidate genes, given that the IL-8 receptor gene cluster lies approximately 130 kb downstream of the *SLC11A1* gene (Shaw *et al.*, 1996) and these receptors play an important role in immune responses.

Thirdly, the variable associations observed between individual studies may also be attributed to the effect of other genes, which may modulate SLC11A1 function. Associations of individual *SLC11A1* polymorphisms with disease may be weak and/or inconsistent across patient populations because additional genes, which may modulate disease risk, will vary among case/control groups being compared. While the clinical manifestations of autoimmune diseases are distinct, the underlying genetics are often similar; namely most show associations with the major histocompatibility complex (MHC) region on chromosome 6, especially MHC class II loci, which confer as much as

50% of disease risk. Interestingly, among patients carrying susceptibility MHC alleles for Type 1 diabetes the frequency of allele 2 has been shown to be lower (Nishino *et al.*, 2005). Furthermore, evidence suggesting that *SLC11A1* promoter polymorphisms modulate both susceptibility to and severity of rheumatoid arthritis in individuals lacking MHC-associated risk factors has also been reported (Rodriguez *et al.*, 2002). Other studies have shown that the susceptibility (and protective) effects of allele 3 (and allele 2) were additive when co-occurring with identified MHC alleles conferring susceptibility (and resistance) to disease development (Sanjeevi *et al.*, 2000). To date, most studies of the association of *SLC11A1* polymorphisms and disease incidence have not investigated the modulating effect of MHC haplotypes that have been correlated with either resistance or susceptibility to disease.

SLC11A1 is an iron-regulated gene and, as such, association studies may show varying results due to the variability in the iron status of the individuals included in the study population, which will likely confound the genetic effect (Atkinson and Barton, 1998, Atkinson *et al.*, 1997). For example, high *SLC11A1* expression in the presence of allele 3 may lead to the depletion of iron from the macrophage, and therefore provide protection against infection. This protective influence of allele 3 will be most potent under conditions of low iron concentration, and increasing iron concentration may negate the effect. Increased iron levels exert many effects on macrophage function resulting in the inhibition of a Th1 pro-inflammatory immune response (Carrasco-Marín *et al.*, 1996, Theurl *et al.*, 2005). Furthermore, while increased stores of iron may unfavourably alter the immunoregulatory balance to facilitate increased growth rates of microbes, they may also operate to decrease susceptibility to autoimmune and inflammatory disease (Kotze *et al.*, 2001, Valberg *et al.*, 1989).

Only one of the association studies included in the present meta-analysis considered the possible environmental influence of iron status among case and controls when determining associations of *SLC11A1* variants and disease incidence (Kotze *et al.*, 2001). Therefore, iron status, which will be heterogeneous across a single population, may determine the probability of identifying associations by modulating the pure genetic effect. To incorporate the confounding factor of iron status in association studies represents a major challenge because hypothetical power calculations indicate that

sample sizes in excess of 10^5 individuals are required when studying such a two-way interaction (McDermid and Prentice, 2006).

Finally, associations may be influenced by the ethnic makeup of the individuals included in the association studies. There are variable frequencies of allele 3 and the incidence of infectious and autoimmune/inflammatory diseases throughout the world. In regions where infectious disease is endemic, allele 3 is maintained at a higher frequency, presumably due to positive selection pressure exerted by conferring enhanced survival of carriers. Thus, associations of *SLC11A1* with the incidence of autoimmune and inflammatory disease may appear stronger depending on the ethnicity of individuals included in the studies. Indeed, *SLC11A1* polymorphic variants have been associated with susceptibility or resistance to multiple autoimmune and inflammatory diseases and ethnic variations have been reported; for example, multiple sclerosis in South African Caucasians, sarcoidosis in African Americans, rheumatoid arthritis in Canadian Caucasians and Koreans, juvenile rheumatoid arthritis in Latvians, T1D in the United Kingdom, and inflammatory bowel disease in Japanese populations. The current data related to the association of *SLC11A1* promoter allele 3 with the incidence of autoimmune and inflammatory disease cannot conclusively support or refute the claim that this allele is associated with resistance to disease.

The results of the present meta-analysis do not wholly corroborate the hypothesis that allele 3 of the *SLC11A1* promoter would be associated with susceptibility to autoimmune and inflammatory disease. Environmental factors, such as infection prevalence and iron status, as well as additional genetic markers, both within (such as -237C/T) and outside (especially MHC class II) of *SLC11A1* will vary among studies and will likely operate to create a complex milieu, which ultimately modulates disease susceptibility.

The present meta-analysis emphasises that caution must be exercised when interpreting association studies using small sample sizes that have low power to detect authentic allelic association, establishing the need for the completion of large, unbiased studies on the relationships between these polymorphisms and autoimmune/inflammatory diseases. However, completion of large studies are hindered by the current genotyping methods which are either time consuming or unable to detect all $(GT)_n$ alleles. Therefore, a

sensitive high-throughput methodology to genotype the $(GT)_n$ promoter polymorphism would facilitate the completion of larger studies (Chapter 4) to enable conclusions to be determined regarding the association of variants at the $(GT)_n$ polymorphisms with disease occurrence.

Additionally, the current study presents evidence that a link between the presence of variants of the $(GT)_n$ microsatellite repeat and the incidence of autoimmune/inflammatory disease exists (i.e. a weak predominance of allele 2 in the absence of disease). The observed association of the current study and the findings of another meta-analysis, which identified an association of $(GT)_n$ allele 3 with pulmonary tuberculosis (Li *et al.*, 2006), suggests that functional analyses on how *SLC11A1* promoter variants may influence disease incidence are warranted (Chapter 5 and 6).

CHAPTER 4 – HIGH-THROUGHPUT GENOTYPING OF *SLC11A1* MICROSATELLITE REPEATS BY HIGH RESOLUTION MELT CURVE ANALYSIS

4.1 INTRODUCTION

Solute carrier family 11A member 1 (SLC11A1) has restricted expression to macrophages, in which it is localised to the phagosomal membrane where it functions as a divalent cation transporter (Sections 1.1.3 and 1.1.4). SLC11A1 classically activates macrophages, which facilitates elimination of macrophage-trophic pathogens (Blackwell *et al.*, 2001). SLC11A1 exerts potent, pleiotropic effects, including increased expression of iNOS and subsequent generation of NO, upregulation of MHC class II expression and enhanced antigen presentation to T cells, increased production of pro-inflammatory cytokines (notably IL-1β and TNF-α), production of reactive species involved in oxidative burst, and upregulation of KC. Collectively, these responses initiate and perpetuate Th1 (pro-inflammatory) immune reactions, which efficiently clear infections. However, these potent Th1 responses putatively increase susceptibility to autoimmune/inflammatory diseases (Section 1.1.6).

Expression of *SLC11A1* is modulated by a complex polymorphic $(GT)_n$ microsatellite promoter repeat. Nine $(GT)_n$ alleles, which differ in both repeat length and sequence composition, have been identified to date (Table 1.3). Alleles 2 and 3, which differ by only a GT repeat, account for over 95% of all *SLC11A1* $(GT)_n$ promoter alleles within populations. The remaining alleles occur at extremely low frequencies, which vary according to ethnicity. Promoter assays using monocytes have shown that allele 3 drives significantly higher *SLC11A1* expression compared to allele 2. Furthermore, classical activation of macrophages by the exogenous stimuli, IFN-γ and LPS, results in a significant increase in *SLC11A1* expression driven by allele 3, but leads to decreased *SLC11A1* expression in the presence of allele 2 (Section 1.3.2). From the gene expression studies it was hypothesised that higher *SLC11A1* expression, driven by allele 3, produces a macrophage phenotype which facilitates pathogen clearance, however, may also increase susceptibility to autoimmune/inflammatory diseases in genetically permissive individuals. Conversely, in the presence of allele 2, resultant low *SLC11A1* expression increases susceptibility to infection, but may confer resistance to autoimmune/inflammatory disease (Searle and Blackwell, 1999)

Association studies have been conducted to assess the strength of association between the occurrence of *SLC11A1* alleles 2 and 3 and the incidence of infectious and

autoimmune/inflammatory diseases (Section 1.3.4, Tables 1.4 and 1.5). However, results of such studies have been inconsistent (Section 1.3.4) and meta-analyses of these case/control association studies highlight these inconsistencies (Li *et al.*, 2006, Nishino *et al.*, 2005, O'Brien *et al.*, 2008) (Chapter 7). A meta-analysis, completed by Li et al. (2005), revealed that allele 3 was associated with resistance to pulmonary tuberculosis infection in African and Asian populations, but not in European populations. The latter cohorts comprised sample sizes of 47 and 101 in which the incidence of allele 3 was associated with both susceptibility and resistance to pulmonary tuberculosis infection. In another meta-analysis, which investigated the association of *SLC11A1* alleles 2 and 3 with the occurrence of autoimmune/inflammatory disease, O'Brien et al. (2008) (Chapter 3) did not find an association between allele 3 and disease incidence, however, a marginal protective effect in the presence of allele 2 was reported. This finding corroborates the results of another smaller meta-analysis (Nishino *et al.*, 2005) and observations from a more comprehensive meta-analysis which is presented in Chapter 7 of this thesis.

The majority of association studies conducted to date have included less than 200 cases, and consequently, the power to detect authentic allelic associations is low (Section 1.3.5). The issue of small sample sizes is further confounded when environmental factors, which modulate the incidence of infectious/autoimmune disease, are considered. Such two-way interactions require sample sizes of 10^5 individuals if genuine associations are to be established (McDermid and Prentice, 2006). Other limitations of studies analysing small sample sizes include genetic bias, as such studies tend to over report the frequency of the less frequent variants (Section 1.3.5).

Although PCR amplicon size determination (Blackwell *et al.*, 1995, Liu *et al.*, 1995) and restriction fragment length polymorphisms (Graham *et al.*, 2000, Kotze *et al.*, 2001) are commonly used to genotype the *SLC11A1* $(GT)_n$ microsatellite, these methodologies are unable to accurately distinguish all alleles. Genotyping based on PCR amplicon size is the most common methodology used, however it cannot differentiate alleles 3 and 5 or alleles 1 and 7, which have identical lengths, but varying sequence composition (Table 1.3). The inability to differentiate alleles has resulted in significant mis-reporting of allelic frequencies by studies relying solely on PCR amplicon size to distinguish alleles. One example is the mis-reporting of allele 7 as allele 1 among Asian cohorts.

Allele 7 has only been identified in Asian populations and is the same length as allele 1. Prior to the identification of allele 7, $(GT)_n$ microsatellite repeat genotyping studies conducted in Asian populations had only reported allele 1. However, cloning and sequencing of PCR amplicons revealed that allele 1 is not present in Asian populations, suggesting that these studies may have mis-reported allele 7 as allele 1 (Kojima *et al.*, 2001).

Collectively, the putative importance of the *SLC11A1* promoter microsatellite in modulating disease susceptibility, coupled with the inconsistent results of association studies and the inability to rapidly and reliably detect all alleles using current genotyping methods, highlights the need for an accurate, rapid, high-throughput genotyping methodology. However, the complexity of the GT repeat polymorphism (Table 1.3) has made this objective difficult to achieve. Prior to this study, cloning and sequencing (Kojima *et al.*, 2001) was the only method sensitive enough to detect all $(GT)_n$ promoter alleles. However, this method is labour intensive, time-consuming, and is therefore is not amenable to the analysis of large sample sizes which are required for association studies.

The $(CAAA)_n$/1729+271del4 polymorphism is another polymorphic microsatellite repeat, located in the 3'UTR of *SLC11A1*, which has not been well characterised. To date, two polymorphic variants have been identified, which differ by a single CAAA repeat and a G to A SNP (Section 1.2.4.2; Figure 1.6). This polymorphism was recently shown to be a marker of mortality after infection with human immunodeficiency virus (HIV) (McDermid *et al.*, 2009) and has been associated with susceptibility to infectious (*Mycobacterium tuberculosis*) (Fitness *et al.*, 2004a) and inflammatory disease (Crohn's disease) (Kotlowski *et al.*, 2008). Although the functional role of the $(CAAA)_n$ polymorphism is yet to be elucidated, it is hypothesised that this polymorphism may modulate mRNA transcript stability, thereby modulating expression levels of *SLC11A1* at the translational level (Section 1.2.4.2). Genotyping of the $(CAAA)_n$ microsatellite is currently carried out by amplicon size determination after capillary electrophoresis of radio- or fluorescently-labeled PCR products (Fitness *et al.*, 2004a, Kotlowski *et al.*, 2008). The aim of this study was to develop a specific, rapid, high throughput methodology to genotype the *SLC11A1* $(GT)_n$ promoter polymorphisms and 3'UTR $(CAAA)_n$ microsatellite repeats using high resolution melt curve analysis.

4.1.1 High-Throughput Genotyping of *SLC11A1* Microsatellite Repeats Using High Resolution Melt Curve Analysis

The conventional methods for differentiating between wild type and mutant alleles using real time PCR have relied upon allele specific fluorescence using fluorescently-labelled primers, probes, or molecular beacons (Mhlanga and Malmberg, 2001). However, these approaches require expensive fluorescently-labeled oligonucleotide probes or primers (Liew *et al.*, 2004). Additionally, the ability to genotype using these methods relies upon the specificity of the primer or probe for the target sequence. The use of fluorescently-labeled primers/probes to genotype the *SLC11A1* microsatellite is therefore unfeasible due to the complex repetitive nature of the $(GT)_n$ microsatellite repeat.

High resolution melt (HRM) curve analysis is a fast and cost effective real-time PCR-based technique with a range of applications, including genotyping and mutation discovery. HRM curve analysis allows post-PCR analysis using unlabelled oligonucleotides coupled with an inexpensive saturating DNA intercalating dye. Ririe et al. (1997) were the first to show that melt curve analysis could be used to assess the quality of amplicons after real-time PCR, while HRM using unlabeled oligonucleotides with a saturating DNA dye was first described by Grundry et al. (2003) and Wittwer et al. (2003). The melting curve is obtained after PCR amplification by monitoring the fluorescence of the intercalating dye as the temperature passes through the denaturation temperature of the PCR product. Upon denaturation, the intercalating dye is released, resulting in a rapid loss of fluorescence (Figure 4.1). Because the melting curve of an amplicon is dependent upon its length, sequence and CG content, PCR products with different lengths and/or base compositions will have different melting characteristics, and therefore different melting temperatures, which can be exploited to distinguish different genotypes (Lay and Wittwer, 1997, Ririe *et al.*, 1997, Wittwer *et al.*, 1997).

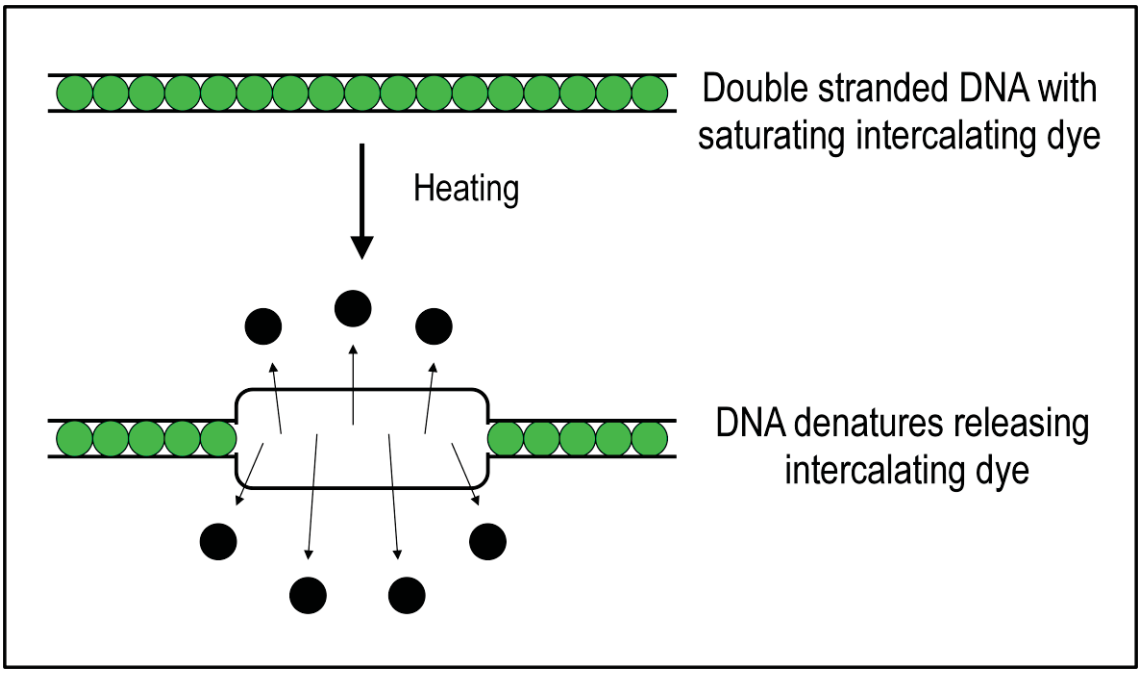

Figure 4.1 Molecular mechanism of melt curve analysis. A double stranded DNA intercalating dye (green circles) binds between the DNA bases. The sample is heated at a fixed rate and denaturation of the double stranded DNA results in a rapid loss of fluorescence.

In the genotyping of SNPs or insertion/deletion mutations by HRM, homozygous samples produce a single melting curve, while heterozygous samples produce more complex melting curves, which arise from the formation of both homoduplexes and heteroduplexes (Figure 4.2) (Liew *et al.*, 2004). Heteroduplexes are formed by the annealing of non-complementary strands of DNA, causing mispairing of the DNA in the non-complementary regions. Such mispairing decreases the stability of heteroduplexes as compared to that of homoduplexes, and therefore the former dissociate earlier in the melting profile (Gundry *et al.*, 2003). The melt curve analysis of heterozygous samples yields four molecular species (two homoduplexes and two heteroduplexes), each possessing unique melting temperatures (Figure 4.2). Because of the formation of these heteroduplex species, heterozygous samples are not genotyped according to their melting temperature, but rather by the shape of the dissociation profile. Liew et al. (2004) tested the melting profile of all possible heteroduplexes formed when a single nucleotide polymorphism is introduced and found that each heterozygote generated a unique melting curve, thereby allowing each heterozygote genotype to be distinguished.

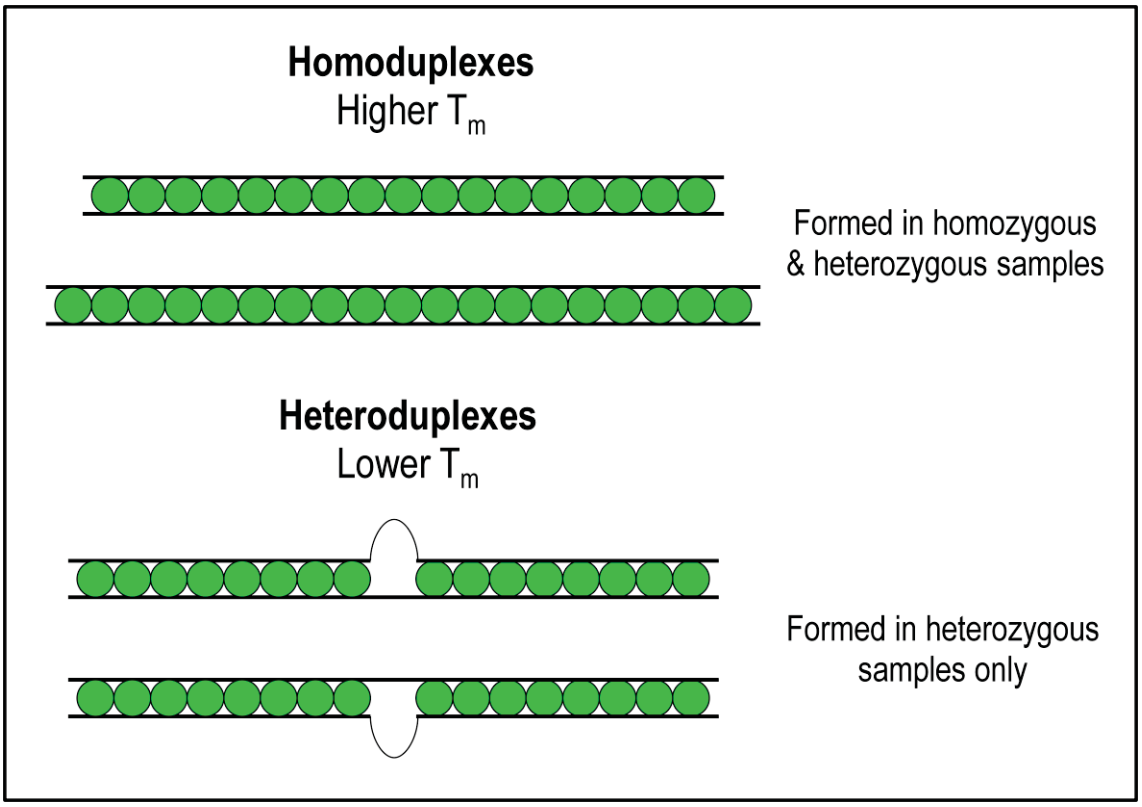

Figure 4.2 Molecular species formed during melting curve analysis of a sample containing heterozygous and homozygous genotypes. Homozygous samples result in the formation of homoduplexes while heterozygous samples result in the formation of a mixture of homoduplexes and heteroduplexes. Heteroduplexes contain regions of base mispairing, which lowers the denaturation temperature as compared to that of homoduplex samples.

Unlike agarose or polyacrylamide gel electrophoresis, melting curve analysis can also distinguish products of equal length but different sequence compositions (Ririe *et al.*, 1997). In the case of the $(GT)_n$ repeat, HRM offers a novel method by which to detect alleles with the same $(GT)_n$ promoter length but different GT sequence compositions, such as alleles 1 and 7 and alleles 3 and 5. Also, HRM analysis should be sufficiently sensitive to detect novel alleles, as these would produce distinct melting profiles.

4.2 MATERIALS AND METHODS

4.2.1 Materials

4.2.1.1 General Materials

FTA Mini Cards and the 2mm Harris Micro Punch were obtained from Whatman International Ltd (Middlesex, United Kingdom). The Twin.tec skirted PCR plates and heat sealing film were purchased from Eppendorf (Hamburg, Germany). The PureLink Genomic DNA Mini Kit, pCR8/GW/TOPO vector, Platinum *Taq* DNA polymerase and High-Fidelity Platinum *Taq* DNA polymerase were purchased from Invitrogen (California, USA), while the Accu-Chek Softclix lancets were purchased from Hoffmann-La Roche Ltd (Basel, Switzerland). The LC Green 1 master mix and the Lightcycler capillary tubes were purchased from Idaho Technologies (Salt Lake City, USA) and Roche Applied Science (Penzberg, Germany), respectively.

4.2.1.2 Oligonucleotides

Multiple primer sets were designed to flank both the $(GT)_n$ promoter (rs34448891) and 3'UTR $(CAAA)_n$ (rs17229009) polymorphisms based on the sequence file AF229613. Primers were designed following the previously described parameters (Section 2.1.3). Table 4.1 lists all of the oligonucleotides designed for the genotyping of the *SLC11A1* polymorphisms by HRM analysis.

The primer sequences that were optimal for genotyping the *SLC11A1* $(GT)_n$ promoter and $(CAAA)_n$ polymorphisms were the HSNRAMPC-F/HSNRAMPC-R (127bp amplicon) and the HSLC11A1-CAAAhr1-F/HSLC11A1-CAAAhr1-R (110bp amplicon) primer pairs, respectively.

Table 4.1 Oligonucleotides used for Genotyping of *SLC11A1* $(GT)_n$ and $(CAAA)_n$ Polymorphisms by HRM Analysis.

Primer name	Sequence	Length
$(GT)_n$ promoter polymorphism		
HSNRAMPA-F	TGAAGACTCGCATTAGGCCAACG	23
HSNRAMPA-R	CCGTGTTCTGTGCCTCCCAAGT	22
HSNRAMPC-F	CCAGATCAAAGAGAATAAGAAAGACC	26
HSNRAMPC-R	CCTGCCCCTTGCGTATTCATGTCA	24
HSNRAMPD-R	CCGTGTTCTGTGCCTCCCAAGTT	23
HSNRAMPE-F	GCATTAGGCCAACGAGGGGTCTT	23
$(CAAA)_n$ polymorphism		
HSNRAMP1-CAAA-F	CCTAGCGCAGCCATGTGATTACC	23
HSNRAMP1-CAAA-R	CCCAAGTCCTCAAGCCCTCACC	22
HSLC11A1-CAAAhr1F	CCACCCTTGCCATGGAGGTTAAG	23
HSLC11A1-CAAAhr1R	CACGCCTGCAGGTGCTCAATAAA	23
HSLC11A1-CAAAhr2R	CACCCTTGGGCTGTCAGGTCAC	22

4.2.2 Methods

4.2.2.1 Genomic DNA Collection

4.2.2.1.1 Buccal Cell Collection

Participants were instructed to chew the inside of their cheeks for 20-30s and then to vigorously swill 10ml of mouthwash (Gatorade Bluebolt) for 30s. The liquid was then expelled into a 50ml centrifuge tube. In the laboratory, all samples were vortexed to obtain a homogenous suspension. Mouthwash samples were either immobilised on FTA cards (Section 4.2.2.1.2) or directly added to PCR reactions (Section 4.2.2.2.3).

4.2.2.1.2 FTA Card Immobilisation of Buccal Cells

FTA card immobilisation of buccal cells was carried out in accordance with a protocol approved by the UTS Human Research Ethics Committee. Mouthwash samples (from 30 participants) were first collected following the buccal cell collection methodology (Section 4.2.2.1.1). FTA cards were dipped into the mouthwash sample and allowed to air-dry. Collected FTA card samples were stored in separate envelopes at RT and gDNA was extracted for PCR amplification when required (Sections 4.2.2.2.1, 4.2.2.2.2 and 4.2.2.3).

4.2.2.1.3 Collection of Blood Cells

Blood (50-100µl) was collected from the finger tip using an Accu-Chek Softclix lancet (10 participants) (Hoffmann-La Roche Ltd, USA). Blood was placed into a sterile 1.7ml centrifuge tube containing 20µl Proteinase K and gDNA was extracted using the PureLink Genomic DNA Mini Kit, according to the manufacturer's instructions. The quality and quantity of extracted gDNA was assessed by agarose gel electrophoresis (Section 2.2.2.5) and NanoDrop quantification (Section 2.2.2.7). The gDNA samples were stored at -20^{o}C until required for PCR amplification (Section 4.2.2.4.2).

4.2.2.2 Genomic DNA Extraction

4.2.2.2.1 Preparation of FTA Card Immobilised gDNA for PCR Analysis

Sample punches of FTA cards containing immobilised gDNA from mouthwash samples (Section 4.2.2.1.1 and 4.2.2.1.2) were prepared using a 2mm Harris Micro punch (Whatman) ensuring the sample area of the card was the only part in direct contact with the cutting mat. Sample punches were then transferred to sterile 1.7ml centrifuge tubes. The 2mm Harris Micro Punch was cleaned after each sample by punching out five 2mm disks from a blank FTA card. The cutting mat was cleaned with 70% (v/v) ethanol between each sample. A simplified method of washing the FTA punches was employed to remove any potential PCR inhibitors and contaminants (Makowski *et al.*, 1995). This involved using sterile H_2O to wash the punches, instead of the manufacturer's protocol of a single wash with FTA purification reagent, followed by two washes in TE buffer (Whatman FTA protocol BD08). Sample punches were washed in 0.5ml of sterile H_2O for 5min (with constant inversion) and were then dried in a heating block (55^{o}C for 15min). The 2mm card punches were then transferred directly to a PCR reaction (Section 4.2.2.4) or stored at 4^{o}C O/N.

4.2.2.2.2 Elution of FTA Card Immobilised gDNA

It was found that the FTA card punches could not be added directly to real-time PCR amplification reactions due to interference with fluorescence measurements. Therefore, elution of gDNA from the FTA card was trialed for use in the PCR. Seven FTA card sample punches (2mm) (Section 4.2.2.2.1) containing immobilised buccal cell gDNA from a single mouthwash sample (Section 4.2.2.1.1 and 4.2.2.1.2), were washed once in 500µl of sterile H_2O and then inverted for 5min. The water was completely removed

and the sample punches were dried in a heating block (55°C for 15min). For the elution of gDNA using TE buffer, sample punches were transferred to a tube containing different volumes (25, 50, 75, 100, 150 and 200µl) of TE buffer and heated at 99°C for 15min to elute the DNA. An aliquot (5µl) of the eluted DNA was then used for PCR (Section 4.2.2.4).

Genomic DNA was also eluted from the FTA cards by RT elution with pH treatment following the published protocol (Whatman application note, 2004 – Eluting genomic DNA from FTA cards using room temperature and pH treatment). Briefly, 35µl of solution 1 (0.1M NaOH, 0.3mM EDTA, pH13) was added to a single or double FTA card punch (Section 4.2.2.2.1) and incubated at RT for 5 min. Following this, 65µl of solution 2 (0.1M Tris-HCl, pH 7.0) was added, the tube vortexed 5 times and then incubated for a further 10min. The FTA card was removed and 5µl of the solution was used for PCR (Section 4.2.2.4), or stored at -20°C until used.

4.2.2.2.3 Direct Addition of Buccal Cells to the PCR

Buccal cells, from frozen (-20°C) or fresh mouthwash samples (Section 4.2.2.1.1), were collected by centrifugation (3min at 10000rpm) and the supernatant was discarded. The cells were washed twice in 4ml of low EDTA TE buffer (0.1mM EDTA) and the buccal cell pellet was resuspended in 1ml of low EDTA TE buffer and transferred to a fresh 1.7ml centrifuge tube. Cells were added directly (5µl) into a PCR (Section 4.2.2.4), or stored at -20°C until needed.

4.2.2.3 Cloning of *SLC11A1* $(GT)_n$ and $(CAAA)_n$ Polymorphic Variants

PCR fragments containing different *SLC11A1* $(GT)_n$ promoter variants (alleles 2, 3, 5 and 9) and $(CAAA)_n$ variants [$(CAAA)_2$ and $(CAAA)_3$] were amplified from FTA card bound buccal cells using oligonucleotides HSNRAMPA-F/R and HSNRAMPCAAA-F/R (Section 2.2.2.1), producing amplicon sizes of 208bp [for $(GT)_n$ allele 3] and 220bp [for $(CAAA)_3$]. PCR products were purified (Section 2.2.2.2) and cloned into the pCR8/GW/TOPO vector (Section 2.2.3.2). Plasmid DNA was extracted (Section 2.2.2.4) and sequenced to identify the cloned alleles (Sections 2.2.2.6 and 2.2.4.2). The plasmids containing the allelic variants of the $(GT)_n$ and $(CAAA)_n$ polymorphisms were used to optimise parameters of the genotyping methodologies (Section 4.3.2 and 4.3.3).

4.2.2.4 PCR Protocols

4.2.2.4.1 PCR 2 – Optimisation of Parameters for Real-Time PCR Analysis

PCRs, for the optimisation of the real-time PCR parameters (Section 4.3.2), were carried out in a 25µl reaction volume, which contained 1U Platinum *Taq* polymerase, 1X LCGreen I Mix (1X LCGreen I, 0.25mg/ml BSA, 0.2mM dNTPs and 1-3mM Mg Buffer), and forward and reverse primers (0.5-9.0µM). Each reaction contained 0.1ng plasmid DNA (Section 4.2.2.3).

PCRs for the optimisation of primer annealing temperature (Section 4.3.2.1) and magnesium chloride concentration (Section 4.3.2.2) were carried out in an Eppendorf Mastercycler Gradient instrument (Eppendorf) using FTA card immobilised gDNA from buccal cells isolated from the same sample card (Sections 4.2.2.1.1, 4.2.2.1.2 and 4.2.2.2.1). The quality of PCR products was assessed by agarose gel electrophoresis (Section 2.2.2.5). The annealing temperature was varied from 56-72^{o}C, while the magnesium chloride concentration was varied from 1.0-3.0mM. The optimal annealing temperature was determined as the temperature which produced a single amplicon with the highest intensity. The optimal magnesium chloride concentration for the different primer sets was the magnesium concentration which produced the most intense band without the presence of additional non-specific bands. All other optimisation steps (Sections 4.3.2.3, 4.3.2.4 and 4.3.3) were carried out by real-time PCR using the Mastercycler ep *realplex*^{2} (Eppendorf).

Primer matrices were completed to determine the optimal primer concentration (Section 4.3.2.3). The primers were tested in all combinations of forward and reverse primer concentrations of 9.0, 6.0, 3.0 and 0.5µM. Cloned and sequenced plasmid DNA, containing the $(GT)_n$ or $(CAAA)_n$ microsatellite repeat region (containing allelic variants $(GT)_n$ allele 3 and $(CAAA)_3$, respectively), were used as the template for the real-time PCR amplification for the determination of optimal primer concentrations (Section 4.2.2.3). Optimal primer concentrations were determined after real-time PCR amplification by analysis of the quantification curves (i.e. low Ct value, steep amplification plot and the absence of an early plateau phase) and the melting profiles (presence of a smooth single peak), on the *realplex* PCR instrument.

To determine the appropriate polymerase for the HRM genotyping methodologies, plasmid DNA, containing the $(GT)_n$ and $(CAAA)_n$ microsatellite regions (Section 4.2.2.3), were amplified with both polymerases (Platinum *Taq* and Platinum *Taq* DNA polymerase High Fidelity) in parallel, and the generated amplicons were then analysed by HRM curve analysis using the HR-1 melting instrument (Section 4.2.2.5).

For all optimisation steps, PCR was initiated by an initial denaturation (95^{o}C, 5min), followed by 40 cycles of 95^{o}C for 15-30s, 56-72^{o}C for 15-30s and 72^{o}C for 15-60s. Real-time PCR included a dissociation/melting step, which consisted of denaturation at 95^{o}C for 15s, rapid cooling to 60^{o}C for 15s, followed by heating at a rate of 0.4^{o}C up to 95^{o}C with fluorescence acquisition. Real-time PCR amplification was assessed using the quantification plots and melting curves.

4.2.2.4.2 PCR 3 – Optimised Real-Time PCR Protocol for the Genotyping of SLC11A1 Microsatellite Repeats by HRM Analysis

Real-time PCR was carried out in a 25µl reaction volume, which contained 1U Platinum *Taq* polymerase (Invitrogen); 1X LCGreen I Mix (1X LCGreen I, 0.25mg/ml BSA, 0.2mM dNTPs and 2mM Mg Buffer) (Idaho Technologies, USA), and forward and reverse primer concentrations of 6.0/9.0µM for the $(GT)_n$ repeat and 3.0/6.0µM for the $(CAAA)_n$ repeat. The template added to each reaction consisted either of plasmid DNA (0.1ng), diluted PCR product (10pg) or extracted gDNA (10-25ng). A minimum of four replicates were completed for each sample. Amplification of the $(GT)_n$ repeat region was initiated by an initial denaturation (95^{o}C, 5min), followed by 40 cycles of 95^{o}C for 15s, 64.5^{o}C for 15s and 72^{o}C for 15s. The $(CAAA)_n$ PCR utilised a 2-step PCR consisting of an initial denaturation (95^{o}C, 5min) followed by 40 cycles of 95^{o}C for 15s and 72^{o}C for 30s. Amplification of both the $(GT)_n$ and $(CAAA)_n$ repeat regions were followed by a dissociation step consisting of a denaturation step of 95^{o}C for 15s, cooling to 60^{o}C for 15s, and then heating at a rate of 0.4^{o}C/s up to 95^{o}C with fluorescence acquisition. Real-time PCR amplification was assessed using the quantification plot and the melting curves from the realplex mastercyler software. Replicate samples were then analysed by HRM curve analysis using the HR-1 (Section 4.2.2.5). Replicate samples, which did not result in efficient amplification or a high Ct value from the analysis of quantification plots and melt curves from the realplex

mastercycler software, were not analysed further by HRM analysis with the HR-1. The raw curves, obtained by high-resolution melting of the samples using the HR-1, were further analysed (Section 4.2.2.6.2) to allow the determination of a samples genotype.

4.2.2.4.3 PCR 4 – Nested PCR Protocol to Increase Starting Template for HRM Genotyping from FTA Card Immobilised gDNA

Direct addition of washed FTA card punches (containing bound gDNA from buccal cells) to the real-time genotyping PCR did not provide adequate starting template for optimal amplification that was required for HRM analysis (Section 4.3.4.1). Therefore, a nested PCR approach was used, which consisted of two rounds of amplification, to increase the starting template concentration for the real-time genotyping PCR (Section 4.2.2.4.2). The first amplification step involved the amplification of the region of interest, and after amplification, the PCR product was diluted and used as the starting template for the second, genotyping PCR (Section 4.2.2.4.2).

The first PCR amplification step was carried out in a final volume of 50µl containing 1U Platinum *Taq* polymerase (Invitrogen); 1X PCR Buffer; 2.5mM $MgCl_2$; 0.25mM dNTPs and 20µM HSNRAMPA-F/R or HSNRAMPCAAA-F/R primers (Table 4.1). Sample punches were added directly to the PCR reaction. PCR consisted of an initial denaturation (95^{o}C for 5min); followed by 34 cycles of denaturation (95^{o}C for 30s), annealing (59^{o}C [for $(GT)_n$ repeat] or 58^{o}C [for $(CAAA)_n$ repeat] for 30s) and extension (72^{o}C for 40s), with a final extension at 72^{o}C for 10min. After PCR purification (Section 2.2.2.2), amplified DNA was diluted to 2pg/µl and 10pg was added to the second amplification reaction (real-time PCR genotyping reaction) (Section 4.2.2.4.2). Following real-time PCR amplification (Section 4.2.2.4.2), genotypes were determined by HRM analysis (Section 4.2.2.5 and 4.2.2.6.2).

4.2.2.5 Genotyping of *SLC11A1* Microsatellite Polymorphisms by HRM Curve Analysis

After amplification by real-time PCR using the Mastercycler ep *realplex*^{2} (Section 4.2.2.4.2), the samples were analysed by HRM curve analysis to genotype samples. The PCR products (15µl) were transferred to LightCycler capillary tubes and HRM was completed using the HR-1 dedicated high resolution melter (Idaho Technologies). For

both the $(GT)_n$ and $(CAAA)_n$ protocols, samples were heated at a rate of 0.1^oC/s with fluorescence acquisition between 75^oC and 95^oC. The raw melting curves were then analysed using the HR-1 Melt Tool Analysis software (Section 4.2.2.6.2) to genotype samples.

4.2.2.6 Software

4.2.2.6.1 Prediction of Amplicon Melting using Poland

Amplicons to be generated by primers designed for real-time PCR amplification and subsequent genotyping by HRM analysis were assessed using the program Poland (http://www.biophys.uni-duesseldorf.de/local/POLAND/poland.html) (Poland, 1974, Steger, 1994). Poland calculates the thermal denaturation profile of double-stranded nucleic acids using nearest-neighbor stacking interactions and loop entropy functions to predict the melting profile of the input sequence. The designed *SLC11A1* amplicons, containing the $(GT)_n$ and $(CAAA)_n$ polymorphisms, were analysed using the standard parameters. The plots obtained (temperature of 50% probability vs. sequence and base pair vs. sequence vs. temperature) were used to determine if the amplicons generated using the designed primers melted as a single transition or if a more complex melting pattern, due to several melting transitions, existed.

4.2.2.6.2 Genotype Determination from Transformed Raw Melt Curve Data

The raw melting curves, obtained by HRM curve analysis (using the HR-1) of real-time PCR amplified samples (Sections 4.2.2.4.2 and 4.2.2.5), were analysed to genotype samples. The raw melting curves were analysed using the HR-1 Melt Analysis Tool software (Idaho Technologies). Raw curves were first normalised by placing the cursor bars in the flat regions above and below the melting transitions. The first cursor bar set, representing 100% fluorescence (every amplicon is double stranded), was placed just prior to the point where the samples started to melt, while the second cursor set, representing 0% fluorescence (all amplicons single stranded), was placed immediately after the melting transition. The distance within each cursor bar set was approximately $0.5\text{-}1.0^oC$ apart. Further analysis of the $(GT)_n$ samples was completed by temperature shifting the normalised melt curves, where the green horizontal cursor was placed at the lowest point of the melting curves and the red bar then placed as close as possible to the green bar. The $(CAAA)_n$ melt curves were not temperature shifted. To further enhance

the difference between each genotype, the normalised and temperature shifted $(GT)_n$ melt curves and the normalised $(CAAA)_n$ melt curves were converted to difference plots. Genotypes were assigned to each sample manually based on their difference plots, after comparison to standards of known genotype that were analysed simultaneously.

4.3 RESULTS

4.3.1 HRM Analysis Assay Design

4.3.1.1 Oligonucleotide Design for Genotyping of the *SLC11A1* $(GT)_n$ and $(CAAA)_n$ Microsatellites by HRM Analysis

Assay design and optimisation are essential in producing a HRM assay that will enable differentiation of genotypes. Optimisation is essential as the intercalacting dye used is not specific. Thus, any non-specific amplification, primer dimers or contaminating DNA will bind the intercalating dye, lowering the resolution and sensitivity of the melting profile, thereby preventing the differentiation of alleles.

Primers for HRM genotyping were designed to allow amplification of the *SLC11A1* promoter region encompassing the $(GT)_n$ microsatellite polymorphism and the 3'UTR surrounding the $(CAAA)_n$ microsatellite polymorphism (Section 4.2.1.2). The design of oligonucleotides within the *SLC11A1* promoter for genotyping of the $(GT)_n$ repeat by HRM analysis was challenging due to the repetitive nature of both the GT tract and the surrounding DNA. Therefore, primers were placed in suitable regions as close as possible to the polymorphic GT tract (Figure 4.3). Three oligonucleotide primer pairs that flanked each of the *SLC11A1* $(GT)_n$ promoter polymorphism and 3'UTR $(CAAA)_n$ polymorphism were designed (Figure 4.3A and 4.4A).

Several studies suggest that shorter amplicons allow for better discrimination of genotypes as the polymorphic region accounts for a larger portion of the amplicon (Liew *et al.*, 2004, Reed and Wittwer, 2004, Wittwer *et al.*, 2003). However, other studies have shown that longer PCR products may be more beneficial due to the presence of multiple melting domains, which yield more complex melting profiles (Gundry *et al.*, 2003, Ririe *et al.*, 1997). Therefore, oligonucleotides were designed to be interchangeable, to allow the production of amplicons of varying length (110-220 bp) to determine the optimal amplicon length that allowed the greatest discrimination between *SLC11A1* $(GT)_n$ and $(CAAA)_n$ genotypes (Figure 4.3B and 4.4B).

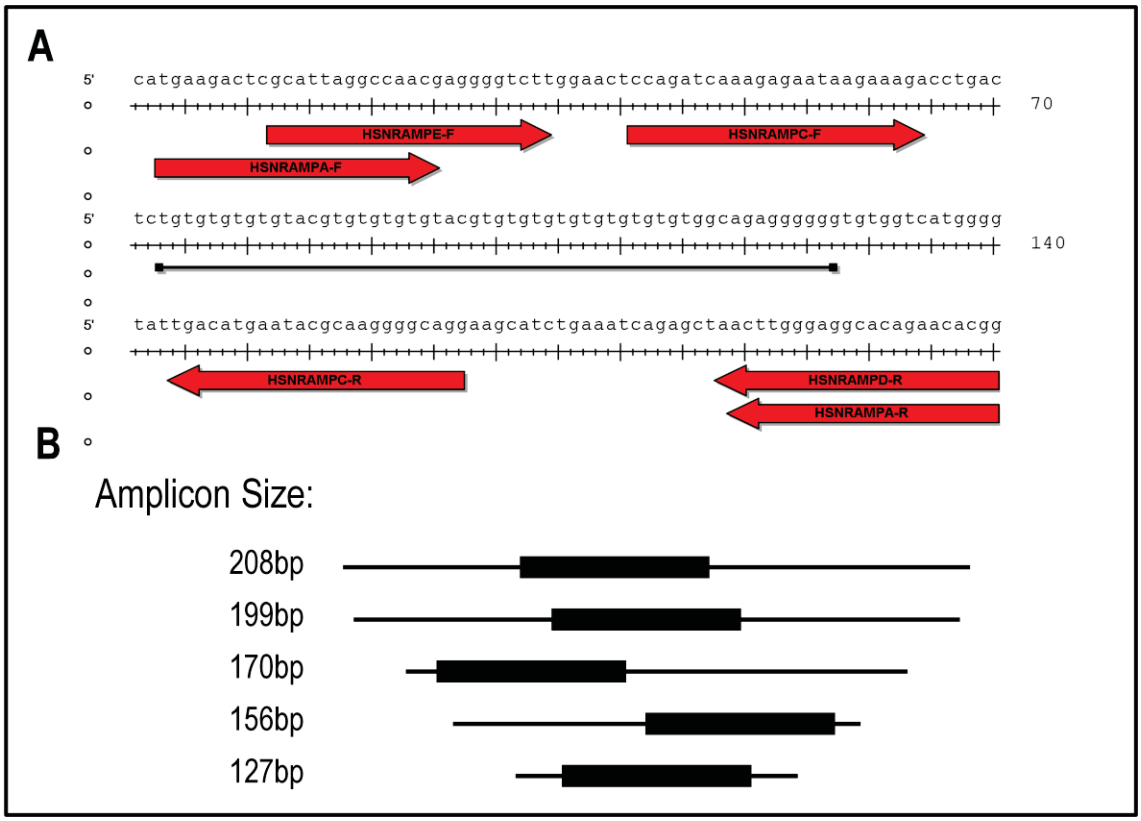

Figure 4.3 Oligonucleotide design for genotyping of the *SLC11A1* $(GT)_n$ promoter polymorphism by HRM. (A) Location of the designed oligonucleotides (red arrows) in relation to the polymorphic GT repeat (thin black line). The primer sets were designed to be interchangeable to allow the production of different amplicon sizes. (B) The different amplicon sizes which can be produced with the designed HRM oligonucleotides and the location of the $(GT)_n$ microsatellite (black box) within each amplicon. Amplicon sizes are based on the presence of $(GT)_n$ allele 3.

The location of the polymorphic region within the amplicon may also influence the ability to discriminate genotypes as the nearest neighbour interactions (Breslauer *et al.*, 1986) around the polymorphism may cause no change in the melting temperature between alleles in the same amplicon. Therefore, the primer sets were designed to produce various fragment sizes in which the location of the polymorphic region within the amplicon varied (Figure 4.3B and 4.4B).

The melting characteristics of all amplicons produced by the designed primer sets were analysed using the program Poland (Section 4.2.2.6.1) (Poland, 1974, Steger, 1994) which showed that all of the designed amplicons for the genotyping of the $(GT)_n$ and $(CAAA)_n$ microsatellites melted in a single transition, and therefore, should result in simple melting curves.

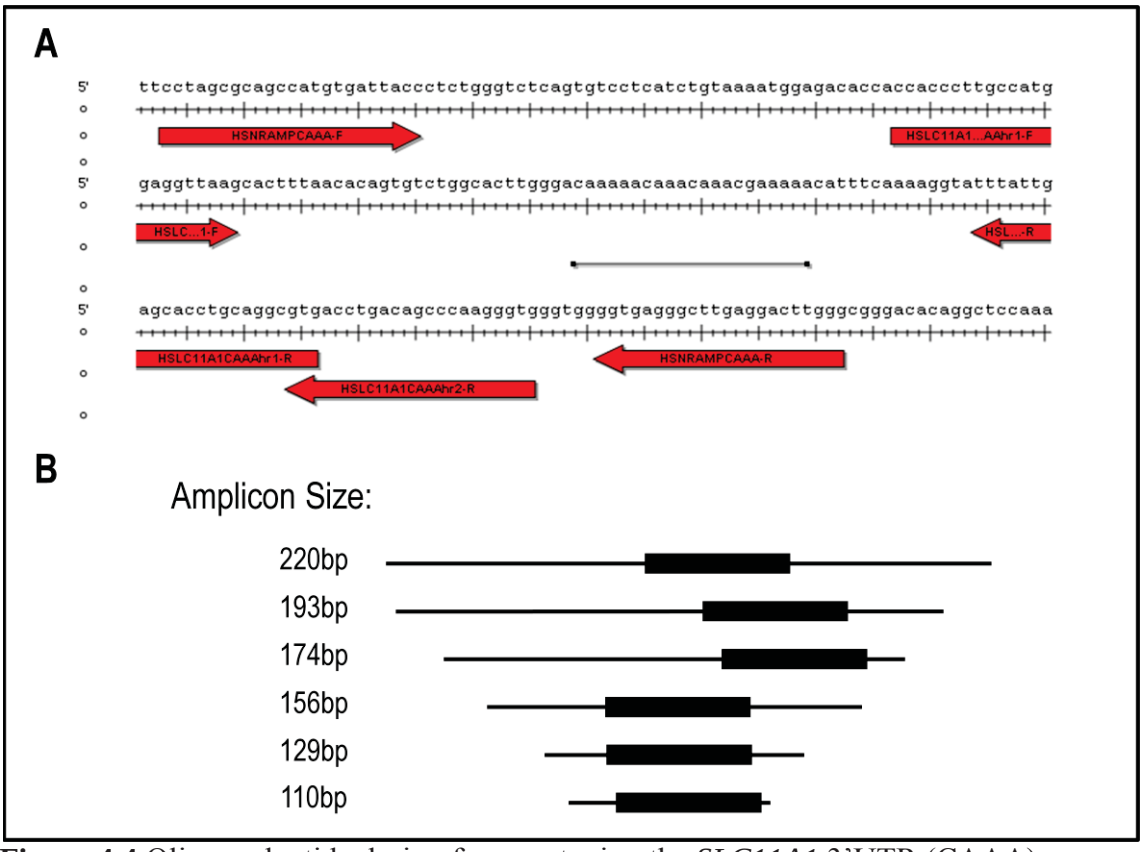

Figure 4.4 Oligonucleotide design for genotyping the *SLC11A1* 3'UTR $(CAAA)_n$ polymorphism by HRM analysis. (A) Location of the designed oligonucleotides (red arrows) in relation to the polymorphic $(CAAA)_n$ repeat (thin black line). The primer sets were designed to be interchangeable to allow the production of a range of different amplicon sizes. (B) The different amplicon sizes which can be produced with the designed HRM oligonucleotides, showing the location of the $(CAAA)_n$ microsatellite (black box) within each amplicon. Amplicon sizes are based on the presence of the allelic variant $(CAAA)_3$.

4.3.1.2 PCR Amplification using the Designed HRM Oligonucleotides Produced Amplicons of the Correct Length and Sequence

The designed oligonucleotides, for the amplification of *SLC11A1* regions containing the $(GT)_n$ and $(CAAA)_n$ polymorphisms, were analysed to ensure that the correct size fragments were amplified (Section 2.2.2.1). An initial annealing temperature of 56^{o}C was employed. Each of the primer combinations, for the amplification of the $(GT)_n$ and $(CAAA)_n$ regions, resulted in the production of a single product of the correct size (Figure 4.5). The PCR products from the different primer combinations were also purified (Section 2.2.2.2) and sequenced (Section 2.2.2.6). Alignment of the amplicon sequences against the predicted amplified sequence using SeqMan (Lasergene) (Section 2.2.4.2) showed that all primer sets had amplified the correct sequence.

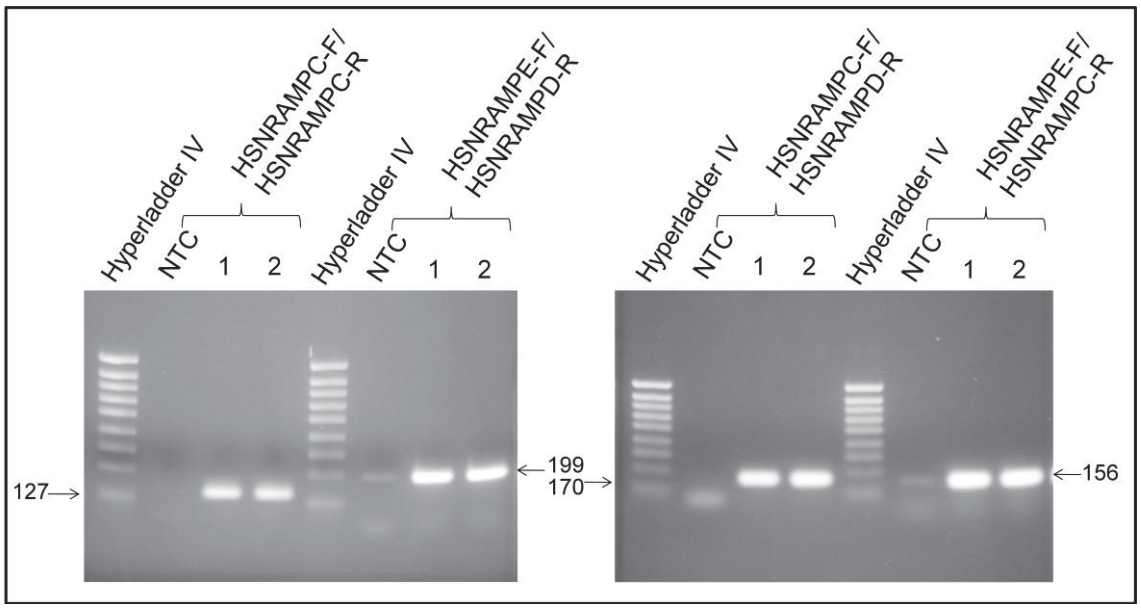

Figure 4.5 Validation of the oligonucleotides designed for HRM analysis for the amplification of $(GT)_n$ and $(CAAA)_n$ microsatellite repeats. Representative $(GT)_n$ amplification results, carried out in duplicate (1 and 2), of the $(GT)_n$ primer sets HSNRAMPC-F/R (127bp), HSNRAMPE-F/D-R (199bp), HSNRAMPC-F/D-R (170bp) and HSNRAMPE-F/C-R (156bp) show the amplification of the correct size fragments. NTC denotes the no template control.

4.3.2 Optimisation of Real-time PCR Parameters for HRM Analysis

All primer combinations for the amplification of the *SLC11A1* regions containing the $(GT)_n$ and $(CAAA)_n$ microsatellite repeats were initially optimised, allowing for the selection of the amplicons which will enable the accurate identification of sample genotypes. All parameters of the real-time genotyping PCR (Section 4.3.2) and the post-PCR HRM analysis (Section 4.3.3.1) were optimised (Table 4.2).

Table 4.2 Optimisation Steps for the Production of the *SLC11A1* HRM Assays.

Optimisation Step	Method	Reason
Annealing temperature of oligonucleotides (Section 4.3.2.1)	Temperature gradient PCR (56-72°C)	Increases the stringency of the PCR reaction as the increased annealing temperature reduces non-specific binding of the primers.
$MgCl_2$ concentration (Section 4.3.2.2)	$MgCl_2$ gradient PCR (1-3mM)	Magnesium is an essential cofactor for *Taq* polymerase and a concentration too low or high will result in no amplification or aberrant amplification, respectively.
Primer concentration (Section 4.2.2.3)	Primer matrices (0.5µM-9.0µM)	Primer concentrations too high result in the formation of non-specific products or primer-dimers, lowering the efficiency of the amplification and sensitivity of the HRM procedure.
Taq polymerase selection (Section 4.2.2.4)	Trial of Platinum *Taq* and High Fidelity Platinum *Taq* Polymerase	A high fidelity polymerase is essential to minimise replication errors during replication to ensure sensitivity of the genotyping methodology to discriminate different genotypes
Cycling parameters (Section 4.2.2.4)	Minimise cycling times	Shorter cycling times reduce the amplification of non-specific products and reduces the time of the genotyping PCR, aiding in the production of a high-throughput genotyping methodology.
Ramp rate of HR-1 instrument (Section 4.3.3.1)	Ramp rate of 0.4°C/s and 0.1°C/s	To determine the optimal rate of heating for the differentiation of genotypes.
Optimisation of HR-1 HRM software analysis parameters (Section 4.3.3.1)	Normalisation and/or temperature shifting	The HRM analysis tool will allow for a greater differentiation between subtle differences in raw melt curves, resulting in greater sensitivity of the HRM genotyping assay.

4.3.2.1 Optimisation of PCR Annealing Temperature

The optimal annealing temperature for PCR using the designed HRM oligonucleotides was determined using a gradient temperature PCR for all primer combinations (Section 4.2.2.4.1). The addition of an intercalating DNA dye for real-time PCR analysis or HRM genotyping, results in a higher stability of double stranded DNA (Gundry *et al.*, 2003). Therefore, the optimal annealing temperature for all primer sets was determined with the inclusion of the saturating double stranded DNA intercalating dye LCGreen1 (Section 4.2.2.4.1). The optimal annealing temperature for the amplification of the $(GT)_n$ repeat was 64.5°C and 66.4°C for the HSNRAMPC-F/R (Figure 4.6) and

HSNRAMPD-F/C-R primer combinations, respectively. The remaining primer combinations for the amplification of the $(GT)_n$ repeat all had optimal amplification with an annealing temperature of 65°C. The optimal annealing temperature for all of the primer sets used for the amplification of the $(CAAA)_n$ polymorphism was 72°C and thus a 2-step PCR protocol was developed.

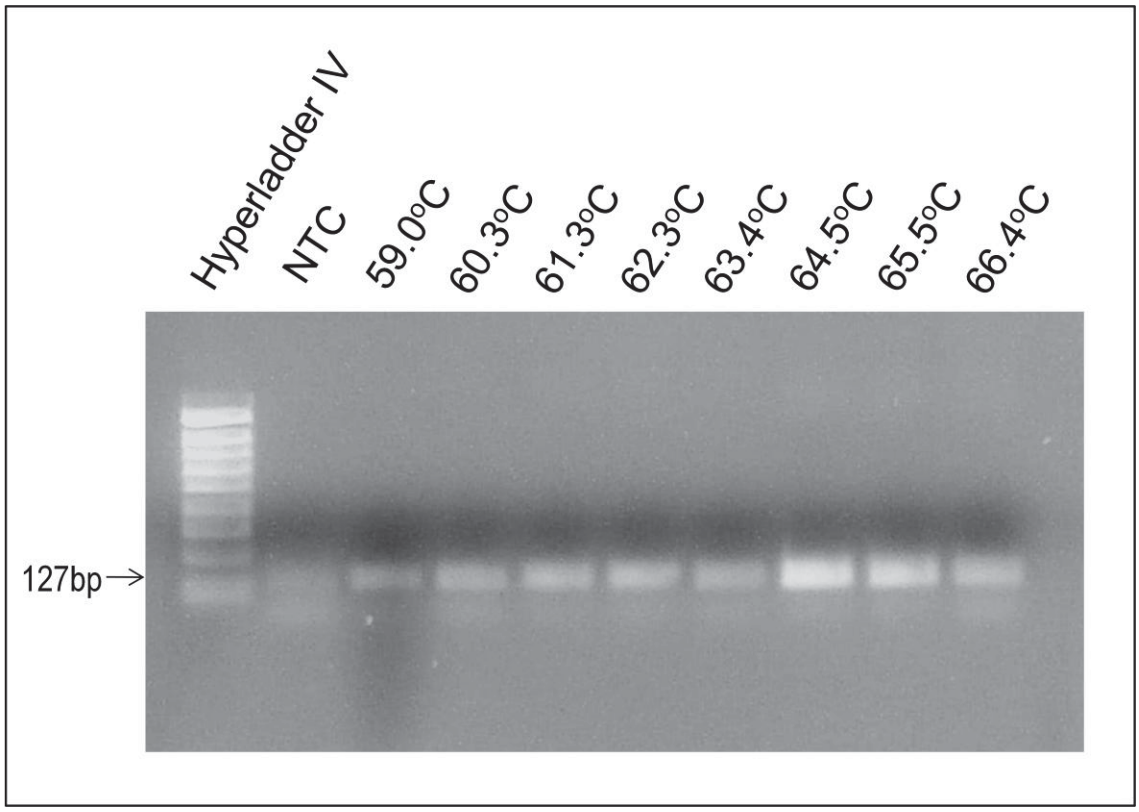

Figure 4.6 Determination of the optimal annealing temperature by gradient temperature PCR. Representative results of the amplification of the primer combination HSNRAMPC-F/R for the amplification of the $(GT)_n$ repeat. The PCR contained buccal cell gDNA immobilised on FTA card, with a temperature gradient of 59-66.4°C and post-PCR analysis of amplicons by agarose gel electrophoresis. NTC denotes the no template control.

4.3.2.2 Optimisation of Magnesium Chloride Concentration

Optimisation of the magnesium chloride concentration was conducted with a magnesium concentration ranging from 1-3mM (Section 4.2.2.4.1) in conjunction with the previously determined optimal annealing temperature (Section 4.3.2.1) (Figure 4.7). The optimal magnesium concentration for all of the primer sets, for the amplification of the $(GT)_n$ and $(CAAA)_n$ repeats, was determined to be 2mM.

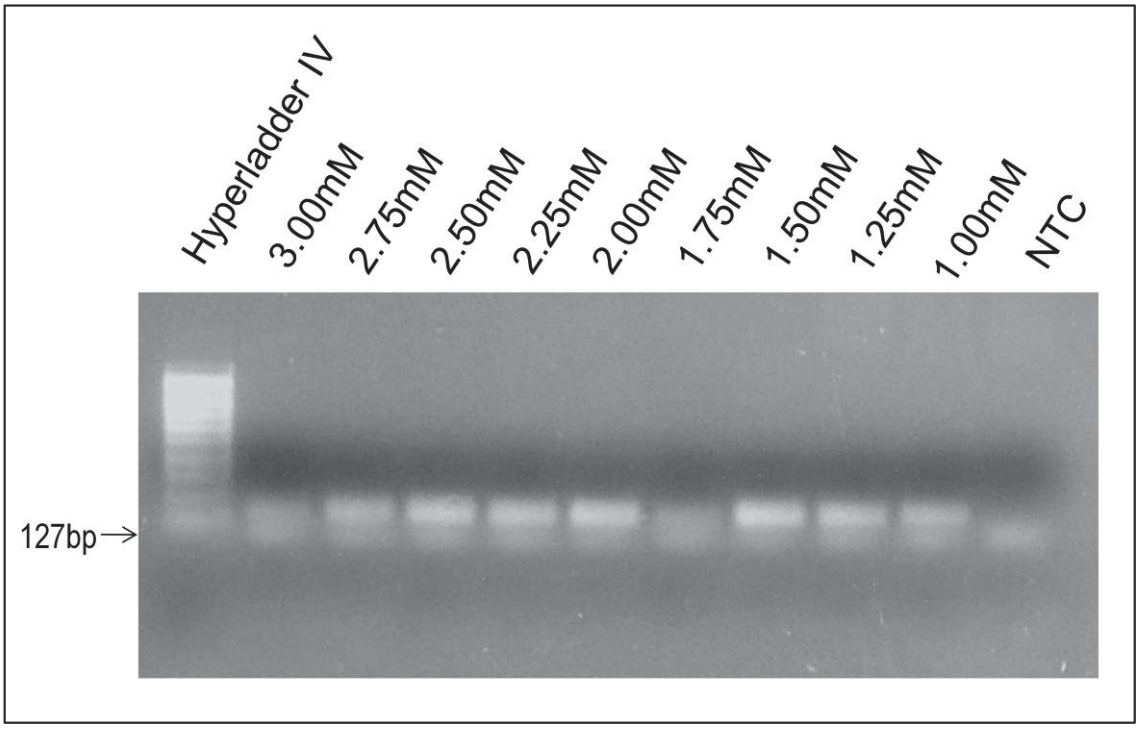

Figure 4.7 Determination of the optimal magnesium chloride concentration using a magnesium concentration gradient PCR. Representative results of the amplification using the HSNRAMPC-F/R primer set for the amplification of the $(GT)_n$ repeat. The PCR contained buccal cell gDNA immobilised on FTA card, with a magnesium gradient of 1-3mM with post-PCR analysis of amplicons by agarose gel electrophoresis. NTC denotes the no template control.

4.3.2.3 Optimisation of Primer Concentrations by Real-time PCR

Once the optimal annealing temperature and magnesium concentration were determined, different combinations of forward and reverse primer concentrations were tested through 4x4 concentration primer matrices to determine the optimal primer concentrations (Section 4.2.2.4.1). Previously cloned and sequenced plasmid DNA was used in these PCRs (Section 4.2.2.3). Optimal primer concentrations were determined after real-time PCR amplification by analysis of the quantification curves (i.e. low Ct value, steep amplification plot and the absence of an early plateau phase) and the melting profiles (presence of a smooth single peak) (Figure 4.8).

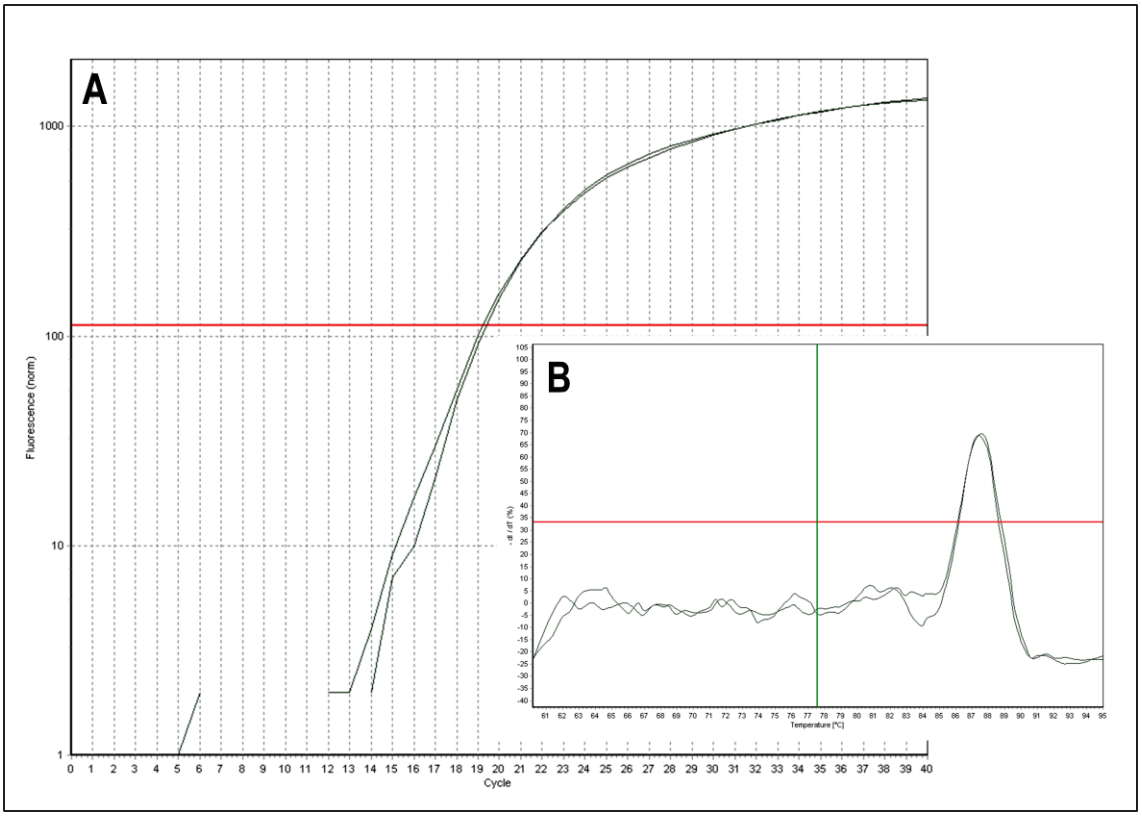

Figure 4.8 Determination of optimal primer concentrations by analysis of different combinations of forward and reverse primer concentrations. Forward and reverse primers were tested at different concentrations (9µM, 6µM, 3µM and 0.5µM). The representative result shown, of the primer set HSNRAMPC-F/R for the amplification of the $(GT)_n$ repeat, shows optimal amplification from forward and reverse primer concentrations of 6µM and 9µM, respectively. (A) Quantification profile displaying optimal amplification. The plot has a low Ct value, steep amplification plot and the absence of an early plateau phase. (B) The melt curve profile displaying the presence of a smooth single peak.

Testing of all combinations of forward and reverse primer concentrations found that the HSNRAMPC-F/R and SLC11A1CAAAhr1-F/R primer sets, for the amplification of regions containing the $(GT)_n$ and $(CAAA)_n$ microsatellite repeats, respectively, produced the optimal and most efficient amplification from all of the primer combinations tested. Furthermore, HRM analysis of post-PCR amplicons (Section 4.2.2.5) found that amplicons generated by the use of the aforementioned primers produced the most consistent melting profiles. Therefore, the primer sets HSNRAMPC-F/R and SLC11A1CAAAhr1-F/R, were selected for use in HRM genotyping of the $(GT)_n$ and $(CAAA)_n$ microsatellites, respectively. The optimal forward and reverse primer concentrations for the HSNRAMPC-F/R primer set were determined to be 6.0µM and 9.0µM (Figure 4.8), respectively, while the optimal SLC11A1CAAAhr1-F/R forward and reverse primer concentrations were 3.0µM and 6.0µM, respectively.

After melting analysis on the realplex instrument (Section 4.2.2.4.1), the amplicons generated from the different primer combinations of the selected HSNRAMPC-F/R and SLC11A1CAAAhr1-F/R primer sets were further analysed by HRM using the HR-1 instrument (Section 4.2.2.5) (Figure 4.9). The change in the position of the melting curve observed with different primer concentrations indicates the sensitivity of HRM to subtle changes in reaction conditions. This highlights the importance of extensive optimisation of amplification parameters to ensure the production of an assay with the ability to accurately and consistently differentiate between genotypes. Furthermore, it was identified that replicates containing inefficient amplification, or a significantly high Ct value (greater than 30) resulted in melting profiles which differed significantly from the expected melting path of that sample. Therefore, samples which did not result in optimal amplification, based on the analysis of the quantification plots, were omitted from HRM analysis.

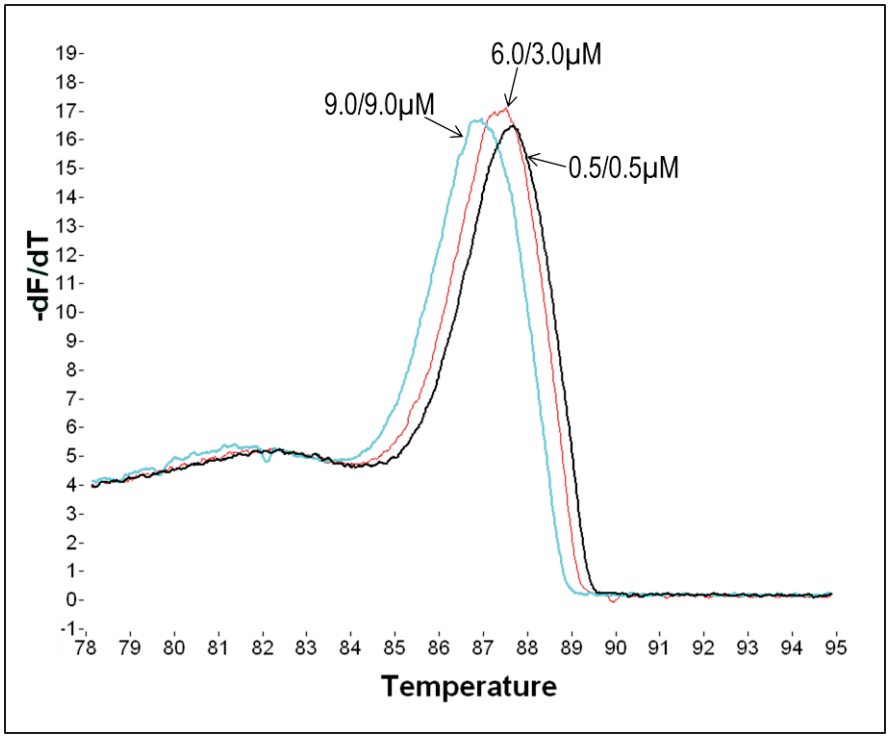

Figure 4.9 HRM curve analysis is sensitive to subtle changes in reaction conditions. The figure displays the first derivative melting profiles from three samples amplified with the HSNRAMPC-F/R primer set, containing different primer concentrations (µM). All samples were amplified from plasmid DNA containing $(GT)_n$ allele 3. Samples were analysed by high resolution melting using the HR-1 instrument. The raw melting data was first normalised before being converted to the negative first derivative plot.

4.3.2.4 Selection of *Taq* Polymerase and Optimisation of Real-time PCR Cycling Parameters

Different *Taq* polymerases were assessed for use in the *SLC11A1* HRM genotyping assays. The repetitive structure of microsatellites results in a much higher replication error rate than that seen with non-repetitive DNA sequences. Therefore, a high fidelity *Taq* polymerase is essential to minimise replication errors during real-time PCR amplification. Two high fidelity polymerases were trialled, the Platinum *Taq* DNA polymerase and the Platinum *Taq* DNA polymerase High Fidelity (Hi-Fi *Taq*) (Section 4.2.2.4.1). The amplification and HRM curve profiles obtained using the Hi-Fi *Taq* were not as optimal as those obtained with Platinum *Taq*. Therefore the Platinum *Taq* polymerase was selected for use with the HRM genotyping methodologies.

Initial real-time PCR analysis utilised cycling parameters of 30s (denaturation, annealing and extension steps) for the $(GT)_n$ promoter methodology and a 30s denaturation step followed by 1min annealing/extension step for the $(CAAA)_n$ methodology (Section 4.2.2.4.1). Optimisation of the cycling parameters was aimed at shortening these times [15s for the $(GT)_n$, and 15 and 30s for denaturation and annealing/extension, respectively, for the $(CAAA)_n$]. For amplification of $(GT)_n$ and $(CAAA)_n$ promoter regions, no difference in the quality of the amplification was observed between the different cycling times and, therefore, the cycling times were reduced. This also enabled the real-time PCR to be completed faster, thereby contributing to the production of an efficient, rapid high-throughput genotyping methodology.

4.3.3 HRM Genotyping of Simulated *SLC11A1* $(GT)_n$ and $(CAAA)_n$ Genotypes

After the parameters of real-time PCR amplification were optimised (Section 4.3.2), the ability of the optimised HRM methodology to genotype the $(GT)_n$ and $(CAAA)_n$ polymorphisms was assessed. To do this, the three most common *SLC11A1* $(GT)_n$ promoter genotypes (homozygous allele 2, homozygous allele 3, heterozygous allele 2/3), which account for greater than 95% of the total promoter allele frequencies, and the $(CAAA)_n$ genotypes (homozygous $(CAAA)_{2/2}$, $(CAAA)_{3/3}$, heterozygous $(CAAA)_{2/3}$) were simulated using the cloned and sequenced $(GT)_n$ and $(CAAA)_n$ alleles (Section 4.2.2.3). The plasmid clones were used individually and in combination to mimic homozygosity and heterozygosity, respectively, for both $(GT)_n$ and $(CAAA)_n$ polymorphisms. All real-time PCRs used the optimised PCR protocol (Section 4.2.2.4.2) followed by HRM analysis (Section 4.2.2.5 and 4.2.2.6.2).

4.3.3.1 Optimisation of HRM Parameters - Ramp Rate and HR-1 Software Analysis Parameters

Initial genotyping experiments utilising the optimised real-time PCR protocol allowed the optimisation of the melting parameters of the HR-1 instrument as well as the software used to analyse the raw melting profiles.

Analysis of the raw melting curves using the HR-1 software is an integral part in accentuating the differences in the melt profiles of the different genotypes (Figure 4.10). Raw melt curves are first normalised, which alters each curve for the variance in the fluorescence intensity of each sample. Normalised curves can then be temperature shifted, which draws all the curves together, forcing the curves to separate based on the shape of the curve. Temperature shifting helps to accentuate heterozygous samples (due to an altered melting curve profile resulting from the presence of heteroduplex species), thereby facilitating their differentiation from homozygous samples (Figure 4.2). These differences are further accentuated by the use of the difference plot that subtracts the fluorescence of all curves from a selected sample. The difference plot, which shows the greatest differentiation between samples, can then be used to assign a genotype to a sample.

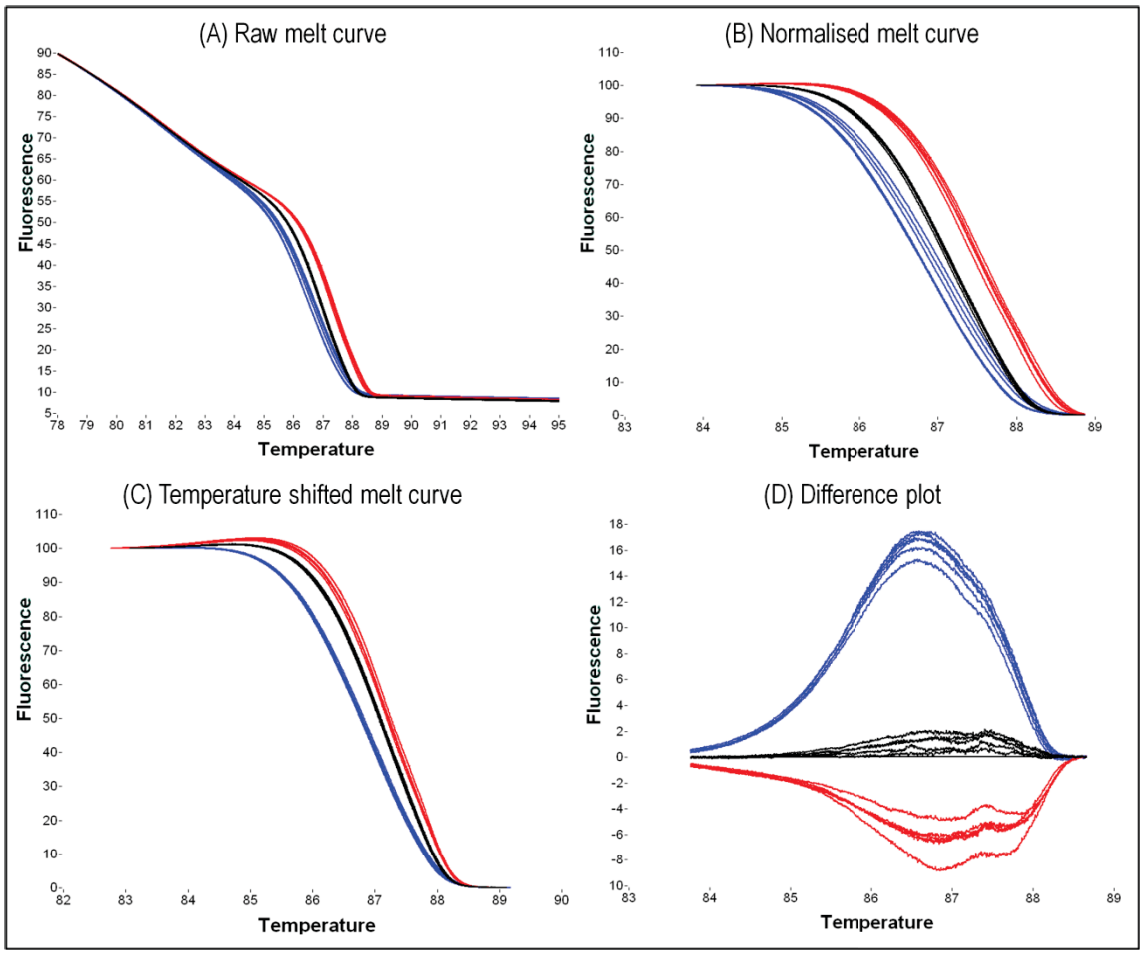

Figure 4.10 HR-1 software analysis of the raw melt curves of simulated $(GT)_n$ genotypes. The raw melt curves (A) are first normalised (B) which removes the variance in fluorescence intensity. Normalised melt curves can then be temperature shifted (C), forcing the samples to separate based on the shape of the curve. The difference plot (D) subtracts the fluorescence intensity from a selected sample and is used to assign a genotype to a sample. The red, black and blue lines represent samples homozygous for alleles 3 and 2, and heterozygous for alleles 2 and 3, respectively.

Analysis of the raw melt curves indicated that normalisation and temperature shifting of the raw melt curves allowed optimal differentiation of the $(GT)_n$ genotypes (Figure 4.10). However, for the $(CAAA)_n$ polymorphism, better differentiation was achieved when the samples were normalised only (Figure 4.11). When the $(CAAA)_n$ melt curves were temperature shifted (after normalisation) the homozygous samples no longer separated as two distinct groups, but melted as one group (Figure 4.11).

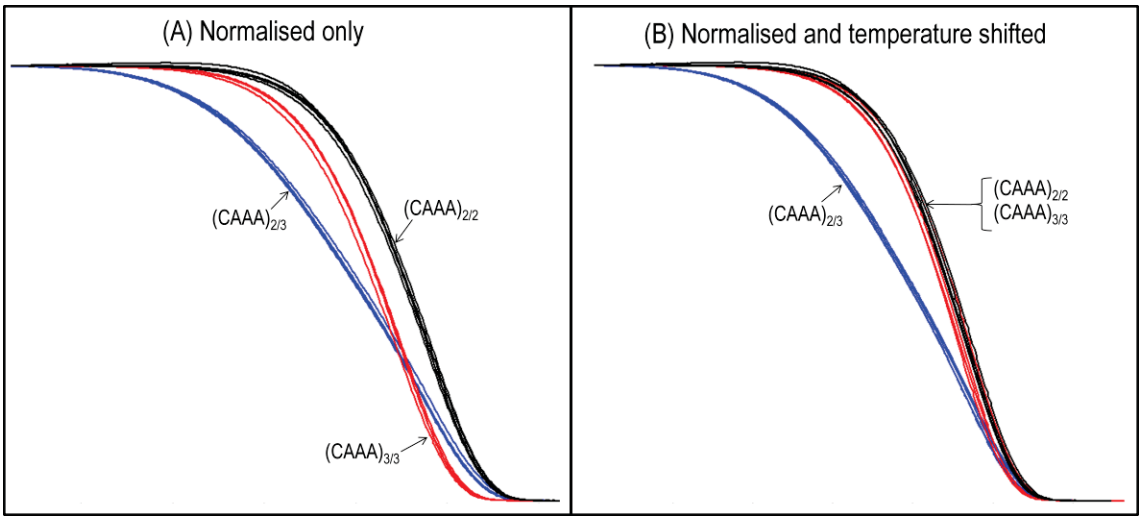

Figure 4.11 Analysis of the $(CAAA)_n$ melting curves using the HR-1 software. (A) Normalised melt curves and (B) normalised and temperature shifted melt curves.

The ramp rate at which the HR-1 instrument melts the post-PCR samples was also optimised. The ramp rate was trialled at two different rates of 0.4°C/s and 0.1°C/s to determine which temperature provided the best differentiation between genotypes. Comparison of the curves obtained at the two resolutions indicated that a rate of 0.1°C/s gave better differentiation between genotypes for both the $(GT)_n$ and $(CAAA)_n$ polymorphisms (Figure 4.12). Therefore, the HR-1 ramp rate of 0.1°C/s was used for the $(GT)_n$ and $(CAAA)_n$ genotyping methodologies.

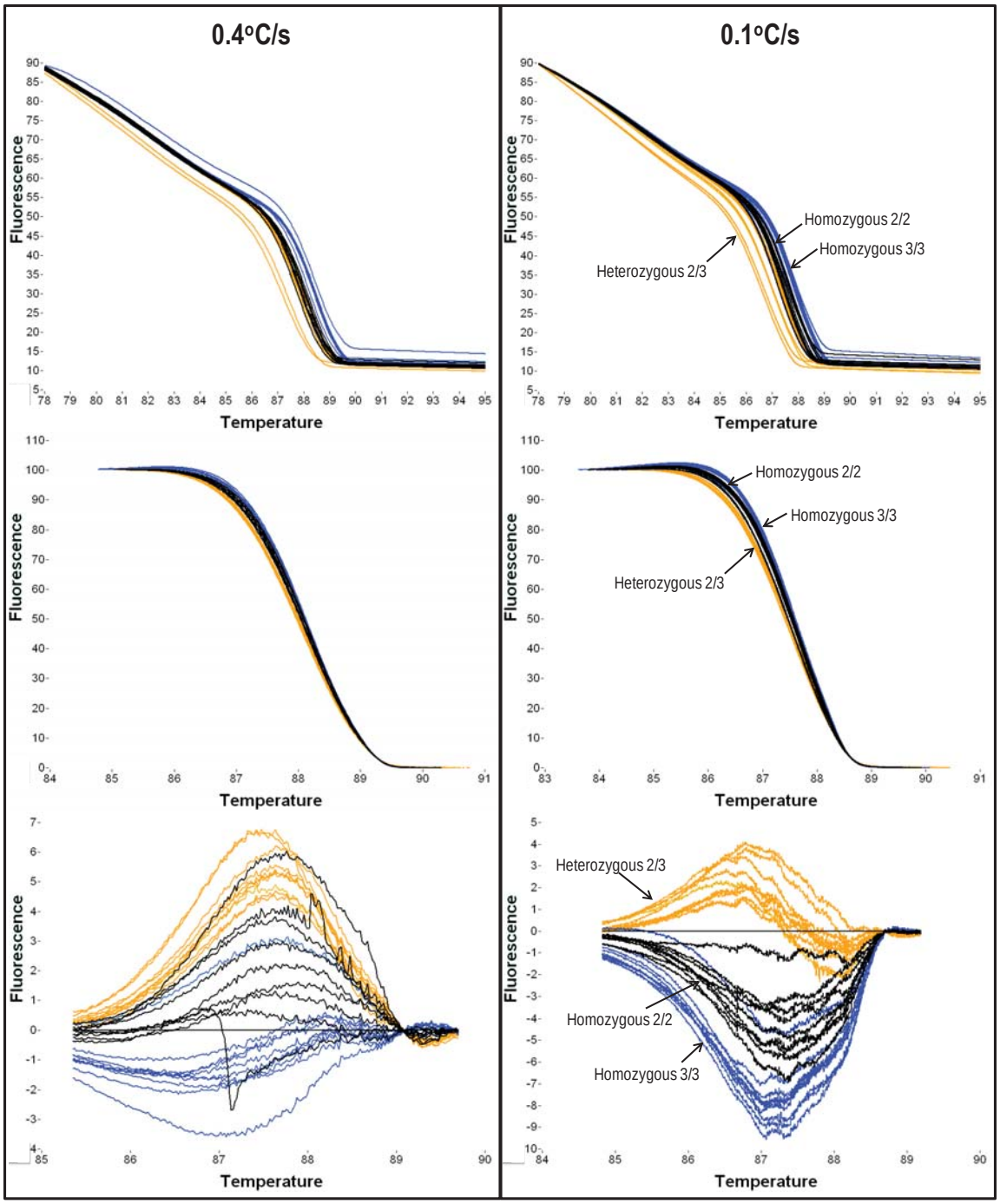

Figure 4.12 Optimisation of the HR-1 ramp rate to enable sensitive differentiation of genotypes. Representative HRM results of the $(GT)_n$ microsatellite with a ramp rate of 0.4°C/s (left panel) and 0.1°C/s (right panel). The raw melt curves are shown at the top of each panel, the normalised and temperature shifted melt curves in the middle and their respective difference plot at the bottom. Greater differentiation of simulated genotypes is observed in the plots of samples melted at 0.1°C/s compared to 0.4°C/s.

4.3.3.2 The Optimised HRM Genotyping Methodologies Successfully Differentiates Simulated $(GT)_n$ and $(CAAA)_n$ Genotypes

Analysis of the simulated homozygote and heterozygote genotypes, using the optimised real-time PCR conditions, in conjunction with the HR-1 HRM parameters, allowed successful genotyping of the $(GT)_n$ and $(CAAA)_n$ polymorphisms. The melt profiles of homozygous and heterozygous genotypes separated into clearly defined groups (Figure 4.13). The optimised HRM genotyping methodology was consistently able to discriminate each of the simulated *SLC11A1* $(GT)_n$ promoter and $(CAAA)_n$ genotypes.

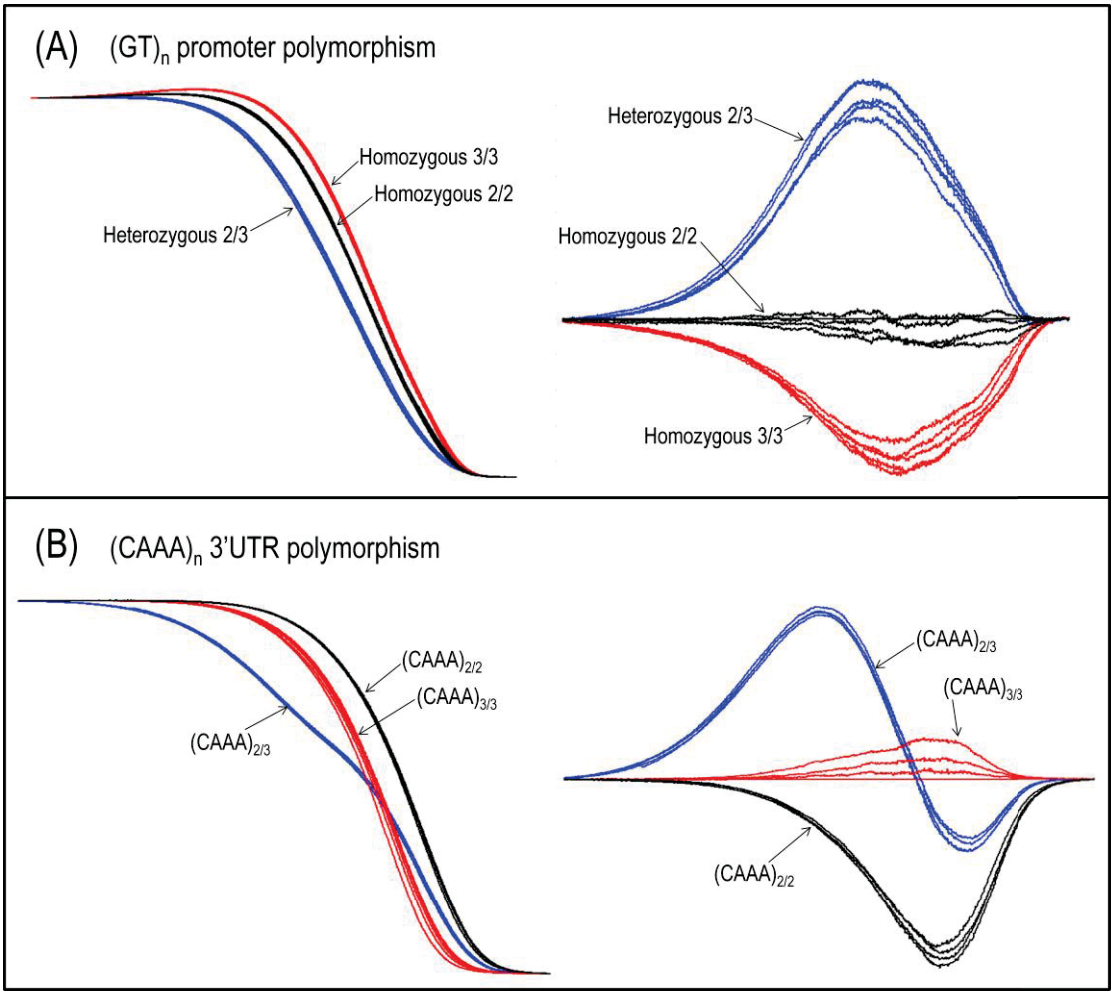

Figure 4.13 HRM analysis of simulated *SLC11A1* $(GT)_n$ and $(CAAA)_n$ genotypes. Plasmids containing different $(GT)_n$ and $(CAAA)_n$ alleles were used individually, or mixed, to represent the various homozygous and heterozygous $(GT)_n$ and $(CAAA)_n$ genotypes. (A) *SLC11A1* $(GT)_n$ melt curves. The normalised and temperature shifted melt curves are shown on the left side of the panel and the respective difference plot is shown on the right. (B) *SLC11A1* $(CAAA)_n$ melt curves. The normalised melt curves are shown on the left with the respective difference plot (right).

4.3.3.3 Differentiation of the Common and Rare $(GT)_n$ Heterozygous Genotypes using the Developed HRM Assay

It has been shown that different heterozygous genotypes, located at the same polymorphic site, can be differentiated according to their melting curves (Graham *et al.*, 2005). Different heterozygous genotypes result in the formation of different homoduplex and heteroduplex species (Section 4.1.1), giving each heterozygous genotype a unique melting profile. To determine if the uncommon $(GT)_n$ alleles, which are infrequently found in a homozygous form, could be differentiated from the more frequently occurring homozygous and heterozygous genotypes (which account for greater than 95% of all genotypes), the less abundant *SLC11A1* heterozygous $(GT)_n$ promoter genotypes were simulated using cloned alleles (corresponding to $(GT)_n$ genotypes 2/5, 2/9, 3/5 and 3/9). Genotyping of the simulated rare heterozygous samples, along with the common simulated homozygous and heterozygous genotypes, showed that the rare heterozygous samples produce melting profiles that can be differentiated from the common genotypes, in particular the heterozygous 2/3 genotype (Figure 4.14). Thus, using this genotyping methodology, samples that do not conform to the common melting groups would be selected for cloning and sequencing to determine the genotype of the sample. This approach may potentially lead to the discovery of novel alleles, which would remain uncharacterised using alternative techniques, such as PCR amplicon size determination and restriction fragment length polymorphisms.

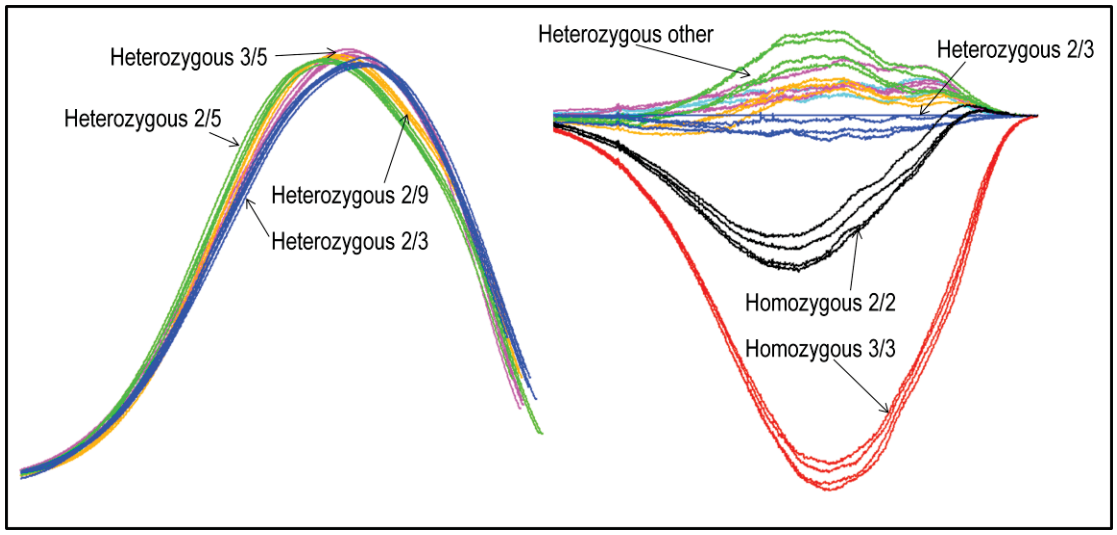

Figure 4.14 Differentiation of rare and common simulated $(GT)_n$ genotypes using HRM analysis. Plasmid alleles containing the *SLC11A1* $(GT)_n$ common (alleles 2 and 3) and rare (alleles 5 and 9) alleles were mixed to simulate different heterozygous genotypes. The first derivative profiles and difference plot, are shown (left and right sides of panels, respectively) with the different colours representing different genotypes.

4.3.4 Validation of the *SLC11A1* $(GT)_n$ and $(CAAA)_n$ HRM Genotyping Methodologies

The successful differentiation of the simulated genotypes showed that the *SLC11A1* $(GT)_n$ and $(CAAA)_n$ microsatellite repeats could be reliably genotyped using the optimised HRM methodology developed in the current study. Validation of the $(GT)_n$ and $(CAAA)_n$ genotyping methods was therefore subsequently conducted using gDNA samples derived from different individuals. During the optimisation of the HRM genotyping methodologies it was found that a reasonable quantity of DNA is required for accurate genotyping to ensure all samples amplify with a similar Ct value.

Blood is the most common source of gDNA for genotyping studies. However, the collection of blood is an invasive technique that may deter individuals from participating in a study, particularly when children are involved in the sample cohort (Harty *et al.*, 2000, Lum and Le Marchand, 1998). A fast and non-invasive method of DNA collection and extraction, in conjunction with the HRM methodology, would be ideal for high-throughput genotyping of samples. Such a high-throughput genotyping technique is required to enable association studies to analyse large enough sample sizes to have the statistical power to identify authentic associations (Section 1.3.5).

4.3.4.1 Direct use of FTA Card Punches in the PCR

A non-invasive source of gDNA is buccal cells. We previously collected buccal cell gDNA samples through a combined method of mouthwash collection followed by FTA card immobilisation (n=30) (Section 4.2.2.1.1 and 4.2.2.1.2). The collected gDNA samples were subsequently genotyped for the $(GT)_n$ and $(CAAA)_n$ microsatellite repeats by cloning and sequencing (unpublished). The combined methodology (mouthwash and FTA card) overcame several problems, which have individually limited the use of these techniques in genotyping studies (London *et al.*, 2001, Milne *et al.*, 2006, Mulot *et al.*, 2005). The combined method of the immobilisation of gDNA from a mouthwash sample on the FTA card resulted in a high yield of DNA, an even distribution of the immobilised DNA across the card and the incorporation of a rapid and less labour intensive DNA extraction technique.

Direct addition of washed FTA cards to the optimised real-time PCR (Section 4.2.2.2.1 and 4.2.2.4.2) to validate the HRM genotyping methodologies, resulted in amplification of the FTA card samples over a wide range of Ct values, with inconsistent results among replicates (Figure 4.15). The varied Ct values were most likely due to the presence of the FTA card punch within each well of the PCR, which inhibited complete fluorescence acquisition from the sample, therefore, not allowing assessment of the quality of the amplification. Also, significant levels of noise were observed early in the amplification process from reactions containing FTA cards, which was absent from the amplification profiles of reactions containing plasmid DNA samples (Figures 4.8 and 4.15). Due to the inability to determine the quality of the amplification, the use of the direct addition of an FTA card punch was not optimal for the $(GT)_n$ and $(CAAA)_n$ HRM genotyping methodologies.

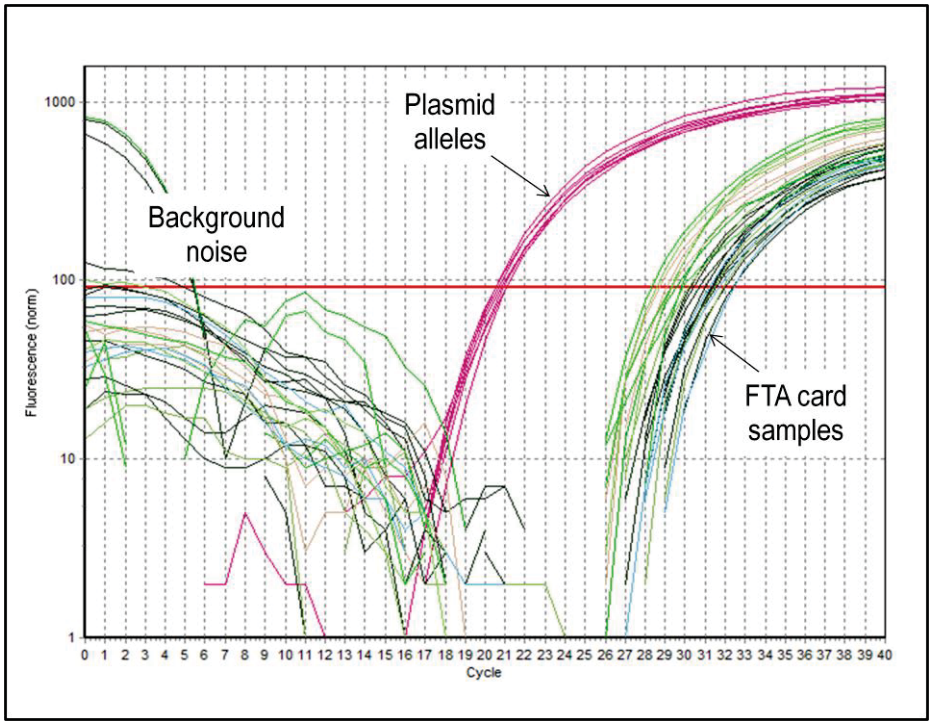

Figure 4.15 Real-time PCR quantification profiles of amplified plasmid alleles and FTA card immobilised gDNA samples. The quantification plots show the substantial background noise and low Ct values for the amplification when FTA card punches were added directly to the PCR as compared to the use of plasmid DNA as template.

4.3.4.2 HRM Genotyping of Samples after Elution of DNA from FTA Cards

As the use of a micropunch from an FTA card as the source of gDNA directly added to the real-time PCR for HRM curve analysis was inadequate, an alternative strategy was explored. Several studies have reported the removal/elution of DNA from the FTA card by enzymatic digestion or elution into an elution solution (Heath *et al.*, 1999, Johanson *et al.*, 2009, Lema *et al.*, 2006, Rajendram *et al.*, 2006), thus allowing the addition of gDNA directly to the PCR without the need for the inclusion of the FTA card. Therefore, the efficacy of eluting the DNA from an FTA card was investigated by the addition of an FTA card punch to different volumes of TE buffer (Section 4.2.2.2.2). PCR amplification of the gDNA eluted using TE buffer resulted in a low level of amplification from the smallest elution volumes (25, 50 and 75µl) (Figure 4.16). While this method overcame the issue of the addition of the FTA card punch directly to the real-time PCR, the level of amplification achieved was much lower than that obtained with the direct addition of the washed FTA card (positive control). Therefore, this approach was not feasible for use in the HRM genotyping methodologies.

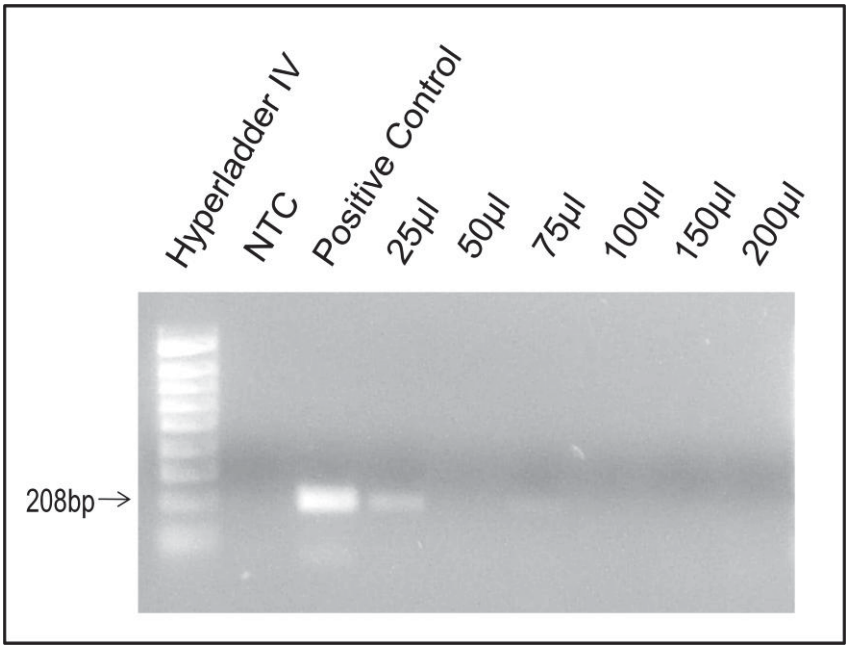

Figure 4.16 PCR amplification of eluted gDNA from FTA cards using different volumes of TE buffer. FTA cards were added to different volumes of TE Buffer (25, 50, 75, 100, 150 and 200µl) and heated (99^{o}C for 15min). A 5µl aliquot of each eluate was added to a PCR for the amplification of a 208bp *SLC11A1* promoter region using the HSNRAMPA-F/R primer set (Section 2.2.2.1). Post-PCR analysis of amplicons by agarose gel electrophoresis is shown. NTC denotes the no template control, while the positive control contained a single 2mm FTA card punch with immobilised gDNA.

Another elution technique was trialled, which used pH treatment with RT elution (Section 4.2.2.2.2). This method has been used to elute high quality DNA with subsequent PCR amplification from 3 year old bacterial DNA samples immobilised on FTA cards (Rajendram *et al.*, 2006). In this method, FTA card punches were exposed to an EDTA solution (pH 13.0) to elute gDNA, followed by the addition of Tris buffer (pH 7.0), resulting in eluted gDNA in TE buffer (Section 4.2.2.2.2). PCR amplification of gDNA (Section 2.2.2.1), eluted using the pH treatment, did not produce any amplification, suggesting that the elution technique failed to elute a sufficient amount of gDNA from the FTA card.

4.3.4.3 Amplification from Buccal Cells Added Directly to the PCR

The elution of gDNA from the FTA cards resulted in insufficient amounts of gDNA being recovered for HRM genotyping applications. The source of the DNA on the FTA cards was buccal cells from a mouthwash sample, which has been shown to result in a very high DNA yield (London *et al.*, 2001, Mulot *et al.*, 2005). Thus, if buccal cells could be added directly to the PCR it would increase the template gDNA concentration in the reactions. Previously collected and frozen mouthwash samples (one year old), as well as fresh mouthwash samples (Section 4.2.2.1.1) containing buccal cells (n=4) were washed (Section 4.2.2.2.3) to remove any PCR inhibitors and 5µl of the washed buccal cells was added directly to the PCR (Section 2.2.2.1) (Figure 4.17). The buccal cells from one of the fresh mouthwash samples would not adhere as a pellet, when repeatedly centrifuged during the washing of the cells and was therefore not analysed any further. The inability to pellet buccal cells from mouthwash samples has been previously reported, where it was suggested that the presence of salivary mucins results in high viscosity of the samples, hindering the collection of buccal cells by centrifugation (Aidar and Line, 2007).

Use of the one year old frozen samples resulted in a very low level of amplification in two out of the four samples (Figure 4.17A), while use of fresh samples resulted in good amplification in only two of the three samples (Figure 4.17B). The direct addition of buccal cells to the PCR appears to result in strong amplification when samples are fresh, however, the reliability of this method is not very good, as only 50% of fresh mouthwash samples resulted in the production of a PCR product.

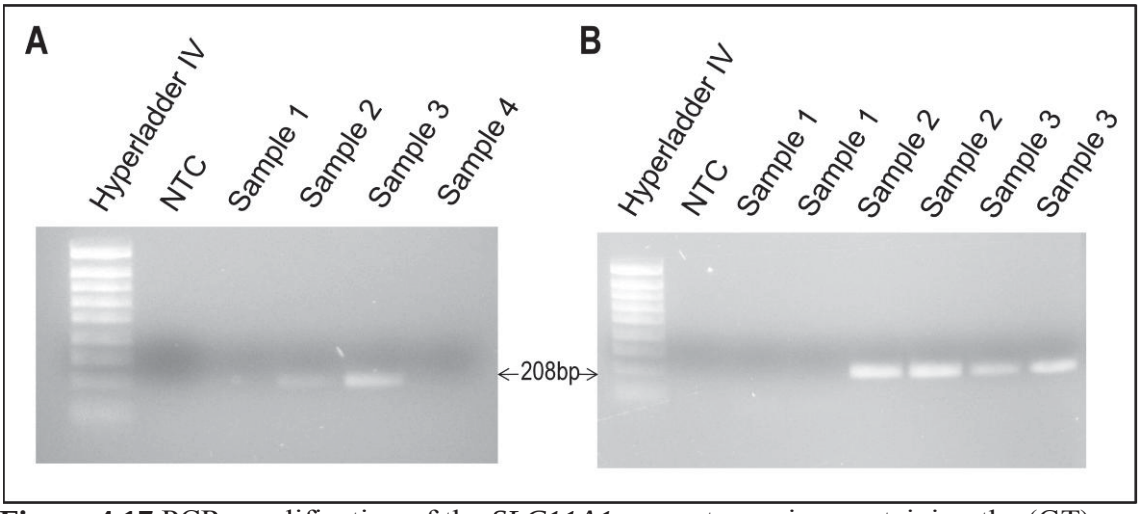

Figure 4.17 PCR amplification of the *SLC11A1* promoter region containing the $(GT)_n$ microsatellite repeat from buccal cells. One year old (A) and fresh (B) buccal cells were added to a PCR containing the HSNRAMPA-F/R primer set to produce a 208bp amplicon. NTC denotes the no template control.

4.3.4.4 Introduction of a Nested PCR Approach to Allow for the Validation of the HRM Assay for the $(CAAA)_n$ Polymorphism

The previously trialled methods of gDNA collection and extraction were insufficient to allow optimal PCR amplification to validate the HRM genotyping assays. Therefore, a nested PCR approach, utilising gDNA immobilised on the FTA card, was employed to allow for enrichment of the sequence of interest for genotyping. A nested PCR uses two successive rounds of amplification where the second round of amplification utilises a second primer set specific to a region within the first generated amplicon (Sections 4.2.2.4.3 and 4.2.2.4.2). In this case, the second round, real-time PCR product, was subsequently analysed by HRM curve analysis using the HR-1 instrument (Sections 4.2.2.5 and 4.2.2.6.2).

This nested PCR approach allowed the successful differentiation of all (n = 30) genotypes of the *SLC11A1* $(CAAA)_n$ polymorphism by HRM analysis using the HR-1 (Figure 4.18). Thus, the nested PCR approach utilising FTA card immobilised gDNA enabled the validation of the $(CAAA)_n$ HRM genotyping methodology. However, using this method the different $(GT)_n$ promoter genotypes could not be distinguished. It was found that all samples melted as a single group and different genotypes could not be distinguished, however, the different simulated $(GT)_n$ plasmid genotypes, could be distinguished using this methodology.

The inability to genotype the $(GT)_n$ promoter polymorphism was likely attributable to the quality of gDNA isolated from buccal cells. Buccal cells are exposed to carcinogens and mutagens and exhibit high rates of cell turnover with rapid cell proliferation and concomitant DNA replication. A positive correlation between age and microsatellite instability in buccal cells has been reported (Slebos *et al.*, 2008). Collectively, these factors may be problematic for the genotyping of a complex microsatellite repeat, such as the $(GT)_n$ polymorphism.

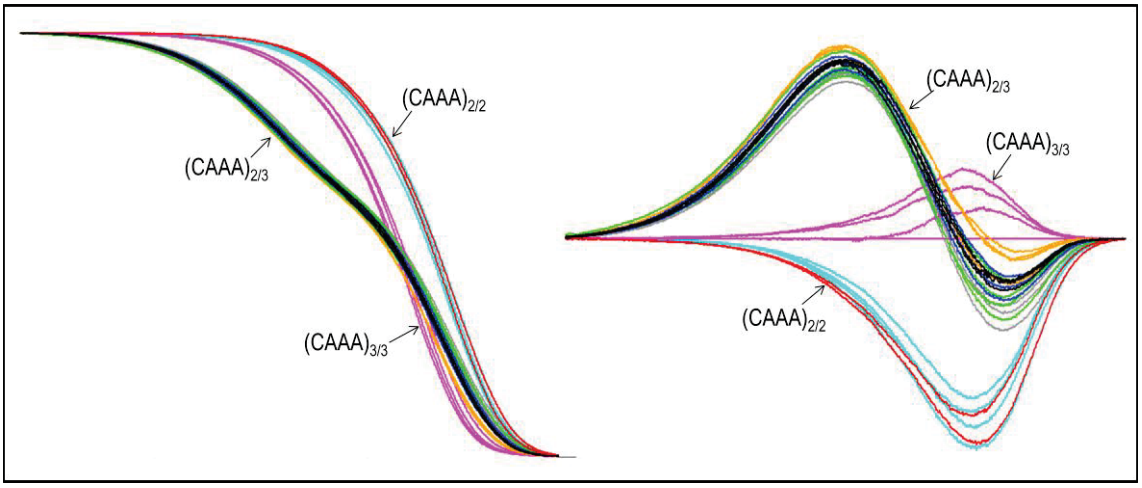

Figure 4.18 Genotyping of the *SLC11A1* $(CAAA)_n$ repeat using a nested PCR protocol utilising FTA card immobilised gDNA from buccal cells. The normalised melting curves and the corresponding difference plot are shown on the left and right, respectively. The different colours represent replicates of the same sample.

4.3.4.5 Validation of the $(GT)_n$ HRM Genotyping Assay using gDNA Isolated from Blood

Due to the inability to successfully genotype the $(GT)_n$ promoter polymorphism using the nested PCR technique, gDNA isolated from blood was trialled to validate the $(GT)_n$ HRM genotyping methodology. The method of gDNA collection utilised a diabetic lancet to draw several drops of blood (total volume of approximately 100µl) followed by gDNA extraction using a commercial extraction kit (Section 4.2.2.1.3). While this is an invasive technique and a more expensive method of gDNA collection, as compared to DNA collected using FTA cards, a high quantity and quality of isolated gDNA was obtained (Figure 4.19).

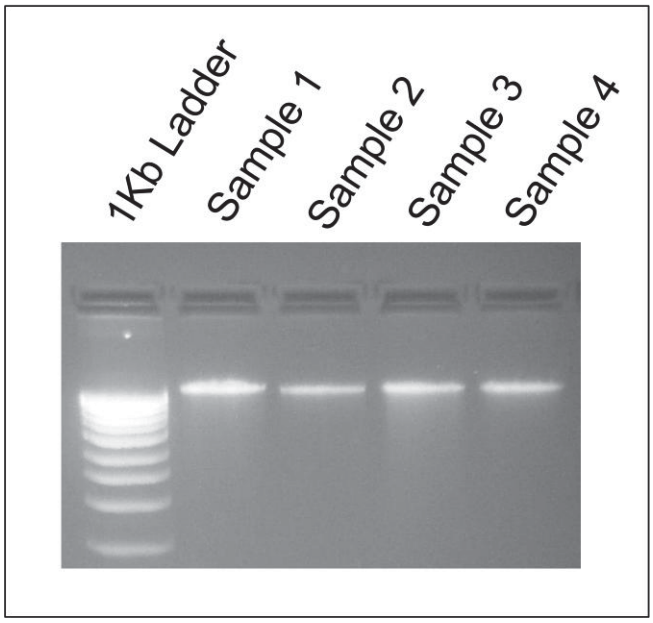

Figure 4.19 Representative image of the gDNA isolated from whole blood collected by diabetic lancet followed by extraction using a commercial spin column system.

Due to the high quality and quantity, the gDNA extracted from whole blood was used to validate the optimised HRM genotyping methodologies for both the $(GT)_n$ and $(CAAA)_n$ microsatellite repeats (Sections 4.2.2.4.2, 4.2.2.5 and 4.2.2.6.2). Using gDNA isolated from the blood allowed for 100% of collected samples (n = 10) to be correctly genotyped for both the $(GT)_n$ and $(CAAA)_n$ polymorphisms. Confirmation of the genotypes of all samples was completed by sequence analysis. Homozygote and heterozygote promoter $(GT)_n$ and $(CAAA)_n$ genotypes separated into distinct melting groups (Figure 14.20). Although homozygosity for $(GT)_n$ allele 2 was not represented in any of the collected samples, the $(GT)_n$ HRM genotyping methodology was able to differentiate the more frequently occurring homozygous allele 3 and heterozygous allele 2/3 genotypes.

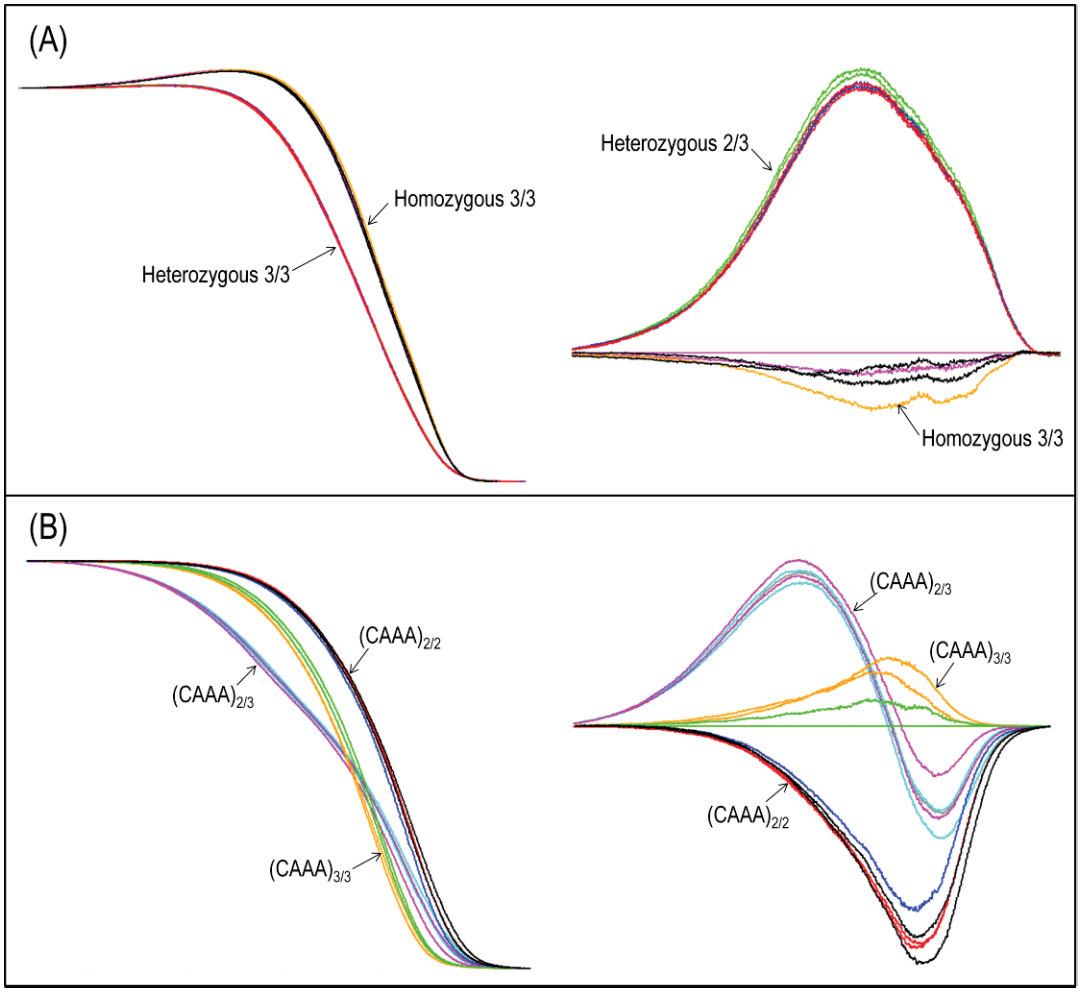

Figure 4.20 Validation of the HRM genotyping methodology using gDNA extracted from blood. $(GT)_n$ (A) and $(CAAA)_n$ (B) normalised and temperature shifted or normalised melting curves, and the respective difference plots, are shown on the left and right, respectively. The different colours represent replicates of the same sample.

4.3.5 Genotypes of the *SLC11A1* $(GT)_n$ and $(CAAA)_n$ Repeat can be Differentiated using the Eppendorf *realplex* Real-Time PCR Instrument

During the optimisation of the HRM genotyping methodology using real-time PCR, it was found that simulated plasmid genotypes of the $(GT)_n$ and $(CAAA)_n$ microsatellite repeats could be differentiated using the melting curve application on the Eppendorf mastercycler *realplex* (a non-dedicated melter) based on the peak maxima of the first derivative profile of the melting curves. Table 4.3 shows the melting temperature and the range of temperatures obtained for seven different experiments. In each experiment the simulated genotypes were consistently discriminated using the realplex instrument,

with no overlap observed between the melting temperature ranges of the different genotypes within each experiment.

Table 4.3 Differentiation of Simulated Common *SLC11A1* $(GT)_n$ Promoter Genotypes using the Eppendorf Mastercycler ep *realplex*.

Run No.	Replicates	Homozygous Allele 2		Homozygous Allele 3		Heterozygous Allele 2/3	
		Temp	Range	Temp	Range	Temp	Range
1	6	88.0	(87.9-88.2)	88.3	(88.2-88.4)	87.6	(87.6-87.8)
2	5	88.0	(87.9-88.2)	88.4	(88.3-88.5)	87.7	(87.5-87.8)
3	5	88.0	(88.0-88.1)	88.4	(88.3-88.5)	87.6	(87.5-87.8)
4	5	88.0	(87.9-88.0)	88.2	(88.1-88.4)	87.6	(87.4-87.8)
5	5	88.0	(87.9-88.0)	88.4	(88.1-88.4)	87.6	(87.4-87.8)
6	5	88.4	(88.4-88.5)	88.9	(88.8-89.0)	87.9	(87.8-88.1)
7	5	87.9	(87.8-88.0)	88.3	(88.3-88.5)	87.5	(87.3-87.7)

The melting parameters of the Eppendorf real-time instrument were varied to identify if different genotypes could be differentiated based on the comparison of the shape of their melting curves. Melting of samples at a rate of $0.1^oC/s$ produced high levels of background noise, which prevented the determination of the true shape of the curve and also resulted in additional peaks being apparent on the first derivative profile that the software would report as a melting transition. When the samples were melted at a rate of $0.4^oC/s$, the majority of the background noise disappeared and this allowed for better discrimination of the different genotypes (Figure 4.21). The different genotypes separate into different groups showing that genotyping of these microsatellite repeats is possible using the Eppendorf ep *realplex* instrument.

The Eppendorf mastercycler ep *realplex* is not a dedicated high resolution melting instrument, suggesting that the designed and optimised HRM genotyping methodologies for the $(GT)_n$ and $(CAAA)_n$ repeats are versatile and can be performed using other non-dedicated melters (i.e. using real-time PCR instruments). This is the first reported case of the Eppendorf instrument being able to differentiate genotypes using melt curve analysis which has led to the preparation of this work as an invited technical application note (Eppendorf Application Note 206).

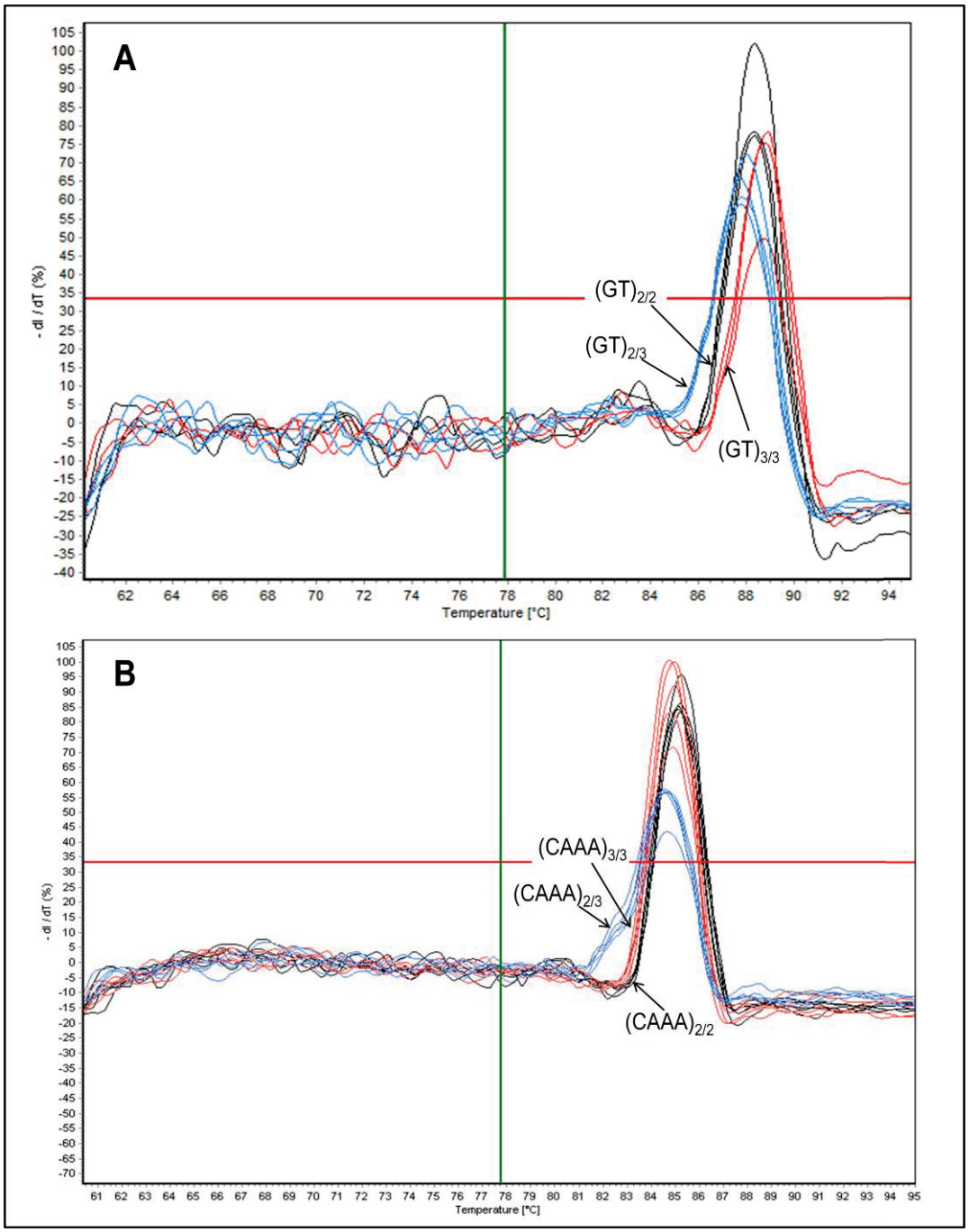

Figure 4.21 First derivative melting profiles for genotyping the *SLC11A1* $(GT)_n$ and $(CAAA)_n$ polymorphisms using the Eppendorf ep *realplex* real-time PCR instrument.

4.4 DISCUSSION

4.4.1 Introduction

Current methods for the genotyping of the *SLC11A1* promoter $(GT)_n$ and $(CAAA)_n$ polymorphisms are inadequate as they do not allow sufficiently large sample sizes to be analysed in a timely manner to allow completion of large association studies, which are required to increase the statistical power to detect authentic associations. Current genotyping methods lack the sensitivity to detect all microsatellite variants and/or are costly, time consuming and laborious. In this chapter an optimised genotyping methodology, based on HRM curve analysis, was developed to genotype polymorphisms within the *SLC11A1* gene: the $(CAAA)_n$ polymorphism and the three most common $(GT)_n$ promoter genotypes.

It was shown, through careful design of the HRM genotyping assays, and the rigorous optimisation of the real-time PCR and HRM parameters, that simulated genotypes of the $(GT)_n$ and $(CAAA)_n$ polymorphisms could be differentiated based on their melting profiles. Furthermore, through the use of simulated genotypes, it was shown that the $(GT)_n$ genotyping methodology is capable of detecting the less common $(GT)_n$ alleles in a heterozygous form. While using the simulated genotypes provided proof of principle of the ability to detect the *SLC11A1* microsatellite genotypes using HRM, validation of the HRM genotyping methodologies was completed using gDNA samples isolated from whole blood and buccal cells.

4.4.2 Design and Optimisation of the HRM Genotyping Assays

The process of amplicon design and optimisation is crucial for the development of a robust HRM methodology (White and Potts, 2006). A range of amplicon lengths, containing the $(GT)_n$ and $(CAAA)_n$ microsatellite repeats, were designed and amplification parameters were optimised for each polymorphism (Sections 4.3.1 and 4.3.2). For both the $(GT)_n$ and $(CAAA)_n$ HRM genotyping assays, the smallest amplicons produced the most consistent amplification and post-PCR melting profiles (Section 4.2.2.3), in accordance with previous observations (Gundry *et al.*, 2003,

Herrmann *et al.*, 2006, Liew *et al.*, 2004, White and Potts, 2006, Wittwer *et al.*, 2003). Smaller amplicons consistently provide the greatest overall fluorescence change between different alleles/genotypes. This would be due to the production of single melting domain curves by smaller amplicons (Gundry *et al.*, 2003, Ririe *et al.*, 1997). In addition to this, the use of a smaller amplicon means that the polymorphism accounts for a greater percentage of the total length of the amplicon and therefore, will show larger differences between different genotypes. It is well noted that amplicons up to 400 bases have the ability to discriminate different genotypes (Reed and Wittwer, 2004, White and Potts, 2006) with scanning sensitivity near 100% with amplicons less than 400bp (Reed and Wittwer, 2004). Larger amplicons tend to have multiple melting domains producing more complex melting curves which are harder to analyse (White and Potts, 2006).

All parameters of the genotyping real-time PCR (Section 4.3.2) and post-PCR HRM analysis (Section 4.3.3.1) were vigorously optimised because the intercalacting dye used is not specific for the amplicon, and will bind to any double stranded DNA present, any non-specific amplification products formed, primer dimers or contaminating DNA, lowering the resolution and sensitivity of the melting profile and preventing the differentiation of genotypes.

It was found that HRM analysis is sensitive to subtle changes in reaction conditions and is highlighted by the observation that the use of different primer concentrations, for the production of the same amplicon, resulted in significant differences in the melting profile for the same plasmid allele (Section 4.3.2.3, Figure 4.9). Furthermore, the melting temperature of an amplicon has been shown to be affected by the $MgCl_2$ concentration of the PCR (Ririe *et al.*, 1997). As heteroduplex products melt, the single stranded DNA produced is able to reanneal with complementary single stranded DNA to produce new homoduplexes (as the melting temperature of these homoduplexes has not yet been reached) causing artificial inflation of the fluorescence level. Grundy et al (2003) have shown that low magnesium concentration limits strand reassociation producing more sensitive melt curves. Additionally, it was also found, and has been previously reported, that the different template sources and methods of gDNA extraction produce melt curves which have subtle differences (White and Potts, 2006). Therefore, consistency of all reaction parameters between individual samples within the

same experiment is important to allow an accurate comparison of the melting characteristics. This ensures that genotypes can be differentiated.

It was also found that the quality of real-time PCR amplification of individual samples had a large effect over the quality of the melt curve achieved. The best melting profiles were observed when the samples produced similar consistent amplification profiles, with low Ct values (20-25), steep amplification plots and a similar level of end fluorescence (Figure 4.8). When these criteria were satisfied, optimal differentiation between the different genotypes of the $(GT)_n$ and $(CAAA)_n$ polymorphisms was achieved. Samples with late amplification (Ct values greater than 30), or lower end fluorescence, and samples resulting in unusual amplification profiles all produced melt curves that were inconsistent with the other replicates of a particular sample. After each real-time PCR experiment was completed, the quality of the amplification of each sample was assessed through the analysis of the quantification plot and the melting curve from the real-time PCR, before the samples were melted using the HR-1. Samples which did not meet the requirements of the optimal real-time amplification were omitted ensuring that the samples that underwent HRM were those that would produce melt curves with the greatest differentiation between genotypes.

4.4.3 Validation of the HRM Genotyping Assays

The quality of the real-time PCR amplification achieved is directly associated with the quantity and quality of the template (gDNA). Successful differentiation of the $(GT)_n$ and $(CAAA)_n$ genotypes was achieved using cloned repeats used to simulate different genotypes (Section 4.3.3.2). However, validation of the genotyping methods with gDNA proved difficult. The initial validation attempts were completed using gDNA isolated from buccal cells. Buccal cells were used as they are a readily available source of gDNA and are commonly used in other applications (for example forensics) but their use is not common in genetic epidemiological studies. Buccal cells and the range of isolation techniques trialled allowed for the collection of gDNA in a fast and non-invasive method which is ideal for the production of a complete high-throughput genotyping methodology, encompassing DNA collection through to HRM analysis.

The direct addition of FTA card bound buccal cell DNA (as FTA card punches) to the real-time PCR resulted in late amplification profiles (Section 4.3.4.1). Previous successful use of the FTA card samples in standard PCR resulted in consistent high amplification, thus it was thought that the poor amplification observed was due to the presence of the FTA card in the reaction inhibiting the total fluorescence acquisition of the samples. A similar conclusion was reported in another publication (Muthukrishnan *et al.*, 2008). Therefore, this method of gDNA collection was not suitable for the HRM genotyping methodology as the quality of the amplification could not be assessed.

Several other methods were trialled to validate the HRM genotyping methodologies using buccal cell DNA. This included elution of the DNA from the FTA card with TE buffer or pH treatment, and the direct addition of buccal cells to the PCR (Sections 4.3.4.2 and 4.3.4.3). All of these methods allowed the addition of liquid gDNA to the PCR and therefore, the inhibition of the fluorescence acquisition observed with the direct addition of the FTA card to the real-time PCR would was eliminated. However, these either resulted in poor or inconsistent amplification.

A nested PCR approach was subsequently employed which allowed for the successful validation of the $(CAAA)_n$ genotyping methodology (Section 4.3.4.4). However, the nested PCR approach did not allow for the successful genotyping of the $(GT)_n$ promoter polymorphism. The inability to genotype the $(GT)_n$ promoter polymorphism by the nested PCR approach was attributable to the quality of the gDNA isolated from the buccal cells. Buccal cells are exposed to carcinogens and mutagens and exhibit high rates of cell turnover with rapid cell proliferation and concomitant DNA replication. Therefore, these cells may be more prone to replication errors, especially at complex microsatellite repeat sites like the *SLC11A1* promoter. There are also a range of environmental factors that can result in allelic alterations in buccal cells (Gabriel *et al.*, 2006, Pai *et al.*, 2006, Pai *et al.*, 2002, Rupa and Eastmond, 1997, Vuyyuri *et al.*, 2006, Yang *et al.*, 2003). A positive correlation between age and microsatellite instability in buccal cells has also been reported (Slebos *et al.*, 2008). Collectively, these factors may be problematic for the genotyping of a complex microsatellite repeat, such as the $(GT)_n$ polymorphism using gDNA isolated from buccal cells.

High quality gDNA appears to be essential to the success of genotyping the $(GT)_n$ promoter polymorphism, as this study is not the first to have encountered issues. In an association study of *SLC11A1* polymorphisms with *M.tuberculosis*, Soborg et al. (2002) were unable to genotype some patients at the promoter $(GT)_n$ polymorphism due to the poor quality of gDNA samples extracted from frozen whole blood. In another association study, PCR products were unobtainable in 39% of the population studied when DNA extracted from blood was used (Paccagnini *et al.*, 2009). The inability to genotype the total population of a study lowers the sample size analysed and, therefore, also the power to find a significant association.

Both the $(GT)_n$ and $(CAAA)_n$ HRM genotyping methods were validated using gDNA isolated from blood obtained through a finger prick using a diabetic lancet and gDNA extraction using a commercial system (Section 4.3.4.5). This technique proved successful as the extracted gDNA was of very high quality and quantity (Figure 4.19). The isolation of gDNA from blood obtained through a fingerprick is an ideal method of DNA extraction and collection as it is rapid and results in a high quantity and quality gDNA, which is required for the collection of large sample numbers for association studies.

4.4.4 Sample Spiking with a Known Genotype May Increase the Robustness of the HRM Assays

In some HRM experiments, different homozygous samples have near identical melt curves, meaning that wild type and mutant homozygous genotypes are indistinguishable. This commonly occurs with SNP genotyping where the nearest neighbor interaction of the immediate bases adjacent to the polymorphism is the same for different variants of the polymorphism (Breslauer *et al.*, 1986). It is predicted that 4-16% of SNPs (and potentially a number of insertion/deletion polymorphisms) fall into this category. A method to differentiate these SNPs has been described where each sample is spiked with a known reference amplicon, usually containing the most frequent (wild type) variant (Palais *et al.*, 2005, Reed *et al.*, 2007). The addition of the reference amplicon to wild type homozygous samples results in no change in the shape of the melting profile, however, the addition of the wild type amplicon to the homozygous mutant samples causes the formation of heteroduplexes, which have lower melting

temperatures, thereby altering the shape of the melting profile to enable differentiation between different homozygous genotypes.

For the $(CAAA)_n$ genotyping methodology, the difference plots were analysed from normalised only melt curves without subsequent temperature shifting (Section 4.3.3.1). When the $(CAAA)_n$ melt curves were temperature shifted, $(CAAA)_{2/2}$ and $(CAAA)_{3/3}$ homozygous genotypes became indistinguishable (Figure 4.11). Therefore, if temperature shifting is a requirement for future analysis when using the $(CAAA)_n$ genotyping methodology, spiking all of the samples with a reference gDNA of known genotype will allow for the differentiation between the different homozygous samples.

It was found that the optimised $(GT)_n$ genotyping methodology is more prone to slight variations in the quality of the melting curves compared to the $(CAAA)_n$ genotyping methodology. This is likely attributable to the number of base pair differences that the two methodologies are detecting, a 2bp and 4bp deletion for the $(GT)_n$ and $(CAAA)_n$ methods, respectively. While it was shown that the genotyping methodology can detect the most common $(GT)_n$ homozygous and heterozygous genotypes, the addition of a reference amplicon, to the real-time PCR, may increase the robustness of the methodology, increasing the differentiation between genotypes. Also, in populations where there is a particularly high frequency of another $(GT)_n$ allele (e.g. allele 7 in Asian populations or allele 5 in Greek populations) (Table 1.3), spiking of the samples with a reference sample of known genotype may provide a way to differentiate genotypes of these ethnic specific alleles from the more common genotypes.

4.4.5 The HRM Genotyping Assays can Detect Novel Variants and Rare $(GT)_n$ Alleles in a Heterozygous Form

Currently, the most common genotyping methodology for the $(GT)_n$ promoter and $(CAAA)_n$ polymorphisms, is through size determination of amplified fragments containing the microsatellite repeats. However, this method is unable to detect all alleles at the $(GT)_n$ repeat (as rare alleles are mis-reported due to the common length of alleles; allele 7 is mis-reported for allele 1 and allele 5 for allele 3) or identify novel sequence variants of the $(GT)_n$ and $(CAAA)_n$ repeats. One of the major advantages of HRM analysis is the ability to simultaneously genotype a polymorphism and also scan for any

novel sequence variants (Liew *et al.*, 2004, Palais *et al.*, 2005, Reed and Wittwer, 2004, Wittwer *et al.*, 2003, Zhou *et al.*, 2005). Through the use of simulated genotypes from cloned variants, it was shown that the $(GT)_n$ genotyping methodology was capable of detecting the less commonly occurring alleles in a heterozygous form compared to the common heterozygous genotype (allele 2/3) (Section 4.3.3.3). Therefore, due to the ability to detect rare alleles, both the $(GT)_n$ and $(CAAA)_n$ HRM genotyping methodologies should also be sensitive enough to reveal novel microsatellite variants. The rare alleles and novel variants, detected using the optimised HRM genotyping methodologies, will appear as samples which have different shaped melting curves compared to the common genotypes. These samples could then be selected for cloning and sequence analysis to determine their genotypes. Cloning and sequencing of $(GT)_n$ polymorphism is the only genotyping method enabling each allele to be separated and analysed individually. Thus, unlike the most common method of genotyping the $(GT)_n$ and $(CAAA)_n$ microsatellites, the designed and optimised HRM methodologies have the ability to identify novel allelic variants and rare $(GT)_n$ alleles, which would be missed or misidentified using current methodologies.

4.4.6 Conclusion

In this chapter, optimised genotyping methodologies have been developed, based on HRM curve analysis, which can successfully genotype the $(GT)_n$ and $(CAAA)_n$ polymorphisms within the *SLC11A1* gene. The optimised HRM genotyping methodologies allow for a conservative estimate of approximately 260 samples a week to be genotyped using the HR-1 instrument. When compared to the 10 samples per week that can be genotyped by traditional cloning and sequencing, the estimate represents a significant increase in the number of samples that can be genotyped. This genotyping methodology has the potential to be further developed and scaled up through the use of a real-time PCR instrument that also has built-in HRM and auto-call genotyping capabilities. These instruments, which include the Lightcycler (Roche Applied Science, USA) or Rotorgene (Qiagen, Germany), allow 96-384 samples to be melted at the same time meaning thousands of samples could be genotyped per week. While the HR-1 instrument is recognised as the gold standard for HRM analysis (Reed *et al.*, 2007), a recent study found that the sensitivity and specificity of the HR-1, the Lightcycler and Rotorgene to assess a range of different SNPs was comparable between

the different platforms (White and Potts, 2006). Furthermore, the ability to differentiate the $(GT)_n$ and $(CAAA)_n$ polymorphisms using the Eppendorf mastercyler ep *realplex* suggests that the designed and optimised HRM genotyping methodologies are versatile and can be performed using other non-dedicated melters (Section 4.3.5).

HRM has most commonly been used for the genotyping of SNPs, however, HRM methodologies are more frequently being used to genotype microsatellites and insertion/deletion mutations (Mackay *et al.*, 2008, Mader *et al.*, 2008, Marziliano *et al.*, 2000, Pirulli *et al.*, 2000, Reed *et al.*, 2007, Vaughn and Elenitoba-Johnson, 2004). For the analysis of polymorphic microsatellites, these HRM methods are commonly used as a scanning technique where unknown samples are compared to a wild type sample to identify variants with different melting profiles. These scanning techniques can identify the presence of sequence variants, however, they do not provide information as to the nature of the variant that has been identified. In a recent review, the ability to use HRM to completely genotype short tandem repeats was suggested to be of significant importance for the next step in HRM technology (Reed *et al.*, 2007). The optimised $(GT)_n$ HRM genotyping methodology is a step towards complete genotyping of short tandem repeats, as the most common $(GT)_n$ genotypes could be successfully genotyped and the identification of rare or novel variants was possible.

The designed and optimised HRM methodologies allow for the sensitive, accurate and rapid determination of *SLC11A1* $(GT)_n$ and $(CAAA)_n$ microsatellite polymorphisms. Therefore, the HRM methodologies will facilitate the completion of association studies analysing larger sample sizes required to identify true or significant associations. The analysis of larger sample sizes, enabled by the high-throughput HRM genotyping methodologies, will aid in the determination of the association between the presence of variants at the $(GT)_n$ promoter microsatellite and $(CAAA)_n$ 3'UTR polymorphisms and the incidence of infectious and autoimmune diseases.

CHAPTER 5 – FUNCTIONAL ANALYSIS OF THE *SLC11A1* PROMOTER

PART 1: Discovery of Important *SLC11A1* Promoter Elements by Bioinformatic Analysis.

PART 2: Design and Construction of *SLC11A1* Promoter Constructs for Functional Analysis.

5.1 INTRODUCTION

5.1.1 The *SLC11A1* Promoter

The *SLC11A1* promoter contains several polymorphisms which have been shown to alter *SLC11A1* expression (Figure 5.1). One of these polymorphisms is the $(GT)_n$ microsatellite repeat, which is located approximately 240bp upstream of the transcription start site. The $(GT)_n$ microsatellite is a complex repeat of GT units interspersed by AC dinucleotides. Of the nine polymorphic variants identified, alleles 2 and 3 account for greater than 95% of the allele frequencies in most populations (Section 1.3.1). The presence of allele 3 results in significantly higher basal level of *SLC11A1* expression compared to allele 2 (Section 1.3.2). The -237C/T polymorphism is another functional polymorphism located 40bp downstream of the $(GT)_n$ microsatellite repeat. The presence of the T variant, which has only been identified in combination with $(GT)_n$ allele 3, results in lower *SLC11A1* expression level, comparable to that driven by $(GT)_n$ allele 2 (Section 1.3.3).

Due to the important role that *SLC11A1* plays in the activation of a Th1 mediated immune response to macrophage specific pathogens, it is thought that these functional promoter polymorphisms may play a role in conferring resistance/susceptibility to infectious and Th1-mediated autoimmune/inflammatory diseases. A large number of association and linkage studies have been conducted to determine the association of *SLC11A1* promoter variants with the incidence of a range of infectious and autoimmune diseases (Section 1.3.4). These studies have attempted to determine if an association exists in a blinded fashion, as functional knowledge of the regulatory mechanisms controlling *SLC11A1* transcription, which ultimately mediates the differential *SLC11A1* expression observed with the functional promoter variants, is lacking.

The work completed in this thesis has adopted a functional approach to gain a greater understanding of the *SLC11A1* promoter. The first aim was to determine the mechanism by which *SLC11A1* is regulated at the level of transcription initiation and to determine if the *SLC11A1* promoter mediates bidirectional transcription. The second aim was to determine the mechanism by which *SLC11A1* expression is altered by the different polymorphic sequence variants.

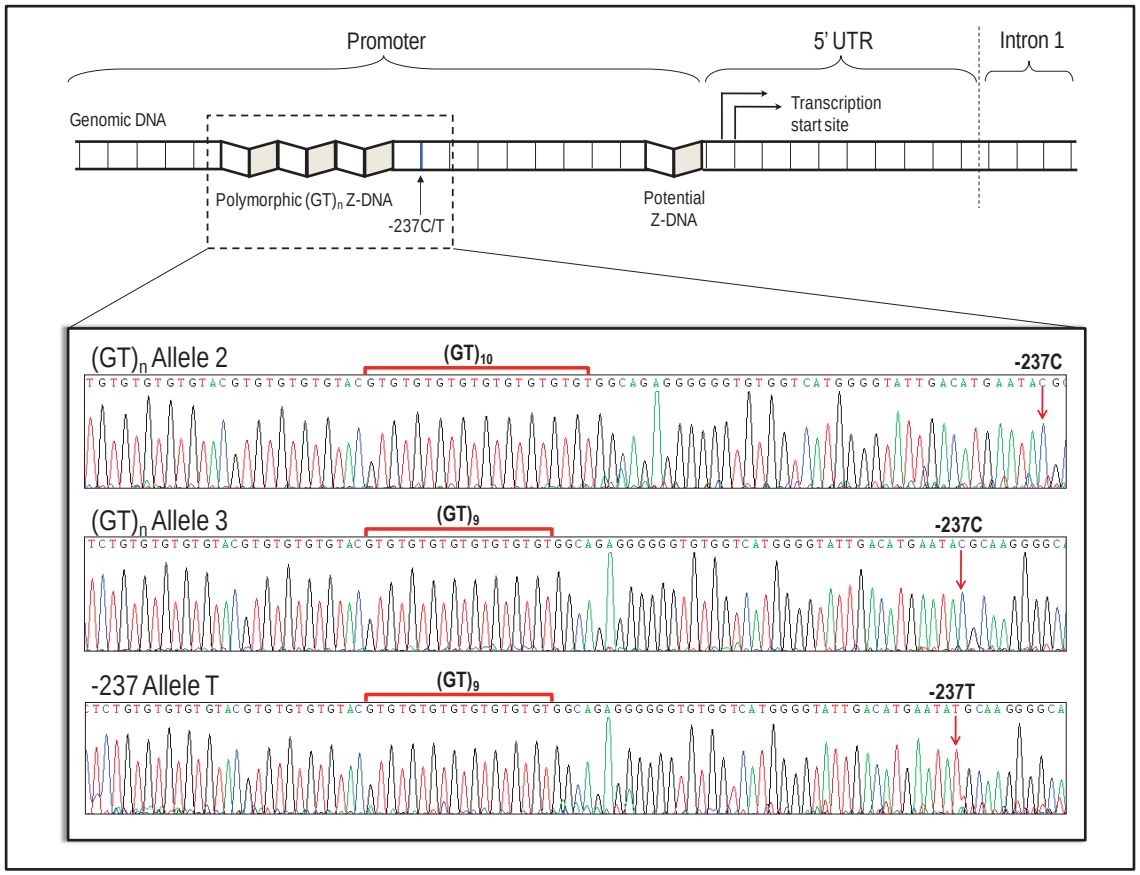

Figure 5.1 *SLC11A1* promoter organisation showing the positions of the *SLC11A1* $(GT)_n$ and -237C/T promoter polymorphisms. The upper panel is a representation of the *SLC11A1* promoter and shows the location of sequence variants relative to the transcription start sites. The lower image shows the sequences of the three common promoter variants, which have been shown to modulate *SLC11A1* expression levels. $(GT)_n$ allele 2 contains a polymorphic repeat of 10 GT repeats and is always associated with the more frequent -237 C variant, while $(GT)_n$ allele 3 contains 9 GT repeats and is associated with both the commonly occurring -237 C and less commonly occurring -237 T variants.

To complete these aims a systematic bioinformatic assessment of the *SLC11A1* promoter, to identify important promoter regions, was undertaken (Chapter 5, Part 1). The findings of the bioinformatic analysis guided the preparation of expression constructs containing promoter regions of varying size and containing regions of putative importance with regard to transcriptional regulation (Chapter 5, Part 2). The promoter expression constructs were tested in human cell lines to determine the functional significance of the putative functional elements (identified *in silico*) (Chapter 6, Part 3). After promoter activity assessment, the sequences of regions identified to play a functional role in the mechanism of *SLC11A1* transcription were re-assessed for transcription factor binding sites to explain the functional effects observed.

5.1.2 Mechanisms of Eukaryotic Transcription Initiation

RNA polymerase II (pol II), which transcribes protein-coding genes into an mRNA transcript, cannot directly recognise (in a sequence specific manner) a target promoter to initiate transcription. Gene promoters contain different sequence elements which bind proteins, in a sequence specific manner, to recruit pol II, thereby facilitating the regulated cell specific expression of a gene. Core promoter elements bind proteins involved in the formation of the basal transcriptional complex, while proximal and distal enhancer/repressor elements (located proximal and distal to core promoter elements, respectively) bind transcription factors which enhance/repress transcription (Latchman, 2004).

5.1.2.1 The Basal Transcriptional Complex

The basal transcriptional complex describes an essential multi-component complex of factors required to recruit pol II, which subsequently binds to this multi-component complex, and initiates transcription (Figure 5.2). In promoters with canonical TATA boxes, the first step in the formation of the transcriptional complex is the binding of TATA-binding protein (TBP) to a TATA consensus sequence (commonly TATAa/tAa/t) located approximately 30bp upstream of the transcription start site (Strubin and Struhl, 1992). Binding of TBP can only occur at consensus sites, which are not packaged into nucleosomes, thus restricting TBP binding to genes/regions required by the cell.

Binding of TBP to DNA results in the recruitment of TBP-associated factors (TAFs) to form a complex, termed transcription factor IID (TFIID). Formation of the TFIID complex at the core promoter results in the sequential recruitment of the factors TFIIA, TFIIB, TFIIE, TFIIF and TFIIH, which assemble with pol II to form the basal transcriptional complex (Figure 5.2). Dissociation of pol II from the basal transcriptional complex then leads to transcription initiation (Latchman, 2004).

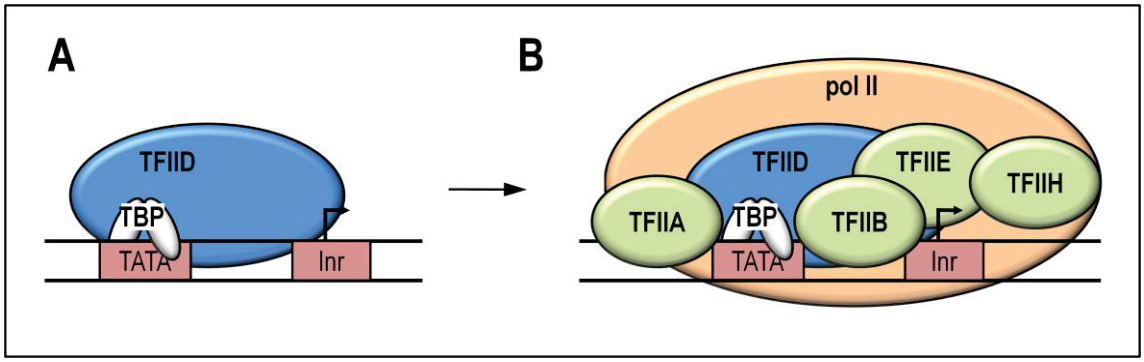

Figure 5.2 Formation of the basal transcriptional complex. (A) TBP binds to the TATA element recruiting TAF to form TFIID. (B) Formation of TFIID then recruits other factors and RNA polymerase II (pol II) allowing initiation of transcription. Key: TATA – TATA box element, Inr – Initiator element, TBP – TATA binding protein, TAF – TBP associated factor, TFIID – transcription factor (for RNA polymerase II recruitment) D.

5.1.2.2 Transcription from Non-Canonical (TATA-less) Promoters

SLC11A1 does not have a conventional TATA or CCAAT box promoter and the mechanism by which *SLC11A1* transcription initiation is mediated is not fully known (Searle and Blackwell et al., 1999). Gene promoters lacking a canonical TATA box element cannot directly interact with TBP to initiate the formation of the basal transcriptional complex. However, in most cases, the binding of TBP is still required for the formation of the basal transcriptional complex (Smale, 1997, Smale and Kadonaga, 2003). Such promoters contain other core promoter elements, which recruit factors that interact with and facilitate the positioning and binding of TBP or TFIID.

An initiator element (Inr) is a core promoter element, which can mediate transcription independently of a TATA element (O'Shea-Greenfield and Smale, 1992). Initiator elements have been suggested to be analogous to TATA elements and are located over the transcription initiation start site where they recruit initiator binding proteins in a sequence specific manner [Py Py A N T/A Py (Py – Pyrimidine, N – A, G, T or C)] (Figure 5.3) (Smale *et al.*, 1990, Zenzie-Gregory *et al.*, 1992). The TFIID complex then forms around, and interacts with, the protein bound at the initiator element (in association with TFIIA), thus modulating the binding or the interaction of TBP with the DNA (Emami *et al.*, 1997). The other factors involved in the formation of the basal transcriptional complex are then recruited. This mechanism is similar to the formation of the basal transcriptional complex in promoters with a TATA element (Section 5.1.2.1).

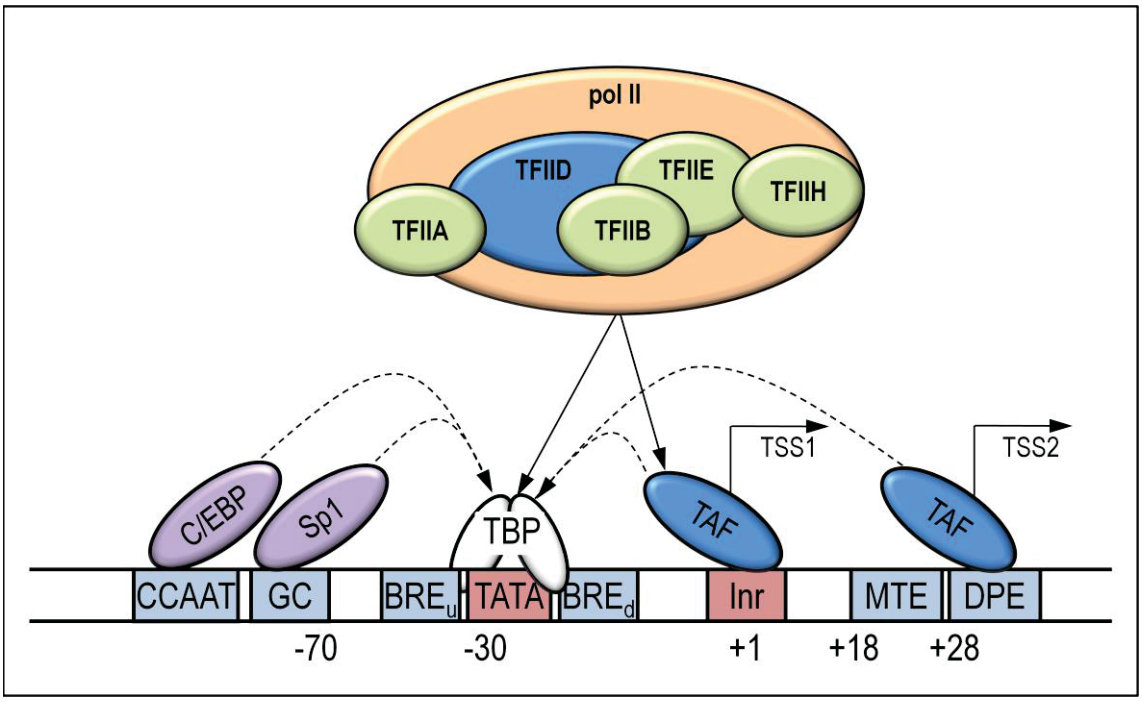

Figure 5.3 Core elements involved in transcription from a non-canonical TATA-less promoter. TATA box and Inr elements are able to mediate transcription initiaition (elements in pink). Other core elements (blue) located upstream and downstream associate with Inr (and TATA elements) to determine the location for the formation of TBP as well as the basal transcriptional complex. Key: TATA – TATA box element, TBP – TATA binding protein, TAF – TBP associated factor, TFIID – transcription factor IID, pol II – RNA polymerase II, Inr – Initiator element, BRE_u – upstream TFIIB response element, BRE_d – downstream TFIIB response element, MTE – motif ten element, DPE – downstream promoter element, Sp1 – specificity protein 1, C/EBP – CCAAT/enhancer binding protein, TSS – transcription start site.

Other essential core elements, located throughout the promoters of genes which lack a TATA element, have also been described. The presence of these other essential core elements alone is not sufficient to mediate the formation of the basal transcriptional complex. Generally these essential core elements are associated with other elements (such as an Inr). These other essential core elements are required to form the basal transcriptional complex, as removal of these elements results in the loss of gene expression. Examples of essential core elements include downstream promoter elements (DPE), which are located 28bp downstream of the transcription initiation start site and are generally found in conjunction with Inr elements, and TFIIB-recognition elements (BRE), which associate in a sequence specific manner to a region analogous to the location of a TATA element (Figure 5.3). Other core promoter elements that have been described include the motif ten element (MTE), downstream core element (DCE) and X

core promoter element 1 (XCPE1). However, to date, these elements have not been well characterised (Juven-Gershon *et al.*, 2008) (Figure 5.3).

The CCAAT and GC box elements are other elements which may also be involved in transcription initiation, and are generally located 70-150bp upstream of the transcription start site (Figure 5.3). The CCAAT box elements recruit CCAAT/enhancer binding protein (C/EBP), a group of proteins expressed in a range of tissues, while GC boxes (consensus GGGCGG) bind the transcription factor Specificity Protein 1 (Sp1) and Kruppel-like factors (KLFs) (Kaczynski *et al.*, 2003, Liu *et al.*, 2009). Multiple Sp1 sites have been shown to mediate transcription initiation in promoters which lack a TATA element (Huber *et al.*, 1998, Smale, 1997, Smale and Kadonaga, 2003). In addition to transcriptional activation, recruitment of C/EBP and Sp1 to CCAAT and GC box elements, respectively, has also been shown to repress transcription.

5.1.2.3 Transcriptional Activators and Repressors

If transcription initiation is restricted to core proteins involved in the formation of the basal transcriptional complex, then transcription proceeds slowly (Burley and Roeder, 1996). The interaction of transcriptional activators with enhancer elements located within the promoter region can increase the rate of transcription. These can be located proximally or distally to the core promoter region. These factors can interact with different components of the basal transcriptional complex, either through direct interaction with, or through non-DNA bound secondary factors which then interact with, the proteins involved in the formation of the basal transcriptional complex (Latchman, 2004). Likewise, these elements can function to enhance transcription through the modification of the chromatin structure. These enhancer proteins function to stabilise or complement core protein interactions, thereby enhancing the rate of formation of the basal transcriptional complex, resulting in an increased rate of transcription. However, unlike TAFs, which direct the location and formation of the assembly of the basal transcriptional complex, transcriptional activators do not directly determine where transcription occurs and binding of an activator is not an essential requirement for transcription initiation.

5.1.3 The *SLC11A1* Promoter and Transcription

Since the determination of the *SLC11A1* sequence (Blackwell *et al.*, 1995, Cellier *et al.*, 1994), a number of *in silico* promoter studies have been conducted to determine the mechanism of transcription initiation and to identify putative transcription factor binding sites (TFBS) within the *SLC11A1* promoter (Awomoyi, 2007, Blackwell *et al.*, 1995, Kishi *et al.*, 1996, Searle and Blackwell, 1999).

The *SLC11A1* promoter lacks consensus TATA, GC or CAAT box elements (Blackwell *et al.*, 1995). However, Kishi et al, (1996) identified a putative non-canonical TATA box (TAAAA located at positions -37 to -33). Transcription from a promoter with a canonical TATA box generally occurs from a single transcription start site, while transcription from a non-canonical promoter results in multiple sites of transcription initiation (Ince and Scotto, 1995). The lack of a TATA element in the *SLC11A1* promoter is consistent with the presence of multiple transcription initiation start sites. This finding is further corroborated by analyses of the murine *Slc11a1* promoter, which also lacks a canonical TATA, GC and CCAAT box elements, and possesses multiple transcription start sites (Govoni *et al.*, 1995, Wyllie *et al.*, 2002). To date, other potential DNA sequence elements involved in the formation of the basal transcriptional complex, such as Inr or DPE, have not been identified within the *SLC11A1* promoter.

The *SLC11A1* promoter has also been assessed for the presence of enhancer elements, which may recruit transcriptional activators (Figure 5.4) (Awomoyi, 2007, Blackwell *et al.*, 1995, Kishi *et al.*, 1996, Searle and Blackwell, 1999). The previously published putative TFBS are correlated with the haemopoietic/monocytic restricted expression of *SLC11A1* and the role of *SLC11A1* a gene involved in immune modulation. Additionally, putative binding sites involved in the regulation of *SLC11A1* expression due to exogenous stimuli IFN-γ and LPS have been reported (Figure 5.4). In addition to the range of TFBS that have been described in the *SLC11A1* promoter (Figure 5.4), a string of heat shock transcription factor motifs have also been described (Blackwell *et al.*, 1995).

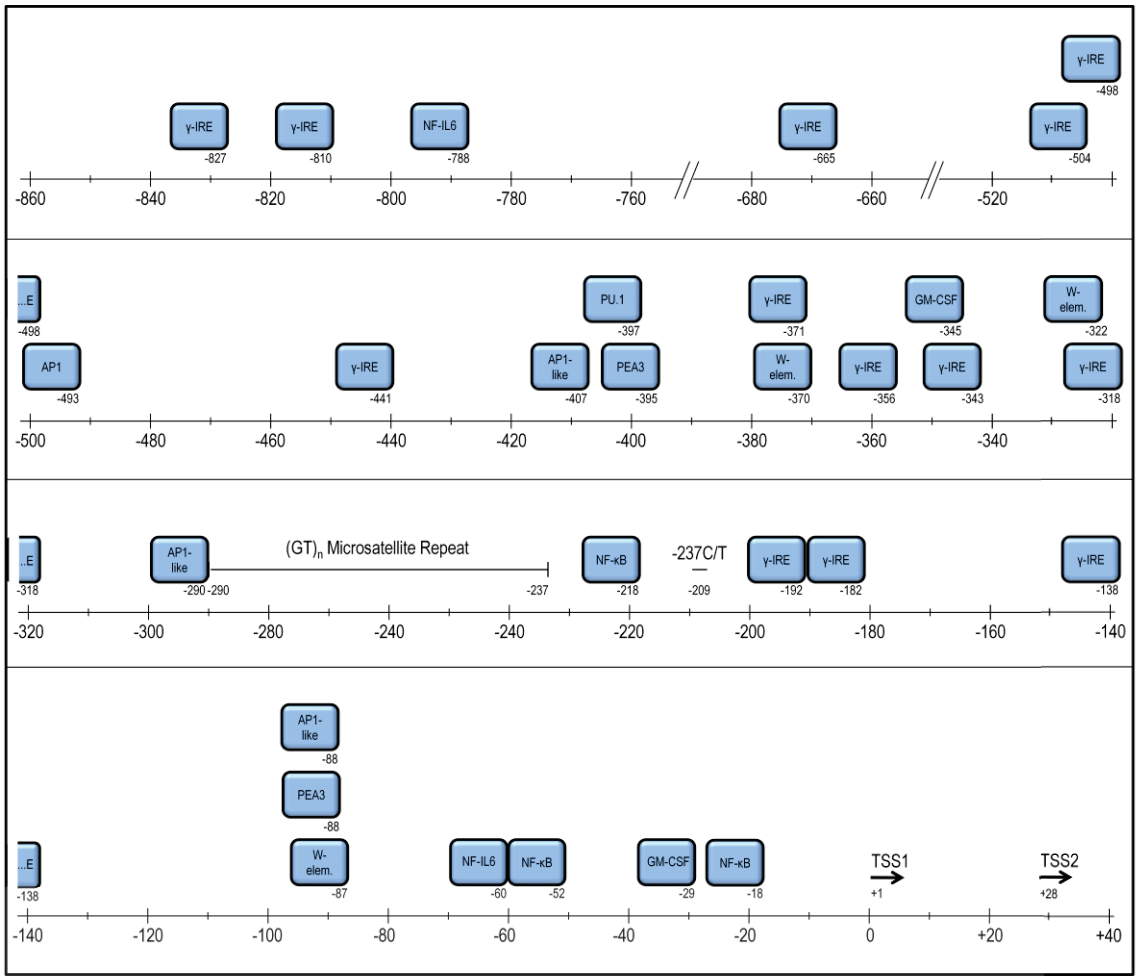

Figure 5.4 Location of previously published putative transcription factor binding sites located within the *SLC11A1* promoter. The blue boxes indicate the location of the putative transcription factors within the *SLC11A1* promoter (the scale located underneath is relative to TSS1). Landmarks of the *SLC11A1* promoter (the transcription start sites and promoter polymorphisms) are also indicated. Numbers located below and to the right of the boxes or landmarks indicate the location of the element (the 3' nucleotide position). Key: TSS – transcription start site; NF-κB – nuclear factor kappa-light-chain-enhancer of activated B cells; GM-CSF - granulocyte macrophage colony-stimulating factor; NF-IL6 – nuclear factor IL-6; W-elem. – W-element; γ-IRE – interferon-γ response element; AP-1 – activator protein 1; PU.1 – protein encoded by *SPI-1* (spleen focus by forming virus proviral integration 1) gene.

5.1.4 *SLC11A1* Promoter Polymorphisms Modulate *SLC11A1* Expression

The mechanism by which the promoter $(GT)_n$ microsatellite repeat and the -237C/T polymorphisms alter expression of *SLC11A1* remains unknown (Figure 1.8). Searle and Blackwell (1999) suggested that the differences in expression levels, due to the presence of $(GT)_n$ allele 2 or 3, may be attributable to a juxtaposition of LPS-related enhancer elements, which are differentially affected by the two microsatellite variants. Furthermore, Zaahl et al. (2004) suggested that the -237 T variant, when in *cis* with $(GT)_n$ allele 3, influences IFN-γ and LPS response elements, resulting in a lower level of expression as compared to the expression of the more common -237 C variant. Both of these explanations suggest that transcription factors activated/expressed during stimulation of monocytes/macrophages by the exogenous stimuli IFN-γ and LPS are responsible for the differences in expression levels between the different promoter variants. However, differences in *SLC11A1* expression, mediated by the allelic variants, also exist in the absence of stimulation (Figure 1.8), suggesting that these differences in expression, mediated by variants at the $(GT)_n$ and -237C/T polymorphisms, exist prior to the activation of cells.

5.1.4.1 The *SLC11A1* $(GT)_n$ Microsatellite has Endogenous Enhancer Activity

The *SLC11A1* $(GT)_n$ microsatellite repeat has been shown to function as an enhancer element. Promoter constructs containing repeat variants differing only in the length of the microsatellite repeat show variation in promoter activity (Searle and Blackwell, 1999). The $(GT)_n$ microsatellite repeat is thought to form an alternative DNA structure, known as Z-DNA (Blackwell *et al.*, 1995). Z-DNA occurs primarily in DNA sequences containing alternating purine/pyrimidine nucleotides, as found in the $(GT)_n$ microsatellite repeat. Potential Z-DNA forming sequences are over represented in the 5' UTR and promoter regions of genes (Schroth *et al.*, 1992), such as *SLC11A1*, where these microsatellite sequences are thought to have enhancer functions to upregulate transcription (Bates and Maxwell, 2005, Kashi and Soller, 1999, Rich and Zhang, 2003). Therefore, the endogenous enhancement ability of the $(GT)_n$ microsatellite repeat is thought to be mediated by the ability to form Z-DNA.

5.1.4.2 Z-DNA Structure and Function

Z-DNA has the potential to form in DNA sequences with alternating purine/pryimidine bases when torsional stress is applied to the sequence (Peck *et al.*, 1982). The most common sequences for the formation of Z-DNA are alternating GC or GT repeats (Ho, 1994, Ho *et al.*, 1986). Z-DNA, unlike the canonical B-DNA structure, has a left handed turn, which can form transiently to reduce the high level of torsional stress/energy held within the DNA (Wang *et al.*, 1979). This conversion from a right handed to a left handed structure is due to an alternation between *anti* (C/T) and *syn* (G) conformation of the nucleotides producing the zig-zag backbone of Z-DNA (Figure 5.5).

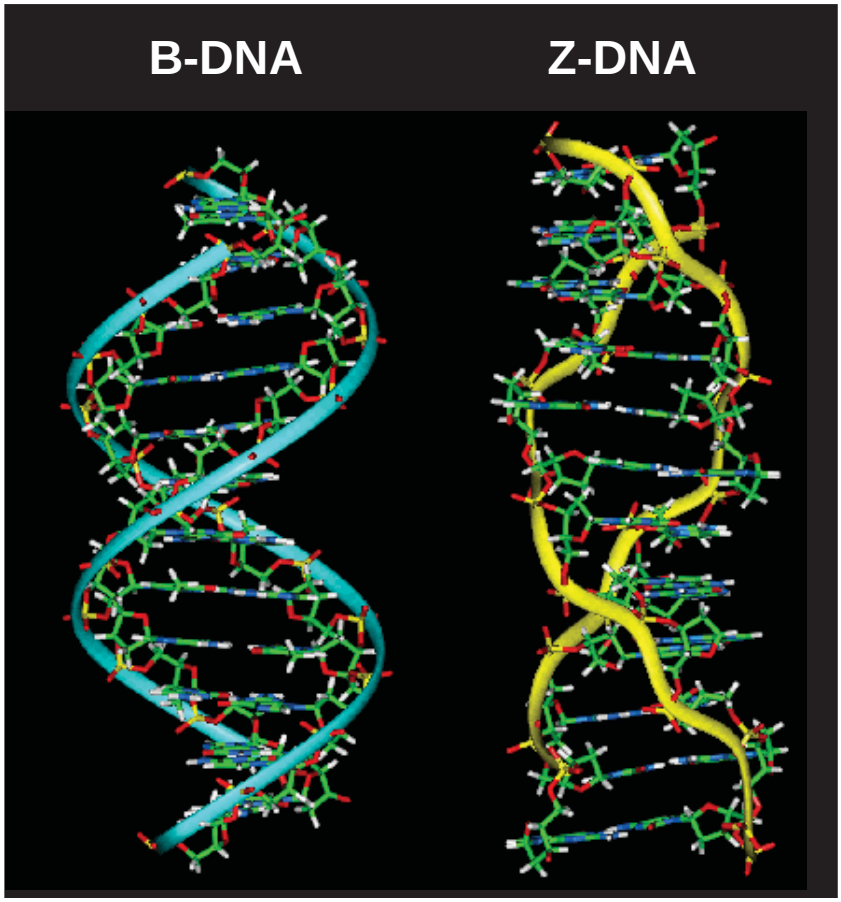

Figure 5.5 Comparison of the structure of right handed B-DNA to the left handed Z-DNA. The primary structure of DNA consists of repeating nucleotides, which stack on each other with a "stagger" due to the asymmetrical nature of nucleotides, causing the strands to coil around each other in a right handed fashion producing the canonical B-DNA, with 10.5 bases per helical turn. B-DNA can transition to Z-DNA in alternating purine/pyrimidine sequences when stress (such as negative supercoiling) is applied. The transition to Z-DNA causes the bases to flip, producing a left hand helical structure with 12 bases per helical turn. A single turn of Z-DNA reduces two turns of negative supercoiling (Herbert and Rich, 1999).

5.1.4.2.1 Z-DNA Formation May Modulate Allelic Differences in SLC11A1 Expression

In vivo, negative supercoiling (the energy held within DNA due to the underwinding of DNA) is maintained in DNA bound to nucleosomes. During transcription, nucleosomes are removed resulting in the release of the energy from the DNA-nucleosome interactions. The level of supercoiling and the amount of energy held within the DNA is not evenly distributed along a chromosome, but is restricted to small DNA regions and is dependent upon many complex factors, including the rate of transcription, the number of active transcription complexes, local topoisomerase activity, the binding of specific proteins, and the chromatin structure of the region (Bates and Maxwell, 2005, Kashi and Soller, 1999).

During transcription, binding of the basal transcriptional complex and melting of the DNA to initiate transcription significantly increases the level of negative supercoiling downstream of the transcription initiation site (Liu and Wang, 1987). Negative supercoiling is a major inhibitor of transcription. An increase in negative supercoiling places the DNA under increasing torsional stress, resulting in an increasing amount of free energy being held by the negatively supercoiled DNA. When this torsional stress, reaches a certain point, known as the critical superhelical density, it causes the bases to flip upside down, forming a left handed helical structure in sequences that have alternating purine/pryimidine residues (Bates and Maxwell, 2005, Kashi and Soller, 1999). The flipping of the bases causes the formation of left-handed Z-DNA resulting in a reduction in the level of negative supercoiling, thereby enhancing the rate of transcription (Herbert and Rich, 1999). When the level of negative supercoiling decreases to a point lower than the critical superhelical density, the left handed Z-DNA transitions back to a right handed DNA conformation.

Observed differences in *SLC11A1* expression levels, mediated by the allelic variants of the *SLC11A1* $(GT)_n$ promoter repeat, may be attributable to differences in the amount of free energy required for Z-DNA transition. For example, allele 3 would theoretically have a greater ability to enhance transcription, as compared to $(GT)_n$ allele 2, due to a greater propensity to form Z-DNA.

5.1.5 Aims

The underlying mechanism of *SLC11A1* transcription initiation, and the location of DNA elements, which recruit transcriptional activators, is unknown. Previous studies suggest that *SLC11A1* does not contain canonical TATA, GC or CCAAT box elements, however, no other core promoter elements have been described to explain the mechanism of transcription initiation.

The aim of this work was to determine a minimal promoter region, in which the essential components for the formation of the basal transcriptional complex are located, and to determine if the *SLC11A1* promoter, either the identified minimal promoter region or larger promoter regions, can mediate bidirectional transcription. Additionally, this work aimed to identify the location of elements which recruit transcriptional activators/repressors that modulate expression and to determine the mechanism by which the common promoter polymorphisms alter *SLC11A1* expression.

This was achieved through initial *in silico* bioinformatic analyses of the *SLC11A1* promoter to identify putatively important regions involved in the regulation of *SLC11A1* transcription (Chapter 5, Part 1). The findings of the *in silico* analysis guided the design of promoter constructs, containing promoter regions of varying size, orientation and allelic variants, to determine the functional importance of the regions identified *in silico* (Chapter 5, Part 2). The designed promoter constructs were tested *in vivo* using human cell lines. Identified promoter regions important in *SLC11A1* transcription were subsequently re-assessed for TFBS, to provide a mechanism for the functional effects observed (Chapter 6, Part 3).

5.2 MATERIALS AND METHODS

5.2.1 Materials

5.2.1.1 General Materials

The dNTPs and the pooled human gDNA were purchased from Promega (Wisconsin, USA). DyNAzyme II DNA Polymerase and Phusion High-Fidelity DNA Polymerase were purchased from Finnzymes (Espoo, Finland). The PCR additives GC melt and dimethyl sulfoxide (DMSO) were obtained from Clontech (California, USA) and Sigma-Aldrich (Missouri, USA), respectively. Size 15 sterile scalpel blades were purchased from Livingstone International (Sydney, Australia) and glycerol was obtained from Sigma-Aldrich (Missouri, USA). The Purelink Quick Gel Extraction Kit, GeneTailor Site-Directed Mutagenesis System, PureLink HiPure Plasmid Maxiprep kit, One-Shot MAX Efficiency DH5α-T1^{R} competent cells, pGeneBLAzer-TOPO plasmid and T4 DNA ligase were purchased from Invitrogen (California, USA). The restriction enzymes, *Sma*I and *Bst*XI, were purchased from Roche Molecular Biosciences (Basel, Switzerland), while *Bsu*36I, *Pst*I, *Nco*I and *Rsa*I were purchased from New England Biolabs (Massachusetts, USA).

5.2.1.2 Oligonucleotides

Multiple oligonucleotides specific for the *SLC11A1* promoter were designed following previously described parameters (Section 2.1.3) based on sequence file AF229613. Due to the presence of previously identified repetitive elements (Alu, SINE and MER elements) within the *SLC11A1* promoter, an Alu element search (Section 5.2.2.1.6) was completed to ensure primers were designed to regions located between these elements (Marquet *et al.*, 2000, Roger *et al.*, 1998). Table 5.1 lists the designed oligonucleotide primers.

Table 5.1 Oligonucleotides Designed for *SLC11A1* Promoter Analyses.

Primer name	Sequence	Length	Name*
Primers for the preparation of promoter constructs and sequencing			
SLC11A1prom1a-F	TCAGCCAGGTGCAGTGGTTCATGC	24	
SLC11A1prom1a-R	AAGGACTCCACCCAGTGAGATTG	23	A
SLC11A1prom1b-F	CCAGCCTGGGCAACATAGTGAGAC	24	
SLC11A1prom1b-R	AAGGACTCCACCCAGTGAGATTGA	24	
SLC11A1prom1c-R	CCGAGTGCCCTGCCTCTTACATC	23	C
SLC11A1promAlu1-F	TGGGGGCCTGTAATCCTCGTGACT	24	1
SLC11A1promAlu2-F	TGGGCATGAGTCAAGCTGGATTTC	24	2
SLC11A1promAlu3-F	CCATCCTTGGGCAGCTACATTTTT	24	3
SLC11A1promAlu4-F	CAGTCAAGCATGGTGGCATAGGTC	24	4
SLC11A1prom1d-F	CAAAAATTAGCCAGGTGTGGTTGG	24	5
SLC11A1prom1e-F	CAGAGCAAGACGCCATCTCAAAGT	24	
SLC11A1prom1f-F	GCACCACTGCACTTCACACCTCAC	24	6
SLC11A1prom1g-F	GAGAAGGGACATGATCTGGTGACA	24	7
SLC11A1prom1h-F	ACAAAGGTCCACTCCATGGGTAAC	24	10
SLC11A1prom1-237C-F	CATGGGGTATTGACATGAATACGCAAGGGGCAG	33	9
HSNRAMPA-F	TGAAGACTCGCATTAGGCCAACG	23	8
HSNRAMPC-R	CCTGCCCCTTGCGTATTCATGTCA	24	D
Primers for sequence analysis			
SLC11A1Seq1	CACTGGGATCTGGTCCTGGTTCAA	24	
SLC11A1Seq2	AGGCTGGTCTCGAACTCCTGGTCT	24	
SLC11A1Seq3	CAGGAAGCAGAGGTTTCAGTTAGC	24	
Primers for *in vitro* site-directed mutagenesis			
SDM-F (SLC11A1prom1-237T-F)	CATGGGGTATTGACATGAATATGCAAGGGGCAG	33	9
SDM-R (SLC11A1prom1-237-R)	ATTCATGTCAATACCCCATGACCACACCCC	30	

*Name used to describe amplicon created from this primer for the production of promoter constructs. Amplicon names were made up of a forward primer number and a reverse primer letter. For example, promoter region 1A is created using forward primer 1 (SLC11A1promAlu1-F) and reverse primer A (SLC11A1prom1a-R).

5.2.2 Methods

5.2.2.1 Bioinformatic Analysis of the *SLC11A1* Promoter

Multiple programs for *in silico* sequence analysis were used to obtain information about the *SLC11A1* promoter. This *in silico* information was then used to guide the design of *SLC11A1* promoter constructs to functionally test identified putative promoter regions important in transcription.

5.2.2.1.1 Bioinformatic Storage and Analysis using LaserGene

GeneQuest file

As a range of *in silico* studies analysing the *SLC11A1* promoter were conducted a large amount of data was generated. To allow for this information to be easily stored and compared, all data from the *in silico* analyses was annotated against the nucleotide sequence AF229163 into a GeneQuest file (from the Lasergene suite of programs).

Throughout the analyses, the transcription start site of *SLC11A1* was used as a reference point to identify different regions of the *SLC11A1* promoter. Several transcription start sites have been described for *SLC11A1*, however, the transcription start site used in the *SLC11A1* sequence file AF229163 (Marquet *et al.*, 2000) and first determined by 5' Random Amplification of cDNA Ends (5'RACE) (Kishi *et al.*, 1996) was used as the reference point and has been referred to as transcription start site 1 (TSS1). Another documented transcription start site, which is 28bp downstream of transcription start site 1, has also been described and is referred to as transcription start site 2 (TSS2) in this study (Richer *et al.*, 2008). The -237C/T polymorphism is located -237bp upstream of TSS2, however, based on the nomenclature used in this study, the location of this polymorphism is 209bp upstream of the TSS1 reference point (-209C/T) (Mohamed *et al.*, 2004). However, the common name for this polymorphism (-237C/T) has been retained.

SeqBuilder – Cloning File

A cloning project was created using SeqBuilder (Lasergene, DNAStar) to allow the sequence files for all of the designed *SLC11A1* expression plasmids to be stored. The sequence for the production of each *SLC11A1* promoter insert was derived from the AF229163 GeneQuest file. The promoter plasmids designed and produced were simulated in SeqBuilder, where *SLC11A1* promoter inserts were TA cloned into the pGeneBLAzer plasmid. The designed plasmids in the file were used to analyse the plasmids produced to determine restriction fragment patterns using different restriction enzymes (Section 2.2.2.3).

5.2.2.1.2 ClustalW Alignment of the Promoter Regions of SLC11A1 Homologs

In order to define regions of high homology, clustalW alignment was carried out using promoter regions of *SLC11A1* homologs. A search of the NCBI database identified nine *SLC11A1* homologs, which were assessed for their inclusion into the alignment. The *Gallus gallus* sequence was excluded from the clustalW alignment as there was significant evidence to suggest that the mechanism of transcriptional regulation differed significantly from the other *SLC11A1* homologs. This was due to the orientation of the *Slc11a1* gene, in relation to the surrounding genes, which was in the opposite direction to the other *SLC11A1* homologs, the absence of a GT or CA microsatellite repeat, and a

lack of restricted expression within the reticuloendothelial system (Section 1.1.3). Therefore, the clustalW alignment included the promoter sequences of eight *SLC11A1* homologs.

From the promoter region of *SLC11A1* (or homolog) 3000 bases were extracted. In most cases this was completed through the NCBI Reference Sequences (from the gene page) and extracted from large sequence files. The extracted data was selected to include 2000 bases upstream of the transcriptional start site (or putative start site) and 1000 bases downstream of the start site. Sequences were copied into the EditSeq Lasergene program (DNASTAR) and then imported into MegAlign. A clustalW alignment was completed of the imported sequences in MegAlign and the resulting alignment was assessed manually for regions of high homology.

5.2.2.1.3 Identification of Conserved SLC11A1 Promoter Elements by WeederH Analysis

The program WeederH was used to identify conserved elements located within the *SLC11A1* promoter. The program WeederH (http://www.beacon.unimi.it/modtools/) is a free web-based program, which identifies conserved TFBS (Pavesi *et al.*, 2007). The 3000bp of the human *SLC11A1* promoter region, as used in the clustalW alignment (Section 5.2.2.1.2), was used as the reference sequence. Three other *SLC11A1* promoter homologs (*mus*, *rattus* and *canis*) were used as a comparison to determine conserved regions. FASTA formatted sequence data was pasted into the appropriate area of the input form and the respective species selected. The results were viewed using the UCSC genome browser (http://genome.ucsc.edu) by entering the appropriate information about species, chromosome and start/stop locations on the chromosome (*Homo sapiens*, Chr2, 21893160-218956160) and the results were entered into the Lasergene GeneQuest file (Section 5.2.2.1.1).

5.2.2.1.4 Analysis of SLC11A1 for Transcription Factor Binding Sites

Transcription Element Search Software (TESS)

The Transcription Element Search Software (TESS) (http://www.cbil.upenn.edu/cgi-bin/tess/tess) (Schug, 2003, Schug and Overton, 1997) is a free web-based program, which searches for putative TFBS using site or consensus strings and positional weight

matrices from the TRANSFAC, JASPAR, IMD and CBIL-GibbsMat databases. Binding sites are determined through the use of a scoring system, with a default minimum score of 12. However, shorter consensus sequences will not reach this score and therefore may be missed. The score can be lowered to find shorter consensus sequences or sequences with a higher mis-match.

The analysis of TFBS was completed by pasting FASTA formatted *SLC11A1* promoter and 5'UTR sequences (AF229163) into the search box and completing a search with default parameters. TFBS search results were generally analysed using the annotated sequence view. Further information about transcription factors was obtained by following hyperlinks for the particular transcription factor and also by using the external database references.

GRAILEXP

GRAILEXP (version 3.3) (http://compbio.ornl.gov/grailexp/) (Xu and Uberbacher, 1997) is a suite of programs commonly used in the discovery and annotation of genes. In addition to predicting the exon/intron structure from a DNA sequence, the program also has the ability to identify promoter regions and CpG islands. The prediction of promoter regions is based around the search for consensus sequences (e.g. TATA, GC and CCAAT elements) within an area of 5000bp of the first codon of a predicted GRAILEXP gene model. One gene element is assigned to each gene model. A FASTA formatted sequence of the whole *SLC11A1* gene and promoter region (AF229163) was entered with all features of the program enabled. The gene predictions and promoter data output were compared to the annotated Genequest sequence file (Section 5.2.2.1.1).

Lasergene – Genequest

A TFBS search was completed in Lasergene Genequest by first creating an EditSeq DNA sequence file containing the *SLC11A1* promoter region and 5'UTR. The file was opened using the Genequest program and the patterns – signals – tfd.dat was dragged from the method curtain onto the assay surface with the source organism 'mammalian' selected and site length 'any' chosen. Further summary information was obtained about individual transcription factors found to bind to the promoter region by analysis of the site description. From this page further information was obtained through the Pubmed ID links.

BioGPS

BioGPS (http://biogps.gnf.org/#goto=welcome) (Wu *et al.*, 2009) is a free online gene annotation source. The gene expression activity chart of the program was used in association with the TFBS searches to look at the expression pattern of identified putative transcription factors in different tissues. This allowed each putative binding site to be assessed, based on the expression profile of the factors, and to be removed if inconsistent with the restricted expression of *SLC11A1* to phagocytic cells. This significantly reduced the number of identified TFBS to those likely relevant to the expression of *SLC11A1*.

5.2.2.1.5 Identification of Z-DNA Forming Sequences in the SLC11A1 Promoter by Z-Hunt Analysis

Z-Hunt is an online program (http://gac-web.cgrb.oregonstate.edu/zDNA/) (Ho *et al.*, 1986) that uses the thermodynamic properties of a DNA sequence to identify regions that have the propensity to form Z-DNA. The program is superior to other programs that determine Z-DNA forming regions as it is able to identify non-classical sequences which deviate from the alternating purine/pyrimidine sequence. The program identifies Z-DNA forming regions within a sequence, providing each identified region with a Z-Score, which is proportional to the ability of that region to form Z-DNA. A cutoff value of 700 is applied, with higher scores indicative of a greater propensity for the formation of Z-DNA.

The Z-Hunt program was used to identify regions of the *SLC11A1* promoter, which have a propensity for the formation of Z-DNA. The *SLC11A1* promoter sequence was obtained from the sequence file AF229163. Genomic sequences were formatted into FASTA format, copied into Microsoft Word and saved in rich text format (rtf). The rtf text file was altered manually to produce the individual $(GT)_n$ allele sequences. Individual rtf files were uploaded onto the Z-Hunt server and submitted to determine the presence of Z-DNA forming sequences and their corresponding Z-scores.

5.2.2.1.6 Dectection of Alu Elements and Other Repetitive Elements within the SLC11A1 Promoter

A search for *Alu* and other repetitive sequence elements, within the *SLC11A1* promoter, was completed to ensure that designed oligonucleotides were located in sequence regions that did not include the repeat sequences (Section 5.2.1.2). Identification of repetitive elements was achieved through a basic nucleotide blast (http://blast.ncbi.nlm.nih.gov/) using the accession number AF229163 with the Human Alu repeat elements chosen as the search set. Repetitive elements located around the *SLC11A1* promoter were mapped into the *SLC11A1* GeneQuest file (Section 5.2.2.1.1) and compared to previous reports describing the presence of repetitive elements in the *SLC11A1* promoter (Marquet *et al.*, 2000, Roger *et al.*, 1998).

5.2.2.2 DNA Techniques

5.2.2.2.1 PCR 5 – Amplification of Promoter Regions for Promoter Analysis

Regions of the *SLC11A1* promoter to be functionally analysed for promoter activity, which were identified through the *in silico* analysis were produced by PCR amplification for cloning into promoter constructs (Sections 5.2.2.2.3 and 5.2.2.2.6). Amplification was carried out in a total volume of 50µl, which contained 2U Phusion Polymerase, 1X Phusion GC Buffer, 0.2mM dNTP, 20µM forward and reverse primers and pooled human gDNA (25ng) or 1A-*bla*(M) plasmid DNA (0.2ng) (Section 5.2.2.2.3). The additives GC melt (2-10%) and DMSO (3%) were added to the PCR when single bands were not obtained using standard PCR conditions. Table 5.5 outlines the optimal PCR conditions for the amplification of the different *SLC11A1* promoter regions. Each PCR experiment included a negative (no template) control in which sterile dH_2O was added to the PCR instead of template DNA. The PCR was carried out in an Eppendorf Mastercycler Gradient instrument (Eppendorf) and was initiated with a denaturation step (98^{o}C, 3min), followed by 34 cycles of denaturation (98^{o}C, 10s), annealing (56-72^{o}C, 20s) and extension [72^{o}C, 10-60s (148bp-3kb fragments)], followed by a final extension step (72^{o}C, 5min). After amplification, amplicons were analysed by agarose gel electrophoresis (0.8-1.4%) (Section 2.2.2.5) of an aliquot (5µl) of the PCR. Amplicons were gel (Section 5.2.2.2.2) or PCR purified (Section 2.2.2.2) and then cloned into the pGeneBLAzer plasmid (Section 5.2.2.2.3 or 5.2.2.2.6) for functional analyses.

5.2.2.2.2 Gel Purification of DNA Fragments for Cloning

Gel purification of restriction fragments (Section 5.2.2.2.9) and PCR products (Section 5.2.2.2.1) was completed to remove any contaminating DNA fragments. Samples for purification were electrophoresed in 1.4-1.8% agarose gels for 1-2h (Section 2.2.2.5). DNA fragments were visualised using a transilluminator set on low intensity UV (Section 2.2.2.5). Bands of interest were excised from the agarose using a size 15 sterile scalpel blade and gel slices were transferred to a sterile centrifuge tube. The DNA fragments were then purified from the agarose using the Purelink Quick Gel Extraction Kit, following the manufacturer's protocol. The purified DNA was eluted in a volume of 50µl and 5µl was then electrophoresed to confirm successful purification. The concentration of purified DNA was determined using the NanoDrop (Section 2.2.2.7) and used immediately or stored at -20^{o}C until required for cloning (Section 5.2.2.2.3 and 5.2.2.2.6).

5.2.2.2.3 Production of the 1A-bla(M) Plasmid

All promoter inserts were cloned into the reporter vector pGeneBLAzer-TOPO plasmid upstream of a modified β-lactamase gene (*bla*) (Section 6.1.1). The 1A-*bla*(M) plasmid (containing the largest *SLC11A1* promoter region, 1A of 3267bp length, cloned upstream of the β-lactamase gene) was prepared first by PCR amplification using pooled human gDNA (Section 5.2.2.2.1). The pooled gDNA was used to obtain as many of the common sequence variants within the *SLC11A1* promoter (at the $(GT)_n$ microsatellite repeat and the -237C/T variants), with each variant cloned into a different plasmid. Sequence variants not obtained through this method were produced by *in vitro* site-directed mutagenesis (Section 5.2.2.2.4). The 1A insert was cloned following the pGeneBLAzer cloning protocol (Section 5.2.2.2.6) (Figure 5.17) producing four different plasmids all containing promoter region 1A, with $(GT)_n$ allele 3 in the forward and reverse orientation and $(GT)_n$ allele 2 in the forward and reverse orientation. Preparation of the same promoter regions with the different sequence variants allowed for the determination of the mechanisms by which the most commonly occurring promoter variants differentially modulated *SLC11A1* expression. Likewise, analysis of the important identified promoter regions in both the forward and reverse orientation were used to determine if the *SLC11A1* promoter mediates bidirectional transcription.

Validation of the cloning of the correct sized insert and determination of the orientation of the insert was completed by restriction analysis using the enzyme *SmaI* (Section 5.2.2.2.8) (Figure 5.17). *In-vitro* site-directed mutagenesis (Section 5.2.2.2.4) was used to modify the 1A-*bla*(M) plasmid containing allele 3 in both the forward and reverse orientation to produce the -237 T variant, thereby producing 2 new plasmids, both containing the 1A promoter region (with $(GT)_n$ allele 3) with the mutant -237 T allele in the forward and reverse orientation.

Complete sequencing of all six 1A-*bla*(M) plasmids was carried out to identify any sequence variants other than the common promoter alleles (Section 5.2.2.2.5). The six verified 1A-*bla*(M) plasmids (allele 2, allele 3 and allele T in both the forward and reverse orientation) were produced on a large scale (Section 5.2.2.3.1) and were used as the template for the amplification of the smaller promoter regions for cloning (Sections 5.2.2.2.1 and 5.2.2.2.6), or for *in vivo* detection of promoter activity in human cell lines (Chapter 6, Part 3).

5.2.2.2.4 In Vitro Site-Directed Mutagenesis

The use of pooled human gDNA to amplify the 1A insert (Section 5.2.2.2.1) did not allow for the less commonly occurring -237 T variant to be obtained as a clone in the pGeneBLAzer-TOPO vector (Section 5.3.2.3). *In vitro* site-directed mutagenesis was used to introduce the -237 T variant.

Primers were designed to introduce the -237 T variant into the target plasmids 1A-*bla*(M) allele 3 in both the forward and reverse orientation (Section 5.2.2.2.3) (Figure 5.18). Primer specifications were as detailed in the GeneTailor Site-Directed Mutagenesis System manual. Briefly, a forward primer was designed that flanked the mutation site with 10 nucleotides downstream of the mutation site, while the reverse primer was designed to be positioned adjacent to the mutation site.

The manufacturer's protocol for the introduction of the -237 T variant was followed. The methylation reaction had a final volume of 16µl, containing 100ng plasmid DNA (1A-*bla*(M) allele 3 in either the forward or reverse orientation), 1.6µl methylation

buffer, 1X freshly diluted SAM and 4U DNA methylase. The reaction was incubated at 37^{o}C for 1h.

The mutagenesis reaction was completed in a total volume of 50µl, which contained 2U Platinum *Taq* DNA Polymerase High Fidelity, 1X HiFi Buffer, 1.2mM dNTP, 1mM $MgSO_4$, 0.3µM forward and reverse mutagenesis primers (Table 5.1), and 2µl of methylated plasmid reaction. The mutagenesis reaction was completed on the Eppendorf Mastercycler Gradient instrument. The reaction was initiated by an initial denaturation step of 94^{o}C for 2min, followed by 20 cycles of 94^{o}C for 30s, 55^{o}C for 30s and 68^{o}C for 8min 30s, and a final extension step of 68^{o}C for 10min. The mutagenesis reaction was checked by electrophoresis of a 5µl aliquot in an agarose gel (Section 2.2.2.5).

The mutagenesis reaction (2µl) was transformed into One-Shot MAX Efficiency DH5α-T1^{R} competent cells (Section 2.2.3.2), clones were grown O/N and plasmid DNA was then isolated (Sections 2.2.3.3 and 2.2.2.4). Verification of the correct base substitution of the commonly occurring -237 C variant for the T variant was completed by restriction digestion of a 208bp amplified promoter region (primers HSNRAMPA-F/R) (Section 2.2.2.1) containing the -237C/T mutation with the enzyme *Msl*I (Section 2.2.2.3) (Figure 5.18). The prepared 1A-*bla*(M) plasmids containing the T variant in the forward and reverse orientation were completely sequenced to ensure that no additional sequence variations were introduced during the mutagenesis reactions (Section 5.2.2.2.5).

5.2.2.2.5 Verification of the 1A-bla(M) Plasmids by Sequence Analysis

The prepared 1A-*bla*(M) plasmids (Section 5.2.2.2.3), for all three allelic variants in both the forward and reverse orientation, were completely sequenced (Section 2.2.2.6). Sequencing of each of the 1A-*bla*(M) plasmids was completed to identify any aberrant polymorphisms (other than the selected common allelic variants), which may have been present in the template DNA (pooled human gDNA), introduced during PCR amplification (Section 5.2.2.2.1), cloning (Section 5.2.2.2.3), or during the site directed mutagenesis reaction to introduce the -237 T variant (Section 5.2.2.2.4). Figure 5.6 shows the location of the six forward primers and five reverse primers used, in relation

to transcription start site 1 (TSS1), to sequence in both directions the 3267bp 1A inserts cloned into the pGeneBLAzer plasmid (primer sequences are detailed in Table 5.1).

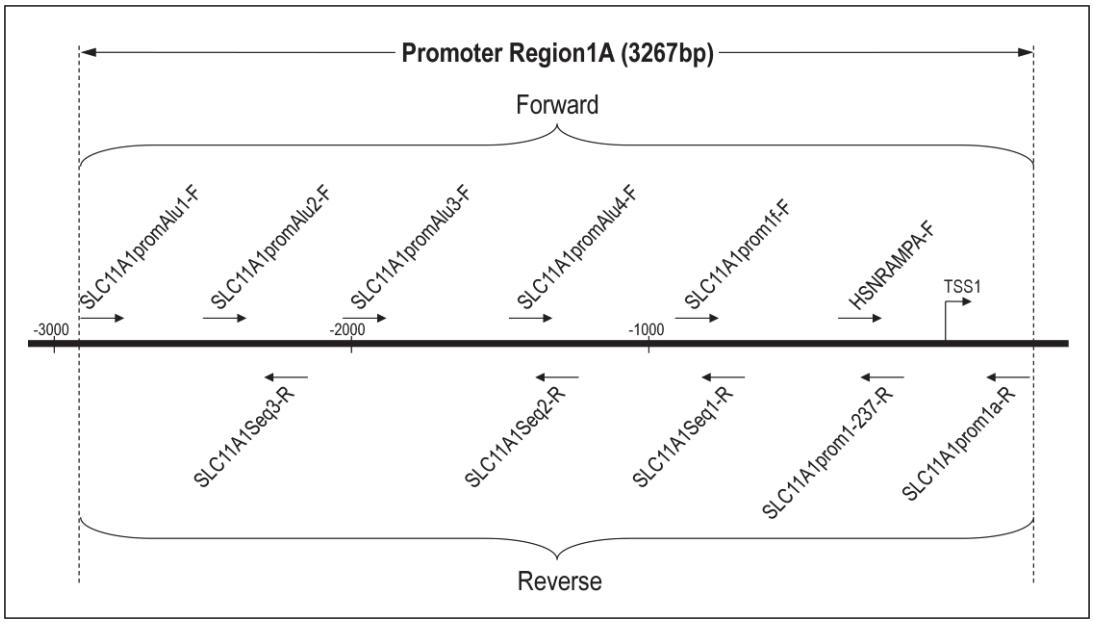

Figure 5.6 Primers used to completely sequence cloned 1A-*bla*(M) plasmids containing the different sequence variants in both the forward and reverse orientation. The 1A insert (3267bp) was sequenced in both directions by six forward primers and five reverse primers. The location of primers are relative to TSS1.

5.2.2.2.6 The pGeneBLAzer Cloning Protocol to Produce the 1A-bla(M) Plasmid and Smaller SLC11A1 Promoter Constructs

The amplification of the 1A promoter region (Section 5.2.2.2.1), for the production of the 1A-*bla*(M) plasmid (Section 5.2.2.2.3), was completed using pooled human gDNA. Once sequenced and verified (Section 5.2.2.2.5), the 1A-bla(M) plasmids, containing the common *SLC11A1* promoter variants (allele 2, allele 3 and allele T), were used as the templates for the amplification of the smaller promoter regions (Section 5.2.2.2.1) for cloning into the pGeneBLAzer expression vector. Figure 5.16 details the size and depicts the different *SLC11A1* promoter regions amplified and cloned for the reporter analyses. Amplification of the smaller promoter regions, using the 1A-*bla*(M) plasmid as template, comprised three separate PCR reactions, with each reaction containing one allelic variant and each variant was cloned and the sequence was verified separately. Additionally, all plasmids were made in both the forward and reverse orientation to determine if the *SLC11A1* promoter mediates bidirectional transcription.

PCR products were PCR (Section 2.2.2.2) or gel (Section 5.2.2.2.2) purified and assessed by agarose gel electrophoresis (Section 2.2.2.5). To allow for compatibility with TOPO cloning, 3' A overhangs were added to the purified products (Section 5.2.2.2.7) before cloning (Section 2.2.3.2) into the pGeneBLAzer-TOPO plasmid. After O/N growth, positive colonies were isolated and cultured (Section 2.2.3.3). Mini-preparations of plasmid DNA were completed (Section 2.2.2.4), and the quality of the purified plasmid DNA was assessed by agarose gel electrophoresis (Section 2.2.2.5). Verification of the production of the correct plasmids, containing inserts of the correct size and orientation, were determined through restriction digestion and sequencing (Section 5.2.2.2.8). Verified plasmids were produced on a large scale (Section 5.2.2.3.1) for *in vivo* detection of promoter activity in human cell lines (Chapter 6, Part 3).

5.2.2.2.7 Addition of A Overhangs for TOPO TA Cloning

TOPO cloning of amplified *SLC11A1* promoter regions (Section 5.2.2.2.1) into the pGeneBLAzer plasmid (Section 5.2.2.2.6) requires inserts to have 3' A overhangs. This allows for efficient ligation into the vector, which is made with a T overhang. Most standard DNA polymerases produce amplicons with A overhangs, however, Phusion polymerase creates blunt end products, which are not directly compatible with TOPO cloning.

The 3' A overhangs were added by incubation of the amplicons to be cloned with DyNAzyme II DNA Polymerase. The reaction was carried out in a total volume of 15µl, which contained DyNAzyme II DNA polymerase (2U), 1X buffer, 2mM dATP and 11µl purified PCR product (Section 5.2.2.2.2). The reaction was incubated at 72^{o}C for 20min and then used immediately for cloning (Section 5.2.2.2.6).

5.2.2.2.8 Verification of SLC11A1 Promoter Constructs

Verification of the cloned *SLC11A1* promoter regions into the pGeneBLAzer plasmid (Sections 5.2.2.2.3 and 5.2.2.2.6) was completed by restriction digestion (Section 2.2.2.3) and sequencing (Section 2.2.2.6). Verification was completed to ensure that the correctly sized *SLC11A1* promoter insert had been cloned, and that all clones contained the correct sequence variant at the $(GT)_n$ microsatellite repeat and -237C/T substitution. Verification was also completed to determine the orientation of the insert cloned into

pGeneBLAzer vector. Appropriate restriction enzymes were selected using the simulated plasmids in the SeqBuilder cloning file (Section 5.2.2.1.1). The criteria used was for the selection of a single enzyme, which had restriction sites located in both the *SLC11A1* promoter insert and the pGeneBLAzer vector. Sequencing (Section 2.2.2.6) of the insert was completed to verify promoter constructs when there were no restriction enzymes which met this criteria. Table 5.2 lists the method of verification for each of the prepared constructs containing different *SLC11A1* promoter regions with each of the common sequence variants (allele 2, allele 3 and allele T) in both the forward and reverse orientation. One of each correct plasmid size, containing each of the individual sequence variants in both the forward and reverse orientation, was selected for functional analyses in human cell lines (Chapter 6, Part 3).

Table 5.2 Method of *SLC11A1* Promoter Plasmid Verification Prior to Functional Analysis.

Plasmid	Enzyme	Fragment sizes (bp)
1A-*bla* (M)-F	*Sma* I	4622, 4025
1A-*bla* (M)-R	*Sma* I	5581, 3062
7A-*bla* (M)-F	*Pst* I	3352, 2927
7A-*bla* (M)-R	*Pst* I	4011, 2268
7C-*bla* (M)-F	*Pst* I	3325, 2609
7C-*bla* (M)-R	*Pst* I	3693, 2268
8A-*bla* (M)-F	*Nco* I	3128, 1774, 735, 472
8A-*bla* (M)-R	*Nco* I	3299, 1774, 735, 301
8C-*bla* (M)-F	*Nco* I	3128, 1774, 735, 154
8C-*bla* (M)-R	*Nco* I	2981, 1774, 735, 301
8D-*bla* (M)-F	*Rsa* I	2418, 2141, 516, 334, 124, 12
8D-*bla* (M)-R	*Rsa* I	2418, 2141, 516, 343, 115, 12
9C-*bla* (M)-F	Sequencing	
9C-*bla* (M)-R	Sequencing	
10C-*bla* (M)-F	Sequencing	
10C-*bla* (M)-R	Sequencing	
emp-*bla* (M)	*Rsa* I	2418, 2141, 516, 292

5.2.2.2.9 Production of the Negative Control Plasmid emp-bla(M)

An empty vector of the pGeneBLAzer plasmid (vector only with no insert), which could be used as a negative control to establish background fluorescence during *in vivo* detection of promoter activity, was constructed as there was no commercially available circular pGeneBLAzer plasmid. The empty vector [termed emp-*bla*(M)] was produced

by the removal of an insert from one of the prepared *SLC11A1* promoter constructs, followed by self-ligation of the vector to produce the empty vector.

Analysis of the prepared *SLC11A1* promoter constructs was completed using the SeqBuilder cloning project file (Section 5.2.2.1.1) to determine restriction digestion patterns. The promoter construct, 8A-*bla*(M) in the forward orientation, was determined to be the most suitable plasmid to produce the empty vector by double digestion (Section 2.2.2.3) with the enzymes *Bsu*36I and *Bst*XI, as each of the individual enzymes cut once on either side of the insert, to completely remove the 8A insert (Figure 5.19). The 8A-bla(M) (1µg) was digested O/N with the restriction enzyme *Bsu*36I and the product was purified (Section 2.2.2.2). The purified product was then digested O/N with the enzyme *Bst*XI and the 5366bp fragment was purified from the smaller insert by gel purification (Section 5.2.2.2.2) (Figure 5.19).

DNA overhangs, produced from restriction digestion, were filled in to produce blunt ends using Phusion Polymerase in a final reaction volume of 50µl, containing 2U Phusion Polymerase, 1X Phusion HF Buffer, 0.2mM dNTP and 10µl gel purified vector incubated at 72^{o}C for 20min. Ligation of blunt ends was completed in 20µl containing 1U T4 ligase (Invitrogen), 1X ligase buffer and 2µl blunt end vector. The reaction was ligated at RT for 4h and transformed into competent TOP10 cells (Section 2.2.3.2). Four positive clones were selected (Section 2.2.3.3) and plasmid was DNA isolated (Section 2.2.2.4). Verification of the removal of the 8A insert and the re-ligation of the pGeneBLAzer plasmid to produce the empty vector was completed by restriction digest using the enzyme *Rsa*I (Section 5.2.2.2.8) (Figure 5.19). One correct clone was selected to grow to a high plasmid stock (Section 5.2.2.3.1) for transfection as a negative control.

5.2.2.3 Microbial Techniques

5.2.2.3.1 Large Scale Preparation of Plasmid DNA (Maxi-prep)

Promoter regions successfully amplified (Section 5.2.2.2.1) and cloned (Section 5.2.2.2.3 and 5.2.2.2.6) in the pGeneBLAzer-TOPO plasmid and verified for insert size, sequence and orientation (Section 5.2.2.2.8) were grown on a large scale to produce high concentration plasmid stocks for *in vivo* detection of promoter activity (Chapter 6, Part 3). Positive clones were inoculated (100-200µl) into 5ml of LB medium (Section

2.2.3.1) containing 100µg/ml ampicillin. Cells were grown O/N at 37^{o}C with agitation (220rpm). After O/N growth, the 5ml of culture was added to a 1l conical flask containing 200ml LB medium (100µg/ml ampicillin) and incubated O/N at 37^{o}C with agitation (200rpm).

After O/N growth, 50ml of the culture was transferred to two 50ml centrifuge tubes and centrifuged using the Megafuge at 4000rcf for 10min at RT. The supernantant was discarded and another 50ml of culture was added to each 50ml centrifuge tube and centrifuged. The supernatant was again discarded and excess media removed. Plasmid DNA was isolated and purified using the PureLink Plasmid Maxiprep kit following the manufacturer's protocol. For the different centrifugation steps, samples were transferred to sterile Sorvall tubes and centrifuged in a Sorvall Super T21 centrifuge at 14000rpm at 4^{o}C for the appropriate time period as outlined in the protocol.

Plasmid DNA was resuspended in 350µl TE buffer and transferred to a 1.7ml centrifuge tube and stored at -20^{o}C. Plasmid quality was determined by agarose gel electrophoresis (Section 2.2.2.5) and the yield was determined by NanoDrop quantification (Section 2.2.2.7), with the average concentration of isolated plasmids approximately 1-4µg/µl. These high concentration plasmid stocks were used for *in vivo* detection of *SLC11A1* promoter activity through transfection into human cell lines (Chapter 6, Part 3).

5.3 RESULTS

PART 1: Discovery of Important *SLC11A1* Promoter Elements by Bioinformatic Analysis.

A number of different bioinformatic software programs were utilised to analyse the *SLC11A1* promoter to identify highly conserved and putatively important regulatory regions. All of the results obtained from these *in silico* studies were compiled into a Lasergene GeneQuest file (Section 5.2.2.1.1). Putative regulatory regions identified were used for the design and production of *SLC11A1* promoter constructs (Chapter 5, Part 2) for functional analyses of the identified elements in human cell lines (Chapter 6, Part 3).

5.3.1.1 A Model of Regulation of *SLC11A1* Expression

Based on previously published findings regarding the positions of putative transcription factor binding sites and the results of reporter assays, a hypothesised model for the regulation of *SLC11A1* expression was developed (Figure 5.7). In previous studies, the factors involved in the formation of the basal transcriptional complex were not identified and therefore, the minimal promoter region had not yet been elucidated. However, due to the detection of multiple transcription start sites, expression of *SLC11A1* is likely controlled through an initiator, or downstream promoter element, which mediates the formation of the basal transcriptional complex (Figure 5.7).

Control of *SLC11A1* expression within cells is likely under both endogenous and exogenous control. Endogenous control of *SLC11A1* expression appears to be through the macrophage-specific transcription factors, PU.1 and GM-CSF, which control the phagocytic cell restricted expression of *SLC11A1* (Figure 5.7). Furthermore, reporter assays of the different $(GT)_n$ microsatellite repeat alleles (which differ only in the length of the repeat) has shown that different $(GT)_n$ sequences differentially enhance transcription, without the addition of exogenous stimuli (i.e. in unstimulated cells $(GT)_n$ allele 3 has a higher level of *SLC11A1* expression compared to allele 2). This suggests that the fundamental DNA sequence of the microsatellite modulates transcription, and therefore, the endogenous transcriptional enhancement would putatively be attributable to the Z-DNA forming ability of the microsatellite, with the expression levels of

different $(GT)_n$ alleles being driven by varying propensities of the sequences to form Z-DNA (Section 5.1.4.2.1).

Exogenous control of *SLC11A1* expression (i.e. modulated by the exogenous stimuli, IFN-γ and LPS) appears to be mediated through the binding of transcription factors to multiple IFN-γ response elements (γ-IRE) and LPS response elements (binding transcription factors NF-κB, NF-IL6 and AP-1) (Figure 5.7). Differential expression levels modulated by the $(GT)_n$ and -237C/T promoter polymorphisms, after the addition of exogenous stimuli, would be due to the polymorphic sequence variants differentially affecting the interaction between and/or binding of transcription factors to promoter enhancer elements.

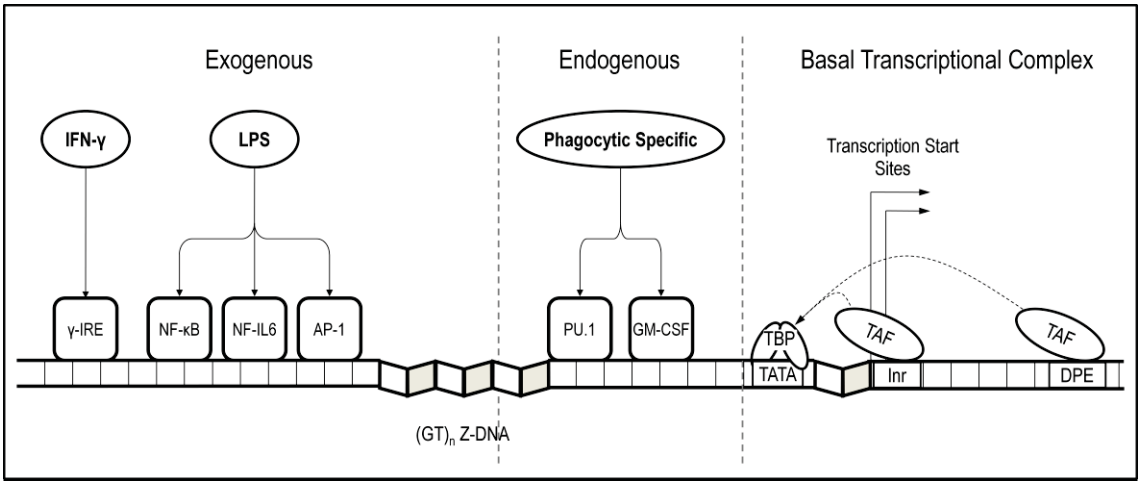

Figure 5.7 Hypothesised mechanism for the control of *SLC11A1* expression based on the findings of previously published studies. *SLC11A1* expression is under both endogenous and exogenous control. Endogenous control is mediated through phagocytic cell specific factors PU.1 and GM-CSF and the Z-DNA forming ability of the $(GT)_n$ microsatellite repeat. Exogenous control (after the exposure to exogenous stimuli) appears to be attributable to multiple IFN-γ response elements (γ-IRE) and LPS response elements (binding transcription factors NF-κB, NF-IL6 and AP-1) located throughout the *SLC11A1* promoter. It is hypothesised that transcription is modulated through initiator (Inr) or downstream promoter element (DPE). The position of factors and elements in the figure does not represent the putative binding location within the *SLC11A1* promoter. Key: IFN-γ – interferon-γ; LPS – lipopolysaccharide; TBP – TATA binding protein; TAF – TBP associated factor; γ-IRE – interferon-γ response element; NF-κB – nuclear factor kappa-light-chain-enhancer of activated B cells; NF-IL6 – nuclear factor IL-6; AP-1 – activator protein 1; PU.1 – protein encoded by *SPI-1* (spleen focus by forming virus proviral integration 1) gene; GM-CSF – granulocyte macrophage colony-stimulating factor.

5.3.1.2 Identification of Conserved Regions within the *SLC11A1* Promoter

A high level of homology is found between protein sequences of different homologs of SLC11A1, suggesting that the protein plays an important evolutionarily conserved function (Section 1.1.2). Due to the restricted expression of SLC11A1 homologs, as well as the similar function the gene plays in immunomodulation (in higher order animals), it would be expected that the mechanisms controlling expression of the different SLC11A1 homologs may be similar. Therefore, a clustalW alignment was conducted to identify highly conserved promoter regions among the different *SLC11A1* homologs. Sequence conservation likely suggests functional significance of the region representing putatively important sites that regulate gene expression (i.e. sequences for the recruitment and binding of transcription factors).

The promoter sequences of eight *SLC11A1* homologs were included in the clustalW alignment. Table 5.3 displays information about the organisms, which were included in the alignment, the accession numbers of the different sequences as well as the selected nucleotide regions. A clustalW alignment was then performed using all 8 promoter regions using the slow and accurate alignment (Section 5.2.2.1.2).

Table 5.3 *SLC11A1* Homologs Included in the ClustalW Analysis.

Organism	Accession No.	First Nucleotide Position	Last Nucleotide Position
Homo sapien	AF229163	4060	7059
Macaca mulatta	NW_001098167	305761	308760
Mus musculus	NT_039170	51946454	51949454
Pan troglodytes	NW_001232114	300017	303017
Equus caballus	NC_009149.1	8047141	8050141
Rattus norvegicus	NW_047816	17141907	17144907
Bos taurus	NW_001494678	284803	287803
Canis familiaris	NC_006619.2	28035951	28038951

The most conserved region identified from the clustalW alignment of *SLC11A1* homologs was approximately 200 bases in length and located just downstream of the $(GT)_n$ microsatellite repeat extending to the first transcription start site (-200 to -1) (Appendix 1). Furthermore, within this identified conserved 200bp region was a region of approximately 40bp (-70 to -28) that approached 100% homology between all eight *SLC11A1* homologs (Figure 5.8A). Conservation of this near perfectly aligned 40bp

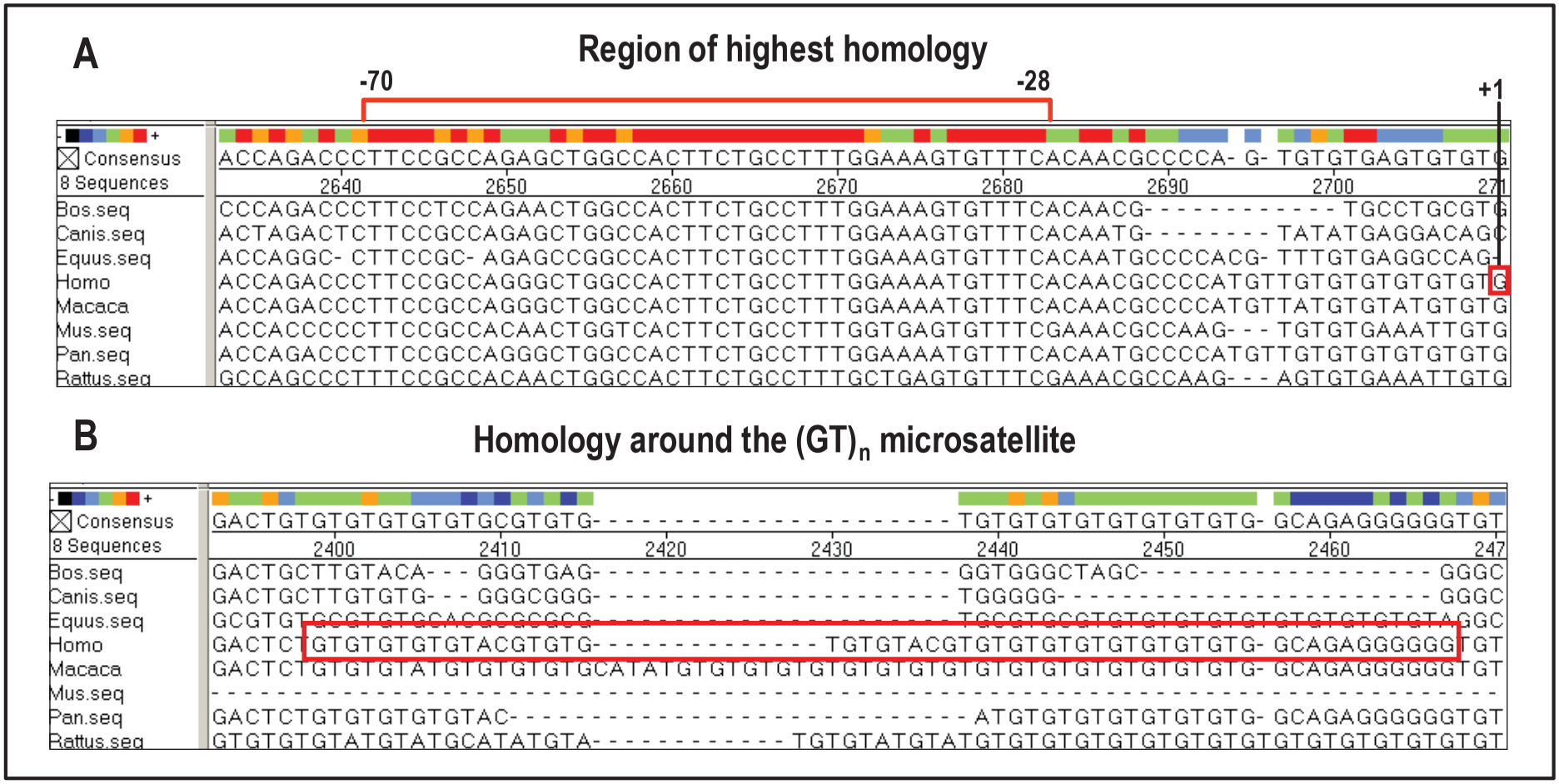

Figure 5.8 ClustalW alignment of the nucleotide sequences of the promoter regions of 8 *SLC11A1* homologs. The coloured bar located at the top of each alignment designates the level of homology (red designates 100% homology, followed by orange and green, while blue designates low homology). (A) The region with the highest level of conservation was located just upstream of the transcription start site (-70 to -28) and may represent the minimal promoter region and the site for the formation of the basal transcriptional complex. (B) Homology around the $(GT)_n$ microsatellite repeat. The box designates the human sequence showing the lack of conservation of the sequence at the $(GT)_n$ repeat.

region, suggested that this site plays an important functional role, and, due to its location, likely represents a minimal promoter region required for the assembly of the basal transcriptional complex. Other areas of high homology were also identified in the 5'UTR and within the first exon of the *SLC11A1* gene at positions +44 to +71 and +199 to +222, respectively (Appendix 1). These regions could represent initiator or downstream core promoter elements, which are required for the formation of the basal transcriptional complex or may represent sites of transcription factor binding.

Further analysis of the clustalW alignment found that the $(GT)_n$ microsatellite tract was not well conserved between the different *SLC11A1* promoter homologs (Figure 5.8B). While nearly all homologs had some form of GT repeat sequences, the location of the repeat within the promoter and the sequence composition was not highly conserved. In murine and rat sequences, the GT microsatellite repeat was shifted upstream approximately 200bp as compared to the human promoter. The bovine sequence did not have a well defined microsatellite of repetitive GT units, however, the region did contain areas of homology to the human microsatellite repeat. This lack of sequence specific conservation suggests that the $(GT)_n$ microsatellite repeat may have a topological or structural influence on transcription (such as the formation of Z-DNA), rather than a sequence specific function, such as transcription factor binding.

A low level of homology was identified at the location of the -237C/T polymorphism (209bp upstream of TSS1), however, a highly homologous 9bp region was located 5-6bp downstream of the -237C/T polymorphic site. Zaahl et al. (2004), showed that the -237 T variant, when in cis with $(GT)_n$ allele 3, results in a lower *SLC11A1* expression level compared to the expression levels normally driven by $(GT)_n$ allele 3 in cis with the frequent -237 C variant (Section 1.3.3). The lower promoter activity driven by the T variant could be due to this base substitution modulating the ability of a transcription factor to bind to the homologous region adjacent to the polymorphic site. Comparison of the sequence of the homologous region with previously published putative TFBS showed that this conserved region may correspond to a γ-IRE binding site. The regions of homology that were identified through the clustalW alignment were loaded into the Genequest sequence file (Section 5.2.2.1.1) used to collect information about the *SLC11A1* promoter.

5.3.1.3 Identification of Conserved Elements within the *SLC11A1* Promoter

The motif discovery program, WeederH, was used to further identify conserved promoter regions within the *SLC11A1* promoter. Like the clustalW alignment, the program uses the concept that conservation of DNA sequences between species implies an important functional role for those sequence regions. This method has been termed *phylogenetic footprinting* (Tagle *et al.*, 1988). However, unlike other programs (such as clustalW), which identify important motifs/conserved regions based on the level of sequence homology alone, WeederH assesses for significant deviation from sequence conservation based on a reference sequence and the other sequence homolog being tested. Identified motifs/elements are then scored relative to the level of conservation observed. Rigorous testing of the program has shown a high correlation between the highest scoring elements identified by WeederH analysis and elements which have been found to bind transcription factors experimentally, thereby validating the predictive value of this *in silico* analysis (Pavesi *et al.*, 2007).

The human *SLC11A1* promoter region was assessed for conserved elements against the promoter regions of three *SLC11A1* promoter homologs (*mus*, *rattus* and *canis*) using WeederH (Section 5.2.2.1.3). This analysis indicated that the majority of the identified elements were located within a few hundred bases of the transcription start site, and that there was a close correlation between the identified elements and conserved regions from the WeederH analyses and clustalW alignment, respectively. Figure 5.9 displays the location of all identified WeederH elements surrounding the transcription start site, with the location of the nine highest scoring WeederH elements identified in the *SLC11A1* promoter.

The highest and sixth highest scoring WeederH elements (scores of 38.08 and 15.67, respectively) were located in the -28 to -70bp region (Site 1 and 6, Figure 5.9), consistent with the area found to exhibit the greatest homology from the clustalW alignment. Therefore, this region likely plays a significant role in modulating *SLC11A1* expression, and may represent a minimal promoter region required for the assembly of the basal transcriptional complex.

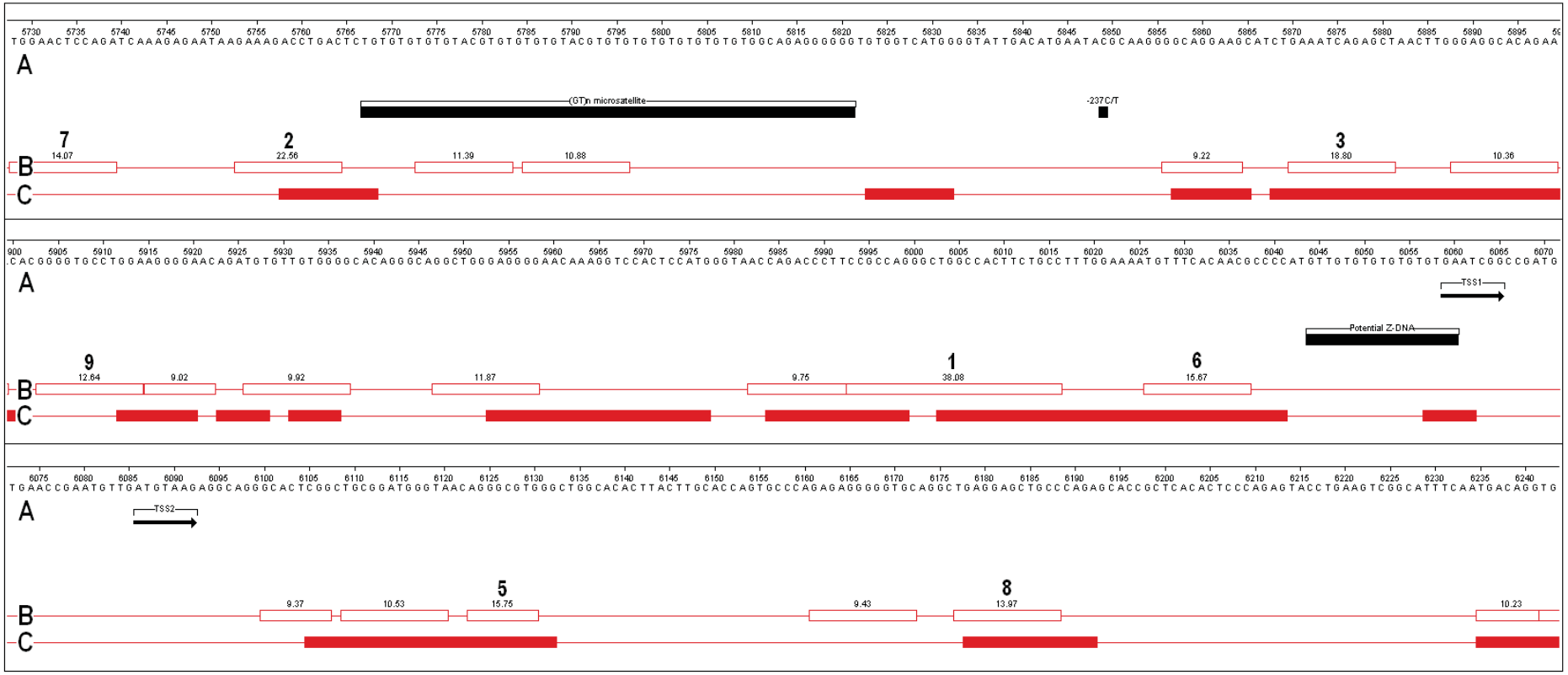

Figure 5.9 The *SLC11A1* promoter showing the location of conserved regions identified from the WeederH analysis and clustalW alignment. (A) Nucleotide sequence, location of the transcription start sites (TSS) and *SLC11A1* promoter polymorphisms. (B) Open red boxes show the location of conserved sequence motifs identified by WeederH analysis. The smaller numbers on top of each box represent the score for the identified motif. Larger numbers designate the location of the nine highest scoring identified motifs in order of significance of conservation (1-9). The fourth highest scoring element is not shown, however is located approximately 200bp upstream of TSS1. (C) Conserved regions, identified by clustalW analysis, showing a high correlation between the identified WeederH elements and conserved regions identified from the clustalW alignment.

The second and third highest scoring elements identified by the WeederH analysis were located adjacent to the 5' end of the $(GT)_n$ microsatellite repeat and 60bp downstream of the $(GT)_n$ microsatellite repeat, respectively (Figure 5.9). Like the highest scoring element, these WeederH elements are consistent with the finding of high conservation from the clustalW alignment and may be elements for the recruitment of transcriptional enhancers.

Several elements were also identified downstream of the transcription start site, in particular, the fourth most conserved region was located in the first intron (+199 to +222), while the fifth highest scoring element (15.75) was located in the 5'UTR (+44 to +77) (Figures 5.9 and 5.10). The identified elements located in the 5'UTR and into the first intron of *SLC11A1* fall within conserved regions identified in the clustalW alignment, suggesting that regions downstream of the transcription start site may represent core promoter elements, other 5' UTR enhancer elements, or may play a post transcriptional role (Figure 5.10).

Consistent with the clustalW analysis, the -237C/T polymorphism was not located in a conserved area (Figure 5.9), suggesting that the altered *SLC11A1* expression observed in the presence of this polymorphism may not be due to the alteration of a TFBS. While a high level of conservation in the $(GT)_n$ microsatellite repeat region was not observed in the clustalW analysis, the WeederH analysis identified two conserved repetitive regions (scores of 11.39 and 10.88), suggesting the presence of a putative element for transcription factor binding (Figure 5.9). Due to its location within the $(GT)_n$ repeat, transcription factor binding to this site within the $(GT)_n$ repeat, or at the second highest scoring WeederH element located adjacent to the microsatellite repeat, may be affected by the rate of Z-DNA formation of the microsatellite, and therefore, may play a role in mediating differential allelic expression of the $(GT)_n$ alleles.

A high level of concordance was observed between clustalW alignment and WeederH analysis suggesting promoter regions identified in these *in silico* analyses may be involved in the control of *SLC11A1* expression (Figure 5.10).

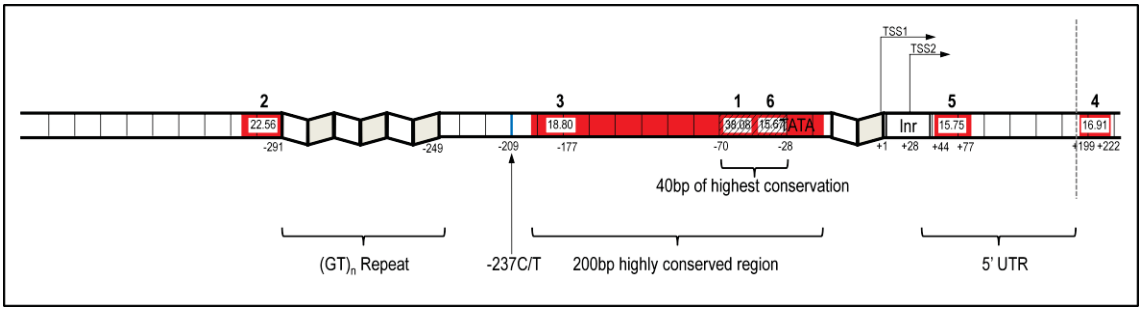

Figure 5.10 Summary of the most significant findings from the clustalW alignment and WeederH analysis of the *SLC11A1* promoter. The landmarks of the *SLC11A1* promoter are shown, including the two transcription start sites (TSS1 and TSS2), the location of the 5'UTR and the exon/intron boundary (grey striped line) and the location of the polymorphic $(GT)_n$ microsatellite repeat and the -237C/T polymorphism. The TATA and Inr indicate the presumptive location of TATA and initiator elements, respectively. Red regions indicate the conserved areas of the *SLC11A1* promoter identified from the clustalW alignment, with the 40bp region showing the highest conservation (-70 to -28), designated by diagonal stripes. The highest scoring WeederH elements are shown as white boxes containing numbers, with the large numbers above ordering these elements sequentially by score (1-6).

5.3.1.4 Identification of Transcription Factor Binding Sites within the *SLC11A1* Promoter

A search for potential TFBS within the *SLC11A1* promoter was completed using several *in silico* bioinformatic programs (Section 5.2.2.1.4). These searches were performed to identify the location of any consensus sequences which may be involved in the formation of the basal transcriptional complex, thereby forming the minimal promoter region. The *in silico* analyses also facilitated the identification of putative transcription factor binding sites located throughout the *SLC11A1* promoter.

5.3.1.4.1 Bioinformatic Analysis Failed to Identify Consensus Sequences for Core Proteins Involved in the Basal Transcriptional Complex

Analysis of the *SLC11A1* promoter using TESS, GRAILEXP or Lasergene programs failed to identify consensus sequences for TBP/TFIID binding (to a TATA element), consistent with previously published reports (Section 5.1.3). Furthermore, analysis of the two major transcription start sites did not identify any initiator elements, which could recruit proteins to mediate the formation of the basal transcriptional complex. The lack of TATA/initiator elements was consistent with visual analysis of the *SLC11A1* promoter sequence for the presence of TATA and initiator elements following published consensus sequence requirements (Javahery *et al.*, 1994, Lo and Smale, 1996, Smale, 1997). Additionally, TFBS searches and visual sequence analysis did not identify other core elements, such as DPE, MTE or BRE, within the *SLC11A1* promoter (Figure 5.3).

While no core promoter sequence elements were identified in the *SLC11A1* promoter, the bioinformatic analysis, using the programs TESS and Lasergene (Section 5.2.2.1.4), identified multiple CCAAT and GC elements for the binding of the factors C/EBP and Sp1. In particular, 15 sites were identified for the binding of Sp1 within the *SLC11A1* promoter. Figure 5.11 displays results of the bioinformatic analysis using the program TESS, highlighting the location of the binding sites for the factors C/EBP and Sp1, with several binding sites located in the conserved regions identified through clustalW and WeederH analysis. It has previously been shown that the transcription factors Sp1 and C/EBP can drive expression from promoters, which lack TATA and other core elements (Huber *et al.*, 1998, Smale, 1997, Smale and Kadonaga, 2003), suggesting that they may mediate the formation of the basal transcriptional complex for *SLC11A1* expression.

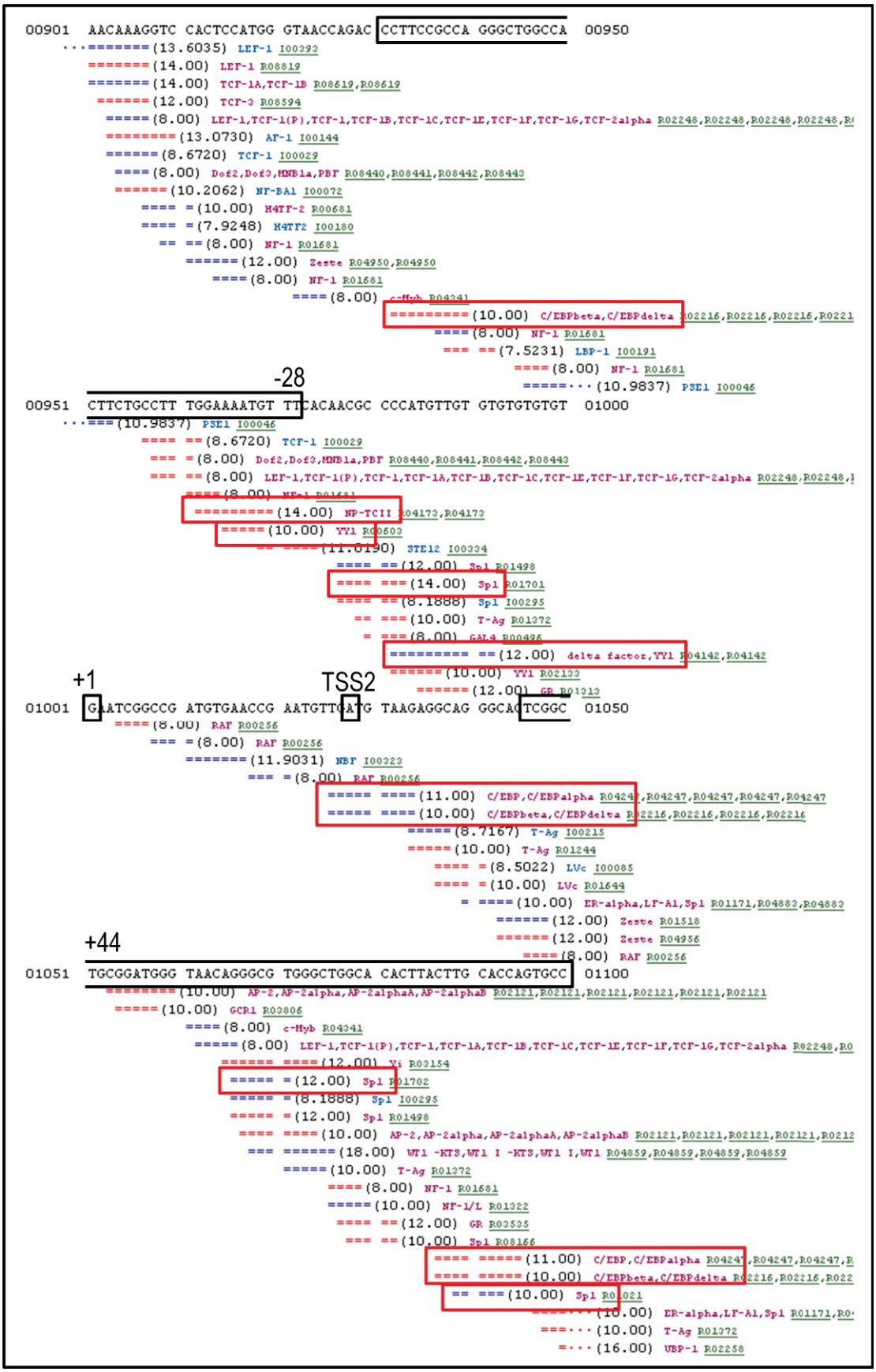

Figure 5.11 TFBS search of the *SLC11A1* promoter centered on the TSS using the program TESS. The black boxes indicate conserved regions identified by clustalW alignment and WeederH analysis, while red boxes indicate putative TFBS.

Several other elements were also identified in the area that showed the highest level of conservation from the clustalW and WeederH analysis (Figure 5.11, black box from position -70 to -28). Consensus sequences for the binding of the transcription factors Ying-Yang 1 (YY1) and NP-TCII were identified. The transcription factor YY1 has been shown to play a role in the formation of the basal transcriptional complex, through binding to an initiator element (Usheva and Shenk, 1996). However, the location of the element relative to the two TSS was inconsistent with a potential role as an initiator element. Located over the YY1 consensus sequence was an NP-TCII element, which binds the transcription factor NF-κB, an LPS response element, which may be involved in the upregulation of *SLC11A1* expression after exposure to LPS. The location of YY1 and NP-TCII elements within the most conserved region and highest scoring elements from the clustalW and WeederH analyses, respectively, suggests they may function as core promoter elements involved in *SLC11A1* expression.

5.3.1.4.2 Identification of Putative TFBS in the SLC11A1 Promoter

The completed TFBS searches (Section 5.2.2.1.4) identified a large number of potential enhancer elements within the *SLC11A1* promoter, which may function to recruit transcription factors that enhance transcription. Due to the large number of identified enhancer elements, it was beyond the scope of this study to analyse all of these elements. Rather, results of the promoter assays focusing on different regions of the *SLC11A1* promoter will narrow the focus to more specific locations within smaller regions of the promoter, which can then be assessed bioinformatically for the presence of putative enhancer elements.

5.3.1.4.3 SLC11A1 Promoter Polymorphisms and Transcription Factor Binding

Transcription factor binding site searches were used to assess if variants at the $(GT)_n$ and -237C/T polymorphisms altered any putative consensus TFBS sequences, which could provide an explanation for the differences in *SLC11A1* expression observed with the different alleles (Section 5.2.2.1.4). Analysis of the $(GT)_n$ microsatellite repeat region did not identify any consensus elements for transcription factor binding using TESS. However, Lasergene analysis did identify two TFBS within the $(GT)_n$ microsatellite repeat region. The identified elements (TACGTG) putatively bind the

factor ARNT. These sites were consistent with two conserved sites identified by WeederH analysis (Figure 5.9), suggesting that a factor might bind to the $(GT)_n$ repeat. However, this finding is inconsistent with the clustalW analysis, which showed a lack of conservation within the $(GT)_n$ microsatellite repeat among *SLC11A1* homologs, suggesting a topological role, rather than a functional role in the binding of a sequence specific transcription factor.

In general, there was a lack of sequence conservation at the site of the -237C/T polymorphism, as identified by the clustalW and WeederH analyses. However, analysis for the presence of TFBS showed some interesting results. Analysis of the region with the wild type -237 C variant included did not identify any transcriptional elements, however, when the analysis was carried out in the presence of the mutant -237 T variant, a site for the binding of the ubiquitously expressed transcription factor Oct-1 (also known as POU2F1) was introduced. Binding of this factor may be involved in the decreased level of *SLC11A1* expression observed in the presence of the -237 T variant.

5.3.1.5 Multiple Regions of the *SLC11A1* Promoter Display a Propensity to Form Z-DNA

The *SLC11A1* promoter region was assessed for the presence of sequences, which have the ability to form Z-DNA. The switch from the canonical B-DNA to the Z-DNA conformation in promoter regions may enhance the rate of transcription (Section 5.1.4.2.1) (Rich and Zhang, 2003). The propensity of a DNA sequence to form Z-DNA is related to the length of the alternating purine/pryimidine tract and the torsional stress placed on the sequence, with longer tracts requiring less torsional stress to form Z-DNA, as compared to shorter sequences (Nordheim *et al.*, 1982).

Assessment of the complete *SLC11A1* promoter region by Z-Hunt analysis (Section 5.2.2.1.5) identified three putative Z-DNA forming sequences (Table 5.4). Located 240bp upstream of the transcription start site, the $(GT)_n$ promoter microsatellite repeat yielded the highest Z-score (12598.14), with the entire 44bp $(GT)_n$ tract possessing the ability to form Z-DNA. The observed Z-score was significantly higher than the cutoff score of 700. This finding is consistent with the observation that the $(GT)_n$ microsatellite repeat forms Z-DNA *in vivo* during transcription (Bayele *et al.*, 2007, Xu *et al.*, 2011).

Two other regions of the *SLC11A1* promoter were also shown to have the propensity to form Z-DNA (Table 5.4). An alternating purine pryimidine sequence was identified 5344bp upstream of the transcription start site (with a Z-score of 2062.84), and another Z-DNA forming sequence was identified over the transcription start site (TSS1) (Z-score of 1276.91) (Table 5.4).

Table 5.4 Identified *SLC11A1* Promoter Sequences with the Potential to Form Z-DNA.

Position*	Location†	Length	Z-Score	Sequence
5768-5811	-240	44	12598.14	$(GT)_5AC(GT)_5AC(GT)_9GG$
715-727	-5344	13	2062.84	TACACGCACACGA
6046-6060	+1	15	1276.91	TGTGTGTGTGTGTGA

*Based on sequence file AF229613 where TSS1 is located at 6059.
†In relation to TSS1.

5.3.1.5.1 The $(GT)_n$ Microsatellite Alleles Differ in their Z-DNA Forming Ability

Having identified the $(GT)_n$ microsatellite repeat as a region possessing Z-DNA forming potential, the ability of each of the different $(GT)_n$ repeat variants to form Z-DNA was further analysed (Section 5.2.2.1.5). Z-Hunt analysis of the individual $(GT)_n$ alleles found that allele 1 had the highest Z-score (18793.69), followed by allele 2 (15167.83), then alleles 3 (12598.14) and 4 (11990.58) (Figure 5.12). Consistent with previous reports (Nordheim *et al.*, 1982), it was found that the longer $(GT)_n$ alleles had a greater potential to form Z-DNA, as allele 1, with 11 GT repeats, had the highest Z-score, followed by allele 2 and allele 3 (10 and 9 GT repeats, respectively). However, the known promoter activity of the $(GT)_n$ repeats, as determined experimentally by reporter assays (Section 1.3.2), does not correlate with the *in silico* predictions of the Z-DNA forming ability of the individual alleles (Figure 5.12). Reporter analyses have shown that $(GT)_n$ allele 3 drives a significantly higher level of *SLC11A1* expression, as compared to $(GT)_n$ allele 2 in monocytic cell lines. This finding contradicts the Z-hunt analysis, which shows that allele 2 has a greater propensity to form Z-DNA, as compared to allele 3 and, therefore, allele 2 would be theoretically predicted to possess a greater transcriptional enhancer activity. This contradictory finding suggests that the ability of allelic variants at the $(GT)_n$ microsatellite repeat to modulate *SLC11A1* expression, in the absence of exogenous stimuli, is not solely attributable to the Z-DNA forming ability of each allele (Sections 5.1.4.2.1 and 5.3.1.1).

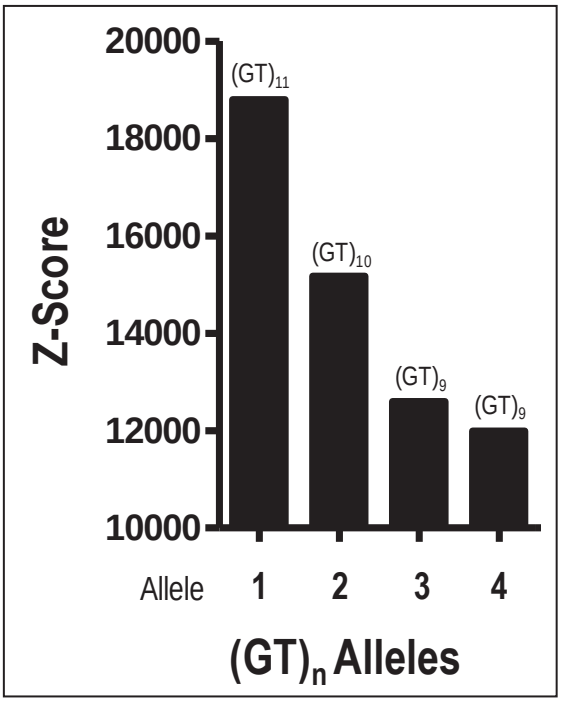

Figure 5.12 Z-Hunt analysis of the *SLC11A1* $(GT)_n$ microsatellite alleles. Each $(GT)_n$ variant has a different number of GT repeats and/or different sequence composition. Above each bar is the number of GT units located at the end of the repeat for that specific allele.

Z-hunt analysis of the *SLC11A1* promoter containing $(GT)_n$ allele 3 in association with either the -237 C or T variant showed that the presence of this polymorphism does not alter the Z-DNA forming ability of the *SLC11A1* promoter $(GT)_n$ microsatellite repeat.

5.3.1.6 *In Silico* Identification of Transcription Factor Binding Sites and Promoter Activity: GeneQuest Summary

All of the data from the bioinformatic analysis of the *SLC11A1* promoter was compiled into a GeneQuest file (Section 5.2.2.1.1). Figure 5.13 displays the findings of the bioinformatic analyses, focusing specifically on the area which displayed the highest level of homology (-469 to +211). The important *SLC11A1* regions identified through the bioinformatic analyses were used as the basis for the design of promoter reporter constructs to determine the promoter activity associated with the different regions (Chapter 5, Part 2).

Since the completion of the bioinformatic analysis (and design of the promoter constructs), three studies which assess the *SLC11A1* promoter for transcription factor

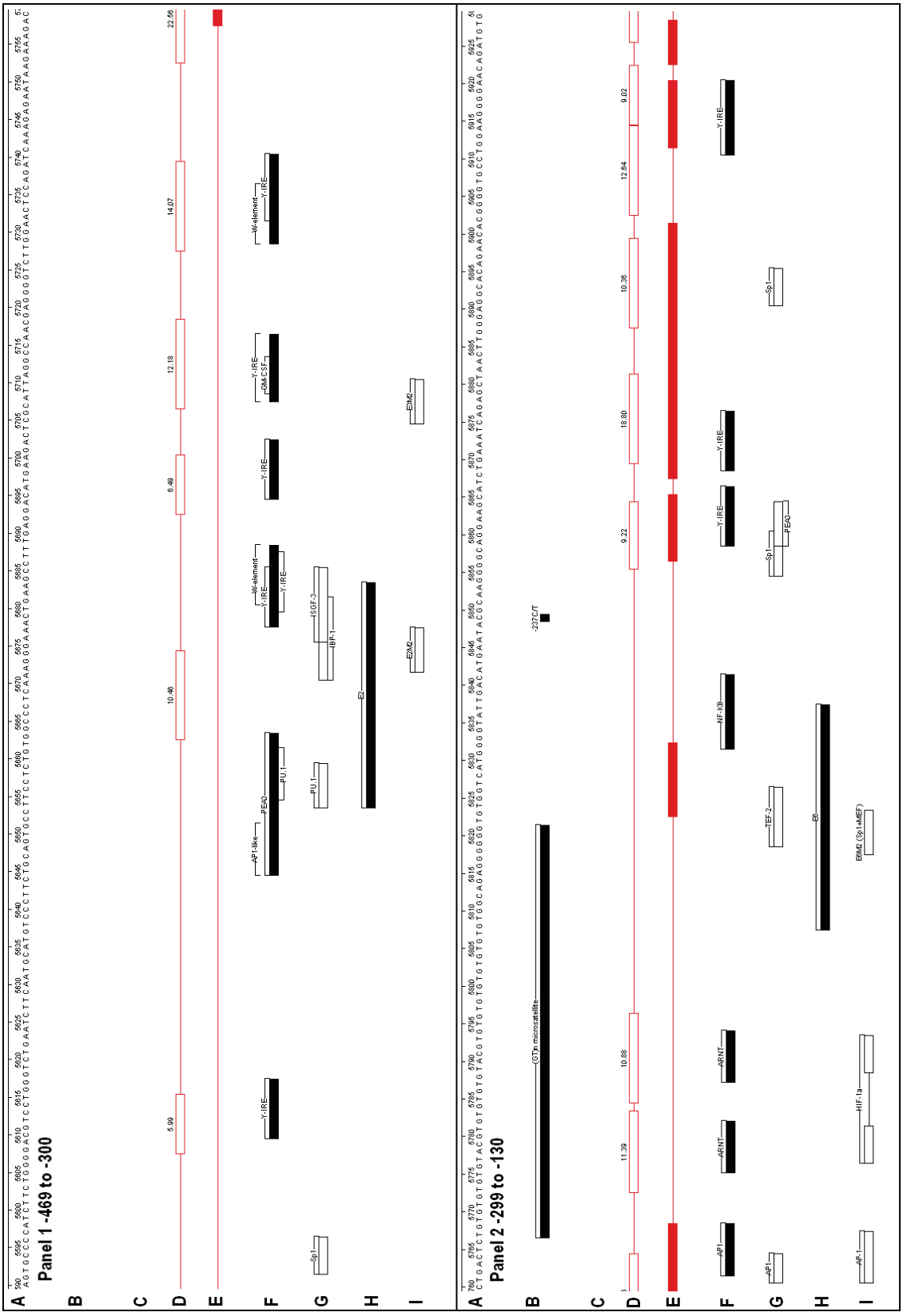
Panel 1 -469 to -300
Panel 2 -299 to -130
Y-IRE
PEA3
PU.1
AP1-like
NF-element
ISGF-3
IBP-1
E2
E2M2
AP1
ARNT
HIF-1a
(GT)n microsatellite
-237C/T
NF-KB
TEF-2
E5
E2M2 (Sp1+MEF)
Sp1
AP-1
11.39
10.88
10.46
6.49
5.99
22.68
14.07
12.18
9.22
18.80
10.36
12.64
9.02

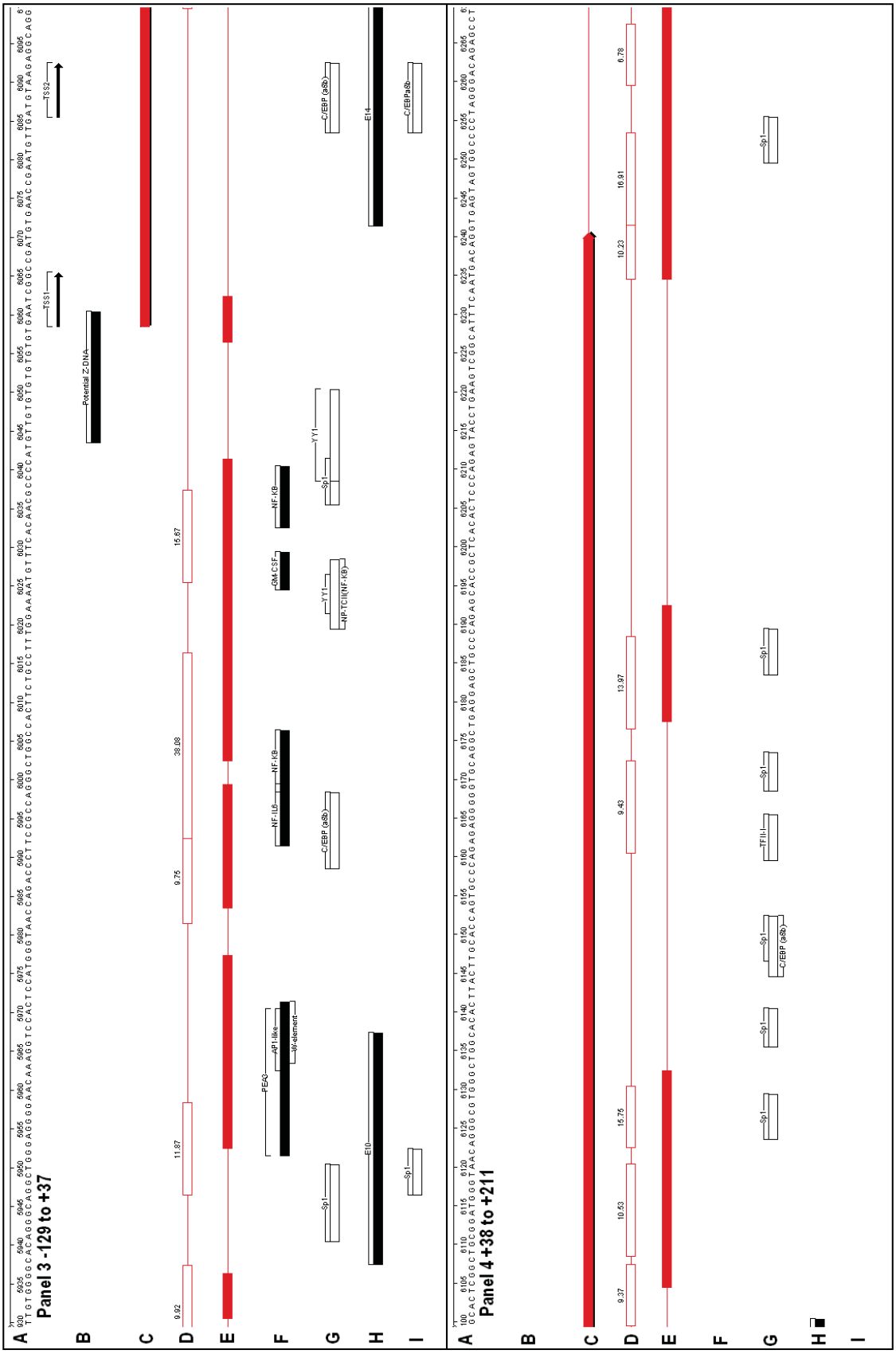
Panel 3 -129 to +37
Panel 4 +38 to +211
Potential Z-DNA
TSS1
TSS2
PEA3
AP1-like
Ik-element
NF-IL6
NF-KB
GM-CSF
C/EBP (a&b)
Sp1
YY1
NP-TCII(NF-KB)
E10
E14
C/EBPa&b
TFIII-I
9.92
11.87
9.75
38.88
15.67
9.37
10.53
15.75
9.43
13.97
10.23
10.91
6.78

Figure 5.13 Compilation of the findings of the bioinformatic analyses of the *SLC11A1* promoter and 5'UTR and comparison with previously published theoretical and experimentally-determined promoter elements. (A) Ruler and *SLC11A1* sequence based on NCBI file AF229163. (B) Landmarks of the *SLC11A1* promoter showing the location of the two transcription start sites, the *SLC11A1* $(GT)_n$ and -237C/T promoter polymorphisms and potential Z-DNA sequences. (C) Location of the *SLC11A1* mRNA transcript. (D) Location of conserved elements identified from the WeederH analysis. The score above each box designates the level of conservation. (E) Conserved regions identified by clustalW alignment of promoter regions of 8 *SLC11A1* homologs. (F) Location of previously published putative TFBS (based on the following papers: Awomoyi, 2007, Blackwell *et al*., 1995, Kishi *et al*., 1996, Searle and Blackwell *et al*., 1999). (G) Location of putative TFBS identified in the current study. (H) Protected sites identified through *in vitro* footprinting suggesting the location of TFBS determined by Richer et al. (2008). (I) Experimentally determined TFBS (Based on the following papers: Bayele *et al*., 2007, Richer *et al*., 2008, Xu *et al*., 2011). Sites E2M2, E3M2 and E6M2 were identified experimentally by Richer et al. (2008) as elements for transcription factor binding.

binding have been published (Bayele *et al.*, 2007, Richer *et al.*, 2008, Xu *et al.*, 2011). The transcription factors identified by these studies are displayed in Figure 5.13, in association with the findings of the current bioinformatic analyses. The recently published experimentally determined sites of transcription factor binding (Figure 5.13I) corroborate the current bioinformatic analysis (Figure 5.13 D, E and G), showing a high predictive ability for identifying important elements using the bioinformatic tools utilised in the current analyses.

Bayele et al. (2007) identified the binding of hypoxia inducible factor 1 alpha (HIF-1α) to a cryptic consensus sequence located within the $(GT)_n$ microsatellite repeat (Figure 5.13, Panel 2, Row I – HIF-1α). While the clustalW alignment identified neither the location of HIF-1α binding, nor the $(GT)_n$ microsatellite repeat as being highly conserved, both WeederH analysis (Row D), as well as the TFBS searches (which identified ARNT, Row G), identified the two repetitive cryptic sites located in the $(GT)_n$ repeat. However, Bayele et al. (2007) showed that HIF-1α binds to the microsatellite *in vivo* only upon cell stimulation (treatment with IFN-γ + LPS or exposure to zymosan particles), showing that binding of this factor could not account for previously reported differences in the level of expression observed in the presence of $(GT)_n$ alleles 2 or 3 (or the rarely occuring alleles), in the absence of exogenous stimulus (Figure 1.8).

Furthermore, Richer et al. (2008) identified vitamin D response elements involved in the upregulation of *SLC11A1* (after vitamin D differentiation of HL-60 cells). *In vitro* footprinting identified 14 protected sites within the *SLC11A1* promoter. Of these, 4 sites were identified by electrophoretic mobility shift assays to contain transcription factor binding sites (Figure 5.13H, E2, E6, E10 and E14). Based on these footprinting experiments, Richer et al. (2008) identified binding of the transcription factors Sp1 (binding -112 to -106) at site E10 (Panel 3, Row I), as well as C/EBP-α/β (located over the second transcription start site +25 to +34) at site E14 (Panel 3, Row I), both of which were also identified in the TFBS searches. While the site for Sp1 binding appeared to be conserved (located within a WeederH element), the C/EBP binding site was not conserved, suggesting that this element may be specific for the human gene. However, while Richer et al. (2008) identified Sp1 and C/EBP binding, transcription factor binding to three other identified elements, E2M2, E3M2 and E6M2, was not determined (Figure 5.13, Panel 1 and 2, Row I).

The most recent paper determining transcription factor binding to the *SLC11A1* promoter reports the binding of an AP1-like transcription factor (ATF-3 and Jun D binding) adjacent the 5' end of the $(GT)_n$ microsatellite repeat (Figure 5.13, Panel 2, Row I). The binding of this factor is consistent with a report from Awoyomi (2007), which first suggested an AP1 site located adjacent to the $(GT)_n$ repeat based on the high level of homology at this site. Furthermore, bioinformatic analysis completed in the current study identified this site as a highly conserved region by clustalW analysis, as the second most conserved region by WeederH analysis (22.56) and also through the TFBS searches.

5.3.1.7 Conclusions of the Bioinformatic Analysis

The bioinformatic analysis identified a number of important regions which could be putatively involved in *SLC11A1* transcription (Figure 5.14). The bioinformatic analysis indicated that the most important elements for *SLC11A1* transcription were located in a 700bp region of the promoter, spanning 500bp upstream of the transcription start site through to the first intron (-500 to +211). Furthermore, within this region, a highly conserved 40bp promoter region located 28bp upstream of TSS1 was determined to be the likely site for the formation of the basal transcriptional complex. Putative important

regions were also identified downstream of the transcription start site in the 5'UTR region and the first intron of *SLC11A1*.

The high correlation observed between the findings of the bioinformatic analysis completed in this study and the location of published transcription factor elements (Section 5.3.1.6), suggests the combined bioinformatic assessment has a significant predictive ability to identify further elements within the *SLC11A1* promoter that are involved in the regulation of *SLC11A1* transcription. Furthermore, this provides a greater confidence that putative areas, identified from the *in silico* analyses (Figure 5.14), which were selected for further analysis through the use of promoter constructs and subsequent reporter assays (Chapter 5, Part 2 and Chapter 6, Part 3), contain functional elements involved in the regulation of *SLC11A1* transcription.

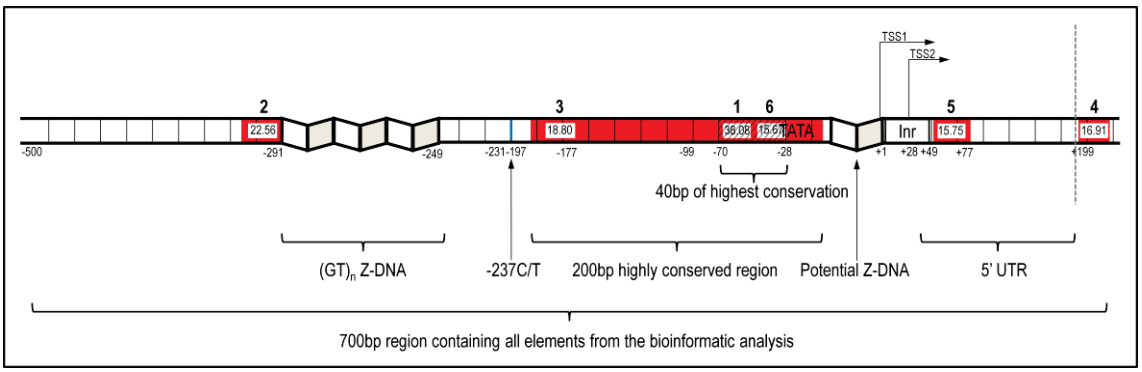

Figure 5.14 Compilation of findings of the bioinformatic analysis of the *SLC11A1* promoter. The landmarks of the *SLC11A1* promoter are shown, including the two transcription start sites (TSS1 and TSS2), the location of the 5'UTR and the exon/intron boundary (grey striped line) and the location of the polymorphic $(GT)_n$ microsatellite repeat and the -237C/T polymorphism. Zig-zag lines identify regions with the potential to form Z-DNA. The TATA and Inr indicate the presumptive location of TATA and initiator elements, respectively. The bioinformatic analysis indicated the important elements for *SLC11A1* transcription were located in a 700bp promoter region, which spanned 500bp upstream of the transcription start site through to the first intron. Red regions identify the areas of the *SLC11A1* promoter which are conserved from the clustalW alignment, with the 40bp region showing the highest conservation (-70 to -28), designated by diagonal stripes. The highest scoring WeederH elements are shown as white boxes containing numbers, with the large numbers above ordering these elements sequentially by score (1-6).

PART 2: Design and Construction of *SLC11A1* Promoter Constructs for Functional Analysis.

5.3.2.1 Primer Site Determination and Primer Design

Based on the findings of the *in silico* bioinformatic analyses of the *SLC11A1* promoter, the promoter was divided into sections to allow the functional assessment of the identified putative regulatory regions. The primers were distributed evenly over a 3.5kb region of the *SLC11A1* promoter to allow a systematic approach to determine important regions which modulate *SLC11A1* transcription (Figure 5.15).

Previous reports have shown that the *SLC11A1* promoter region contains highly repetitive elements (Alu, SINE and MER elements) (Marquet *et al.*, 2000, Roger *et al.*, 1998). Therefore, to ensure that the designed primers for the amplification of different segments of the promoter were not located within these repetitive elements (thus making amplification of promoter regions difficult), an *in silico* BlastN search was completed to locate all repetitive elements within the *SLC11A1* promoter (Section 5.2.2.1.6). These regions were mapped in the GeneQuest file of the *SLC11A1* promoter (Section 5.2.2.1.1) (Figure 5.15D). Primers for the production of *SLC11A1* promoter constructs for reporter analyses were then designed, which were located in the regions between the identified repetitive elements (Figure 5.15E).

Ten forward and three reverse primers were designed to amplify different regions of the *SLC11A1* promoter (Figure 5.15F). Due to the numerous forward and reverse primers designed, and the subsequent amplicons produced, a nomenclature was devised to systematically identify each amplicon. Amplicon names were based on the forward and reverse primers used. Each forward primer was numbered sequentially based on its location from 1, designating the primer with the furthest location from the transcription start site (SLC11A1promAlu1), through to 10, for the forward primer located closest to the transcription start site (SLC11A1prom1h-F). A letter was used to signify the reverse primer used, with A, C and D referring to the primers SLC11A1prom1a-R, SLC11A1prom1c-R and HSNRAMPC-R, respectively (Table 5.1) (Figure 5.15G). For example, the largest promoter region designed is termed 1A, as the forward primer 1 and reverse primer A was used to produce this amplicon.

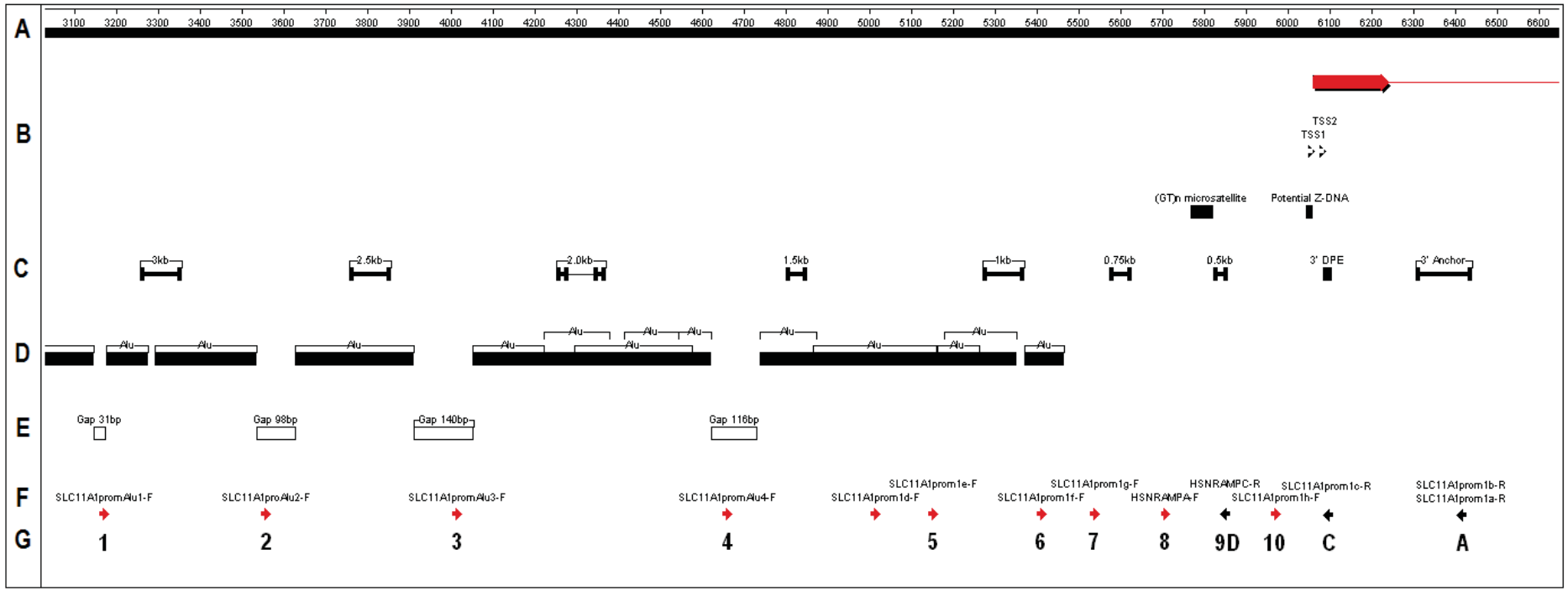

Figure 5.15 Location of designed primers for the amplification of different promoter regions for subsequent production of *SLC11A1* promoter plasmids. (A) Ruler. (B) Landmarks of the *SLC11A1* promoter showing the location of the mRNA transcript (red arrow), the two transcription start sites (TSS), the *SLC11A1* $(GT)_n$ promoter polymorphisms and potential Z-DNA sequence. (C) Ideal location of promoter regions for production of primers for PCR amplification. The regions were selected to break the *SLC11A1* promoter into evenly spaced regions centered around the putative elements identified by the *in silico* analyses. (D) Location of identified Alu repetitive elements from an *in silico* Alu search. (E) The location of gaps between the Alu elements for the design of primers. (F) Location of designed *SLC11A1* primers (arrows), designed based on the findings gathered from the bioinformatic analysis of the *SLC11A1* promoter and located between Alu elements, with primer names located above each primer. Red arrows pointing right indicate forward primers, while black arrows pointing left indicate reverse primers. (G) Large numbers and letters beneath designed primers designate the nomenclature used to name inserts for cloning. The name of a promoter region is based on the number and letter of the forward and reverse primer used to amplify that promoter region.

5.3.2.1.1 Optimisation of PCR Conditions for the Amplification of SLC11A1 Promoter Regions

The PCR conditions (annealing temperature and the inclusion of PCR additives if required) for the amplification of the different *SLC11A1* promoter regions were optimised using pooled human gDNA to allow for the production of single PCR products for each promoter segment (Section 5.2.2.2.1). Table 5.5 displays the optimal PCR conditions for the production of the different *SLC11A1* promoter amplicons and the primers used to produce the amplicons. Sequencing of each amplicon verified the amplification of the correct *SLC11A1* promoter sequence (Section 2.2.2.6).

Table 5.5 Optimised PCR Conditions for the Amplification of the Different *SLC11A1* Promoter Amplicons for Subsequent Cloning.

Amplicon	Annealing Temperature	Forward	Reverse	Size(bp)
1A	72+ 5µl GC melt	SLC11A1promAlu1-F	SLC11A1prom1a-R	3267
1C	72+ 2µl GC melt	SLC11A1promAlu1-F	SLC11A1prom1c-R	2949
2A	72	SLC11A1promAlu2-F	SLC11A1prom1a-R	2879
2C	72+ 5µl GC melt	SLC11A1promAlu2-F	SLC11A1prom1c-R	2562
3A	72 + DMSO	SLC11A1promAlu3-F	SLC11A1prom1a-R	2425
3C	72 + DMSO	SLC11A1promAlu3-F	SLC11A1prom1c-R	2107
4A	64.4	SLC11A1promAlu4-F	SLC11A1prom1a-R	1777
4C	64.4	SLC11A1promAlu4-F	SLC11A1prom1c-R	1459
5A	70.4	SLC11A1prom1d-F	SLC11A1prom1a-R	1422
5C	70.4	SLC11A1prom1d-F	SLC11A1prom1c-R	1104
6A	64.4	SLC11A1prom1f-F	SLC11A1prom1a-R	1024
6C	64.4	SLC11A1prom1f-F	SLC11A1prom1c-R	706
7A	64.4	SLC11A1prom1g-F	SLC11A1prom1a-R	899
7C	64.4	SLC11A1prom1g-F	SLC11A1prom1c-R	580
8A	64.4	HSNRAMPA-F	SLC11A1prom1a-R	729
8C	64.4	HSNRAMPA-F	SLC11A1prom1c-R	411
8D	64.4	HSNRAMPA-F	HSNRAMPC-R	165
9A	64.4	SLC11A1prom1-237C/T-F	SLC11A1prom1a-R	597
9C	64.4	SLC11A1prom1-237C/T-F	SLC11A1prom1c-R	280
10A	64.4	SLC11A1prom1h-F	SLC11A1prom1a-R	465
10C	64.4	SLC11A1prom1h-F	SLC11A1prom1c-R	148

5.3.2.2 Selection of *SLC11A1* Promoter Regions for Cloning and Reporter Analyses

Figure 5.16 summarises the identified elements potentially regulating *SLC11A1* expression as identified from the bioinformatic analyses, the location of designed primers to amplify the different promoter regions, and the *SLC11A1* promoter regions, which were cloned for the production of reporter constructs. The *SLC11A1* promoter regions were designed to functionally determine multiple aspects of *SLC11A1* transcription (Sections 5.3.2.2.1, 5.3.2.2.2 and 5.3.2.2.3). Once amplified, these promoter regions were cloned into the pGeneBLAzer expression vector (Sections 5.3.2.3 and 5.3.2.4) for functional assessment (Chapter 6, Part 3).

Results of the bioinformatic analyses indicated that the location of elements controlling *SLC11A1* expression were within a 700bp region surrounding the transcription start sites (approximately -500 to +210). Therefore, all promoter regions designed (except promoter region 1A) were located within this 700bp region (Figure 5.16). The promoter region 1A was the largest *SLC11A1* promoter region cloned (3267bp) to determine if there were transcriptional elements located upstream of the identified 700bp region which may influence *SLC11A1* transcription. As shown in Figure 5.16, the designed primers allowed the production of amplicons with sequential shortening of the *SLC11A1* promoter in both directions, thus allowing the functional assessment of the different regions of the *SLC11A1* promoter to determine which regions specifically regulated *SLC11A1* expression.

5.3.2.2.1 Identification of SLC11A1 Promoter Regions Containing Core Elements for the Formation of the Basal Transcriptional Complex

The bioinformatic analysis identified a highly conserved region between -70 and -28, suggesting that this site may mediate the formation of the basal transcriptional complex. The sequential shortening of the designed *SLC11A1* promoter regions was centered around this identified site, with a 148bp promoter region (10C) the smallest *SLC11A1* region cloned (Figure 5.16). These analyses would indicate whether this region contains the core elements for the formation of the basal transcriptional complex.

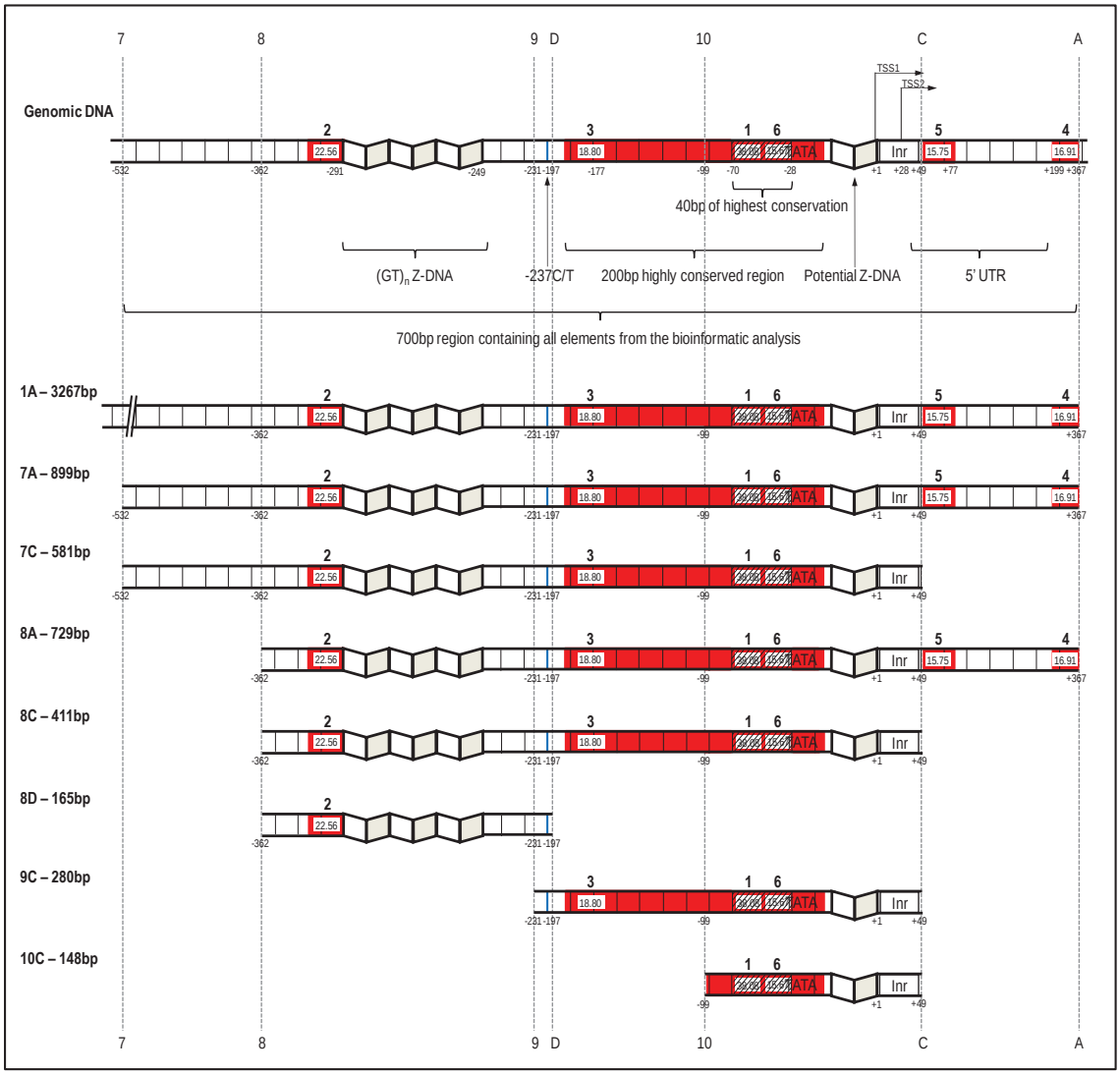

Figure 5.16 Designed *SLC11A1* promoter regions for cloning into reporter constructs to functionally test the different elements identified bioinformatically. Located at the top is a summary of the findings of the bioinformatic analyses and location of important identified promoter elements. The landmarks of the *SLC11A1* promoter are shown, including the transcription start sites (TSS1 and TSS2), the location of the 5'UTR and the polymorphic $(GT)_n$ microsatellite repeat and the -237C/T polymorphism (blue line). Red regions identify the areas of the *SLC11A1* promoter shown to be conserved from the clustalW alignment, with the 40bp region showing the highest conservation (-70 to -28), designated by diagonal stripes. The highest scoring WeederH elements are shown as white boxes containing numbers, with the large numbers above ordering these elements sequentially by score (1-6). TATA and Inr (initiator) identify the presumptive location of these elements. The grey dashed lines designate the location of the designed primers, with the numbers and letters signifying forward and reverse primers, respectively. Below the summary the designed *SLC11A1* promoter regions containing the identified bioinformatic elements are shown. The name (primer number and letter used to produce amplicon) and size of the different promoter regions are shown to the left.

The bioinformatic analysis of the *SLC11A1* promoter also identified conserved elements which may play a role in *SLC11A1* transcription within the 5'UTR, and into the first intron (Figure 5.16). Two reverse primers were designed (reverse primers A and C), to allow the production of amplicons which included (1A, 7A and 8A) or excluded (7C and 8C) the 5'UTR and the small portion of the first intron from the analysis (Figure 5.16), to determine whether the these regions contain core promoter elements and/or elements for the recruitment of transcriptional enhancers.

5.3.2.2.2 Determination of the Effect of Variants at the $(GT)_n$ and -237C/T Polymorphisms on SLC11A1 Expression

To determine how promoter variants modulate differential *SLC11A1* promoter activity, multiple plasmids for each of the same *SLC11A1* promoter region cloned (Figure 5.16) were created, which only differed by the allelic variant present at the $(GT)_n$ and -237C/T polymorphism. This enabled identification of *SLC11A1* promoter regions which may be responsible for the differences in the level of expression driven by the different variants. When a promoter region contained both the $(GT)_n$ microsatellite and -237C/T polymorphisms, three different plasmids were produced to mimic the possible combinations of allelic variants at $(GT)_n$ and -237C/T polymorphisms, which contained either $(GT)_n$ allele 2 (10 GT repeats with -237 C), allele 3 (9 GT repeats with -237 C), or allele T (10 GT repeats [allele 3] with -237 T) (Figure 5.1). The effect of the allelic variants at the $(GT)_n$ repeat were determined by comparing promoter activity between plasmid variants allele 2 and allele 3, while the effect of the variants at the -237C/T polymorphisms were determined by comparing plasmid variants allele 3 with allele T. Likewise, if a promoter region contained only the -237C/T polymorphism (promoter region 9C) then two plasmid variants were produced and termed allele C and allele T. The designed promoter region 9C was produced to exclude the $(GT)_n$ repeat in order to allow the analysis of the effects of variants at the -237C/T polymorphisms separately from the $(GT)_n$ microsatellite repeat.

5.3.2.2.3 Determination of the Ability of the SLC11A1 Promoter to Mediate Bidirectional Transcription

All of the designed *SLC11A1* promoter regions (Figure 5.16), containing the different *SLC11A1* promoter variants (Section 5.3.2.2.2), were cloned in both the forward and

reverse orientation to determine if the *SLC11A1* promoter could mediate bidirectional transcription. Furthermore, if bidirectional transcription was present, then use of the promoter constructs could establish if the different promoter variants altered the rate of forward transcription as compared to reverse transcription, which may account for observed differences in *SLC11A1* promoter activity mediated by the different promoter variants.

5.3.2.3 Construction of the Largest *SLC11A1* Promoter Plasmid: 1A-*bla*(M)

The designed *SLC11A1* promoter regions (Figure 5.16) were cloned into the pGeneBLAzer expression plasmid upstream of a β-lactamase gene (*bla*) (Section 6.1.1). The largest *SLC11A1* promoter region designed, 1A (3267bp), was first amplified using pooled human gDNA and cloned, into the pGeneBLAzer vector (Section 5.2.2.2.3) to produce the plasmid 1A-*bla*(M) (Figure 5.17A). The pooled human gDNA was used as template for the production of the 1A promoter region to enable each common sequence variant at the $(GT)_n$ and -237C/T polymorphisms to be cloned independently. The 1A-*bla*(M) plasmids, each containing a common *SLC11A1* promoter sequence variant, were created, sequenced and used as the template for the production of the shorter designed promoter segments (Figure 5.16). To increase the probability of isolating the different promoter variants in the 1A-*bla*(M) constructs, 30 colonies were selected and plasmid DNA was isolated (Figure 5.17B). Validation of the cloning of the correct sized insert and determination of the orientation of the insert in the isolated 1A-*bla*(M) plasmids was determined by restriction digestion, using the enzyme *SmaI* (Section 5.2.2.2.8) (Figure 5.17C).

Sequencing of the isolated 1A-*bla*(M) plasmids was carried out to determine which *SLC11A1* promoter variants had been cloned (Section 2.2.2.6). The use of pooled human gDNA allowed the cloning of 1A-*bla*(M) plasmids containing $(GT)_n$ alleles 2 and 3 both in the forward and reverse orientation. However, the -237 T variant was not obtained from any of the plasmids, with all clones possessing the wild type -237 C variant.

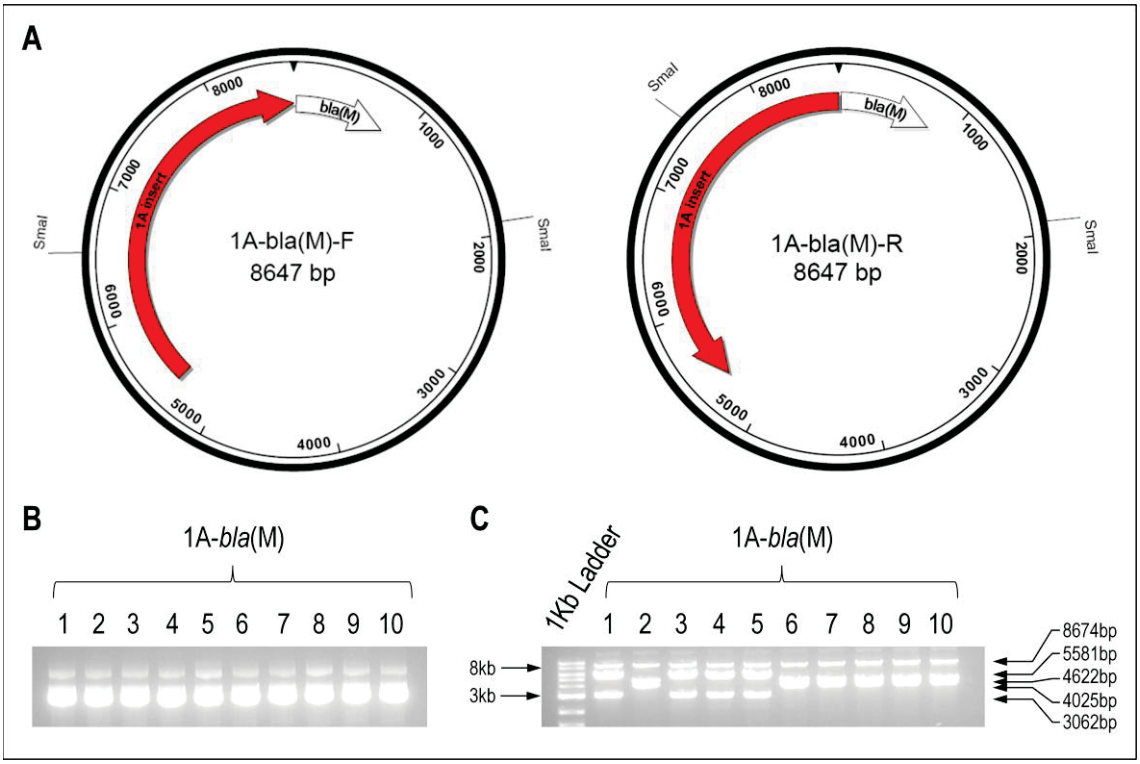

Figure 5.17 Production of the *SLC11A1* expression plasmid 1A-*bla*(M). (A) Maps of the 1A-*bla*(M) plasmids in the forward and reverse orientation showing the *SLC11A1* promoter insert 1A cloned upstream of the β-lactamase gene [*bla*(M)] and location of the *Sma*I restriction sites. (B) Isolated 1A-*bla*(M) plasmid DNA obtained from mini-prep (Section 2.2.2.4). (C) Restriction digestion of 1A-*bla*(M) plasmids with *Sma*I to verify that the cloned insert was the correct size and to determine the orientation of the insert. Forward orientation insert produced bands 4025 and 4622bp while reverse orientation plasmids produced bands 3062 and 5581bp.

5.3.2.3.1 In Vitro Site-Directed Mutagenesis to Generate the -237 T Variant

The use of the pooled human gDNA to obtain the common *SLC11A1* promoter variants did not result in the isolation of the -237 T variant. *In vitro* site-directed mutagenesis of the prepared 1A-*bla*(M) plasmid was used to generate the -237 T substitution in cis with $(GT)_n$ allele 3 in both forward and reverse orientations (Section 5.2.2.2.4) (Figure 5.18). The introduction of the T variant was validated by restriction digestion as the substitution of the C to a T introduces a cleavage site for the enzyme, *Msl*I (Figure 5.18B). Restriction digestion of a 208bp amplicon containing the -237C/T polymorphism confirmed that the *in vitro* site-directed mutagenesis successfully introduced the -237 T variant (in *cis* with $(GT)_n$ allele 3) in the forward and reverse orientation (Section 5.2.2.2.4) (Figure 5.18C).

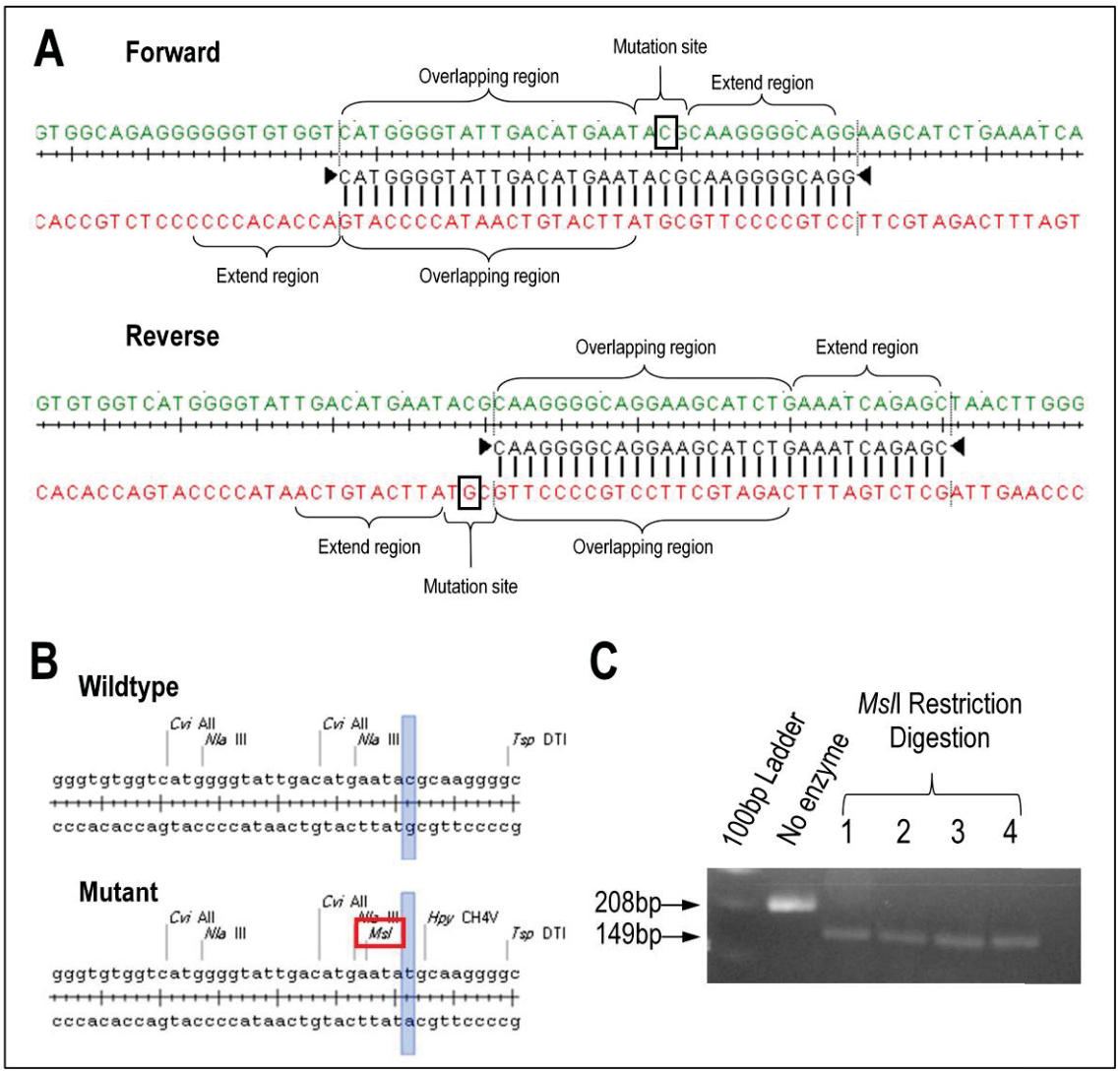

Figure 5.18 *In vitro* site directed mutagenesis for the production of the -237 T variant in *cis* with $(GT)_n$ allele 3. (A) Designed forward and reverse site-directed mutagenesis primers for the production of the -237 C to T substitution. The mutation site was introduced by the forward primer. (B) Restriction enzyme digestion map of mutagenesis site. The introduced T nucleotide (highlighted) introduces an *Msl*I restriction site. (C) Restriction digestion of plasmid clones after site directed mutagenesis. Cleavage of the 208bp product by *Msl*I into 149bp and 59bp signifies the presence of the -237 T variant.

5.3.2.3.2 Verification of 1A-bla(M) Clones by Sequence Analysis

Isolated 1A-*bla*(M) plasmids, for each of the common sequence variants (1A-*bla*(M) allele 2, allele 3 and allele T in the forward and reverse orientation), were selected for use in the *SLC11A1* promoter expression assays. Complete sequencing of selected plasmids was carried out (Section 5.2.2.2.5), to ensure that no other sequence variations, other than the selected common *SLC11A1* polymorphisms had been introduced. With the exception of a polymorphic $G(T)_n$ microsatellite, located 2474bp upstream the transcription start site (Section 5.3.2.6), complete sequencing of the selected 1A-*bla*(M)

plasmids did not identify sequence variants other than the selected variants at the $(GT)_n$ and -237C/T promoter polymorphisms. The 1A-*bla*(M) plasmid variants containing either $(GT)_n$ allele 2 or allele 3 contained the $G(T)_n$ microsatellite variants $G(T)_8G(T)_3$ or $G(T)_{11}$, respectively (analogous to that found naturally from the pooled human gDNA) (Section 5.3.2.6).

5.3.2.4 Production of the Smaller *SLC11A1* Promoter Plasmids

The smaller *SLC11A1* promoter regions designed to functionally test elements identified through the bioinformatic analysis (Figure 5.16) (Section 5.3.2.2) were cloned into the pGeneBLAzer-TOPO plasmid. The cloned and sequence verified 1A-*bla*(M) plasmids (allele 2, allele 3 and allele T in the forward orientation) (Section 5.3.2.3) were used as the template to produce the smaller *SLC11A1* promoter inserts (Section 5.2.2.2.1). These were subsequently cloned, isolated (Section 5.2.2.2.6), and verified for the incorporation of the correct insert and insert orientation (Section 5.2.2.2.8).

The amplification, cloning and verification of expression constructs resulted in the production of 42 different plasmids, containing the eight designed *SLC11A1* promoter regions (Table 5.6) (Figure 5.16). Promoter regions 1A, 7A, 7C, 8A, 8C and 8D contained both $(GT)_n$ and -237C/T polymorphisms (Figure 5.16). Therefore, six different promoter constructs were prepared for each of these regions (variants: allele 2, allele 3 and allele T in the forward and reverse orientation) (Table 5.6). Four different plasmids were produced for the promoter region 9C, containing only the -237C/T polymorphism (variants: allele C and allele T in the forward and reverse orientation), while the promoter region 10C did not contain any polymorphisms and, therefore, was only produced in the forward and reverse orientation (Table 5.6). The created *SLC11A1* promoter expression constructs were transfected into human cell lines to determine the influence of bioinformatically identified putative regulatory elements involved in *SLC11A1* transcription (Chapter 6, Part 3).

Table 5.6 Description of Variants of the Manufactured *SLC11A1* Reporter Constructs.

Plasmid Insert Size	Variants	
	Number	Description
1A-*bla* (M) 3267bp	6	Allele 2, Allele 3 and Allele T in the forward and reverse orientation.
7A-*bla* (M) 898bp	6	Allele 2, Allele 3 and Allele T in the forward and reverse orientation.
7C-*bla* (M) 581bp	6	Allele 2, Allele 3 and Allele T in the forward and reverse orientation.
8A-*bla* (M) 729bp	6	Allele 2, Allele 3 and Allele T in the forward and reverse orientation.
8C-*bla* (M) 411bp	6	Allele 2, Allele 3 and Allele T in the forward and reverse orientation.
8C-*bla* (M) 411bp	6	Allele 2, Allele 3 and Allele T in the forward and reverse orientation.
8D-*bla* (M) 165bp	6	Allele 2, Allele 3 and Allele T in the forward and reverse orientation.
9C-*bla* (M) 280bp	4	Allele C and Allele T in the forward and reverse orientation.
10C-*bla* (M) 148bp	2	Forward and reverse orientation.

5.3.2.5 Production of the Control Plasmids

An empty vector negative control was required for the *SLC11A1* promoter assays to determine a baseline expression level, thus allowing for correction of background fluorescence. However, due to the presence of the topoisomerases at each end of the linear vector (which allows for fast TOPO ligation of the insert), re-circularisation of the vector was not possible. There was neither a commercially available circular *bla*(M) plasmid nor literature documenting the removal of the topoisomerases enzymatically or chemically (and subsequent self-ligation) of any of the TOPO vectors. LaGier et al. (2007) used an empty vector as a control [empty-*bla*(M)], however, the paper did not specify how the empty vector was prepared. Restriction enzyme analysis of all the *SLC11A1* reporter plasmids (Sections 2.2.4.1 and 5.2.2.1.1) determined an empty vector [emp-*bla*(M)] plasmid could be produced using the 8A-*bla*(M) plasmid cut with the restriction enzymes *Bsu*36I and *Bst*XI to remove the insert (Figure 5.19A). Therefore, the emp-*bla*(M) plasmid was prepared (Section 5.2.2.2.9) by sequential digestion of the

8A-*bla*(M) plasmid, followed by self-ligation of the vector (Figure 5.19B). Restriction digestion, with the enzyme *RsaI*, verified that the correct emp-*bla*(M) plasmid had been created (Figure 5.19D).

Provided with the transfection kit was a positive control plasmid, UBC-*bla*(M), which has the ubiquitously expressed, ubiquitinase C promoter, located upstream of the β-lactamase gene. This provided a positive control for use in the transfection studies.

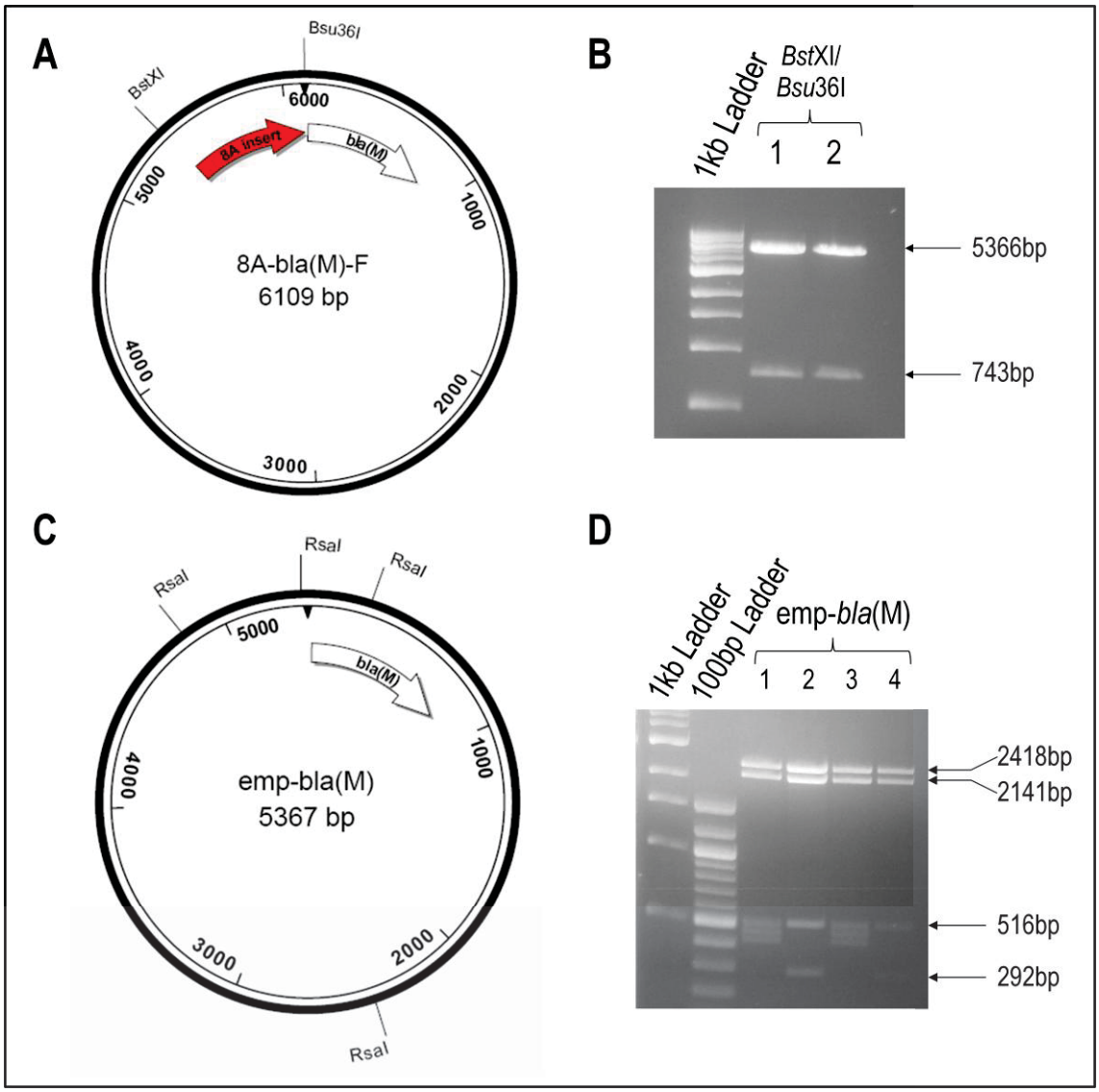

Figure 5.19 Production of the negative control emp-*bla*(M) plasmid. (A) Restriction map of the 8A-*bla*(M) plasmid with the enzymes *Bst*XI and *Bsu*36I allowing the removal of the 8A insert. (B) Double restriction digestion showing the removed insert (743bp) and the linear vector (5366bp). (C) Restriction map of the ligated emp-*bla*(M) plasmid showing the positions of *Rsa*I sites. (D) Restriction digestion of isolated plasmids with clones 2 and 4 showing the correct banding pattern and successful production of the emp-*bla*(M) plasmid.

5.3.2.6 Identification of Novel Sequence Variants within the *SLC11A1* Promoter

Sequencing and alignment of the sequences of the different isolated 1A-*bla*(M) plasmid clones (Section 5.3.2.3.2) resulted in the identification of several novel promoter variants. A putative single base substitution was detected in one of the cloned *SLC11A1* promoter inserts. This was a base substitution of an A for a C at position -2578 (designated -2578A/C) (Figure 5.20A). Another substitution (G to A) was detected in the non-coding region of the first exon at position +128 (47 bases upstream of the translation start site). This is the first polymorphism to be reported within the 5'UTR of *SLC11A1* (Figure 5.20B) (Section 1.2.4.2). Each of these single base substitutions was identified in only one of the sequenced plasmids, suggesting that these identified substitutions may be rare novel polymorphisms. Alternatively, they may represent artifacts of the amplification and cloning process to produce the plasmid clones. Further sampling and sequencing is required to validate the identified novel sequence variants.

In addition to the two identified single base substitutions, a polymorphic $G(T)_n$ tract $[G(T)_nG(T)_3G(T)_3G(T)_5G(T)_2G(T)_2G(T)_6]$ was also identified 2474 bases upstream of the *SLC11A1* transcription start site (rs13035487) (Figure 5.20C). Three novel polymorphic variants [$G(T)_{14}$, $G(T)_{11}$ and $G(T)_{10}$], in addition to two previously reported variants [$G(T)_{12}$ and $G(T)_8G(T)_3$] were identified. The large region (3267bp) of the *SLC11A1* promoter amplified and cloned in the pGeneBLAzer plasmid to produce the 1A-*bla*(M) plasmid, allowed for the analysis of haplotype patterns between the different polymorphisms within the *SLC11A1* promoter (Table 5.7).

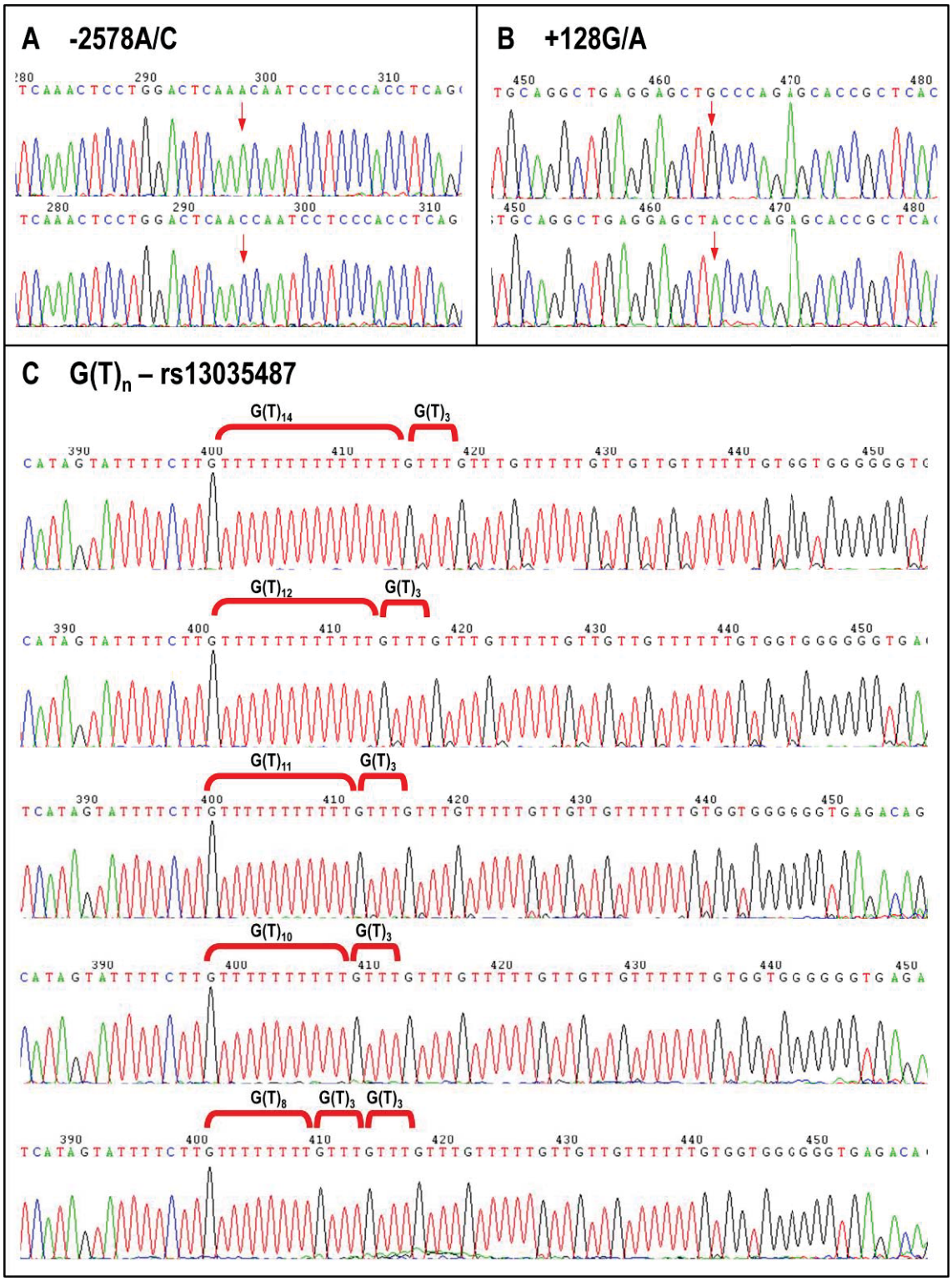

Figure 5.20 Sequencing electrophoregrams of novel *SLC11A1* promoter sequence variants. Two single base substitutions were identified, one 2578bp upstream of the transcription start site (A), resulting in the substitution of an A nucleotide for a C, and a second at position +128 and 47 bases before the translation start site (B), resulting in a G to A substitution. (C) Five alleles (of which three are novel) of a $G(T)_n$ microsatellite (rs13035487) were identified.

From the 17 1A-*bla*(M) plasmids, which were sequenced, the allelic variants $G(T)_8G(T)_3$ and $(GT)_n$ allele 2 were always identified in *cis* with each other (5 of 17 plasmids), while $(GT)_n$ allele 3 was only identified with the four other identified $G(T)_n$ alleles, notably $G(T)_{11}$ (8 of 17 plasmids) (Table 5.7). It is not known if polymorphic variants at the $G(T)_n$ polymorphism (at -2474) have an effect on the expression levels of *SLC11A1*, however, due to the high level of LD that exists within the *SLC11A1* promoter (especially $(GT)_n$ allele 2 and $G(T)_8G(T)_3$), the observed association of the *SLC11A1* promoter microsatellite $(GT)_n$ alleles with infectious and autoimmune disease may be due to potential LD with the $G(T)_n$ polymorphism located further upstream.

Table 5.7 *SLC11A1* Promoter Haplotypes at the $G(T)_n$, Promoter $(GT)_n$ and -237C/T Polymorphic Sites.

$G(T)_n$ Allele	$(GT)_n$ Allele	-237	Number*
$G(T)_{14}$	3	C	1
$G(T)_{12}$	3	C	1
$G(T)_{11}$	3	C	8
$G(T)_{10}$	3/9	C	2
$G(T)_8G(T)_3$	2	C	5

*Number of plasmids with polymorphism combination (n=17)

Further sampling and sequencing is required to validate the identified novel sequence variants and to determine the extent of LD between promoter variants. However, validation of these novel sequence variants was beyond the scope of this current study (Section 6.4.6.6).

5.4 DISCUSSION

5.4.1 *In Silico* Identification of Putative Elements Involved in *SLC11A1* Transcription

Bioinformatic analyses were used to assess the *SLC11A1* promoter to identify important regions for the binding of putative regulatory elements that may modulate *SLC11A1* expression. The findings of the bioinformatic studies guided the design of promoter constructs to functionally determine whether identified putative promoter regions could regulate *SLC11A1* expression. The majority of data from the bioinformatic assessment indicated that the important *SLC11A1* promoter elements/regions were located within a 700bp region, surrounding the transcription start site (-500bp to +200) (Figure 5.14). Therefore, this 700bp region formed the focus of the reporter analyses (Section 5.3.2.2).

The bioinformatic studies showed that a high level of conservation existed upstream of TSS1 (-28 to -70). While TFBS searches did not identify elements associated with the formation of the basal transcriptional complex (for example TATA box or TAF/TFIID elements) (Section 5.3.1.4.1), the positioning, as well as the extremely high level of conservation (Sections 5.3.1.2 and 5.3.1.3) suggested that this region could be the site for the formation of the basal transcriptional complex. Furthermore, a high level of homology was also identified after the two transcription start sites in the 5' UTR and first intron of *SLC11A1* (Section 5.3.1.2). In particular, the fourth and fifth highest scoring WeederH elements were located after the transcription start site (Section 5.3.1.3), suggesting either the presence of a core promoter element (i.e. DPE) or non-core elements (Figure 5.14). The *SLC11A1* promoter expression constructs were designed to determine a minimal promoter region through the systematic shortening of the *SLC11A1* promoter around the region displaying the highest level of conservation (*SLC11A1* promoter region 10C, Figure 5.16). Furthermore, constructs were designed to determine if the identified putative elements, located after the transcription start site, modulated *SLC11A1* expression. The *SLC11A1* promoter constructs were designed to also allow for the systematic determination of *SLC11A1* promoter regions which enhance expression (Figure 5.16). Once these regions were identified, they could be further assessed, according to the bioinformatic data collected, to determine putative transcription factor candidates (Section 5.3.1.4.2).

From the bioinformatic analyses completed in this study, and conclusions from other studies, there is conflicting evidence regarding the level of conservation at the $(GT)_n$ microsatellite repeat, and therefore, the mechanism by which the microsatellite functions to enhance transcription. While a repetitive GT unit was identified in the promoter region of all *SLC11A1* homologs (Section 5.3.1.2), the clustalW alignment indicated poor conservation of the repetitive sequence (Figure 5.8), suggesting that the repeat may play a topological role, as opposed to being involved in the binding of transcription factors in a sequence specific manner. However, another previously published alignment of four *SLC11A1* homologs, which only included the GT repeat region, showed a high level of conservation at the microsatellite repeat (Awomoyi, 2007), consistent with conserved elements identified from the WeederH analysis (Figure 5.9) and recruitment of the transcription factor HIF-1α to these elements (Bayele *et al.*, 2007) (Figure 5.13). The clustalW alignment, completed in this study, failed to identify conservation within the $(GT)_n$ microsatellite region due to the large 3000bp region selected for the analysis. While other features of the selected 3000bp *SLC11A1* homolog promoters were well aligned (for example the translation start site), the differing locations of the GT repeats between the different homolog promoters meant they were not aligned in the current analysis, thus accounting for the observed lack of conservation. Therefore, it appears that the $(GT)_n$ microsatellite repeat functions to modulate *SLC11A1* expression through both a topological function (i.e. transcriptional enhancement due to the formation of Z-DNA [Section 5.3.1.5]), as well as recruitment of the transcription factor HIF-1α to conserved sequence elements, in a sequence specific manner.

The bioinformatic analysis of the *SLC11A1* promoter identified a significant number of putative elements located throughout the promoter region (Figure 5.13). A comparison of identified elements from the different *in silico* programs showed a high degree of correlation (Figure 5.14). Since the compilation of this data, three subsequent studies have identified transcription factor binding to sequence elements within the *SLC11A1* promoter (Section 5.3.1.6). Comparison of the *in silico* data with these experimentally determined promoter elements indicates a significant level of concordance between the published sites and those identified by bioinformatic analyses in the current study. The level of concordance suggests that the bioinformatic assessment completed has significant predictive ability to discover other elements within the *SLC11A1* promoter

involved in transcriptional regulation. This provides greater confidence in the methodology employed for the design and production of the promoter constructs and a high level of confidence that the prepared promoter constructs will likely identify functional regions involved in the regulation of *SLC11A1* expression.

5.4.2 Mechanism of Differential *SLC11A1* Expression Mediated by the Functional Promoter Polymorphisms

Allelic variants at the $(GT)_n$ microsatellite and -237C/T promoter polymorphisms have been shown to differentially regulate *SLC11A1* expression. At the $(GT)_n$ microsatellite repeat, reporter constructs indicated that allele 3, with 9 GT repeats, mediated a higher level of *SLC11A1* expression, as compared to allele 2 (10 GT repeats) (and the other alleles that occur at low frequencies), with or without exposure to exogenous stimuli (Figure 1.8). Due to the role *SLC11A1* plays in the activation of a Th1 mediated immune response, the $(GT)_n$ alleles have been the focus of a significant number of studies assessing the association of this microsatellite with the incidence of disease (infection, autoimmune/inflammatory disease and cancer), with growing evidence showing that $(GT)_n$ allele 3 confers susceptibility to autoimmune disease (but resistance to infection), while allele 2 predisposes an individual to infectious disease (but resistance to autoimmune disease). Similarly, the -237 T variant resulted in a significantly lower level of *SLC11A1* expression (comparable to the expression level of $(GT)_n$ allele 2), as compared to the wild type -237 C variant (Section 1.3.3). The mechanism by which the promoter variants at these polymorphisms modulate differential levels of *SLC11A1* expression is yet to be elucidated.

The transcriptional enhancement modulated by the $(GT)_n$ microsatellite repeat has been attributed, in part, to the ability of the microsatellite to form Z-DNA (Blackwell, 1996, Searle and Blackwell, 1999). Z-DNA is an alternative DNA conformation, which has been shown to enhance transcription (Section 5.1.3.2). Bioinformatic (Section 5.3.1.5) and experimental analyses have shown the ability of the $(GT)_n$ microsatellite form to Z-DNA *in vivo* during *SLC11A1* transcription (Bayele *et al.*, 2007, Xu *et al.*, 2011). Therefore, it was hypothesised that the ability of the $(GT)_n$ promoter alleles to modulate differing *SLC11A1* expression levels would be attributable to differences in the ability of each allele to form Z-DNA (Sections 5.1.4.2.1 and 5.3.1.1). Thus, high *SLC11A1*

expression, driven by $(GT)_n$ allele 3, would be due to an increased propensity to transition to Z-DNA, compared to allele 2. Bioinformatic analysis of allelic variants at the $(GT)_n$ microsatellite repeat for their Z-DNA forming propensity, found the ability of the individual $(GT)_n$ alleles to form Z-DNA did not correlate with previously reported promoter activity for the individual alleles, but was associated with the length of the microsatellite repeat, consistent with previous observations (Nordheim *et al.*, 1982) (Section 5.3.1.5.1). The Z-Hunt analysis of the different $(GT)_n$ microsatellite alleles found that $(GT)_n$ allele 2 (15167.83), with 10 GT repeats, had a higher Z-score than allele 3 (12598.14) (9 GT repeats) (Section 5.3.1.5.1), suggesting that allele 2 would have an increased propensity to form Z-DNA, and therefore, would drive higher *SLC11A1* expression, as compared to allele 3. The contradictory findings between the Z-Hunt analysis (which suggested that allele 2 possessed greater transcriptional activity) and the previously determined promoter activity of the $(GT)_n$ alleles (which show allele 3 drives higher *SLC11A1* expression), suggests that the ability of the individual $(GT)_n$ alleles to modulate differential *SLC11A1* expression is not mediated by differences in the ability of the alleles to form Z-DNA to enhance transcription, but due to an alternative mechanism(s).

Bioinformatic analysis aimed at understanding the mechanism underlying the difference in the level of expression mediated by the -237C/T polymorphism found that the presence of the -237 C or T variant did not affect the Z-score of the $(GT)_n$ microsatellite repeat (Section 5.3.1.5.1). This suggests that differences in the level of expression of *SLC11A1*, mediated through variants at the -237C/T polymorphism, are not due to these sequence variants bringing about differences in the propensity of the microsatellite repeat to form Z-DNA. Furthermore, this suggests that the -237C/T polymorphism may function to alter *SLC11A1* expression independently of the differential level of expression modulated by allelic variants at the $(GT)_n$ repeat. Further bioinformatic analysis did not identify transcription factor binding at the location of the -237C/T polymorphism in the presence of the commonly occurring C variant, however, TFBS searches identified an element for the recruitment of the ubiquitously expressed transcription factor, Oct-1, in the presence of the T variant (Section 5.3.1.4.3). The introduction of this element and recruitment of Oct-1 to the *SLC11A1* promoter during transcription may be responsible for the lower *SLC11A1* expression level observed in the presence of the -237 T variant.

To further assess the mechanism by which the $(GT)_n$ and -237C/T polymorphisms alter *SLC11A1* expression, multiple *SLC11A1* promoter constructs were produced for each promoter region designed (Figure 5.16), with each plasmid differing only by the allelic variant present (Section 5.3.2.4). The promoter constructs containing the different allelic variants were designed to enable the identification of promoter regions, where transcription factors may be located, which are differentially regulated by the different promoter variants. This may lead to the identification of the mechanism by which variants at the $(GT)_n$ and -237C/T modulate differential levels of *SLC11A1* expression.

5.4.3 Conclusion

Results of the completed *in silico* analysis of the *SLC11A1* promoter were used as a guide for the functional experiments aimed at understanding the mechanisms of *SLC11A1* transcription and how allelic variants within the promoter function to modulate differential *SLC11A1* expression. The design of the promoter constructs, based on the findings of the bioinformatic analysis has enabled a focused approach (as opposed to the random cloning of different promoter segments), to facilitate the determination of the functional importance of the identified putative promoter elements. The promoter activity of the 42 designed and prepared *SLC11A1* promoter constructs were determined *in vivo* using human cell lines. The results of the reporter assays are presented in Chapter 6.

CHAPTER 6 – FUNCTIONAL ANALYSIS OF THE *SLC11A1* PROMOTER

PART 3: Analysis of the *SLC11A1* Promoter using Promoter Assays.

6.1 INTRODUCTION

Studies assessing the association of functional variants of the *SLC11A1* promoter with the incidence of infectious and autoimmune diseases have produced conflicting observations (Section 1.3.4). These studies have attempted to determine if there is an association with disease incidence in the absence of functional knowledge of the regulatory mechanisms controlling *SLC11A1* transcription, and the mechanisms mediating the differential expression of *SLC11A1* observed in the presence of the different promoter variants. The current study adopted an integrated approach utilising a combination of *in silico* and *in vivo* analyses, to gain an understanding of *SLC11A1* promoter function and regulation.

In the previous chapter, *in silico* bioinformatic analyses of the *SLC11A1* promoter were completed to identify putative regulatory regions/elements involved in the expression of *SLC11A1* (Chapter 5, Part 1). The *in silico* analyses indicated that the important *SLC11A1* promoter elements/regions were located within a 700bp region (-500 to +200) surrounding the transcription start site. Furthermore, a highly conserved 40bp region upstream of the transcription start site (-70 to -28), and putative elements in the 5'UTR and into the first intron were also identified (Figure 5.14). Based on the findings of the bioinformatic analyses, *SLC11A1* promoter regions of varying lengths (Figure 5.16) were cloned into a reporter vector to empirically determine the promoter activity driven by each of the elements identified *in silico* (Chapter 5, Part 2).

Where the *SLC11A1* promoter regions contained either the $(GT)_n$ or -237C/T polymorphisms, multiple promoter constructs which contained the different polymorphic variants were designed and cloned for each promoter length. This strategy was aimed at identifying promoter regions containing elements for the recruitment of transcription factors that may interact differently with the polymorphic variants to modulate *SLC11A1* expression. Where promoter regions contained both the $(GT)_n$ and -237C/T polymorphisms, three promoter constructs were prepared to contain the different combinations of polymorphic variants. These were termed allele 2 [combined $(GT)_n$ allele 2 and -237 C], allele 3 [combined $(GT)_n$ allele 3 and -237 C] and allele T [combined $(GT)_n$ allele 3 and -237 T] (Section 5.3.2.2.2). When the cloned promoter region contained only the -237C/T polymorphism (*SLC11A1* promoter region 9C,

Figure 5.16), two plasmid variants were produced, and named allele C and allele T. Additionally, the different promoter regions, containing the different polymorphic variants, were cloned into the expression constructs in both the forward and reverse orientation to determine if the *SLC11A1* promoter could mediate bidirectional transcription (Section 5.3.2.2.3). In total, 42 different *SLC11A1* promoter constructs were designed and prepared (Table 5.6).

In the current chapter, the 42 *SLC11A1* promoter constructs were transfected into monocytic and non-monocytic human cell lines, in parallel with the negative and positive control plasmids, emp-*bla*(M) and UBC-*bla*(M), respectively, to functionally determine the promoter activity of different regions of the *SLC11A1* promoter (Chapter 6, Part 3). Furthermore, the mechanism by which promoter variants differentially modulate *SLC11A1* expression, and whether the *SLC11A1* promoter could mediate bidirectional transcription were also investigated. The *SLC11A1* promoter regions identified to alter promoter activity were further assessed based on the bioinformatic data, to identify candidate TFBS.

6.1.1 Detection of *SLC11A1* Promoter Activity using the GeneBLAzer Reporter System

The different *SLC11A1* promoter regions were cloned into the pGeneBLAzer reporter vector upstream of a β-lactamase gene (*bla*) (Figure 6.1A). β-lactamase is a bacterial enzyme which has been developed as a reporter to quantify promoter activity in the pGeneBLAzer plasmid in mammalian cells. After transfection, β-lactamase expression is directed by the cloned promoter region within the construct. Promoter activity (i.e. expression level of β-lactamase) is measured by the addition of a fluorescence resonance energy transfer (FRET) molecule, CCF2-AM, composed of a coumarin (donor) and fluorescein (acceptor) moiety (Oosterom *et al.*, 2005, Zlokarnik *et al.*, 1998). When added to live cells, the CCF2-AM FRET molecule passes freely into the cell, where cytoplasmic esterase's modify the molecule and concentrate the substrate within the cell (Figure 6.1B). When excited at 409nm, the intact CCF2-AM molecule results in a green fluorescence emission at 520nm. The expressed β-lactamase cleaves the CCF2-AM substrate resulting in the physical separation of the coumarin and fluorescein moieties, which, upon excitation at 409nm, produces a blue fluorescence

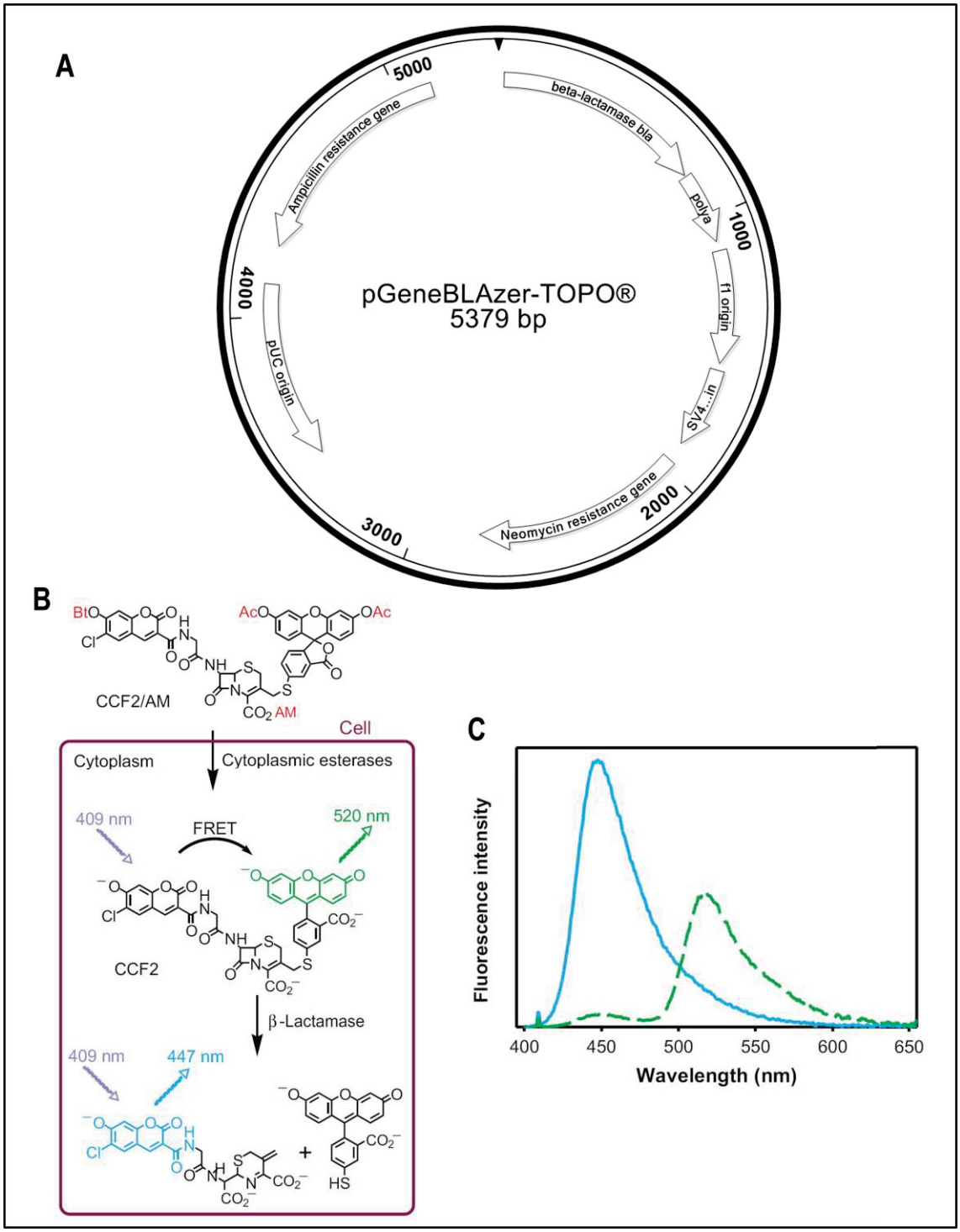

Figure 6.1 GeneBLAzer detection of promoter activity. (A) Map of the pGeneBLAzer reporter plasmid (Section 5.2.2.1.1). (B) After diffusion across the cell membrane, the CCF2-AM substrate is concentrated within the cell, due to modification of the FRET molecule. Excitation of CCF2 at 409nm results in a transfer of energy from the donor to the acceptor, generating green fluorescence emission at 520nm. β-lactamase expression, driven by the cloned promoter region, cleaves the CCF2 molecule (removal of the acceptor), where excitation at 409nm results in the emission of blue fluorescence at 447nm (Zlokarnik *et al.*, 1998). (C) Cleaved (blue) and uncleaved (green) CCF2 substrate have different emission peaks (Zlokarnik *et al.*, 1998).

emission at 447nm (Figure 6.1C) (Zlokarnik *et al.*, 1998). Promoter activity is determined by the ratio of blue to green fluorescence (i.e. cleaved and uncleaved substrate, respectively). This ratiometric determination reduces experimental well to well variation, which may arise from variation in cell density, cell size or signal intensity (Oosterom *et al.*, 2005, Qureshi, 2007). Therefore, by extension, the observed fluorescence intensity (due to β-lactamase expression driven by the cloned promoter region) is a measure of *SLC11A1* promoter activity.

6.2 MATERIALS AND METHODS

6.2.1 Materials

Dulbecco's Modified Eagle Medium (DMEM), RNase AWAY, Roswell Park Memorial Institute (RPMI) 1640 medium, HEPES buffer, L-gluatamine, amino acids, TrypLE Express, fetal bovine serum (FBS), Recovery Cell Culture Freezing Medium, Hanks buffered salt solution (HBSS), OPTIMEM, Accutase, Lipofectamine 2000, Lipofectamine LTX, SuperScript III First-Strand Synthesis Supermix, SYBR GreenER qPCR SuperMix Universal, and the CCF2-AM Loading Kit were purchased from Invitrogen (California, USA). Methanol, formaldehyde (37%), phorbol myristate acetate (PMA), 0.4% trypan blue, LPS, and recombinant human IFN-γ were purchased from Sigma-Aldrich. Tissue culture flasks (T75 and T175) for the culture of U937 and THP-1 cell lines were purchased from Sarstedt (Nümbrecht, Germany). Tissue culture flasks for the culture of 293T cells, 6-well tissue culture plates, 15ml and 50ml centrifuge tubes and 20 gauge needles were purchased from BD Biosciences (New Jersey, USA). Costar 96 well optically clear black walled tissue culture plates were purchased from Corning (Massachusett, USA). The Amaxa Human Monocyte Nucelofection system was purchased from Lonza (Basel, Switzerland). The 50μm gauze was obtained from Sefar Filter Specialist (Thal, Switzerland) and the RNeasy Plus Mini Kit from Qiagen (Maryland, USA).

6.2.1.1 Cell Lines

The cell lines used for transfection of *SLC11A1* promoter constructs to determine promoter activity included:

- 293T cells (human embryonic kidney cell line) (kindly donated by Lisa Sedger, University of Technology Sydney).
- U937 (histiocytic cell line) (kindly donated by Stella Valenzuala, University of Technology Sydney).
- THP-1 (monocytic leukaemia cell line) (purchased from the European Collection of Cell Cultures).

6.2.2 Methods

6.2.2.1 Cell Culture Techniques

6.2.2.1.1 Sterility and Containment

All mammalian cell culture work was conducted in a class II laminar flow cell culture cabinet. Sterilisation of equipment and the working area of the cabinet was completed by cleaning with 70% (v/v) ethanol followed by exposure to UV light for 15min prior to the commencement of any cell culture work. After UV sterilisation, all media, cells or equipment were thoroughly cleaned with 70% (v/v) ethanol when moved in or out of the cell culture cabinet. Unless otherwise stated, all media was warmed to 37^{o}C prior to use. All cell lines were grown at 37^{o}C in a humidified chamber with 5% CO_2.

6.2.2.1.2 Culture and Maintenance of Human Embryonic Kidney 293T Cells

The human embryonic kidney 293T cell line (293T) was created by adenoviral transformation of healthy human aborted fetus embryonic kidney cells (Graham *et al.*, 1977). The 293T cell line is an adherent cell line, which was maintained in DMEM supplemented with 20mM HEPES, 2mM L-glutamine and 10% (v/v) FBS. Cells were passaged every 3-4 days with a 1 in 10 to 1 in 20 split (doubling time ~18-20h) (Section 6.2.2.1.5).

6.2.2.1.3 Culture and Maintenance of U937 Cells

The cell line U937 is a histiocytic cell line originating from an individual suffering from diffuse histiocytic lymphoma (Sundström and Nilsson, 1976). The U937 cell line is a non-adherent cell line and was maintained in DMEM supplemented with 20mM HEPES, 2mM L-glutamine and 10% (v/v) FBS. Cells were maintained at a density of between 0.3-1.0×10^{6}cells/ml and subcultured every 3-4 days (doubling time of ~30h) (Section 6.2.2.1.5).

6.2.2.1.4 Culture and Maintenance of THP-1 Cells

The THP-1 cell line, a non-adherent acute monocytic leukaemia cell line (Tsuchiya *et al.*, 1980), was originally obtained at a passage number of 14. THP-1 cells were cultured in RPMI 1640 medium supplemented with 20mM HEPES, 2mM L-glutamine and 10%

(v/v) FBS. Cells were maintained at a density of between 0.3-0.8×10^6cells/ml and passaged every 3-5 days using a 1 in 4 to 1 in 5 split (doubling time ~40h) (Section 6.2.2.1.5). Cells between passage number 14 and 25 were used for experiments.

6.2.2.1.5 Passaging of Cell Lines

Enumeration of Cell Density

For the passage of cell lines and for experimental work, cell density was determined using a haemocytometer. Cells were loaded by capillary action into a haemocytometer and viewed under an inverted microscope. The cell density was determined using the mean number of cells within the four large corner squares on the counting grid, multiplied by a factor of 10^4 and the dilution factor (if applicable).

Adherent Cell Lines

To subculture adherent cells, the media was removed and 3ml of TrypLE Express was washed over the cell monolayer and then removed. A further 8ml of TrypLE Express was then added to the flask, which was incubated at 37^{o}C for approximately 4min. Cell detachment was verified by viewing the cells using an inverted microscope. Cells were dispersed using a pipette and 1ml of cell suspension was removed and added to a 50ml centrifuge tube containing 5ml of media. After centrifugation (1000rpm, 2min), the supernatant was removed and the cells were resuspended in 10ml of fresh culture medium. The appropriate volume (generally 1-5ml) of cell suspension was then seeded into new T75 flasks and fresh culture medium was added to the flask to a final volume of 20ml. The cells were incubated at 37^{o}C with 5% CO_2.

Non-adherent Cell Lines

Non-adherent cells were subcultured by removing 5-10ml of confluent cell suspension (0.8×10^6cells/ml) and adding it to a centrifuge tube. After centrifugation (1000g, 4min) the cells were resuspended in fresh media (5-10ml) and the required number of cells were transferred to new T75 tissue culture flasks. Fresh culture medium was added to the flask for a final volume of 20ml and the cells were incubated at 37^{o}C with 5% CO_2.

6.2.2.1.6 Determination of Cell Viability

The trypan blue viability assay was used as a relative measure of cell death. The vital dye trypan blue (0.4%) was added to an equal volume of media containing suspended cells, loaded into a haemocytometer, and cells were observed immediately. The number of blue (dead) cells counted in a total of 100 cells represented the percentage of non-viable cells.

6.2.2.1.7 Reviving Mammalian Cell Lines

Cell stocks, maintained in liquid nitrogen, were thawed rapidly in a 37^{o}C water bath. Once thawed, all of the media containing the cells was removed and added dropwise to 4ml of media (containing 20% (v/v) FBS) with gentle mixing. Cells were pelleted (500rpm, 8min) and resuspended in 5ml of fresh culture medium (containing 20% (v/v) FBS) and transferred to a T25 tissue culture flask, and incubated at 37^{o}C and 5% CO_2. Flasks containing THP-1 cells were maintained in an upright position to concentrate cells for 5-7 days.

6.2.2.1.8 Storage of Mammalian Cell Lines

Cells were frozen down when in the log phase of growth. Cells were removed from the tissue culture flasks (Section 6.2.2.1.5), resuspended in Recovery Cell Culture Freezing Medium at a density of 1×10^{6}cells/ml, and 1ml of the cell suspension was added to individual cryogenic tubes. To achieve a slow rate of freezing, cryogenic tubes were placed in a freezing apparatus containing isopropanol and frozen at -80^{o}C for 24h. Cells were then transferred to storage in liquid nitrogen.

6.2.2.1.9 Differentiation and Cytokine Stimulation of THP-1 Cells

Differentiation of THP-1 cells was completed by the addition of PMA to the culture medium to achieve a final concentration of 5ng/ml or 100ng/ml. Cells were observed for adherence 24h after initiation of differentiation. Removal of adherent, PMA-differentiated THP-1 cells, after 48h, was achieved using Accutase following the same procedure used for the removal of adherent cells (Section 6.2.2.1.5). However, cells were washed with phosphate buffered saline (PBS) prior to the addition of the Accutase. Stimulation of THP-1 cells was achieved by supplementation of the culture medium with IFN-γ (100U/ml) and LPS (0.1μg/ml) prior to the addition of cells.

6.2.2.2 Transfection Protocols

6.2.2.2.1 Transfection of 293T Cells using Lipofectamine 2000

The 293T cells were seeded into 96 well optically clear bottom black walled plates or 6-well tissue culture plates (for flow cytometric analysis) 24h prior to transfection of cells with the *SLC11A1* promoter constructs (Figure 5.16). For the 96 or 6 well plates, 2.5×10^4 or 2.5×10^6 cells were added to each well, respectively. Plates were incubated at 37^{o}C with 5% CO_2 until the cells were transfected.

Lipofectamine 2000 was used to transfect 293T cells with the *SLC11A1* promoter constructs (Section 5.2.3.4), or the positive and negative control plasmids [UBC-*bla*(M) and emp-*bla*(M), respectively] (Section 5.3.2.5). After 24h, cells were observed for adherence using an inverted microscope. Transfections in 96 well plates were conducted in replicates of four. For each plasmid transfected, solution A (2µg plasmid DNA in a final volume 50µl OPTIMEM) and solution B (4µl Lipofectamine 2000 and 46µl OPTIMEM) were prepared separately, then mixed together and allowed to stand for 20min. The media was then carefully removed from all wells and cells were washed in 100µl of OPTIMEM. The OPTIMEM was removed completely and 20µl of lipid/DNA complexes (combined solution A and B) was added in each well, followed by the addition of 100µl fresh culture medium. Transfection of 293T cells in 6 well plates was completed in a similar fashion to cells in 96-well plates, however, increased volumes were used: solution A (4µg DNA in 250µl OPTIMEM) and solution B (10µl Lipofectamine 2000 and 240µl OPTIMEM). After transfection, the cells were incubated (37^{o}C, 5% CO_2) and, after 24h, the cells were loaded with substrate (Section 6.2.2.2.4) and fluorescence was detected using a plate reader (Section 6.2.2.3.3) or flow cytometer (Section 6.2.2.3.4).

6.2.2.2.2 Transfection of THP-1 Cells with Lipofectamine LTX

Prior to transfection (24h), THP-1 cells were passaged into fresh media to ensure that the cells were in log phase growth (Section 6.2.2.1.5). At the time of transfection, cells were approximately 50% confluent (4×10^5cells/ml). Liposomes were prepared by the addition of 1µg plasmid DNA (*SLC11A1* promoter constructs or control plasmids) to 200µl of OPTIMEM, followed by the addition of 1µl of PLUS reagent. The sample was mixed gently, incubated at RT for 5min and 2.5µl of Lipofectamine LTX was added.

The sample was mixed gently and incubated at RT for 30min. THP-1 cells were removed from the flask, washed in OPTIMEM, counted (Section 6.2.2.1.5) and resuspended in OPTIMEM at a density of 2×10^5cells/ml. Cells were seeded into 12 well tissue culture plates (2×10^5cells/well) and 200µl of the DNA-lipid complexes were added dropwise into the well and mixed gently. Cells were incubated at 37°C with 5% CO_2 and, 24h post-transfection, cells were loaded with CCF2-AM substrate (Section 6.2.2.2.4) and fluorescence was detected using a plate reader (Section 6.2.2.3.3) or flow cytometer (Section 6.2.2.3.4).

6.2.2.2.3 Transfection of THP-1 Cells Using Nucleofection

Prior to transfection (24h), THP-1 cells were split into fresh culture medium to ensure that cells were in log phase growth. At the time of transfection, cells were approximately 50% confluent. Prior to transfection, 6 well tissue culture plates, containing 3ml human monocyte nucleofector media (supplemented with 20% (v/v) FBS and 1% amino acids), were incubated at 37°C with 5% CO_2 until required. Following the optimised protocol of Schnoor et al. (2009), THP-1 cells were transfected using the Amaxa Human Monocyte Nucelofection Kit. Each transfection was conducted using 2.5×10^6cells in 100µl human monocyte nucleofector solution. The appropriate *SLC11A1* promoter plasmid, or supplied pmaxGFP vector (0.5µg), was then added to the cells in nucleofector solution, mixed well and transferred to the nucleofection cuvette. The cells were electroporated using a Nucleofector (Lonza) set to the Y-001 program, and 500µl of human monocyte nucleofector media (supplemented with 20% (v/v) FBS and 1% amino acid) was added to the cuvette (post-nucleofection) and the contents were mixed well. Cells were removed from the cuvette using a sterile pipette and transferred to a single well of the pre-incubated 6 well tissue culture plate, containing human monocyte nucleofector media. Cells were mixed well and incubated at 37°C with 5% CO_2 and, 24h post-transfection, cells were loaded with substrate (Section 6.2.2.2.4) and promoter activity was determined by flow cytometry (Section 6.2.2.3.4).

6.2.2.2.4 Addition of Substrate (CCF2-AM) For Reporter Analysis

To detect promoter activity of cells transfected with *SLC11A1* promoter constructs (Sections 6.2.2.2.1, 6.2.2.2.2 and 6.2.2.2.3), the transfected cells were initially analysed

for cellular morphology and/or adherence using an inverted microscope. Loading of the coumarin cephalosporin fluorescein (CCF2-AM) substrate was carried out according to the manufacturer's general loading protocol for *in vivo* detection. Firstly, 6X loading solution was prepared (solution A was added to solution B, mixed well, and then solution C was added) and wrapped in aluminium foil to avoid light exposure. When cells were analysed by flow cytometry or confocal microscopy, HBSS was substituted for solution C.

For substrate loading of 293T cells in 96 well plates (Section 6.2.2.2.1), the media was removed, cells were washed once with 100µl HBSS, and 100µl of fresh HBSS was added to each well. With the light in the class II laminar flow cabinet turned off, 20µl of the 6X loading solution was added to each well. Control wells, which did not contain cells, were prepared in parallel and these contained 100µl HBSS and 20µl 6X loading solution. The 96 well plate was incubated at RT for 60min, protected from light exposure. Promoter activity was determined by measurement of fluorescence intensity (blue and green) using a fluorescence plate reader (Section 6.2.2.3.3) or cells were analysed by confocal microscopy (Section 6.2.2.3.2).

For substrate loading of Lipofectamine LTX transfected THP-1 cells (Section 6.2.2.2.2), the cells were removed from the 12 well tissue culture plate, transferred to centrifuge tubes, washed once in HBSS, and resuspended in 400µl HBSS. Samples were split into replicates of four by transferring 100µl of cells from each well to a 96 well optically clear bottom black walled plate. The substrate was then loaded, as previously described for the 293T cells. Prior to the measurement of fluorescence intensity using the plate reader, the plate was centrifuged (1000g, 1min) to ensure that cells were located at the base of each well.

For flow cytometric analysis of the adherent, cell line 293T (Section 6.2.2.2.1), the media was removed from the 6 well tissue culture plates and the cells were removed from the wells by the addition of 1ml TrypLE Express. After 4min incubation (37^{o}C with 5% CO_2) the cells were transferred to 15ml centrifuge tubes and 3ml fresh medium was added to each tube followed by centrifugation (1000g, 4min). After removal of the supernatant, the cells were washed in 4ml of HBSS and 2ml of fresh HBSS was added followed by the addition of 6X loading solution. The cells were resuspended and passed

through 50µm gauze to remove any clumped cells or cellular debris. The cells were then incubated for 1h at RT (protected from light) and the promoter activity was determined by flow cytometry (Section 6.2.2.3.4).

For THP-1 cells transfected by nucleofection (Section 6.2.2.2.3), the cells were transferred to 15ml centrifuge tubes 24h post-transfection. The cells were centrifuged (1000g, 4min) and the supernatant was removed. The cells were resuspended in 1ml HBSS and divided into triplicate samples in a 96 well U-bottom plate, which was centrifuged (1000g, 4min), and the supernatant removed. Cells were resuspended in 100µl of HBSS and transferred to bullet tubes containing 200µl HBSS. Next, 60µl of 6X loading solution was added to each bullet tube and mixed well. The cells were incubated for 1h at RT (protected from light) and promoter activity determined by flow cytometry (Section 6.2.2.3.4). For analysis by confocal microscopy, 50µl of the washed and substrate loaded THP-1 cells were loaded into a well of a 96 well optically clear black wall plate. The plate was centrifuged (1000g, 4min at RT) to ensure cells were located at the bottom of the wells and cells were visualised by confocal microscopy (Section 6.2.2.3.2).

6.2.2.3 Analyses of Human Cell Lines Transfected with *SLC11A1* Promoter Constructs

6.2.2.3.1 Fluorescence/Light Microscopy Analysis of Human Cell Lines Transfected with the SLC11A1 Promoter Constructs

Analysis of *SLC11A1* promoter constructs transfected into human cell lines was completed using the Olympus BX-51 microscope using the X20 and X40 air objectives and the X60 and X100 oil immersion objective. For fluorescence analysis, excitation was completed using a mercury burner (Olympus U-RFL-T) with a peak at 404.7nm and WIB (bandpass 460-490 – blue) and WIG (bandpass 520-550 – green) emission filter cubes.

6.2.2.3.2 Confocal Microscopy Analysis of Human Cell Lines Transfected with the SLC11A1 Promoter Constructs

Confocal microscopy was conducted to assess the promoter activity of the *SLC11A1* promoter constructs after transfection into 293T (Section 6.2.2.2.1) and THP-1 (Section 6.2.2.2.2 and 6.2.2.2.3) cells, using a X40 air objective. Fluorescence analysis was

carried out with excitation at 405nm (UV) and two channels were used to detect the fluorescence emission, a blue filter cube (425-475nm, with the laser power set low and the gain adjusted to a medium level), and a green filter cube (500-550nm, with no laser power and the gain set at a medium level). The laser power and gain adjustments were varied for each experiment and the settings were determined by analysis of the untransfected cells. The green channel gain was set to ensure that the level of green fluorescence was below the level of saturation. The blue channel gain value was set so that no blue fluorescence was observable. Cells transfected with the negative and positive control plasmids (Section 5.3.2.5) and the *SLC11A1* promoter plasmids (Section 5.3.2.4) were then assessed for green and blue fluorescence levels (i.e. promoter activity). Cells were imaged in the Z-series and maximum intensity profile images of the Z-series were produced in NIS-Elements (Nikon).

6.2.2.3.3 Fluorescence Plate Reader Analysis of Human Cell Lines Transfected with the SLC11A1 Promoter Constructs

Fluorescence detection of promoter activity of transfected cells (in 96 well plates) was completed 60min after loading cells with the CCF2-AM substrate (Section 6.2.2.2.4). Fluorescence detection was carried out using the bottom-read Synergy HT plate reader (BioTek, Vermont, USA). The plate was analysed with 10 sample reads per well with an excitation filter of 400/30nm and detection was completed using 460/40 (blue fluorescence) and 528/20 (green fluorescence) emission filters, with sensitivities of 80 and 75, respectively.

Raw fluorescence intensity data was exported into Microsoft Excel and background fluorescence was subtracted, based on the mean value of the control wells which did not contain any cells, for both blue and green fluorescence data. The ratio of blue to green fluorescence was then determined for each well and the mean of the replicate samples represented the level of promoter activity for each *SLC11A1* promoter region. Graphs of promoter activity were generated by transferring the data from replicate samples into Graphpad Prism 5. The promoter activity of cells transfected with *SLC11A1* promoter constructs reported represents the trend from a minimum of three independent experiments. The level of promoter activity was assessed between each of the promoter constructs based on the fold change in fluorescence intensity between different constructs.

6.2.2.3.4 Flow Cytometric Analysis of Human Cell Lines Transfected with the SLC11A1 Promoter Constructs

Fluorescence detection of promoter constructs transfected into 293T (Section 6.2.2.2.1) and THP-1 (Section 6.2.2.2.2 and 6.2.2.2.3) cells was carried out using the BD LSR II flow cytometer with FACSDiva software (BD Biosciences). The cells were analysed with the following channels (and voltages): forward (326) and side (263) scatter and the fluorescence channels 530/30 (244) and 450/50 (262 and 230 for 293T and THP-1 cells, respectively). Generally, 3-5×10^4 events were acquired. Data was exported as FCS files from the FACSDiva software and imported into CellQuest (BD Biosciences) for analysis. From the forward and side scatter histogram, a gate (R1) was placed around the cell population of interest and events within R1 were further analysed according to fluorescence intensity.

For the analysis of the 293T cells transfected with promoter constructs, the cells in gate R1 were assessed through a dot plot of green (530/30) versus blue (450/50) fluorescence. A second gate (R2) was placed around the β-lactamase expressing cell population (the gate location was determined by analysis of CCF2-AM loaded untransfected cells and negative control emp-*bla*(M) plasmid transfected cells). Mean fluorescence intensity of cells within gate R2 was then determined (Figure 6.11).

For the analysis of THP-1 cells transfected with promoter constructs, the cells selected in gate R1 were displayed as a dot plot of green fluorescence (on x-axis) versus forward scatter. A second gate, R2, was placed around the high green fluorescing cell population, which represented the viable cell population. A dot plot of green versus blue fluorescence was then created for cells located in gate R2. The mean fluorescence intensity was determined for each sample by placing a gate, R3, around the transfected β-lactamase expressing cells using a similar method to that used to analyse 293T cells (Figure 6.13).

Raw mean fluorescence intensity data was imported into Microsoft Excel and the mean fluorescence intensity of untransfected cells was subtracted from the replicate raw data samples. The adjusted mean fluorescence intensities were tabulated using Graphpad Prism 5 to allow graphical representation of the data. The promoter activity of each of the *SLC11A1* promoter construct presented is representative of a minimum of three

independent experiments. The level of promoter activity was assessed between each of the promoter constructs based on the fold change in fluorescence intensity between different constructs. All flow cytometric dot plots shown were prepared by importing the FCS files into the software program FlowJo Flow Cytometry Analysis software (FlowJo, USA) where the gating parameters were replicated.

6.2.2.4 Staining Techniques for the Characterisation of the THP-1 Cell Line

SLC11A1 displays restricted expression to monocytes/macrophages (and other phagocytic cells, Section 1.1.3) and expression levels increase upon differentiation and stimulation. Characterisation of the THP-1 cell line was undertaken to determine if the cell line was representative of monocyte/macrophages, thereby providing a good model in which to study *SLC11A1* expression. The THP-1 cell line was assessed through the use of morphological and cytochemical stains. Furthermore, quantitative reverse transcriptase real-time PCR (Section 6.2.2.5) was carried out to ensure that *SLC11A1* was expressed in THP-1 cells.

6.2.2.4.1 Morphological Assessment of THP-1 Cells

Slides were prepared for May-Grunwald Giemsa staining by spreading approximately 0.6×10^6 THP-1 cells (in RPMI medium) across a glass slide and allowing cells to air dry. Slides were then fixed in methanol for 10min and placed in May-Grunwald stain for 5min. Slides were then transferred to Giemsa stain for 10min, rinsed in buffered water, and then the slides were placed in buffered water for 5min. Stained slides were allowed to air dry and mounted using a coverslip and DPX. Cells were analysed using the Olympus BX-51 microscope (Section 6.2.2.4.7).

6.2.2.4.2 Slide Preparation for Cytochemical Analyses

THP-1 cells (5×10^4 cells) were cytospun (Hettich Universal 32 centrifuge) onto glass slides (1250rpm, 4min) and slides were then air dried and fixed. Positive control slides, kindly donated by Gillian Rozenburg (Prince of Wales Hospitial, Australia), were stained in parallel with the THP-1 cells.

6.2.2.4.3 Periodic Acid-Schiff Staining

The periodic acid-schiff (PAS) stain tests for the presence of glycogen. A magenta colour denotes a positive result due to the Schiff stain combining with stable aldehyde groups (Figure 6.8A). Air dried cytospin slides (Section 6.2.2.4.2) were fixed in formal methanol (5ml 37% formaldehyde mixed with 45ml 100% methanol) for 15s and then rinsed with water for 10s and allowed to air dry. Slides were stained in periodic acid for 10min, rinsed in water and placed in Schiff's reagent for 30min. Slides were then rinsed in water for 5min and counterstained with Harris haematoxylin for 2min and rinsed again in water for 1min. Once air dried, slides were mounted using a coverslip and DPX. Cells were analysed using the Olympus BX-51 microscope (Section 6.2.2.4.7). Granulocytes at all stages of development stain positive (AML+), while 10-40% of lymphocytes show granular positivity on a negative background (ALL-). Monocytes and their precursors show variable diffuse positivity with superimposed fine granules (Hanly, 2001, Matutes *et al.*, 2006).

6.2.2.4.4 Sudan Black B Staining of THP-1 Cells

Sudan black B (SBB) is a lipophilic stain that binds irreversibly to an unknown granule component in granulocytes. A positive result is denoted by a black granular pattern in the cytoplasm (Figure 6.8B). Prepared THP-1 cells (Section 6.2.2.4.2) were fixed in concentrated formalin (formalin vapour) for 10min. To complete this, Whatman filter paper (size 14) was placed at the base of a perspex staining dish and a few drops of 37% formaldehyde were placed on the filter paper (until completely damp), which was allowed to stand for 10min with the lid on to produce the vapour. Slides were then placed into the staining dish supported on applicator sticks placed above the formalin soaked filter paper and allowed to stand for 10min. The fixed films were placed into the Sudan black B staining solution for 60min, washed in 70% (v/v) ethanol for 2min, and then rinsed briefly in water. Slides were counterstained in haematoxylin for 10min, washed in running water for 5min and allowed to air dry before cells were mounted with a coverslip and DPX. Cells were analysed using the Olympus BX-51 microscope (Section 6.2.2.4.7). Developing and mature granulocytes show a strong positive result (AML+), while lymphocytes and lymphoblasts are negative (ALL-), and monocytes/monoblasts show a negative result (Hanly, 2001, Matutes *et al.*, 2006).

6.2.2.4.5 Myeloperoxidase Staining of THP-1 Cells

Myeloperoxidase is located in the primary and secondary granules of granulocytes and their precursors. A positive result is denoted by the presence of a blue granular pattern in the cytoplasm (Figure 6.8C). Air dried cytospin slides (Section 6.2.2.4.2) were fixed in formal ethanol (5ml 37% formaldehyde mixed with 45ml 100% ethanol) for 1min and washed in running tap water for 20s and allowed to air dry. Washed fixed slides were placed into the peroxidase stain for 30s, washed in water for 30s, and then allowed to air dry before being mounted with DPX and a coverslip. Cells were analysed using the Olympus BX-51 microscope (Section 6.2.2.4.7). Developing and mature granulocytes are strongly positive (AML+) while lymphoblasts and lymphocytes are negative (ALL-). Monoloblasts are negative while monocytes stain positive or negative. The myeloperoxidase stain reflects results obtained from the SBB stain (Hanly, 2001, Matutes *et al.*, 2006).

6.2.2.4.6 Combined α-Naphthyl butyrate and AS-D Chloroacetate esterase Staining of THP-1 Cells

The combined α-naphthyl butyrate and AS-D chloroacetate esterase stain allows the differentiation of myeloid and monocytic cells on a single slide. It is commonly used to detect acute myelomonocytic leukaemia (AMML), which displays a dual phenotype (both granulocytic and monocytic). The combined stain is therefore a good way to differentiate between acute leukaemias of myeloid or monocytic origin or a mixture of the two (AMML). This stain was kindly completed by Prince of Wales Hospital Haematology Department. Fresh slides (Section 6.2.2.4.2) were fixed in formalin vapour for 4min and then incubated in α-NBE working solution for 45min. Slides were rinsed with distilled water and then placed into the chloroacetate esterase working solution for 10min. The slides were rinsed with distilled water, counterstained with Harris haematoxylin for 5min, and then rinsed in water for 10min. Once air dried, slides were mounted using a coverslip and DPX. Cells were analysed using the Olympus BX-51 microscope (Section 6.2.2.4.7). Myeloid cells stain a dark-blue colour while monocytic cells stain a red-brown colour (megakaryocytes and platelets also stain a red-brown colour) (Hanly, 2001, Matutes *et al.*, 2006).

6.2.2.4.7 Analysis of THP-1 Cell Morphology and Cytochemistry by Light Microscopy

Stained cells (Sections 6.2.2.4.1 and 6.2.2.4.3-6) were examined and images were captured on an Olympus BX-51 microscope. Positive control slides were first analysed to ensure the stains had worked correctly prior to analysing the stained THP-1 cells. Unless otherwise stated, images of stained THP-1 cells were obtained using the X60 oil objective.

6.2.2.5 Techniques for Quantiation of *SLC11A1* Expression

6.2.2.5.1 RNA extraction

Quantitative reverse transcriptase real-time PCR was completed to verify that THP-1 cells expressed *SLC11A1*. THP-1 cells (untreated, PMA differentiated or IFN-γ and LPS stimulated [Section 6.2.2.1.9]) were removed from the tissue culture flask (3×10^6 cells), centrifuged, the supernatant removed, and the cell pellet was stored at -80^{o}C until RNA was extracted. Prior to RNA extraction, all surfaces and pipettes were treated with RNase AWAY to deactivate any contaminating RNases. RNA was extracted using the RNeasy Plus Mini Kit, following the manufacturer's protocol. Homogenisation of the cell lysate was completed by passing the lysate through a 20 gauge needle five times. The purified RNA was eluted from the spin column in 50µl of supplied RNase free water. The concentration of the extracted RNA was quantified using the NanoDrop (Section 2.2.2.7), and cDNA was synthesised immediately after extraction (Section 6.2.2.5.2).

6.2.2.5.2 Synthesis of cDNA

Synthesis of cDNA was carried out using the SuperScript III First-Strand Synthesis Supermix, following the manufacturer's protocol. Firstly, 5µg of isolated RNA (Section 6.2.2.5.1) was added to 50µM oligo(dT) and annealing buffer in a final volume of 8µl. Samples were incubated at 65^{o}C for 5min, placed on ice for 1min, and 1X First Strand Reaction Mix and Superscript III were added. The reactions were mixed well and incubated for 50min at 50^{o}C followed by an incubation at 85^{o}C for 5min to terminate the reaction. The synthesised cDNA was stored at -20^{o}C until used for quantitative real-time PCR (Section 6.2.2.5.3).

6.2.2.5.3 PCR 6 – Quantitation of SLC11A1 Expression by Real-time PCR

Quantitative real-time PCR was carried out to quantitate *SLC11A1* expression (target gene) relative to the reference gene, RPL36AL (ribosomal protein L36a-like), using the SYBR GreenER qPCR SuperMix Universal. The PCR was carried out in a 25µl reaction volume, which contained 1X SYBR GreenER qPCR SuperMix Universal, 6.0µM forward and reverse primer concentrations and 50ng cDNA template (Section 6.2.2.5.2). Four replicate reactions were completed for each sample. Real-time PCR was conducted on the Mastercycler ep *realplex*^{2} instrument (Eppendorf). The PCR was initiated by an UDG incubation (50^{o}C for 2min), followed by an initial denaturation (95^{o}C, 5min) and 40 cycles of denaturation (95^{o}C for 30s), annealing (61^{o}C for 30s), and extension (72^{o}C for 30s). Amplification was followed by a dissociation step consisting of a denaturation step at 95^{o}C for 15s and then 60^{o}C for 15s, followed by fluorescence acquisition as the samples were heated to 95^{o}C for 10min. Real-time PCR amplification was assessed using quantification plots and melting curves.

Differences in expression were calculated by first determining the mean Ct value of the four replicates of each sample for the target and reference gene. The ΔCt (difference between the Ct values of the target and reference gene) was determined by subtracting the mean Ct value of the target gene from the mean Ct value of the reference gene for both mean Ct values of untreated and treated samples (equation 1 and 2, respectively). The difference in expression was then determined using the equation $2^{-\Delta\Delta Ct}$, where ΔΔCt equals $\Delta Ct_{(treated)}$ minus the $\Delta Ct_{(untreated)}$ (equation 3).

$$\Delta Ct_{(untreated)} = Ct_{(target)} - Ct_{(reference)} \quad [1]$$

$$\Delta Ct_{(treated)} = Ct_{(target)} - Ct_{(reference)} \quad [2]$$

$$\Delta\Delta Ct = \Delta Ct_{(treated)} - \Delta Ct_{(untreated)} \quad [3]$$

6.3 RESULTS

PART 3: Analysis of the *SLC11A1* Promoter using Promoter Assays.

6.3.1 Determination of the Promoter Activity of *SLC11A1* Constructs Transfected into 293T Cells

6.3.1.1 Characterisation of the 293T Cell Line

The *SLC11A1* promoter constructs were first tested in the non-monocytic cell line 293T (Graham *et al.*, 1977). Being of non-monocytic lineage, 293T cells do not express *SLC11A1*. Therefore, the data gathered from the transfection of *SLC11A1* promoter constructs into 293T cells enabled the identification of promoter regions containing non-monocytic specific factors which regulate *SLC11A1* transcription. For example, data from the 293T cell transfections may enable the determination of a minimal promoter region, as the core components for the formation of the basal transcriptional complex that mediates pol II transcription are located in all cells, or may identify *SLC11A1* promoter regions which could recruit general, ubiquitously expressed transcription factors. Additionally, the results obtained from the transfection of the promoter constructs into 293T cells could be compared to the transfection results obtained from a monocytic cell line, where *SLC11A1* exhibits restricted expression, allowing the identification of *SLC11A1* promoter regions containing elements for the recruitment of monocyte specific regulators of transcription.

The 293T cell line was initially analysed by fluorescence microscopy (Section 6.2.2.3.1) to assess the suitability for use with the Geneblazer technology. Promoter activity generated from the expression constructs is based on cleavage of a green fluorescing molecule to generate a blue fluorescing molecule (Figure 6.1). Therefore, to enable sensitive determination of promoter activity, it was first established that the 293T cells did not generate green or blue autofluorescence. No autofluorescence was observed from untransfected 293T cells, thereby establishing that the 293T cells were suitable candidates for use with the Geneblazer technology (Figure 6.2A).

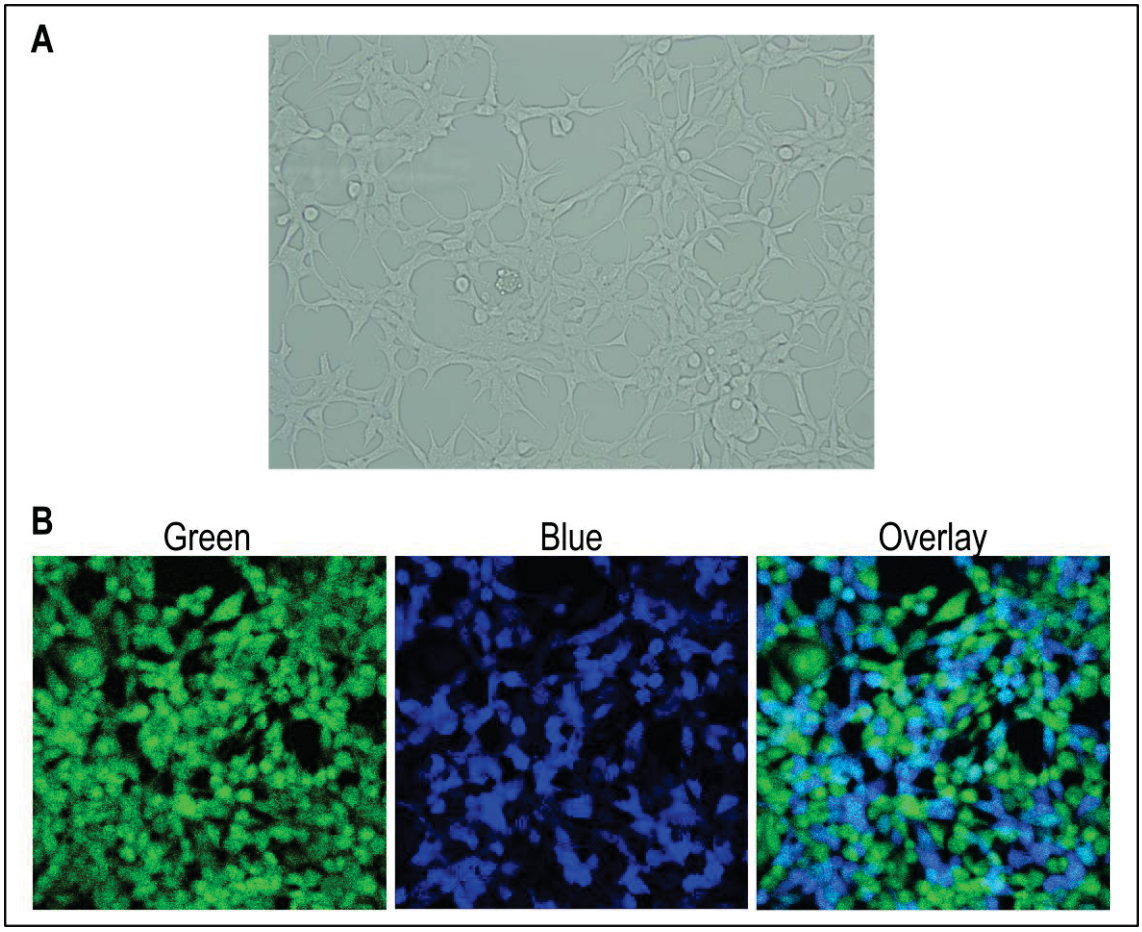

Figure 6.2 Microscopic analysis of 293T cells. (A) Bright field microscopy of untransfected 293T cells grown on glass coverslips. No blue or green autofluorescence was observed when untransfected 293T cells were assessed by fluorescence microscopy (X60 magnification). (B) Confocal microscopy analysis of 293T cells transfected with the positive control, UBC-*bla*(M) (X40 magnification). After seeding 293T cells into 96-well plates (24h), 293T cells were transfected with the *SLC11A1* promoter constructs and controls using Lipofectamine 2000, and, 24h post transfection, the CCF2-AM substrate was loaded into the transfected 293T cells. Cells were analysed for green (left panel) and blue (centre panel) fluorescence (representing uncleaved and cleaved substrate, respectively). The overlay (right panel) shows colocalisation of blue and green fluorescence.

6.3.1.2 Transfection of *SLC11A1* Promoter Constructs into 293T Cells

The *SLC11A1* promoter constructs were transfected into the 293T cell line using Lipofectamine 2000 (Section 6.2.2.2.1). Transfections of promoter constructs were completed in replicates of four in 96-well plates, with the negative and positive control plasmids (emp-*bla*(M) and UBC-*bla*(M), respectively) included in all transfection experiments. After substrate loading (Section 6.2.2.2.4), detection of green and blue fluorescence levels of transfected 293T cells was performed using a fluorescence plate reader (Section 6.2.2.3.3).

Analysis of transfected 293T cells by confocal microscopy showed that the procedure did not induce morphological changes and the transfected cells showed a homogenous distribution of green and blue fluorescence (Figure 6.2B) (Section 6.2.2.3.2). The post-transfection cell viability remained high (between 95 and 100%) (Section 6.2.2.1.6) and the transfection efficiency was also high, with 60-75% of cells fluorescing blue (Figure 6.2B). The positive control, UBC-*bla*(M) plasmid, exhibited the highest fluorescence ratio (i.e. the highest promoter activity), while the negative control plasmid emp-*bla*(M) (Section 5.3.2.5) resulted in low promoter activity, with a similar level of green fluorescence compared to other *SLC11A1* promoter plasmids, but low blue fluorescence. Variable promoter activities were observed after 293T cells were transfected with constructs containing different segments of the *SLC11A1* promoter (Figure 6.3).

6.3.1.2.1 Determination of Important Promoter Regions Driving SLC11A1 Transcription in 293T Cells

The *SLC11A1* constructs containing different lengths of the *SLC11A1* promoter, all harbouring the variant allele 3 [$(GT)_n$ allele 3 with -237 C] in the forward orientation (Section 5.3.2.2), were first transfected into 293T cells (Figure 6.3). Transfection of the 293T cells with *SLC11A1* promoter plasmids showed that promoter region 7C (-532 to +49) consistently resulted in the highest promoter activity, while promoter regions 1A (-2900 to +367) and 8C (-362 to +49) resulted in the lowest promoter activity.

The smallest *SLC11A1* promoter regions, 9C (-231 to +49) and 10C (-99 to +49), resulted in a high level of promoter activity, just below that observed for *SLC11A1* promoter region 7C (which exhibited the highest promoter activity). This suggests that

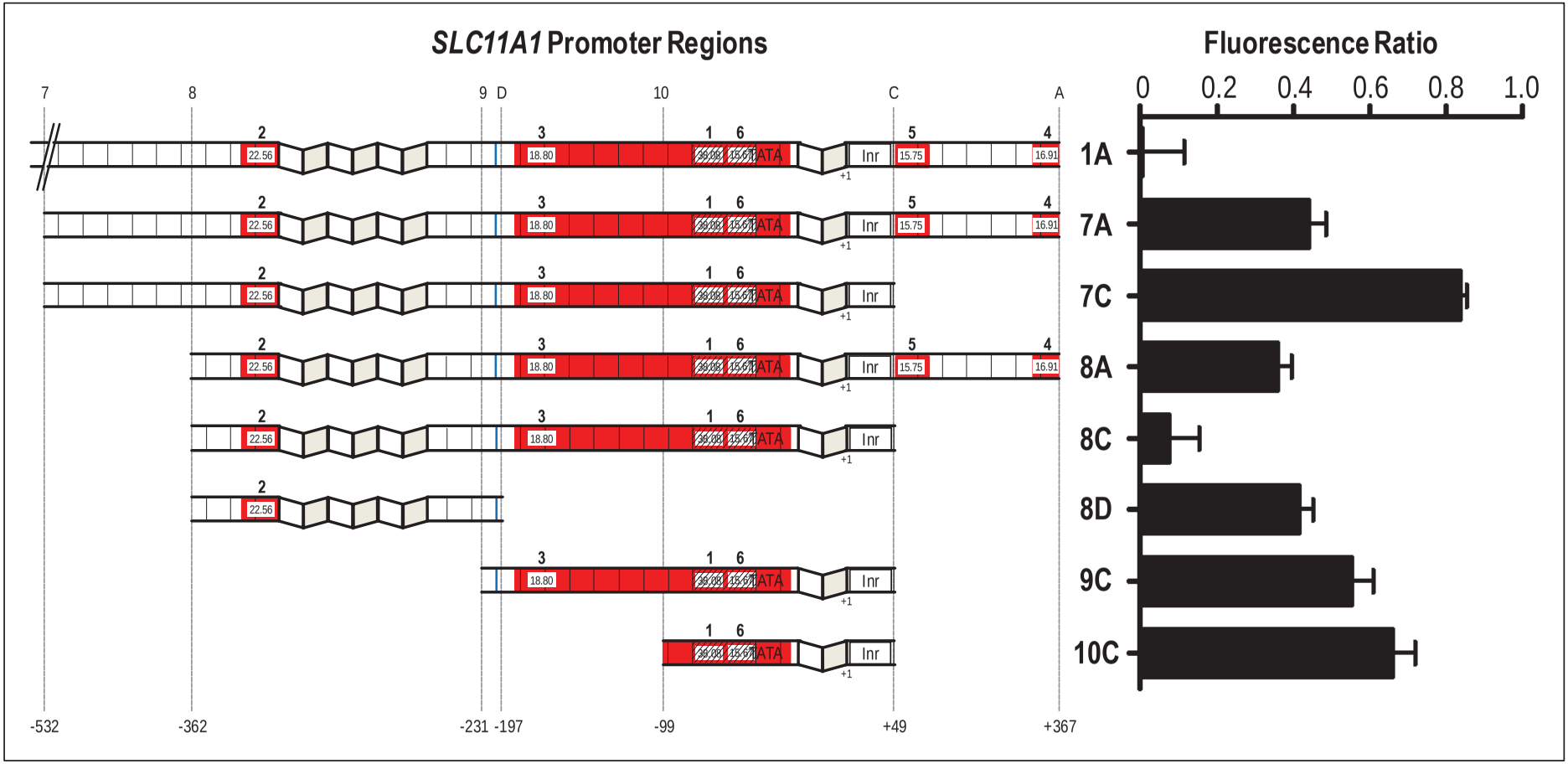

Figure 6.3 Promoter activity of *SLC11A1* constructs, containing different lengths of the *SLC11A1* promoter, after transfection into 293T cells. 293T cells were transiently transfected with the promoter constructs, with all plasmids containing variant allele 3 [$(GT)_n$ allele 3 with -237 C] in the forward orientation. Cells were loaded with the CCF2-AM substrate 24h post-transfection and fluorescence intensity measured using a fluorescent plate reader. The promoter activities of the different promoter constructs (right) are shown adjacent to the respective *SLC11A1* promoter regions cloned into the pGeneBLAzer plasmid (left).

the minimal promoter region, and the site of the formation of the basal transcriptional complex, is located within the 10C promoter region (-99 to +49) (Figure 6.3). This is consistent with the results obtained from the bioinformatic analyses (Sections 5.3.1.2 and 5.3.1.3).

The bioinformatic analyses also identified elements within the 5'UTR, and extending into the first intron, which could function as core promoter elements. Core elements are essential in the formation of the basal transcriptional complex, and their removal results in a loss of gene expression. However, *SLC11A1* promoter activity was not lost in any of the plasmids containing promoter regions, which lacked the 5'UTR and first intron (plasmids 7C, 8C, 8D, 9C and 10C) (region +49 to +367). This finding suggests that *SLC11A1* expression is not modulated by a core promoter element downstream of the transcription start site. However, while no core promoter elements were identified, the decrease in the level of promoter activity driven by promoter regions 8A to 8C suggests that the region +49 to +367 may contain an element for transcription factor binding, which enhances transcription (Sections 5.3.1.2 and 5.3.1.3).

The promoter region 8C resulted in a low level of promoter activity, however, the 7C promoter region drove the highest promoter activity, with a four to five fold increase in expression over that observed in the presence of promoter region 8C. Therefore, another element for the binding of a transcription factor may be located within the -532 to -362 region. Likewise, the 3 fold decrease in promoter activity observed in the presence of promoter region 8C, as compared to that driven by the smaller 9C region, suggests that the -362 to -231 region contains an element for the recruitment of a transcription factor which negatively regulates *SLC11A1* expression.

6.3.1.2.2 Assessment of the Ability of the SLC11A1 Promoter to Mediate Bidirectional Transcription

Promoter constructs with inserts cloned in the forward and reverse orientation (all containing variant allele 3), were transfected into 293T cells to assess the ability of the *SLC11A1* promoter to mediate bidirectional transcription (Figure 6.4). The majority of inserts cloned in the reverse orientation showed no promoter activity, with the exception of promoter regions 8A and 8D. While the promoter region 8A (-326 to +367) showed similar promoter activity in the forward and reverse orientation, bidirectionality of the

SLC11A1 promoter likely does not occur *in vivo*, as the largest promoter regions (7A and 7C) did not exhibit bidirectional promoter activity (Figure 6.4). This suggests that the *SLC11A1* promoter contains or recruits factors, which co-ordinate regulated expression in the forward orientation.

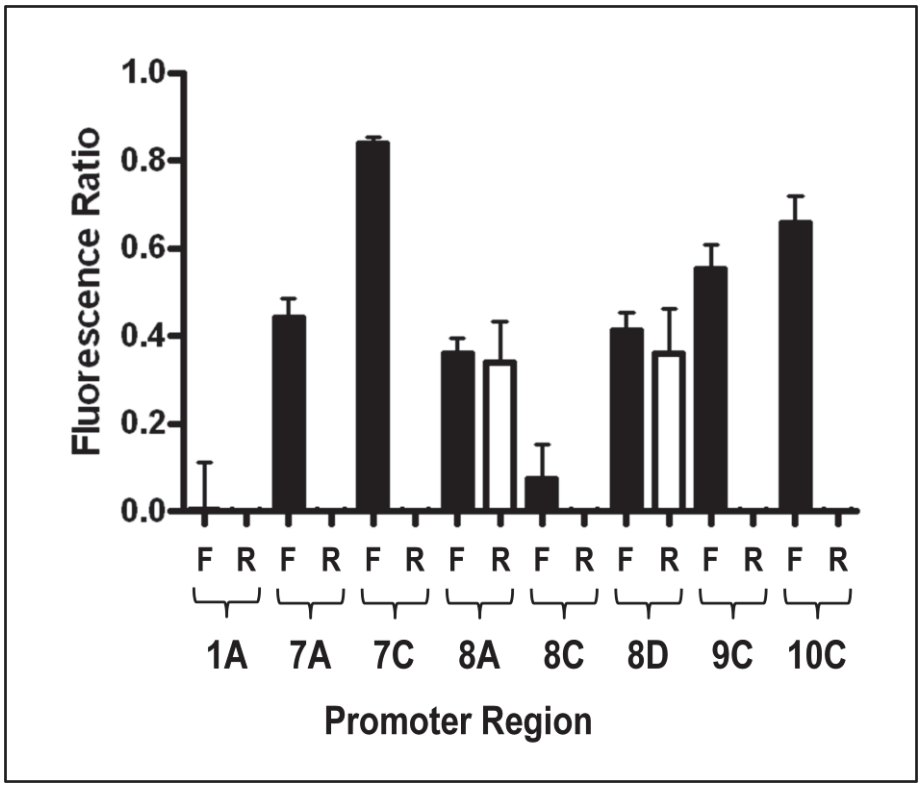

Figure 6.4 Assessment of the ability of the *SLC11A1* promoter region to mediate bidirectional transcription in non-monocytic (293T) cells. The black and white bars represent *SLC11A1* promoter regions cloned into the pGeneBLAzer vector in the forward (F) and reverse (R) orientation, respectively.

The *SLC11A1* promoter region 8D (-326 to -231) resulted in a comparable fluorescence ratio in both the forward and reverse orientation. This plasmid contained only the $(GT)_n$ microsatellite repeat (with a minimal amount of sequence either side) and lacks the region 9C/10C where the formation of the basal transcriptional machinery occurs (Figure 6.3). The promoter activity of the 8D plasmid in the forward and reverse orientation is likely attributable to the intrinsic ability of the alternating purine/prymidine sequence to enhance transcription due to the formation of Z-DNA, thereby confirming previous reports that the microsatellite repeat has endogenous enhancer ability (Searle and Blackwell, 1999).

6.3.1.2.3 The Promoter Variants Allele 2 and Allele T Drive Higher Promoter Activity Compared to the Allele 3 Variant in 293T Cells

The effect of variants at the $(GT)_n$ and -237C/T polymorphisms on *SLC11A1* promoter activity was assessed. The different *SLC11A1* promoter lengths, containing the allelic variants, allele 2, allele 3 and allele T (or allele C and allele T for promoter region 9C) (Sections 5.3.2.2, 5.3.2.4), were transfected into 293T cells (Section 6.2.2.2.1) to elucidate the mechanism(s) by which promoter variants modulate differential *SLC11A1* expression (Figure 6.5).

Interestingly, $(GT)_n$ allele 2 drove a 1.3 to 6 fold higher level of *SLC11A1* promoter activity as compared to $(GT)_n$ allele 3, in all *SLC11A1* promoter regions tested (Figure 6.5). This finding is in contrast with previous studies, which have shown that $(GT)_n$ allele 3 drives a higher level of *SLC11A1* expression as compared to $(GT)_n$ allele 2 in monocytic cell lines (Searle and Blackwell, 1999, Zaahl *et al.*, 2004). This finding also challenges the current hypothesis explaining the association of the different $(GT)_n$ alleles with the incidence of disease (Section 1.3), namely, that increased *SLC11A1* expression, driven by allele 3, confers resistance and susceptibility to infectious and autoimmune disease, respectively, due to the generation of a heightened Th1 mediated immune response. However, the current finding that $(GT)_n$ allele 2 exhibits a greater promoter activity than $(GT)_n$ allele 3, in non-monocytic 293T cells, is consistent with the findings of the Z-Hunt analysis (Section 5.3.1.5.1, Figure 5.12), which identified that $(GT)_n$ allele 2 had a greater propensity to form Z-DNA and accordingly would exert greater transcriptional enhancement of *SLC11A1* as compared to allele 3.

The presence of the -237 T variant resulted in a 1.3 to 5 fold higher level of promoter activity as compared to that observed for the more common -237 C variant in all *SLC11A1* promoter regions tested (Figure 6.5). This trend was also observed for the 9C promoter region (-231 to +49) (Figure 6.3), which lacked the $(GT)_n$ microsatellite repeat, suggesting that this polymorphism may alter *SLC11A1* expression independently of the $(GT)_n$ microsatellite repeat. The higher promoter activity driven by the -237 T variant, as compared to the -237 C variant, is in contrast to a previous transfection study, carried out in monocytic cell lines, which showed that the C variant drove enhanced *SLC11A1* expression compared to the T variant (Zaahl *et al.*, 2004).

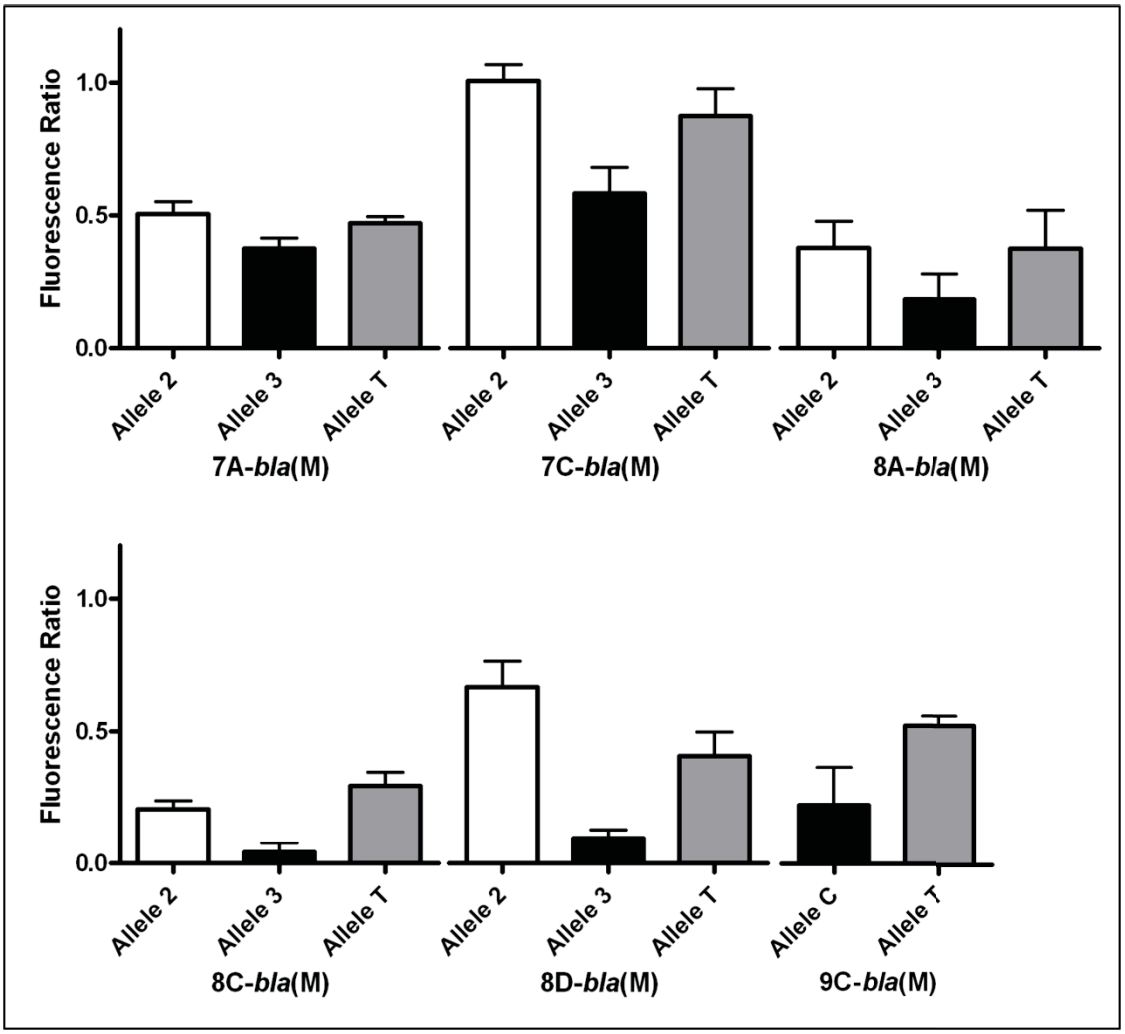

Figure 6.5 Effect of the *SLC11A1* plasmid variants, allele 2, allele 3 and allele T, on *SLC11A1* promoter activity in 293T cells. Multiple plasmids of the same *SLC11A1* promoter region, differing only by the promoter variant present, either allele 2 [$(GT)_n$ allele 2 with -237 C], allele 3 [$(GT)_n$ allele 3 with -237 C] or allele T [$(GT)_n$ allele 3 with -237 T] (Section 5.3.2.2.2), were transfected into 293T cells. Promoter region 9C contained only the -237C/T polymorphism, therefore, had two variants, allele C and allele T.

Previously published transfection experiments, determining the promoter activity mediated by variants within the *SLC11A1* promoter, have been completed in monocytic cell lines where *SLC11A1* has restricted expression. The results presented are based on expression of promoter constructs in non-monocytic cells, which do not express *SLC11A1*. Therefore, there may be other factors, such as the presence of transcription factors, Z-DNA binding proteins or DNA topology changes, that are specific to monocytic cells, which may account for the differences in expression patterns observed.

6.3.2 Determination of the Promoter Activity of *SLC11A1* Constructs Transfected into THP-1 Cells

6.3.2.1 Selection of a Monocytic Cell Line with *SLC11A1* Expression

SLC11A1 has restricted expression to phagocytic cells, notably monocytes and macrophages (Section 1.1.3). To elucidate the monocyte-specific factors which influence *SLC11A1* expression, a cell line that exhibited the phenotypic characteristics of monocytes/macrophages and also expressed *SLC11A1* was required. Previous publications assessing *SLC11A1* expression have utilised THP-1, U937 and HL-60 cell lines (Richer *et al.*, 2008, Roig *et al.*, 2002, Searle and Blackwell, 1999, Zaahl *et al.*, 2004), with the THP-1 and U937 cell lines exhibiting *SLC11A1* expression in the absence of differentiation/stimulation. Therefore, the THP-1 and U937 cells were assessed for their suitability for use with the *in vivo* detection of *SLC11A1* promoter activity using the Geneblazer technology.

As the expression of *SLC11A1* differs according to the stage of monocyte/macrophage development (Figure 1.3), different transcription factors are likely involved in modulating *SLC11A1* expression. Therefore, a cell line which could be induced to differentiate from a monocyte-like cell to a macrophage-like cell would be ideal to test the prepared *SLC11A1* promoter constructs. Accordingly, THP-1 and U937 cells were analysed with or without PMA, resulting in differentiated (i.e. macrophage-like) and undifferentiated (i.e. monocyte-like) cells, respectively (Section 6.2.2.1.9) (Auwerx, 1991, Tsuchiya *et al.*, 1982). After PMA induced differentiation, THP-1 cells became adherent as single cells within 24h, with no observable green or blue auto-fluorescence in either undifferentiated or differentiated THP-1 cells (Figure 6.6A). When U937 cells were PMA differentiated, the cells adhered as large masses of cells, with evidence of continued cell division (which is not a feature of monocyte differentiation to macrophages) (Figure 6.6B). Additionally, a low level of green auto-fluorescence and a high level of blue auto-fluorescence were observed (Figure 6.6B). Therefore, the monocytic-like THP-1 cells, which lacked auto-fluorescence and exhibited monocyte to macrophage differentiation, were the most suitable candidate to assess promoter activity of the *SLC11A1* promoter constructs using the Geneblazer technology.

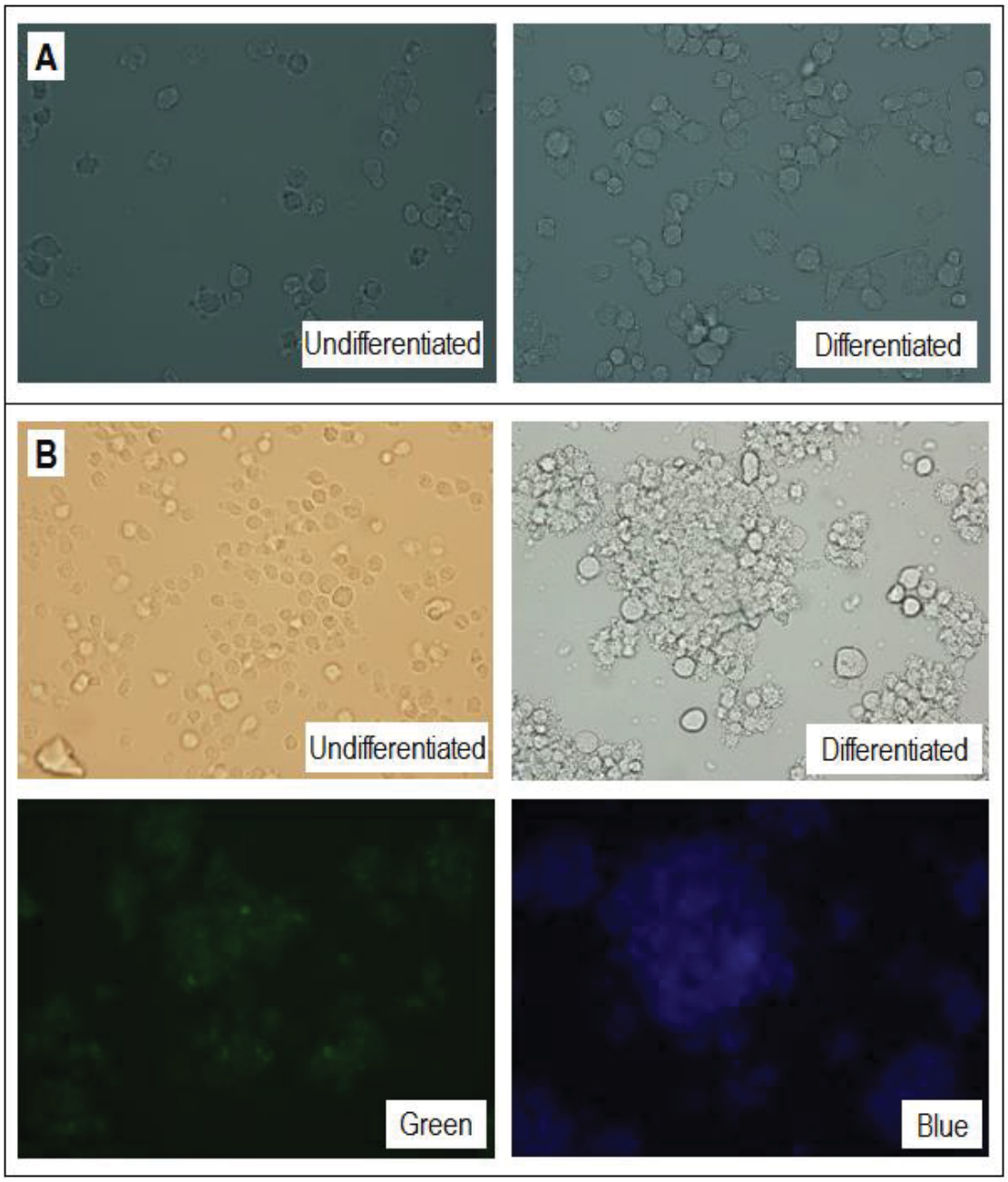

Figure 6.6 Analysis of THP-1 and U937 cell lines for suitability for use with the Geneblazer technology. (A) Undifferentiated (left panel) and PMA differentiated (right panel) THP-1 cells (X40 magnification). (B) Undifferentiated (middle left panel) and PMA differentiated U937 cells (middle right panel) and the green (bottom left panel) and blue (bottom right panel) auto-fluorescence of differentiated U937 cells (X40 magnification).

6.3.2.2 Characterisation of the THP-1 Cell Line

THP-1 cells were established in the 1980s from a patient with acute monocytic leukaemia (Tsuchiya *et al.*, 1980). THP-1 cells are non-adherent and analysis of the cellular morphology by electron microscopy and cytochemical stains suggests that the cells have a monocyte-like phenotype (Tsuchiya *et al.*, 1980). The THP-1 cell line was characterised to validate that the cells possessed a monocytic-like phenotype (and not another leukaemic cell type) and possessed *SLC11A1* expression, by morphological/ cytochemical analyses and reverse transcriptase real-time PCR, respectively.

6.3.2.2.1 Morphological/Cytochemical Characterisation of THP-1 Cells

Morphological analysis of THP-1 cells by May-Grunwald Giemsa staining (Section 6.2.2.4.1) found that the cells were predominantly round with cell diameters ranging between 12 and 18µm (Figure 6.7). The cytoplasm was slightly basophilic with intracellular vacuoles and nuclei staining lightly and being round in appearance, with most having an an indent. The morphological appearance after May-Grunwald Giemsa staining was consistent with the findings of Tsuchiya et al. (1980), suggesting that the cells resembled a monocytic leukaemia.

Cytochemistry was further used to validate that the THP-1 cell line represented a monocytic leukaemia and did not contain features of other haemopoietic malignancies. Consistent with the findings of Tsuchiya et al. (1980), the cytochemical analysis determined that the THP-1 cells were PAS negative (Figure 6.8A) (Section 6.2.2.4.3),

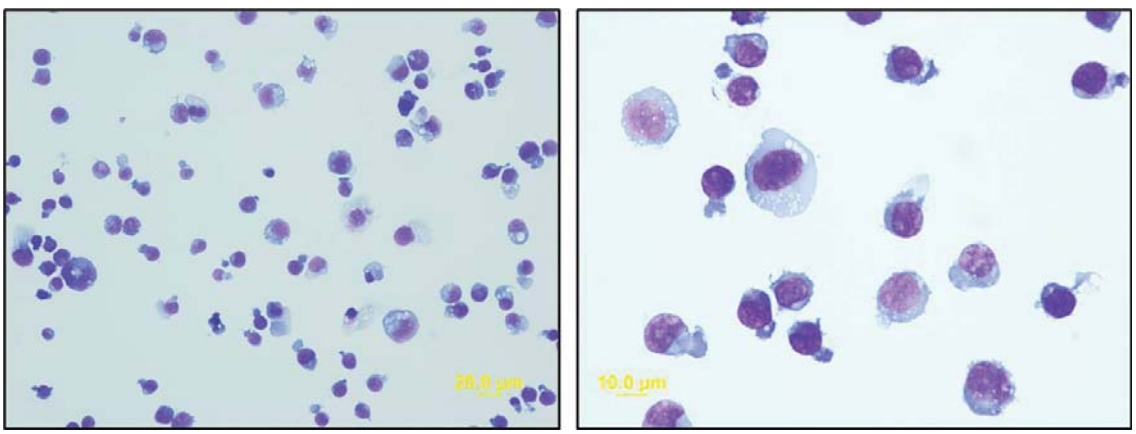

Figure 6.7 Analysis of THP-1 cell morphology by May-Grunwald Geimsa staining (left panel X20 magnification, right panel X60 magnification).

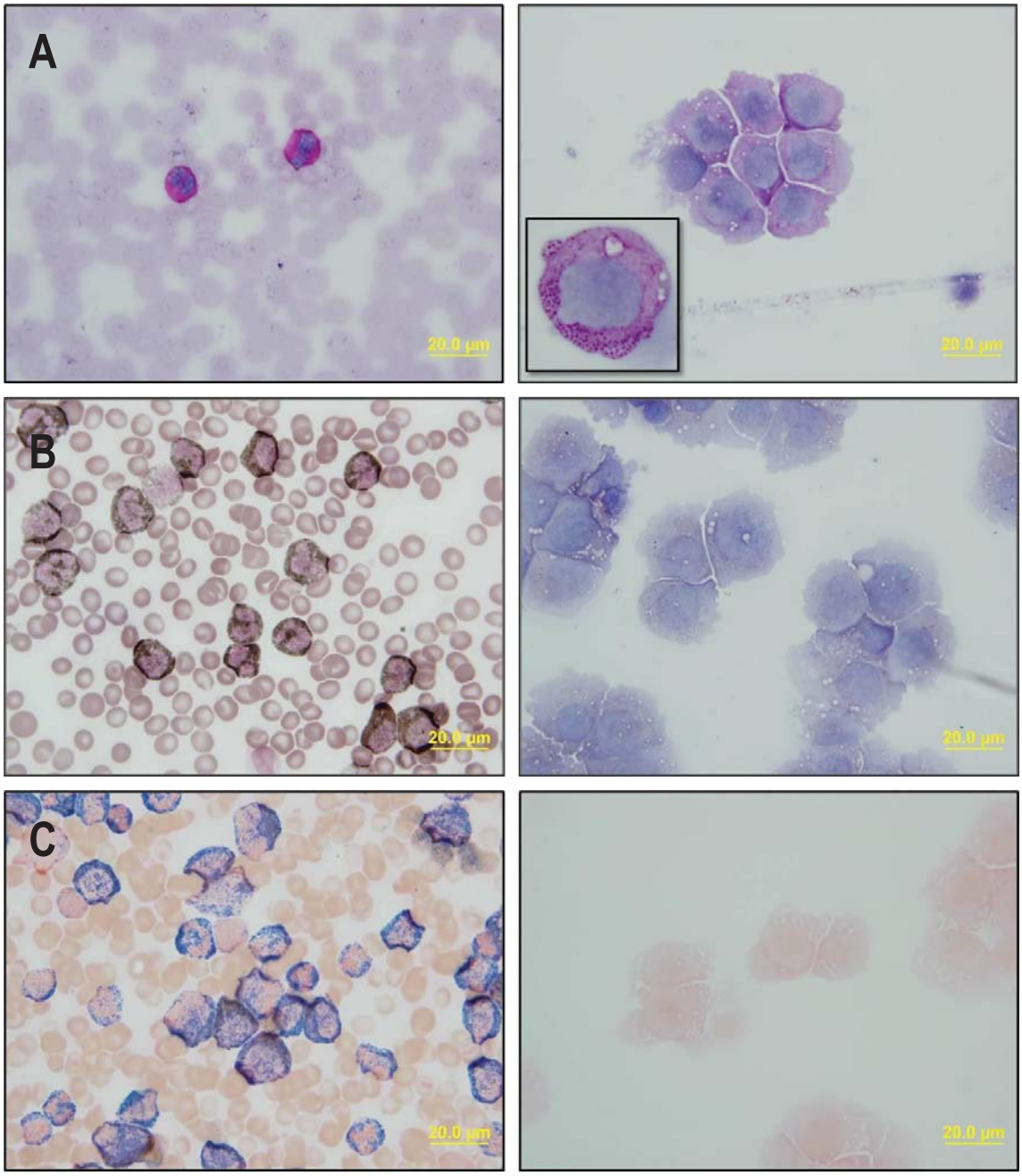

Figure 6.8 Cytochemical analyses of THP-1 cells. The THP-1 cells are shown in the right panels and the respective positive controls in the left panels. (A) Periodic acid-schiff stain (left panel: normal peripherial blood showing two neutrophils with intense positive magenta staining). Inset in the right panel is a higher magnification image of a THP-1 cell displaying the positive fine granules (Section 6.2.2.4.3). (B) Sudan Black B stain (left panel: acute myeloid leukaemia with granulocytic cells showing positive black granular pattern in the cytoplasm). (C) Myleoperoxidase stain (left panel: acute myeloid leukameia showing myeloblasts/myelocytes containing the expected blue granular pattern in the cytoplasm).

SBB negative (Figure 6.8B) (Section 6.2.2.4.4) and myeloperoxidase negative (Figure 6.8C) (Section 6.2.2.4.5). The combined α-Naphthyl butyrate and AS-D chloroacetate esterase staining of THP-1 cells (Section 6.2.2.4.6) resulted in the production of an intense red/brown colour within the cytoplasm with no blue colouration produced, validating that the cells were of monocytic origin and not myeloid or biphenotypic AMML (mixed myeloid/monocytic phenotype) (Figure 6.9) (Matutes *et al.*, 2006).

Verfication of the THP-1 cell line suggests, based on morphological and cytochemical features, that the cells were of monocytic origin and do not contain features characteristic of other leukaemias. This observation is consistent with a previously reported characterisation of THP-1 cells (Tsuchiya *et al.*, 1980).

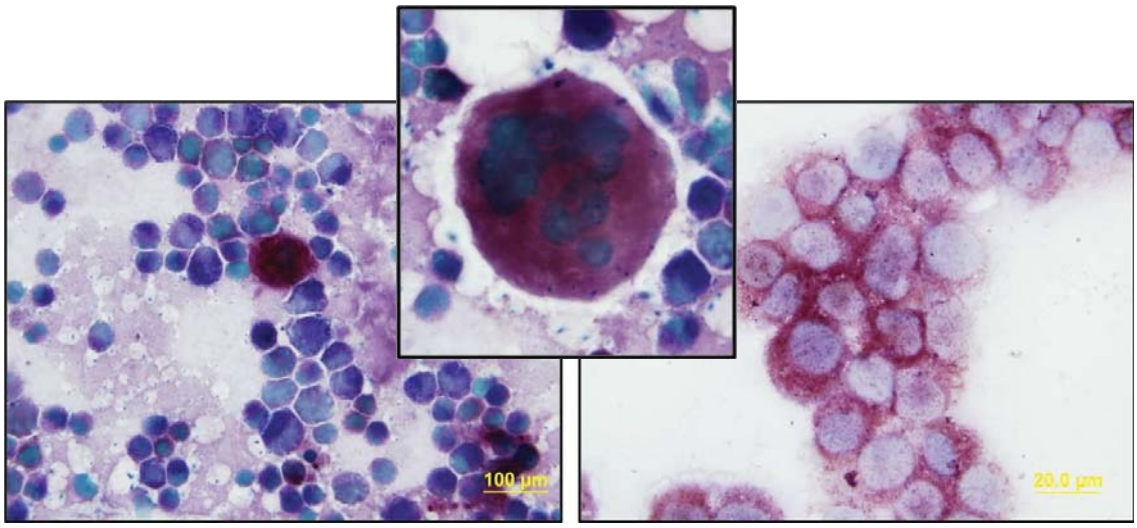

Figure 6.9 Combined α-naphthyl butyrate and AS-D chloroacetate esterase stain. The left hand panel is the positive control of bone marrow (X40 magnification) showing positive results for the combined esterase stain with the majority of cells containing dark blue granules indicating a myeloid origin and few cells staining a red/brown colour indicating a monocyte/megakaryocyte origin. A higher magnification image of a megakaryocyte shows the red/brown colouration observed (centre). The THP-1 cells (right hand side) contain red/brown colouration in the cytoplasm.

6.3.2.2.2 Quantitation of SLC11A1 Expression in THP-1 Cells

A model monocyte/macrophage cell line for the analysis of promoter regions driving *SLC11A1* expression should exhibit similar kinetics as observed in primary monocytes and macrophages in the level of *SLC11A1* expression when differentiated or stimulated. Therefore, quantitative real-time RT-PCR was carried out to determine the level of expression of *SLC11A1* in THP-1 cells after differentiation and stimulation. THP-1 cells were either treated with PMA (5ng/ml or 100ng/ml) for 48h to stimulate differentiation into macrophage-like cells or stimulated with IFN-γ and LPS (either individually or in combination) for 6h (Section 6.2.2.1.9). RNA was extracted from the cells (Section 6.2.2.5.1), cDNA synthesised (Section 6.2.2.5.2) and quantitative real-time RT-PCR was used to determine the level of *SLC11A1* expression (Section 6.2.2.5.3).

Analysis of the untreated cells verified that THP-1 cells expressed *SLC11A1*. When THP-1 cells were differentiated with PMA (5ng/ml or 100ng/ml), *SLC11A1* expression increased 24 and 29 fold, respectively, as compared to undifferentiated cells. This increase in *SLC11A1* expression suggested that the pattern of expression is similar to that seen during the differentiation of primary monocytes to macrophages (Figure 1.3). Furthermore, stimulation of the cells with LPS, IFN-γ, and LPS + IFN-γ resulted in an increase in *SLC11A1* expression (2.7, 5.7 and 1.3 fold increase, respectively). The increase in *SLC11A1* expression following differentiation or stimulation suggests that the THP-1 cell line exhibited the changes in *SLC11A1* expression observed *in vivo*, indicating that THP-1 cells represented an appropriate model to elucidate the mechanisms that modulate *SLC11A1* transcription.

6.3.2.3 Optimisation of THP-1 Cell Transfection with the *SLC11A1* Promoter Constructs

6.3.2.3.1 Detection of SLC11A1 Promoter Activity using a Fluorescence Plate Reader

Initially, transfection of the THP-1 cell line to determine promoter activity of the *SLC11A1* promoter constructs was completed using a similar methodology to that used for the 293T cells. However, Lipofectamine LTX transfection of THP-1 cells (Section 6.2.2.2.2), followed by CCF2-AM substrate loading (Section 6.2.2.2.4), and subsequent detection using a fluorescence plate reader (Section 6.2.2.3.3) failed to identify any differences in promoter activity between the different *SLC11A1* promoter constructs, including expected differences between the positive and negative control plasmids, UBC-*bla*(M) and emp-*bla*(M), respectively.

Trypan blue exclusion staining (Section 6.2.2.1.6) of THP-1 cells throughout the transfection protocol showed that 97% of cells were viable prior to transfection, however, 24h post Lipofectamine LTX transfection, cell viability was significantly decreased to 40-50%. The low cell viability was also evident when the transfected THP-1 cells were analysed by confocal microscopy (Section 6.2.2.3.2), which identified two cell populations, according to the intensity of green fluorescence (Figure 6.10); a high and a low fluorescing population, representing viable and non-viable (non-viable cells can not retain the CCF2-AM substrate and therefore exhibit low green fluorescence) cell populations, respectively.

Additionally, confocal microscopy analysis of transfected THP-1 cells showed that transfection efficiency was low. Of the viable cells (high green fluorescence), only 1-2% of cells transfected with the positive control plasmid [UBC-*bla*(M)] showed blue fluorescence greater than that observed for the negative control plasmid [emp-*bla*(M)] (Figure 6.10), indicating that only 1-2% of viable cells were transfected. Therefore, the inability to detect differences between the Lipofectamine LTX transfected promoter constructs was attributable to both low cell viability and transfection efficiency. The difficulty of transfecting the THP-1 cells identified in this study corroborates previous reports (Martinet *et al.*, 2003, Schnoor *et al.*, 2009).

The inability to detect differences in promoter activity between the *SLC11A1* promoter constructs was further compounded by the use of a plate reader for fluorescence detection, as all cell populations (viable and non-viable) contributed to the overall fluorescence detected. Therefore, a method to increase the cell viability and transfection efficiency, as well as a method, capable of detecting only the transfected cell population was required to determine the promoter activity driven by each of the *SLC11A1* promoter constructs.

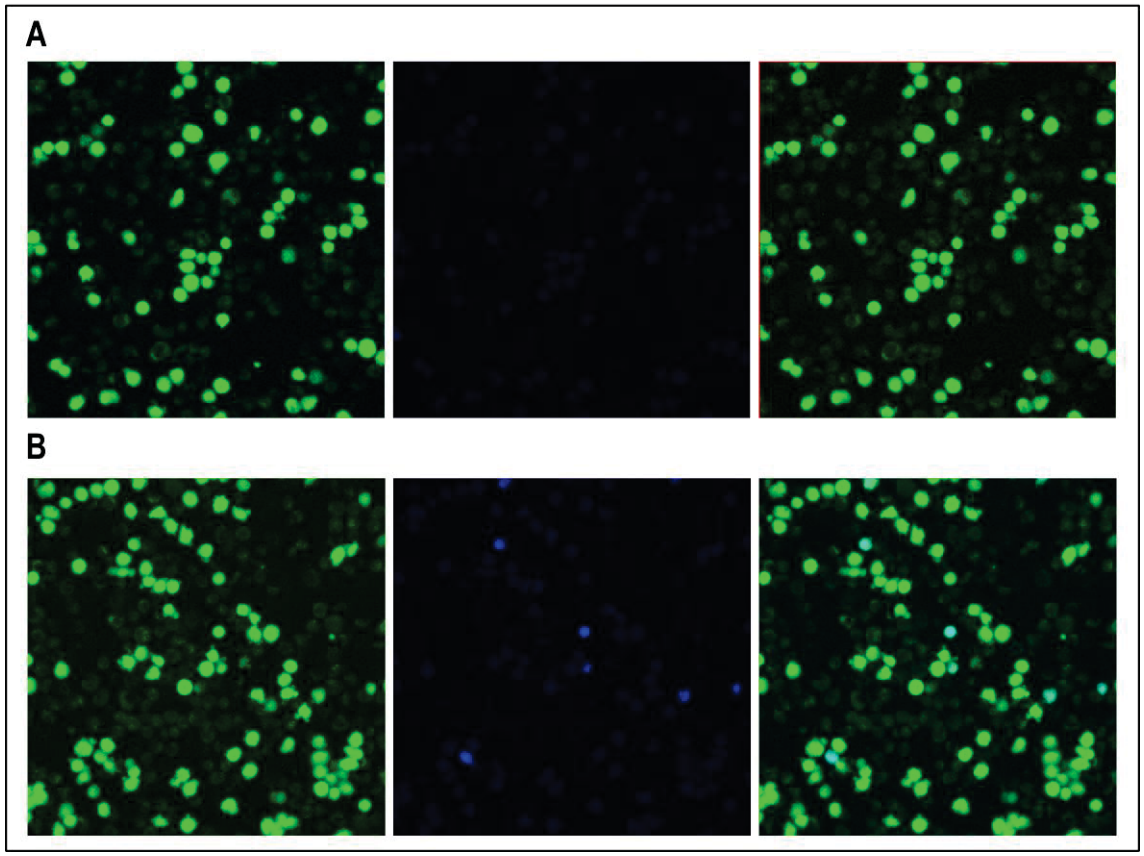

Figure 6.10 Lipofectamine LTX transfected THP-1 cells showing low cell viability and low transfection efficiency. Cells were analysed by confocal microscopy (X40 magnification) after transfection and substrate loading. (A) THP-1 cells transfected with the negative control emp-*bla*(M) plasmid. (B) THP-1 cells transfected with the positive control UBC-*bla*(M) plasmid. Cells were analysed for green (left panel) and blue (centre panel) fluorescence (representing uncleaved and cleaved substrate, respectively). The overlay (right panel) shows colocalisation of both blue and green fluorescing cells.

6.3.2.3.2 Flow Cytometric Analysis Enabled the Selective Detection of Transfected THP-1 Cells

Flow cytometry has been used to detect rare events in β-lactamase expressing stably transfected Jurkat cells using the CCF2-AM substrate (Knapp *et al.*, 2003). Due to the ability to gate on specific cell populations of interest (i.e. only the viable transfected cells in this case), flow cytometry offered a more specific and sensitive detection method, as compared to fluorescence measurements conducted using a plate reader. Confocal microscopy of Lipofectamine LTX transfected THP-1 cells found that the non-viable cell population emitted low green fluorescence as compared to the viable cells (Figure 6.10). Flow cytometry would enable the exclusion of the non-viable cell population by gating specifically on the high green fluorescing (viable) cells. Furthermore, viable, non-transfected cells would result in no, or very low blue fluorescence as they lack the ability to cleave the substrate, and could also be excluded from the analysis. This approach would enable the assessment of promoter activity exclusively from the viable transfected cell population.

To test the flow cytometric method of detection and quantification of fluorescence intensity, the *SLC11A1* promoter constructs were first transfected into the 293T cells and subsequently analysed by flow cytometry (Sections 6.2.2.2.1, 6.2.2.3.4). As the promoter activity of the *SLC11A1* promoter constructs had already been determined in 293T cells using the fluorescence plate reader (Section 6.3.1.2), fluorescence detection by flow cytometry, allowed a direct comparison of promoter activity determined by the two methods. Transfection of the *SLC11A1* promoter constructs into 293T cells (Section 6.2.2.2.1) and detection by flow cytometry (Section 6.2.2.3.4) produced a similar trend in promoter activity, driven by the different constructs, as observed using the plate reader (Figure 6.11), thus validating the determination of promoter activity using flow cytometry.

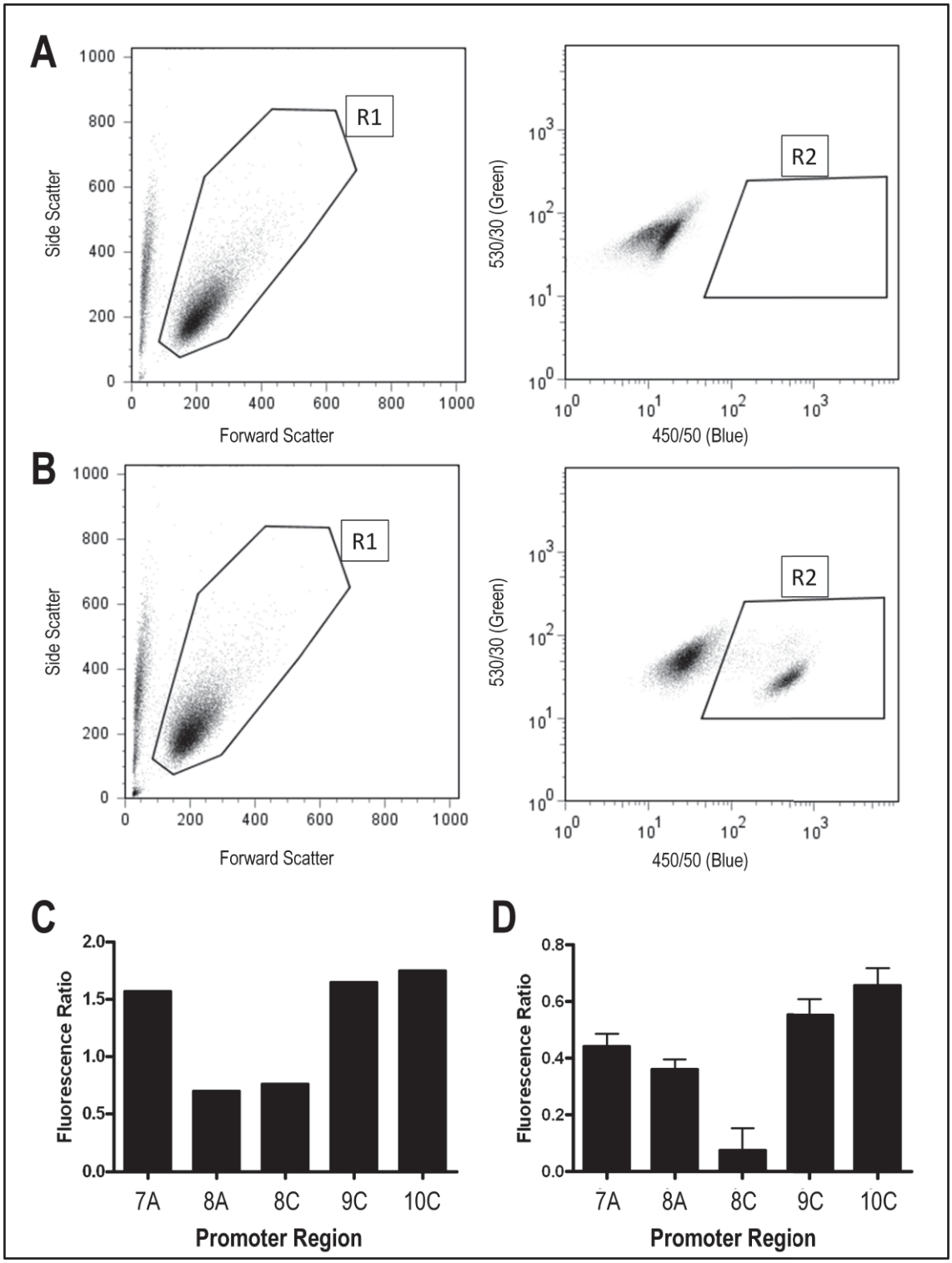

Figure 6.11 Validation of flow cytometric analyses to quantitate promoter activity driven by the different *SLC11A1* promoter constructs using 293T cells. (A) Gating procedure used to detect promoter activity of negative control emp-*bla*(M) and (B) positive control UBC-*bla*(M) plasmids. Gate R1 was first selected to exclude cellular debris using the forward and side scatter plot (left panels). Promoter activity was determined as the mean fluorescence intensity of a gate R2 from scatter plots of blue and green fluorescence (Section 6.2.2.3.4). (C) Promoter activity of *SLC11A1* promoter constructs transfected into 293T cells with flow cytometry or (D) fluorescence plate reader detection.

6.3.2.3.3 Nucleofection of THP-1 Cells Resulted in Increased Cell Viability and Transfection Efficiency as Compared to Lipofectamine LTX

The use of Lipofectamine LTX to transfect THP-1 cells resulted in low transfection efficiency and viability of the THP-1 cells post-transfection, thereby prohibiting comparisons of promoter activity driven by the different *SLC11A1* promoter constructs. Consistent with previous findings (Section 6.3.2.3.1), flow cytometry analysis of Lipofectamine LTX transfected THP-1 cells (Figure 6.12, left panel) showed that the majority of the cells were non-viable (approximately 80%), and of the viable cell population, only 1-2% were transfected. Nucleofection has previously been shown to allow transfection of THP-1 cells with high efficiency while maintaining cell viability (Martinet *et al.*, 2003, Schnoor *et al.*, 2009). The modified nucleofection protocol of Schnoor et al. (2009), reported transfection efficiencies and cell viability of 55-56% and 62-81%, respectively.

Transfection of THP-1 cells using nucleofection (Section 6.2.2.2.3) with subsequent flow cytometric analysis (Section 6.2.2.3.4) resulted in significantly higher cell viability (approximately 70%) and transfection efficiency (30% of viable cells) as compared to transfection using Lipofectamine LTX (Figure 6.12A). Consistent with this finding, confocal microscopy analysis of THP-1 cells, transfected using nucleofection, also showed a significant increase in the number of green and blue fluorescing cells, indicating a high cell viability and transfection efficiency, respectively (Figure 6.12B). Due to the lower post-transfection cell viability of THP-1 cells, the gating parameters used to assess promoter activity (Figure 6.13) differed from those used for the analysis of 293T cells (Figure 6.11).

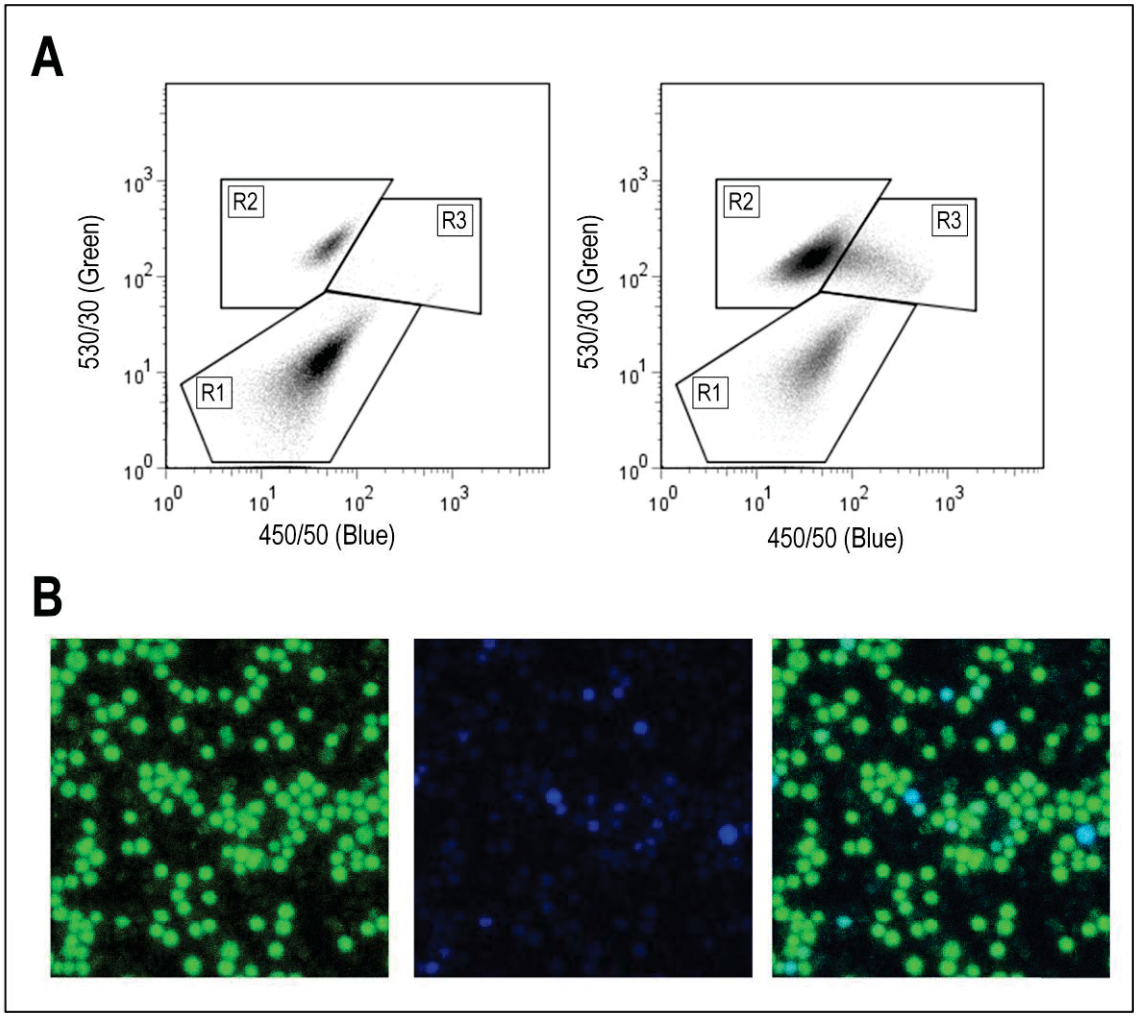

Figure 6.12 Nucleofection of THP-1 cells increases cell viability and transfection efficiency. (A) Comparison of THP-1 cells transfected with the positive control plasmid [UBC-*bla*(M)] using either lipofectamine LTX (left panel) or Nucleofection (right panel) (all captured events are shown). R1: non-viable THP-1 cells, R2: viable untransfected cells, R3: viable transfected cells. (B) Confocal microscopy analysis of THP-1 cells transfected by nucleofection with the positive control plasmid UBC-*bla*(M) (X40 magnification). Cells were analysed for green (left panel) and blue (centre panel) fluorescence (representing uncleaved and cleaved substrate, respectively). The overlay (right panel) shows colocalisation of both blue and green fluorescing cells.

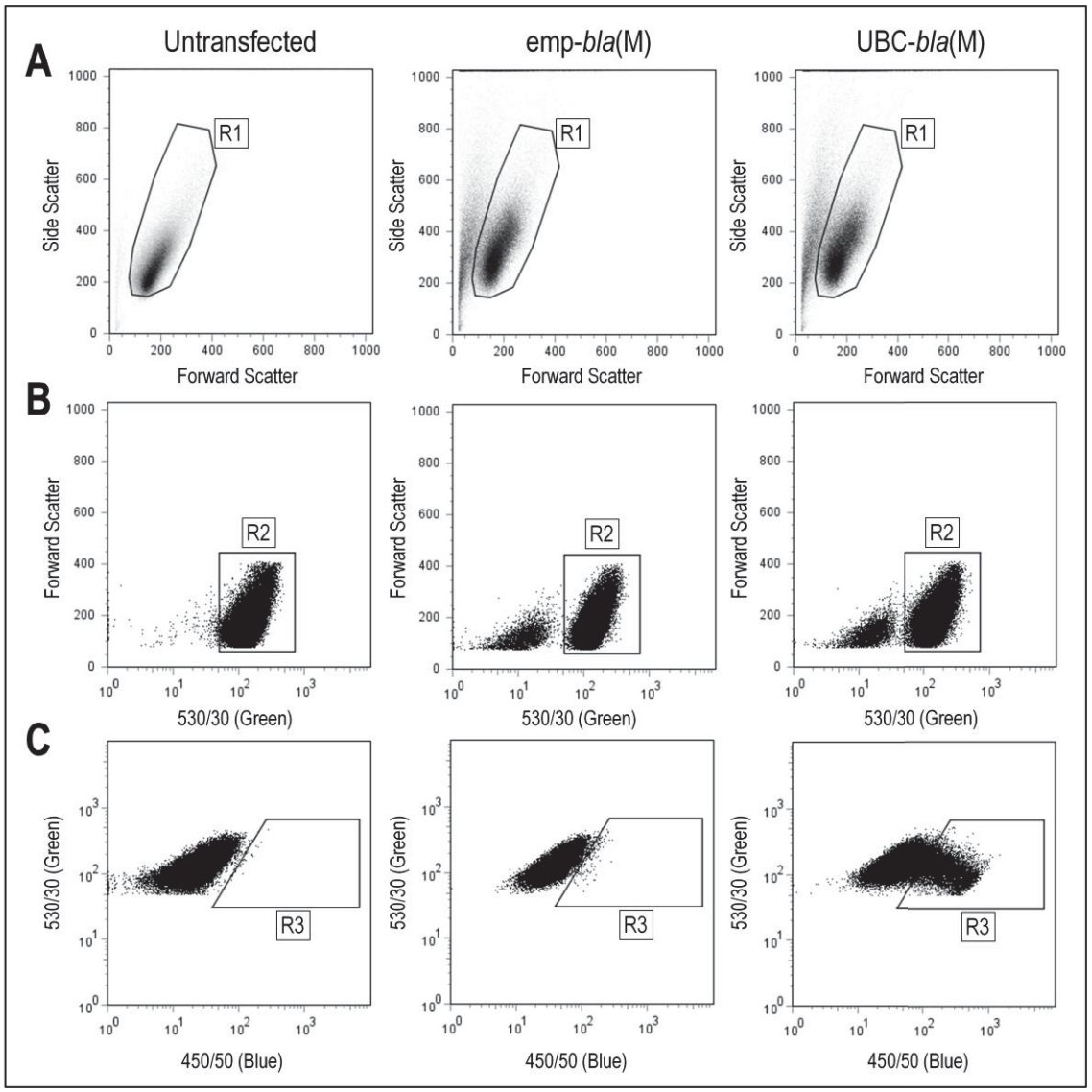

Figure 6.13 Gating protocol for determining promoter activity after nucleofection of THP-1 cells with *SLC11A1* promoter constructs. Gates were determined according to scatter plots of untransfected cells (left panels), negative control [emp-*bla*(M)] transfected THP-1 cells (middle panels), and the positive control [UBC-*bla*(M)] transfected THP-1 cells (right panels). On the forward and side scatter plot (A), a gate R1 was used to select only intact cells (removing cell debris). To remove the non-viable cells, a gate R2 was used to select viable cells, which had high green fluorescence on a forward versus green fluorescence scatter plot (B). Promoter activity was then determined by the mean fluorescence intensity of gate R3, which was positioned after analysis of untransfected cells and cells transfected with the negative control plasmid, emp-*bla*(M), to gate specifically on the transfected cell population (C). The mean fluorescence intensity of the viable untransfected cell population of the negative control plasmid [emp-*bla*(M)] was used to correct for background fluorescence for each *SLC11A1* promoter construct.

6.3.2.4 Transfection of *SLC11A1* Promoter Constructs into THP-1 Cells

Using the optimised THP-1 transfection method involving nucleofection (Section 6.2.2.2.3) and flow cytometric analysis (Section 6.2.2.3.4), *SLC11A1* promoter constructs were transfected into undifferentiated THP-1 cells (monocyte phenotype). Overall, the level of *SLC11A1* promoter activity driven by the different promoter constructs was higher in THP-1 cells as compared to 293T cells, when comparisons were made using the positive control plasmid [UBC-*bla*(M)]. The negative control plasmid, emp-*bla*(M), resulted in a similar level of green fluorescence, compared to other *SLC11A1* promoter plasmids, however, there was no or low blue fluorescence. Variable promoter activities were observed after nucleofection of the different *SLC11A1* promoter constructs into THP-1 cells.

6.3.2.4.1 Determination of Important Promoter Regions Driving SLC11A1 Transcription in Monocyte-Like THP-1 Cells

The different *SLC11A1* promoter lengths, containing only the variant allele 3 [$(GT)_n$ allele 3 with -237 C] in the forward orientation (Section 5.3.2.2), were assessed for their promoter activity in THP-1 cells. Similar to results obtained using 293T cells, promoter region 7C (-532 to +49) had the highest promoter activity in the THP-1 cells (Figure 6.14). However, promoter region 8A (-362 to +367) had the lowest promoter activity (Figure 6.14). In THP-1 cells, increasing promoter region size correlated with increasing promoter activity. For example, the promoter activity of construct 7C was higher than that of 8C, which had higher promoter activity than 9C, which, in turn, was greater than 10C (the smallest promoter region) (Figure 6.14).

Determination of the Minimal *SLC11A1* Promoter Region and Mechanism of Transcription Initiation

The smallest *SLC11A1* promoter region, 10C, was able to activate transcription, albeit at a medium to low level (Figure 6.14). This 148bp region, spanning from -99 to +49, represents the minimal promoter region and, therefore, the site of the formation of the basal transcriptional complex. The location of the minimal promoter region within this 148bp region confirmed the *in silico* clustalW and WeederH analysis, which identified this region as the most conserved (Section 5.3.1.2 and 5.3.1.3). This finding also

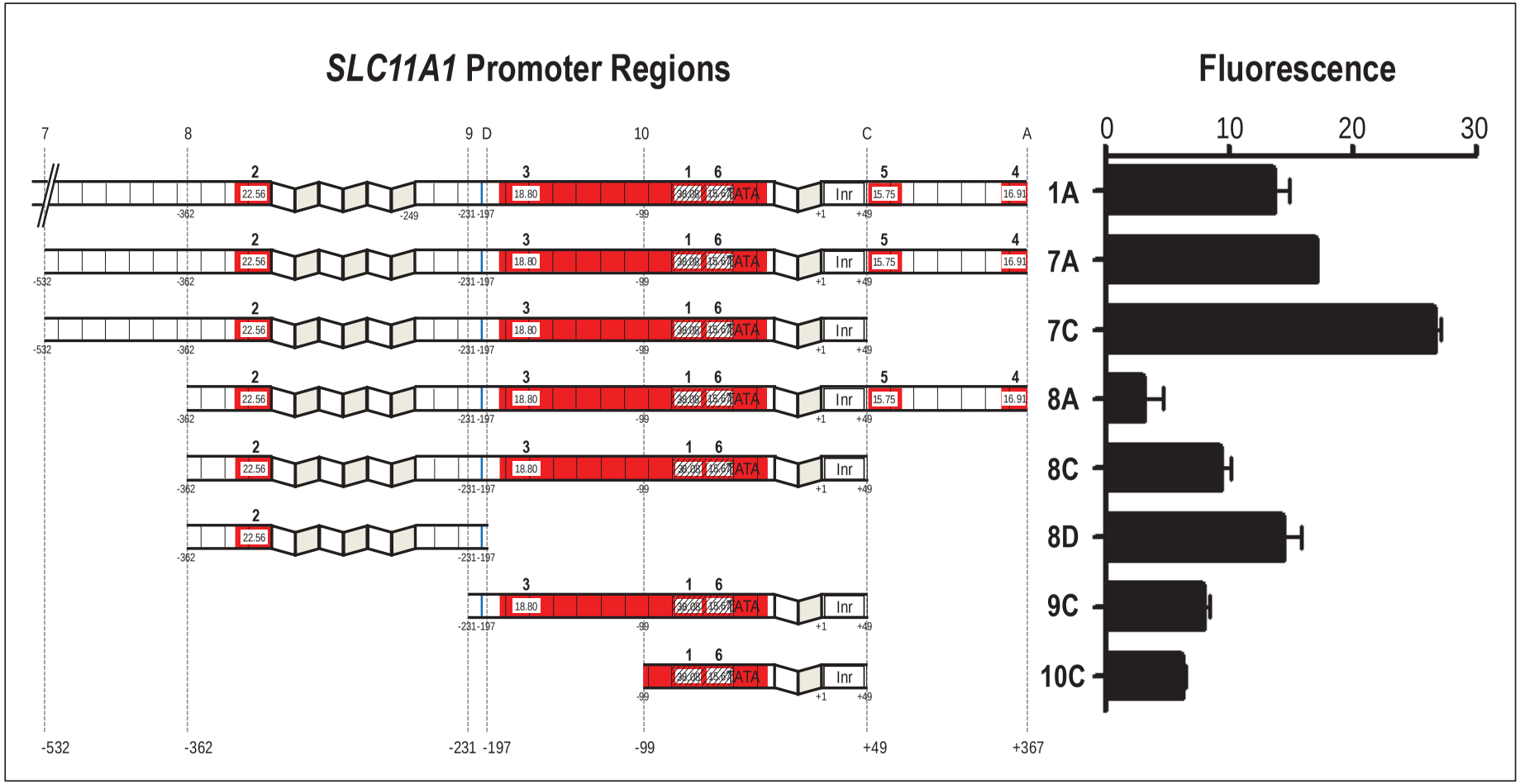

Figure 6.14 Promoter activity of *SLC11A1* constructs, containing different lengths of the *SLC11A1* promoter, after transfection into THP-1 cells. Nucleofection of *SLC11A1* promoter constructs, containing only allelic variant allele 3 [$(GT)_n$ allele 3 with -237 C] in the forward orientation, was used to transiently transfect THP-1 cells. Cells were loaded with the CCF2-AM substrate 24h post-nucleofection and fluorescence intensity measured by flow cytometry. The promoter activity of the promoter constructs in THP-1 cells (right) are shown adjacent to the respective *SLC11A1* promoter regions cloned into the pGeneBLAzer plasmid (left).

corroborates the data obtained after transfection of the *SLC11A1* promoter constructs into 293T cells (Figure 6.15) (Section 6.3.1.2.1). The observation that the minimal promoter region of *SLC11A1* is shared by both non-monocytic (293T) and monocytic (THP-1) cells suggests that the essential factors involved in the formation of the basal transcriptional complex may not be monocyte specific.

Transfection of the *SLC11A1* promoter constructs into THP-1 cells also showed that a downstream promoter element, or other core elements downstream of the transcription start site (+50 to +369), are not involved in the formation of the basal transcriptional complex as a loss of promoter activity from promoter regions lacking the 5'UTR was not observed (Figure 6.14). The absence of core elements located within this region is consistent with the results after the transfection of promoter constructs into 293T cells (Figure 6.15) (Section 6.3.1.2.1) and corroborates the findings of TFBS searches (Section 5.3.1.4.1).

Location of Potential Transcriptional Enhancers/Repressors

The observation that enhanced promoter activity correlated with increasing promoter length (Figure 6.14) suggests the presence of TFBS, and/or regions of altered DNA topology, located throughout the *SLC11A1* promoter. Such regions would likely exert synergistic effects to enhance *SLC11A1* expression. However, an increase in promoter activity was not observed between the larger 1A promoter region (3267bp region spanning -2900 to +369) compared to the smaller 7A promoter region (-533 to +369). A similar level of promoter activity was observed from both of these *SLC11A1* promoter regions, suggesting that there are no transcriptional elements which influence *SLC11A1* transcription in monocytes, located within the -2900 to -533 region.

Of particular interest was the -532 to -362 region of the *SLC11A1* promoter. Both the 7A (-533 to +369) and 7C (-533 to +49) promoter regions drove a high level of promoter activity, however, the 8A (-362 to +369) and 8C (-362 to +49) regions resulted in promoter activity that was 3 to 5 fold lower (Figure 6.14). This 170bp region (-532 to -362), located upstream of the $(GT)_n$ microsatellite repeat, likely contains a factor(s), which enhance *SLC11A1* transcription. These factors may interact directly to facilitate formation of the basal transcriptional complex, thereby enhancing *SLC11A1*

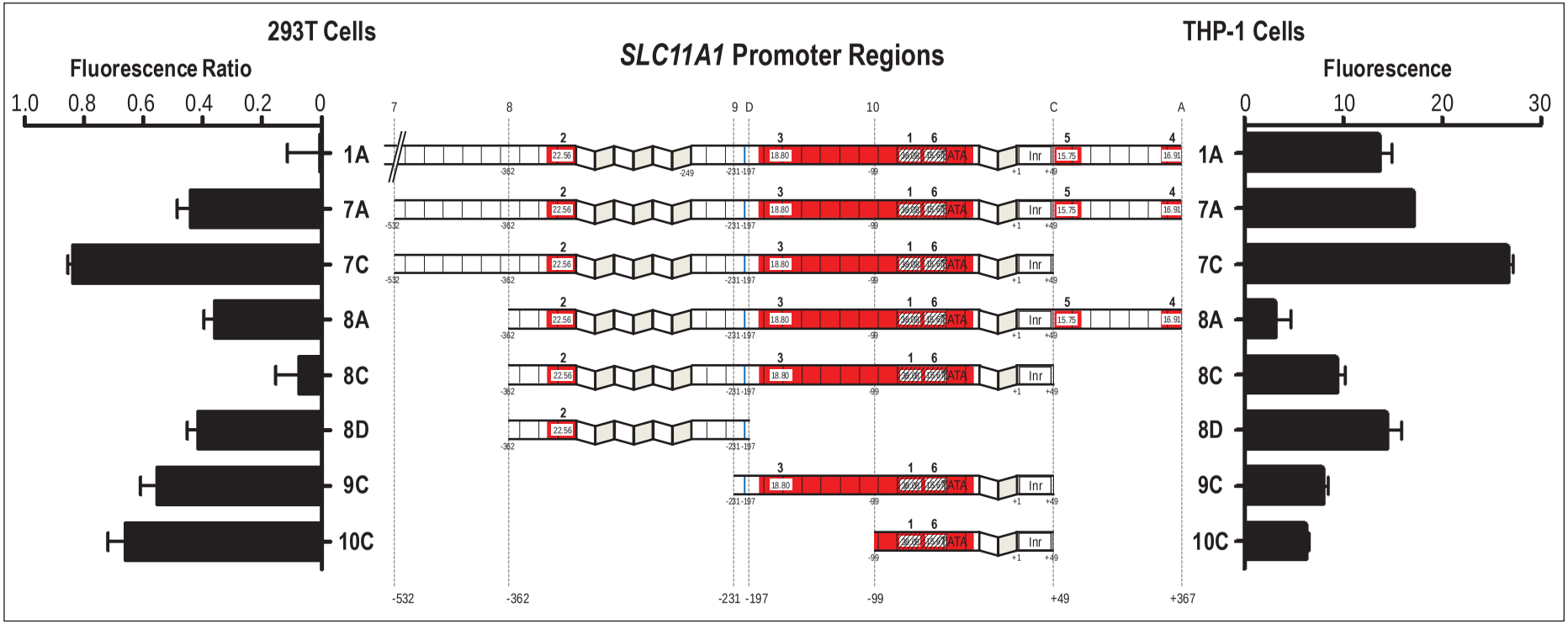

Figure 6.15 Comparison of promoter activity of *SLC11A1* constructs, containing different lengths of the *SLC11A1* promoter, in 293T cells and THP-1 cells. The cell lines were transiently transfected with the promoter constructs, with all plasmids containing only variant allele 3 [$(GT)_n$ allele 3 with -237 C] in the forward orientation, and 24h post transfection loaded with the CCF2-AM substrate with detection of promoter activity using a fluorescent plate reader (293T) or flow cytometry (THP-1). The promoter activity of the different promoter constructs in the THP-1 (right) and 293T (left) cells are shown adjacent to the respective promoter regions cloned into the pGeneBLAzer plasmid (centre).

expression. Alternatively, due to the location of this region 300-500bp upstream of the minimal promoter region, a synergistic effect with another transcription factor(s) located closer to the transcription start site may result, thereby accounting for the high promoter activity observed with the 7C promoter region. This region was also shown to drive higher promoter activity in 293T cells, however, the effect of this region on *SLC11A1* promoter activity was more pronounced in THP-1 cells (Figure 6.15) (Section 6.3.1.2.1).

The bioinformatic analyses of the *SLC11A1* promoter coupled with observations after the transfection of promoter constructs into 293T cells suggested the presence of transcriptional enhancer elements located within the 5'UTR and the first intron (+50 to +369) (Sections 5.3.1.7 and 6.3.1.2.1). However, after transfection of the *SLC11A1* promoter constructs into THP-1 cells, a 1.5 and 3 fold decrease in promoter activity was observed between regions 7C and 7A and regions 8C and 8A, respectively (Figure 6.14), indicating that the +50 to +369 region does not contain any functional transcriptional enhancer(s). However, the decreased promoter activity observed for the +50 to +369 promoter region suggests that this region serves to recruit a factor, which inhibits *SLC11A1* transcription in monocytes. The transcriptional effect of the -362 to -231 region also differed between the non-monocytic (293T) and monocytic (THP-1) cells. While this region appears to recruit a transcription factor which inhibits transcription in 293T cells (Section 6.3.1.2.1), the higher promoter activity driven by 8C (-362 to +49) as compared to 9C (-231 to +49) in THP-1 cells, suggested that this region did not contain an inhibitory element in monocytic cells (Figure 6.15).

6.3.2.4.2 The SLC11A1 Promoter Shows Evidence of Bidirectional Transcription

Analysis of promoter activity in the forward and reverse orientation (containing the allele 3 variant) indicated that the *SLC11A1* promoter may mediate bi-directional transcription, as the larger promoter regions (1A, 7A and 7C) exhibited promoter activity when cloned in the opposite orientation (Figure 6.16). The promoter activity of these larger promoter regions, in the reverse orientation, was 25-50% of the activity driven by the respective inserts in the forward orientation. While the larger *SLC11A1* promoter regions showed evidence of bidirectional promoter activity *in vivo*, the smaller promoter regions did not show any evidence of promoter activity in the reverse

orientation. The bidirectional activity of the 1A, 7A and 7C promoter regions in THP-1 cells was not observed in 293T cells (Section 6.3.1.2.2), in which only promoter regions 8A and 8D mediated bidirectional expression (Figure 6.16).

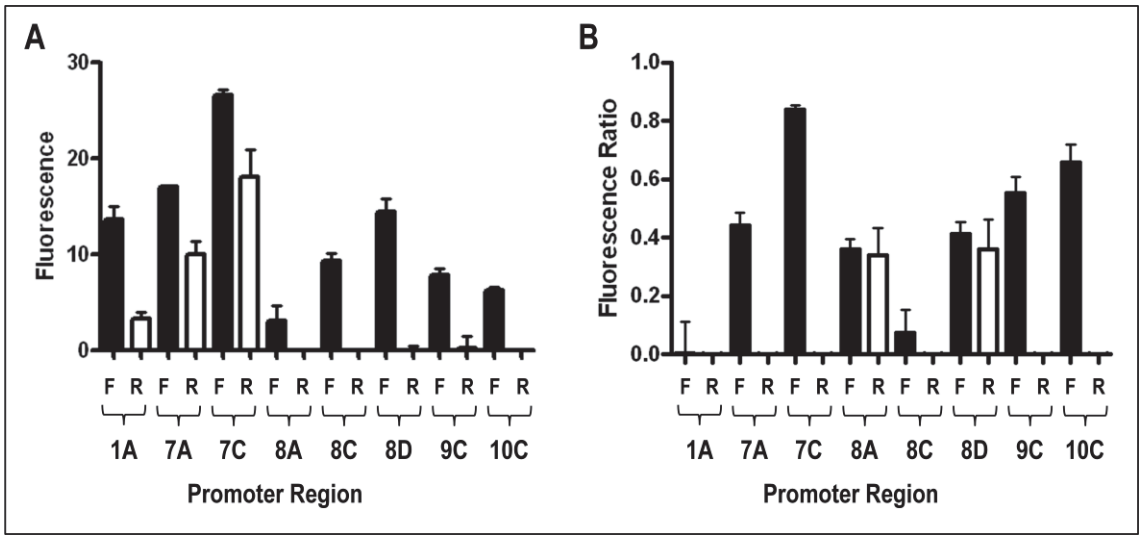

Figure 6.16 Assessment of the ability of the *SLC11A1* promoter region to mediate bidirectional transcription. The black and white bars represent *SLC11A1* promoter regions, all containing variant allele 3 [$(GT)_n$ allele 3 with -237 C] cloned into the pGeneBLAzer vector in the forward (F) and reverse (R) orientation, respectively. Promoter activity observed when promoter constructs were tested in monocyte-like THP-1 (A) and the non-monocyte 293T (B) cells.

A Monocyte Specific Factor Binds to the 8D Promoter Region

Consistent with findings using 293T cells, the 8D promoter region (-362 to -197), which contains the $(GT)_n$ microsatellite repeat and a small amount of surrounding DNA, showed a medium level of promoter activity, suggesting that the $(GT)_n$ microsatellite repeat may have endogenous enhancement ability (Figure 6.15). However, unlike the findings using the 293T cell line (Section 6.3.1.2.2), the 8D promoter region only enhanced transcription when in the forward orientation in THP-1 cells, with no promoter activity observed in the reverese orientation (Figure 6.16). This suggests that there may be a monocyte specific transcription factor, which binds within the 8D region to co-ordinate expression only in the forward orientation.

6.3.2.4.3 Promoter Constructs Containing Allele 3 Drive Higher Promoter Activity Compared to Allele 2 and Allele T in THP-1 Cells

The different *SLC11A1* promoter lengths, containing the variants allele 3 [$(GT)_n$ allele 3 with -237 C], allele 2 [$(GT)_n$ allele 2 with -237 C], and allele T [$(GT)_n$ allele 3 with -237 T] were transfected into THP-1 cells to determine the effects of the common promoter variants on *SLC11A1* promoter activity and locate factors which may mediate the differential expression levels observed in the presence of the different variants (Figure 1.8) (Section 5.3.2.2.2).

Of the different promoter lengths transfected into THP-1 cells, promoter regions 7C, 8C and 8D resulted in a 2 to 2.5 fold increase in promoter activity in the presence of $(GT)_n$ allele 3 as compared to $(GT)_n$ allele 2 (Figure 6.17A). Promoter regions 7A and 8A displayed a similar trend to the other *SLC11A1* promoter regions tested, where $(GT)_n$ allele 3 drove higher expression as compared to allele 2, however the differences in the level of expression were not as pronounced (Figure 6.17B). While the higher promoter activity observed in the presence of allele 3 is consistent with previous reports, which have assessed the promoter activity of the $(GT)_n$ microsatellite repeat in monocytic cell lines (Searle and Blackwell, 1999, Zaahl *et al.*, 2004), it does not corroborate the results observed after transfection of the promoter constructs in 293T cells (Section 6.3.1.2.3) or the *in silico* Z-Hunt analysis (Section 5.3.1.5.1). Both of the latter analyses found that $(GT)_n$ allele 2 possessed greater enhancer ability as compared to allele 3.

Analysis of the effect of the -237C/T polymorphism on promoter activity in THP-1 cells found that the more frequent -237 C variant drove a 1.5 to 6 fold increase in promoter activity as compared to the -237 T variant (Figure 6.17A). The trend for higher promoter activity in the presence of the -237 C variant was also observed for the 9C promoter region, which lacks the $(GT)_n$ microsatellite repeat, suggesting that this polymorphism may modulate *SLC11A1* expression independently of the $(GT)_n$ microsatellite (Figure 6.17C). However, the lower promoter activity of the -237 T variant, as compared to the -237 C variant, in the 9C region was not as high (1.5 fold increase) as that seen in the other promoter regions containing both the $(GT)_n$ microsatellite and the -237C/T polymorphisms. This suggested that the -237C/T polymorphism may alter *SLC11A1* expression both independently of, and in association with, the $(GT)_n$ microsatellite repeat. The effect of the -237C/T polymorphism on

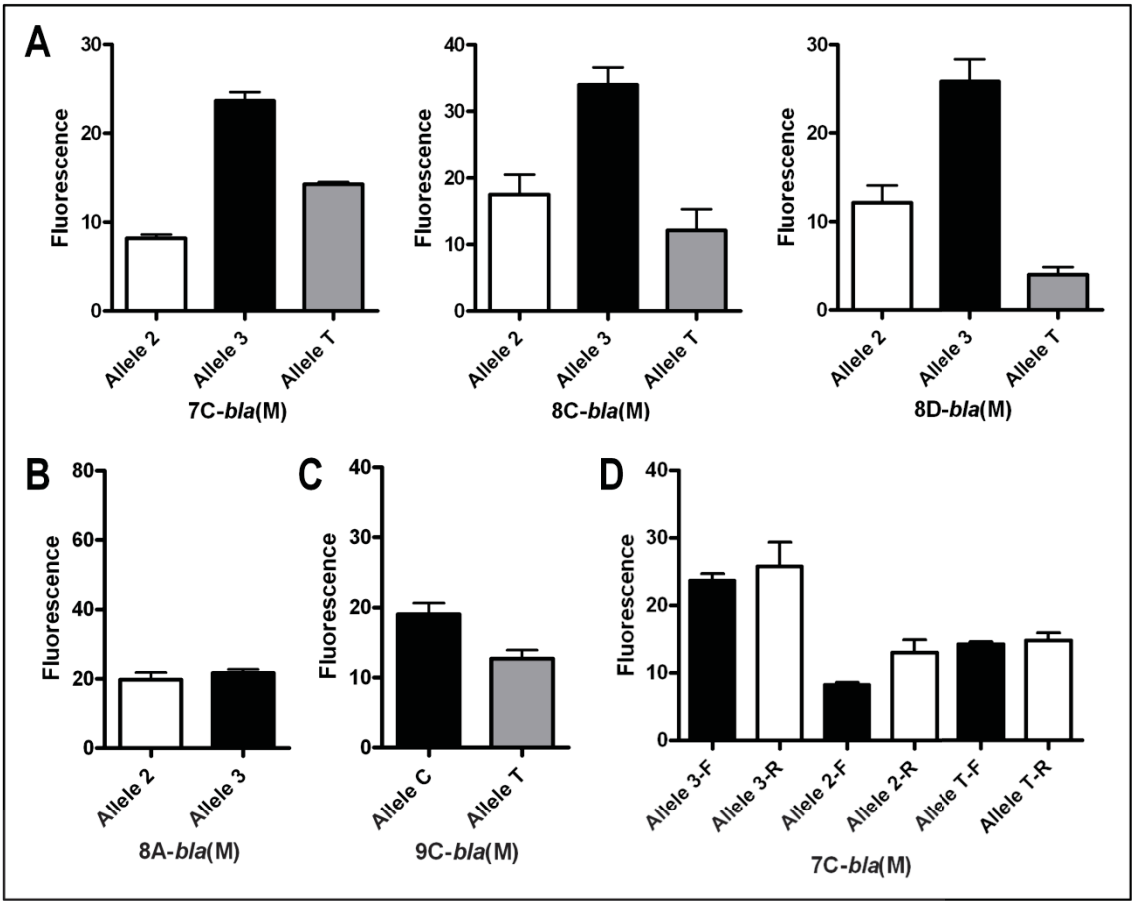

Figure 6.17 Analysis of the effect of the variants at the *SLC11A1* promoter $(GT)_n$ and -237C/T polymorphisms on promoter activity in THP-1 cells. Multiple plasmids of the same *SLC11A1* promoter region, differing only by the allelic variant present, either allele 2 [$(GT)_n$ allele 2 with -237 C], allele 3 [$(GT)_n$ allele 3 with -237 C] or allele T [$(GT)_n$ allele 3 with -237 T], were transfected into THP-1 cells. Promoter region 9C contained only the -237C/T polymorphism, therefore, had two variants, allele C and allele T. Promoter activity of the allelic variants observed in the 7C, 8C, 8D (A), 8A (B) and 9C (C) *SLC11A1* promoter regions. (D) Assessment for bias in the direction of transcription due to the presence of different allelic variants. Promoter regions 1A, 7A and 7C, containing the different allelic variants, were transfected into THP-1 cells in both the forward and reverse orientation.

promoter activity in THP-1 cells differed to that observed in the 293T cells. While a decrease in promoter activity was observed in the presence of the -237 T variant in THP-1 cells, the presence of this variant led to an increase in promoter activity in 293T cells (Section 6.3.1.2.3).

Analysis of the larger promoter regions, 1A, 7A and 7C, suggested that the *SLC11A1* promoter may mediate transcription in a bidirectional fashion (Section 6.3.2.4.2). Therefore, modulation of *SLC11A1* promoter activity by the different promoter variants

could be due to the variant altering the rate of transcription in the forward direction as compared to transcription in the reverse orientation, with increased reverse direction transcription resulting in a decrease in *SLC11A1* expression. Analysis of the 1A, 7A and 7C promoter constructs containing the common promoter variants in the forward and reverse orientation, did not detect any differences in promoter activity of forward and reverse orientation constructs between the different variants (Figure 6.17D).

6.3.2.5 Further Bioinformatic Analysis of Important *SLC11A1* Promoter Regions Identified by the Reporter Assays

Based on the findings of the *in vivo* promoter analyses (Sections 6.3.1.2 and 6.3.2.4), the identified important *SLC11A1* promoter regions were analysed further to identify putative DNA elements which may recruit transcription factors to these regions that may be involved in modulating *SLC11A1* transcription. Analyses were carried out by reviewing the previously obtained *in silico* data and by conducting further analyses (Sections 5.2.2.1.4 and 5.3.1.4)

6.3.2.5.1 The Basal Transcriptional Complex Assembles within a 148bp Region (-99 to +49) of the SLC11A1 Promoter

The *SLC11A1* promoter reporter assays identified a minimal promoter region of 148bp located at -99 to +49 within the *SLC11A1* promoter (Section 6.3.2.4.1). While this region showed high homology among *SLC11A1* homologs, as determined by the clustalW and WeederH analyses (Figure 6.18A), no elements for the formation of the basal transcriptional complex (for example TATA box, Inr, DPE etc) were identified when this region was analysed using TFBS searches or by visual sequence analysis (Section 5.3.1.4.1). Kishi et al. (1996) reported a non-canonical TATA box (GAAAA) located at -38 to -33, however this site is not as highly conserved as the surrounding regions, casting doubt on the significance of this site (Figure 6.18A). Located adjacent to this site is an area of high homology, which was identified by clustalW analysis and was the 6th highest scoring element from the WeederH analysis (15.67). The location of this region at -33 to -22 (TGTTTCACAACG) is in keeping with the positioning of a TATA element and may therefore represent the site for TBP interaction (Figure 6.18).

Located upstream of the putative TBP element, within the *SLC11A1* promoter region which displayed the highest level of conservation (-70 to -28) (Section 5.3.1.2), is the highest scoring WeederH element (38.08) (Section 5.3.1.3) (Figure 6.18). Based on its location, this highly conserved sequence may correspond to a region where a transcription factor(s) binds, as either part of the TFIID complex, or other TAFs, which would bind first and then recruit TBP to the highly conserved -33 to -22 region. Also located within this region are predicted C/EBP (NF-IL6) (Figure 6.18) and Sp1 sites, which may further modulate the formation of the basal transcriptional complex.

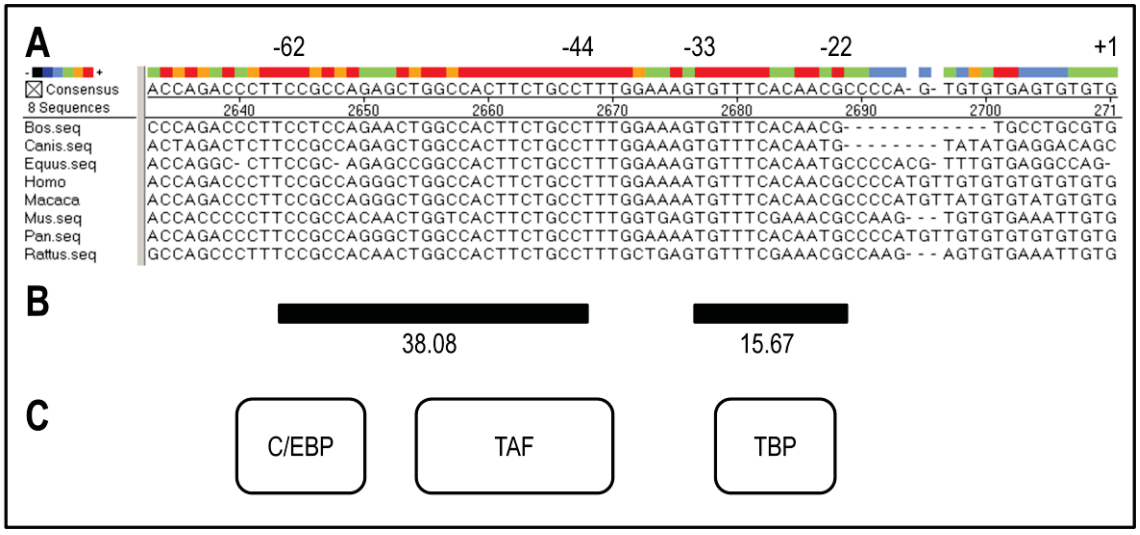

Figure 6.18 Identified *SLC11A1* minimal promoter region and putative mechanism of *SLC11A1* expression. (A) ClustalW alignment of the promoter regions of 8 *SLC11A1* homologs. (B) The location of WeederH elements and their respective scores. (C) Location of putative TFBS. Transcription is initiated by TAF binding to the region displaying the highest level of homology and highest scoring WeederH element. TAF would then recruit TBP to a region -33 to -22 from which the basal transcriptional complex would form.

6.3.2.5.2 Analysis of the 170bp Region (-532 to -362) Exerting the Highest SLC11A1 Promoter Activity

The promoter assays identified a 170bp region (-532 to -362) as having the greatest transcriptional activity (Figure 6.14) (Section 6.3.2.4.1). This region was assessed for potential TFBS that could account for the high promoter activity observed. A range of transcription factor elements, potentially able to regulate monocyte-specific expression, were identified within this region. These included binding sites for transcription factors involved in immune cell development or haemopoietic cell proliferation (c-Myb, PU.1, PEA3, GATA2 and GM-CSF), in interferon response (IRF-1, IRF-2 and IRF-9) or LPS response (CSPB1), and more generalised transcription factor binding sites (AP1, AP2 and Sp1) (Figure 6.19).

In the vicinity of the described 170bp region were two sites (E2M2 and E3M2), previously identified by Richer et al. (2008), as elements for the binding of transcription factors (Figure 6.19). While these sites were identified as putative transcriptional elements, the specific transcription factors which bound these sites were not determined (Richer *et al.*, 2008). The site E3M2, located at the border of the identified 170bp region, was located close to a high scoring WeederH element (12.18) (Figure 6.19). Bioinformatic analysis did not identify any transcription factors at the E3M2 site, however, previous studies have suggested that GM-CSF may bind at this site. The site E2M2 also coincides with another identified WeederH element (10.46) and analysis of this site located a number of putative interferon response elements (ISGF3 – IRF9, IRF2) (Figure 5.19). Furthermore, visual sequence analysis of this site revealed a perfect match for an IFN-stimulated response element (ISRE) [(A/G)NGAAANNGAAACT] (Darnell *et al.*, 1994), specifically an IRF-Ets composite sequence (IECS) [GAAANN(N)GGAA] (Tamura *et al.*, 2005, Tamura *et al.*, 2008).

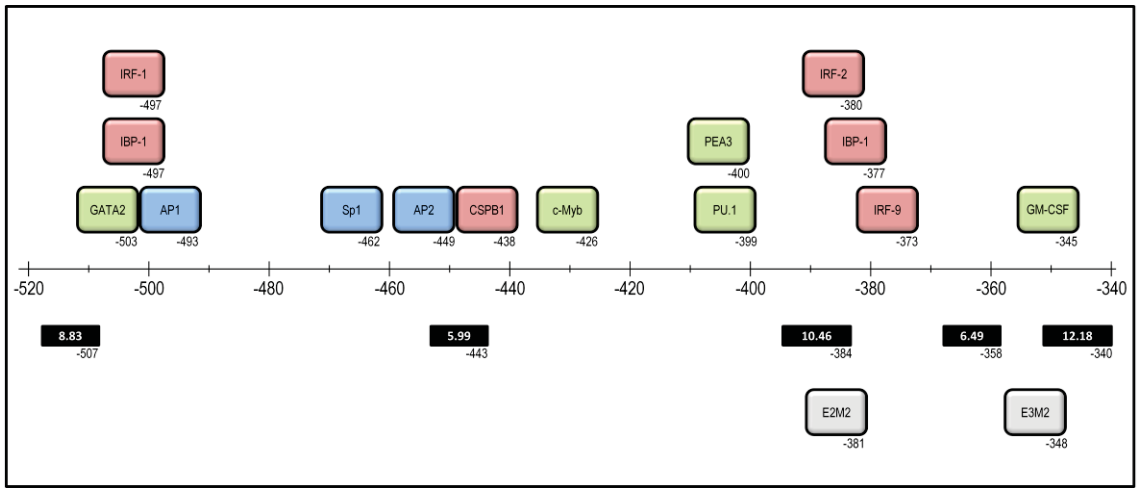

Figure 6.19 Location of putative transcription factor binding sites within the -520 to -340 region of the *SLC11A1* promoter. This region drove the greatest level of transcriptional enhancement. The coloured boxes indicate the location of putative TFBS within the *SLC11A1* promoter (the scale located underneath is relative to TSS1). The green, red and blue colours indicate transcription factors present in immune cell development, IFN/LPS responsiveness and general transcription factors, respectively. The black boxes indicate the location of elements identified by WeederH analysis, with the respective score indicated inside the box. The grey boxes indicate the location of sites E2M2 and E3M2 (identified by Richer *et al*., 2008). Numbers located below to the right of boxes indicate the location of the element (the 3' nucleotide position).

The promoter analyses showed a trend towards increasing *SLC11A1* promoter activity with increasing length of the *SLC11A1* promoter region assessed. From the bioinformatic analysis, multiple elements for the binding of the transcription factors, Sp1 and C/EBP, were identified. Binding of these transcription factors has been shown to drive expression from promoters, which lack canonical TATA box elements (Huber *et al.*, 1998, Smale, 1997, Smale and Kadonaga, 2003). Specifically, 15 sites for Sp1 binding were identified within the *SLC11A1* promoter, suggesting that *SLC11A1* transcription may be further modulated by Sp1 and C/EBP sites dispersed throughout the promoter, which would account for the increased expression levels observed with increasing promoter size.

6.3.2.5.3 Binding of a Monocyte Specific Transcription Factor within the -362 to -197 Region Mediates Allelic Differences in SLC11A1 Expression

Z-Hunt analysis indicated that $(GT)_n$ allele 2 had a greater propensity to form Z-DNA as compared to $(GT)_n$ allele 3, suggesting that allele 2 would provide greater transcriptional enhancement (Section 5.3.1.5.1). This finding was corroborated by the promoter analyses conducted using 293T cells (Section 6.3.1.2.3). However, when the promoter plasmids were transfected into the THP-1 monocytic cell line, $(GT)_n$ allele 3 possessed a higher promoter activity as compared to $(GT)_n$ allele 2 (Section 6.3.2.4.3), and was consistent with previous studies assessing the transcriptional enhancement ability of the different $(GT)_n$ variants in monocytic cell lines (Searle and Blackwell, 1999, Zaahl *et al.*, 2004). Therefore, these results indicate that monocyte-specific factor(s) interact with (or are differentially affected by) the $(GT)_n$ microsatellite repeat to mediate the differences in *SLC11A1* expression observed for the different promoter variants. Furthermore, the monocyte-specific factor(s) would be located within the -362 to -197 region (165bp), as this region was common to all of the promoter constructs assessing the effects of the $(GT)_n$ microsatellite repeat.

Analysis of the -362 to -197 promoter region identified a number of transcription factor elements, which may play a role in modulating *SLC11A1* transcription in monocytic cells (Figure 6.20). This region contains the experimentally determined sites for the binding of HIF-1α and AP1 (ATF3) located within, and adjacent to, the $(GT)_n$ microsatellite repeat, respectively (Bayele *et al.*, 2007, Xu *et al.*, 2011) (Figure 6.20). This region also contained two sites, identified by Richer et al. (2008), which could mediate transcription factor binding. These include the previously described E3M2 region (putative GM-CSF binding) (Figures 6.19 and 6.20) and the E6M2 site, which, from the *in silico* analysis, correlated with elements for the binding of the transcription factors, Sp1 and KLF (Figure 6.20). Also located within the -362 to -197 region were sites for additional Sp1 and KLF binding as well as a PEA3 site. A few highly conserved WeederH elements were also located within this 165bp region (Figure 6.20) and several of these corresponded with experimentally determined sites for transcription factor binding. However, no transcription factor binding candidates were identified for two high scoring WeederH elements, in particular the seventh highest scoring element (14.08), which was located within the 165bp 8D region, and another element (18.08, the third highest scoring element) located just outside of the 8D region.

Analysis of the effect of the -237C/T polymorphism on transcriptional activity suggested that the lower level of promoter activity driven by the -237 T variant in THP-1 cells was independent of the $(GT)_n$ microsatellite repeat (Section 6.3.2.4.3). Analysis of wild type (-237 C) sequence for potential TFBS did not identify any transcriptional elements in the vicinity of the -237C/T polymorphism. However, a TFBS search carried out with the introduction of the -237 T variant, resulted in the production of a transcriptional element for the binding of the ubiquitously-expressed transcription factor Oct-1 (Figure 6.20) (Section 5.3.1.4.3). The introduction of the Oct-1 element in the presence of the -237 T variant may explain the differences in promoter activity mediated by variants at the -237C/T polymorphism.

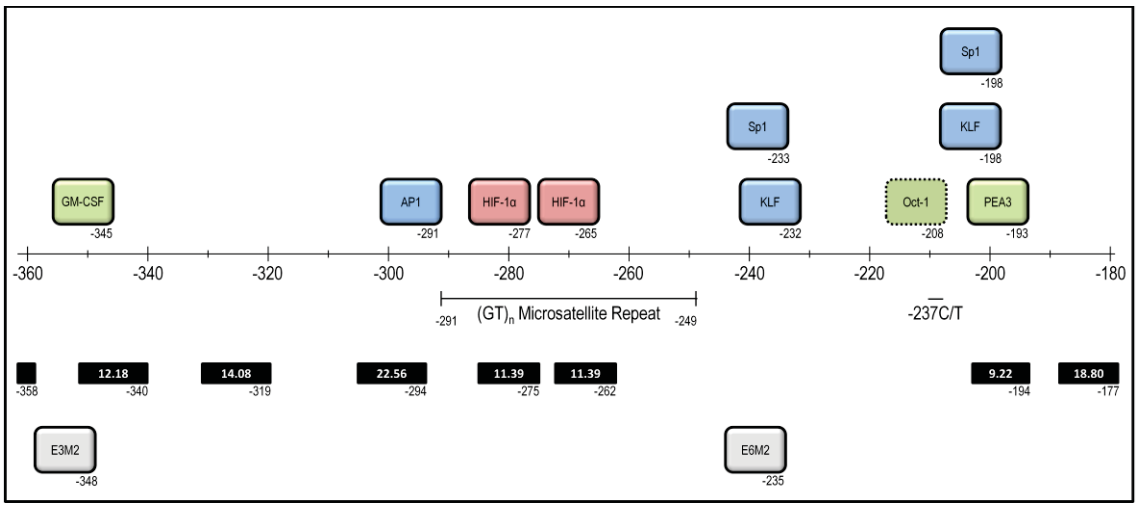

Figure 6.20 Location of putative monocyte-specific TFBS within the -360 to -180 region of the *SLC11A1* promoter. The coloured boxes indicate the location of putative transcription factor binding within the *SLC11A1* promoter (the scale bar located underneath is relative to TSS1). The green, red and blue colours indicate transcription factors expressed during immune cell development, IFN/LPS responsiveness and general transcription factors, respectively. The black boxes indicate the location of elements identified by WeederH analysis, with the respective score indicated inside the box. The grey boxes indicate the location of sites E3M2 and E6M2 (identified by Richer *et al*., 2008). Numbers located below to the right of boxes indicate the location of the element (the 3' nucleotide position).

6.4 DISCUSSION

6.4.1 Overview

The current study has utilised an integrated approach, based on *in silico* bioformatics and *in vivo* functional assays, to elucidate promoter regions involved in the transcriptional regulation of *SLC11A1*. Firstly, bioinformatic analyses of the *SLC11A1* promoter were completed to identify highly conserved and putative regulatory regions involved in *SLC11A1* transcription (Chapter 5, Part 1). These regulatory regions were then used to define *SLC11A1* promoter regions, for cloning into promoter reporter assays, allowing the functional assessment of the regions for their involvement in *SLC11A1* transcriptional regulation (Chapter 5, Part 2). A number of different variants of each *SLC11A1* promoter length, differing only at the $(GT)_n$ microsatellite and the -237C/T polymorphisms, were cloned. Additionally, these promoter regions were cloned in both the forward and reverse orientation. The prepared *SLC11A1* promoter constructs were then functionally assessed for promoter activity in monocyte-like (THP-1) and non-monocyte (293T) cell lines (Chapter 6, Part 3). Testing of the promoter constructs allowed: the identification of a minimal *SLC11A1* promoter region and promoter regions mediating transcriptional enhancement of *SLC11A1*, the determination of the ability of the *SLC11A1* promoter to mediate bidirectional transcription, and the elucidation of the mechanism by which promoter variants mediate differential levels of *SLC11A1* expression.

6.4.2 THP-1 Cells are an Appropriate Model for the Investigation of *SLC11A1* Expression

To determine promoter activity of the designed and manufactured *SLC11A1* promoter constructs, it was important to select a cell line which displays the restricted expression of *SLC11A1 in vivo*. Furthermore, it would be advantageous that the selected cell line mimics the kinetics of *SLC11A1* expression during monocyte to macrophage differentiation or upon stimulation (with IFN-γ or LPS), thereby ensuring that the factors involved in modulating *SLC11A1* expression are present as cells progress along the monocyte/macrophage lineage.

THP-1 cells were found, by morphological/cytochemical analysis and quantitative real time PCR, to resemble a monocyte-like cell, which expressed *SLC11A1* (Section 6.3.2.2.1 and 6.3.2.2.2). Furthermore, the observed increase in *SLC11A1* expression during cellular differentiation of THP-1 cells was consistent with that observed during the differentiation of primary monocytes to macrophages. A PMA concentration of 5ng/ml was found to be adequate to allow differentiation and a concomitant increase in *SLC11A1* expression, in the absence of off target effects observed using higher concentrations (Park *et al.*, 2007). Stimulation of THP-1 cells with IFN-γ and LPS also resulted in an increase in *SLC11A1* expression (Section 6.3.2.2.2), consistent with observations after stimulation of primary monocytes. Overall, the morphological and cytochemical analyses coupled with increased expression of *SLC11A1* during monocyte to macrophage differentiation or stimulation established that the THP-1 cell line constituted an appropriate model for the analysis of the mechanisms of *SLC11A1* expression.

6.4.3 *SLC11A1* Promoter Analysis

6.4.3.1 A 148bp Region of the *SLC11A1* Promoter Defines the Minimal Promoter Region

Transfection of promoter constructs containing different lengths of the *SLC11A1* promoter, into 293T and THP-1 cells, showed that the minimal promoter region able to activate transcription was a 148bp region (located from -99 to +49), which represents the site for the formation of the basal transcriptional complex (Figure 6.21). The location of the minimal promoter (-99 to +49) corresponds to the region predicted by the bioinformatic analyses (WeederH analysis and the clustalW alignment) (Section 5.3.1.2 and 5.3.1.3). Furthermore, the 148bp minimal promoter region identified in the current analysis is the smallest region identified to date, which is able to mediate *SLC11A1* transcription. Prior to this study, a 180bp region (-161 to +19) was the smallest identified *SLC11A1* promoter region, which could mediate transcription (Xu *et al.*, 2011).

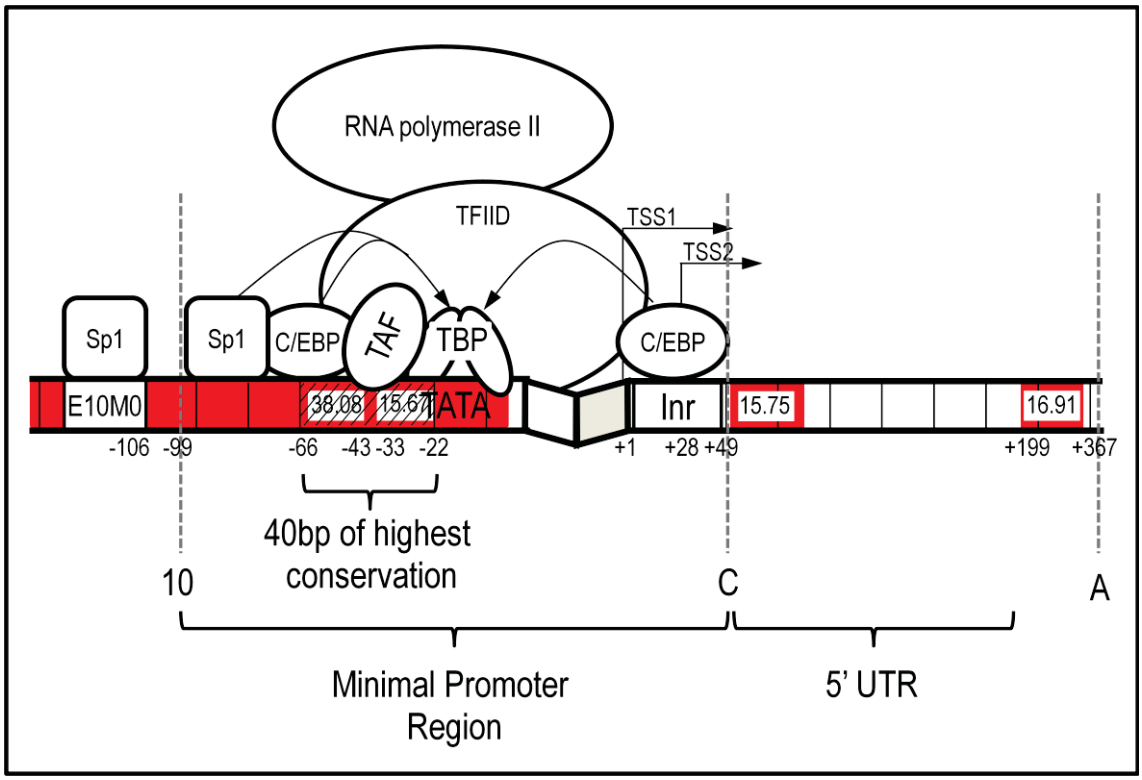

Figure 6.21 *SLC11A1* transcription appears to be initiated by a mechanism different to that observed from canonical promoters. Landmarks of the *SLC11A1* promoter are shown, including the two transcription start sites (TSS1 and TSS2) and putative Z-DNA forming sequence identified at TSS1 (Section 5.3.1.5). Red regions indicate the conserved areas of the *SLC11A1* promoter identified from the clustalW alignment and white boxes containing numbers indicate the high scoring WeederH elements (Section 5.3.1.2 and 5.3.1.3). A 148bp region was identified as the minimal promoter region (-99 to +49) and the site for the formation of the basal transcriptional complex. No core promoter elements were identified in the 5' UTR or first intron of *SLC11A1*. Recruitment of C/EBP binding has been experimentally determined to occur over TSS2 (+24) and functions as a core promoter element, while Sp1 binding just outside of the minimal promoter region (located at -106 to site E10M0) has also been experimentally shown to occur (Richer *et al*., 2008). Initiation of the formation of the basal complex is likely due to Sp1 and C/EBP binding first within the minimal promoter region. Sp1 and C/EBP binding would recruit TBP and TAF's to the promoter to mediate TFIID formation and then subsequent recruitment of the basal transcriptional complex.

6.4.3.2 Mechanism of the Formation of the Basal Transcriptional Complex

The results obtained from the *in silico* bioinformatic analysis and reporter assays suggests that *SLC11A1* transcription is initiated by a mechanism different to that observed for canonical promoters containing TATA, Inr or DPE elements (Figure 6.21). Core promoter elements were not identified in the 5'UTR and first intron of *SLC11A1*, thus confirming the location of the minimal promoter region, and core elements

involved in transcription intiation, to the region between -99 to +49 of the *SLC11A1* promoter (Section 6.3.2.4.1). Consistent with previous *in silico* studies, *SLC11A1* was not found to contain a TATA element (Blackwell *et al.*, 1995, Searle and Blackwell, 1999) and further *in silico* and visual sequence analysis of the identified minimal promoter region did not identify other core elements, including an initiator element, DPE, MTE or $BRE_{u/d}$ (Section 5.3.1.4.1). These observations are consistent with the finding that non-canonical, TATA-less promoters generally have multiple transcription initiation start sites, as observed with *SLC11A1* (Smale and Kadonaga, 2003).

However, analysis of the *SLC11A1* promoter identified multiple transcription factor binding sites for Sp1 and C/EBP (Section 5.3.1.4.1 and 6.3.2.5.1). The data from the current study, and that of previous reports, suggest that *SLC11A1* transcription may be initiated through the binding of transcription factors C/EBP and Sp1 to CCAAT box and GC box elements, respectively (Bowen *et al.*, 2003, Richer *et al.*, 2008, Yeung *et al.*, 2004).

Richer et al. (2008) identified a consensus site for the CCAAT-binding factors located over the second transcription start site (28bp upstream of TSS1) of *SLC11A1* (Figure 6.21) and showed that the transcription factors C/EBPα and C/EBPβ (also known as NF-IL6) are able to bind at this site. The transcription factors C/EBPα and C/EBPβ are important in the differentiation of immature cells into monocytes and then into macrophages (Friedman, 2007, Studzinski *et al.*, 2006). Interestingly, *SLC11A1* transcription was completely abolished when the site of C/EBP binding was mutated, suggesting that this transcription factor functions as a core promoter element, which is essential for the formation of the basal transcriptional complex. While C/EBP has not been reported to function as a core initiator like protein (Smale, 1997, Smale and Kadonaga, 2003), the location of C/EBP binding over the transcription start site has been reported in another promoter (Jiang and Zarnegar, 1997). The transcription factor C/EBP has been shown to directly activate transcription through interaction with the core factors, TBP and TFIIB (Chevneval *et al.*, 1991, Nerlov and Ziff, 1995, Pedersen *et al.*, 2001) and, aside from *SLC11A1*, it has been shown to play a role in the expression of other immune-related genes, such as IL-6 (Akira *et al.*, 1992, Natsuka *et al.*, 1992), IL-12p40 (Plevy *et al.*, 1997), IL-1β (Yang *et al.*, 2000b), and iNOS (Sakitani *et al.*, 1998).

In addition to the C/EBP binding site, Richer et al. (2008) identified a Sp1 site located, 106bp upstream of the transcription start site and just outside the minimal promoter area identified in the current study (Figure 6.21). While this site was not identified as a core element for transcription, multiple putative Sp1 sites have been identified throughout the *SLC11A1* promoter, with potentially one of the sites located within the minimal promoter region, being essential for *SLC11A1* expression. Interestingly, *Slc11a1* expression has been shown to be inhibited after the knockdown of Sp1 expression by RNA interference in mice (Yeung *et al.*, 2004). Furthermore, a Sp1 site, located in the core promoter region, was found to be essential for expression of *Slc11a1* during macrophage differentiation and upon stimulation with IFN-γ and LPS. Therefore, Sp1 potentially plays an important role in modulating *SLC11A1* expression (Bowen *et al.*, 2003).

The transcription factor Sp1 is ubiquitously expressed, however it exerts cell- and tissue-specific control over the genes whose transcription it regulates. This high level of control is mediated through the wide range of protein modifications to Sp1, altering transcription factor interactions and the ability of Sp1 to bind DNA (Resendes and Rosmarin, 2004, Suske, 1999, Tan and Khachigian, 2009). Sp1 can mediate transcription through direct interaction with TBP, TAF4 and TAF7, to initiate the formation of the basal complex, and multiple Sp1 sites have been shown to initiate the expression of genes which lack TATA and other core elements (Huber *et al.*, 1998, Smale, 1997, Smale and Kadonaga, 2003, Wierstra, 2008). Interaction of Sp1 with other transcription factors occurs through multiple binding domains, resulting in synergistic effects. In particular, Sp1 can interact with other Sp1 factors as well as the monocytic transcription factors, PU.1 and C/EBP. Sp1 has been shown to be involved in the expression of important myeloid genes (Resendes and Rosmarin, 2004) as well as CD14 and C/EBP expression in both monocytes and macrophages (Berrier *et al.*, 1998, Zhang *et al.*, 1994).

Therefore, the mechanism of *SLC11A1* transcription initiation appears to be controlled through the binding of transcription factors, C/EBPα or C/EBPβ and Sp1, to the minimal promoter region (Figure 6.21). Both Sp1 and C/EBP can bind to nucleosome bound DNA recruiting chromatin modifiers to alter the local topological structure, thereby activating transcription (Wierstra, 2008). Formation of the basal transcriptional

complex would then be mediated through the direct interaction of C/EBP and Sp1 with TBP and TAFs (and potentially TFIIB) leading to the formation of TFIID, recruitment of the other core proteins and RNA polymerase II (Section 5.1.2), and thus *SLC11A1* transcription. Other genes, whose expression has been shown to be mediated through the combined effects of Sp1 and C/EBP binding, include CD11c (CD18) (López-Rodríguez *et al.*, 1997), human reduced folate carrier promoter C (Payton *et al.*, 2005) and lactoferrin (Khanna-Gupta *et al.*, 2000).

6.4.3.3 The 5'UTR and First Intron do not Function to Enhance *SLC11A1* Transcription in Monocytic Cells

The current study is the first to determine if the *SLC11A1* 5'UTR contains any core promoter elements, or elements involved in the binding of transcription factors. The *in silico* analysis identified several elements in the 5'UTR and the first intron, in particular the fourth and fifth highest scoring WeederH elements (scores 16.91 and 15.75) (Section 5.3.1.3) (Figure 6.21). Additionally, the promoter assays suggested the 5'UTR and first intron contained elements which could enhance transcription in 293T cells (Section 6.3.1.2.1). However, the same region did not provide transcriptional enhancement in THP-1 cells (Section 6.3.2.4.1). Interestingly, the presence of the 5'UTR and first intron region resulted in a decrease in promoter activity in THP-1 cells (Figure 6.14), suggesting that this region may contain a monocyte-specific transcriptional repressor.

It is not uncommon for the 5'UTR and the first intron to contain elements for transcription factor binding (Bianchi *et al.*, 2009, McKeon *et al.*, 1997). However, while regions identified in the 5'UTR and the first intron were found not to mediate any transcriptional enhancement in monocytic cells, these highly conserved sites may be active at other stages of macrophage differentiation or stimulation, potentially mediating the increase in *SLC11A1* expression observed. *In silico* analysis of murine *Slc11a1* identified transcriptional elements in the first intron, homologous to the conserved region of the first intron in the human gene (16.91, Figure 6.21), suggesting that transcription factor binding may occur at this site during the classical activation of macrophages or in response to IFN-γ stimulation (Govoni *et al.*, 1995).

6.4.3.4 Identification of *SLC11A1* Promoter Regions Important in the Recruitment of Transcription Factors

In the THP-1 cell line it was found that the smallest promoter region tested had the lowest promoter activity, with promoter activity increasing as the *SLC11A1* promoter regions increased in length (Figure 6.14). This is consistent with published studies assessing *SLC11A1* expression in HL-60 cells, which showed that increasing promoter activity was correlated with increasing promoter size, with the region showing the highest promoter activity being of similar size and location to the region with the highest promoter activity identified in the current study (region 7C, located from -532 to +49) (Figure 6.14) (Roig *et al.*, 2002, Xu *et al.*, 2011).

Initiation of transcription is slow when restricted to the core proteins involved in the formation of the basal transcriptional complex (Burley and Roeder, 1996). This would account for the low promoter activity mediated by the smallest *SLC11A1* promoter region (+99 to -49) used in the current study. This region likely only contains sites for the binding of core proteins involved in the formation of the basal complex. Promoter activity increased, as larger promoter regions were assessed, presumably due to the introduction of elements for the binding of additional transcriptional enhancers, thereby, increasing the rate of transcription through direct or indirect interaction with the basal transcriptional complex (Latchman, 2004).

It has previously been suggested that negative elements, which inhibit *SLC11A1* expression, may be located upstream of the *SLC11A1* promoter in the -3451 to -469 region (Roig *et al.*, 2002). While increasing promoter size correlated with increasing promoter activity in the current study, there was no difference in the level of expression between the largest (1A) and second largest (7A) promoter regions tested (Figure 6.14) (Section 6.3.2.4.1). This suggests that no transcriptional enhancers or negative regulators of expression are located within the -2900 to -533 region of the *SLC11A1* promoter. Furthermore, when combined with the previous observation of a lack of transcriptional enhancement by the 5'UTR, these findings suggest that the components required for *SLC11A1* transcription in monocytic cells are located within a 581bp region (from -532 to +49) (Figure 6.22).

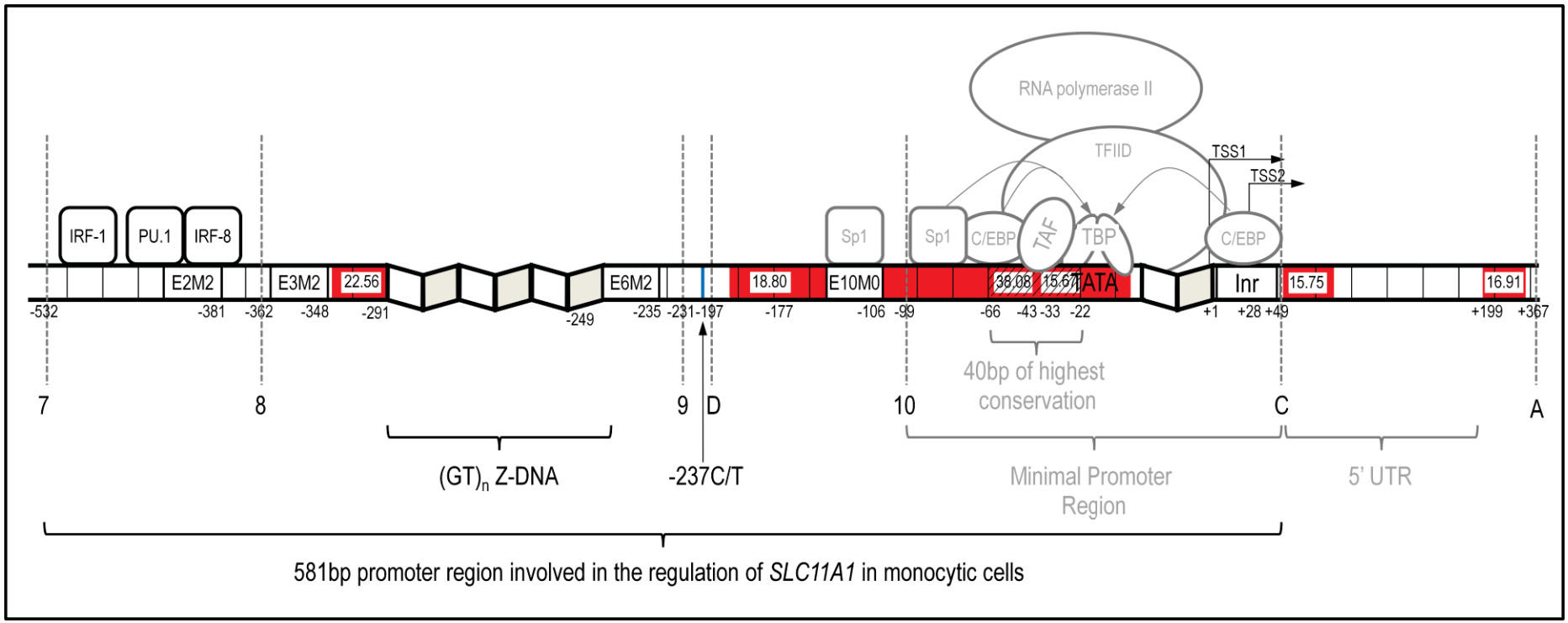

Figure 6.22 Transfection of the promoter constructs into THP-1 cells revealed that a 581bp region is involved in expression of *SLC11A1* in monocytic cells. The *SLC11A1* promoter region from -532 to -362 exerted the greatest transcriptional enhancement over *SLC11A1* expression. Within this region, combined binding of transcription factors, IRF-8 and PU.1 to an IECS element, are the likely candidates mediating the increase in expression observed. Also identified within this region is a putative site for IRF-1 binding. Sites E2M2, E3M2, E6M2 and E10M0 identify TFBS identified by Richer et al. (2008). Landmarks of the *SLC11A1* promoter are shown, including the two transcription start sites (TSS1 and TSS2) and the location of the polymorphic $(GT)_n$ microsatellite repeat and -237C/T polymorphism (blue line). Red regions indicate the conserved areas of the *SLC11A1* promoter identified from the clustalW alignment and white boxes containing numbers indicate the high scoring WeederH elements (Section 5.3.1.2 and 5.3.1.3). The grey dashed lines designate the *SLC11A1* promoter regions cloned for production of the promoter constructs. A description of the minimal promoter region (promoter regions and transcription factors shown in grey) is detailed in Figure 6.21.

6.4.3.4.1 Transcription Factors IRF and PU.1 are Candidates for the Transcriptional Enhancement of the -532 to -362 SLC11A1 Promoter Region

It was found that a 170bp region (-532 to -362), located upstream of the $(GT)_n$ repeat, displayed the greatest enhancement of promoter activity in monocytes (Section 6.3.2.4.1). A similar region was also reported to drive increased *SLC11A1* expression in HL-60 cells after vitamin D stimulation (Richer *et al.*, 2008, Roig *et al.*, 2002). While the identified -532 to -362 region did not contain a high level of homology from the clustalW alignment and WeederH analysis (Figure 5.13), the *in silico* analyses for putative TFBS identified a number of elements for the recruitment of transcription factors, which could account for the high *SLC11A1* promoter activity that occurs in the presence of this 170bp promoter region (Figure 6.19).

The most significant of the identified TFBS, located in the 170bp region, were two ISRE for the binding of interferon regulatory factors (IRF) (Figure 6.19). The IRF family, which consists of nine members (IRF-1-9), plays an important role in immune cells, where IRF members are involved in signal transduction, initiation of gene expression during IFN stimulation and in responding to pathogen- associated molecular patterns (PAMPs), such as LPS and viral DNA (Tamura *et al.*, 2008). Of the nine members of the IRF family, IRF-1, IRF-2, IRF-4, and IRF-8 are expressed in monocytes and macrophages (Friedman, 2007). In addition to the role that these transcription factors play in the activation and maintenance of an immune response, they are also involved in myeloid development and macrophage function (Tamura *et al.*, 2005, Tamura *et al.*, 2008).

IRF-8 is an essential transcription factor involved in the commitment of developing myeloid cells to a monocyte/macrophage lineage, as IRF-8 null progenitor cells are unable to differentiate into macrophages (Scheller *et al.*, 1999, Tamura and Ozato, 2002, Tsujimura *et al.*, 2002). While the TFBS searches identified parallel consensus sequences for IRF-2 and IRF-9 (Figure 6.19), these transcription factors do not play a role in myeloid differentiation. Closer visual analysis of the sequence of this region identified an IRF-Ets composite sequence (IECS) for the combined binding of transcription factors, IRF-8 and PU.1 (an Ets transcription factor) (Section 6.3.2.5.2) (Tamura *et al.*, 2005, Tamura *et al.*, 2008). The IECS elements were first identified to

be active during the differentiation of macrophages, resulting in the transactivation of a number of genes, in particular those encoding several lysosomal/endosomal proteins (Tamura *et al.*, 2005). The identified IECS, in the *SLC11A1* promoter, correlated with a previously identified protected site (E2M2) found during vitamin D differentiation of HL-60 cells, suggesting that transcription factor binding occurs at this site during monocyte to macrophage differentiation (Figure 6.22) (Richer *et al.*, 2008). However, the study could not identify the specific transcription factor that bound to this region. Due to the observation that *SLC11A1* has increasing expression during macrophage activation (Section 1.1.3.2), as well as restricted localisation to the endosome/lysosome (Section 1.1.3.1), the identified IECS site in the *SLC11A1* promoter, which binds the interacting factors IRF-8 and PU.1, is a strong candidate element for the observed increase in expression driven in the presence of this 170bp promoter region. Furthermore, the transcription factors, IRF-8 and PU.1, have been shown to interact to drive *Slc11a1* transcription in mice (Alter-Koltunoff *et al.*, 2003, Alter-Koltunoff *et al.*, 2008, Govoni *et al.*, 1995, Turcotte *et al.*, 2007, Turcotte *et al.*, 2005).

The second ISRE that was identified in the 170bp region of the *SLC11A1* promoter was a putative IRF-1 transcription factor located at -497bp (Figure 6.22). The transcription factor IRF-1 also plays a role in myeloid development and, therefore, may also be associated with the higher promoter activity which occurs in the presence of this 170bp region (Friedman, 2007, Tamura *et al.*, 2008).

6.4.3.4 The *SLC11A1* Promoter Shows Evidence of Bidirectional Transcription

Results of the transfection of the *SLC11A1* promoter constructs in both the forward and reverse orientation in THP-1 cells suggests that the *SLC11A1* promoter may function to direct transcription in a bidirectional manner (Section 6.3.2.4.2). The shortest *SLC11A1* promoter constructs showed orientation-specific promoter activity only in the forward direction, while the larger promoter constructs (1A, 7A and 7C), showed orientation-independent promoter activity (Figure 6.16). This is consistent with previous findings that a larger *SLC11A1* promoter region (386bp located at -338 to +48) showed evidence of bidirectional transcription, however, a smaller region (263bp located at -85 to +178) showed expression only in the forward orientation (Bayele *et al.*, 2007, Roig *et al.*, 2002).

A bidirectional promoter is characterised by gene pairs orientated head to head on opposite DNA strands, with less than 1000bp separating their transcription start sites (Trinklein *et al.*, 2004). Transcriptional expression of the gene pair is mediated by a common promoter region. While a gene located within 1000bp upstream of *SLC11A1*, on the opposite strand is not apparent at the *SLC11A1* locus, the current finding is consistent with a study into the level of bidirectional transcription, which found that 52% of random promoters showed transcriptional activity in both directions (Trinklein *et al.*, 2004). This suggests that half of all human promoters do not exhibit strong directionality in transcription initiation. This lack of directional transcription was found to be more common in TATA-less promoters, as the presence of a TATA element regulates the directionality of transcription (Trinklein *et al.*, 2004).

The bidirectional nature of the *SLC11A1* promoter may be of functional significance due to a currently unidentified, regulatory transcript such as a gene for a regulatory microRNA, or another type of non-coding RNA, located in the opposite direction. Such regulatory non-coding RNAs are increasingly being shown to play important roles in the coordination of gene expression (Mattick, 2007, Neil *et al.*, 2009, Wei *et al.*, 2011). The coexpression of a regulatory non-coding RNA, with the *SLC11A1* transcript, may explain (and be responsible for) the pleiotropic effects attributable to increased *SLC11A1* expression levels.

Likewise, the bidirectional nature of the *SLC11A1* promoter may be attributable to the increased rate of *SLC11A1* expression observed from the larger *SLC11A1* promoter regions, as compared to the smaller promoter regions. The smaller *SLC11A1* promoter regions drive low promoter activity, which would allow sufficient time to correctly orientate the formation of the basal transcriptional complex. However, the larger promoter regions, by mediating more rapid expression due to the presence of additional transcriptional activators, may result in decreased stringency with respect to the orientation of the basal transcriptional complex (Neil *et al.*, 2009). In this case the co-expressed transcript, known as a cryptic unstable transcript, does not play a functional role and would be rapidly degraded (Neil *et al.*, 2009, Wei *et al.*, 2011, Xu *et al.*, 2009).

6.4.4 The Influence of *SLC11A1* Promoter Polymorphisms on *SLC11A1* Promoter Activity

The *SLC11A1* promoter contains several polymorphisms, which have been shown to alter *SLC11A1* expression. To determine the mechanism underlying the ability of the different promoter polymorphisms to alter *SLC11A1* expression, various lengths of the *SLC11A1* promoter, containing the different polymorphic variants, were cloned for reporter assays. The promoter constructs were designed to contain $(GT)_n$ allele 2 or allele 3, as well as either the C or T variant at the -237C/T polymorphism (both in cis with $(GT)_n$ allele 3). These were transfected into 293T and THP-1 cells, to assess if interacting factors were located within the different promoter regions, which may associate with, or be differentially modulated by, the different promoter variants.

6.4.4.1 The $(GT)_n$ Variants Mediate Differential Transcription Through the Binding of a Monocyte-Specific Transcription Factor to the -362 to -197 Region

Of the nine identified alleles of the $(GT)_n$ microsatellite repeat, the most frequently occurring $(GT)_n$ allele 3 has also been shown to mediate significantly higher *SLC11A1* expression in monocytic cell lines as compared to $(GT)_n$ allele 2 (Figure 1.8) (Searle and Blackwell, 1999, Zaahl *et al.*, 2004). The mechanism by which the 2bp difference between $(GT)_n$ alleles 3 and 2 mediates a significant difference in *SLC11A1* expression remains unknown.

It was hypothesised, and has recently been shown, that the polymorphic $(GT)_n$ microsatellite repeat can form Z-DNA during transcription of *SLC11A1* (Bayele *et al.*, 2007, Blackwell *et al.*, 1995, Xu *et al.*, 2011). Z-DNA has been shown to enhance transcription by reducing the negative supercoiling, thereby allowing transcription factor binding and unwinding of the DNA to allow pol II transcription (Section 5.1.4.2.1) (Bates and Maxwell, 2005, Kashi and Soller, 1999). Due to the ability of the $(GT)_n$ microsatellite to form Z-DNA during transcription, it would be hypothesised that the difference in the basal level of *SLC11A1* expression (in the absence of exogenous stimuli) between the $(GT)_n$ alleles would be mediated through the differing ability of the $(GT)_n$ repeats to form Z-DNA. However, in the current study, Z-Hunt analysis found that allele 2, with 10 GT repeats, had a greater propensity to form Z-DNA than allele 3

(9 GT repeats), inferring that allele 2 would possess greater transcriptional enhancement (Figure 5.12). This finding is consistent with reports which show that longer alternating purine/pryimidine tracts have an increased ability to form Z-DNA, and accordingly, a greater ability to enhance transcription (Nordheim *et al.*, 1982). However, this finding contradicts previously completed reporter assays, showing that allele 3 drives a higher level of *SLC11A1* expression than allele 2. This contradiction suggests that the ability of alleles 2 and 3 to mediate different levels of *SLC11A1* expression is not attributable to their propensity to form Z-DNA.

Transfection of promoter constructs containing the different $(GT)_n$ alleles into non-monocytic 293T cells indicated that the presence of allele 2 resulted in a higher promoter activity as compared to allele 3 (Figure 6.23) (Section 6.3.1.2.3). This corroborated the results of the Z-Hunt analysis, which ascribed a higher Z-score to allele 2. When the promoter constructs containing the different microsatellite alleles were transfected into the monocyte-like THP-1 cell line, $(GT)_n$ allele 3 was shown to drive higher promoter activity in all of the promoter regions tested (Figure 6.23) (Section 6.3.2.4.3), contradicting the findings of the Z-Hunt analysis and the results of the transfection of promoter constructs in 293T cells.

The findings from the current analysis suggests that $(GT)_n$ allele 2 has a greater transcriptional enhancement ability compared to allele 3, as observed from the Z-Hunt analysis and the transfection of promoter constructs into the non-monocytic 293T cells. However, in monocytic cells, *SLC11A1* expression is modulated by a monocyte-specific factor(s), which are differentially regulated by the $(GT)_n$ alleles to result in a higher level of expression in the presence of $(GT)_n$ allele 3. Putatively, the 9 GT repeat length and/or the Z-DNA forming ability of allele 3 is optimal for the binding of a monocytic-specific factor(s). Alternatively, a monocytic specific factor may initially bind and then alter the propensity for the GT repeat to form Z-DNA. Furthermore, the results of the reporter assays suggested that the location of the element(s) for the recruitment of monocyte-specific transcription factor(s) is within a 165bp promoter region between -362 to -197, as all larger promoter regions tested showed the same expression profile (Figures 6.5, 6.17 and 6.23).

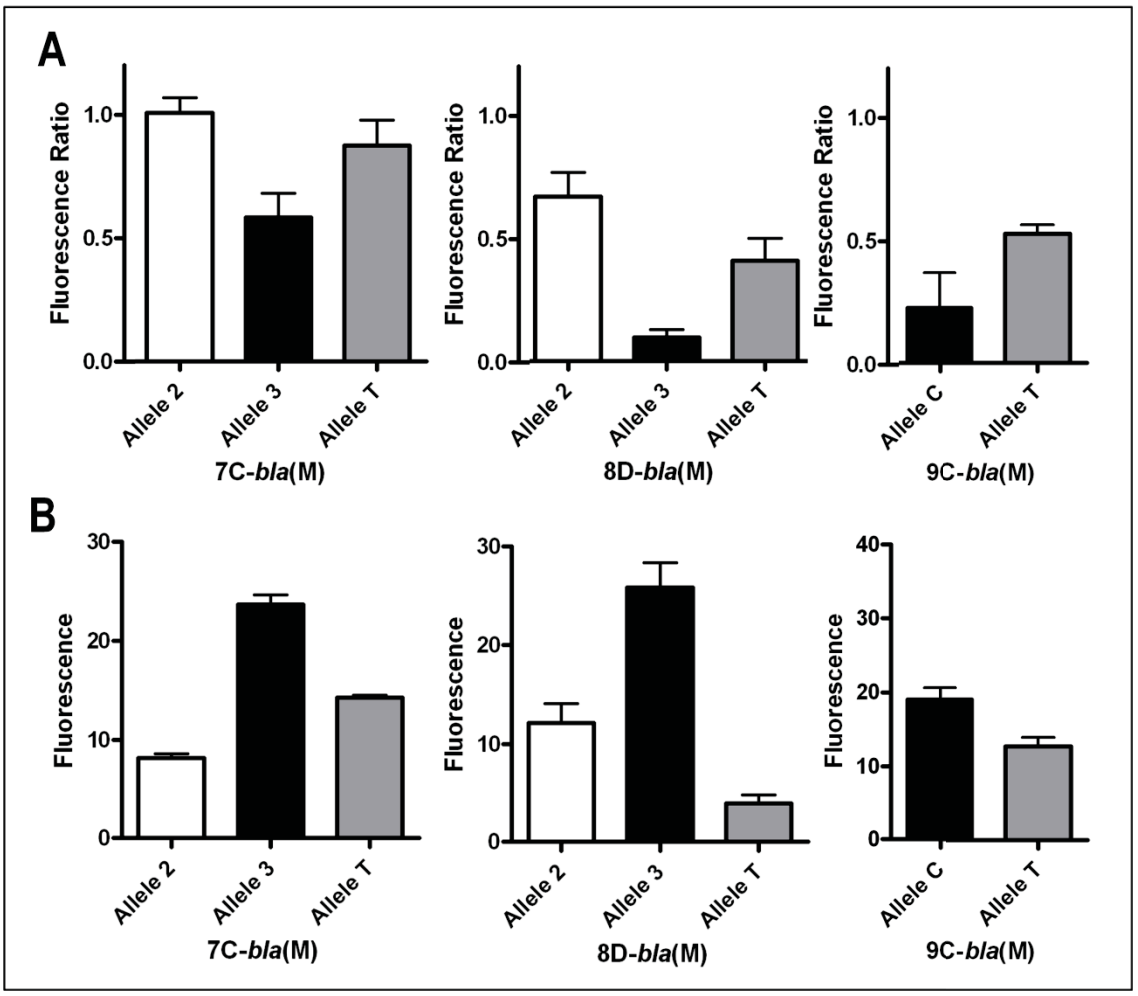

Figure 6.23 Comparison of the promoter activity of the *SLC11A1* promoter constructs, containing the common allelic variants, in non-monocytic and monocyte-like cells. Multiple plasmids of the same *SLC11A1* promoter region, differing only by the promoter variant present, either allele 2 [$(GT)_n$ allele 2 with -237 C], allele 3 [$(GT)_n$ allele 3 with -237 C] or allele T [$(GT)_n$ allele 3 with -237 T], were transfected into 293T cells (A) or monocyte-like THP-1 cells (B). Promoter region 9C contained only the -237C/T polymorphism, therefore, had two variants, allele C and allele T.

The modulation of *SLC11A1* expression by the $(GT)_n$ alleles in monocytic cells may be mediated by the binding of the recently described transcription factors, ATF-3 and JunB, to an AP-1-like element (identified as the second highest scoring WeederH element [22.56]; Section 5.3.1.3) located within the 165bp region adjacent to the microsatellite repeat (Xu *et al.*, 2011) (Figure 6.24). Xu et al. (2011) used the HL-60 (pre-monocytic) cell line, which does not endogenously express *SLC11A1*, to show that after PMA differentiation, binding of ATF-3 to the AP1-like element recruited BRG1 (SWI/SNF complex) and β-actin to modulate the removal of nucleosomes within the *SLC11A1* promoter (Figure 6.24). Removal of the nucleosomes allows the formation of

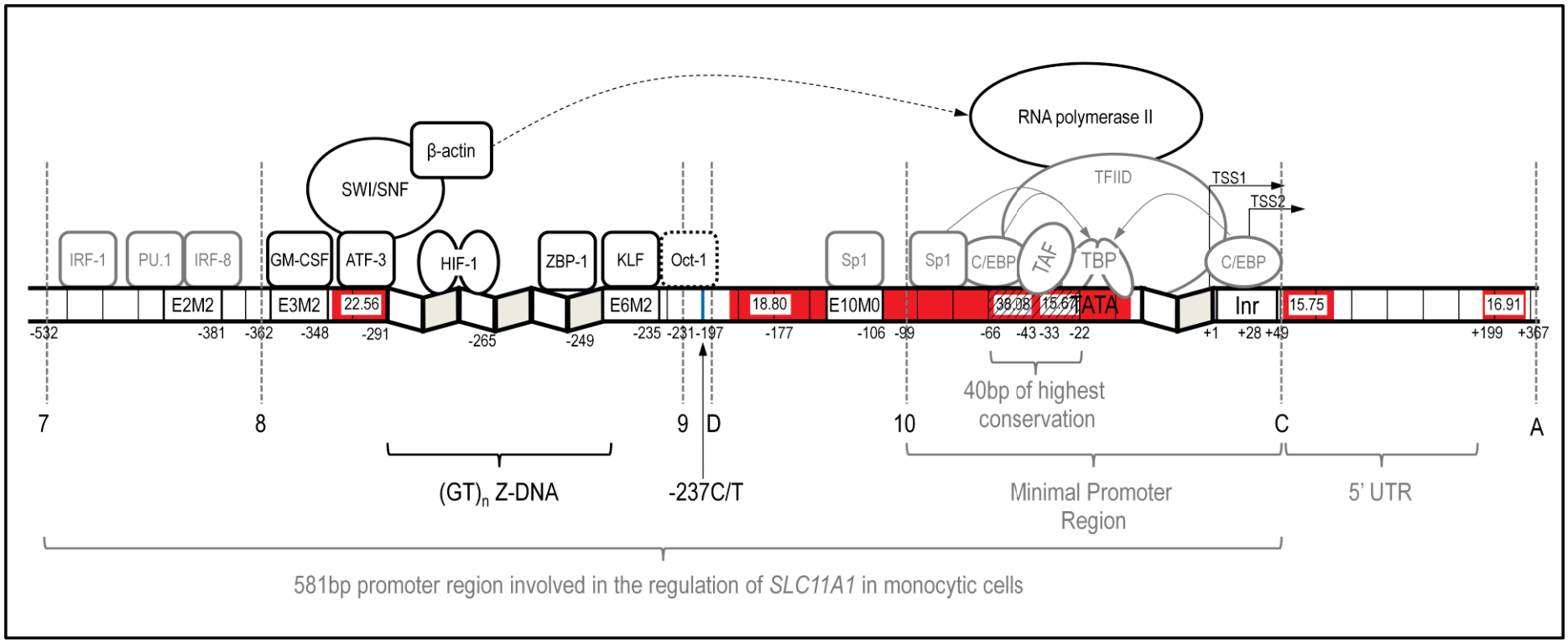

Figure 6.24 Monocytic-specific factor(s), binding within the -362 to -197 region, were identified as the mechanism controlling differences in promoter activity in the presence of allelic variants at the $(GT)_n$ repeat. ATF-3 and Jun D binding to an AP-1-like element adjacent to the $(GT)_n$ microsatellite repeat have been shown to promote an open chromatin structure of the *SLC11A1* promoter (through recruitment of SWI/SNF) and enhance transcription by recruitment of pol II (through direct interaction with β-actin) (Xu *et al.*, 2011, Xu *et al.*, 2010). Therefore ATF-3 is a candidate factor controlling differences in promoter activity in the presence of variants at the $(GT)_n$ repeat. Other candidate factors include GM-CSF, KLF, Sp1 and ZBP-1. While HIF-1 has been shown to bind to the $(GT)_n$ repeat to enhance *SLC11A1* transcription, HIF-1 is not a candidate to explain differences in promoter activity in monocytes (Bayele *et al.*, 2007). The -237C/T polymorphism functions to alter *SLC11A1* promoter activity independently of the $(GT)_n$ repeat. The candidate transcription factor, Oct-1, binding over the site of the -237C/T polymorphism in the presence of the -237 T variant, could be responsible for the observed differences in promoter activity mediated by the variants at the -237C/T polymorphism. Descriptions of promoter regions and transcription factors shown in grey are detailed in Figures 6.21 and 6.22.

an open chromatin structure (and recruitment of pol II to the basal transcriptional complex), thereby facilitating transcription (Figure 6.24) (Xu *et al.*, 2011, Xu *et al.*, 2010). The study found that ATF-3 binding and recruitment of BRG1 were essential for Z-DNA formation at the $(GT)_n$ microsatellite repeat (Xu *et al.*, 2011). Therefore, ATF-3 binding to the AP-1-like site in the *SLC11A1* promoter is the likely candidate responsible for modulation of *SLC11A1* expression in the presence of the different $(GT)_n$ variants in monocytic cells.

Transcription factor binding site searches identified several additional transcription factors, which may also bind within the 165bp promoter region to modulate *SLC11A1* expression in the presence of the different $(GT)_n$ alleles (Figure 6.20). These transcription factors include binding of Sp1 and KLF downstream of, and adjacent to, the $(GT)_n$ microsatellite repeat, GM-CSF binding to the previously identified E3M2 site (Richer *et al.*, 2008) and PEA3 (Figure 6.24). In addition to these factors, the ability of the microsatellite repeat to form Z-DNA could result in the recruitment of transcription factors, which may bind to a Z-DNA conformation. The transcription factor Z-DNA binding protein 1 (ZBP-1) is a cytosolic based immune sensor involved in interferon signaling (IFN-γ) (Takaoka *et al.*, 2007) and may bind to the 3' end of the microsatellite repeat (Figure 6.24). Due to the different abilities of the $(GT)_n$ alleles to form Z-DNA, modulation of different levels of *SLC11A1* expression, may be attributable to the differing propensity for ZBP-1 (or another similar factor which can bind Z-DNA) to bind and enhance transcription.

The transcription factor HIF-1α has also been shown to bind, within the identified 165bp region, to a cryptic element located in the middle of the $(GT)_n$ microsatellite repeat (Bayele *et al.*, 2007) (Figure 6.24). However, HIF-1α is not stably expressed in normoxic (normal oxygen concentration) monocytic cells (which represents the stage of *SLC11A1* expression in THP-1 cells investigated in the current study) and was shown to transactivate *SLC11A1* expression only after cytokine stimulation or the induction of phagocytosis (Bayele *et al.*, 2007), thereby discounting the potential for HIF-1α to mediate the higher *SLC11A1* expression observed in the presence of $(GT)_n$ allele 3 in monocytic cells.

6.4.4.2 The -237C/T Polymorphism Functions Independently of the $(GT)_n$ Microsatellite Repeat to Modulate *SLC11A1* Expression

Transfection of promoter constructs containing different lengths of the *SLC11A1* promoter, which only differed at the -237 polymorphic site (209 bases upstream of TSS1; Section 5.2.2.1.1), into 293T cells found that a higher promoter activity was observed in the presence of the -237 T variant, as compared to the -237 C variant for all promoter regions tested (Section 6.3.1.2.3) (Figure 6.23). This finding is consistent with a previous analysis of this polymorphism in 293T cells, which found the less frequent -237 T variant drove a 1.6 fold increase in promoter activity as compared to the more common C variant (Donninger *et al.*, 2004).

However, when the promoter constructs were transfected into THP-1 cells, the -237 C variant resulted in a greater transcriptional enhancement compared to the -237 T variant with all promoter regions tested (Section 6.3.2.4.3). This finding is also consistent with reporter studies assessing the effect of the -237C/T polymorphism in THP-1 and U937 cells (Zaahl *et al.*, 2004). Furthermore, it was found that the transcriptional enhancement occurring in the presence of the -237 C variant, compared to the T variant, was independent of the $(GT)_n$ microsatellite repeat. This is consistent with the results of the Z-Hunt analysis, which showed that the -237C/T polymorphism did not alter the ability of the $(GT)_n$ microsatellite to form Z-DNA and suggests that the -237C/T polymorphism may modulate *SLC11A1* expression by altering transcription factor binding to the region. However, *in silico* analysis of the sequence at the -237C/T polymorphism found that the region was not highly conserved (Section 6.3.1.2 and 6.3.1.3) and did not identify any potential TFBS, which would potentially recruit transcription factors to the region of the polymorphic site (Section 5.3.1.4.3). This suggests that substitution of C to T does not result in the loss of a transcriptional element that could explain the drop in promoter activity observed.

While no elements for the recruitment of transcription factors were lost at the location of the -237C/T polymorphism, TFBS searches did identify the formation of a new element for the recruitment of the ubiquitously expressed transcription factor, octamer binding protein 1 (Oct-1, also known as POU2FI), when the common -237 C variant was substituted with the T variant (Section 5.3.1.4.3) (Figure 6.24). The formation of this TFBS is in agreement with the findings of Donninger et al. (2004) and binding of

this transcription factor may explain the increased promoter activity observed in the presence of the less frequent -237 T variant, compared to the C variant, in 293T cells. The Oct1 site is 89bp upstream of an identified Sp1 site (Richer *et al.*, 2008) (Figure 6.24) and direct protein interaction of promoter bound Oct1 and Sp1 have been shown to regulate (and increase) transcriptional activity (Strom *et al.*, 1996, Zwilling *et al.*, 1994).

The decrease in *SLC11A1* promoter activity observed in the presence of the -237 T variant, compared to the C variant, in THP-1 cells, may also be due to the binding of Oct-1 to this site (Figure 6.24). While the introduction of this sequence element may enhance promoter activity in 293T cells, the recruitment of Oct-1 in monocytic cells, may out-compete/inhibit binding of other transcription factors located in adjacent DNA regions important in *SLC11A1* expression, thus resulting in the observed decrease in *SLC11A1* expression. For example Oct-1 binding at the site of the -237C/T polymorphism, in the presence of the -237 T variant, may inhibit the recruitment of a transcription factor to the site E6M2 (Richer *et al.*, 2008) thereby lowing the promoter activity.

6.4.5 Conclusion

This study has functionally analysed the *SLC11A1* promoter to determine the mechanisms of transcriptional regulation and the way in which promoter variants function to modulate differential expression of *SLC11A1*. The study was completed using an integrated approach, where bioinformatic analyses were first completed to identify putative transcriptional regulatory elements (Chapter 5, Part 1). Based on the findings of the bioinformatic analyses, promoter constructs of varying lengths were designed to functionally test the elements identified *in silico* (Chapter 5, Part 2). The promoter activities of the prepared constructs were tested using the human cell lines, 293T and THP-1 (Chapter 6, Part 3). Figure 6.25 displays a summary of the findings from the *in silico* and functional analyses of the *SLC11A1* promoter.

The current study has identified a 581bp region of the *SLC11A1* promoter that was involved in transcriptional enhancement of *SLC11A1* in monocytic cells (-532 to +49) (Figure 6.25). Furthermore, within this region, a 148bp minimal promoter region (-99 to

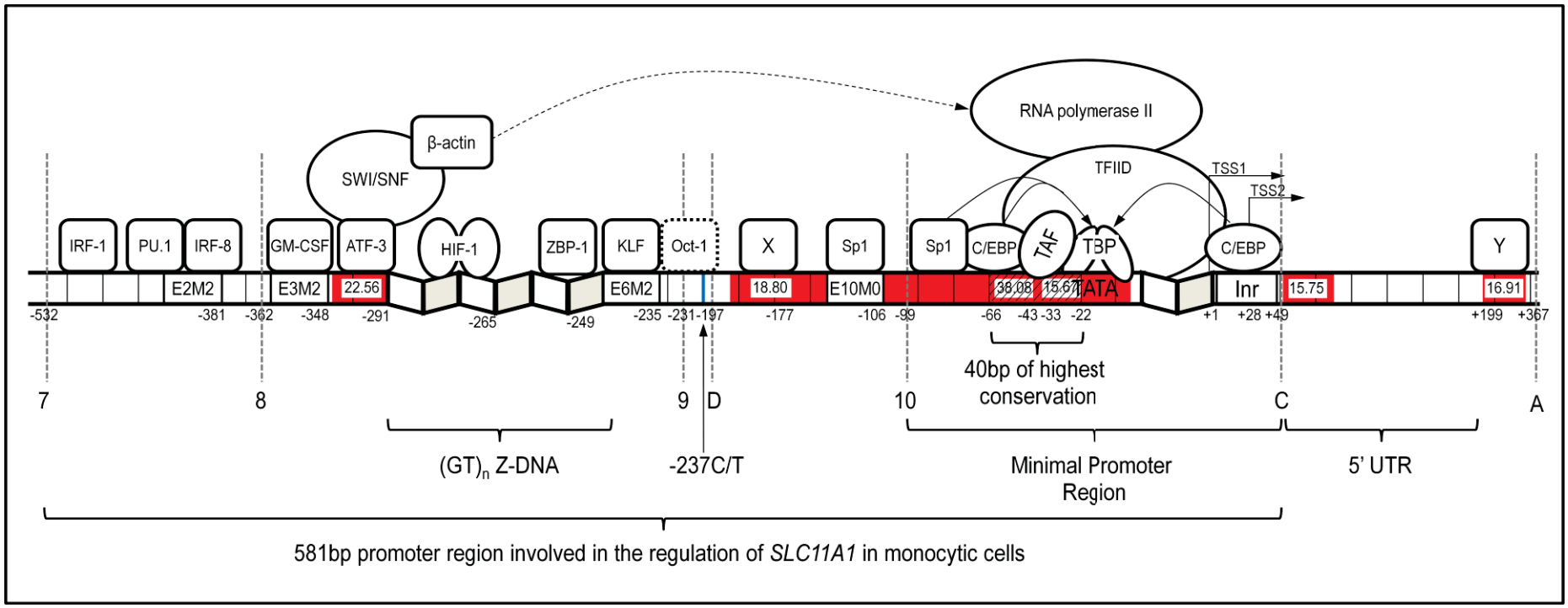

Figure 6.25 Summary of the putative mechanisms of *SLC11A1* expression and location of experimentally determined transcription factors. The transfection of the promoter constructs into THP-1 cells suggested that a 581bp region was involved in expression of *SLC11A1* in monocytic cells. Within this region a 148bp region was identified as the minimal promoter region and the site for the formation of the basal transcriptional complex. Initiation of the formation of the basal complex appears to be due to Sp1 and C/EBP binding to the minimal promoter region which directly interact with TBP and TAF's to mediate TFIID formation and then subsequent recruitment of the basal transcriptional complex. The *SLC11A1* promoter region from -532 to -362 exerted the greatest transcriptional enhancement over *SLC11A1* expression. Within this region, combined binding of transcription factors, IRF-8 and PU.1 to an IECS element, are the likely candidates to mediate the increase in expression observed. Also identified within this region is a putative site for IRF-1 binding. A putative monocytic specific factor, binding within the 8D region (-362 to -197), was identified as the mechanism controlling the differential level of SLC11A1 expression in monocytic cells. WeederH analysis of the *SLC11A1* promoter identified several high scoring elements, however transcription factor binding site searches could not identify putative elements recruited to the identified elements (factors X and Y located at elements with scores 18.80 and 16.91).

+49) was identified, which contained the core elements for the formation of the basal transcriptional complex. This study is the first to analyse the 5'UTR and first intron of *SLC11A1*, showing that this region does not contain core elements essential for transcription initiation. The current findings suggest that *SLC11A1* transcription is initiated by a mechanism different to that observed for canonical promoters (i.e. not through TATA, Inr or DPE elements), with the formation of the basal transcriptional complex putatively mediated by the transcription factors, Sp1 and C/EBP, which directly interact with TAFs to recruit other core proteins, allowing transcription of *SLC11A1* to occur (Figure 6.25). Additionally, the current analysis has identified a 170bp region (-532 to -362), upstream of the $(GT)_n$ microsatellite repeat, which has the greatest transcriptional enhancement on *SLC11A1* promoter activity. Within the 170bp region, a novel IECS element, for the combined recruitment of IRF8 and PU.1, was identified as the candidate responsible for the increased promoter activity observed (Figure 6.25).

Analysis of promoter constructs containing the *SLC11A1* promoter regions cloned in the forward and reverse orientation determined that the *SLC11A1* promoter could mediate bidirectional transcription. However, the functional significance of bidirectional transcription at the *SLC11A1* locus is currently unclear. Such bidirectional transcription may mediate the expression of a putative regulatory transcript or may produce a cryptic unstable transcript, which is rapidly degraded.

This study is the first to show that the ability of the $(GT)_n$ alleles to differentially modulate *SLC11A1* expression, in monocytes, is not attributable to their differing abilities to form Z-DNA. Rather, differential expression is due to monocyte-specfic factor(s), binding to a 165bp region of the *SLC11A1* promoter (-362 to -197) (Figure 6.25). Furthermore, it is hypothesised that removal of this monocyte-specific factor would result in $(GT)_n$ allele 2 driving a higher level of *SLC11A1* expression than allele 3, as predicted by the *in silico* Z-Hunt analysis and determined by the analysis of promoter constructs in 293T cells.

Additionally, this study is the first to show that differences in *SLC11A1* expression, mediated by the -237C/T polymorphism, occur independently of the $(GT)_n$ microsatellite repeat, suggesting that the -237C/T polymorphism alters an element for

the recruitment of a transcription factor. While no TFBS were identified over the site of the polymorphism in the presence of the common -237 C variant, it is hypothesised that the introduction of a sequence element and recruitment of the transcription factor, Oct-1, in the presence of the -237 T variant, may out compete/inhibit binding of another transcription factor, resulting in the loss of *SLC11A1* expression observed in monocytic cells (Figure 6.25).

Therefore, through the combined *in silico* analysis and the subsequent design, production and analysis of promoter constructs, the current study has been able to determine the mechanism by which *SLC11A1* is regulated at the level of transcription initiation and furthermore, has elucidated a mechanism which explains the variation in *SLC11A1* expression mediated by polymorphic variants within the *SLC11A1* promoter. The work completed in this study will ultimately help to determine the mechanism by which *SLC11A1* and the functional promoter polymorphisms confer susceptibility/resistance to infectious, autoimmune and other diseases.

6.5 Future Directions

6.5.1 Assessment of the Minimal Promoter Region to Determine the Location of Core Elements

Future work will further characterise the identified 148bp minimal promoter region, to determine the exact location of core elements involved in the formation of the basal transcriptional complex and to elucidate the precise mechanism of transcription initiation. This would involve site-directed mutagenesis of the *SLC11A1* promoter constructs, to introduce base substitutions in identified putative core elements to determine their functional significance. Electrophoretic mobility shift assays (EMSA) and chromatin immunoprecipitation assays could be used to assess the interaction of transcription factors, Sp1 and C/EBP, with the minimal promoter region. Furthermore, the role of Sp1 and C/EBP in transcription initiation could then be further assessed by co-transfection of reporter constructs with plasmids expressing the Sp1 and C/EBP proteins to test the putative mechanism of transcription initiation.

6.5.2 Analysis of the 170bp Promoter Region Driving High Promoter Activity

The current study identified that high promoter activity occurred in the presence of a 170bp region of the *SLC11A1* promoter, located from -532 to -362 (Section 6.3.2.4.1). Further work will be aimed at determining the location of transcriptional element(s) within this region through the use of *in vivo* footprinting. Chromatin immunoprecipitation assays and EMSAs could be completed to determine the identity of transcription factors recruited to protected sites identified from the *in vivo* footprinting assays. Furthermore, site directed mutagenesis of the identified IECS element, for the recruitment of the transcription factors, IRF-8 and PU.1, within the *SLC11A1* promoter constructs may determine what role this candidate element plays in *SLC11A1* expression in monocytes. Co-transfection of reporter constructs with plasmids expressing the identified transcription factors could be competed to determine what effect the factors, binding within the identified 170bp promoter region, exert on *SLC11A1* promoter activity.

6.5.3 Determination of the Monocyte-Specific Transcription Factor Interacting with Allelic Variants to Modulate Differential Levels of *SLC11A1* Expression

Another future direction will be to determine the monocyte-specific factor(s) which interact with variants of the $(GT)_n$ microsatellite repeat, within a 165bp region of the promoter, to mediate differential levels of *SLC11A1* promoter activity (Section 6.4.4.1). In 293T cells, a higher promoter activity was observed in the presence of allele 2, as compared to allele 3, which was consistent with the prediction of the Z-Hunt analysis, while allele 3 drove an increased promoter activity in monocyte-like (THP-1) cells, compared to allele 2. It is hypothesised, that in the absence of the monocyte-specific factor(s), the promoter activity of allelic variants at the $(GT)_n$ microsatellite repeat in monocytic cells would be consistent with the predicted promoter activity observed in non-monocytic (293T) cells and identified by Z-Hunt analysis (i.e. allele 2 drives higher promoter activity as compared to allele 3). Therefore, site directed mutagenesis of reporter constructs at putative elements within the identified 165bp promoter region could be completed to determine the location of elements, which result in a higher promoter activity of allele 3 compared to allele 2 when promoter assays are completed in monocytic cells. Furthermore, chromatin imunoprecipitation assays and EMSAs could be completed to determine the identity of the monocyte-specific transcription factor(s).

Validation of the identification of the monocyte-specific transcription factor(s), which interact with the $(GT)_n$ alleles to mediate differential *SLC11A1* promoter activity, could be completed by several methods. Firstly, co-transfection of the different promoter constructs containing $(GT)_n$ allele 2 or allele 3, with or without plasmids expressing the identified transcription factor(s), would be transfected into non-monocytic (293T) cells. If the identified transcription factor was responsible for the observed differences in promoter activity, then in the presence of the plasmid expressing the monocytic transcription factor, $(GT)_n$ allele 3 would mediate higher promoter activity compared to allele 2, while in the absence of the monocyte transcription factor, allele 2 would mediate higher expression. Alternatively, RNA interference in monocytic cells, to knockdown the expression of the identified monocytic transcription factor, should result in $(GT)_n$ allele 2 driving a higher promoter activity as compared to allele 3.

6.5.4 Analysis of Sequence Elements Identified by the WeederH Analysis

The WeederH program has a high predictive ability in locating elements for transcription factor binding (Section 5.3.1.6) (Pavesi *et al.*, 2007). Therefore, further work should aim to determine if the high scoring elements, identified in the current study, do in fact modulate *SLC11A1* expression through the recruitment of transcription factors. In particular, no transcription factor binding sites were located to bind at the site of the third and fourth highest scoring elements (18.80 and 16.91), located at 177bp upstream the transcription start site and in the first intron of SLC11A1, respectively (Figure 6.25, Factors X and Y). Site-directed mutagenesis of promoter constructs at the high scoring WeederH elements will determine if these sites function to mediate *SLC11A1* expression in monocytic cells. If these sites do not play a role in monocytic cells then they may function to mediate *SLC11A1* expression at another stage of cellular differentiation or activation.

6.5.5 Analysis of the Mechanisms of *SLC11A1* Transcription at Different Stages of Monocyte/Macrophage Differentiation and Stimulation

The current study has identified important promoter regions involved in *SLC11A1* transcription initiation, and furthermore, the mechanisms by which the allelic variants within the *SLC11A1* promoter are able to alter *SLC11A1* expression, specifically in undifferentiated and unstimulated monocyte-like cells (THP-1). Therefore, only transcriptional information at the monocytic stage of cell development was determined.

The level of *SLC11A1* expression changes at different stages of the monocyte and macrophage differentiation process, in which *SLC11A1* expression increases as the cells gain greater phagocytic ability (Figure 1.3). The level of *SLC11A1* is further modulated after the classical activation of macrophages and also upon exposure to EPO (Soe-Lin *et al.*, 2008). Concomitant with the changes in *SLC11A1* expression, would also be alterations in the milieu of transcription factors. Therefore, the transcription factors which regulate expression of *SLC11A1* in monocytes, as analysed in this study, may not play a role in *SLC11A1* expression at other stages of cellular differentiation and

activation. For example, binding of HIF-1α to the *SLC11A1* promoter only occurs after cytokine stimulation or induction of phagocytosis (Bayele *et al.*, 2007) (Section 6.4.4.1).

Therefore, the designed constructs used in the current study, containing different *SLC11A1* promoter regions and the common polymorphisms, could be transfected into THP-1 cells at different stages of differentiation or activation, to determine the location of elements for the recruitment of transcription factors which mediate *SLC11A1* expression at that time point. Additionally, it has been found that upon IFN-γ and LPS stimulation, *SLC11A1* expression is downregulated in the presence of $(GT)_n$ allele 2 (as compared to IFN-γ alone), while an increase in *SLC11A1* expression is observed in the presence of allele 3 (Figure 1.8). It is hypothesised that the expression differences are due to the juxtaposition of IFN-γ and LPS response elements which are affected by the microsatellite repeat length (Searle and Blackwell, 1999). Therefore, the promoter constructs may provide a way to locate these elements.

6.5.6 Validation of Novel Sequence Variants of the *SLC11A1* Promoter Identified During the Preparation of the Promoter Constructs

Validation of the promoter constructs by sequencing resulted in the identification of novel sequence variants, with two putative single point mutations detected, one in the promoter region (designated -2578A/C), and another 128bp downstream of the transcription start site (+128G/A) (Section 5.3.2.6). Each of the variants was only identified once, therefore, further sampling and sequencing is required to validate these sequence variants and determine their frequencies. Additionally, three novel variants of a previously identified $G(T)_n$ repeat (rs13035487) were also identified, bringing the total number of variants identified at this site to five. Additional sampling and sequencing is required to validate the observed LD identified between repeat lengths at the $G(T)_n$ repeat and the *SLC11A1* promoter $(GT)_n$ microsatellite repeat (Section 5.3.2.6).

CHAPTER 7 - META-ANALYSES ASSESSING THE ASSOCIATION OF *SLC11A1* POLYMORPHISMS WITH THE OCCURRENCE OF AUTOIMMUNE AND INFECTIOUS DISEASE

7.1 INTRODUCTION

SLC11A1 expression is restricted to macrophages where it plays a major role in the elimination of macrophage-tropic pathogens by initiating and perpetuating a Th1 pro-inflammatory immune response. While murine models show a strong correlation between the expression of functional *Slc11a1* with both resistance to macrophage-tropic pathogens and susceptibility to autoimmune disease (Govoni *et al.*, 1996, Kissler *et al.*, 2006, Malo *et al.*, 1994, Vidal *et al.*, 1995), studies analysing the association of *SLC11A1* with disease incidence in humans have produced inconsistent results (Sections 1.3.4.1 and 1.3.4.2). This inconsistency is attributable, in part, to the absence of a naturally occurring polymorphism within the human *SLC11A1* locus, which produces a functionally null protein (Vidal *et al.*, 1996). Rather, polymorphisms that alter the levels of functional *SLC11A1* expressed have been described (Section 1.2).

Of the *SLC11A1* polymorphisms identified to date, the polymorphic $(GT)_n$ microsatellite repeat has been shown to alter the level of *SLC11A1* expressed (Section 6.3.2.4.3) (Searle and Blackwell, 1999, Zaahl *et al.*, 2004), and is therefore, a strong candidate for influencing disease incidence. Several alleles of different repeat length have been identified, with $(GT)_n$ allele 2 resulting in lower *SLC11A1* expression compared to the more commonly occurring $(GT)_n$ allele 3. It has therefore been hypothesised that allele 3 would provide protection against infectious disease by driving high *SLC11A1* expression and a resultant Th1 mediated immune response. However, allele 3 would also be associated with susceptibility to Th1-mediated autoimmune diseases.

Over 110 association studies, which aimed to assess the association of different *SLC11A1* polymorphisms (Figure 7.1) with the incidence of infectious, autoimmune/inflammatory and other diseases, have been conducted to date. These studies have shown inconsistent results, which are largely attributable to the small sample sizes of the individual studies that lack the statistical power to determine bonafide associations. Furthermore, studies with small sample sizes also have a tendency to over report allele frequencies (Section 1.3.5). Other reasons for the inconsistent findings could be due to population stratification or publication biases.

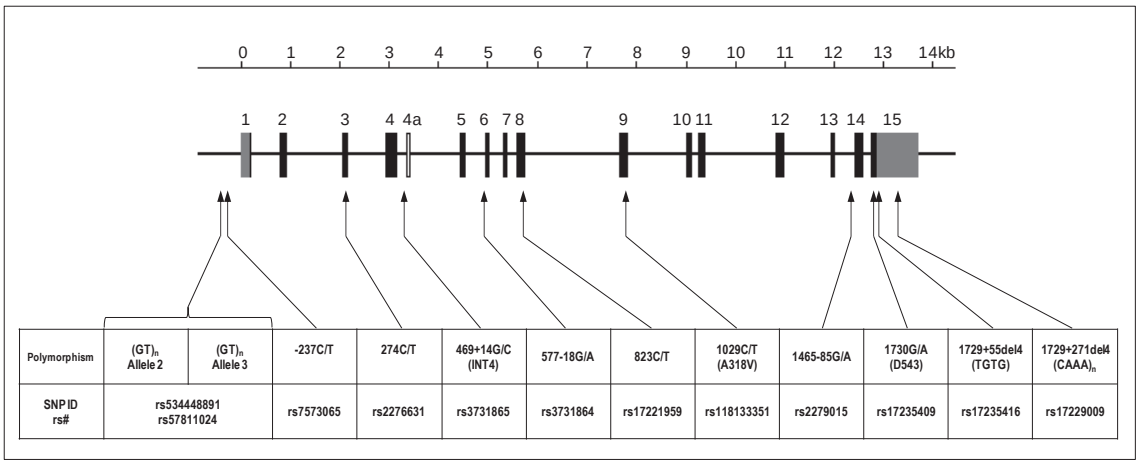

Figure 7.1 Location of *SLC11A1* polymorphisms analysed in the meta-analysis. Associations between the occurrence of these polymorphisms and the incidence of autoimmune/inflammatory, infectious disease and tuberculosis alone was analysed by a meta-analysis. The 15 exons of the gene are shown as black boxes with their respective numbers. The corresponding scale above indicates the length (kb) of the gene. The grey boxes indicate the 3' and 5' untranslated regions and the introns and flanking regions are represented by a thin line. The arrows indicate the position of sequence variants. Below each polymorphism is the reference SNP (rs#) identification number.

The aim of the present study was to use meta-analyses to determine the association of *SLC11A1* polymorphisms with the incidence of infectious and autoimmune disease (Figure 7.1). A meta-analysis is a powerful tool which combines individual association studies to determine the strength of an association. By pooling the individual association studies, a meta-analysis increases the sample size, which therefore increases the statistical power to determine the magnitude of associations.

The current meta-analysis was undertaken for several reasons. Firstly, there has been at least a doubling in the number of case control association studies (and in some cases a 3-4 fold increase) that have been completed since the previously published meta-analysis of the association of *SLC11A1* polymorphisms with pulmonary tuberculosis infection (Li *et al.*, 2006) and with autoimmune/inflammatory diseases (Chapter 3) (Nishino *et al.*, 2005, O'Brien *et al.*, 2008). This represents a significant increase in the number of studies to be included (or eligible for inclusion) in the meta-analysis, which will increase the likelihood of identifying associations, or the lack thereof, between *SLC11A1* polymorphisms and disease incidence. Secondly, the current meta-analysis assessing the association of *SLC11A1* polymorphisms with infectious disease incidence has been more inclusive (as all infectious diseases, except HIV, were included in the

analysis) compared to the previous meta-analysis, which only assessed pulmonary tuberculosis publications (Li *et al.*, 2006). The aforementioned analysis included 14 publications assessing pulmonary tuberculosis, while the current analysis includes 26 studies assessing the association of *SLC11A1* polymorphisms with infectious disease, published during the same time period (1998-2004), and 59 publications all together (1995-2010).

Additionally, this meta-analysis assessed a number of polymorphisms, within the *SLC11A1* gene, for which meta-analyses to determine disease association had not been previously performed. This study is the first to assess the association of polymorphisms other than the $(GT)_n$ promoter repeat with the occurrence of autoimmune disease. The current analysis includes the assessment of a further 10 polymorphisms, which could not be previously analysed as there were insufficient association studies to enable a meta-analysis to be completed (O'Brien *et al.*, 2008). This analysis is also the first to assess the association of $(GT)_n$ allele 2, the -273C/T, 274C/T, 1465-85G/A and 1729+271del4 polymorphisms with the incidence of infectious disease or tuberculosis alone. Overall, the present study constitutes the largest and most inclusive meta-analysis of *SLC11A1* polymorphisms with the incidence of infectious and autoimmune diseases conducted to date.

7.2 METHODS

7.2.1 Criteria for Study Inclusion

Publications included in the meta-analysis were identified by searching literature databases (PubMed, Medline and Ovid) using the search terms “SLC11A1”, “NRAMP1”, “autoimmunity”, “inflammation”, “tuberculosis” and “infection”, individually and in combination using the Boolean characters "OR" or “AND”. Additional papers were sourced by cross-referencing original and review publications. Inclusion criteria for the meta-analysis were that studies assessed *SLC11A1* polymorphisms in patients diagnosed with a specific autoimmune/inflammatory or infectious disease and used non-familial subjects as controls. Furthermore, all publications included in the meta-analyses had to assess HIV negative cases and controls.

Information regarding the disease studied, the population analysed and the study findings was extracted from all publications meeting the inclusion criteria. Total study numbers (individuals and alleles) and allelic frequencies (numbers and percentages) were also tabulated for all relevant datasets within a publication. When a publication contained several datasets/associations for a single polymorphism, each dataset was assessed as an individual association when the populations/diseases were different between the datasets. Alternatively, data were pooled if the same population/disease was analysed. Allele frequencies were inferred when genotype frequencies were reported. In the few cases where carrier frequencies were reported, the genotype frequencies were first determined and then allele frequencies were inferred (as described in Appendix 2). Corresponding authors were contacted by email if the information to determine the odds ratio (OR) was unavailable or if the published data was ambiguous. When publications assessed specific *SLC11A1* polymorphisms, but concluded that an analysis was not completed due to a low frequency of the less commonly occurring variant, the data was omitted from the analysis. The data extracted from all publications satisfying the inclusion criteria for the meta-analysis was reanalysed to ensure that the extracted data was correct. Only polymorphisms that had been investigated in five or more individual association studies were included in the analysis. The only exception was the analysis of the association of the 1729+271del4

[$(CAAA)_n$] polymorphism with the incidence of autoimmune disease, which included only three associations. Where a large number of datasets were available for a particular polymorphism, smaller meta-analyses were completed, where possible, analysing the association of individual diseases (for example T1D, tuberculosis) or geographical location with the *SLC11A1* polymorphisms. In these cases analyses were performed from as many as two association studies.

Although nine *SLC11A1* promoter microsatellite $(GT)_n$ alleles have been identified to date, seven of these alleles (alleles 1 and 4-9) occur at extremely low frequencies (Table 1.3). Therefore, association studies have focused on the association of the common alleles (alleles 2 and 3), which have a combined allele frequency of greater than 95%, with disease incidence. Meta-analyses of both $(GT)_n$ allele 3 and allele 2 were completed to determine the association of these alleles with the incidence of autoimmune/inflammatory and infectious disease. For the analysis of allele 3, the frequency data for alleles 1, 2 and 4-9 were pooled and compared against the frequency of allele 3. Likewise, for the analysis of allele 2, the frequencies of alleles 1 and 3-9 were pooled and compared against the frequency of allele 2.

7.2.2 Statistical analysis

The program R (R Core Development Team, 2008) was used to perform the statistical analysis utilising the program Rmeta (Lumley, 2009). Data tables, containing the number of cases and controls and allele frequencies, were created in Microsoft excel and saved in .csv format which can be recognised by R. Figure 7.2 shows the methodology used to analyse the individual datasets. Using the relevant data sets, the OR and 95% confidence intervals (CI) were determined for each individual association included in each of the meta-analyses.

The combined association of a polymorphism with autoimmune or infectious disease incidence, from the individual associations, was completed by the determination of a pooled OR estimate. The fixed-effects pooled OR estimate (Mantel-Haenszel method) was first determined (Figure 7.2). A pooled OR estimate of 1 indicates a lack of association between the polymorphism of interest and the disease state analysed, while a pooled OR estimate higher or lower than 1 indicates susceptibility or resistance to the

disease state analysed, respectively. Furthermore, the fixed-effects pooled OR estimate was deemed to be significant if the 95% CI did not include 1.

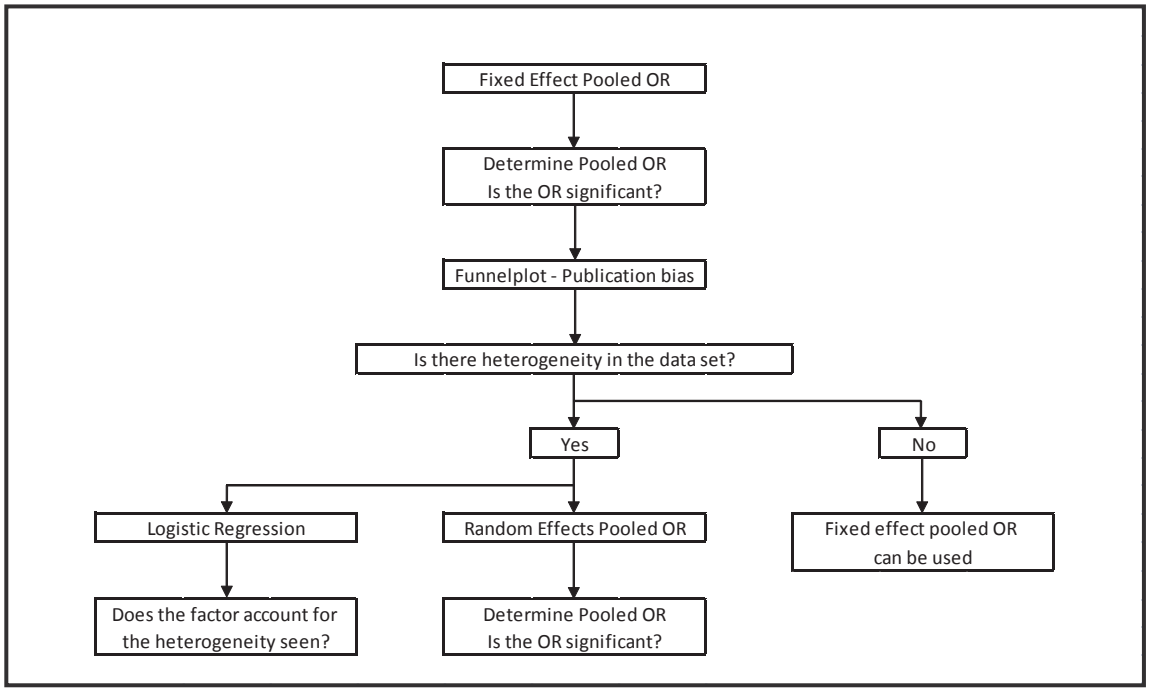

Figure 7.2 Flow chart outlining the methodology used to determine pooled OR estimates for the association of *SLC11A1* polymorphisms with the occurrence of infectious or autoimmune disease. The fixed effects pooled OR estimate was first determined. The OR was determined to be significant if the 95% CI did not include 1. If heterogeneity was identified in the dataset, as determined by the Cochran Q test, then the random effects pooled OR estimate was completed and the underlying cause of the heterogeneity was assessed by logistic regression. The funnel plot was used to assess for bias within the dataset.

The fixed-effects OR has an underlying assumption that the individual ORs from each dataset included in the meta-analysis are homogenous (i.e. all publications report the same findings with regard to the association being assessed). When analysing a number of studies in a meta-analysis, ideally, all variables would be consistent across studies. For example, consistency with respect to diagnostic criteria for the inclusion of cases, criteria for the selection of controls and population background, infers that the outcome measured for each study (in this case the OR) would be consistent across studies, which are combined to determine the overall association. Therefore, the pooled OR estimate reflects only the effect of the association being analysed, and is not attributable to

additional variables which are not consistent across all populations analysed (Berman and Parker, 2002).

The Cochran Q test was utilised to determine whether heterogeneity was present in the analysed data set and was completed in association with the determination of the fixed-effects pooled OR estimate. The null hypothesis of the Cochran Q test is that the studies included are heterogeneous. Therefore, a p-value less than 0.05 (or a Chochran Q value, which is greater than the degrees of freedom of the analysis) indicates the existence of heterogeneity within the studies included in the meta-analysis. If the Cochran Q test revealed that heterogeneity was present, then the fixed-effect pooled OR estimate was not used as the underlying assumption of homogeneity was not satisfied (Figure 7.2). In this case, the random-effects pooled OR estimate (DerSimonian-Laird method), which differs from the fixed-effect model in that there is no underlying assumption of homogeneity within the dataset, was used to determine the pooled OR. The random-effects pooled OR estimate was deemed significant if the 95% CI did not include 1 (with a p-value of less than 0.05).

Pooled OR estimates are a weighted method, which takes into account the sample size of the individual studies. Larger studies have a greater influence over the pooled OR estimate, and therefore, inclusion of studies with very large sample sizes, as compared to the other studies in the analysis, may bias the pooled OR estimate. To assess the influence of studies with large sample sizes, pooled OR estimates were determined in the presence and absence of the large study. Additionally, funnel plots (Section 7.2.3) were analysed to determine if the OR estimate was reflective of all publications. Where a large sample size study was found to exert significant bias over the pooled OR estimate (i.e. the reversal of the direction of the pooled OR estimate), the large publication was omitted from the analyses.

7.2.2.1 Determination of the Source of Heterogeneity using Logistic Regression Analysis

If significant heterogeneity of ORs was identified within a dataset when the fixed-effects pooled OR estimate was calculated, logistic regression analysis was used to explore the cause of the observed heterogeneity, provided the number of publications included in the analysis were sufficiently large. Logistic regression analysis was

conducted using the program R to determine if the observed heterogeneity was attributable to the ethnic/geographical location of the population analysed or the range of diseases assessed. To assess for heterogeneity due to the disease analysed, comparable diseases were grouped. For the analysis of autoimmune disease, the publications assessing inflammatory bowel disease, ulcerative colitis and Crohn's disease were collectively classified as inflammatory bowel disease; while rheumatoid arthritis and juvenile rheumatoid arthritis were classified as rheumatoid arthritis. For the analysis of infectious disease, individual studies were separated into four groups: tuberculosis, leprosy, *M. avium* and other. To assess heterogeneity due to the ethnicity/geographical location of the population, datasets were classified as Asian, African, European, Mediterranean and South American. If the p-value was less than 0.05, then the heterogeneity was deemed attributable to differences in ORs across the grouping analysed (i.e. due to the diseases or ethnicities analysed).

7.2.3 Detection of Bias using the Funnel Plot

The data sets used for the meta-analyses were also assessed for bias through the use of a funnel plot. A funnel plot is a graphical representation (scatter plot) of the sample size versus ORs (logOR). Therefore, an OR of one (i.e. no association) equates to zero on the funnel plot and each point on the plot represents a single association. Due to the ability of larger studies to more accurately estimate true associations of the variables tested, the OR estimates of smaller studies are scattered at the base of the funnel plot, with a narrowing at the top of the plot where the larger studies reside. This produces a plot, which has an inverted funnel shape, with symmetry of publications on both sides of the pooled OR estimate (if bias is absent). Bias is present in the dataset when the funnel plot is asymmetric (gap in inverted funnel shape), and for publication bias, the gap is usually located at the bottom of the funnel plot, where the smaller studies with non-significant findings are located (Sterne *et al.*, 2001).

Bias is introduced by a range of factors. Publication bias arises due to a preference to publish results with significant findings in English based journals, while smaller studies, with non-significant findings, are either not published or published in smaller (non-English) local journals (Jüni *et al.*, 2002, Sterne *et al.*, 2001). Other sources of bias could be due to heterogeneity in the data (due to a lack of stringent inclusion criteria) or

random variation attributable to chance. When bias exists in the dataset, the pooled OR estimate can overestimate the true strength of the association.

7.2.4 Continuity Corrections for Zero Observations

Studies which have zero observations for both cases and controls were excluded from the current meta-analyses, as it has been shown that these studies do not contribute to the pooled OR estimate (Sweeting *et al.*, 2004). However, studies with a zero observation in only the case or control frequencies were included. The inclusion of datasets with zero events (in either the case or control frequencies) to meta-analyses has been shown to decrease heterogeneity within a dataset and reduce the confidence interval of the pooled OR estimate (Friedrich *et al.*, 2007). To allow the inclusion of studies containing zero observations, a continuity correction was added to the frequencies. The reciprocal of the opposite treatment size method was used to allow studies with a zero observation to be included. In this method, the reciprocal of the sample size of the opposite arm was added (i.e. for cases the reciprocal of the control sample size was added to the case frequencies, while for controls, the reciprocal of the case sample size was added to the control frequencies). The use of the reciprocal of the opposite treatment arm size provides a more conservative estimate, which does not bias the pooled OR estimate compared to other methods such as the addition of a standard constant (i.e. 0.5) (Sweeting *et al.*, 2004).

7.3 RESULTS

A total of 34 and 59 publications, which determined the association of *SLC11A1* polymorphisms with the incidence of autoimmune/inflammatory and infectious disease, respectively, met the criteria for inclusion into the meta-analyses (Appendix 3 and 4). From the 34 identified publications of autoimmune/inflammatory disease, 11 *SLC11A1* polymorphisms had been investigated in a sufficient number of association studies to warrant completion of a meta-analysis (a total of 162 associations) (Table 7.1), while 8 polymorphisms, from the 59 publications investigating infectious disease, had a sufficient number of association studies completed to be included (224 associations in total). Table 7.1 summarises the number of publications and datasets for each polymorphism, the number of datasets analysed after the exclusion of publications (Appendix 5-9), and the number of cases and controls. The literature search identified a greater number of *SLC11A1* polymorphisms, where association studies assessing the incidence with autoimmune and infectious disease had been completed, however, the number of data sets for these polymorphisms were insufficient to complete a meaningful meta-analysis.

Table 7.1 Summary of Identified Publications, Datasets Analysed and Number of Cases and Controls.

Polymorphism	Autoimmune Disease					Infectious Disease				
	Publications*	Datasets#	Analysed†	Cases	Control	Publications*	Datasets#	Analysed†	Cases	Control
$(GT)_n$ Allele 3	30	32	29	10932	11023	29	29	24	4497	5175
$(GT)_n$ Allele 2	30	32	29	11210	10969	29	29	18	2837	2683
-237C/T	7	9	9	6371	6963	7	7	5	380	433
274C/T	9	9	9	6546	7074	10	12	11	1726	2347
469+14G/C	14	14	14	10122	12006	39	43	39	5490	6498
577-18G/A	6	6	5	711	691					
823C/T	8	8	8	922	952					
1029C/T	8	8	4	949	873					
1465-85G/A	9	9	8	6342	6639	6	7	6	771	713
1730G/A	16	16	15	7050	7588	42	46	44	5490	6498
1729+55del4	16	16	14	10116	11340	43	45	43	6669	8030
1729+271del4	3	3	3	480	309	5	6	6	868	1581

*Total number of published studies identified from the literature search meeting the inclusion criteria of the meta-analysis.

#Total number of datasets from the identified publications for inclusion into the meta-analysis.

†The number of datasets analysed in the meta-analysis after the removal of datasets containing zero observation for both cases and controls and when data to determine OR was not forthcoming from corresponding authors.

7.3.1 Associations of *SLC11A1* Polymorphisms with the Incidence of Autoimmune Disease

The analysis of *SLC11A1* polymorphisms with autoimmune/inflammatory disease included 11 polymorphisms (Table 7.1) (Figure 7.1). Table 7.2 displays a summary of the pooled OR estimates for each polymorphism (Section 7.2.2).

As part of a larger study of the association of six previously identified T1D susceptibility genes, Maier et al. (2005) completed a case control association study of several *SLC11A1* polymorphisms with T1D. However, the paper did not provide allele frequencies of cases and controls. Correspondence with the authors resulted in the receipt of a more comprehensive analysis (Yang *et al.*, unpublished), which assessed an extended sample size, and accordingly, the Maier et al. (2005) paper was excluded from all meta-analyses. Care was taken to incorporate the Yang et al. (unpublished) study into the individual meta-analyses of *SLC11A1* polymorphisms, due to the large sample sizes analysed in this study (which ranged from 5498-10611 individual cases or controls) (Section 7.2.2), which could bias the estimated pooled OR.

Table 7.2 Meta-analyses of the Association of *SLC11A1* Polymorphisms with the Incidence of Autoimmune/Inflammatory Disease.

Polymorphism	Fixed-Effects Pooled OR					
Association	Complete dataset	Cochrane Q test	Absence of Yang[†]	Cochrane Q test	Random-Effects	Significance
$(GT)_n$ Allele 3						
Autoimmune/autoinflammatory	1.07 (1.03-1.12)	82.59 (P=0)	1.09 (1.01-1.18)	82.42 (P=0)	**1.08 (0.96-1.21)**	**P=0.22**
Autoimmunity	1.08 (1.03-1.13)	75.13 (P=0)			**1.11 (0.98-1.26)**	**P=0.09**
$(GT)_n$ Allele 2						
Autoimmune/autoinflammatory	0.93 (0.89-0.97)	59.01 (P=0)	0.91 (0.83-0.99)	58.73 (P=0)	**0.92 (0.83-1.03)**	**P=0.22**
Autoimmunity	0.93 (0.89-0.97)	54.73 (P=0)			**0.90 (0.81-1.00)**	**P=0.06**
-237C/T						
Autoimmunity	0.92 (0.83-1.02)	12.43 (P=0.13)	**0.61 (0.46-0.81)****	**5.87 (P=0.55)**		
IBD	**0.60 (0.43-0.84)****	**5.82 (P=0.32)**				
274C/T						
Autoimmunity	0.97 (0.92-1.03)	18.41 (P=0.02)	**1.25 (1.07-1.47)****	**7.50 (P=0.38)**		
469+14G/C						
Autoimmune/autoinflammatory	0.93 (0.89-0.97)	58.92 (P=0)	1.37 (1.18-1.59)	31.09 (P=0.02)	**1.32 (1.03-1.71)***	**P=0.02****
577-18G/A						
Autoimmunity	**0.74 (0.50-1.09)**	**2.87 (P=0.58)**	N/A	N/A		
823C/T						
Autoimmunity	0.90 (0.75-1.08)	23.71 (P=0)	N/A	N/A	**1.02 (0.67-1.56)**	**P=0.93**
1029C/T (A318V)						
Autoimmunity	**0.48 (0.21-1.11)**	**1.57 (P=0.67)**	N/A	N/A		
1465-85G/A						
Autoimmunity	0.98 (0.93-1.03)	10.97 (P=0.14)	**1.11 (0.95-1.29)**	**8.19 (P=0.22)**		
1730G/A						
Autoimmune/autoinflammatory	1.23 (1.09-1.39)	46.48 (P=0)	1.23 (1.04-1.45)	46.49 (P=0)	**1.15 (0.84-1.58)**	**P=0.39**
Autoimmunity	1.25 (1.10-1.41)	45.33 (P=0)	1.26 (1.05-1.49)	45.29 (P=0)	**1.17 (0.83-1.66)**	**P=0.37**
1729+55del4						
Autoimmune/autoinflammatory	1.10 (0.98-1.25)	29.36 (P=0.01)	0.97 (0.80-1.17)	26.16 (P=0.01)	**1.17 (0.83-1.64)***	**P=0.37**
Autoimmunity	1.10 (0.98-1.25)	29.25 (P=0)	0.96 (0.80-1.16)	25.43 (P=0)	**1.17 (0.82-1.67)***	**P=0.38**
1729+271del4						
Autoimmunity	**0.98 (0.80-1.22)**	**1.79 (P=0.41)**	N/A	N/A		

Bolded pooled OR estimates represent the final pooled OR estimate for the association of the *SLC11A1* polymorphism.

[†]Pooled OR estimate with the omission of the large sample sized Yang *et al*. (unpublished) study.

N/A - The publication did not assess this polymorphism.

*Random-effects OR determined in the absence of Yang *et al*. (unpublished).

**Statistically significant

7.3.1.1 Association of the $(GT)_n$ Promoter Alleles with the Incidence of Autoimmune/Inflammatory Disease

Meta-analyses were completed for both $(GT)_n$ allele 3 and allele 2 to determine the association of these variants with the incidence of autoimmune/inflammatory disease (Section 7.2.1). Of the 32 datasets identified from literature searches, 29 datasets were included in the meta-analysis (Appendix 5a and 5b). The meta-analyses of $(GT)_n$ allele 3 and allele 2 showed a marginal trend towards susceptibility and resistance to autoimmune/inflammatory disease incidence, with pooled OR estimates of 1.08 and 0.92, respectively (Table 7.2). However, the CI interval of both estimates included 1, indicating that neither $(GT)_n$ allele 2 or 3 are associated with the incidence of autoimmune/inflammatory disease (Table 7.3). Re-analysis of the pooled OR estimate, omitting the study conducted by Yang et al. (unpublished), resulted in little change in the observed OR estimate, showing that the large study did not bias the pooled OR estimate, and therefore, this large study was retained in the analyses (Table 7.2) (Section 7.2.2). Furthermore, analysis of the funnel plots from the meta-analysis of $(GT)_n$ allele 2 and 3 with autoimmune/inflammatory disease did not indicate bias within the datasets (Figure 7.3).

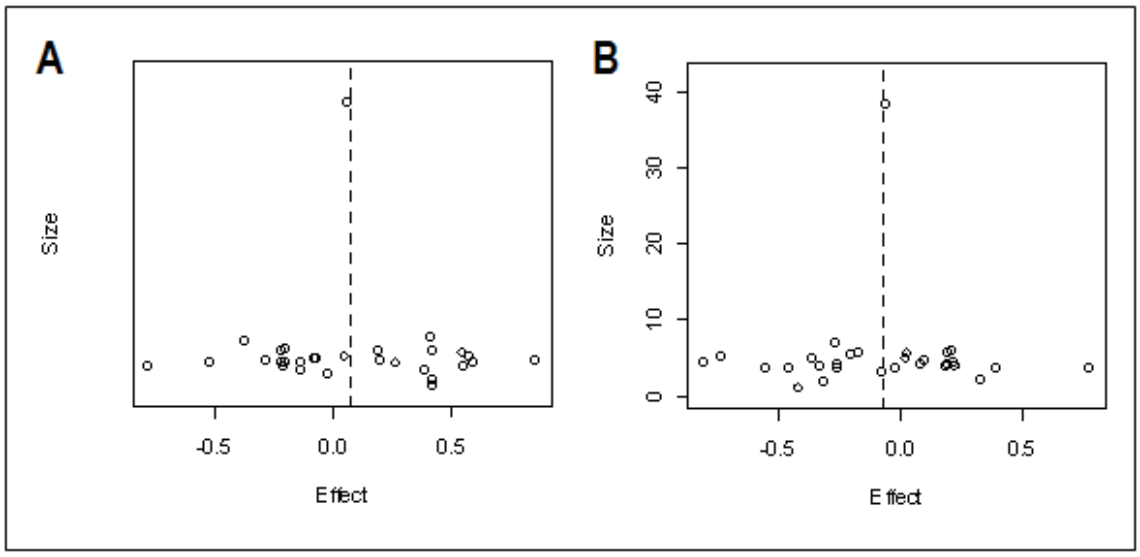

Figure 7.3 Funnel plots of the meta-analyses assessing the association of the $(GT)_n$ alleles with the incidence of autoimmune/inflammatory disease. (A) Allele 3. (B) Allele 2. The dashed lines indicate the location of the random-effects pooled OR estimate.

7.3.1.1.1 $(GT)_n$ Allele 2 is Associated with Marginal Protection Against the Occurrence of Autoimmune Disease

Further analysis was completed by assessing the association of *SLC11A1* $(GT)_n$ allele 2 and 3 with autoimmune diseases only. Behçet's disease is a systemic vasculitis of unknown aetiology, characterised by relapsing ulcers/lesions. Unlike the other diseases assessed in the meta-analyses, Behçet's disease does not exhibit the classical features of autoimmune disease and is described as an autoinflammatory disease (an inherited disorder of inflammatory attacks of innate nature) (Direskeneli, 2006, Mendes *et al.*, 2009). Therefore, the association of the $(GT)_n$ alleles was completed using only the association studies analysing autoimmune diseases.

Re-analysis of the pooled OR estimate, assessing the association of the $(GT)_n$ alleles with autoimmune disease only, yielded an increased pooled OR estimate for $(GT)_n$ allele 3 of 1.11 with a 95% CI, which just included 1 (0.98-1.26), thereby strengthening the association of *SLC11A1* $(GT)_n$ allele 3 with the incidence of autoimmune disease, however, this value did not reach significance (*P*=0.09) (Table 7.2). Analysis of the association of $(GT)_n$ allele 2 with the incidence of autoimmune disease resulted in an OR estimate of 0.90 with a 95% CI which included 1 (0.81-1.00), thus increasing the strength of the association of allele 2 with protection from the development of autoimmune disease. However, this putative association was just outside statistical significance (P=0.06) (Table 7.2).

7.3.1.1.2 The $(GT)_n$ Allelic Variants are Associated with the Incidence of Sarcoidosis and Type 1 Diabetes

Further analysis of the association of $(GT)_n$ allele 3 with individual autoimmune diseases found a significant association with the incidence of both sarcoidosis and T1D with pooled OR estimates of 1.65 (CI: 1.30-2.08) and 1.07 (CI: 1.01-1.12), respectively (Table 7.3). Conversely, a significant protective effect was observed when the association of $(GT)_n$ allele 2 with the incidence of sarcoidosis [OR=0.73 (CI: 0.54-0.98)] and Type 1 diabetes [OR=0.93 (CI: 0.89-0.98)] was analysed (Table 7.3). No association was observed between $(GT)_n$ alleles 2 and 3 and the occurrence of inflammatory bowel disease, rheumatoid arthritis and multiple sclerosis.

Table 7.3 Pooled OR Estimates of the Association of $(GT)_n$ Alleles 3 and 2 with Disease Occurrence and Ethnicity.

	Allele 3	Allele 2
Disease		
Type 1 diabetes	1.07 (1.01-1.12)**	0.93 (0.89-0.98)**
Sarcoidosis	1.65 (1.30-2.08)**	0.73 (0.54-0.98)**
Multiple sclerosis	1.22 (0.80-1.85)	0.84 (0.53-1.33)
Inflammatory bowel disease	1.05 (0.81-1.37)	0.91 (0.78-1.06)
Rheumatoid athritis	1.06 (0.75-1.51)	0.91 (0.65-1.26)
Ethnicity		
African	1.75 (1.19-2.59)**	0.66 (0.13-3.43)
European	1.17 (0.97-1.42)	0.82 (0.67-1.00)
Mediterranean	1.10 (0.98-1.24)	1.06 (0.89-1.26)
Asian	0.80 (0.67-0.96)**	0.88 (0.73-1.06)

**Statistically significant

The difference in $(GT)_n$ allele frequencies between different populations has been well documented (Awomoyi, 2007, Yip *et al.*, 2003). Therefore, further analysis was completed assessing the association of the allelic variants of the $(GT)_n$ repeat, in individual ethnicities/geographical locations, with the occurrence of autoimmune disease (Table 7.3).

From these analyses, allele 3 was found to be significantly associated with the onset of autoimmune disease in African populations, with a fixed-effects pooled OR of 1.75 (CI: 1.19-2.59), and just outside of statistical significance in European and Mediterranean populations. A significant association of allele 3 with autoimmune disease was also found in the Asian population, with a fixed-effects pooled OR estimate of 0.80 (CI: 0.67-0.96) (Table 7.3). Surprisingly, this finding, which included 6 datasets, is opposite to the overall pooled OR trend of the other populations studied. This suggests that in Asian populations $(GT)_n$ allele 3 putatively exerts a protective effect against the development of autoimmune disease, while in the other populations analysed, allele 3 is associated with an increased propensity to develop autoimmune disease. No significant associations were identified from the analysis of allele 2 with autoimmune disease when data was analysed according to ethnicity (Table 7.3).

Ideally, the current meta-analyses would be completed based on the individual populations and diseases assessed, thereby removing confounding factors which exist when studies from different populations and diseases are pooled (as in the current meta-analysis). The juxtaposition in the association of different populations with autoimmune diseases highlights the requirement for the completion of more association studies, with sufficiently large sample sizes, to allow the study of single diseases and populations enabling the identification of authentic associations.

7.3.1.2 The -237C/T, 274C/T and 469+14G/C Polymorphisms are Associated with the Incidence of Autoimmune Disease

The meta-analyses of the -237C/T, 274C/T and 469+14G/C polymorphism included 9, 9 and 14 datasets, respectively (Appendix 6a). When all datasets were assessed for each polymorphism, the meta-analyses found a non-significant protective effect of the less frequent variants at the -237C/T, 274C/T and 469+14G/C polymorphisms (Table 7.2). However, it was found that inclusion of the large Yang et al. (unpublished) dataset biased the pooled OR estimates (Section 7.2.2). Analysis of the funnel plots for each of the meta-analyses showed that the dataset from Yang et al. (unpublished) significantly influenced the pooled OR estimate for each of the polymorphisms by skewing the OR towards a value of 1 (Figure 7.4). In the -237C/T funnel plot, the large study was the only dataset located to the right of the OR estimate. In funnel plots showing data for the 274C/T and the 469+14G/C polymorphisms, only 2 out of 9 and 4 out of 14 publications were located to the right of the pooled OR estimate, respectively (Figure 7.4). Therefore, the resultant OR was not representative of the overall trend of all studies included in the meta-analyses and this large dataset was omitted from the calculation of the pooled OR estimates for the -237C/T, 274C/T and 469+14G/C polymorphisms. Re-analysis of the pooled OR estimates in the absence of Yang et al. (unpublished) resulted in funnel plots which showed no evidence of bias.

Re-analysis of the pooled OR estimate found that the less frequent T variant at the -237C/T polymorphism exerts a putative protective effect against the occurrence of autoimmune disease, with a statistically significant pooled OR estimate of 0.61 (CI: 0.46-0.81) (Table 7.2). The less frequent -237 T variant has only been identified in *cis* with $(GT)_n$ allele 3, where it results in a significant reduction in *SLC11A1* expression, to levels comparable to those expression levels driven by $(GT)_n$ allele 2 (Chapter 6)

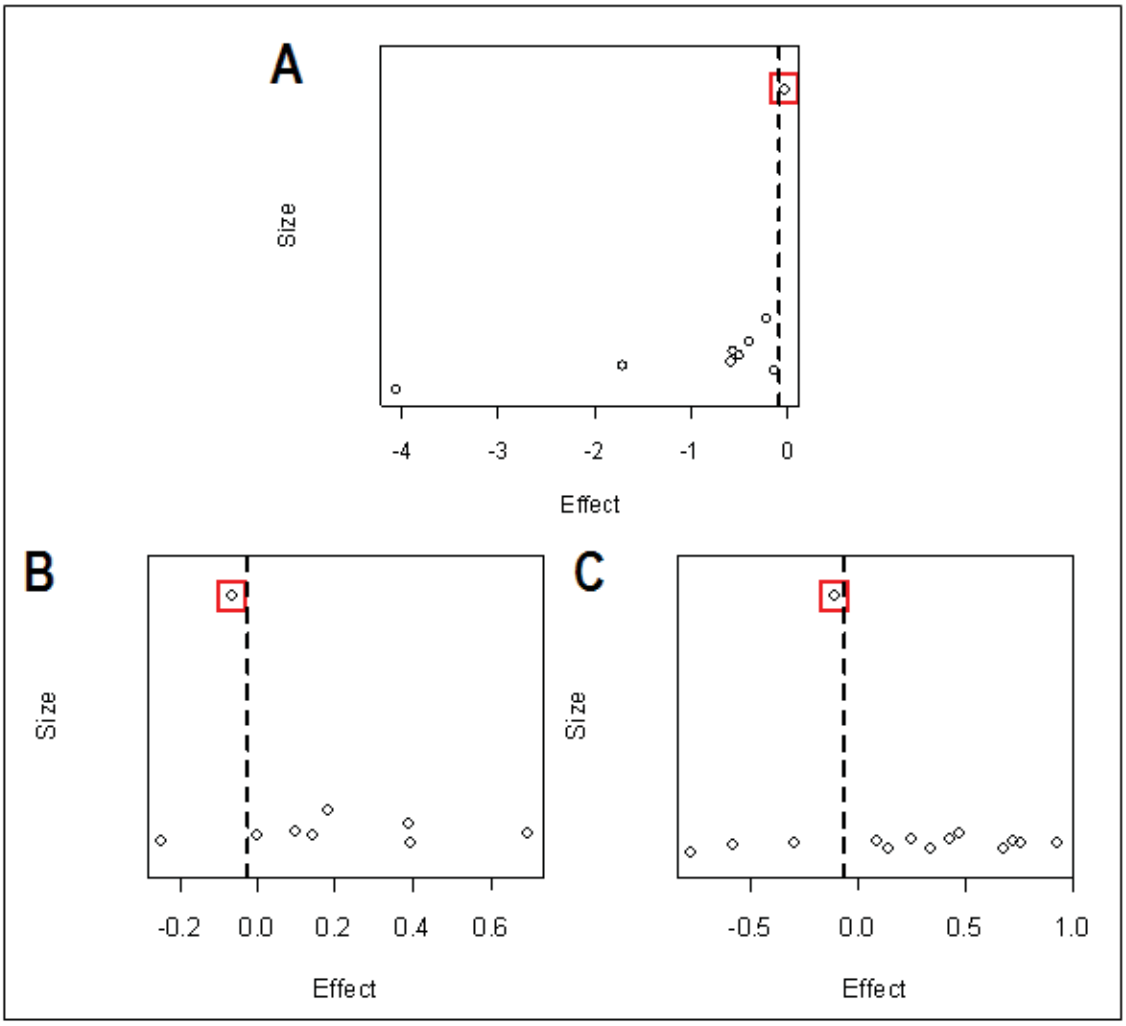

Figure 7.4 Funnel plots of the meta-analyses of the -237C/T (A), 274C/T (B) and 469+14G/C (C) polymorphisms with the occurrence of autoimmune disease. The odds ratios (logOR) for each study included in the meta-analyses was plotted against its sample size. The dashed lines indicate the location of the pooled OR estimate when all datasets were analysed. For each polymorphism, the large Yang et al. (unpublished) dataset (dot located in the red box) biased the pooled OR estimate.

(Zaahl *et al.*, 2004). Therefore, the identified protective effect of the -237 T variant, observed in the current meta-analysis, is consistent with functional data suggesting that this variant would afford protection against autoimmune disease by driving decreased *SLC11A1* expression and concomitant decreased Th1 immune response. Furthermore, analysis of the association of the -237C/T polymorphism with inflammatory bowel disease (combined Crohn's disease and ulcerative colitis) found that the mutant T variant exerted a putative protective effect over disease onset (OR=0.60) (Table 7.2).

Analysis of the 274C/T and 469+14G/C polymorphisms, omitting the dataset of Yang et al. (unpublished), resulted in a reversal of the direction of the previously determined

pooled OR estimates. In both cases the less frequent variants were associated with the occurrence of autoimmune disease, with statistically significant pooled OR estimates of 1.25 (CI: 1.07-1.47) and 1.32 (CI: 1.03-1.71) for the 274C/T and 469+14G/C polymorphisms, respectively.

7.3.1.3 Polymorphisms Within the 3' Region of *SLC11A1* are Not Associated with the Incidence of Autoimmune Disease

No significant associations were identified between the *SLC11A1* polymorphisms, 577-18G/A, 823C/T, 1029C/T, 1465-85G/A, 1729+55del4 and 1729+271del4, and the incidence of autoimmune disease (Table 7.2) (Appendix 6). Again, the large Yang *et al*. (unpublished) dataset skewed the pooled OR estimate for the 1465-85G/A and 1729+55del4 meta-analyses, and therefore this dataset was omitted. However, the large Yang et al. (unpublished) dataset was retained in the meta-analysis of the 1730G/A (D543N) polymorphisms as no bias was observed, as determined by analysis of the funnel plot and resultant pooled OR estimates (Section 7.2.2).

Interestingly, all of the polymorphisms located in the 3' region of the *SLC11A1* gene showed no association with the incidence of autoimmune disease, while polymorphisms in the 5' end of *SLC11A1* [$(GT)_n$,-237C/T, 247C/T and 469+14G/C] were all found to be significantly associated (or just outside the values required for statistical significance) with the incidence of autoimmune disease (Figure 7.1) (Table 7.2).

7.3.1.4 Logistic Regression Analysis to Determine the Source of Heterogeneity Identified in the Meta-Analyses

Heterogeneity of pooled OR estimates was observed within the datasets used for the meta-analyses of the *SLC11A1* $(GT)_n$, 469+14G/C, 823C/T, 1730G/A and 1729+55del4 polymorphisms with autoimmune disease (based on the Cochran Q value) (Table 7.2) (Section 7.2.2). Logistic regression analysis was used to determine if the different diseases or different ethnicity/populations analysed accounted for the source of the heterogeneity observed within the datasets for each polymorphism (Section 7.2.2.1). Logistic regression analysis found that the different diseases analysed and the different ethnicity/populations studied were not the source of the observed heterogeneity within the datasets.

7.3.2 Associations of *SLC11A1* Polymorphisms with the Incidence of Infectious Disease

The analysis of the association of *SLC11A1* polymorphisms with the incidence of infectious disease included the assessment of 8 polymorphisms (Table 7.1) (Figure 7.1). Table 7.4 displays the pooled OR estimates for each polymorphism. Where possible, additional meta-analyses were completed assessing the association of the *SLC11A1* polymorphisms with tuberculosis or leprosy alone (Table 7.4). Additionally, the association of the *SLC11A1* polymorphisms with the incidence of infectious disease according to ethnicity was also analysed.

Table 7.4 Meta-analyses of the Association of *SLC11A1* Polymorphisms with the Incidence of Infectious Disease.

Polymorphism	Pooled OR Estimate			
Association	Fixed-Effects	Cochrane Q test	Random-Effects	Significance
$(GT)_n$ Allele 3				
Infectious disease	0.82 (0.76-0.88)	59.00 (P=0)	**0.82 (0.72-0.93)**	**P=0.002****
Tuberculosis	0.75 (0.69-0.82)	40.54 (P=0)	**0.76 (0.65-0.89)**	**P=0.0005****
$(GT)_n$ Allele 2				
Infectious disease	**1.32 (1.20-1.46)****	**25.52 (P=0.08)**		
Tuberculosis	**1.47 (1.30-1.66)****	**12.23 (P=0.27)**		
-237C/T				
Infectious disease	**0.66 (0.41-1.06)**	**2.11 (P=0.71)**		
274C/T				
Infectious disease	**1.07 (0.95-1.20)**	**11.28 (P=0.34)**		
Tuberculosis	**1.15 (0.93-1.41)**	**10.03 (P=0.12)**		
469+14G/C				
Infectious disease	1.21 (1.12-1.31)	56.54 (P=0.03)	**1.22 (1.10-1.36)**	**P=0.0003****
Tuberculosis	1.23 (1.13-1.33)	47.63 (P=0.01)	**1.24 (1.09-1.40)**	**P=0.001****
1465-85G/A				
Infectious disease	**1.05 (0.89-1.24)**	**2.86 (P=0.70)**		
1730G/A				
Infectious disease	1.17 (1.08-1.26)	102.58 (P=0)	**1.21 (1.05-1.39)**	**P=0.007****
Tuberculosis	1.18 (1.08-1.29)	75.97 (P=0)	**1.22 (1.04-1.42)**	**P=0.01****
1729+55del4				
Infectious disease	1.18 (1.11-1.26)	83.39 (P=0)	**1.22 (1.10-1.36)**	**P=0.0003****
Tuberculosis	1.23 (1.14-1.33)	51.98 (P=0)	**1.28 (1.14-1.44)**	**P=0.00003****
Leprosy	**1.06 (0.89-1.26)**	**1.63 (P=0.80)**		
1729+271del4				
Infectious disease	**1.06 (0.89-1.24)**	**2.92 (P=0.71)**		
Tuberculosis	**1.02 (0.87-1.19)**	**2.12 (P=0.71)**		

Bolded OR estimates represent the final pooled OR estimate for the association of the *SLC11A1* polymorphism.
**Statistically significant

7.3.2.1 *SLC11A1* $(GT)_n$ Allele 2 and Allele 3 are Associated with Susceptibility and Resistance to Infectious Disease and Tuberculosis Alone

The meta-analysis of the association of $(GT)_n$ allele 2 and allele 3 with infectious disease included 18 and 24 datasets, respectively (Table 7.1) (Appendix 7a and 7b). The meta-analyses showed that $(GT)_n$ allele 2 was strongly associated with the incidence of infectious disease, with a statistically significant fixed-effects pooled OR estimate of 1.32 (CI: 1.20-1.46). On the other hand, $(GT)_n$ allele 3 was shown to play a protective role against the occurrence of infectious disease, with a random-effects pooled OR of 0.82 (CI: 0.72-0.93) (Table 7.4). Further analysis, assessing the association of the $(GT)_n$ alleles with the incidence of tuberculosis alone, revealed a stronger association than those observed with the occurrence of infectious disease *per se*, with fixed and random-effects pooled OR of 1.47 (CI: 1.30-1.66) and 0.76 (CI: 0.65-0.89) for allele 2 and 3, respectively (Table 7.4).

A meta-analysis assessing the association of $(GT)_n$ allele 2 with the occurrence of infectious disease or tuberculosis alone has not been completed prior to the current study. A previous meta-analysis, and case control association studies have focused primarily on the incidence of allele 3 with infectious disease, and disease associations with allele 2 have not been investigated (Li *et al.*, 2006). However, the results of the current meta-analysis show that the association of $(GT)_n$ allele 2 with the incidence of infectious disease and tuberculosis susceptibility alone is more significant than the protective effect putatively exerted by $(GT)_n$ allele 3. Additionally, the $(GT)_n$ allele 2 dataset was found to be homogenous, as the Chochran Q value did not identify heterogeneity of OR within the dataset. Conversely, heterogeneity was identified within the $(GT)_n$ allele 3 dataset (Table 7.4). It would be envisaged that a sequence variant, which alters the propensity of an individual to contract an infectious disease (i.e. the variant provides a selective advantage or disadvantage to the carrier) would be common to all studies irrespective of other factors responsible for heterogeneity (for example ethnicity and nutritional status). In such a case, the ORs for the individual studies in the meta-analysis would be expected to be homogenous, as is observed with the meta-analysis of allele 2 with the incidence of infectious disease. Therefore, the meta-analysis data suggests that allele 2 may exert a greater influence on the incidence of infectious disease than the previously thought $(GT)_n$ allele 3.

Analysis of the funnel plots from the meta-analyses of $(GT)_n$ allele 2 and 3 with the incidence of infectious disease indicated the presence of bias within the datasets (Figure 7.5). While the use of the trim and fill method was previously used to adjust for bias (Chapter 3), in the current analysis the use of the trim and fill method does not appear to be needed, as if the funnel plots for both the $(GT)_n$ allele 2 and 3 analyses did not show bias (i.e. the "missing" studies were filled in), these missing studies would be located in a position that would strengthen the pooled OR estimate.

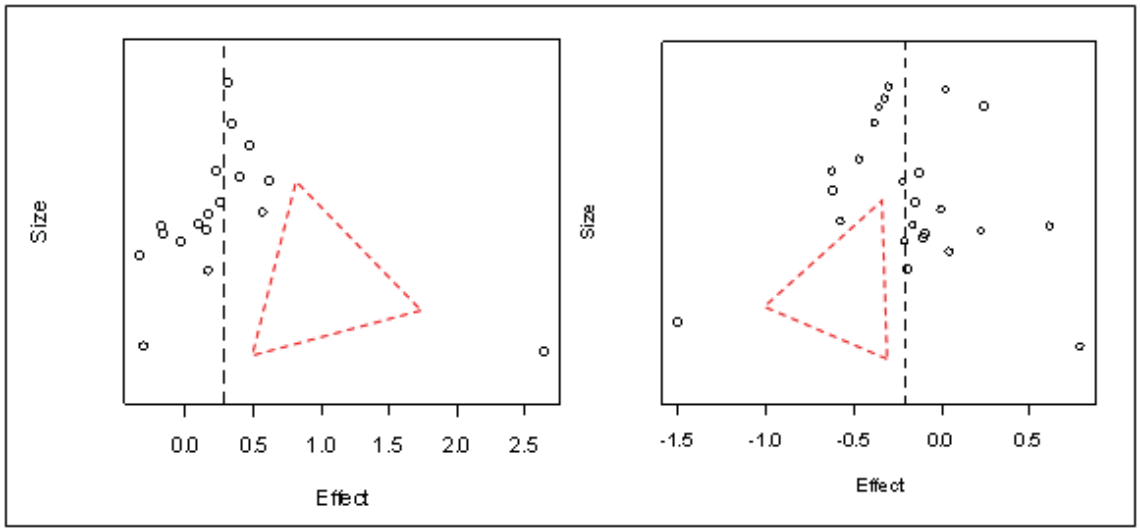

Figure 7.5 Funnel plots of the meta-analyses of allelic variants at the $(GT)_n$ repeat with the incidence of infectious disease. The odds ratios (logOR) for each study included in the meta-analyses was plotted against the sample size of the study. The dashed lines indicate the location of the pooled OR estimate. Slight bias is evident in the analysis of $(GT)_n$ allele 2 (A) and allele 3 (B) due to small gaps to the right and left of the pooled OR estimates, respectively. The dotted triangles indicate the location of missing studies.

7.3.2.1.1 The Association of the $(GT)_n$ Alleles with Infectious Disease According to Ethnicity

Further analysis, based on ethnicity, found that $(GT)_n$ allele 2 was significantly associated with infectious disease susceptibility in the African population, with a susceptibility trend, which failed to reach significance, among Asian and European populations (Table 7.5). Furthermore, no association was found in the South American population (Table 7.5). Allele 3 was found to be significantly associated with resistance to infectious disease in African and Asian populations, however, no association was found among European and South American populations (Table 7.5). While the lack of association of both $(GT)_n$ allele 2 and 3 with the occurrence of infectious disease in the

South American population may be due to the small number of publications completed to date (n=2), conflicting results were observed with the association of the $(GT)_n$ alleles with infectious disease in the European population. The results from the European population indicate that allele 2 may be associated with the incidence of infectious disease (OR=1.24), while allele 3 appears to play no role in affording disease protection (OR=1.01). This result suggests that in the European population allele 2 exerts a greater influence over infectious disease susceptibility compared to allele 3.

Table 7.5 Analysis of the Association of $(GT)_n$ Allele 2 and 3 with the Incidence of Infectious Disease According to Ethnicity.

Ethnicity	Allele 3	Allele 2
African	0.81 (0.74-0.90)**	1.45 (1.22-1.71)**
Asian	0.72 (0.63-0.83)**	1.28 (0.98-1.66)
European	1.01 (0.69-1.48)	1.24 (0.97-1.57)
South American	1.02 (0.74-1.41)	1.00 (0.72-1.40)

**Statistically significant

7.3.2.2 The 469+14G/C, 1730G/A and 1729+55del4 Polymorphisms are Associated with the Incidence of Infectious Disease

The meta-analyses assessing the association of the 469+14G/C, 1730G/A and 1729+55del4 polymorphisms with the incidence of infectious disease included 39, 44 and 43 datasets, respectively (Table 7.1) (Appendix 8a, 8b and 8c). The meta-analyses found that the presence of the less frequent variant for each polymorphism was significantly associated with the incidence of infectious disease, with random effects pooled OR estimates of 1.22 (CI: 1.10-1.36), 1.21 (CI: 1.05-1.39) and 1.22 (CI: 1.10-1.36) for the 469+14G/C, 1730G/A and 1729+55del4 polymorphisms, respectively (Table 7.4). Furthermore, analysis of the association of the 469+14G/C, 1730G/A and 1729+55del4 polymorphisms with the incidence of tuberculosis alone identified a stronger association than that observed with infectious disease *per se*, with pooled OR estimates of 1.24 (CI: 1.09-1.40), 1.22 (CI: 1.04-1.42) and 1.28 (CI: 1.14-1.44), respectively (Table 7.4). Significant heterogeneity, as determined by the Cochran Q value, was identified within the datasets of the meta-analyses assessing both infectious disease and tuberculosis alone for all three polymorphisms (469+14G/C, 1730G/A and

1729+55del4) (Table 7.4). The association of the incidence of leprosy with *SLC11A1* polymorphisms was only completed for the 1729+55del4 polymorphism, as there were insufficient association studies to warrant an analysis of the other polymorphisms. No association between the occurrence of the 1729+55del4 polymorphism and the incidence of leprosy was identified (Table 7.4). No asymmetry was identified from the analysis of the funnel plots for the 469+14G/C, 1730G/A and 1729+55del4 polymorphisms.

7.3.2.2.1 Association of SLC11A1 Polymorphisms with the Incidence of Infectious Disease According to Geographical Location/Ethnicity

Analysis of the association of the 469+14G/C, 1730G/A and 1729+55del4 polymorphisms with the occurrence of infectious disease among different ethnicities, identified a trend in which the less frequent variant for each polymorphism was associated with the incidence of infectious disease (Table 7.6). In particular, a significant association was identified between each polymorphism and the incidence of infectious disease in the Asian population. The 469+14C/C and 1729+55del4 polymorphisms were significantly associated with the incidence of infectious disease in the African population. However, a protective effect appeared to be conferred by the less frequent 1730 A variant in the Mediterranean population (Table 7.6). However, this analysis incorporated only two publications, suggesting that the observed association may be largely attributable to random variation.

Table 7.6 Analysis of the Association of the 469+14G/C, 1730G/A and 1729+55del4 Polymorphisms with the Incidence of Infectious Disease Based on Ethnicity.

Ethnicity	469+14G/C	1730G/A	1729+55del4
African	1.37 (1.14-1.65)**	1.26 (0.82-1.93)	1.11 (1.01-1.23)**
Asian	1.35 (1.10-1.66)**	1.23 (1.11-1.36)**	1.30 (1.08-1.57)**
European	1.03 (0.88-1.21)	1.19 (0.79-1.78)	1.66 (0.90-3.05)
South American		1.18 (0.98-1.43)	1.21 (1.00-1.47)
Mediterrianean	1.19 (0.75-1.87)	0.37 (0.23-0.61)**	1.16 (0.40-3.40)

**Statistically significant

7.3.2.3 The -237C/T, 274C/T, 1485-85G/A and 1729+271del4 Polymorhisms are not Associated with the Incidence of Infectious Disease

No significant association was identified between the occurrence of the -237C/T, 274C/T, 1485-85G/A and 1729+271del4 polymorphisms and the incidence of infectious disease or tuberculosis alone (Table 7.4) (Appendix 9). The association of the -237C/T polymorphism with infectious disease failed to reach statistical significance and this is likely attributable to the small number of publications, which have been completed to date. The results suggest that promoter -237C/T polymorphism may be associated with the occurrence of infectious disease, however more association studies are required.

7.3.2.4 Logistic Regression Analysis to Determine the Source of Heterogeneity Identified in the Meta-Analyses

Heterogeneity of OR was observed within datasets from the meta-analyses of the *SLC11A1* $(GT)_n$ allele 3, 469+14G/C, 1730G/A and 1729+55del4 polymorphisms with infectious disease (Table 7.4) (Section 7.2.2). Therefore, only $(GT)_n$ allele 2 was found to be significantly associated with the incidence of infectious disease with an absence of significant heterogeneity of OR within the datasets included in the analysis. Logistic regression analysis was used to determine if the different diseases or different ethnicity/populations analysed accounted for the source of the heterogeneity observed within the datasets for each polymorphism (Section 7.2.2.1). Logistic regression analysis found that the different diseases analysed and the different ethnicity/populations were not the source of the observed heterogeneity within the datasets of the *SLC11A1* polymorphisms.

7.3.3 Summary

Of the associations found between *SLC11A1* polymorphisms and disease occurrence, $(GT)_n$ allele 2 showed the strongest association with both infectious disease and tuberculosis alone. Significant associations were also observed with the 469+14G/C, 1730G/A and 1729+55del4 polymorphisms and the incidence of infectious disease and tuberculosis alone (Table 7.4). In contrast to the observation that polymorphisms throughout the *SLC11A1* gene were associated with the occurrence of infectious disease, meta-analyses of the association of *SLC11A1* polymorphisms with the incidence of

autoimmune disease, revealed that polymorphisms in the 5’ end of *SLC11A1* were associated with disease incidence, while polymorphisms in the 3’ end showed no association (Section 7.3.1.3) (Table 7.2 and 7.4) (Figure 7.6).

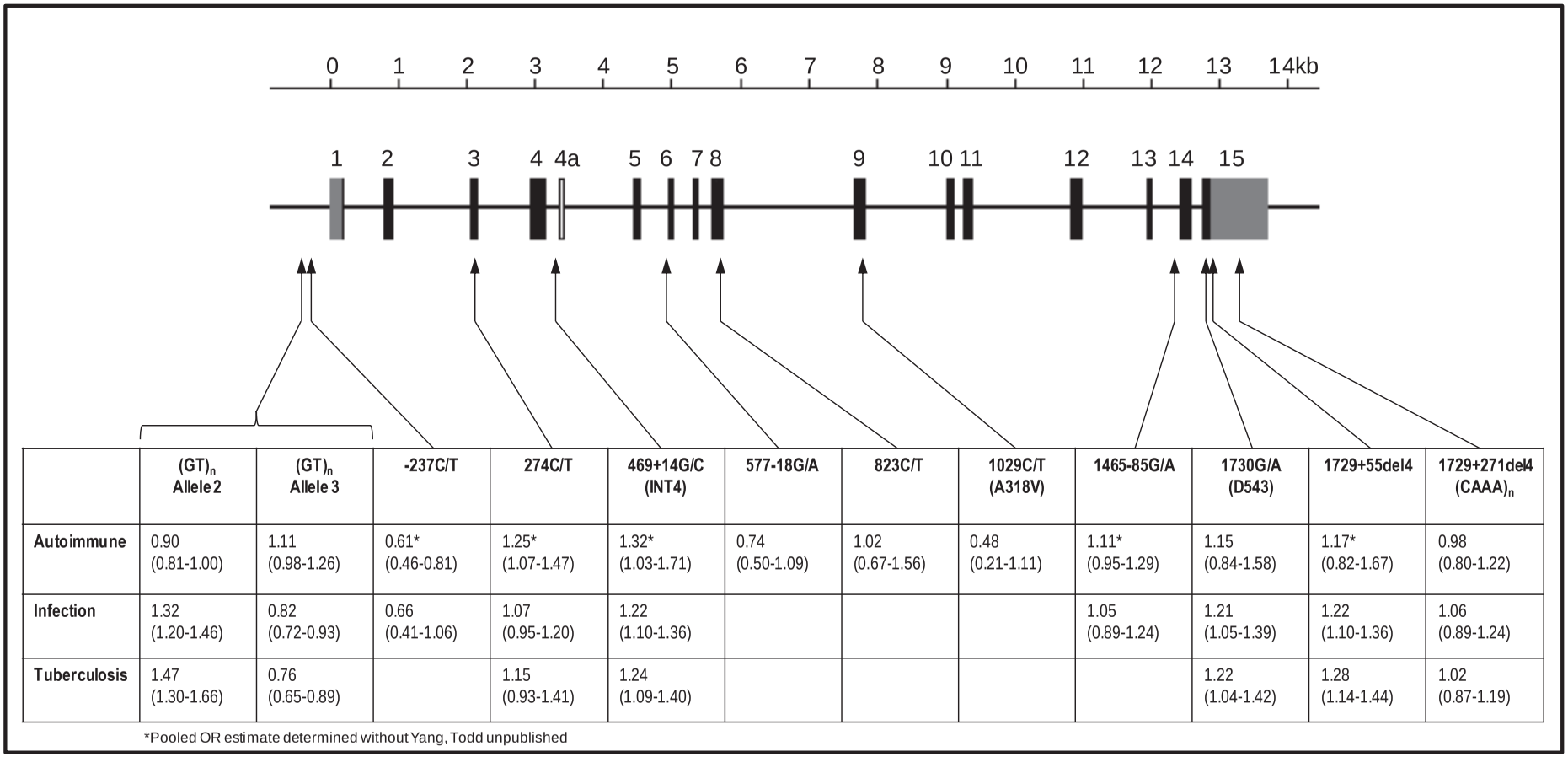

	$(GT)_n$ Allele 2	$(GT)_n$ Allele 3	-237C/T	274C/T	469+14G/C (INT4)	577-18G/A	823C/T	1029C/T (A318V)	1465-85G/A	1730G/A (D543)	1729+55del4	1729+271del4 $(CAAA)_n$
Autoimmune	0.90 (0.81-1.00)	1.11 (0.98-1.26)	0.61* (0.46-0.81)	1.25* (1.07-1.47)	1.32* (1.03-1.71)	0.74 (0.50-1.09)	1.02 (0.67-1.56)	0.48 (0.21-1.11)	1.11* (0.95-1.29)	1.15 (0.84-1.58)	1.17* (0.82-1.67)	0.98 (0.80-1.22)
Infection	1.32 (1.20-1.46)	0.82 (0.72-0.93)	0.66 (0.41-1.06)	1.07 (0.95-1.20)	1.22 (1.10-1.36)				1.05 (0.89-1.24)	1.21 (1.05-1.39)	1.22 (1.10-1.36)	1.06 (0.89-1.24)
Tuberculosis	1.47 (1.30-1.66)	0.76 (0.65-0.89)		1.15 (0.93-1.41)	1.24 (1.09-1.40)					1.22 (1.04-1.42)	1.28 (1.14-1.44)	1.02 (0.87-1.19)

*Pooled OR estimate determined without Yang, Todd unpublished

Figure 7.6 Summary of the results from the meta-analyses (pooled OR estimates and 95% CI interval) assessing the association of the *SLC11A1* polymorphisms with the incidence of autoimmune disease, infectious disease and tuberculosis alone.

7.4 DISCUSSION

7.4.1 Summary

Due to the role of SLC11A1 in driving a Th1 pro-inflammatory immune response, a significant number of case-control association studies have been completed to determine if polymorphisms within the *SLC11A1* locus are associated with the incidence of infectious and autoimmune disease. These studies have produced inconsistent results (Section 1.3.4). Therefore, through the use of meta-analyses, the current study aimed to determine the association of several polymorphisms within the *SLC11A1* locus with the occurrence of infectious and autoimmune disease. The current study incorporates the largest number of publications and the largest number of *SLC11A1* polymorphisms investigated to date, with 11 and 8 *SLC11A1* polymorphisms analysed with the occurrence of autoimmune and infectious disease, respectively (Figure 7.6).

From the current meta-analysis, the association of $(GT)_n$ alleles 2 and 3 with reduced and increased incidence of autoimmune disease, respectively, fell just outside of statistical significance (Table 7.2). The findings of the current analysis that allele 2 is associated with a reduced incidence of autoimmune disease is consistent with two smaller meta-analyses assessing the association of the $(GT)_n$ alleles with autoimmune disease, which included 7 and 15 datasets (Nishino *et al.*, 2005, O'Brien *et al.*, 2008) (Table 7.7). However, the OR estimates of the association of allele 3 with autoimmune disease have been inconsistent (Table 7.7). An estimate was not reported by Nishino et al. (2005), suggesting that no association was found. The pooled OR estimate determined by O'Brien et al. (2008), in the absence of asymmetry within the dataset, was 0.88 (CI: 0.65), suggesting no association (Table 7.7). In the current analysis, a trend for the association of allele 3 with increased incidence of autoimmune disease was observed. While the finding was not significant, the direction of the pooled OR estimate was opposite to that reported in O'Brien et al. (2008) but consistent with the hypothesis of Searle and Blackwell. (1999) (Section 1.3.4). The current study has the largest sample size to date, suggesting that the observed estimate is reflective of the true association.

Table 7.7 Comparison of Pooled OR Estimates between the Current and Previously Completed Meta-analyses with the Incidence of Autoimmune Disease and Tuberculosis.

Polymorphism	Autoimmune			Tuberculosis	
	Nishino et al., 2005	O'Brien et al., 2008	Current Analysis	Li et al., 2006	Current Analysis
$(GT)_n$ Allele 2	0.71 (0.53-0.96)**	0.80 (0.22)	0.90 (0.81-1.00)		1.47 (1.30-1.66)**
$(GT)_n$ Allele 3		0.88 (0.66)	1.11 (0.98-1.26)	0.76 (0.60-0.97)**	0.76 (0.65-0.89**
469+14G/C			1.32 (1.03-1.71)**	1.14 (0.69-1.35)	1.24 (1.09-1.40)**
1730G/A			1.15 (0.84-1.58)	1.67 (1.36-2.05)**	1.22 (1.04-1.42)**
1729+55del4			1.17 (0.82-1.67)	1.33 (1.08-1.63)**	1.28 (1.14-1.44)**

**Statistically significant

Prior to the completion of the current study, meta-analyses of only 4 *SLC11A1* polymorphisms with the incidence of tuberculosis had been completed (Table 7.7) (Li *et al.*, 2006). The pooled OR estimates observed in the current meta-analyses were similar to the OR estimates reported previously (Table 7.7). However, the magnitude of the association at the 1730G/A polymorphism was significantly different (Table 7.8). The current meta-analysis included 32 associations, compared to 9, and therefore is probably more reflective of the true association (Appendix 8b). The increase in the number of datasets in the current analyses would also account for the observed significant association between the 469+14G/C polymorphism and the incidence of tuberculosis, which was not observed in the previous meta-analysis (Table 7.7) (Li *et al.*, 2006).

The current study completed 15 new meta-analyses (10 for autoimmune disease and 5 for infectious disease). Previously, only the $(GT)_n$ alleles had been assessed in meta-analyses to determine their association with the occurrence of autoimmune disease, as there were insufficient studies to allow a meaningful analysis of the other polymorphisms (Chapter 3). The current meta-analysis is the first to identify an association of the T variant of the -237C/T polymorphism with a reduced incidence of autoimmune disease. Furthermore, the less frequent variants of the 274C/T and 469+14G/C polymorphisms were significantly associated with the incidence of autoimmune disease (Table 7.2). Additionally, the current analysis is the first to show a strong association between $(GT)_n$ allele 2 and the incidence of tuberculosis alone and infectious disease *per se* (Table 7.4).

Attempts to determine the source of heterogeneity of OR by logistic regression analysis, found that factors such as the specific disease analysed, or the ethnicity/geographical location of the population analysed, could not account for the observed heterogeneity identified in the majority of datasets (Sections 7.3.1.4 and 7.3.2.4). This may have been attributable, in part, to the classification of studies into groups, which did not adequately reflect the heterogeneity present within the dataset. For example, the combined grouping of multiple disease entities (each with their own unique pathogenesis) as a single syndrome (e.g. inflammatory bowel disease or group "other" in the analysis of autoimmune and infectious disease, respectively), or grouping studies based on ethnicity/geographical location which may not take into full account the underlying population stratifications present (Section 7.2.2.1) (Cardon and Palmer, 2003).

Alternatively, the source of the heterogeneity may be due to other confounding factors not assessed in the logistic regression analysis, which may play a greater role in influencing disease incidence (and thus alter the OR of the individual studies). These may include shared environmental factors such as nutritional status and poverty, as well as other host genetic factors (Stein and Baker, 2011, Stein *et al.*, 2007). The identification of heterogeneity within the datasets shows the need for the completion of additional studies with large sample sizes conducted within a specific ethnicity and disease type, enabling subsequent meta-analyses greater power to determine the association of *SLC11A1* polymorphisms with the occurrence of a specific disease state.

7.4.2 Functional Variants within the 5' and 3' LD Haplotype Regions of *SLC11A1* Influence Autoimmune and Infectious Disease Susceptibility

The meta-analyses found that polymorphisms in the 5' region of *SLC11A1*, but not the 3' region, were associated with susceptibility/resistance to autoimmune disease (Section 7.3.1.3), while polymorphisms located throughout *SLC11A1* were associated with the incidence of infectious disease and tuberculosis alone (Section 7.3.3) (Figure 7.7).

It has previously been shown that significant LD exists around *SLC11A1* (Dunstan *et al.*, 2001, Kim *et al.*, 2008, Yip *et al.*, 2003). Yip et al. (2003) found that the *SLC11A1* locus contained two LD blocks (in the current study these are termed 5' LD haplotype

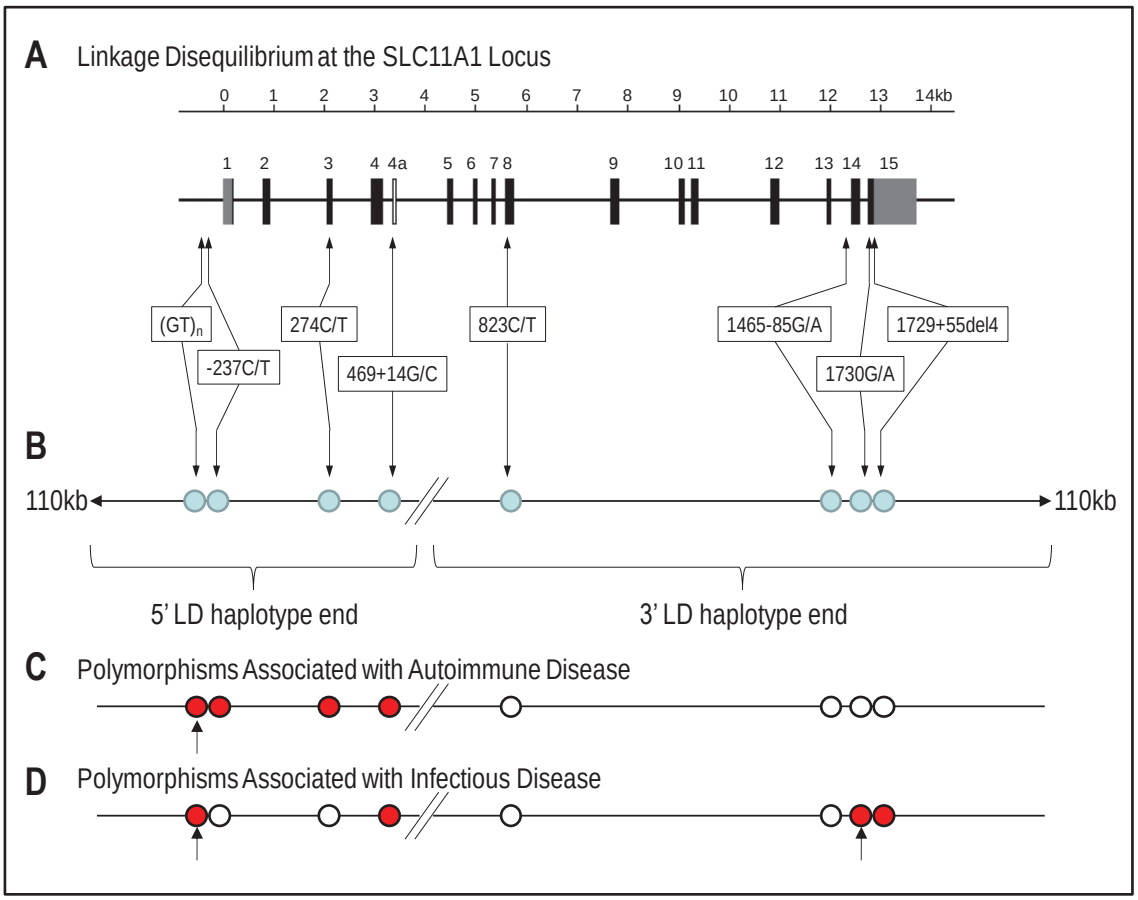

Figure 7.7 Linkage disequilibrium at the *SLC11A1* locus and location of polymorphisms associated with the incidence of autoimmune and infectious disease. (A) Genomic organisation of *SLC11A1* and location of studied sequence variants. The 15 exons of the gene are shown as black boxes with their respective numbers and the corresponding scale above indicates the length (kb) of the gene. The grey boxes indicate the 3' and 5' untranslated regions and the introns and flanking regions are represented by a thin line. The arrows indicate the position of sequence variants. (B) LD located within the *SLC11A1* locus. The blue circles indicate the location of the *SLC11A1* polymorphisms, with the thin line representing the flanking DNA regions. The two LD blocks, identified by Yip et al. (2003) (termed 5' LD haplotype end and 3' LD haplotype end) are shown, with the double dashed line designating the weak LD observed between 5' and 3' *SLC11A1* regions. (C) Polymorphisms within the 5' LD haplotype end but not the 3' end are associated with the incidence of autoimmune disease (red circles indicate an association, while white circles indicate no association). (D) Polymorphisms in both the 5' and 3' LD haplotype blocks were found to be associated with infectious disease. The $(GT)_n$ and 1730G/A are candidate polymorphisms in the *SLC11A1* locus influencing autoimmune and infectious disease susceptibility at the 5' and 3' LD haplotype ends, respectively (arrows).

end and 3' LD haplotype end) (Figure 7.7). The study identified that significant LD existed between the $(GT)_n$, -237C/T, 274C/T and 469+14G/C polymorphisms and markers 110kb upstream of the *SLC11A1* locus, including the IL8Rb locus (termed 5'LD haplotype end). Additional LD was found to exist between the 823C/T, 1465-85G/A, 1730G/A and 1729+55del4 polymorphisms and markers 110kb downstream of the *SLC11A1* locus (termed 3'LD haplotype end). However, LD was not observed between polymorphisms located in the 5' and 3' LD haplotype ends of the *SLC11A1* locus (Figure 7.7) (Yip *et al.*, 2003).

The *SLC11A1* polymorphisms identified in the current analysis to be significantly associated with disease incidence may be the functional cause of the association(s) seen in that the polymorphism(s) results in an altered phenotype which influences disease susceptibility. Alternatively, the association observed may be due to the polymorphism being positively or negatively selected because it is in linkage disequilibrium with the true disease causing variant. In the latter case, a genetic variant which alters disease incidence provides a positive/negative selective pressure for the inheritance of all of the polymorphisms within that LD block (known as the hitchhiker effect).

The findings of the meta-analyses suggest that at least one functional polymorphism at the 5' end of *SLC11A1* (or a polymorphism(s) in LD with the 5' end of *SLC11A1*), influences susceptibility to autoimmune disease, while at least two functional polymorphisms, one at the 5' end and one at the 3' end (or in LD with each region), influences infectious disease susceptibility. Polymorphisms in LD with the significantly associated *SLC11A1* polymorphisms should also be considered as potential functional candidates for disease susceptibility. Functional tests are required to identify the polymorphic variants which may result in an altered cellular phenotype to influence infectious/autoimmune disease susceptibility.

Due to the role that SLC11A1 plays in the activation of a Th1 (pro-inflammatory) immune response, it would be most likely that the observed associations identified with infectious and autoimmune disease is mediated by a polymorphism(s) within the *SLC11A1* locus, and not due to a polymorphism(s) located in LD, but outside of *SLC11A1* locus (i.e. a variant in a non-immune gene). However, a significant level of LD was found to exist between the 5' end of *SLC11A1* and the neutrophil expressed

Interleukin-8 receptor, beta (*IL8RB*) (Yip *et al.*, 2003). Therefore, polymorphisms located within the *IL8RB* locus may be responsible for the association identified at the 5' end of *SLC11A1*. Further work is required to determine whether polymorphisms located within the *IL8RB* locus are responsible for the observed association of the 5' end of *SLC11A1* with infectious and autoimmune disease.

7.4.2.1 The $(GT)_n$ and 1730G/A Polymorphisms are Functional Candidates Altering the Cellular Phenotype of SLC11A1 to Influence Autoimmune/Infectious Disease Susceptibility

Within the *SLC11A1* locus, the $(GT)_n$ and the 1730G/A polymorphisms are the most probable candidates for the alteration of disease incidence observed at the 5' and 3' LD ends, respectively (Figure 7.7). These two polymorphisms are the likely candidates as they have putative functional effects being able to either influence the level of *SLC11A1* expressed or altering the ability of *SLC11A1* to transport divalent cations, respectively. These putative functional effects result in an altered phenotype which may explain the reason for the associations with infectious and autoimmune disease identified in this study (Decobert *et al.*, 2006, Gazouli *et al.*, 2008a).

Furthermore, the findings from the meta-analyses also suggest that the $(GT)_n$ and 1730G/A polymorphisms are the candidate variants at the 5' and 3' ends of *SLC11A1*, respectively, responsible for influencing disease incidence. The meta-analyses of the $(GT)_n$ and 1730G/A polymorphisms were the only analyses in which the large data set analysed by Yang et al. (unpublished) could justifiably be retained. In both of the $(GT)_n$ and 1730G/A meta-analyses the pooled OR estimates were not biased/skewed by the inclusion of the large study, which was not the case when this study was included in analyses of the other *SLC11A1* polymorphisms (Table 7.2). It would be expected that in a gene that is essential for host survival, the magnitude of the effect of mutations, which have either a detrimental or positive effect would be similar across different populations. The fact that the Yang et al. (unpublished) study did not skew the pooled OR estimates of the $(GT)_n$ and 1730G/A meta-analyses suggests that these polymorphisms (and not the other polymorphisms which were skewed by the inclusion of the analysis) are likely responsible for the observed associations at the 5' and 3' LD haplotype ends of *SLC11A1*.

The putative functional $(GT)_n$ and 1730G/A polymorphisms, responsible for observed association at the 5' and 3' LD haplotype ends, respectively, are located in different regions of the *SLC11A1* locus, and therefore, may function to alter disease susceptibility through differing mechanisms. The $(GT)_n$ promoter polymorphism would influence disease susceptibility by modulating *SLC11A1* expression. During an infection, or in the development of autoimmunity, transcription factor binding to the *SLC11A1* promoter, in association with different functional $(GT)_n$ alleles (which mediate differential expression of *SLC11A1*), would alter the level of *SLC11A1* expressed. Therefore, the differing SLC11A1 levels would exert phenotypic effects to alter the Th1 pro-inflammatory immune response elicited. Conversely, the 1730G/A polymorphism, located in the coding region, would alter the ability of SLC11A1 to transport divalent cations out of the phagosome. Therefore, the phenotypic effects of this polymorphism to alter disease susceptibility may be due to the retention of higher iron levels within the phagosome, allowing replication of a pathogen within the phagosome. Therefore, the $(GT)_n$ polymorphism, through the alteration of *SLC11A1* expression, and 1730G/A polymorphism, through the mediation of altered SLC11A1 function, may work to influence disease susceptibility through differing mechanisms. While these polymorphisms may function independently to alter the cellular phenotype, functional variants which influence disease susceptibility may be present together, with the genetic contribution of *SLC11A1* to disease being likely due to a summation of the functional effects of polymorphisms throughout the *SLC11A1* locus (Section 7.4.4). Functional tests are required to elucidate the mechanisms by which the $(GT)_n$ and 1730G/A polymorphisms may influence infectious and autoimmune disease susceptibility.

7.4.3 $(GT)_n$ Allele 2 Exerts the Selective Pressure at the 5' End to Influence Infectious and Autoimmune Disease Susceptibility

The $(GT)_n$ microsatellite repeat is the most likely candidate at the 5' LD haplotype end for influencing infectious and autoimmune disease susceptibility. Consistent with previous reports, $(GT)_n$ allele 3 and allele 2 were significantly associated with resistance and susceptibility to infectious disease, respectively (Li *et al.*, 2006, Searle and Blackwell, 1999). Overall, the most significant result identified from the current study was the association of $(GT)_n$ allele 2 with the incidence of infectious disease (OR=1.32)

and specifically the incidence of tuberculosis (OR=1.47). The strength of the association of $(GT)_n$ allele 2 with the incidence of infectious disease was greater than the protective effect afforded by $(GT)_n$ allele 3 (Table 7.4), as the relative magnitude of the OR and 95% CI for allele 2 is further from 1, than allele 3. Consistent with these findings, a stronger association of allele 2 with reduced incidence of autoimmune disease was also observed, compared to an increased incidence observed with allele 3 (Table 7.2).

Reporter studies have shown that different lengths of the $(GT)_n$ microsatellite repeat alter *SLC11A1* expression levels, with $(GT)_n$ allele 3 driving higher expression than $(GT)_n$ allele 2. Due to the important role SLC11A1 plays in initiating and perpetuating a Th1 immune response, it was hypothesised that over expression of *SLC11A1* driven by $(GT)_n$ allele 3 would result in a heightened Th1 immune response and a subsequent "chronic hyperactivation of macrophages" (i.e. classical activation) (Searle and Blackwell, 1999, Shaw *et al.*, 1996). This chronic hyperactivation of macrophages would confer resistance to infectious disease, but also susceptibility to autoimmune diseases (Searle and Blackwell, 1999). This hypothesis suggests that allele 3 is the disease causing variant of the $(GT)_n$ microsatellite repeat, which exerts a selective pressure within the *SLC11A1* locus to modulate of disease susceptibility.

Due to the hypothesis that allele 3 is the disease causing variant at the $(GT)_n$ microsatellite, case-control association studies have focused specifically on the association of allele 3 with disease incidence, commonly grouping the other $(GT)_n$ alleles together to report a combined allele frequency "other" (Bellamy *et al.*, 1998, Fitness *et al.*, 2004a, Fitness *et al.*, 2004b, Leung *et al.*, 2007, Soborg *et al.*, 2002, Soborg *et al.*, 2007). However, the findings of the current meta-analysis suggest that $(GT)_n$ allele 2, and not $(GT)_n$ allele 3, has the strongest association with infectious and autoimmune disease. Thus, it appears that $(GT)_n$ allele 2 is the disease causing variant at the $(GT)_n$ microsatellite influencing the incidence of disease. Furthermore, homogeneity of OR for individual studies of the meta-analysis suggest that $(GT)_n$ allele 2 is responsible for the observed association with infectious disease (Section 7.3.2.1). Such homogeneity of OR was absent within the allele 3 dataset (Table 7.4). Therefore, the meta-analysis data suggests that $(GT)_n$ allele 2, and not allele 3, is the disease causing variant at the $(GT)_n$ microsatellite, which exerts the selective pressure at the *SLC11A1* locus to influence infectious and autoimmune disease susceptibility.

7.4.3.1 $(GT)_n$ Allele 2 May Influence Disease Incidence Due to a Heightened Anti-inflammatory Immune Response Mediated Through Increased IL-10 Expression

The findings of the current meta-analysis that allele 2 is the disease variant at the $(GT)_n$ repeat, does not support the current hypothesis that a chronic hyperactivation of macrophages driving a heightened Th1 pro-inflammatory immune response (elicited by allele 3) is responsible for the observed associations with disease incidence (Searle and Blackwell, 1999, Shaw *et al.*, 1996). Therefore, how does $(GT)_n$ allele 2 function to alter infectious and autoimmune disease susceptibility?

Human and murine studies suggest that $(GT)_n$ allele 2 may alter disease susceptibility through higher expression of the anti-inflammatory cytokine IL-10. Macrophages or dendritic cells, isolated from mice which lack functional *Slc11a1*, have higher IL-10 expression after infectious challenge or induction of a model of autoimmune disease, compared to macrophages/dendritic cells containing functional *Slc11a1* (Fritsche *et al.*, 2008, Jiang *et al.*, 2009, Pie *et al.*, 1996, Rojas *et al.*, 1999, Smit *et al.*, 2003, Stober *et al.*, 2007). While the loss of functional Slc11a1 in the murine model does not correlate with the observed phenotype occurring with the $(GT)_n$ repeat in humans (i.e. a reduced level of *SLC11A1* expression rather than loss of function), a human based study has also shown that individuals who carry allele 2 have a significantly increased expression of the anti-inflammatory cytokine IL-10, compared to individuals who do not carry allele 2 (Awomoyi *et al.*, 2002).

Therefore, it is hypothesised that allele 2 is the disease causing variant at the $(GT)_n$ microsatellite repeat driving low *SLC11A1* expression and a subsequent increase in IL-10 expression. The increased IL-10 expression would produce a heightened anti-inflammatory immune response, inhibiting the production of an adequate Th1 pro-inflammatory immune response. Specifically, IL-10 has been shown to inhibit innate macrophage anti-microbial molecules involved in a pro-inflammatory immune response and has also been shown to reduce antigen processing, antigen presentation and T cell activation (Asadullah *et al.*, 2003, Couper *et al.*, 2008, de Waal Malefyt *et al.*, 1991, Gazzinelli *et al.*, 1992, Moore *et al.*, 2001). Thus, the inhibition of a Th1 pro-inflammatory immune response, in the presence of allele 2, would confer susceptibility

to infectious disease, however, due to the inhibition of Th1 effector molecules and T cell activation, would confer resistance to Th1 mediated autoimmune diseases.

While the results of the meta-analyses suggest that $(GT)_n$ allele 2 is the disease causing variant at the $(GT)_n$ repeat, putatively through increased IL-10 production and inhibition of a pro-inflammatory immune response, it is hypothesised that $(GT)_n$ allele 3 would drive an adequate level of *SLC11A1* expression, high enough to produce a Th1 pro-inflammatory immune response to allow efficient resolution of infectious disease and, due to the lack of inhibition of a pro-inflammatory immune response (as seen with allele 2), would maintain the effector molecules and cells to initiate Th1 mediated autoimmune diseases (in genetically and environmentally permissive individuals).

7.4.4 Future Association Studies Should Complete Haplotype Analysis of the *SLC11A1* Locus

The complex LD pattern at the *SLC11A1* locus, and the current finding that functional polymorphisms in both 5' and 3' LD haplotype ends of *SLC11A1* are associated with the incidence of infectious disease provides evidence that future association studies should ideally analyse cases and controls through haplotype analyses, as opposed to adopting a narrow binomial approach of analysing only a single polymorphism. For example, while the current meta-analyses suggest an association between the $(GT)_n$ repeat with the incidence of infectious and autoimmune disease susceptibility, the $(GT)_n$ repeat does not function independently to alter *SLC11A1* expression levels. For example, reporter studies have shown that both the $(GT)_n$ and -237C/T polymorphisms function synergistically to determine the level of *SLC11A1* expressed (Zaahl *et al.*, 2004) (Chapter 6). Therefore, association studies which analyse the effect of the $(GT)_n$ repeat and -237C/T polymorphisms independently are not assessing the complex interaction which is occurring to determine the level of SLC11A1 expressed. Additionally, there are other polymorphisms within *SLC11A1* which putatively exert phenotypic effects to alter SLC11A1 expression/function (e.g. 1730G/A Section 7.4.2.1). Therefore, an individual's propensity to develop disease would be determined by a summation of the effects of each of the individual polymorphisms within the *SLC11A1* locus, with association studies which complete haplotype analyses able to

identify the complex additive factors which would be missed in association studies which analyse single polymorphisms.

Therefore, future analyses of the association of *SLC11A1* with the incidence of disease should complete haplotype analyses based around a 5' LD haplotype end and a 3' LD haplotype end (and potentially over the whole *SLC11A1* locus), thus providing greater power to identify which haplotypes, and potentially which polymorphisms, are functionally linked to disease incidence. Testament to this, association studies, which assess *SLC11A1* haplotypes have identified more robust associations as compared to when these studies analysed individual polymorphisms (Bellamy *et al.*, 1998, Kim *et al.*, 2003, Merza *et al.*, 2009, Qu *et al.*, 2007, Runstadler *et al.*, 2005, Yen *et al.*, 2006).

7.4.5 Conclusion

The findings of the current meta-analysis have identified a positive association of polymorphisms within the 5' region of *SLC11A1* with autoimmune disease, while polymorphisms located in the 5' and 3' region were associated with the incidence of infectious disease. Due to the LD pattern, which exists at the *SLC11A1* locus, the findings of the current study suggest that at least one functional polymorphism exists at the 5' LD region, which is associated with autoimmune disease, while at least two functional polymorphisms, one in the 5' region and a second in the 3' region, influence the occurrence of infectious disease (Figure 7.7). The $(GT)_n$ repeat and the 1730G/A polymorphisms are the strongest functional candidates influencing disease incidence at the 5' and 3' LD ends, respectively.

Furthermore, the findings of the current analysis suggest that allele 2, and not allele 3, is the disease causing variant of the functional $(GT)_n$ promoter polymorphism exerting the selective pressure at the 5' LD region to alter infectious and autoimmune disease susceptibility. The identification of allele 2 as the disease-associated variant challenges the hypothesis of how the $(GT)_n$ promoter polymorphism modulates disease susceptibility. It is hypothesised that allele 2, which drives low *SLC11A1* expression, would influence disease susceptibility through a heightened anti-inflammatory immune response due to increased IL-10 expression and subsequent inhibition of a Th1 pro-

inflammatory immune response, mediating susceptibility to infectious disease, but resistance to Th1 mediated autoimmune disease.

In the current analysis, consistent findings were observed when assessing the association of *SLC11A1* polymorphisms with infectious disease *per se* as compared to studies assessing tuberculosis alone (Table 7.5). The findings suggest that *SLC11A1* polymorphisms may be associated with infectious diseases other than tuberculosis. However, the over representation of tuberculosis studies, among the association studies, reveals the need for the completion of analyses assessing the association of *SLC11A1* polymorphisms with the occurrence of infectious diseases other than tuberculosis. A priority should be on infectious diseases which have restricted localisation to macrophages, or infectious diseases to which *SLC11A1* has been strongly associated using animal models (for example Salmonella and Leishmania).

Additionally, while some polymorphisms have been assessed in a large number of association studies to allow the completion of a meaningful meta-analysis, insufficient association studies have been completed on several polymorphisms, which show a trend with disease incidence, however, the pooled OR does not reach significance. Had more association studies been completed significance may have been attained. This includes, for example, analyses of the -237C/T and 1029C/T (A318V) polymorphisms with the incidence of infectious and autoimmune disease, respectively (Figure 7.6). Both of these polymorphisms may exert effects on SLC11A1 expression/function and show a significant trend with disease incidence, but with a lack of sufficient numbers of studies, the determination of the existence of a significant association cannot be made (Table 7.1).

The aim of the work presented in this chapter was to determine, based on previously published case/control association studies, the association of *SLC11A1* polymorphisms with disease incidence. Based on the findings of the current meta-analyses, the *SLC11A1* locus does play a role in influencing susceptibility to infectious and autoimmune diseases. Further functional analyses are required to determine the exact polymorphisms which produce phenotypic changes that influence disease susceptibility. While the observed association of the *SLC11A1* locus identified may only be a modest contribution to autoimmune/infectious disease incidence, as compared to other

identified genetic loci, for example the large role the HLA locus plays in a number of diseases (Blackwell *et al.*, 2009, Davies *et al.*, 1994, Shilna *et al.*, 2009), the current findings of the meta-analysis are significant in helping to determine the multiple host genetic factors involved in complex diseases. Identification of these host genetic factors will help to prevent, control and treat these complex diseases.

CHAPTER 8 - GENERAL DISCUSSION

8.1 Introduction

With restricted localisation to the phagosomal membrane of monocytes/macrophages, SLC11A1 elicits a range of pleiotropic effects to initiate and perpetuate a Th1 pro-inflammatory immune response. In murine models, a strong link between Slc11a1 function and the development of autoimmune and infectious disease has been observed, thereby suggesting that *SLC11A1* is also a strong candidate gene for influencing the occurrence of infectious and autoimmune diseases in humans. However, a strong association, similar to that observed in murine models, is yet to be identified in humans. This may be attributable, in part, to the absence of a loss of function mutation in *SLC11A1*, like the G169D mutation observed in murine *Slc11a1*. Due to the essential role that SLC11A1 plays in macrophage function to drive pro-inflammatory immune responses, such loss of function mutations would be detrimental to the host and would therefore be predicted to be rare. Rather, promoter polymorphisms provide a more subtle way of altering the cellular phenotype of the level of functional SLC11A1 expressed.

Variants at the promoter $(GT)_n$ microsatellite repeat and the -237C/T polymorphisms have been shown to modulate *SLC11A1* expression. Based on these observations, it was hypothesised that increased *SLC11A1* expression, in the presence of $(GT)_n$ allele 3, would mediate a heightened activation status of classically activated macrophages affording resistance to infectious diseases, but susceptibility to autoimmune diseases. Conversely, decreased *SLC11A1* expression, in the presence of $(GT)_n$ allele 2, or the less frequent -237 T variant, would result in a low activation status of macrophages, thereby conferring susceptibility to infectious diseases, but resistance to autoimmune diseases. Prior to the completion of this study, the mechanism by which variants at the $(GT)_n$ microsatellite and -237C/T polymorphisms alter *SLC11A1* expression was unknown.

Familial and case control association studies have shown inconsistent relationships between the presence of particular *SLC11A1* polymorphisms and the incidence of infectious and autoimmune disease. The majority of these studies have included less than 200 cases and, therefore, lack sufficient power to detect authentic associations. Additionally, these studies attempt to determine if *SLC11A1* polymorphisms are

associated with disease incidence without functional knowledge of the mechanism(s) by which SLC11A1 expression/function may be modulated by these variants.

The overall aim of this project was to characterise the *SLC11A1* promoter and the mechanisms by which the $(GT)_n$ and -237C/T promoter polymorphisms regulate *SLC11A1* expression to putatively influence susceptibility to autoimmune and infectious disease. This was achieved through several diverse approaches; namely meta-analyses, the development and validation of a HRM genotyping methodology, and combined *in silico* analyses and reporter assays.

8.2 Association of $(GT)_n$ Alleles 2 and 3 with the Incidence of Autoimmune/Inflammatory Diseases

Initial meta-analyses of case/control association studies (conducted between 1991 and 2006; 15 datasets) were performed to determine the association of *SLC11A1* promoter $(GT)_n$ alleles 2 and 3 with the incidence of autoimmune/inflammatory disease (Chapter 3). The meta-analyses found no association between the presence of $(GT)_n$ allele 3 and the incidence of autoimmune disease, with a random effects pooled OR of 0.88 (CI = 0.66), however, a fixed effects pooled OR of 0.80 (95% CI = 0.22) suggested a weak predominance of disease in the absence of $(GT)_n$ allele 2. The finding that allele 2, but not allele 3, is associated with autoimmune disease is consistent with subsequent meta-analyses suggesting allele 2 is the disease causing variant of the $(GT)_n$ microsatellite repeat.

The observed inconsistent findings of the individual association studies, assessing the presence of a particular *SLC11A1* $(GT)_n$ allele with the incidence of autoimmune/inflammatory disease, were determined to be attributable, in part, to the limited statistical power (due to small sample sizes), selection bias, and/or population diversity of the association studies. The meta-analyses highlighted the requirement for the completion of large unbiased studies to determine the relationship between *SLC11A1* polymorphisms and the occurrence of autoimmune/inflammatory and infectious disease.

8.3 Genotyping of *SLC11A1* Microsatellite Polymorphisms Using HRM

The completion of large-scale unbiased association studies have, prior to this study, been impractical because the conventional *SLC11A1* $(GT)_n$ genotyping methodologies are time consuming, costly and cannot detect all $(GT)_n$ variants. A novel HRM methodology for the genotyping of the *SLC11A1* $(GT)_n$ and $(CAAA)_n$ microsatellite repeats was designed, optimised, and validated (Chapter 4). This HRM methodology is the first report of a technique enabling high-throughput genotyping of the $(GT)_n$ microsatellite repeat with the sensitivity to differentiate all genotypes and the ability to detect novel sequence variants. Furthermore, assay validation, using gDNA isolated from blood or buccal cells, yielded a 100% success rate for genotyping the $(GT)_n$ and $(CAAA)_n$ microsatellites. The HRM methodologies will facilitate the completion of association studies analysing larger sample sizes, which are required to identify significant associations between $(GT)_n$ promoter and $(CAAA)_n$ variants and disease occurrence.

8.4 Localisation and Functional Evaluation of the *SLC11A1* Promoter

To characterise the *SLC11A1* promoter, and determine how the promoter variants may mediate differential *SLC11A1* expression, an integrated approach was undertaken, using *in silico* bioinformatic analyses and *in vivo* reporter assays. Firstly, bioinformatic analyses of the *SLC11A1* promoter were completed to identify putative regulatory regions involved in *SLC11A1* transcription (Chapter 5, Part 1). The putative regulatory regions were then used to define *SLC11A1* promoter regions for the preparation of promoter constructs containing different *SLC11A1* promoter lengths (Chapter 5, Part 2). Constructs containing different *SLC11A1* promoter lengths enabled the identification of promoter regions important for *SLC11A1* transcription initiation and transcriptional enhancement (Figure 5.16). The *SLC11A1* promoter lengths were also cloned in both the forward and reverse orientation to determine whether the *SLC11A1* promoter could mediate bidirectional transcription. Additionally, multiple constructs containing the same *SLC11A1* promoter length, which differed only by the variant at the $(GT)_n$ or -237C/T polymorphism, were prepared to determine how promoter variants modulate differential *SLC11A1* promoter activity. In total 42 *SLC11A1* promoter constructs were

prepared (Table 5.6). Promoter constructs were functionally assessed for promoter activity in a monocyte-like (THP-1) and a non-monocytic (293T) cell line, to identify the location of promoter regions containing elements for the recruitment of monocytic and non-monocytic factors involved in *SLC11A1* transcription, respectively (Chapter 6, Part 3).

8.4.1 Characterisation of the *SLC11A1* Promoter

8.4.1.1 A 148bp Region of the SLC11A1 Promoter Defines the Minimal Promoter Region

A 148bp minimal *SLC11A1* promoter region (-99 to +49) was identified, which contained the core elements involved in the formation of the basal transcriptional complex, and corroborated the findings of the bioinformatic analyses. The identified 148bp minimal promoter region is the smallest identified to date, which is able to mediate *SLC11A1* transcription. Within the minimal promoter region, a 40bp region that approached near 100% homology between eight *SLC11A1* homologs (Figure 5.8), was identified as the likely site for the formation of the basal transcriptional complex. However, TFBS searches of this highly conserved 40bp region, and the other regions of the *SLC11A1* promoter, failed to identify any canonical core promoter elements.

The results from the current analysis suggest that *SLC11A1* transcription is initiated through a mechanism which differs from that observed for canonical promoters containing TATA, Inr or DPE elements (Figure 6.21). This is consistent with the observation that transcription from these non-canonical promoters is generally from multiple transcription start sites, as observed with *SLC11A1*. However, TFBS searches did identify multiple sites for the recruitment of the transcription factors, Sp1 and C/EBP, within the minimal promoter region, suggesting that recruitment of these factors may be responsible for the initiation of *SLC11A1* transcription. This hypothesis is consistent with observations that Sp1 is essential in Slc11a1 expression in mice (Bowen *et al.*, 2003, Yeung *et al.*, 2004). Both Sp1 and C/EBP can recruit chromatin modifiers to activate transcription, and furthermore, can directly interact with TBP and TAFs to initiate the formation of the basal transcriptional complex.

8.4.1.2 Transcription Factors IRF-8 and PU.1 are Candidates for the Transcriptional Enhancement of the -532 to -362 Promoter Region of SLC11A1

It was determined that increasing promoter length was correlated with increasing promoter activity, suggesting that multiple elements for the recruitment of transcription factors are located throughout the *SLC11A1* promoter, and function synergistically to enhance transcription. Furthermore, it was found that a 170bp region (-532 to -362), located upstream of the $(GT)_n$ repeat, displayed the greatest enhancement of promoter activity in monocytes. Within this region, a novel IECS element, for the combined recruitment of the transcription factors, IRF-8 and PU.1, was identified as the candidate responsible for the increased promoter activity observed. IECS elements are localised in genes involved in the differentiation of macrophages, especially those encoding lysosomal/endosomal proteins (Tamura *et al.*, 2005). Therefore, the identified IECS element is the likely candidate for the observed increase in *SLC11A1* promoter activity by this 170bp region.

8.4.1.3 The SLC11A1 Promoter Mediates Bidirectional Transcription

Analysis of the *SLC11A1* constructs containing the different promoter regions cloned in the forward and reverse orientation determined that the *SLC11A1* promoter may function to direct transcription in a bidirectional manner. While the shorter promoter regions displayed orientation specific promoter activity in the forward direction, the larger *SLC11A1* promoter regions showed orientation independent promoter activity. Such bidirectional transcription may mediate the expression of a putative regulatory transcript or may produce a cryptic unstable transcript, which is rapidly degraded (Neil *et al.*, 2009, Wei *et al.*, 2011, Xu *et al.*, 2009).

8.4.2 The Influence of Variants at the $(GT)_n$ and -237C/T Promoter Polymorphisms on *SLC11A1* Promoter Activity

8.4.2.1 The -362 to -197 Region Mediates Differential SLC11A1 Expression in the Presence of Different $(GT)_n$ Alleles in Monocytes

Variants of the $(GT)_n$ and -237C/T polymorphisms have been shown to alter *SLC11A1* expression, however, the mechanism by which these variants alter expression is unknown. The $(GT)_n$ repeat has been shown to form Z-DNA *in vivo* (Bayele *et al.*,

2007, Blackwell *et al.*, 1995, Xu *et al.*, 2011) and formation of Z-DNA has been shown to enhance transcription by reducing the level of negative supercoiling, allowing transcription factor binding and pol II transcription (Bates and Maxwell, 2005, Kashi and Soller, 1999, Rich and Zhang, 2003). Therefore, it was previously thought that differences in the basal level of *SLC11A1* expression in the presence of different $(GT)_n$ alleles were mediated through the differing abilities of the $(GT)_n$ repeats to form Z-DNA. However, the current study has shown that the ability of the $(GT)_n$ repeats to modulate *SLC11A1* expression is not attributable to the differing propensities for the specific alleles to form Z-DNA.

The results from the current study indicate that $(GT)_n$ allele 2 should provide a greater transcriptional enhancement, as compared to allele 3. This observation is based on the greater propensity of $(GT)_n$ allele 2 to form Z-DNA, and the higher promoter activity of promoter constructs containing $(GT)_n$ allele 2, compared to allele 3, when tested in the non-monocytic 293T cell line (Sections 5.3.1.5.1 and 6.3.1.2.3). However, when tested in the monocyte-like THP-1 cell line, the promoter constructs containing $(GT)_n$ allele 3 drove a higher *SLC11A1* promoter activity, compared to allele 2 (Section 6.3.2.4.3). Together, these results indicate that *SLC11A1* expression is modulated by a monocyte-specific factor, binding to a 165bp region of the *SLC11A1* promoter (-362 to -197), which is differentially regulated by the $(GT)_n$ alleles to mediate higher promoter activity in the presence of allele 3. Furthermore, it is hypothesised that removal of this monocyte-specific factor would result in allele 2 driving higher *SLC11A1* promoter activity compared to allele 3, in monocytes. Candidate transcription factors responsible for the modulation of *SLC11A1* expression in the presence of different $(GT)_n$ alleles include ATF-3, Sp1, KLF, GM-CSF, PEA-3 and ZBP-1.

8.4.2.2 The -237C/T Polymorphism Alters SLC11A1 Promoter Activity Independently of the $(GT)_n$ Microsatellite Repeat

The current study identified that the -237C/T polymorphism functions to modulate *SLC11A1* expression independently of the $(GT)_n$ microsatellite repeat. This suggests that rather than altering the endogenous enhancer ability of the $(GT)_n$ microsatellite, the -237C/T polymorphism alters an element for the recruitment of a transcription factor. While no TFBS were identified at the site of this polymorphism in the presence of the more common -237 C variant, the introduction of a sequence element for the

recruitment of the transcription factor, Oct-1, was observed in the presence of the -237 T variant (Section 5.3.1.4.3). Recruitment of Oct-1, in the presence of the T variant, may out-compete, or inhibit, the binding of another transcription factor, which is required for the high *SLC11A1* promoter activity in monocytes.

Overall, the promoter assays enabled the characterisation of the *SLC11A1* promoter and the determination of the mechanism(s) by which the promoter variants modulate expression of *SLC11A1*. The work completed from the *in silico* bioinformatic analyses and the functional reporter assays provides a basis for the determination of the mechanism by which *SLC11A1* promoter variants alter the cellular phenotype to influence the incidence of infectious, autoimmune and other diseases.

8.5 Association of *SLC11A1* Polymorphisms with the Occurrence of Infectious and Autoimmune Disease

Since the completion of previous meta-analyses (Chapter 3) (Li *et al.*, 2006), there has been a significant increase in the number of case/control association studies assessing the incidence of *SLC11A1* polymorphisms with disease occurrence. Therefore, a second meta-analysis of the association of polymorphisms located throughout the *SLC11A1* locus with the incidence of both infectious and autoimmune disease was completed (studies conducted between 1996 to the present; 83 publications containing 386 datasets) (Chapter 7). To date, this meta-analysis represents the largest and most comprehensive completed assessing the association of *SLC11A1* polymorphisms with disease occurrence. This analysis was undertaken as there was at least a doubling in the number of association studies that had been completed since the previously published meta-analyses. Additionally, 15 polymorphisms (10 for the association with autoimmune disease and 5 for infectious disease) which had not been previously assessed, now had a significant number of association studies completed to warrant a meta-analysis.

The meta-analyses identified an association between the presence of $(GT)_n$ alleles 2 and 3 with reduced and increased incidence of autoimmune disease, respectively, however, this did not reach statistical significance. A significant association was identified between the presence of alleles 2 and 3 and the occurrence of T1D and sarcoidosis. Furthermore, it was determined for the first time, that the less common T variant at the -

237C/T polymorphism was associated with a reduced incidence of autoimmune disease, and the less frequent variants of the 274C/T and 469+14G/C polymorphisms were significantly associated with the incidence of autoimmune disease (Table 7.2).

The current study identified an association between $(GT)_n$ allele 2 and the incidence of infectious disease *per se* and specifically tuberculosis, with random effects pooled OR estimates of 1.32 (CI = 1.20-1.46) and 1.47 (CI = 1.30-1.66), respectively. A significant association of $(GT)_n$ allele 3 in protection against infectious disease *per se* and tuberculosis alone was also identified, however, this association was not as strong as that observed for allele 2. A significant association between the less frequently occurring variants at the 469+14G/C, 1730G/A and 1729+55del4 polymorphisms and the incidence of infectious disease *per se*, and tuberculosis alone, was also identified (Table 7.4).

8.5.1 Variants within the 5' and 3' LD Haplotype Regions of *SLC11A1* Influence Autoimmune and Infectious Disease Susceptibility

The current meta-analysis identified a positive association between polymorphisms within the 5' region of *SLC11A1*, but not the 3' region, and the incidence of autoimmune disease, while polymorphisms located in the 5' and 3' region were associated with the incidence of infectious disease. Due to the complex LD pattern which exists at the *SLC11A1* locus (Dunstan *et al.*, 2001, Kim *et al.*, 2008, Yip *et al.*, 2003), the findings suggested that at least one functional polymorphism exists within the 5' LD region of *SLC11A1*, which alters the cellular phenotype to influence autoimmune disease susceptibility, while at least two functional polymorphisms, one in the 5' region and a second in the 3' region, influence the occurrence of infectious disease (Figure 7.7). Of the polymorphisms located in the different LD regions, the $(GT)_n$ repeat and the 1730G/A polymorphisms are the strongest functional candidates at the 5' and 3' LD ends, respectively, influencing disease incidence. Due to the complex LD pattern at the *SLC11A1* locus, and the finding that polymorphisms located in both the 5' and 3' regions of *SLC11A1* are associated with disease occurrence, future association studies should ideally conduct haplotype analyses.

8.5.2 $(GT)_n$ Allele 2 Influences Disease Incidence Through a Heightened Anti-Inflammatory Immune Response Mediated by Increased IL-10 Expression

The strongest association found from the meta-analysis was that of $(GT)_n$ allele 2 with the incidence of infectious disease and tuberculosis alone. Surprisingly, the observed association of $(GT)_n$ allele 2 with the increased incidence of infectious disease and tuberculosis was stronger than the protective effect conferred in the presence of $(GT)_n$ allele 3. Therefore, it is now hypothesised that allele 2, and not allele 3, is the disease causing variant of the functional $(GT)_n$ promoter polymorphism. The identification of allele 2 as the disease-associated variant challenges the hypothesis that a heightened activation status of classically activated macrophages, in the presence of $(GT)_n$ allele 3, is responsible for the observed association with infectious and autoimmune disease occurrence (Searle and Blackwell, 1999, Shaw *et al.*, 1996).

How might $(GT)_n$ allele 2 function to modulate disease susceptibility? Allele 2, which drives low *SLC11A1* expression, may influence disease susceptibility through a heightened anti-inflammatory immune response due to increased IL-10 expression and subsequent inhibition of a Th1 pro-inflammatory immune response, thereby mediating susceptibility to infectious disease, but resistance to Th1 mediated autoimmune disease.

8.6 Conclusions

Infectious and autoimmune diseases are complex multifactorial diseases, where multiple genetic (both host and pathogen) and environmental factors play an aetiological role. Elucidation of host genetic factors involved in these complex diseases will help to develop new preventative and therapeutics strategies, ultimately lowering the burden of these diseases. Prior to the completion of this study, a strong link between *SLC11A1* and disease occurrence had not been observed in humans, due to the inconsistent findings of association studies. The findings presented in this thesis suggest that SLC11A1 does play a role in influencing susceptibility to both infectious and autoimmune diseases. While the observed association identified may only be a modest contribution to disease incidence, as compared to other genetic loci (i.e. HLA locus), the current findings are significant in elucidating the multiple host genetic factors involved in these complex diseases.

The findings of the current study suggest that the presence of at least one polymorphism in the 5' LD region of *SLC11A1* is responsible for altering the host phenotype to influence the occurrence of both infectious and autoimmune disease. Of the polymorphisms located in the 5' LD region, the promoter $(GT)_n$ microsatellite repeat and the -237C/T polymorphism, identified in this and previous studies to alter *SLC11A1* expression levels, are the most likely candidates for the observed association (Decobert *et al.*, 2006, Gazouli *et al.*, 2008a, Searle and Blackwell, 1999, Zaahl *et al.*, 2004). Furthermore, based on the findings of the bioinformatic analyses, functional reporter assays and meta-analyses, it was observed that $(GT)_n$ allele 2 is likely to be the disease causing variant of the $(GT)_n$ repeat, driving low *SLC11A1* expression (compared to allele 3) to putatively alter disease susceptibility due to a heightened anti-inflammatory immune response, attributable to increased IL-10 expression. Through the use of murine models, it has been observed that modest reductions in *Slc11a1* expression can result in significant phenotypic consequences (Kissler *et al.*, 2006, Soe-Lin *et al.*, 2009, Soe-Lin *et al.*, 2008). This suggests that a similar reduction in *SLC11A1* promoter activity, as identified with $(GT)_n$ allele 2, compared to allele 3, will also result in an altered cellular phenotype to influence disease susceptibility.

While significant associations were observed in the meta-analyses between the $(GT)_n$ alleles and the incidence of specific diseases (i.e. tuberculosis and Type 1 diabetes), there is a pressing need for the completion of large unbiased studies assessing the association of the $(GT)_n$ alleles with other specific diseases (e.g. leprosy and salmonella). The completion of such studies will be aided through the use of the sensitive and high-throughput HRM genotyping methodology designed and optimised in the current study. The completion of these large studies will ensure that studies have the power to detect true associations.

While this study has identified important regions involved in *SLC11A1* expression, what is clear is that the mechanisms controlling *SLC11A1* expression are complex and this study is the first phase in the understanding of these mechanisms. The level of *SLC11A1* expression changes at different stages of monocyte to macrophage differentiation. Furthermore, SLC11A1 plays a role in both the development of a Th1 pro-inflammatory immune reponse and erythrophagocytosis, and the cellular levels of SLC11A1 are altered by a range of exogenous factors (e.g. LPS, IFN-γ, EPO and iron). Putatively, the

mechanisms controlling expression of *SLC11A1* at different stages of cellular differentiation and function differ, adding further complexity to the regulation of *SLC11A1* expression. The current study has characterised the *SLC11A1* promoter specifically at the monocytic stage of cellular development. Due to the complexity of *SLC11A1* expression and the ability of SLC11A1 to influence disease susceptibility, further examination of the *SLC11A1* promoter is required to determine the mechanisms by which SLC11A1 alters disease occurrence.

Through the use of multiple techniques, the current study has characterised the *SLC11A1* promoter and the mechanisms by which variants at the $(GT)_n$ and -237C/T promoter polymorphisms regulate *SLC11A1* expression. The work completed in this thesis provides a basis for the determination of the mechanism by which *SLC11A1* promoter variants alter the cellular phenotype through modulation of *SLC11A1* expression to influence the incidence of infectious, autoimmune and other diseases. The work completed in this study is significant in helping to determine the multiple host genetic factors involved in infectious and autoimmune diseases, of which, the involvement of *SLC11A1* has become more evident.

APPENDIX

Appendix 1

Appendix 1 ClustalW alignment of the promoter regions of 8 *SLC11A1* homologs showing highly conserved regions.

Appendix 2

Allele frequency determination from carrier frequency.

Carrier frequency describes the number of individuals who carry that allele. The allele frequency can be determined from carrier frequency if the carrier frequency and the total study numbers are known. If the carrier frequency of the wild type allele is A% and the mutant is B%, then 100-B% describes the percent frequency of individuals who are homozygous for A/A. Likewise, 100-A% describes the percent frequency of individuals who are homozygous for B/B. Based on this, the overlap between A% and B% is then equal to the percent frequency of individuals who are heterozygous A/B. Taking into account the total number of individuals included in the study (n) then:

$$\frac{(100-B\%)}{100} \times n = \text{number of individuals who are homozygous A}$$

$$\frac{(100-A\%)}{100} \times n = \text{number of individuals who are homozygous B}$$

$$\frac{100-(100-B\%)+(100-A\%)}{100} \times n = \text{number of individuals who are heterozygous A/B}$$

Appendix 3

Publications identified for inclusion in the meta-analysis of *SLC11A1* polymorphisms with the incidence of autoimmune disease

Study*	Disease	Population
John *et al* ., 1997	Rheumatoid arthritis	English
Stokkers *et al* ., 1999	Inflammatory bowel disease	Dutch
Graham *et al* ., 2000	Primary biliary cirrhosis	English
Maliarik *et al* ., 2000	Sarcoidosis	African Americans
Sanjeevi *et al* ., 2000	Juvenile rheumatoid arthritis	Latvian/Russian
Singal *et al* ., 2000	Rheumatoid arthritis	Canadian
Yang *et al* ., 2000a	Rheumatoid arthritis	Korean
Kojima *et al* ., 2001	Inflammatory bowel disease	Japanese
Kotze *et al* ., 2001	Multiple sclerosis	South African
Bassuny *et al* ., 2002	Type 1 diabetes	Japanese
Rodriguez *et al* ., 2002	Rheumatoid arthritis	Spanish
Akahoshi *et al* ., 2004	Sarcoidosis	Japanese
Comabella *et al* ., 2004	Multiple sclerosis	Spanish
Takahashi *et al* ., 2004	Type 1 diabetes	Japanese
Crawford *et al* ., 2005	Inflammatory bowel disease	Caucasian
Dubaniewicz *et al* ., 2005	Sarcoidosis	Polish
Maier *et al* ., 2005	Type 1 diabetes	Mixed
Nishino *et al* ., 2005	Type 1 diabetes	Japanese
Runstadler *et al* ., 2005	Juvenile rheumatoid arthritis	Finnish
Kim *et al* ., 2006	Behcet's disease	Korean
Sechi *et al* ., 2006	Crohn's disease	Sardinians
Yen *et al* ., 2006	Rheumatoid arthritis	Taiwanese
Zaahl *et al* ., 2006	Inflammatory bowel disease	South African (mixed)
Chermesh *et al* ., 2007	Crohn's disease	Ashkenazi Jews
Gazouli *et al* ., 2007	Sarcoidosis	Greek
Ates *et al* ., 2008	Systemic sclerosis	Turkish
Gazouli *et al* ., 2008a	Crohn's disease	Greek
Gazouli *et al* ., 2008b	Multiple sclerosis	Sardinians
Kotlowski *et al* ., 2008	Ulcerative colitis	Canadian
Ates *et al* ., 2009a	Behcet's disease	Turkish
Ates *et al* ., 2009b	Rheumatoid arthritis	Dutch
Paccagnini *et al* ., 2009	Type 1 diabetes	Italian
Ates *et al* ., 2010	Multiple sclerosis	Turkish
Yang *et al* ., unpublished	Type 1 diabetes	Great Britain

* Publications listed in chronological order and by first author.

Appendix 4

Publications identified for inclusion in the meta-analysis of *SLC11A1* polymorphisms with the incidence of infectious disease.

Publication	Population	Disease
Liu *et al* ., 1995	Hong Kong/Canadian	Tuberculosis
Blackwell *et al* ., 1997	Brazilian	Tuberculosis
Bellamy *et al* ., 1998	Gambian	Tuberculosis
Huang *et al* ., 1998	American	Mycobacterium avium
Roy *et al* ., 1999	Indian	Leprosy
Gao *et al* ., 2000	Japanese	Tuberculosis
Ryu *et al* ., 200	Korean	Tuberculosis
Calzada *et al* ., 2001	Peruvian	Chagas' disease (T. Cruzi)
Dunstan *et al* ., 2001	Vietnamese	Typhoid Fever
Meisner *et al* ., 2001	Malian	Leprosy
Awomoyi *et al* ., 2002	Gambian	Tuberculosis
Delgado *et al* ., 2002	Cambodian	Tuberculosis
Ma *et al* ., 2002	American	Tuberculosis
Liaw *et al* ., 2002	Chinese Han & Aboriginal	Tuberculosis
Puzyrev *et al* ., 2002	Slavonic	Tuberculosis
Selvaraj *et al* ., 2002	Indian	Tuberculosis
Soborg *et al* ., 2002	Danish	Tuberculosis
Abe *et al* ., 2003	Japanese	Tuberculosis
Duan *et al* ., 2003	Chinese Han	Tuberculosis
Kim *et al* ., 2003	Korean	Tuberculosis
Liu *et al* ., 2003	Chinese Han	Tuberculosis
Ouchi *et al* ., 2003	Japanese	Kawasaki
Akahoshi *et al* ., 2004	Japanese	Tuberculosis
Ferreria *et al* ., 2004	Brazil	Leprosy/Mitsuda reacion
Fitness *et al* ., 2004a	Malawian	Leprosy
Fitness *et al* ., 2004b	Malawian	Tuberculosis
Hoal *et al* ., 2004	South African coloured	Tuberculosis
Liu *et al* ., 2004	Chinese Han	Tuberculosis
Dubaniewicz *et al* ., 2005	Polish	Tuberculosis
Koh *et al* ., 2005	South Korean	Non-tuberculosis mycobacteria
Zhang *et al* ., 2005	Chinese	Tuberculosis
An *et al* ., 2006	Chinese Han	Tuberculosis
Bravo *et al* ., 2006	Spanish	Brucellosis
Druszcynska *et al* ., 2006	Polish	Tuberculosis
Freidin *et al* ., 2006	Tuvinians	Tuberculosis
Hsu *et al* ., 2006	Taiwanese Aboriginals/Han	Tuberculosis
Stienstra *et al* ., 2006	Ghanaian	Mycobacteria ulcerans
Taype *et al* , 2006	Peruvian	Tuberculosis
Leung *et al* ., 2007	Chinese	Tuberculosis
Nino-Moreno *et al* ., 2007	Mexican	Tuberculosis
Sahiratmadja *et al* ., 2007	Indonesian	Tuberculosis
Soborg *et al* ., 2007	Tanzanian	Tuberculosis
Tanaka *et al* ., 2007	Japanese	Mycobacterium avium
Qu *et al* ., 2007	Chinese	Tuberculosis
Vejbaesya *et al* ., 2007a	Thai	Tuberculosis
Vejbaesya *et al* ., 2007b	Thai	Leprosy
Asai *et al* ., 2008	Japanese	Tuberculosis/Mycobacterium avium
Doorduyn et al., 2008	Dutch	Salmonella/Campylobacter
Farnia *et al* ., 2008	Iranian	Tuberculosis
Ates *et al* ., 2009b	Dutch	Tuberculosis
Chen *et al* ., 2009	Tibetian	Tuberculosis
Jin *et al* ., 2009	Chinese Han	Pediatric TB
Merza *et al* ., 2009	Iranian	Tuberculosis
Castellucci *et al* ., 2010	Brazilian	Leishmania
de Wit *et al* ., 2010	South African coloured	Tuberculosis
Hatta *et al* ., 2010	Indonesian	Tuberculosis
Haverkamp *et al* ., 2010	Dutch	Non-tuberculosis mycobacteria
Motsinger-Reif *et al* ., 2010	American	Tuberculosis
Samaranayake *et al* ., 2010	Sri Lankan	Cutaneous Leishmania

* Publications listed in chronological order and by first author.

Appendix 5

Appendix 5a *SLC11A1* allele 3 frequencies (case versus controls) of all the individual association studies included in the meta-analysis.

	Population	Study Numbers				Allele Frequencies				Allele Frequencies				OR (95% CI)
		n (# people)		2n (# alleles)		Allele 3 +		Allele 3 -		Allele 3 +		Allele 3 -		
		Case	Control	Case	Control	Case	Control	Case	Control	Case	Control	Case	Control	
Inflammatory bowel disease														
Kojima *et al* ., 2001	Japanese	215	324	430	648	317	520	113	128	74	80	26	20	0.69 (0.52-0.92)
Crawford *et al* ., 2005	Caucasian	277	90	554	180	423	136	131	44	76	76	24	24	1.04 (0.71-1.55)
Zaahl *et al* ., 2006	European/African	77	110	154	220	118	176	36	44	77	80	23	20	0.82 (0.50-1.35)
Zaahl *et al* ., 2006	European	16	57	32	114	27	89	5	25	84	78	16	22	1.52 (0.53-4.34)
Zaahl *et al* ., 2006	African	9	25	18	50	16	42	2	8	89	84	11	16	1.52 (0.29-7.96)
Sechi *et al* ., 2006	Sardians	37	34	74	68	53	49	21	19	72	72	28	28	0.98 (0.47-2.04)
Chermesh *et al* ., 2007	Israeli	174	131	348	262	244	173	104	89	70	66	30	34	1.21 (0.86-1.70)
Gazouli *et al* ., 2008a	Greek	274	200	548	400	324	196	224	204	59	49	41	51	1.51 (1.16-1.95)
Kotlowski *et al* ., 2008	Canadian	Requested data not forthcoming.												
Multiple sclerosis														
Kotze *et al* ., 2001	African (Caucasian)	104	329	208	658	160	434	48	224	77	66	23	34	1.72 (1.20-2.47)
Comabella *et al* ., 2004	Spanish	195	125	390	250	260	178	130	72	67	71	33	29	0.81 (0.57-1.14)
Gazouli *et al* ., 2008b	Sardians	60	66	120	132	72	60	48	72	60	45	40	55	1.80 (1.09-2.97)
Ates *et al* ., 2010	Turkish	100	104	200	208	139	148	61	60	69.5	71	30.5	29	0.92 (0.60-1.41)
Primary biliary cirrhosis														
Graham *et al* ., 2000	British	53	78	106	156	70	110	36	46	66	71	34	29	0.81 (0.48-1.38)
Rheumatoid arthritis														
John *et al* ., 1997	American	85	96	170	192	129	136	41	56	76	71	24	29	1.30 (0.81-2.07)
Singal *et al* ., 2000	Canadian	92	88	184	176	132	131	52	45	72	74	28	26	0.87 (0.55-1.39)
Yang *et al* ., 2000a	Korean	74	50	148	100	115	80	33	20	78	80	22	20	0.87 (0.47-1.63)
Rodriguez *et al* ., 2002	Spanish	141	194	282	388	189	277	93	111	67	71	33	29	0.81 (0.58-1.13)
Ates *et al* ., 2009b	Dutch	98	133	196	266	151	217	45	49	77	82	23	18	0.76 (0.48-1.19)
Juvenile rhumatoid arthritis														
Sanjeevi *et al* ., 2000	Latvian/Russian	119	111	238	222	201	155	37	67	84	70	16	30	2.35 (1.49-3.69)
Runstadler *et al* ., 2005	Finnish	Requested data not forthcoming.												
Sarcoidosis														
Maliarik *et al* ., 2000	African American	157	112	314	224	253	157	61	67	81	70	19	30	1.77 (1.19-2.64)
Dubaniewicz *et al* ., 2005	Polish	86	91	172	182	144	136	28	46	84	75	16	25	1.74 (1.03-2.94)
Gazouli *et al* ., 2007	Greek	100	200	200	400	114	186	86	214	57	46.5	43	53.5	1.53 (1.08-2.15)
Type 1 diabetes														
Bassuny *et al* ., 2002	Japanese	Requested data not forthcoming.												
Takahashi *et al* ., 2004	Japanese	95	224	190	448	150	359	40	89	79	80	21	20	0.93 (0.61-1.41)
Nishino *et al* ., 2005	Japanese	114	130	228	260	187	205	41	55	82	79	18	21	1.22 (0.78-1.92)
Paccagnini *et al* ., 2009	Italian	46	38	92	76	68	50	24	26	74	66	26	34	1.47 (0.76-2.86)
Yang *et al* ., unpublished	Great Britain	7697	7371	15394	14742	11395	10732	3999	4010	74	73	26	27	1.06 (1.01-1.12)
Systemic Sclerosis														
Ates *et al* ., 2008	Turkish	52	136	104	272	75	231	29	41	72	85	28	15	0.46 (0.27-0.79)
Behcet's disease														
Kim *et al* ., 2006	Korean	99	98	198	196	141	158	57	38	71	81	29	19	0.59 (0.37-0.95)
Ates *et al* ., 2009a	Turkish	102	102	204	204	161	168	43	36	79	82	21	18	0.80 (0.49-1.31)

"+" and "-" indicate the presence of allele 3 or the absence of allele 3, respectively.

Appendix 5b *SLC11A1* allele 2 frequencies (case versus controls) of all the individual association studies included in the meta-analysis.

	Population	Study Numbers				Allele Frequencies				Allele Frequencies				OR (95% CI)
		n (# people)		2n (# alleles)		Allele 2 +		Allele 2 -		Allele 2 +		Allele 2 -		
		Case	Control	Case	Control	Case	Control	Case	Control	Case	Control	Case	Control	
Inflammatory bowel disease														
Kojima *et al* ., 2001	Japanese	215	324	430	648	65	96	365	552	15	15	85	85	1.02 (0.73-1.44)
Crawford *et al* ., 2005	Caucasian	277	90	554	180	131	42	423	138	24	23	76	77	1.02 (0.68-1.51)
Zaahl *et al* ., 2006	European/African	77	110	154	220	34	42	120	178	22	19	78	81	1.20 (0.72-2.00)
Zaahl *et al* ., 2006	European	16	57	32	114	5	23	27	91	16	20	84	80	0.73 (0.25-2.11)
Zaahl *et al* ., 2006	African	9	25	18	50	2	8	16	42	11	16	89	84	0.66 (0.13-3.43)
Sechi *et al* ., 2006	Sardians	37	34	74	68	13	9	61	59	18	13	82	87	1.40 (0.56-3.51)
Chermesh *et al* ., 2007	Israeli	174	131	348	262	99	84	249	178	28	32	72	68	0.84 (0.59-1.19)
Gazouli *et al* ., 2008a	Greek	274	200	548	400	150	132	398	268	27	33	73	67	0.77 (0.58-1.01)
Kotlowski *et al* ., 2008	Canadian	Requested data not forthcoming.												
Multiple sclerosis														
Kotze *et al* ., 2001	African (Caucasian)	104	329	208	658	41	223	167	435	20	34	80	66	0.48 (0.33-0.70)
Comabella *et al* ., 2004	Spanish	195	125	390	250	127	71	263	179	33	28	67	72	1.22 (0.86-1.72)
Gazouli *et al* ., 2008b	Sardians	60	66	120	132	35	46	85	86	29	35	71	65	0.77 (0.45-1.31)
Ates *et al* ., 2010	Turkish	100	104	200	208	58	56	142	152	29	27	71	73	1.11 (0.72-1.71)
Primary biliary cirrhosis														
Graham *et al* ., 2000	British	53	78	106	156	28	42	78	114	26	27	74	73	0.97 (0.56-1.70)
Rheumatoid Arthritis														
John *et al* ., 1997	American	85	96	170	192	41	56	129	136	41	56	129	136	0.77 (0.48-1.23)
Singal *et al* ., 2000	Canadian	92	88	184	176	50	45	134	131	27	25	73	74	1.09 (0.68-1.74)
Yang *et al* ., 2000a	Korean	74	50	148	100	25	18	123	82	17	18	83	82	0.93 (0.48-1.80)
Rodriguez *et al* ., 2002	Spanish	141	194	282	388	91	108	191	280	32	28	68	72	1.24 (0.88-1.73)
Ates *et al* ., 2009b	Dutch	98	133	196	266	43	49	153	217	22	18	78	82	1.24 (0.79-1.97)
Juvenile rhumatoid arthritis														
Sanjeevi *et al* ., 2000	Latvian/Russian	119	111	238	222	37	65	201	157	16	29	84	71	0.44 (0.28-0.70)
Runstadler *et al* ., 2005	Finnish	Requested data not forthcoming.												
Sarcoidosis														
Maliarik *et al* ., 2000	African American	Requested data not forthcoming.												
Dubaniewicz *et al* ., 2005	Polish	86	91	172	182	28	46	144	136	16	25	84	75	0.57 (0.34-0.97)
Gazouli *et al* ., 2007	Greek	100	200	200	400	62	142	138	258	31	35.5	69	64.5	0.82 (0.57-1.17)
Type 1 diabetes														
Bassuny *et al* ., 2002	Japanese	206	200	412	400	49	65	363	335	12	16	88	84	0.70 (0.47-1.04)
Takahashi *et al* ., 2004	Japanese	95	224	190	448	22	69	168	379	12	15	88	85	0.72 (0.43-1.20)
Nishino *et al* ., 2005	Japanese	114	130	228	260	21	36	207	224	9	14	91	86	0.63 (0.36-1.12)
Paccagnini *et al* ., 2009	Italian	59	72	118	144	67	75	77	43	47	64	53	36	1.21 (0.74-1.97)
Yang *et al* ., unpublished	Great Britain	7697	7371	15394	14742	3999	4010	11395	10732	26	27	74	73	0.94 (0.89-0.99)
Systemic Sclerosis														
Ates *et al* ., 2007b	Turkish	52	136	104	272	29	41	75	231	28	15	72	85	2.18 (1.27-3.75)
Behcet's disease														
Kim *et al* ., 2006	Korean	99	98	198	196	38	27	160	169	19	14	81	86	1.49 (0.87-2.55)
Ates *et al* ., 2008a	Turkish	102	102	204	204	43	36	161	168	21	18	79	82	1.25 (0.76-2.04)

"+" and "-" indicate the presence of allele 2 or the absence of allele 2, respectively.

Appendix 6

Appendix 6a *SLC11A1* frequencies (case versus controls) of all the individual association studies included in the meta-analyses.

	Population	Study Numbers				Allele Frequencies				Allele Frequencies				OR (95% CI)
		n (# people)		2n (# alleles)		Wildtype		Mutant		% Wildtype		% Mutant		
		Case	Control	Case	Control	Case	Control	Case	Control	Case	Control	Case	Control	
-237C/T														
Inflammatory bowel disease														
Zaahl *et al* ., 2006	SAfr/EurAfr desc	77	110	154	220	151	198	3	22	98	90	2	10	0.18 (0.05-0.61)
Zaahl *et al* ., 2006	SAfr/Eur desc	16	57	32	114	30	106	2	8	94	93	6	7	0.88 (0.18-4.38)
Zaahl *et al* ., 2006	SAfr/Afr desc	9	25	18	50	18	47	0	3	100	94	0	6	0.02 (0.0-18875)
Gazouli *et al* ., 2008a	Greek	274	200	548	400	537	386	11	14	98	96.5	2	3.5	0.56 (0.25-1.26)
Kotlowski *et al* ., 2008	Canadian	200	100	400	200	340	164	60	36	85	82	15	18	0.80 (0.51-1.26)
Sarcoidosis														
Gazouli *et al* ., 2007	Greek	100	200	200	400	196	386	4	14	98	96.5	2	3.5	0.56 (0.18-1.73)
Type 1 diabetes														
Paccagnini *et al* ., 2009	Italian	46	38	92	76	68	50	24	26	74	66	26	34	0.68 (0.35-1.32)
Yang *et al* ., unpublished	Great Britain	5649	6233	11298	12466	10651	11734	647	732	94	94	6	6	0.97 (0.87-1.09)
274C/T														
Inflammatory bowel disease														
Stokkers *et al* ., 1999	Dutch	187	255	374	510	251	362	123	148	67	71	33	29	1.20 (0.90-1.60)
Gazouli *et al* ., 2008a	Greek	274	200	548	400	460	354	88	46	84	88.5	16	11.5	1.47 (1.00-2.16)
Rheumatoid Arthritis														
Yang *et al* ., 2000a	Korean	74	53	148	106	124	85	24	21	84	80	16	20	0.94 (0.89-0.99)
Singal *et al* ., 2000	Canadian	92	88	184	176	128	126	56	50	69	72	31	28	1.10 (0.70-1.74)
Yen *et al* ., 2006	Taiwanese	113	74	226	148	202	137	24	11	89	93	11	7	1.48 (0.70-3.12)
Sarcoidosis														
Dubaniewicz *et al* ., 2005	Polish	69	84	138	168	105	132	33	36	76	79	24	21	1.15 (0.67-1.97)
Gazouli *et al* ., 2007	Greek	100	200	200	400	177	354	23	46	88.5	88.5	11.5	11.5	1.00 (0.59-1.70)
Type 1 diabetes														
Paccagnini *et al* ., 2009	Italian	59	72	118	144	43	77	75	67	36	53	64	47	2.00 (1.22-3.30)
Yang *et al* ., unpublished	Great Britain	5578	6048	11156	12096	8223	8765	2933	3331	74	72	26	28	0.94 (0.89-0.99)
469+14G/C (INT4)														
Inflammatory bowel disease														
Sechi *et al* ., 2006	Sardinian	37	34	74	68	49	54	25	14	66	79	34	21	1.97 (0.92-4.21)
Gazouli *et al* ., 2008a	Greek	274	200	548	400	450	352	98	48	82	88	18	12	1.60 (1.10-2.32)
Multiple sclerosis														
Ates *et al* ., 2010	Turkish	100	104	200	208	153	168	47	40	76.5	81	23.5	19	1.29 (0.80-2.07)
Rheumatoid Arthritis														
Yang *et al* ., 2000a	Korean	73	52	146	104	127	92	19	12	87	88	13	12	1.15 (0.53-2.48)
Singal *et al* ., 2000	Canadian	92	88	184	176	123	133	61	43	67	76	33	24	1.53 (0.97-2.43)
Yen *et al* ., 2006	Taiwanese	113	74	226	148	203	137	23	11	90	93	10	7	1.41 (0.67-2.99)
Ates *et al* ., 2009b	Dutch	98	133	196	266	153	234	43	32	78	88	22	12	2.06 (1.25-3.39)
Sarcoidosis														
Maliarik *et al* ., 2000	African American	157	112	314	224	285	197	29	27	78	88	22	12	0.74 (0.43-1.29)
Dubaniewicz *et al* ., 2005	Polish	78	88	156	176	137	141	19	35	91	88	9	12	0.56 (0.30-1.02)
Gazouli *et al* ., 2007	Greek	100	200	200	400	174	352	26	48	88	80	12	20	1.10 (0.66-1.83)
Type 1 diabetes														
Paccagnini *et al* ., 2009	Italian	59	72	118	144	43	77	75	67	36	53	64	47	0.46 (0.18-1.15)
Yang *et al* ., unpublished	Great Britain	8787	10611	17574	21222	12883	15106	4691	6116	73	71	27	29	0.90 (0.86-0.94)
Systemic Sclerosis														
Ates *et al* ., 2008	Turkish	52	136	104	272	77	239	27	33	87	88	13	12	2.54 (1.44-4.49)
Behcet's disease														
Ates *et al* ., 2009a	Turkish	102	102	204	204	157	179	47	25	77	88	23	12	2.14 (1.26-3.64)
577-18G/A														
Rheumatoid arthritis														
Yang *et al* ., 2000a	Korean	73	53	146	106	138	103	8	3	95	97	5	3	1.99 (0.52-7.69)
Singal *et al* ., 2000	Canadian	92	88	184	176	184	176	0	0	100	100	0	0	Zero observation
Yen *et al* ., 2006	Taiwanese	113	74	226	148	217	141	9	7	96	95	4	5	0.84 (0.30-2.29)
Sarcoidosis														
Gazouli *et al* ., 2007	Greek	100	200	200	400	189	376	11	24	94.5	94	5.5	6	0.91 (0.44-1.90)
Inflammatory bowel disease														
Gazouli *et al* ., 2008a	Greek	274	200	548	400	526	376	22	24	96	94	4	6	0.66 (0.36-1.19)
Type 1 diabetes														
Paccagnini *et al* ., 2009	Italian	59	76	118	152	118	144	0	8	100	95	0	5	0.00 (0-3.1×10^{7})
823C/T														
Inflammatory bowel disease														
Stokkers *et al* ., 1999	Dutch	189	238	378	476	352	450	26	26	93	95	7	5	1.28 (0.73-2.24)
Sechi *et al* ., 2006	Sardinian	37	34	74	68	58	66	16	2	78	97	22	3	9.10 (2.01-41.28)
Gazouli *et al* ., 2008a	Greek	274	200	548	400	403	278	145	122	74	69.5	26	30.5	0.82 (0.62-1.09)
Rheumatoid arthritis														
Yang *et al* ., 2000a	Korean	73	48	146	96	132	95	14	1	90	99	10	1	10.08 (1.30-77.94)
Singal *et al* ., 2000	Canadian	92	88	184	176	170	159	14	17	93	90	7	10	0.77 (0.37-1.61)
Yen *et al* ., 2006	Taiwanese	113	74	226	148	187	102	39	46	83	69	17	31	0.46 (0.28-0.75)
Sarcoidosis														
Gazouli *et al* ., 2007	Greek	100	200	200	400	143	278	57	122	71.5	69.5	28.5	30.5	0.91 (0.63-1.32)
Type 1 diabetes														
Paccagnini *et al* ., 2009	Italian	44	70	88	140	88	139	0	1	100	99	0	1	0.01 (0-1.8×10^{8})

Appendix 6b *SLC11A1* frequencies (case versus controls) of all the individual association studies included in the meta-analyses.

	Population	Study Numbers				Allele Frequencies				Allele Frequencies				OR (95% CI)
		n (# people)		2n (# alleles)		Wildtype		Mutant		% Wildtype		% Mutant		
		Case	Control	Case	Control	Case	Control	Case	Control	Case	Control	Case	Control	
1029C/T A318V														
Rheumatoid arthritis														
Yang *et al* ., 2000a	Korean	74	53	148	106	148	106	0	0	100	100	0	0	Zero observation
Singal *et al* ., 2000	Canadian	92	88	184	176	184	176	0	0	100	100	0	0	Zero observation
Yen *et al* ., 2006	Taiwanese	113	74	226	148	224	147	1	2	99	99	1	1	0.32 (0.03-3.61)
Sarcoidosis														
Maliarik *et al* ., 2000	Afr American	157	112	314	224	314	224	0	0	100	100	0	0	Zero observation
Gazouli *et al* ., 2007	Greek	100	200	200	400	197	394	3	6	98.5	98.5	1.5	1.5	1.00 (0.25-4.04)
Behcet's disease														
Kim *et al* ., 2006	Korean	99	98	198	196	198	196	0	0	100	100	0	0	Zero observation
Inflammatory bowel disease														
Gazouli *et al* ., 2008a	Greek	274	200	548	400	544	394	4	6	99	98.5	1	1.5	0.48 (0.14-1.72)
Type 1 diabetes														
Paccagnini *et al* ., 2009	Italian	40	48	80	96	80	92	0	4	100	96	0	4	0.01 (0.00-4664)
1465-85G/A														
Rheumatoid arthritis														
Yang *et al* ., 2000a	Korean	74	53	148	106	100	84	48	22	68	79	32	21	1.83 (1.02-3.28)
Singal *et al* ., 2000	Canadian	92	88	184	176	113	113	71	63	61	64	39	36	1.13 (0.73-1.73)
Runstadler *et al* ., 2005	Finnish	Requested data not forthcoming.												
Yen *et al* ., 2006	Taiwanese	113	74	226	148	153	100	73	48	68	68	32	32	0.99 (0.64-1.55)
Sarcoidosis														
Dubaniewicz *et al* ., 2005	Polish	82	93	164	186	122	127	42	59	74	68	26	32	0.74 (0.46-1.18)
Gazouli *et al* ., 2007	Greek	100	200	200	400	130	270	70	130	65	67.5	35	32.5	1.12 (0.78-1.60)
Inflammatory bowel disease														
Gazouli *et al* ., 2008a	Greek	274	200	548	400	363	270	185	130	66	67.5	34	32.5	1.06 (0.80-1.39)
Type 1 diabetes														
Paccagnini *et al* ., 2009	Italian	58	59	116	118	63	78	53	40	54	66	46	34	1.64 (0.97-2.78)
Yang *et al* ., unpublished	Great Britian	5549	5872	11098	11744	6786	7086	4312	4658	61	60	39	40	0.97 (0.92-1.02)
1730G/A (D543N)														
Inflammatory bowel disease														
Sechi *et al* ., 2006	Sardinian	37	34	74	68	57	52	17	16	77	76	23	24	0.97 (0.44-2.11)
Gazouli *et al* ., 2008a	Greek	274	200	548	400	316	302	232	98	58	75.5	42	24.5	2.26 (1.70-3.01)
Multiple sclerosis														
Comabella *et al* ., 2004	Spanish	195	125	390	250	377	245	13	5	97	98	3	2	1.69 (0.59-4.80)
Ates *et al* ., 2010	Turkish	100	104	200	208	195	203	5	5	97.5	98	2.5	2	1.04 (0.30-3.65)
Rheumatoid Arthritis														
Yang *et al* ., 2000a	Korean	74	51	148	102	126	98	22	4	85	96	15	4	4.28 (1.43-12.82)
Singal *et al* ., 2000	Canadian	92	88	184	176	184	169	0	7	100	96	0	4	0.00 (0.0-94237)
Yen *et al* ., 2006	Taiwanese	113	74	226	148	185	106	41	42	82	72	18	28	0.56 (0.34-0.91)
Ates *et al* ., 2009b	Dutch	98	133	196	266	188	261	8	5	96	98	4	2	2.22 (0.72-6.90)
Sarcoidosis														
Maliarik *et al* ., 2000	African American	157	112	314	224	296	203	18	21	94	91	6	9	0.59 (0.31-1.13)
Akahoshi *et al* ., 2004	Japanese	Requested data not forthcoming.												
Gazouli *et al* ., 2007	Greek	100	200	200	400	160	302	40	98	80	75.5	20	24.5	0.77 (0.51-1.17)
Type 1 diabetes														
Paccagnini *et al* ., 2009	Italian	59	69	118	138	115	136	3	2	97	99	3	1	1.77 (0.29-10.80)
Yang *et al* ., unpublished	Great Britain	5498	6062	10996	12124	10755	11908	241	216	98	98	2	2	1.24 (1.03-1.49)
Systemic Sclerosis														
Ates *et al* ., 2008	Turkish	52	136	104	272	103	267	1	5	99	98	1	2	0.52 (0.06-4.49)
Behcet's disease														
Kim *et al* ., 2006	Korean	99	98	198	196	176	172	22	24	89	88	11	12	0.90 (0.48-1.66)
Ates *et al* ., 2009a	Turkish	102	102	204	204	157	179	47	25	77	88	23	12	1.51 (0.25-9.12)
1729+55del4 (TGTG ins/del)														
Sarcoidosis														
Maliarik *et al* ., 2000	Afr American	157	112	314	224	257	171	57	53	82	76	18	24	0.72 (0.47-1.09)
Gazouli *et al* ., 2007	Greek	100	200	200	400	175	356	25	44	87.5	89	12.5	11	1.16 (0.68-1.95)
Rheumatoid arthritis														
Yang *et al* ., 2000a	Korean	74	51	148	102	125	98	23	4	84	96	16	4	4.51 (1.51-13.48)
Singal *et al* ., 2000	Canadian	92	88	184	176	184	169	0	7	100	96	0	4	0.00 (0.00-94237)
Runstadler *et al* ., 2005	Finnish	Requested data not forthcoming.												
Yen *et al* ., 2006	Taiwanese	113	74	226	148	154	82	72	66	68	55	32	45	0.58 (0.38-0.89)
Ates *et al* ., 2009b	Dutch	98	133	196	266	188	261	8	5	96	98	4	2	2.22 (0.72-6.90)
Multiple sclerosis														
Comabella *et al* ., 2004	Spanish	195	125	390	250	377	247	13	3	97	99	3	1	2.84 (0.80-10.07)
Ates et al., 2010	Turkish	100	104	200	208	195	203	5	5	97.5	98	2.5	2	1.04 (0.30-3.65)
Inflammatory bowel disease														
Sechi *et al* ., 2006	Sardinian	37	34	74	68	52	58	22	10	70	85	30	15	2.45 (1.06-5.66)
Kotlowski *et al* ., 2008	Canadian	200	100	400	200	382	191	18	9	95.5	95.5	4.5	4.5	1.00 (0.44-2.27)
Gazouli *et al* ., 2008a	Greek	274	200	548	400	491	356	57	44	90	89	10	11	0.94 (0.62-1.42)
Type 1 diabetes														
Paccagnini *et al* ., 2009	Italian	59	46	118	92	118	92	0	0	100	100	0	0	Zero observation
Yang *et al* ., unpublished	Great Britian	8463	9835	16926	19670	16614	19371	312	299	98	98	2	2	1.22 (1.04-1.43)
Systemic sclerosis														
Ates *et al* ., 2008	Turkish	52	136	104	272	103	267	1	5	99	98	1	2	0.52 (0.06-4.49)
Behcet's disease														
Ates *et al* ., 2009a	Great Britian	102	102	204	204	201	202	3	2	99	99	1	1	1.51 (0.25-9.12)
1729+271del4 (CAAA)n														
Multiple sclerosis														
Comabella *et al* ., 2004	Spanish	195	125	390	250	236	160	154	90	61	64	39	36	1.16 (0.84-1.61)
Sarcoidosis														
Dubaniewicz *et al* ., 2005	Polish	85	84	170	168	114	110	56	58	67	65	33	35	0.93 (0.59-1.46)
Inflammatory bowel disease														
Kotlowski *et al* ., 2008	Canadian	200	100	400	200	264	124	136	76	66	62	34	38	0.84 (0.59-1.20)

Appendix 7

Appendix 7a *SLC11A1* allele 3 frequencies (case versus controls) of all the individual association studies included in the meta-analysis.

	Population	Study Numbers				Allele Frequencies				Allele Frequencies				OR (95% CI)
		n (# people)		2n (# alleles)		Allele 3 +		Allele 3 -		Allele 3 +		Allele 3 -		
		Case	Control	Case	Control	Case	Control	Case	Control	Case	Control	Case	Control	
Mycobacterium leprae														
Roy *et al* ., 1999	Indian	227	165	454	330	357	271	97	59	79	82	21	18	0.80 (0.56-1.15)
Meisner *et al* ., 2001	Malian	Requested data not forthcoming.												
Ferreria *et al* ., 2004	Brazil	90	61	180	122	113	70	67	52	63	57	37	43	1.25 (0.78-2.00)
Fitness *et al* ., 2004b	Malawian	249	423	498	846	391	627	107	219	79	74	21	26	1.28 (0.98-1.66)
Mycobacterium avium														
Huang *et al* ., 1998	American	Requested data not forthcoming.												
Tanaka *et al* ., 2007	Japanese	111	177	222	354	176	281	46	73	79	79	21	21	0.99 (0.66-1.50)
Mycobacterium tuberculosis														
Liu *et al* ., 1995	Hong Kong/Canadian	12	18	24	36	22	30	2	6	92	83	8	17	2.20 (0.41-11.95)
Blackwell *et al* ., 1997	Brazilian	Requested data not forthcoming.												
Bellamy *et al* ., 1998	Gambian	401	410	802	820	651	705	151	115	81	86	19	14	0.70 (0.54-0.92)
Gao *et al* ., 2000	Japanese	267	202	534	404	405	345	129	59	76	85	24	15	0.54 (0.38-0.75)
Awomoyi *et al* ., 2002	Gambian	329	324	658	648	514	544	144	104	78	84	22	16	0.68 (0.52-0.90)
Ma *et al* ., 2002	American	113	108	226	216	158	174	68	42	70	81	30	19	0.56 (0.36-0.87)
Selvaraj *et al* ., 2002	Indian	Requested data not forthcoming.												
Soborg *et al* ., 2002	Danish	70	176	140	352	109	231	31	121	78	66	22	34	1.84 (1.17-2.90)
Fitness *et al* ., 2004a	Malawian	232	778	464	1556	361	1204	103	352	78	77	22	23	1.02 (0.80-1.31)
Hoal *et al* ., 2004	South African coloured	226	261	452	522	349	441	103	81	77	84	23	16	0.62 (0.45-0.86)
Dubaniewicz *et al* ., 2005	Polish	83	91	166	182	121	136	45	46	73	75	27	25	0.91 (0.56-1.47)
Hsu *et al* ., 2006	Taiwanese (Aboriginals)	101	88	202	176	183	172	19	4	91	98	9	2	0.22 (0.07-0.67)
Hsu *et al* ., 2006	Taiwainese (Han)	110	78	220	156	190	138	30	18	86	88	14	12	0.83 (0.44-1.54)
Leung *et al* ., 2007	Chinese	278	282	556	564	478	493	78	71	86	87	14	13	0.88 (0.62-1.25)
Soborg *et al* ., 2007	Tanzanian	428	427	856	834	676	697	180	137	79	84	21	16	0.74 (0.58-0.94)
Ates *et al* ., 2009b	Dutch	112	80	224	160	186	132	38	28	83	82.5	17	17.5	1.04 (0.61-1.78)
Chen *et al* ., 2009	Tibetian	140	139	280	278	184	217	96	61	66	78	34	22	0.54 (0.37-0.78)
de Wit *et al* ., 2010	South African coloured	498	315	996	630	776	523	220	107	78	83	22	17	0.72 (0.56-0.93)
Motsinger-Reif *et al* ., 2010	American	Requested data not forthcoming.												
Other														
Calzada *et al* ., 2001	Peru	79	85	158	170	97	111	61	59	61	65	39	35	0.85 (0.54-1.33)
Dunstan *et al* ., 2001	Vietnam	214	288	428	576	378	517	50	59	88	90	12	10	0.86 (0.58-1.29)
Ouchi *et al* ., 2003	Japansese	71	110	142	220	107	174	35	46	75	79	25	21	0.81 (0.49-1.33)
Bravo *et al* ., 2006	Spanish	56	89	112	178	71	117	41	61	63	66	37	34	0.90 (0.55-1.48)

"+" and "-" indicate the presence of allele 3 or the absence of allele 3, respectively.

Appendix 7b *SLC11A1* allele 2 frequencies (case versus controls) of all the individual studies association included in the meta-analysis.

	Population	Study Numbers				Allele Frequencies				Allele Frequencies				OR (95% CI)
		n (# people)		2n (# alleles)		Allele 2 +		Allele 2 -		Allele 2 +		Allele 2 -		
		Case	Control	Case	Control	Case	Control	Case	Control	Case	Control	Case	Control	
Mycobacterium leprae														
Roy *et al* ., 1999	Indian	227	165	454	330	97	59	357	271	21	18	79	82	1.25 (0.87-1.79)
Meisner *et al* ., 2001	Malian	Requested data not forthcoming.												
Ferreria *et al* ., 2004	Brazilian	90	61	180	122	59	45	121	77	33	37	67	63	0.83 (0.52-1.35)
Fitness *et al* ., 2004b	Malawian	Requested data not forthcoming.*												
Mycobacterium avium														
Huang *et al* ., 1998	American	Requested data not forthcoming.												
Tanaka *et al* ., 2007	Japanese	111	177	222	354	26	48	196	306	12	14	88	86	0.85 (0.51-1.41)
Mycobacterium tuberculosis														
Liu *et al* ., 1995	Hong Kong/Canadian	12	18	24	36	2	4	22	32	8	11	92	89	0.73 (0.12-4.32)
Blackwell *et al* ., 1997	Brazilian	Requested data not forthcoming.												
Bellamy *et al* ., 1998	Gambian	Requested data not forthcoming.*												
Gao *et al* ., 2000	Japanese	267	202	534	404	93	50	441	354	17	12	83	88	1.49 (1.03-2.16)
Awomoyi *et al* ., 2002	Gambian	329	324	658	648	121	89	537	559	18	14	82	86	1.42 (1.05-1.91)
Ma *et al* ., 2002	American	113	108	226	216	67	42	159	174	30	19	70	81	1.75 (1.12-2.72)
Selvaraj *et al* ., 2002	Indian	Requested data not forthcoming.												
Soborg *et al* ., 2002	Danish	Requested data not forthcoming.*												
Fitness *et al* ., 2004a	Malawian	Requested data not forthcoming.*												
Hoal *et al* ., 2004	South African coloured	226	261	452	522	103	81	349	441	23	16	77	84	1.61 (1.16-2.22)
Dubaniewicz *et al* ., 2005	Polish	83	91	166	182	45	46	121	136	27	25	73	75	1.10 (0.68-1.77)
Hsu *et al* , 2006	Taiwanese (Aboriginals)	101	88	202	176	15	1	187	175	7	1	93	99	14.04 (1.83-107)
Hsu *et al* , 2006	Taiwanese (Han)	110	78	220	156	26	16	194	140	12	10	88	90	1.17 (0.61-2.27)
Leung *et al* ., 2007	Chinese	Requested data not forthcoming.*												
Soborg *et al* ., 2007	Tanzanian	Requested data not forthcoming.*												
Ates *et al* ., 2009b	Dutch	112	80	224	160	38	28	186	132	17	17.5	83	82.5	0.96 (0.56-1.65)
Chen *et al* ., 2009	Tibetian	140	139	280	278	96	61	184	217	34	22	66	78	1.86 (1.27-2.70)
de Wit *et al* ., 2010	South African coloured	498	315	996	630	217	106	779	524	22	17	78	83	1.38 (1.06-1.78)
Motsinger-Reif *et al* ., 2010	American	Requested data not forthcoming.												
Other														
Calzada *et al* ., 2001	Peruvian	79	85	158	170	60	58	98	112	38	34	58	66	1.18 (0.75-1.86)
Dunstan *et al* ., 2001	Vietnamese	214	288	428	576	46	49	382	527	11	9	89	91	1.30 (0.85-1.98)
Ouchi *et al* ., 2003	Japansese	71	110	142	220	19	39	123	181	13	18	87	82	0.72 (0.40-1.30)
Bravo *et al* ., 2006	Spanish	56	89	112	178	41	59	71	119	37	33	63	67	1.16 (0.71-1.91)

"+" and "-" indicate the presence of allele 2 or the absence of allele 2, respectively. *Allele frequencies could not be determined as placed in group "other".

Appendix 8

Appendix 8a *SLC11A1* 469+14G/C frequencies (case versus controls) of all the individual association studies included in the meta-analysis.

	Population	Study Numbers				Allele Frequencies				Allele Frequencies				OR (95% CI)
		n (# people)		2n (# alleles)		Wildtype		Mutant		% Wildtype		% Mutant		
		Case	Control	Case	Control	Case	Control	Case	Control	Case	Control	Case	Control	
Mycobacterium leprae														
Roy *et al* ., 1999	Indian	220	162	440	324	379	284	61	40	86	88	14	12	1.14 (0.75-1.75)
Meisner *et al* ., 2001	Malian	Requested data not forthcoming.												
Vejbaesya *et al* ., 2007b	Thai	37	140	74	280	72	265	2	15	97	95	3	5	0.49 (0.11-2.20)
Hatta *et al* ., 2010	Indonesian	42	198	84	396	74	375	10	21	88	95	12	5	2.41 (1.09-5.33)
Mycobacterium avium														
Tanaka *et al* ., 2007	Japanese	111	177	222	354	195	306	27	48	88	86	12	14	0.88 (0.53-1.46)
Asai *et al* ., 2008	Japanese	17	51	34	102	31	93	3	9	91	91	9	9	1.00 (0.25-3.93)
Non-TB Mycobacteria														
Koh *et al* ., 2005	South Korean	41	50	82	100	64	89	18	11	78	89	22	11	2.28 (1.01-5.15)
Stienstra *et al* ., 2006	Ghanaian	169	184	338	368	319	350	19	18	94	95	6	5	1.16 (0.60-2.25)
Haverkamp *et al* ., 2010	Dutch	81	212	162	424	112	311	50	113	69	73	31	27	1.23 (0.83-1.83)
Mycobacterium tuberculosis														
Lui *et al* ., 1995	Hong Kong/Canadian	12	18	24	36	22	33	2	3	92	92	8	8	1.00 (0.15-6.48)
Bellamy *et al* ., 1998	Gambian	401	411	802	822	718	768	84	54	90	93	10	7	1.66 (1.16-2.38)
Ryu *et al* , 2000	Korean	Requested data not forthcoming.												
Puzyrev *et al* , 2002	Slavonic	58	104	116	208	94	164	22	44	81	79	19	21	0.87 (0.49-1.54)
Soborg *et al* ., 2002	Danish	104	176	208	352	154	239	54	113	74	68	26	32	0.74 (0.51-1.09)
Abe *et al* , 2003	Japanese	95	90	190	180	164	154	26	26	86	86	14	14	0.94 (0.52-1.69)
Kim *et al* ., 2003	Korean	41	45	82	90	62	86	20	4	76	96	24	4	6.94 (2.26-21.30)
Liu *et al* ., 2003	Chinese Han	110	171	220	342	199	321	21	21	90	94	10	6	1.61 (0.86-3.03)
Hoal *et al* ., 2004	South African coloured	239	291	478	582	396	505	82	77	83	87	17	13	1.36 (0.97-1.90)
Liu *et al* ., 2004	Chinese	120	240	240	480	193	377	47	103	80	79	20	21	0.89 (0.61-1.31)
Dubaniewicz *et al* ., 2005	Polish	79	88	158	176	132	141	26	35	84	80	16	20	0.79 (0.45-1.39)
Zhang *et al* ., 2005	Chinese	127	91	254	182	219	167	35	15	86	92	14	8	1.78 (0.94-3.37)
An *et al* ., 2006	Chinese Han	Requested data not forthcoming.												
Druszcynska *et al* ., 2006	Polish	126	114	252	228	196	180	56	48	78	79	22	21	1.07 (0.69-1.66)
Freidin *et al* ., 2006	Tuvinians	233	263	466	526	428	484	38	42	92	92	8	8	1.02 (0.65-1.62)
Freidin *et al* ., 2006	Russian	279	137	558	274	452	232	106	42	81	85	19	15	1.30 (0.88-1.91)
Hsu *et al* , 2006	Taiwanese (Aboriginals)	105	93	210	186	197	184	13	2	94	99	6	1	6.07 (1.35-27.27)
Hsu *et al* , 2006	Taiwanese (Han)	108	92	216	184	190	165	26	19	88	90	12	10	1.19 (0.63-2.23)
Taype *et al* , 2006	Peruvian	630	513	1260	1026	777	681	483	345	62	66	38	34	1.23 (1.03-1.46)
Sahiratmadja *et al* ., 2007	Indonesian	211	360	422	720	419	704	3	16	99	98	1	2	0.32 (0.09-1.09)
Soborg *et al* ., 2007	Tanzanian	442	431	884	862	778	777	106	85	88	90	12	10	1.25 (0.92-1.68)
Vejbaesya *et al* ., 2007a	Thai	149	147	298	294	279	278	19	16	94	95	6	5	1.18 (0.60-2.35)
Qu *et al* ., 2007	Chinese	61	122	122	244	99	222	23	22	81	91	19	9	2.34 (1.25-4.40)
Asai *et al* ., 2008	Japanese	57	51	114	102	91	93	23	9	80	91	20	10	2.61 (1.15-5.95)
Farnia *et al* ., 2008	Iranian	71	39	142	78	111	65	31	13	78	83	22	17	1.40 (0.68-2.86)
Ates *et al* ., 2009b	Dutch	112	80	224	160	189	141	35	19	84	88	16	12	1.37 (0.75-2.50)
Chen *et al* ., 2009	Tibetian	140	139	280	278	267	272	13	6	95	98	5	2	2.21 (0.83-5.89)
Jin *et al* ., 2009	Chinese Han	136	435	272	870	226	747	46	123	83	86	17	14	1.24 (0.85-1.79)
Merza *et al* ., 2009	Iranian	117	60	234	120	193	100	41	20	82	83	18	17	1.06 (0.59-1.91)
Hatta *et al* ., 2010	Indonesian	58	198	116	396	110	375	6	21	95	95	5	5	0.97 (0.38-2.47)
Motsinger-Reif et al., 2010	American	42	52	84	104	73	92	11	12	87	88	13	12	1.16 (0.48-2.77)
Other														
Dunstan *et al* ., 2001	Vietnamese	112	75	224	150	203	136	21	14	91	91	9	9	1.00 (0.49-2.04)
Castellucci *et al* ., 2010	Brazilian	Requested data not forthcoming.												
Samaranayake *et al* ., 2010	Sri Lankan	197	198	394	396	372	374	22	22	94	94	6	6	1.01 (0.49-2.04)

Appendix 8b *SLC11A1* 1730G/A frequencies (case versus controls) of all the individual association studies included in the meta-analysis.

	Population	Study Numbers				Allele Frequencies				Allele Frequencies				OR (95% CI)
		n (# people)		2n (# alleles)		Wildtype		Mutant		% Wildtype		% Mutant		
		Case	Control	Case	Control	Case	Control	Case	Control	Case	Control	Case	Control	
Mycobacterium leprae														
Vejbaesya *et al* ., 2007b	Thai	37	140	74	280	61	238	13	42	82	85	18	15	1.21 (0.61-2.39)
Hatta *et al* ., 2010	Indonesian	41	198	82	396	62	307	20	89	76	78	24	22	1.11 (0.64-1.94)
Mycobacterium avium														
Huang *et al* ., 1998	American	8	4	16	8	16	8	0	0	100	100	0	0	Zero observation
Tanaka *et al* ., 2007	Japanese	111	424	222	848	211	756	11	92	95	89	5	11	0.43 (0.23-0.82)
Asai *et al* ., 2008	Japanese	17	51	34	102	29	100	5	2	85	98	14	2	8.62 (1.59-46.77)
Non-TB Mycobacteria														
Koh *et al* ., 2005	South Korean	41	50	82	100	71	97	11	3	87	97	13	3	5.01 (1.35-18.62)
Stienstra *et al* ., 2006	Ghanaian	144	153	288	306	259	292	29	14	90	95	10	5	2.34 (1.21-4.52
Haverkamp *et al* ., 2010	Dutch	80	214	160	428	157	420	3	8	98	98	2	2	1.00 (0.26-3.83)
Mycobacterium tuberculosis														
Lui *et al* ., 1995	Hong Kong/Canadian	12	18	24	36	20	30	4	6	83	83	17	17	1.00 (0.25-4.00)
Bellamy *et al* ., 1998	Gambian	405	417	810	834	742	791	68	43	92	95	8	5	1.69 (1.14-2.50)
Gao *et al* ., 2000	Japanese	267	202	534	404	471	377	63	27	88	93	12	7	1.87 (1.17-2.99)
Ryu *et al* , 2000	Korean	192	192	384	384	335	355	49	29	87	92	13	8	1.79 (1.10-2.90)
Delgado *et al* ., 2002	Cambodian	355	106	710	212	571	163	139	49	80	77	20	23	0.81 (0.56-1.17)
Ma *et al* ., 2002	American	135	108	270	216	268	215	2	1	99	100	1	0	1.60 (0.14-17.81)
Liaw *et al* ., 2002	Chinese (Han/Aboriginal)	49	48	98	96	79	82	19	14	81	85	19	15	1.41 (0.66-3.00)
Salvaraj *et al* , 2002	Indian	157	112	314	224	284	205	30	19	90	92	10	8	1.14 (0.62-2.08)
Soborg *et al* ., 2002	Danish	104	176	208	352	191	342	17	10	92	97	8	3	3.04 (1.37-6.78)
Abe *et al* , 2003	Japanese	95	90	190	180	170	166	20	14	89	92	11	8	1.39 (0.68-2.85)
Liu *et al* ., 2003	Chinese Han	110	171	220	342	203	329	17	13	92	96	8	4	2.12 (1.01-4.46)
Kim *et al* ., 2003	Korean	37	45	74	90	68	88	6	2	92	98	8	2	3.88 (0.76-19.84)
Liu *et al* ., 2004	Chinese Han	120	240	240	480	229	471	11	9	95	98	5	2	1.22 (0.63-2.40)
Zhang *et al* ., 2005	Chinese	127	91	254	182	215	165	39	17	85	91	15	9	1.76 (0.96-3.22)
Freidin *et al* ., 2006	Tuvinians	236	263	472	526	421	453	51	73	89	86	11	14	0.75 (0.51-1.10)
Freidin *et al* ., 2006	Russian	278	139	556	278	540	266	16	12	97	96	3	4	0.66 (0.31-1.41)
Hsu *et al* , 2006	Taiwanese (aboriginals)	88	90	176	180	145	148	31	32	82	82	18	18	0.99 (0.57-1.70)
Hsu *et al* , 2006	Taiwanese (Han)	83	86	166	172	137	147	29	25	83	85	17	15	1.24 (0.69-2.23)
Taype *et al* , 2006	Peruvian	630	513	1260	1026	1030	868	230	158	82	85	18	15	1.23 (0.98-1.53)
Leung *et al* ., 2007	Chinese	278	282	556	564	462	497	94	67	83	88	17	12	1.51 (1.08-2.12)
Nino-Moreno *et al* ., 2007	Mexican	94	110	188	220	144	174	44	46	77	79	23	21	1.16 (0.72-1.85)
Sahiratmadja *et al* ., 2007	Indonesian	205	350	410	700	334	546	76	154	81	78	19	22	0.81 (0.59-1.10)
Soborg *et al* ., 2007	Tanzanian	442	427	884	854	778	756	106	98	88	89	12	11	1.05 (0.76-1.41)
Vejbaesya *et al* ., 2007a	Thai	149	147	298	294	246	246	52	48	83	84	17	16	1.08 (0.70-1.67)
Qu *et al* ., 2007	Chinese	61	122	122	244	104	217	18	27	85	89	15	11	1.39 (0.73-2.64)
Asai *et al* ., 2008	Japanese	57	51	114	102	103	100	11	2	90	98	10	2	5.34 (1.15-24.70)
Farnia *et al* ., 2008	Iranian	71	39	142	78	105	46	37	32	74	59	26	41	0.51 (0.28-0.91)
Ates *et al* ., 2009b	Dutch	112	80	224	160	220	159	4	1	98	99	2	1	2.89 (0.32-26.11)
Chen *et al* ., 2009	Tibetian	140	139	280	278	243	257	37	21	87	92	13	8	1.86 (1.06-3.27)
Merza *et al* ., 2009	Iranian	117	60	234	120	228	104	6	16	97	87	3	13	0.17 (0.07-0.45)
Hatta *et al* ., 2010	Indonesian	58	198	116	396	86	307	30	89	74	78	26	22	1.20 (0.75-1.94)
Motsinger-Reif *et al* ., 2010	American	40	52	80	104	75	97	5	7	94	93	6	7	0.92 (0.28-3.03)
Other														
Calzada *et al* ., 2001	Peruvian	79	85	158	170	133	142	25	28	84	84	16	16	0.95 (0.53-1.72)
Dunstan *et al* ., 2001	Vietnamese	111	77	222	154	189	130	33	24	85	84	15	16	0.95 (0.53-1.67)
Ouchi *et al* ., 2003	Japansese	71	110	142	220	125	198	17	22	88	90	12	10	1.22 (0.63-2.40)
Bravo *et al* ., 2006	Spanish	65	89	130	178	129	173	1	5	99	97	1	3	0.27 (0.03-2.32)
Castellucci *et al* ., 2010	Brazilian	Requested data not forthcoming.												
Samaranayake *et al* ., 2010	Sri Lankan	199	196	398	392	362	363	36	29	91	93	9	7	1.24 (0.75-2.07)

Appendix 8c *SLC11A1* 1729+55del4 frequencies (case versus controls) of all the individual association studies included in the meta-analysis.

	Population	Study Numbers				Allele Frequencies				Allele Frequencies				OR (95% CI)
		n (# people)		2n (# alleles)		Wildtype		Mutant		% Wildtype		% Mutant		
		Case	Control	Case	Control	Case	Control	Case	Control	Case	Control	Case	Control	
Mycobacterium leprae														
Roy *et al* ., 1999	Indian	222	154	444	308	422	292	22	16	95	95	5	5	0.95 (0.49-1.84)
Meisner *et al* ., 2001	Malian	273	201	546	402	420	307	126	95	77	76	23	24	0.97 (0.72-1.31)
Fitness *et al* ., 2004b	Malawian	258	402	516	804	356	570	160	234	69	71	31	29	1.09 (0.86-1.39)
Vejbaesya *et al* ., 2007b	Thai	37	140	74	280	61	238	6	13	82	85	8	5	1.81 (0.66-4.94)
Hatta *et al* ., 2010	Indonesian	41	198	82	396	62	307	20	89	76	78	24	22	1.11 (0.64-1.94)
Mycobacterium avium														
Huang *et al* ., 1998	American	8	4	16	8	16	8	0	0	100	100	0	0	Zero observation
Tanaka *et al* ., 2007	Japanese	111	424	222	848	211	755	11	93	95	89	5	11	0.42 (0.22-0.81)
Asai *et al* ., 2008	Japanese	17	51	34	102	23	77	11	25	68	75	32	25	1.47 (0.63-3.44)
Non-TB Mycobacteria														
Koh *et al* ., 2005	South Korean	41	50	82	100	60	97	22	3	73	97	27	3	11.86 (3.40-41.32)
Stienstra *et al* ., 2006	Ghanaian	150	174	300	348	224	256	76	92	75	74	25	26	0.94 (0.66-1.34)
Mycobacterium tuberculosis														
Lui *et al* ., 1995	Hong Kong/Canadian	12	18	24	36	20	30	4	6	83	83	17	17	1.00 (0.25-4.00)
Bellamy *et al* ., 1998	Gambian	405	417	810	834	638	702	172	132	79	84	21	16	1.43 (1.12-1.84)
Ryu *et al* ., 2000	Korean	192	192	384	384	335	355	49	29	87	92	13	8	1.79 (1.10-2.90)
Delgado *et al* ., 2002	Cambodian	355	106	710	212	571	163	139	49	80	77	20	23	0.81 (0.56-1.17)
Liaw *et al* ., 2002	Chinese (Han/Aboriginal)	49	48	98	96	80	78	18	18	82	81	18	19	0.98 (0.47-2.01)
Ma *et al* ., 2002	American	135	108	270	216	269	215	1	1	100	100	0	0	0.80 (0.05-12.85)
Salvaraj *et al* ., 2002	Indian	157	112	314	224	282	194	32	30	90	87	10	13	0.73 (0.43-1.25)
Soborg *et al* ., 2002	Danish	104	176	208	352	194	344	14	8	93	98	7	2	3.10 (1.28-7.53)
Abe *et al* ., 2003	Japanese	95	90	190	180	170	166	20	14	89	92	11	8	1.39 (0.68-2.85)
Duan *et al* ., 2003	Chinese Han	147	145	294	290	240	259	54	31	82	89	18	11	1.88 (1.17-3.02)
Kim *et al* ., 2003	Korean	38	45	76	90	68	88	8	2	89	98	11	2	5.18 (1.06-25.17)
Liu *et al* ., 2003	Chinese Han	110	170	220	340	175	292	45	48	80	86	20	14	1.56 (1.00-2.45)
Akahoshi *et al* ., 2004	Japanese	Requested data not forthcoming.												
Fitness *et al* ., 2004a	Malawian	218	709	436	1418	315	993	121	425	72	70	28	30	0.90 (0.71-1.14)
Hoal *et al* ., 2004	South African coloured	190	239	380	478	320	422	60	56	84	88	16	12	(1.41) 0.95-2.09)
Liu *et al* ., 2004	Chinese	120	240	240	480	192	412	48	68	80	86	20	14	1.51 (1.01-2.28)
An *et al* ., 2006	Chinese Han	Requested data not forthcoming.												
Taype *et al* ., 2006	Peruvian	630	513	1260	1026	1031	876	229	150	82	85	18	15	1.30 (1.04-1.62)
Leung *et al* ., 2007	Chinese	278	282	556	564	462	497	94	67	83	88	17	12	1.51 (1.08-2.12)
Nino-Moreno *et al* ., 2007	Mexican	73	83	146	166	104	119	42	47	71	72	29	28	1.02 (0.62-1.67)
Sahiratmadja *et al* ., 2007	Indonesian	214	363	428	726	348	568	80	158	81	78	19	22	0.83 (0.61-1.12)
Soborg *et al* ., 2007	Tanzanian	442	431	884	862	648	646	236	216	73	75	27	25	1.09 (0.88-1.35)
Vejbaesya *et al* ., 2007a	Thai	149	147	298	294	246	246	52	48	83	84	17	16	1.81 (0.66-4.94)
Asai *et al* ., 2008	Japanese	57	51	114	102	76	77	38	25	67	75	33	25	1.54 (0.85-2.79)
Farnia *et al* ., 2008	Iranian	71	39	142	78	138	76	4	2	97	97	3	3	1.10 (0.20-6.15)
Ates *et al* ., 2009b	Dutch	112	80	224	160	220	159	4	1	98	99	2	1	2.89 (0.32-26.11)
Chen *et al* ., 2009	Tibetian	140	139	280	278	218	238	62	40	78	86	22	14	1.69 (1.09-2.62)
Merza *et al* ., 2009	Iranian	117	60	234	120	227	117	7	3	97	97.5	3	2.5	1.20 (0.31-4.74)
Jin *et al* ., 2009	Chinese Han	136	435	272	870	238	814	34	56	87.5	94	12.5	6	2.08 (1.32-3.26)
de Wit *et al* ., 2010	South African coloured	492	312	984	624	871	570	113	54	89	91	11	9	1.37 (0.97-1.93)
Hatta *et al* ., 2010	Indonesian	58	198	116	396	86	307	30	89	74	78	26	22	1.20 (0.75-1.94)
Other														
Calzada *et al* ., 2001	Peruvian	79	85	158	170	133	142	25	28	84	84	16	16	0.95 (0.53-1.72)
Ouchi *et al* ., 2003	Japansese	71	110	142	220	125	198	17	22	88	90	12	10	1.22 (0.63-2.40)
Bravo *et al* ., 2006	Spanish	65	89	130	178	129	173	1	5	99	97	1	3	0.27 (0.03-2.32)
Castellucci *et al* ., 2010	Brazilian	Requested data not forthcoming.												

Appendix 9

Appendix 9 *SLC11A1* polymorphisms frequencies (case versus controls) of all the individual association studies included in the meta-analysis of infectious disease.

	Population	Disease	Study Numbers				Allele Frequencies				Allele Frequencies				OR (95% CI)
			n (# people)		2n (# alleles)		Wildtype		Mutant		% Wildtype		% Mutant		
			Case	Control	Case	Control	Case	Control	Case	Control	Case	Control	Case	Control	
-237C/T															
Bellamy *et al* ., 1998	Gambian	Tuberculosis	Requested data not forthcoming.												
Calzada *et al* ., 2001	Peruvian	Trypanosoma	79	85	158	170	157	167	1	3	99	98	1	2	0.35 (0.04-3.44)
Hoal *et al* ., 2004	South African	Tuberculosis	65	81	130	162	119	147	11	15	92	91	8	9	0.91 (0.40-2.05)
Bravo *et al* ., 2006	Spanish	Brucellosis	65	89	130	178	125	171	5	7	96	96	4	4	0.98 (0.30-3.15)
Hsu *et al* , 2006	Taiwanese	Tuberculosis	88	93	176	186	173	180	3	6	98	97	2	3	0.52 (0.13-2.11)
Hsu *et al* , 2006	Taiwanese (Han)	Tuberculosis	83	85	166	170	158	153	8	17	95	90	5	10	0.46 (0.19-1.09)
Castellucci *et al* ., 2010	Brazilian	Leishmainia	Requested data not forthcoming.												
274C/T															
Liu *et al* ., 1995	Hong Kong/Canadian	Tuberculosis	12	18	24	36	22	33	2	3	92	92	8	8	1.00 (0.15-6.48)
Dunstan *et al* ., 2001	Vietnamese	Typhiod Fever	112	77	224	154	203	138	21	16	91	90	9	10	0.89 (0.45-1.77)
Puzyrev *et al* , 2002	Slavonic	Tuberculosis	55	121	110	242	86	185	24	57	78	76	22	24	0.91 (0.53-1.56)
Liaw *et al* ., 2002	Chinese	Tuberculosis	49	48	98	96	92	95	6	1	94	99	6	1	6.20 (0.73-52.47
Dubaniewicz *et al* ., 2005	Polish	Tuberculosis	80	89	160	178	116	132	44	46	72.5	74	27.5	26	1.09 (0.67-1.76)
Freidin *et al* ., 2006	Tuvinians	Tuberculosis	236	263	472	526	425	463	47	63	90	88	10	12	0.81 (0.54-1.21)
Freidin *et al* ., 2006	Russian	Tuberculosis	299	116	598	232	448	194	150	38	75	84	25	16	1.71 (1.15-2.53)
Doorduyn *et al* ., 2008	Dutch	Salmonella	193	683	386	1366	272	993	114	373	70	73	30	27	1.12 (0.87-1.43)
Doorduyn *et al* ., 2008	Dutch	Campylobacter	454	683	908	1366	655	993	253	373	72	73	28	27	1.03 (0.85-1.24)
Castellucci *et al* ., 2010	Brazilian	Leishmainia	Requested data not forthcoming.												
Motsinger-Reif et al., 2010	American	Tuberculosis	38	50	76	100	61	81	15	19	80	81	20	19	1.05 (0.49-2.23)
Samaranayake *et al* ., 2010	Sri Lankan	Leishmania	198	199	396	398	344	342	52	56	87	86	13	14	0.92 (0.62-1.39)
1465-85G/A															
Lui *et al* ., 1995	Hong Kong/Canadian	Tuberculosis	12	18	24	36	19	25	5	11	79	69	21	31	0.60 (0.18-2.01)
Dunstan *et al* ., 2001	Vietnamese	Salmonella	112	77	224	154	163	114	61	40	73	74	27	26	1.07 (0.67-1.70)
Puzyrev *et al* , 2002	Slavonic	Tuberculosis	56	127	112	254	74	181	38	73	66	71	34	29	1.27 (0.79-2.05)
Dubaniewicz *et al* ., 2005	Polish	Tuberculosis	79	93	158	186	111	127	47	59	70	68	30	32	0.91 (0.58-1.44)
Freidin *et al* ., 2006	Tuvinians	Tuberculosis	233	263	466	526	369	412	97	114	79	78	21	22	0.95 (0.70-1.29)
Freidin *et al* ., 2006	Russian	Tuberculosis	279	135	558	270	378	193	180	77	68	71	32	29	1.19 (0.87-1.64)
Castellucci *et al* ., 2010	Brazilian	Leishmainia	Requested data not forthcoming.												
1729+271del4 (CAAA)n															
Fitness *et al* ., 2004a	Malawian	Tuberculosis	239	762	478	1524	324	1001	154	523	68	66	32	34	0.91 (0.73-1.13)
Fitness *et al* ., 2004b	Malawian	Leprosy	258	429	516	858	329	575	187	283	64	67	36	33	1.15 (0.92-1.45)
Hoal *et al* ., 2004	South African	Tuberculosis	119	132	238	264	164	190	74	74	69	72	31	28	1.16 (0.79-1.70)
Dubaniewicz *et al* ., 2005	Polish	Tuberculosis	82	84	164	168	103	110	61	58	63	65	37	35	1.12 (0.72-1.76)
Hsu *et al* ., 2006	Taiwanese	Tuberculosis	85	95	170	190	129	150	41	40	76	79	24	21	1.19 (0.73-1.96)
Hsu *et al* ., 2006	Taiwanese (Han)	Tuberculosis	85	79	170	158	126	120	44	38	74	76	26	24	1.10 (0.67-1.82)

REFERENCES

Abe, T., Iinuma, Y., Ando, M., Yokoyama, T., Yamamoto, T., Nakashima, K., Takagi, N., Baba, H., Hasegawa, Y. & Shimokata, K. (2003) 'NRAMP1 polymorphisms, susceptibility and clinical features of tuberculosis', *The Journal of Infection,* **46**(4): 215-20.

Agranoff, D.D. & Krishna, S. (1998) 'Metal ion homeostasis and intracellular parasitism', *Molecular Microbiology,* **28**(3): 403-12.

Aidar, M. & Line, S.R. (2007) 'A simple and cost-effective protocol for DNA isolation from buccal epithelial cells', *Brazilian Dental Journal,* **18**(2): 148-52.

Akahoshi, M., Ishihara, M., Remus, N., Uno, K., Miyake, K., Hirota, T., Nakashima, K., Matsuda, A., Kanda, M., Enomoto, T., Ohno, S., Nakashima, H., Casanova, J.L., Hopkin, J.M., Tamari, M., Mao, X.Q. & Shirakawa, T. (2004) 'Association between IFNA genotype and the risk of sarcoidosis', *Human Genetics,* **114**(5): 503-9.

Akira, S., Isshiki, H., Nakajima, T., Kinoshita, S., Nishio, Y., Natsuka, S. & Kishimoto, T. (1992) 'Regulation of expression of the interleukin 6 gene: structure and function of the transcription factor NF-IL6', *Ciba Foundation Symposium,* **167**(47-62): 62-7.

Alter-Koltunoff, M., Ehrlich, S., Dror, N., Azriel, A., Eilers, M., Hauser, H., Bowen, H., Barton, C.H., Tamura, T., Ozato, K. & Levi, B.Z. (2003) 'Nramp1-mediated Innate Resistance to Intraphagosomal Pathogens Is Regulated by IRF-8, PU.1, and Miz-1', *The Journal of Biological Chemistry,* **278**(45): 44025-32.

Alter-Koltunoff, M., Goren, S., Nousbeck, J., Feng, C.G., Sher, A., Ozato, K., Azriel, A. & Levi, B.Z. (2008) 'Innate immunity to intraphagosomal pathogens is mediated by IRF-8 that stimulates the expression of macrophage specific NRAMP1 through antagonizing repression by C-MYC', *The Journal of Biological Chemistry,* **283**(5): 2724-33.

Altet, L., Francino, O., Solano-Gallego, L., Renier, C. & Sanchez, A. (2002) 'Mapping and Sequencing of the Canine NRAMP1 Gene and Identification of Mutations in Leishmaniasis-Susceptible Dogs', *Infection and Immunity,* **70**(6): 2763-71.

An, Y.C., Feng, F.M., Yuan, J.X., Ji, C.M., Wang, Y.H., Guo, M., Deng, X.J., Gao, B.X., Wang, D. & Liu, Q. (2006) 'Study on the association of INT4 and 3'UTR polymorphism of natural-resistance-associated macrophage protein 1 gene with susceptibility to pulmonary tuberculosis', *Zhonghua Liu Xing Bing Xue Za Zhi,* **27**(1): 37-40.

Asadullah, K., Sterry, W. & Volk, H.D. (2003) 'Interleukin-10 Therapy-Review of a New Approach', *Pharmaceutical Reviews,* **55**(2): 241-69.

Asai, S., Abe, Y., Fujino, T., Masukawa, A., Arami, S., Furuya, H. & Miyachi, H. (2008) 'Association of the SLC11A1 Gene Polymorphisms With Susceptibility to Mycobacterium Infections in a Japanese Population', *Infectious Diseases in Clinical Practice,* **16**(4): 230-34.

Ateş, O., Dalyan, L., Hatemi, G., Hamuryudan, V. & Topal-Sarıkaya, A. (2009a) 'Genetic susceptibility to Behçet's syndrome is associated with NRAMP1 (SLC11A1) polymorphism in Turkish patients', *Rheumatology International,* **29**(7): 787-91.

Ateş, O., Dalyan, L., Müsellim, B., Hatemi, G., Türker, H., Ongen, G., Hamuryudan, V. & Topal-Sarıkaya, A. (2009b) 'NRAMP1 (SLC11A1) gene polymorphisms that correlate with autoimmune versus infectious disease susceptibility in tuberculosis and rheumatoid arthritis', *International Journal of Immunogenetics,* **36**(1): 15-9.

Ateş, O., Kurt, S., Bozkurt, N. & Karaer, H. (2010) 'NRAMP1 (SLC11A1) Variants: Genetic Susceptibility to Multiple Sclerosis', *Journal of Clinical Immunology,* **30**(4): 583-6.

Ateş, O., Müsellim, B., Öngen, G. & Topal-Sarıkaya, A. (2008) 'NRAMP1 (SLC11A1): A Plausible Candidate Gene for Systemic Sclerosis (SSc) with Interstitial Lung Involvement', *Journal of Clinical Immunology,* **28**(1): 73-7.

Atkinson, P.G. & Barton, C.H. (1998) 'Ectopic expression of *Nramp1* in COS-1 cells modulates iron accumulation', *FEBS Letters,* **425**(2): 239-42.

Atkinson, P.G. & Barton, C.H. (1999) 'High level of expression of *Nramp1*^{G169} in RAW264.7 cell transfectants: analysis of intracellular iron transport', *Immunology,* **96**(4): 656-62.

Atkinson, P.G., Blackwell, J.M. & Barton, C.H. (1997) 'Nramp1 locus encodes a 65kDa interferon-γ-inducible protein in murine macrophages', *The Biochemical Journal,* **325**(3): 779-86.

Auwerx, J. (1991) 'The human leukemia cell line, THP-1: a multifacetted model for the study of monocyte-macrophage differentiation', *Experientia,* **47**(1): 22-31.

Awomoyi, A.A. (2007) 'The human solute carrier family 11 member 1 protein (SLC11A1): linking infections, autoimmunity and cancer?' *FEMS Immunology and Medical Microbiology,* **49**(3): 324-9.

Awomoyi, A.A., Marchant, A., Howson, J.M., Mcadam, K.P., Blackwell, J.M. & Newport, M.J. (2002) 'Interleukin-10, Polymorphism in SLC11A1 (formerly NRAMP1), and Susceptibility to Tuberculosis.' *Journal of Infectious Diseases,* **186**(12): 1808.

Awomoyi, A.A., Sirugo, G., Newport, M.J. & Tishkoff, S. (2006) 'Global distribution of a novel trinucleotide microsatellite polymorphism (ATA)n in intron 8 of the SLC11A1 gene and susceptibility to pulmonary tuberculosis', *International Journal of Immunogenetics,* **33**(1): 11-5.

Azar, S.T., Tamim, H., Beyhum, H.N., Habbal, M.Z. & Almawi, W.Y. (1999) 'Type I (Insulin-Dependent) Diabetes Is a Th1- and Th2-Mediated Autoimmune Disease', *Clinical and Diagnostic Laboratory Immunology,* **6**(3): 306-10.

Bakshi, R., Benedict, R.H.B., Bermel, R.A., Caruthers, S.D., Puli, S.R., Tjoa, C.W., Fabiano, A.J. & Jacobs, L. (2002) 'T2 Hypointensity in the Deep Gray Matter of Patients With Multiple Sclerosis: A Quantitative Magnetic Resonance Imaging Study', *Archives of Neurology,* **59**(1): 62-8.

Bakshi, R., Dmochowski, J., Shaikh, Z.A. & Jacobs, L. (2001) 'Gray matter T2 hypointensity is related to plaques and atrophy in the brains of multiple sclerosis patients', *Journal of the Neurological Sciences,* **185**(1): 19-26.

Barrera, L.F., Kramnik, I., Skamene, E. & Radzioch, D. (1997) 'I-A beta gene expression regulation in macrophages derived from mice susceptible or resistant to infection with M. bovis BCG', *Molecular Immunology,* **34**(4): 343-55.

Barton, C.H., Biggs, T.E., Baker, S.T., Bowen, H. & Atkinson, P.G. (1999) 'Nramp1: a link between intracellular iron transport and innate resistance to intracellular pathogens', *Journal of Leukocyte Biology,* **66**(5): 757-62.

Barton, C.H., White, J.K., Roach, T.I. & Blackwell, J.M. (1994) 'NH2-terminal sequence of macrophage-expressed natural resistance-associated macrophage protein (Nramp) encodes a proline/serine-rich putative Src homology 3-binding domain', *The Journal of Experimental Medicine,* **179**(5): 1683-7.

Barton, C.H., Whitehead, S.H. & Blackwell, J.M. (1995) 'Nramp transfection transfers Ity/Lsh/Bcg-related pleiotropic effects on macrophage activation: influence on oxidative burst and nitric oxide pathways', *Molecular medicine,* **1**(3): 267-79.

Bassuny, W.M., Ihara, K., Matsuura, N., Ahmed, S., Kohno, H., Kuromaru, R., Miyako, K. & Hara, T. (2002) 'Association study of the NRAMP1 gene promoter polymorphism and early-onset type 1 diabetes', *Immunogenetics,* **54**(4): 282-5.

Bates, A.D. & Maxwell, A. (2005) *DNA Topology,* New York, Oxford University Press.

Bayele, H.K., Peyssonnaux, C., Giatromanolaki, A., Arrais-Silva, W.W., Mohamed, H.S., Collins, H., Giorgio, S., Koukourakis, M., Johnson, R.S., Blackwell, J.M., Nizet, V. & Srai, S.K.S. (2007) 'HIF-1 regulates heritable variation and allele expression phenotypes of the macrophage immune response gene SLC11A1 from a Z-DNA-forming microsatellite', *Blood,* **15**(8): 3039-48.

Begg, C.B. & Mazumdar, M. (1994) 'Operating characteristics of a rank correlation test for publication bias', *Biometrics,* **50**(4): 1088-101.

Bellamy, R., Ruwende, C., Corrah, T., Mcadam, K., Whittle, H.C. & Hill, A.V.S. (1998) 'Variations in the Nramp1 gene and susceptibility to tuberculosis in West Africans', *The New England Journal of Medicine,* **338**(10): 640-4.

Berman, N.G. & Parker, R.A. (2002) 'Meta-analysis: neither quick nor easy', *BMC Medical Research Methodology,* **2**:10.

Berrier, A., Siu, G. & Calame, K. (1998) 'Transcription of a minimal promoter from the NF-IL6 gene is regulated by CREB/ATF and Sp1 proteins in U937 promonocytic cells', *The Journal of Immunology,* **161**(5): 2267-75.

Bianchi, M., Crinelli, R., Giacomini, E., Carloni, E. & Magnani, M. (2009) 'A potent enhancer element in the 5'-UTR intron is crucial for transcriptional regulation of the human ubiquitin C gene', *Gene,* **488**(1): 88-101.

Biggs, T.E., Baker, S.T., Botham, M.S., Dhital, A., Barton, C.H. & Perry, V.H. (2001) 'Nramp1 modulates iron homoeostasis in vivo and in vitro: evidence for a role in cellular iron release involving de-acidification of intracellular vesicles', *European Journal of Immunology,* **31**(7): 2060-70.

Blackwell, J.M. (1989) 'The macrophage resistance gene Lsh/Ity/Bcg', *Research in Immunology,* **140**(8): 767-9.

Blackwell, J.M. (1996) 'Structure and function of the natural-resistance-associated macrophage protein (Nramp1), a candidate protein for infectious and autoimmune disease susceptibility', *Molecular Medicine Today,* **2**(5): 205-11.

Blackwell, J.M. (2001) 'Genetics and genomics in infectious disease susceptibility', *Trends in Molecular Medicine,* **7**(11): 521-26.

Blackwell, J.M., Barton, C.H., White, J.K., Roach, T.I., Shaw, M.A., Whitehead, S.H., Mock, B.A., Searle, S., Williams, H. & Baker, A.M. (1994) 'Genetic regulation of leishmanial and mycobacterial infections: the Lsh/Ity/Bcg gene story continues', *Immunology Letters,* **43**(1-2): 99-107.

Blackwell, J.M., Barton, C.H., White, J.K., Searle, S., Baker, A.M., Williams, H. & Shaw, M.A. (1995) 'Genomic organization and sequence of the human NRAMP gene: identification and mapping of a promoter region polymorphism.' *Molecular Medicine,* **1**(2): 194-205.

Blackwell, J.M., Black, G.F., Peacock, C.S., Miller, E.N., Sibthorpe, D., Gnananandha, D., Shaw, J.J., Silveira, F., Lins-Lainson, Z., Ramos, F., Collins, A. & Shaw, M.A. (1997) 'Immunogenetics of leishmanial and mycobacterial infections: the Belem Family Study', *Philosophical Transactions: Biological Sciences,* **352**(1359): 1331-45.

Blackwell, J.M., Goswami, T., Evans, C.A.W., Sibthorpe, D., Papo, N., White, J.K., Searle, S., Miller, E.N., Peacock, C.S., Mohammed, H. & Ibrahim, M. (2001) 'SLC11A1 (formerly NRAMP1) and disease resistance', *Cellular Microbiology,* **3**(12): 773-84.

Blackwell, J.M., Jamieson, S.E. & Burgner, D. (2009) 'HLA and Infectious Diseases', *Clinical Microbiology Reviews,* **22**(2): 370-85.

Blackwell, J.M., Searle, S., Mohamed, H. & White, J.K. (2003) 'Divalent cation transport and susceptibility to infectious and autoimmune disease: continuation of the Ity/Lsh/Bcg/Nramp1/Slc11a1 gene story', *Immunology Letters,* **85**(2): 197-203.

Blackwell, J.M., Toole, S., King, M., Dawda, P., Roach, T.I. & Cooper, A. (1988) 'Analysis of Lsh gene expression in congenic B10.L-Lshr mice', *Current Topics in Microbiology and Immunology,* **137**:301-9.

Bowen, H., Lapham, A., Phillips, E., Yeung, I., Alter-Koltunoff, M., Levi, B.Z., Perry, V.H., Mann, D.A. & Barton, C.H. (2003) 'Characterization of the murine *Nramp1* promoter: requirement for transactivation by Miz-1', *The Journal of Biological Chemistry,* **278**(38): 36017-26.

Bowlus, C.L. (2003) 'The role of iron in T cell development and autoimmunity', *Autoimmunity Reviews,* **2**(2): 73-8.

Bradley, D.J. (1977) 'Regulation of Leishmania populations within the host II. Genetic control of acute susceptibility of mice to *Leishmania donovani* infection.' *Clinical & Experimental Immunology,* **30**(1): 130-40.

Bravo, M.J., Colmenero, J.D., Martin, J., Alonso, A. & Caballero Gonzalez, A. (2006) 'Variation in the NRAMP1 gene does not affect susceptibility or protection in human brucellosis', *Microbes and Infection,* **8**(1): 154-6.

Breslauer, K.J., Frank, R., Blocker, H. & Marky, L.A. (1986) 'Predicting DNA duplex stability from the base sequence', *Proceedings of the National Academy of Sciences of the United States of America,* **83**(11): 3746-50.

Bucheton, B., Abel, L., Kheir, M.M., Mirgani, A., El-Safi, S.H., Chevillard, C. & Dessein, A. (2003) 'Genetic control of visceral leishmaniasis in a Sudanese population: candidate gene testing indicates a linkage to the NRAMP1 region', *Genes & Immunity,* **4**(2): 104-9.

Bullen, J.J. (1981) 'The Significance of Iron in Infection', *Reviews of Infectious Diseases,* **3**(6): 1127-38.

Burley, S.K. & Roeder, R.G. (1996) 'Biochemistry and Structural Biology of Transcription Factor IID (TFIID)', *Annual Review of Biochemistry,* **65**(1): 769-99.

Bussmann, V., Lantier, I., Pitel, F., Patri, S., Nau, F., Gros, P., Elsen, J.M. & Lantier, F. (1998) 'cDNA cloning, structural organization, and expression of the sheep NRAMP1 gene', *Mammalian Genome,* **9**(12): 1027-31.

Buu, N.T., Cellier, M., Gros, P. & Schurr, E. (1995) 'Identification of a highly polymorphic length variant in the 3'UTR of NRAMP1', *Immunogenetics,* **42**(5): 428-9.

Calzada, J.E., Nieto, A., Lopez-Nevot, M.A. & Martin, J. (2001) 'Lack of association between NRAMP1 gene polymorphisms and Trypanosoma cruzi infection', *Tissue Antigens,* **57**(4): 353-57.

Canonne-Hergaux, F., Calafat, J., Richer, E., Cellier, M., Grinstein, S., Borregaard, N. & Gros, P. (2002) 'Expression and subcellular localization of NRAMP1 in human neutrophil granules', *Blood,* **100**(1): 268-75.

Canonne-Hergaux, F., Fleming, M.D., Levy, J.E., Gauthier, S., Ralph, T., Picard, V., Andrews, N.C. & Gros, P. (2000) 'The Nramp2/DMT1 iron transporter is induced in the duodenum of microcytic anemia mk mice but is not properly targeted to the intestinal brush border ', *Blood,* **96**(12): 3964-70.

Canonne-Hergaux, F., Levy, J.E., Fleming, M.D., Montross, L.K., Andrews, N.C. & Gros, P. (2001) 'Expression of the DMT1 (NRAMP2/DCT1) iron transporter in mice with genetic iron overload disorders', *Blood,* **97**(4): 1138-40.

Cardon, L.R. & Palmer, L.J. (2003) 'Population stratification and spurious allelic association', *The Lancet,* **361**(9357): 598-604.

Carrasco-Marín, E., Alvarez-Domínguez, C., López-Mato, P., Martínez-Palencia, R. & Leyva-Cobián, F. (1996) 'Iron Salts and Iron-Containing Porphyrins Block Presentation of Protein Antigens by Macrophages to MHC Class II-Restricted T Cells', *Cellular Immunology,* **171**(2): 173-85.

Castellucci, L., Jamieson, S., Miller, E., Menezes, E., Oliveira, J., Magalhaes, A., Guimaraes, L., Lessa, M., Ribeiro De Jesus, A., Carvalho, E. & Blackwell, J.M. (2010) 'CXCR1 and SLC11A1 polymorphisms affect susceptibility to cutaneous leishmaniasis in Brazil: a case-control and family-based study', *BMC Medical Genetics,* **11**(1): 10.

Cellier, M., Govoni, G., Vidal, S., Kwan, T., Groulx, N., Liu, J., Sanchez, F., Skamene, E., Schurr, E. & Gros, P. (1994) 'Human natural resistance-associated macrophage protein: cDNA cloning, chromosomal mapping, genomic organization, and tissue-specific expression', *The Journal of Experimental Medicine,* **180**(5): 1741-52.

Cellier, M., Shustik, C., Dalton, W., Rich, E., Hu, J., Malo, D., Schurr, E. & Gros, P. (1997) 'Expression of the human NRAMP1 gene in professional primary phagocytes: studies in blood cells and in HL-60 promyelocytic leukemia', *Journal of Leukocyte Biology,* **61**(1): 96-105.

Cervino, A.C.L., Lakiss, S., Sow, O. & Hill, A.V.S. (2000) 'Allelic association between the NRAMP1 gene and susceptibility to tuberculosis in Guinea-Conakry', *Annals of Human Genetics,* **64**(6): 507-12.

Chen, X.R., Feng, Y.L., Ma, Y., Zhang, Z.D., Li, C.Y., Wen, F.Q., Tang, X.Y. & Su, Z.G. (2009) 'A study on the haplotype of the solute carrier family 11 member 1 gene in Tibetan patients with pulmonary tuberculosis in China', *Zhonghua Jie He He Hu Xi Za Zhi,* **32**(5): 360-4.

Chermesh, I., Azriel, A., Alter-Koltunoff, M., Eliakim, R., Karban, A. & Levi, B.Z. (2007) 'Crohn's disease and SLC11A1 promoter polymorphism', *Digestive Disease and Sciences,* **52**(7): 1632-5.

Chevneval, D., Christy, R.J., Geiman, D., Cornelius, P. & Lane, M.D. (1991) 'Cell-free transciption directed by the 422 adipose P2 gene promoter: activation by the CCAAT/enhancer binding protein', *Proceedings of the National Academy of Sciences,* **88**(19): 8465-9.

Comabella, M., Altet, L., Peris, F., Villoslada, P., Sánchez, A. & Montalban, X. (2004) 'Genetic analysis of SLC11A1 polymorphisms in multiple sclerosis patients', *Multiple Sclerosis,* **10**(6): 618-20.

Couper, K.N., Blount, D.G. & Riley, E.M. (2008) 'IL-10: The Master Regulator of Immunity to Infection', *The Journal of Immunology,* **180**(9): 5771-7.

Crawford, N.P., Eichenberger, M.R., Colliver, D.W., Lewis, R.K., Cobbs, G.A., Petras, R.E. & Galandiuk, S. (2005) 'Evaluation of SLC11A1 as an inflammatory bowel disease candidate gene', *BMC Medical Genetics,* **6**:10.

Curie, C., Alonso, J.M., Le Jean, M., Ecker, J.R. & Briat, J.F. (2000) 'Involvement of NRAMP1 from Arabidopsis thaliana in iron transport', *Biochemistry Journal,* **347**(3): 749-55.

Darnell, J.E., Kerr, I.M. & Stark, G.R. (1994) 'Jak-STAT pathways and transcriptional activation in response to IFNs and other extracellular signalling proteins', *Science,* **264**(5164): 1415-21.

Davies, J.L., Kawaguchi, Y., Bennett, S.T., Copeman, J.B., Cordell, H.J., Pritchard, L.E., Reed, P.W., Gough, S.C.L., Jenkins, S.C., Palmer, S.M., Balfour, K.M., Rowe, B.R., Farrall, M., Barnett, A.H., Bain, S.C. & Todd, J.A. (1994) 'A genome-wide search for human type 1 diabetes susceptibility genes', *Nature,* **371**(6493): 130-6.

de Chastellier, C., Fréhel, C., Offredo, C. & Skamene, E. (1993) 'Implication of phagosome-lysosome fusion in restriction of Mycobacterium avium growth in bone marrow macrophages from genetically resistant mice', *Infection and Immunity,* **61**(9): 3775-84.

de Waal Malefyt, R., Haanen, J., Spits, H., Roncarolo, M.G., Te Velde, A., Figdor, C., Johnson, K., Kastelein, R., Yssel, H. & De Vries, J.E. (1991) 'Interleukin 10 (IL-10) and viral IL-10 strongly reduce antigen-specific human T cell proliferation by diminishing the antigen-presenting capacity of monocytes via downregulation of class II major histocompatibiltiy complex expression', *The Journal of Experimental Medicine,* **174**(4): 915-24.

de Wit, E., van der Merwe, L., van Helden, P. & Hoal, E. (2010) 'Gene-gene interaction between tuberculosis candidate genes in a South African population', *Mammalian Genome,* **22**(1-2): 100-10.

Decobert, M., Larue, H., Bergeron, A., Harel, F., Pfister, C., Rousseau, F., Lacombe, L. & Fradet, Y. (2006) 'Polymorphisms of the human NRAMP1 gene are associated with response to bacillus Calmette-Guerin immunotherapy for superficial bladder cancer', *The Journal of Urology,* **175**(4): 1506-11.

Deeks, J.J., Macaskill, P. & Irwig, L. (2005) 'The performance of tests of publication bias and other sample size effects in systematic reviews of diagnostic test accuracy was assessed', *Journal of Clinical Epidemiology,* **58**(9): 882-93.

Delgado, J.C., Baena, A., Thim, S. & Goldfeld, A.E. (2002) 'Ethnic-specific genetic associations with pulmonary tuberculosis', *The Journal of Infectious Diseases,* **186**(10): 1463-8.

Denis, M., Forget, A., Pelletier, M. & Skamene, E. (1988) 'Pleiotropic effects of the Bcg gene: III. Respiratory burst in Bcg-congenic macrophages', *Clinical and Experimental Immunology,* **73**(3): 370-5.

Direskeneli, H. (2006) 'Autoimmunity vs autoinflammation in Behcet's disease: do we oversimplify a complex disorder?' *Rheumatology,* **45**(12): 1461-5.

Dong, C. & Flavell, R.A. (2000) 'Cell fate decision: T-helper 1 and 2 subsets in immune responses', *Arthritis Research,* **2**(3): 179-88.

Donninger, H., Cashmore, T.J., Scriba, T., Petersen, D.C., Janse van Rensburg, E. & Hayes, V.M. (2004) 'Functional analysis of novel SLC11A1 (NRAMP1) promoter variants in susceptibility to HIV-1', *Journal of Medical Genetics,* **41**(4): e49.

Donovan, A., Brownlie, A., Dorschner, M.O., Zhou, Y., Pratt, S.J., Paw, B.H., Phillips, R.B., Thisse, C., Thisse, B. & Zon, L.I. (2002) 'The zebrafish mutant gene chardonnay (cdy) encodes divalent metal transporter 1 (DMT1)', *Blood,* **100**(13): 4655-9.

Doorduyn, Y., van Pelt, W., Siezen, C.L., van der Horst, F., van Duynhoven, Y.T., Hoebee, B. & Janssen, R. (2008) 'Novel insight in the association between salmonellosis or campylobacteriosis and chronic illness, and the role of host genetics in susceptibility to these diseases', *Epidemiology and Infection* **136**(9): 1225-34.

Druszczyńska, M., Strapagiel, D., Kwiatkowska, S., Kowalewicz-Kulbat, M., Rózalska, B., Chmiela, M. & Rudnicka, W. (2006) 'Tuberculosis bacilli still posing a threat. Polymorphism of genes regulating anti-mycobacterial properties of macrophages', *Polish Journal of Microbiology,* **55**(1): 7-12.

Duan, H.F., Zhou, X.H., Ma, Y., Li, C.Y., Chen, X.Y., Gao, W.W. & Zheng, S.H. (2003) 'A study on the association of 3'UTR polymorphisms of NRAMP1 gene with susceptibility to tuberculosis in Hans', *Zhonghua Jie He He Hu Xi Za Zhi,* **26**(5): 286-9.

Dubaniewicz, A., Jamieson, S.E., Dubaniewicz-Wybieralska, M., Fakiola, M., Nancy Miller, E. & Blackwell, J.M. (2005) 'Association between SLC11A1 (formerly NRAMP1) and the risk of sarcoidosis in Poland', *European Journal of Human Genetics,* **13**(7): 829-34.

Dunstan, S.J., Ho, V.A., Duc, C.M., Lanh, M.N., Phuong, C.X., Luxemburger, C., Wain, J., Dudbridge, F., Peacock, C.S., House, D., Parry, C., Hien, T.T., Dougan, G., Farrar, J. & Blackwell, J.M. (2001) 'Typhoid Fever and Genetic Polymorphisms at the Natural Resistance Associated Macrophage Protein 1', *The Journal of Infectious Diseases,* **183**(7): 1156-60.

Duval, S. & Tweedie, R. (2000a) 'A non-parametric 'trim and fill' method of assessing publication bias in meta-analysis', *Journal of the American Statistical Association,* **95**(499): 89-98.

Duval, S. & Tweedie, R. (2000b) 'Trim and fill: A simple funnel-plot-based method of testing and adjusting for publication bias in meta-analysis', *Biometrics,* **56**(2): 455-63.

Egger, M., Smith, G.D., Schneider, M. & Minder, C. (1997) 'Bias in meta-analysis detected by a simple, graphical test', *British Medical Journal,* **315**(7109): 629-34.

El Baghdadi, J., Remus, N., Benslimane, A., El Annaz, H., Chentoufi, M., Abel, L. & Schurr, E. (2003) 'Variants of the human NRAMP1 gene and susceptibility to tuberculosis in Morocco', *The International Journal of Tuberculosis and Lung Disease,* **7**(6): 599-602.

Emami, K.H., Jain, A. & Smale, S.T. (1997) 'Mechanism of synergy between TATA and initiator: synergistic binding of TFIID following a putative TFIIA-induced isomerization', *Genes & Development,* **11**(22): 3007-19.

Esposito, L., Hill, N.J., Pritchard, L.E., Cucca, F., Muxworthy, C., Merriman, M.E., Wilson, A., Julier, C., Delepine, M., Tuomilehto, J., Tuomilehto-Wolf, E., Ionesco-Tirgoviste, C., Nistico', L., Buzzetti, R., Pozzilli, P., Ferrari, M., Bosi, E., Pociot, F., Nerup, J., Bain, S.C. & Todd, J.A. (1998) 'Genetic analysis of chromosome 2 in type 1 diabetes: analysis of putative loci IDDM7, IDDM12, and IDDM13 and candidate genes NRAMP1 and IA-2 and the interleukin-1 gene cluster', *Diabetes,* **47**(11): 1797-9.

Evans, C.A.W., Harbuz, M.S., Ostenfeld, T., Norrish, A. & Blackwell, J.M. (2001) 'Nramp1 is expressed in neurons and is associated with behavioural and immune responses to stress', *Neurogenetics,* **3**(2): 69-78.

Farnia, P., Pajand, O., Anoosheh, S., Tabarsi, P., Dizaji, M.K., Mohammadi, F., Varahram, M., Baghaei, P., Bahadori, M., Masjedi, M.R. & Velayati, A.A. (2008) 'Comparison of Nramp1 gene polymorphism among TB Health Care workers and recently infected cases; Assessment of Host susceptibility ', *Tanaffos,* **7**(1): 19-24.

Feng, J., Li, Y., Hashad, M., Schurr, E., Gros, P., Adams, L.G. & Templeton, J.W. (1996) 'Bovine natural resistance associated macrophage protein 1 (Nramp1) gene', *Genome Research,* **6**(10): 956-64.

Ferreira, F.R., Goulart, L.R., Silva, H.D. & Goulart, I.M. (2004) 'Susceptibility to leprosy may be conditioned by an interaction between the NRAMP1 promoter polymorphisms and the lepromin response', *International Journal of Leprosy,* **72**(4): 457-67.

Fitness, J., Floyd, S., Warndorff, D.K., Sichali, L., Malema, S., Crampin, A.C., Fine, P.E. & Hill, A.V. (2004a) 'Large-scale candidate gene study of tuberculosis susceptibility in the Karonga district of northern Malawi', *The American Journal of Tropical Medicine and Hygiene,* **71**(3): 341-9.

Fitness, J., Floyd, S., Warndorff, D.K., Sichali, L., Mwaungulu, L., Crampin, A.C., Fine, P.E.M. & Hill, A.V.S. (2004b) 'Large-scale candidate gene study of leprosy susceptibility in the Karonga district of northern Malawi', *The American Journal of Tropical Medicine and Hygiene,* **71**(3): 330-40.

Forbes, J.R. & Gros, P. (2001) 'Divalent-metal transport by NRAMP proteins at the interface of host-pathogen interactions', *Trends in Microbiology,* **9**(8): 397-403.

Forbes, J.R. & Gros, P. (2003) 'Iron, manganese, and cobalt transport by Nramp1 (Slc11a1) and Nramp2 (Slc11a2) expressed at the plasma membrane', *Blood,* **102**(5): 1884-92.

Formica, S., Roach, T.I. & Blackwell, J.M. (1994) 'Interaction with extracellular matrix proteins influences Lsh/Ity/Bcg (candidate Nramp) gene regulation of macrophage priming/activation for tumour necrosis factor-alpha and nitrite release', *Immunology,* **82**(1): 42-50.

Frehel, C., Canonne-Hergaux, F., Gros, P. & de Chastellier, C. (2002) 'Effect of Nramp1 on bacterial replication and on maturation of Mycobacterium avium-containing phagosomes in bone marrow-derived mouse macrophages', *Cellular Microbiology,* **4**(8): 541-56.

Freidin, M., Rudko, A., Kolokolova, O., Ondar, E., Strelis, A. & Puzyrev, V. (2006) 'Comparative analysis of the tuberculosis susceptibility genetic make-up in Tuvinians and Russians', *Molecular Biology,* **40**(2): 218-27.

Friedman, A.D. (2007) 'Transcriptional control of granulocyte and monocyte development', *Oncogene,* **26**(47): 6816-28.

Friedrich, J., Adhikari, N. & Beyene, J. (2007) 'Inclusion of zero total event trials in meta-analyses maintains analytic consistency and incorporates all available data', *BMC Medical Research Methodology,* **7**:5.

Fritsche, G., Nairz, M., Werner, E.R., Barton, H.C. & Weiss, G. (2008) 'Nramp1-functionality increases iNOS expression via repression of IL-10 formation', *European Journal of Immunology,* **38**(11): 3060-7.

Fritz, P., Saal, J.G., Wicherek, C., König, A., Laschner, W. & Rautenstrauch, H. (1996) 'Quantitative photometrical assessment of iron deposits in synovial membranes in different joint diseases', *Rheumatology International,* **15**(5): 211-6.

Fu, J., Ikegami, H., Kawaguchi, Y., Fujisawa, T., Kawabata, Y., Hamada, Y., Ueda, H., Shintani, M., Nojima, K., Babaya, N., Shen, Q.J., Uchigata, Y., Urakami, T., Omori, Y., Shima, K. & Ogihara, T. (1998) 'Association of distal chromosome 2q with IDDM in Japanese subjects', *Diabetologia,* **41**(2): 228-32.

Gabriel, H.E., Crott, J.W., Ghandour, H., Dallal, G.E., Choi, S.W., Keyes, M.K., Jang, H., Liu, Z., Nadeau, M., Johnston, A., Mager, D. & Mason, J.B. (2006) 'Chronic cigarette smoking is associated with diminished folate status, altered folate form distribution, and increased genetic damage in the buccal mucosa of healthy adults', *The American Journal of Clinical Nutrition,* **83**(4): 835-41.

Gao, P.S., Fujishima, S., Mao, X.Q., Remus, N., Kanda, M., Enomoto, T., Dake, Y., Bottini, N., Tabuchi, M., Hasegawa, N., Yamaguchi, K., Tiemessen, C., Hopkin, J.M., Shirakawa, T. & Kishi, F. (2000) 'Genetic variants of NRAMP1 and active tuberculosis in Japanese populations', *Clinical Genetics,* **58**(1): 74-6.

Garrick, L.M., Dolan, K.G., Romano, M.A. & Garrick, M.D. (1999) 'Non-transferrin-bound iron uptake in Belgrade and normal rat erythroid cells', *Journal of Cellular Physiology,* **178**(3): 349-58.

Gazouli, M., Atsaves, V., Mantzaris, G., Economou, M., Nasioulas, G., Evangelou, K., Archimandritis, A.J. & Anagnou, N.P. (2008a) 'Role of functional polymorphisms of NRAMP1 gene for the development of Crohn's disease', *Inflammatory Bowel Diseases,* **14**(10): 1323-30.

Gazouli, M., Koundourakis, A., Ikonomopoulos, J., Gialafos, E.J., Papaconstantinou, I., Nasioulas, G., Lukas, J.C. & Gorgoulis, V.G. (2007) 'The functional polymorphisms of NRAMP1 gene in Greeks with sarcoidosis', *Sarcoidosis, Vasculitis, and Diffuse Lung Diseases* **24**(2): 153-4.

Gazouli, M., Sechi, L., Paccagnini, D., Sotgiu, S., Arru, G., Nasioulas, G. & Vassilopoulos, D. (2008b) 'NRAMP1 polymorphism and viral factors in Sardinian multiple sclerosis patients', *The Canadian Journal of Neurological Sciences,* **35**(4): 491-4.

Gazzinelli, R.T., Oswald, I.P., James, S.L. & Sher, A. (1992) 'IL-10 inhibits parasite killing and nitrogen oxide production by IFN-gamma-activated macrophages', *Journal of Immunology,* **148**(6): 17292-96.

Gomes, M.S. & Appelberg, R. (1998) 'Evidence for a link between iron metabolism and Nramp1 gene function in innate resistance against Mycobacterium avium', *Immunology,* **95**(2): 165-168.

Gordon, S. (2003) 'Alternative activation of macrophages', *Nature Reviews Immunology,* **3**(1): 23-35.

Goswami, T., Bhattacharjee, A., Babal, P., Searle, S., Moore, E., Li, M. & Blackwell, J.M. (2001) 'Natural-resistance-associated macrophage protein 1 is an H+/bivalent cation antiporter', *Biochemical Journal,* **354**(3): 511–19.

Govoni, G., Canonne-Hergaux, F.O., Pfeifer, C.G., Marcus, S.L., Mills, S.D., Hackam, D.J., Grinstein, S., Malo, D., Finlay, B.B. & Gros, P. (1999) 'Functional Expression of Nramp1 In Vitro in the Murine Macrophage Line RAW264.7', *Infection and Immunity,* **67**(5): 2225-32.

Govoni, G., Vidal, S., Cellier, M., Lepage, P., Malo, D. & Gros, P. (1995) 'Genomic Structure, Promoter Sequence, and Induction of Expression of the Mouse Nramp1 Gene in Macrophages', *Genomics,* **27**(1): 9-19.

Govoni, G., Vidal, S., Gauthier, S., Skamene, E., Malo, D. & Gros, P. (1996) 'The Bcg/Ity/Lsh locus: genetic transfer of resistance to infections in C57BL/6J mice transgenic for the Nramp1 Gly169 allele', *Infection and Immunity,* **64**(8): 2923-9.

Graham, A.M., Dollinger, M.M., Howie, S.E.M. & Harrison, D.J. (2000) 'Identification of novel alleles at a polymorphic microsatellite repeat region in the human NRAMP1 gene promoter: analysis of allele frequencies in primary biliary cirrhosis', *Journal of Medical Genetics,* **37**(2): 150-52.

Graham, F.L., Smiley, J., Russell, W.C. & Nairn, R. (1977) 'Characteristics of a Human Cell Line Transformed by DNA from Human Adenovirus Type 5', *Journal of General Virology,* **36**(1): 59-72.

Graham, R., Liew, M., Meadows, C., Lyon, E. & Wittwer, C.T. (2005) 'Distinguishing different DNA heterozygotes by high-resolution melting', *Clinical Chemistry,* **51**(7): 1295-8.

Greenwood, C.M., Fujiwara, T.M., Boothroyd, L.J., Miller, M.A., Frappier, D., Fanning, E.A., Schurr, E. & Morgan, K. (2000) 'Linkage of tuberculosis to chromosome 2q35 loci, including NRAMP1, in a large aboriginal Canadian family.' *American Journal of Human Genetics,* **67**(2): 405-16.

Gruenheid, S., Canonne-Hergaux, F., Gauthier, S., Hackam, D.J., Grinstein, S. & Gros, P. (1999) 'The Iron Transport Protein NRAMP2 Is an Integral Membrane Glycoprotein That Colocalizes with Transferrin in Recycling Endosomes', *The Journal of Experimental Medicine,* **189**(5): 831-41.

Gruenheid, S., Cellier, M., Vidal, S. & Gros, P. (1995) 'Identification and characterization of a second mouse Nramp gene', *Genomics,* **25**(2): 514-25.

Gruenheid, S. & Gros, P. (2000) 'Genetic susceptibility to intracellular infections: Nramp1, macrophage function and divalent cations transport', *Current Opinion in Microbiology,* **3**(1): 43-8.

Gruenheid, S., Pinner, E., Desjardins, M. & Gros, P. (1997) 'Natural Resistance to Infection with Intracellular Pathogens: The Nramp1 Protein Is Recruited to the Membrane of the Phagosome', *The Journal of Experimental Medicine,* **185**(4): 717-30.

Gundry, C.N., Vandersteen, J.G., Reed, G.H., Pryor, R.J., Chen, J. & Wittwer, C.T. (2003) 'Amplicon melting analysis with labeled primers: a closed-tube method for differentiating homozygotes and heterozygotes', *Clinical Chemistry,* **49**(3): 396-406.

Ha, S.C., Lowenhaupt, K., Rich, A., Kim, Y.G. & Kim, K.K. (2005) 'Crystal structure of a junction between B-DNA and Z-DNA reveals two extruded bases', *Nature,* **437**(706): 1183-6.

Hackam, D.J., Rotstein, O.D., Zhang, W.J., Gruenheid, S., Gros, P. & Grinstein, S. (1998) 'Host Resistance to Intracellular Infection: Mutation of Natural Resistance-associated Macrophage Protein 1 (Nramp1) Impairs Phagosomal Acidification', *The Journal of Experimental Medicine,* **188**(2): 351-64.

Hanly, M.G. (2001) Methods in Leukocyte Cytochemistry. *Hematologic Malignancies: Methods and Techniques.* New Jersey, Humana Press.

Harty, L.C., Garcia-Closas, M., Rothman, N., Reid, Y.A., Tucker, M.A. & Hartge, P. (2000) 'Collection of buccal cell DNA using treated cards', *Cancer Epidemiology, Biomarkers & Prevention* **9**(5): 501-6.

Hatta, M., Ratnawati, Tanaka, M., Ito, J., Shirakawa, T. & Kawabata, M. (2010) 'NRAMP1/SLC11A1 gene polymorphisms and host susceptibility to Mycobacterium tuberculosis and M. leprae in South Sulawesi, Indonesia', *The Southeast Asian Journal of Tropical Medicine and Public Health,* **41**(2): 386-94.

Haverkamp, M.H., Lindeboom, J.A., de Visser, A.W., Kremer, D., Kuijpers, T.W., van de Vosse, E. & van Dissel, J.T. (2010) 'Nontuberculous mycobacterial cervicofacial lymphadenitis in children from the multicenter, randomized, controlled trial in The Netherlands: Relevance of polymorphisms in candidate host immunity genes', *International Journal of Pediatric Otorhinolaryngology,* **74**(7): 752-4.

Heath, E.M., O'Brien, D.P., Banas, R., Naylor, E.W. & Dobrowolski, S. (1999) 'Optimization of an automated DNA purification protocol for neonatal screening', *Archives of Pathology & Laboratory Medicine,* **123**(12): 1154-60.

Herbert, A. & Rich, A. (1999) 'Left-handed Z-DNA: structure and function', *Genetica,* **106**(1-2): 37-47.

Herrmann, M.G., Durtschi, J.D., Bromley, L.K., Wittwer, C.T. & Voelkerding, K.V. (2006) 'Amplicon DNA melting analysis for mutation scanning and genotyping: cross-platform comparison of instruments and dyes', *Clinical Chemistry,* **52**(3): 494-503.

Hill, N.J., Lyons, P.A., Armitage, N., Todd, J.A., Wicker, L.S. & Peterson, L.B. (2000) 'NOD Idd5 locus controls insulitis and diabetes and overlaps the orthologous CTLA4/IDDM12 and NRAMP1 loci in humans', *Diabetes,* **49**(10): 1744-7.

Ho, P.S. (1994) 'The non-B-DNA structure of d(CA/TG)n does not differ from that of Z-DNA', *Proceedings of the National Academy of Sciences of the United States of America,* **91**(20): 9549-53.

Ho, P.S., Ellison, M.J., Quigley, G.J. & Rich, A. (1986) 'A computer aided thermodynamic approach for predicting the formation of Z-DNA in naturally occurring sequences', *The EMBO Journal,* **5**(10): 2737-44.

Hoal, E.G., Lewis, L.A., Jamieson, S.E., Tanzer, F., Rossouw, M., Victor, T., Hillerman, R., Beyers, N., Blackwell, J.M. & Van Helden, P.D. (2004) 'SLC11A1 (NRAMP1) but not SLC11A2 (NRAMP2) polymorphisms are associated with susceptibility to tuberculosis in a high-incidence community in South Africa', *The International Journal of Tuberculosis and Lung Disease* **8**(12): 1464-71.

Hsu, Y.H., Chen, C.W., Sun, H.S., Jou, R., Lee, J.J. & Su, I.J. (2006) 'Association of NRAMP 1 gene polymorphism with susceptibility to tuberculosis in Taiwanese aboriginals', *Journal of the Formosan Medical Association,* **105**(5): 363-9.

Hu, J., Bumstead, N., Skamene, E., Gros, P. & Malo, D. (1996) 'Structural organization, sequence, and expression of the chicken NRAMP1 gene encoding the natural resistance-associated macrophage protein 1', *DNA and Cell Biology,* **15**(2): 113-23.

Huang, J.H., Oefner, P.J., Adi, V., Ratnam, K., Ruoss, S.J., Trako, E. & Kao, P.N. (1998) 'Analyses of the NRAMP1 and IFN-gammaR1 genes in women with Mycobacterium avium-intracellulare pulmonary disease', *American Journal of Respiratory and Critical Care Medicine,* **157**(2): 377-81.

Huber, R., Schlessinger, D. & Pilia, G. (1998) 'Multiple Sp1 sites efficiently drive transcription of the TATA-less promoter of the human glypican 3 (GPC3) gene', *Gene,* **214**(1-2): 35-44.

Ince, T.A. & Scotto, K.W. (1995) 'A conserved downstream element defines a new class of RNA polymerase II promoters', *The Journal of Biological Chemistry,* **270**(51): 30249-52.

Jabado, N., Jankowski, A., Dougaparsad, S., Picard, V., Grinstein, S. & Gros, P. (2000) 'Natural resistance to intracellular infections: natural resistance-associated macrophage protein 1 (NRAMP1) functions as a pH-dependent manganese transporter at the phagosomal membrane', *The Journal of Experimental Medicine,* **192**(9): 1237-48.

Javahery, R., Khachi, A., Lo, K., Zenzie-Gregory, B. & Smale, S.T. (1994) 'DNA sequence requirements for transcriptional initiator activity in mammalian cells', *Molecular Cell Biology,* **14**(1): 116-27.

Jiang, H.R., Gilchrist, D.S., Popoff, J.-F., Jamieson, S.E., Truscott, M., White, J.K. & Blackwell, J.M. (2009) 'Influence of *Slc11a1* (formerly *Nramp1*) on DSS-induced colitis in mice', *Journal of Leukocyte Biology,* **85**(4): 703-10.

Jiang, J.G. & Zarnegar, R. (1997) 'A novel transcriptional regulatory region within the core promoter of the hepatocyte growth factor gene is responsible for its inducibility by cytokines via the C/EBP family of transcription factors', *Molecular and Cell Biology,* **17**(10): 5758-70.

Jin, J., Sun, L., Jiao, W., Zhao, S., Li, H., Guan, X., Jiao, A., Jiang, Z. & Shen, A. (2009) 'SLC11A1 (Formerly NRAMP1) gene polymorphisms associated with pediatric tuberculosis in China', *Clinical Infectious Diseases,* **48**(6): 733-8.

Johanson, H.C., Hyland, V., Wicking, C. & Sturm, R.A. (2009) 'DNA elution from buccal cells stored on Whatman FTA Classic Cards using a modified methanol fixation method', *Biotechniques,* **46**(4): 309-11.

John, S., Marlow, A., Hajeer, A., Ollier, W., Silman, A. & Worthington, J. (1997) 'Linkage and association studies of the natural resistance associated macrophage protein 1 (NRAMP1) locus in rheumatoid arthritis', *The Journal of Rheumatology,* **24**(3): 452-7.

Jüni, P., Holenstein, F., Sterne, J., Bartlett, C. & Egger, M. (2002) 'Direction and impact of language bias in meta-analyses of controlled trials: empirical study', *International Journal of Epidemiology,* **31**(1): 115-23.

Juven-Gershon, T., Hsu, J.Y., Theisen, J.W.M. & Kadonaga, J.T. (2008) 'The RNA polymerase II core promoter -- the gateway to transcription', *Current Opinion in Cell Biology,* **20**(3): 253-9.

Kaczynski, J., Cook, T. & Urrutia, R. (2003) 'Sp1- and Kruppel-like transcription factors', *Genome Biology,* **4**(2): 206.

Karupiah, G., Hunt, N.H., King, N.J. & Chaudhri, G. (2000) 'NADPH oxidase, Nramp1 and nitric oxide synthase 2 in the host antimicrobial response', *Reviews in Immunogenetics,* **2**(3): 387-415.

Kashi, Y. & Soller, M. (1999) Functional roles of microsatellites and minisatellites. IN Goldstein, D.B. & Schlötterer, C. (Eds.) *Microsatellites: evolution and applications.* New York, Oxford University Press.

Kaye, P.M. & Blackwell, J.M. (1989) 'Lsh, antigen presentation and the development of CMI', *Research in Immunology,* **140**(8): 810-22.

Kaye, P.M., Patel, N.K. & Blackwell, J.M. (1988) 'Acquisition of cell-mediated immunity to Leishmania. II. LSH gene regulation of accessory cell function', *Immunology,* **65**(1): 17-22.

Khanna-Gupta, A., Zibello, T., Simkevich, C., Rosmarin, A.G. & Berliner, M. (2000) 'Sp1 and C/EBP are necessary to activate the lactoferrin gene promoter during myeloid differentiation', *Blood,* **95**(12): 3734-41.

Kim, E., Kim, K., Park, S., Kim, J., Lee, W., Cha, S., Kim, C., Kang, Y., Han, S., Jung, T. & Park, J. (2008) 'SLC11A1 Polymorphisms Are Associated with the Risk of Chronic Obstructive Pulmonary Disease in a Korean Population', *Biochemical Genetics,* **46**(7): 506-19.

Kim, J.H., Lee, S.Y., Lee, S.H., Sin, C., Shim, J.J., In, K.H., Yoo, S.H. & Kang, K.H. (2003) 'NRAMP1 genetic polymorphisms as a risk factor of tuberculous pleurisy', *The International Journal of Tuberculosis and Lung Disease,* **7**(4): 370-375.

Kim, S.K., Jang, W.C., Park, S.B., Park, D.Y., Bang, K.T., Lee, S.S., Jun, J.B., Yoo, D.H. & Chang, H.K. (2006) 'SLC11A1 gene polymorphisms in Korean patients with Behcet's disease', *Scandinavian Journal of Rheumatology,* **35**(5): 398-401.

Kishi, F. (1994) 'Isolation and Characterization of Human NRAMP cDNA', *Biochemical and Biophysical Research Communications,* **204**(3): 1074-80.

Kishi, F. & Nobumoto, M. (1995) 'Identification of natural resistance-associated macrophage protein in peripheral blood lymphocytes', *Immunology Letters,* **47**(1): 93-6.

Kishi, F., Tanizawa, Y. & Nobumoto, M. (1996) 'Structural analysis of human natural resistance-associated macrophage protein 1 promoter', *Molecular Immunology,* **33**(3): 265-8.

Kissler, S., Stern, P., Takahashi, K., Hunter, K., Peterson, L.B. & Wicker, L.S. (2006) 'In vivo RNA interference demonstrates a role for Nramp1 in modifying susceptibility to type 1 diabetes', *Nature Genetics,* **38**(4): 479-83.

Knapp, T., Hare, E., Feng, L., Zlokarnik, G. & Negulescu, P. (2003) 'Detection of beta-lactamase reporter gene expression by flow cytometry', *Cytometry,* **51A**(2): 68-78.

Knutson, M. & Wessling-Resnick, M. (2003) 'Iron Metabolism in the Reticuloendothelial System', *Critical Reviews in Biochemistry and Molecular Biology,* **38**(1): 61-88.

Knutson, M.D., Vafa, M.R., Haile, D.J. & Wessling-Resnick, M. (2003) 'Iron loading and erythrophagocytosis increase ferroportin 1 (FPN1) expression in J774 macrophages', *Blood,* **102**(12): 4191-7.

Koay, E.S.C. & Walmsley, N. (1996) *A Primer of Chemical Pathology,* Singapore, World Scientific Publishing.

Koh, W.J., Kwon, O.J., Kim, E.J., Lee, K.S., Ki, C.S. & Kim, J.W. (2005) 'NRAMP1 gene polymorphism and susceptibility to nontuberculous mycobacterial lung diseases', *Chest,* **128**(1): 94-101.

Kojima, Y., Kinouchi, Y., Takahashi, S., Negoro, K., Hiwatashi, N. & Shimosegawa, T. (2001) 'Inflammatory bowel disease is associated with a novel promoter polymorphism of natural resistance-associated macrophage protein 1 (NRAMP1) gene', *Tissue Antigens,* **58**(6): 379-84.

Kotlowski, R., Bernstein, C.N., Silverberg, M.S. & Krause, D.O. (2008) 'Population-based case-control study of alpha 1-antitrypsin and SLC11A1 in Crohn's disease and ulcerative colitis', *Inflammatory Bowel Diseases,* **14**(8): 1112-7.

Kotze, M.J., De Villiers, J.N.P., Rooney, R.N., Grobbelaar, J.J., Mansvelt, E.P.G., Bouwens, C.S.H., Carr, J., Stander, I. & du Plessis, L. (2001) 'Analysis of the NRAMP1 Gene Implicated in Iron Transport: Association with Multiple Sclerosis and Age Effects', *Blood Cells, Molecules, and Diseases* **27**(1): 44-53.

Lagier, A.J., Yoo, S.H., Alfonso, E.C., Meiners, S. & Fini, M.E. (2007) 'Inhibition of human corneal epithelial production of fibrotic mediator TGF-beta2 by basement membrane-like extracellular matrix', *Investigative Ophthalmology and Visual Science,* **48**(3): 1061-71.

Lang, T., Prina, E., Sibthorpe, D. & Blackwell, J.M. (1997) 'Nramp1 transfection transfers Ity/Lsh/Bcg-related pleiotropic effects on macrophage activation: influence on antigen processing and presentation', *Infection and Immunity,* **65**(2): 380-86.

Latchman, D.S. (2004) Eukaryotic Transcription Factors. New York, Academic Press.

Lay, M.J. & Wittwer, C.T. (1997) 'Real-time fluorescence genotyping of factor V Leiden during rapid-cycle PCR', *Clinical Chemistry,* **43**(12): 2262-7.

Le Naour, F., Hohenkirk, L., Grolleau, A., Misek, D.E., Lescure, P., Geiger, J.D., Hanash, S. & Beretta, L. (2001) 'Profiling changes in gene expression during differentiation and maturation of monocyte-derived dendritic cells using both oligonucleotide microarrays and proteomics', *The Journal of Biological Chemistry,* **267**(21): 17920-30.

Lehtonen, A., Ahlfors, H., Veckman, V., Miettinen, M., Lahesmaa, R. & Julkunen, I. (2007) 'Gene expression profiling during differentiation of human monocytes to macrophages or dendritic cells', *Journal of Leukocyte Biology,* **82**(3): 710-20.

Lema, C., Kohl-White, K., Lewis, L.R. & Dao, D.D. (2006) 'Optimized pH method for DNA elution from buccal cells collected in Whatman FTA cards', *Genetic Testing,* **10**(2): 126-30.

Leung, K.H., Yip, S.P., Wong, W.S., Yiu, L.S., Chan, K.K., Lai, W.M., Chow, E.Y., Lin, C.K., Yam, W.C. & Chan, K.S. (2007) 'Sex- and age-dependent association of SLC11A1 polymorphisms with tuberculosis in Chinese: a case control study', *BMC Infectious Diseases,* **7**:19.

Lewis, L.A., Victor, T.C., Helden, E.G., Blackwell, J.M., da Silva-Tatley, F., Tullett, S., Ehlers, M., Beyers, N., Donald, P.R. & van Helden, P.D. (1996) 'Identification of C to T mutation at position -236bp in the human NRAMP1 gene promoter', *Immunogenetics,* **44**(4): 309-11.

Li, H.T., Zhang, T.T., Zhou, Y.Q., Huang, Q.H. & Huang, J. (2006) 'SLC11A1 (formerly NRAMP1) gene polymorphisms and tuberculosis susceptibility: a meta-analysis', *The International Journal of Tuberculosis and Lung Disease* **10**(1): 3-12.

Liaw, Y.S., Tsai-Wu, J.J., Wu, C.H., Hung, C.C., Lee, C.N., Yang, P.C., Luh, K.T. & Kuo, S.H. (2002) 'Variations in the NRAMP1 gene and susceptibility of tuberculosis in Taiwanese', *The International Journal of Tuberculosis and Lung Disease* **6**(5): 454-60.

Liew, M., Pryor, R., Palais, R., Meadows, C., Erali, M., Lyon, E. & Wittwer, C.T. (2004) 'Genotyping of single-nucleotide polymorphisms by high-resolution melting of small amplicons', *Clinical Chemistry,* **50**(7): 1156-64.

Liu, H., Mulholland, N., Fu, H. & Zhao, K. (2006) 'Co-operative activity of BRG1 and Z-DNA formation in chromatin remodeling', *Molecular and Cell Biology,* **26**(7): 2550-9.

Liu, J., Fujiwara, T.M., Buu, N.T., Sanchez, F.O., Cellier, M., Paradis, A.J., Frappier, D., Skamene, E., Gros, P. & Morgan, K. (1995) 'Identification of polymorphisms and sequence variants in the human homologue of the mouse natural resistance-associated macrophage protein gene', *American Journal of Human Genetics,* **56**(4): 845-53.

Liu, L.F. & Wang, J.C. (1987) 'Supercoiling of the DNA template during transcription', *Proceedings of the National Academy of Sciences of the United States of America,* **84**(20): 7024-7.

Liu, W., Cao, W.C., Zhang, C.Y., Tian, L., Wu, X.M., Habbema, J.D.F., Zhao, Q.M., Zhang, P.H., Xin, Z.T., Li, C.Z. & Yang, H. (2004) 'VDR and NRAMP1 gene polymorphisms in susceptibility to pulmonary tuberculosis among the Chinese Han population: a case-control study', *The International Journal of Tuberculosis and Lung Disease,* **8**(4): 428-34.

Liu, W., Zhang, C.Y., Tian, L., Li, C.Z., Wu, X.M., Zhao, Q.M., Zhang, P.H., Yang, S.M., Yang, H. & Cao, W.C. (2003) 'A case-control study on natural-resistance-associated macrophage protein 1 gene polymorphisms and susceptibility to pulmonary tuberculosis', *Zhonghua Yu Fang Yi Xue Za Zhi,* **37**(6): 408-11.

Liu, Y., Nonnemacher, M.R. & Wigdahl, B. (2009) 'CCAAT/enhancer-binding proteins and the pathogenesis of retrovirus infection', *Future Microbiology,* **4**(3): 299-321.

Lo, K. & Smale, S.T. (1996) 'Generality of a functional initiator consensus sequence', *Gene,* **182**(1-2): 13-22.

Lohmueller, K.E., Pearce, C.L., Pike, M., Lander, E.S. & Hirschhorn, J.N. (2003) 'Meta-analysis of genetic association studies supports a contribution of common variants to susceptibility to common disease', *Nature Genetics,* **33**(2): 177-182.

London, S.J., Xia, J., Lehman, T.A., Yang, J.H., Granada, E., Chunhong, L., Dubeau, L., Li, T., David-Beabes, G.L. & Li, Y. (2001) 'Collection of Buccal Cell DNA in Seventh-Grade Children Using Water and a Toothbrush', *Cancer Epidemiology Biomarkers and Prevention,* **10**(11): 1227-30.

López-Rodríguez, C., Botella, L. & Corbí, A.L. (1997) 'CCAAT/enhancer binding proteins (C/EBP) regulate the tissue specific activity of the CD11c integrin gene promoter through functional interactions with Sp1 proteins', *The Journal of Biological Chemistry,* **272**(46): 29120-6.

Lum, A. & Le Marchand, L. (1998) 'A simple mouthwash method for obtaining genomic DNA in molecular epidemiological studies', *Cancer Epidemiology, Biomarkers & Prevention,* **7**(8): 719-24.

Lumley, T. (2009) Rmeta version 2.14, R package, http://cran.r-project.org.

Ma, J., Chen, T., Mandelin, J., Ceponis, A., Miller, N.E., Hukkanen, M., Ma, G.F. & Konttinen, Y.T. (2003) 'Regulation of macrophage activation', *Cellular and Molecular Life Sciences,* **60**(11): 2334-46.

Ma, X., Dou, S., Wright, J.A., Reich, R.A., Teeter, L.D., El Sahly, H.M., Awe, R.J., Musser, J.M. & Graviss, E.A. (2002) '5 dinucleotide repeat polymorphism of NRAMP1 and susceptibility to tuberculosis among Caucasian patients in Houston, Texas', *The International Journal of Tuberculosis and Lung Disease,* **6**(9): 818-23.

Mackay, J., Wright, C. & Bonfiglioli, R. (2008) 'A new approach to varietal identification in plants by microsatellite high resolution melting analysis: application to the verification of grapevine and olive cultivars', *Plant Methods,* **4**(1): 8.

Mackenzie, B. & Hediger, M.A. (2004) 'SLC11 family of H+-coupled metal-ion transporters NRAMP1 and DMT1', *Pflügers Archiv European Journal of Physiology,* **447**(5): 571-9.

Mader, E., Lukas, B. & Novak, J. (2008) 'A Strategy to Setup Codominant Microsatellite Analysis for High-Resolution-Melting-Curve-Analysis (HRM)', *BMC Genetics,* **9**:69.

Maier, L.M., Smyth, D.J., Vella, A., Payne, F., Cooper, J.D., Pask, R., Lowe, C., Hulme, J., Smink, L.J., Fraser, H., Moule, C., Hunter, K.M., Chamberlain, G., Walker, N., Nutland, S., Undlien, D.E., Ronningen, K.S., Guja, C., Ionescu-Tirgoviste, C., Savage, D.A., Strachan, D.P., Peterson, L.B., Todd, J.A., Wicker, L.S. & Twells, R.C. (2005) 'Construction and analysis of tag single nucleotide polymorphism maps for six human-mouse orthologous candidate genes in type 1 diabetes', *BMC genetics* **6**:9.

Makowski, G.S., Davis, E.L., Aslanzadeh, J. & Hopfer, S.M. (1995) 'Enhanced direct amplification of Guthrie card DNA following selective elution of PCR inhibitors', *Nucleic Acids Research,* **23**(18): 3788-9.

Maliarik, M.J., Chen, K.M., Sheffer, R.G., Rybicki, B.A., Major, M.L., Popovich, J., Jr. & Iannuzzi, M.C. (2000) 'The Natural Resistance-Associated Macrophage Protein Gene in African Americans with Sarcoidosis', *American Journal of Respiratory Cell and Molecular Biology,* **22**(6): 672-5.

Malo, D., Vogan, K., Vidal, S., Hu, J., Cellier, M., Schurr, E., Fuks, A., Bumstead, N., Morgan, K. & Gros, P. (1994) 'Haplotype Mapping and Sequence Analysis of the Mouse Nramp Gene Predict Susceptibility to Infection with Intracellular Parasites', *Genomics,* **23**(1): 51-61.

Marquet, S., Lepage, P., Hudson, T.J., Musser, J.M. & Schurr, E. (2000) 'Complete nucleotide sequence and genomic structure of the human NRAMP1 gene region on Chromosome region 2q35', *Mammalian Genome,* **11**(9): 755-62.

Marquet, S., Sanchez, F.O., Arias, M., Rodriguez, J., Parks, S.C., Skamene, E., Schurr, E. & Garcia, L.F. (1999) 'Variants of the Human NRAMP1 Gene and Altered Human Immunodeficiency Virus Infection Susceptibility', *Journal of Infectious Diseases,* **180**(5): 1521-25.

Martinet, W., Schrijvers, D.M. & Kockx, M.M. (2003) 'Nucleofection as an efficient nonviral transfection method for human monocytic cells', *Biotechnology Letters,* **25**(13): 1025-29.

Marziliano, N., Pelo, E., Minuti, B., Passerini, I., Torricelli, F. & Da Prato, L. (2000) 'Melting temperature assay for a UGT1A gene variant in Gilbert syndrome', *Clinical Chemistry,* **46**(3): 423-5.

Mattick, J.S. (2007) 'A new paradigm for developmental biology', *The Journal of Experimental Biology,* **210**(9): 1526-47.

Matutes, E., Morilla, R. & Catovsky, D. (2006) Chapter 14 - Immunophenotyping. *Dacie and Lewis Practical Haematology (Tenth Edition).* Philadelphia, Churchill Livingstone.

McDermid, J.M. & Prentice, A.M. (2006) 'Iron and infection: effects of host iron status and the iron-regulatory genes haptoglobin and NRAMP1 (SLC11A1) on host-pathogen interactions in tuberculosis and HIV', *Clinical Science,* **110**(5): 503-24.

McDermid, J.M., van der Loeff, M.F.S., Jaye, A., Hennig, B.J., Bates, C., Todd, J., Sirugo, G., Hill, A.V., Whittle, H.C. & Prentice, A.M. (2009) 'Mortality in HIV infection is independently predicted by host iron status and SLC11A1 and HP genotypes, with new evidence of a gene-nutrient interaction', *The American Journal of Clinical Nutrition,* **90**(1): 225-33.

McKeon, C., Accili, D., Chen, H., Pham, T. & Walker, G.E. (1997) 'A Conserved Region in the First Intron of the Insulin Receptor Gene Binds Nuclear Proteins during Adipocyte Differentiation', *Biochemical and Biophysical Research Communications,* **240**(3): 701-6.

Meisner, S.J., Mucklow, S., Warner, G., Sow, S.O., Lienhardt, C. & Hill, A.V. (2001) 'Association of NRAMP1 polymorphism with leprosy type but not susceptibility to leprosy per se in west Africans ', *American Journal of Tropical Medicine and Hygiene,* **65**(6): 733-5.

Mendes, D., Correia, M., Barbedo, M., Vaio, T., Mota, M., Gonçalves, O. & Valente, J. (2009) 'Behçet's disease - a contemporary review', *Journal of Autoimmunity,* **32**(3-4): 178-88.

Merza, M., Farnia, P., Anoosheh, S., Varahram, M., Kazampour, M., Pajand, O., Saeif, S., Mirsaeidi, M., Masjedi, M.R., Velayati, A.A. & Hoffner, S. (2009) 'The NRAMP1, VDR and TNF-alpha gene polymorphisms in Iranian tuberculosis patients: the study on host susceptibility', *The Brazilian Journal of Infectious Diseases,* **13**(4): 252-6.

Mhlanga, M.M. & Malmberg, L. (2001) 'Using molecular beacons to detect single-nucleotide polymorphisms with real-time PCR', *Methods,* **25**(4): 463-71.

Milne, E., van Bockxmeer, F.M., Robertson, L., Brisbane, J.M., Ashton, L.J., Scott, R.J. & Armstrong, B.K. (2006) 'Buccal DNA collection: comparison of buccal swabs with FTA cards', *Cancer Epidemiology, Biomarkers & Prevention,* **15**(4): 816-9.

Mohamed, H.S., Ibrahim, M.E., Miller, E.N., White, J.K., Cordell, H.J., Howson, J.M., Peacock, C.S., Khalil, E.A., El Hassan, A.M. & Blackwell, J.M. (2004) 'SLC11A1 (formerly NRAMP1) and susceptibility to visceral leishmaniasis in The Sudan', *European Journal of Human Genetics,* **12**(1): 66-74.

Moore, K.W., de Waal Malefyt, R., Coffman, R.L. & O'Garra, A. (2001) 'Interleukin-10 and the interleukin-10 receptor', *Annual Review of Immunology,* **19**(1): 683-765.

Morahan, G., Huang, D., Tait, B.D., Colman, P.G. & Harrison, L.C. (1996) 'Markers on distal chromosome 2q linked to insulin-dependent diabetes mellitus', *Science,* **272**(5269): 1811-3.

Motsinger-Reif, A., Antas, P., Oki, N., Levy, S., Holland, S. & Sterling, T. (2010) 'Polymorphisms in IL-1beta, vitamin D receptor Fok1, and Toll-like receptor 2 are associated with extrapulmonary tuberculosis', *BMC Medical Genetics,* **11**:37.

Mulero, V., Searle, S., Blackwell, J.M. & Brock, J.H. (2002) 'Solute carrier 11a1 (Slc11a1; formerly Nramp1) regulates metabolism and release of iron acquired by phagocytic, but not transferrin-receptor-mediated, iron uptake', *The Biochemical Journal,* **363**(1): 89-94.

Mulot, C., Stucker, I., Clavel, J., Beaune, P. & Loriot, M.A. (2005) 'Collection of human genomic DNA from buccal cells for genetics studies: comparison between cytobrush, mouthwash, and treated card', *Journal of Biomedicine & Biotechnology,* **2005**(3): 291-6.

Muthukrishnan, M., Singanallur, N.B., Ralla, K. & Villuppanoor, S.A. (2008) 'Evaluation of FTA cards as a laboratory and field sampling device for the detection of foot-and-mouth disease virus and serotyping by RT-PCR and real-time RT-PCR', *Journal of Virological Methods,* **151**(2): 311-6.

Natsuka, S., Akira, S., Nishio, Y., Hashimoto, S., Sugita, T., Isshiki, H. & Kishimoto, T. (1992) 'Macrophage differentiation-specific expression of NF-IL6, a transcription factor for interleukin-6', *Blood,* **79**(2): 460-6.

Neil, H., Malabat, C., d'Aubenton-Carafa, Y., Xu, Z., Steinmetz, L.M. & Jacquier, A. (2009) 'Widespread bidirectional promoters are the major source of cryptic transcripts in yeast', *Nature,* **457**(7232): 1038-42.

Nerlov, C. & Ziff, E.B. (1995) 'CCAAT/enhancer binding protein-α amino acid motifs with dual TBP and TFIIB binding abitiy co-operate to activate transcription in both yeast and mammalian cells', *The EMBO Journal,* **14**(17): 4318-28.

Newport, M., Levin, M., Blackwell, J.M., Shaw, M.A., Williamson, R. & Huxley, C. (1995) 'Evidence for exclusion of a mutation in NRAMP as the cause of familial disseminated atypical mycobacterial infection in a Maltese kindred', *Journal of Medical Genetics* **32**(11): 904-6.

Niedergang, F. & Chavrier, P. (2004) 'Signaling and membrane dynamics during phagocytosis: many roads lead to the phagos(R)ome', *Current Opinion in Cell Biology,* **16**(4): 422-8.

Nielsen, O.J., Andersen, L.S., Hansen, N.E. & Hansen, T.M. (1994) 'Serum transferrin receptor levels in anaemic patients with rheumatoid arthritis', *Scandinavian Journal of Clinical & Laboratory Investigation,* **54**(1): 75-82.

Nino-Moreno, P., Portales-Perez, D., Hernandez-Castro, B., Portales-Cervantes, L., Flores-Meraz, V., Baranda, L., Gomez-Gomez, A., Acuna-Alonzo, V., Granados, J. & Gonzalez-Amaro, R. (2007) 'P2X(7) and NRAMP1/SLC11A1 gene polymorphisms in Mexican mestizo patients with pulmonary tuberculosis', *Clinical and Experimental Immunology,* **148**(3): 469-77.

Nishimura, M. & Naito, S. (2008) 'Tissue-specific mRNA expression profiles of human solute carrier transporter superfamilies', *Drug Metabolism and Pharmacokinetics,* **23**(1): 22-44.

Nishino, M., Ikegami, H., Fujisawa, T., Kawaguchi, Y., Kawabata, Y., Shintani, M., Ono, M. & Ogihara, T. (2005) 'Functional polymorphism in Z-DNA–forming motif of promoter of SLC11A1 gene and type 1 diabetes in Japanese subjects: Association study and meta-analysis ', *Metabolism Clinical and Experimental,* **54**(5): 628-33.

Nordheim, A., Lafer, E.M., Peck, L.J., Wang, J.C., Stollar, B.D. & Rich, A. (1982) 'Negatively supercoiled plasmids contain left-handed Z-DNA segments as detected by specific antibody binding', *Cell,* **31**(1): 309-18.

O'Brien, B.A., Archer, N.S., Simpson, A.M., Torpy, F.R. & Nassif, N.T. (2008) 'Association of SLC11A1 promoter polymorphisms with the incidence of autoimmune and inflammatory diseases: A meta-analysis', *Journal of Autoimmunity,* **31**(1): 42-51.

O'Shea-Greenfield, A. & Smale, S. (1992) 'Roles of TATA and initiator elements in determining the start site location and direction of RNA polymerase II transcription', *The Journal of Biological Chemistry,* **267**(2): 1391-402.

Oosterom, J., van Doornmalen, E.J., Lobregt, S., Blomenröhr, M. & Zaman, G.J.R. (2005) 'High-Throughput Screening Using beta-Lactamase Reporter-Gene Technology for Identification of Low-Molecular-Weight Antagonists of the Human Gonadotropin Releasing Hormone Receptor', *ASSAY and Drug Development Technologies,* **3**(2): 143-54.

Ouchi, K., Suzuki, Y., Shirakawa, T. & Kishi, F. (2003) 'Polymorphism of SLC11A1 (Formerly NRAMP1) Gene Confers Susceptibility to Kawasaki Disease', *Journal of Infectious Diseases,* **187**(2): 326-29.

Paccagnini, D., Sieswerda, L., Rosu, V., Masala, S., Pacifico, A., Gazouli, M., Ikonomopoulos, J., Ahmed, N., Zanetti, S. & Sechi, L.A. (2009) 'Linking Chronic Infection and Autoimmune Diseases: *Mycobacterium avium* Subspecies *paratuberculosis*, *SLC11A1* Polymorphisms and Type-1 Diabetes Mellitus', *PLoS ONE,* **4**(9): e7109.

Pai, C.Y., Hsieh, L.L., Lee, T.C., Yang, S.B., Linville, J., Chou, S.L. & Yang, C.H. (2006) 'Mitochondrial DNA sequence alterations observed between blood and buccal cells within the same individuals having betel quid (BQ)-chewing habit', *Forensic Science International,* **156**(2): 124-30.

Pai, C.Y., Hsieh, L.L., Tsai, C.W., Chiou, F.S., Yang, C.H. & Hsu, B.D. (2002) 'Allelic alterations at the STR markers in the buccal tissue cells of oral cancer patients and the oral epithelial cells of healthy betel quid-chewers: an evaluation of forensic applicability', *Forensic Science International,* **129**(3): 158-67.

Palais, R.A., Liew, M.A. & Wittwer, C.T. (2005) 'Quantitative heteroduplex analysis for single nucleotide polymorphism genotyping', *Analytical Biochemistry,* **346**(1): 167-75.

Park, E., Jung, H., Yang, H., Yoo, M., Kim, C. & Kim, K. (2007) 'Optimized THP-1 differentiation is required for the detection of responses to weak stimuli', *Inflammation Research,* **56**(1): 45-50.

Pavesi, G., Zambelli, F. & Pesole, G. (2007) 'WeederH: an algorithm for finding conserved regulatory motifs and regions in homologous sequences', *BMC Bioinformatics,* **7**(8): 46-59.

Payne, S.M. (1993) 'Iron acquisition in microbial pathogenesis', *Trends in Microbiology,* **1**(2): 66-9.

Payton, S.G., Whetstine, J.R., Ge, Y. & Matherly, L.H. (2005) 'Transcriptional regulation of the human reduced folate carrier promoter C: synergistic transactivation by Sp1 and C/EBP β and identification of a downstream repressor', *Biochimica et Biophysica Acta (BBA) - Gene Regulatory Mechanisms,* **1727**(1): 45-57.

Peck, L.J., Nordheim, A., Rich, A. & Wang, J.C. (1982) 'Flipping of cloned d(pCpG)n.d(pCpG)n DNA sequences from right- to left-handed helical structure by salt, Co(III), or negative supercoiling', *Proceedings of the National Academy of Sciences of the United States of America,* **79**(15): 4560-64.

Pedersen, T.A., Kowenz-Leutz, E., Leutz, A. & Nerlov, C. (2001) 'Cooperation between C/EBPalpha TBP/TFIIB and SWI/SNF recruiting domains is required for adipocyte differentiation', *Genes and Development,* **15**(23): 3208-16.

Pie, S., Matsiota-Bernard, P., Truffa-Bachi, P. & Nauciel, N. (1996) 'Gamma interferon and interleukin-10 gene expression in innately susceptible and resistant mice during the early phase of *Salmonella typhimurium* infection', *Infection and Immunity,* **162**(3): 6122-31.

Pirulli, D., Boniotto, M., Puzzer, D., Spano, A., Amoroso, A. & Crovella, S. (2000) 'Flexibility of melting temperature assay for rapid detection of insertions, deletions, and single-point mutations of the AGXT gene responsible for type 1 primary hyperoxaluria', *Clinical Chemistry,* **46**(11): 1842-4.

Plant, J. & Glynn, A.A. (1974) 'Genetics of resistance to infection with *Salmonella typhimurium* in mice', *The Journal of Infectious Diseases,* **133**(1): 72-8.

Plevy, S.E., Gemberling, J.H., Hsu, S., Dorner, A.J. & Smale, S.T. (1997) 'Multiple control elements mediate activation of the murine and human interleukin 12 p40 promoters: evidence of functional synergy between C/EBP and Rel proteins', *Molecular and Cell Biology,* **17**(8): 4572-88.

Poland, D. (1974) 'Recursion relation generation of probability profiles for specific-sequence macromolecules with long-range correlations', *Biopolymers,* **13**(9): 1859-71.

Puzyrev, V.P., Freĭdin, M.B., Rudko, A.A., Strelis, A.K. & Kolokolova, O.V. (2002) 'Polymorphisms of the candidate genes for genetic susceptibility to tuberculosis in the Slavic population of Siberia: a pilot study', *Molecular Biology,* **36**(5): 788-91.

Qu, Y., Tang, Y., Cao, D., Wu, F., Liu, J., Lu, G., Zhang, Z. & Xia, Z. (2007) 'Genetic polymorphisms in alveolar macrophage response-related genes, and risk of silicosis and pulmonary tuberculosis in Chinese iron miners', *International Journal of Hygiene and Environmental Health,* **210**(6): 679-89.

Qureshi, S.A. (2007) 'Beta-lactamase: an ideal reporter system for monitoring gene expression in live eukaryotic cells', *Biotechniques,* **42**(1): 91-6.

R Development Core Team (2008) R: A language and environment for statistical computing, Vienna, Austria, http://www.R-project.org.

Radzioch, D., Kramnik, I. & Skamene, E. (1994) 'Molecular mechanisms of natural resistance to mycobacterial infections', *Circulatory Shock,* **44**(3): 115-20.

Rajendram, D., Ayenza, R., Holder, F.M., Moran, B., Long, T. & Shah, H.N. (2006) 'Long-term storage and safe retrieval of DNA from microorganisms for molecular analysis using FTA matrix cards', *Journal of Microbiological Methods,* **67**(3): 582-92.

Reed, G.H., Kent, J.O. & Wittwer, C.T. (2007) 'High-resolution DNA melting analysis for simple and efficient molecular diagnostics', *Pharmacogenomics,* **8**(6): 597-608.

Reed, G.H. & Wittwer, C.T. (2004) 'Sensitivity and specificity of single-nucleotide polymorphism scanning by high-resolution melting analysis', *Clinical Chemistry,* **50**(10): 1748-54.

Resendes, K.K. & Rosmarin, A.G. (2004) 'Sp1 Control of Gene Expression in Myeloid Cells', *Critical Reviews in Eukaryotic Gene Expression,* **14**(3): 171-81.

Rich, A. & Zhang, S. (2003) 'Z-DNA: The long road to biological function', *Nature Reviews Genetics,* **4**(7): 566-72.

Richer, E., Campion, C.G., Dabbas, B., White, J.H. & Cellier, M.F. (2008) 'Transcription factors Sp1 and C/EBP regulate NRAMP1 gene expression', *The FEBS Journal,* **275**(20): 5074-89.

Rioja, I., Clayton, C., Graham, S., Life, P. & Dickson, M. (2005) 'Gene expression profiles in the rat streptococcal cell wall-induced arthritis model identified using microarray analysis', *Arthritis Research and Therapy,* **7**(1): R101-7.

Ririe, K.M., Rasmussen, R.P. & Wittwer, C.T. (1997) 'Product differentiation by analysis of DNA melting curves during the polymerase chain reaction', *Analytical Biochemistry,* **245**(2): 154-60.

Roach, T.I., Barton, C.H., Chatterjee, D. & Blackwell, J.M. (1993) 'Macrophage activation: lipoarabinomannan from avirulent and virulent strains of Mycobacterium tuberculosis differentially induces the early genes c-fos, KC, JE, and tumor necrosis factor-alpha', *Journal of Immunology* **150**(5): 1886-96.

Roach, T.I., Chatterjee, D. & Blackwell, J.M. (1994) 'Induction of early-response genes KC and JE by mycobacterial lipoarabinomannans: regulation of KC expression in murine macrophages by Lsh/Ity/Bcg (candidate Nramp)', *Infection and Immunity,* **62**(4): 1176-84.

Rodriguez, M.R., Gonzalez-Escribano, M.F., Aguilar, F., Valenzuela, A., Garcia, A. & Nunez-Roldan, A. (2002) 'Association of NRAMP1 promoter gene polymorphism with the susceptibility and radiological severity of rheumatoid arthritis', *Tissue Antigens,* **59**(4): 311-15.

Roger, M., Levee, G., Chanteau, S., Gicquel, B. & Schurr, E. (1997) 'No evidence for linkage between leprosy susceptibility and the human natural resistance-associated macrophage protein 1 (NRAMP1) gene in French Polynesia', *International Journal of Leprosy and Other Mycobacterial Diseases* **65**(2): 197-202.

Roger, M., Sanchez, F.O. & Schurr, E. (1998) 'Comparative study of the genomic organization of DNA repeats within the 5'-flanking region of the natural resistance-associated macrophage protein gene (NRAMP1) between humans and great apes', *Mammalian genome,* **9**(6): 435-9.

Roig, E.A., Richer, E., Canonne-Hergaux, F., Gros, P. & Cellier, M.F. (2002) 'Regulation of NRAMP1 gene expression by 1alpha,25-dihydroxy-vitamin D(3) in HL-60 phagocytes', *Journal of Leukocyte Biology,* **71**(5): 890-904.

Rojas, M., Olivier, M., Gros, P., Barrera, L.F. & Garcia, L.F. (1999) 'TNF-α and IL-10 Modulate the Induction of Apoptosis by Virulent Mycobacterium tuberculosis in Murine Macrophages', *The Journal of Immunology,* **162**(10): 6122-31.

Roy, S., Frodsham, A., Saha, B., Hazra, S.K., Mascie-Taylor, C.G. & Hill, A.V. (1999) 'Association of Vitamin D Receptor Genotype with Leprosy Type', *The Journal of Infectious Diseases,* **179**(1): 187-91.

Runstadler, J.A., Säilä, H., Savolainen, A., Leirisalo-Repo, M., Aho, K., Tuomilehto-Wolf, E., Tuomilehto, J. & Seldin, M.F. (2005) 'Association of SLC11A1 (NRAMP1) with persistent oligoarticular and polyarticular rheumatoid factor-negative juvenile idiopathic arthritis in Finnish patients: Haplotype analysis in Finnish families', *Arthritis & Rheumatism,* **52**(1): 247-56.

Rupa, D.S. & Eastmond, D.A. (1997) 'Chromosomal alterations affecting the 1cen-1q12 region in buccal mucosal cells of betel quid chewers detected using multicolor fluorescence in situ hybridization', *Carcinogenesis,* **18**(12): 2347-51.

Ryu, S., Park, Y.K., Bai, G.H., Kim, S.J., Park, S.N. & Kang, S. (2000) '3'UTR polymorphisms in the NRAMP1 gene are associated with susceptibility to tuberculosis in Koreans', *The International Journal of Tuberculosis and Lung Disease* **4**(6): 577-80.

Sahiratmadja, E., Wieringa, F.T., van Crevel, R., de Visser, A.W., Adnan, I., Alisjahbana, B., Slagboom, E., Marzuki, S., Ottenhoff, T.H., van de Vosse, E. & Marx, J.J. (2007) 'Iron deficiency and NRAMP1 polymorphisms (INT4, D543N and 3'UTR) do not contribute to severity of anaemia in tuberculosis in the Indonesian population', *The British Journal of Nutrition,* **98**(4): 684-90.

Sakitani, K., Nishizawa, M., Inoue, K., Masu, Y., Okumura, T. & Ito, S. (1998) 'Synergistic regulation of inducible nitric oxide synthase gene by CCAAT/enhancer-binding protein β and nuclear factor-κB in hepatocytes', *Genes to Cells,* **3**(5): 321-30.

Samaranayake, T.N., Fernando, S.D. & Dissanayake, V.H.W. (2010) 'Candidate gene study of susceptibility to cutaneous leishmaniasis in Sri Lanka', *Tropical Medicine & International Health,* **15**(5): 632-8.

Sanjeevi, C.B., Miller, E.N., Dabadghao, P., Rumba, I., Shtauvere, A., Denisova, A., Clayton, D. & Blackwell, J.M. (2000) 'Polymorphism at NRAMP1 and D2S1471 loci associated with juvenile rheumatoid arthritis', *Arthritis & Rheumatism,* **43**(6): 1397-404.

Scheller, M., Foerster, J., Heyworth, C.M., Waring, J.F., Löhler, J., Gilmore, G.L., Shadduck, R.K., Dexter, T.M. & Horak, I. (1999) 'Altered development and cytokine responses to myeliod progenitors in the absence of transcription factor, interferon consensus sequence binding protein', *Blood,* **94**(11): 3764-71.

Schnoor, M., Buers, I., Sietmann, A., Brodde, M.F., Hofnagel, O., Robenek, H. & Lorkowski, S. (2009) 'Efficient non-viral transfection of THP-1 cells', *Journal of Immunological Methods,* **344**(2): 109-15.

Schroth, G.P., Chou, P.J. & Ho, P.S. (1992) 'Mapping Z-DNA in the human genome. Computer-aided mapping reveals a nonrandom distribution of potential Z-DNA-forming sequences in human genes', *Journal of Biological Chemistry,* **267**(17): 11846-55.

Schug, J. (2003) Using TESS to Predict Transcription Factor Binding Sites in DNA Sequence. IN Baxevanis, A.D. (Ed.) *Current Protocols in Bioinformatics.* J. Wiley and Sons.

Schug, J. & Overton, C.G. (1997) 'TESS: Transcription Element Search Software on the WWW', (Technical Report): http://www.cbil.upenn.edu/TESS.

Schurr, E., Skamene, E., Morgan, K., Chu, M.L. & Gros, P. (1990) 'Mapping of Col3a1 and Col6a3 to proximal murine chromosome 1 identifies conserved linkage of structural protein genes between murine chromosome 1 and human chromosome 2q', *Genomics,* **8**(3): 477-86.

Searle, S. & Blackwell, J.M. (1999) 'Evidence for a functional repeat polymorphism in the promoter of the human NRAMP1 gene that correlates with autoimmune versus infectious disease susceptibility', *Journal of Medical Genetics,* **36**(4): 295-9.

Searle, S., Bright, N.A., Roach, T.I., Atkinson, P.G., Barton, C.H., Meloen, R.H. & Blackwell, J.M. (1998) 'Localisation of Nramp1 in macrophages: modulation with activation and infection', *Journal of Cell Science,* **111**(19): 2855-66.

Sechi, L.A., Gazouli, M., Sieswerda, L.E., Molicotti, P., Ahmed, N., Ikonomopoulos, J., Scanu, A.M., Paccagnini, D. & Zanetti, S. (2006) 'Relationship between Crohn's disease, infection with Mycobacterium avium subspecies paratuberculosis and SLC11A1 gene polymorphisms in Sardinian patients', *World Journal of Gastroenterology* **12**(44): 7161-4.

Selvaraj, P. (2000) 'Role of human leucocyte antigen (HLA) and non-HLA genes in susceptibility or resistance to pulmonary tuberculosis ', *The Indian Journal of Tuberculosis,* **47**(3): 133-8.

Selvaraj, P., Chandra, G., Kurian, S.M., Reetha, A.M., Charles, N. & Narayanan, P.R. (2002) 'NRAMP1 gene polymorphism in pulmonary and spinal tuberculosis', *Current Science,* **82**(4): 451-4.

Shaw, M.A., Clayton, D., Atkinson, S.E., Williams, H., Miller, N., Sibthorpe, D. & Blackwell, J.M. (1996) 'Linkage of rheumatoid arthritis to the candidate gene NRAMP1 on 2q35', *Journal of Medical Genetics,* **33**(8): 672-7.

Shaw, M.A., Clayton, D. & Blackwell, J.M. (1997a) 'Analysis of the candidate gene NRAMP1 in the first 61 ARC National Repository families for rheumatoid arthritis', *The Journal of Rheumatology,* **24**(1): 212-4.

Shaw, M.A., Collins, A., Peacock, C.S., Miller, E.N., Black, G.F., Sibthorpe, D., Lins-Lainson, Z., Shaw, J.J., Ramos, F., Silveira, F. & Blackwell, J.M. (1997b) 'Evidence that genetic susceptibility to Mycobacterium tuberculosis in a brazilian population is under oligogenic control: Linkage study of the candidate genes NRAMP1 and TBFA', *Tubercle and Lung Disease,* **78**(1): 35-45.

Shilna, T., Hosomichi, K., Inoko, H. & Kuiski, J.K. (2009) 'The HLA genomic loci map: expression, interaction, diversity and disease', *Journal of Human Genetics,* **54**(1): 15-39.

Singal, D.P., Li, J., Zhu, Y. & Zhang, G. (2000) 'NRAMP1 gene polymorphisms in patients with rheumatoid arthritis', *Tissue Antigens,* **55**(1): 44-7.

Skamene, E. (1994) 'The Bcg gene story', *Immunobiology,* **191**(4-5): 451-60.

Skamene, E., Gros, P., Forget, A., Kongshavn, P.L.A., St Charles, C. & Taylor, B.A. (1982) 'Genetic regulation of resistance to intracellular pathogens', *Nature,* **297**(5866): 506-9.

Slebos, R.J.C., Li, M., Vadivelu, S., Burkey, B.B., Netterville, J.L., Sinard, R., Gilbert, J., Murphy, B., Chung, C.H., Shyr, Y. & Yarbrough, W.G. (2008) 'Microsatellite mutations in buccal cells are associated with aging and head and neck carcinoma', *British Journal of Cancer,* **98**(3): 619-26.

Smale, S.T. (1997) 'Transcription initiation from TATA-less promoters within eukaryotic protein-coding genes', *Biochimica et Biophysica Acta,* **1351**(1-2): 73-88.

Smale, S.T. & Kadonaga, J.T. (2003) 'The RNA polymerase II core promoter', *Annual Review of Biochemistry,* **72**:449-79.

Smale, S.T., Schmidt, M.C., Berk, A.J. & Baltimore, D. (1990) 'Transcriptional activation by Sp1 as directed through TATA or initiator: specific requirement for mammalian transcription factor IID', *Proceedings of the National Academy of Sciences of the United States of America,* **87**(12): 4509-13.

Smit, J.J., Folkerts, G. & Nijkamp, F.P. (2004) 'Ramp-ing up allergies: Nramp1 (Slc11a1), macrophages and the hygiene hypothesis', *Trends in Immunology,* **25**(7): 342-7.

Smit, J.J., van Loveren, H., Hoekstra, M.O., Nijkamp, F.P. & Bloksma, N. (2003) 'Influence of the macrophage bacterial resistance gene Nramp1 (Slc11a1) on the induction of allergic asthma in the mouse', *The FASEB Journal,* **17**(8): 958-60.

Soborg, C., Andersen, A.B., Madsen, H.O., Kok-Jensen, A., Skinhoj, P. & Garred, P. (2002) 'Natural resistance-associated macrophage protein 1 polymorphisms are associated with microscopy-positive tuberculosis', *Journal of Infectious Diseases,* **186**(4): 517-21.

Soborg, C., Andersen, A.B., Range, N., Malenganisho, W., Friis, H., Magnussen, P., Temu, M.M., Changalucha, J., Madsen, H.O. & Garred, P. (2007) 'Influence of candidate susceptibility genes on tuberculosis in a high endemic region', *Molecular Immunology,* **44**(9): 2213-20.

Soe-Lin, S., Apte, S.S., Andriopoulos, B.J., Andrews, M.C., Schranzhofer, M., Kahawita, T., Garcia-Santos, D. & Ponka, P. (2009) 'Nramp1 promotes efficient macrophage recycling of iron following erythrophagocytosis in vivo', *Proceedings of the National Academy of Sciences of the United States of America,* **106**(14): 5960-5.

Soe-Lin, S., Apte, S.S., Mikhael, M.R., Kayembe, L.K., Nie, G. & Ponka, P. (2010) 'Both Nramp1 and DMT1 are necessary for efficient macrophage iron recycling', *Experimental Hematology,* **38**(8): 609-17.

Soe-Lin, S., Sheftel, A.D., Wasyluk, B. & Ponka, P. (2008) 'Nramp1 equips macrophages for efficient iron recycling', *Experimental Hematology,* **36**(8): 929-37.

Soo, S.S., Villarreal-Ramos, B., Khan, C.M.A., Hormaeche, C.E. & Blackwell, J.M. (1998) 'Genetic Control of Immune Response to Recombinant Antigens Carried by an Attenuated Salmonella typhimurium Vaccine Strain: Nramp1 Influences T-Helper Subset Responses and Protection against Leishmanial Challenge', *Infection and Immunity,* **66**(5): 1910-7.

Steger, G. (1994) 'Thermal denaturation of double-stranded nucleic acids: prediction of temperatures critical for gradient gel electrophoresis and polymerase chain reaction', *Nucleic Acids Research,* **22**(14): 2760-8.

Stein, C. & Baker, A. (2011) 'Tuberculosis as a complex trait: impact of genetic epidemiological study design', *Mammalian Genome,* **22**(1-2): 91-9.

Stein, C., Zalwango, S., Chiunda, A., Millard, C., Leontiev, D., Horvath, A., Cartier, K., Chervenak, K., Boom, W., Elston, R., Mugerwa, R., Whalen, C. & Iyengar, S. (2007) 'Linkage and association analysis of candidate genes for TB and TNFα cytokine expression: evidence for association with IFNGR1, IL-10, and TNF receptor 1 genes', *Human Genetics,* **121**(6): 663-73.

Sterne, J.A.C., Egger, M. & Smith, G.D. (2001) 'Systematic reviews in health care: Investigating and dealing with publication and other biases in meta-analysis', *British Medical Journal,* **323**(7304): 101-5.

Stienstra, Y., van der Werf, T.S., Oosterom, E., Nolte, I.M., van der Graaf, W.T., Etuaful, S., Raghunathan, P.L., Whitney, E.A., Ampadu, E.O., Asamoa, K., Klutse, E.Y., Te Meerman, G.J., Tappero, J.W., Ashford, D.A. & van der Steege, G. (2006) 'Susceptibility to Buruli ulcer is associated with the SLC11A1 (NRAMP1) D543N polymorphism', *Genes and Immunity,* **7**(3): 185-9.

Stober, C.B., Brode, S., White, J.K., Popoff, J.F. & Blackwell, J.M. (2007) 'Slc11a1, Formerly Nramp1, Is Expressed in Dendritic Cells and Influences Major Histocompatibility Complex Class II Expression and Antigen-Presenting Cell Function', *Infection and Immunity,* **75**(10): 5059-67.

Stokkers, P.C., de Heer, K., Leegwater, A.C., Reitsma, P.H., Tytgat, G.N. & van Deventer, S.J. (1999) 'Inflammatory bowel disease and the genes for the natural resistance-associated macrophage protein-1 and the interferon-gamma receptor 1.' *International Journal of Colorectal Disease* **14**(1): 13-7.

Strom, A.C., Forsberg, M., Lillhager, P. & Westin, G. (1996) 'The transcription factors Sp1 and Oct-1 interact physically to regulate human U2 snRNA gene expression', *Nucleic Acid Research,* **24**(11): 1981-6.

Strubin, M. & Struhl, K. (1992) 'Yeast and human TFIID with altered DNA-binding specificity for TATA elements', *Cell,* **68**(4): 721-30.

Studzinski, G.P., Garay, E., Patel, R., Zhang, J. & Wang, X. (2006) 'Vitamin D Receptor Signaling of Monocytic Differentiation in Human Leukemia Cells: Role of MAPK Pathways in Transcription Factor Activation', *Current Topics in Medicinal Chemistry,* **6**(12): 1267-71.

Sundström, C. & Nilsson, K. (1976) 'Establishment and characterization of a human histiocytic lymphoma cell line (U-937)', *International Journal of Cancer,* **17**(5): 565-77.

Supek, F., Supekova, L., Nelson, H. & Nelson, N. (1997) 'Function of metal-ion homeostasis in the cell division cycle, mitochondrial protein processing, sensitivity to mycobacterial infection and brain function', *Journal of Experimental Biology,* **200**(2): 321-30.

Suske, G. (1999) 'The Sp-family of transcription factors', *Gene,* **238**(2): 291-300.

Sweeting, J.M., Sutton, J.A. & Lambert, C.P. (2004) 'What to add to nothing? Use and avoidance of continuity corrections in meta-analysis of sparse data', *Statistics in Medicine,* **23**(9): 1351-75.

Tagle, D.A., Koop, B.F., Goodman, M., Slightom, J.L., Hess, D.L. & Jones, R.T. (1988) 'Embryonic epsilon and gamma globin genes of a prosimian primate (Galago crassicaudatus) : Nucleotide and amino acid sequences, developmental regulation and phylogenetic footprints', *Journal of Molecular Biology,* **203**(2): 439-55.

Takahashi, K., Hasegawa, Y., Abe, T., Yamamoto, T., Nakashima, K., Imaizumi, K. & Shimokata, K. (2008) 'SLC11A1 (formerly NRAMP1) polymorphisms associated with multidrug-resistant tuberculosis', *Tuberculosis,* **88**(1): 52-7.

Takahashi, K., Satoh, J., Kojima, Y., Negoro, K., Hirai, M., Hinokio, Y., Kinouchi, Y., Suzuki, S., Matsuura, N., Shimosegawa, T. & Oka, Y. (2004) 'Promoter polymorphism of SLC11A1 (formerly NRAMP1) confers susceptibility to autoimmune type 1 diabetes mellitus in Japanese', *Tissue Antigens,* **63**(3): 231-6.

Takaoka, A., Wang, Z., Choi, M.K., Yanai, H., Negishi, H., Ban, T., Lu, Y., Miyagishi, M., Kodama, T., Honda, K., Ohba, Y. & Taniguchi, T. (2007) 'DAI (DLM-1/ZBP1) is a cytosolic DNA sensor and an activator of innate immune response', *Nature,* **448**(7152): 501-5.

Tamura, T. & Ozato, K. (2002) 'ICSBP/IRF-8: its regulatory roles in the development of myeloid cells', *Journal of Interferon and Cytokine Research,* **22**(1): 145-52.

Tamura, T., Thotakura, P., Tanaka, T.S., Ko, M.S. & Ozato, K. (2005) 'Identification of target genes and a unique cis element regulated by IRF-8 in developing macrophages', *Blood,* **106**(6): 1938-47.

Tamura, T., Yanai, H., Savitsky, D. & Taniguchi, T. (2008) 'The IRF Family Transcription Factors in Immunity and Oncogenesis', *Annual Review of Immunology,* **26**(1): 535-84.

Tan, N.Y. & Khachigian, L.M. (2009) 'Sp1 Phosphorylation and Its Regulation of Gene Transcription', *Molecular and Cell Biology,* **29**(10): 2483-8.

Tanaka, G., Shojima, J., Matsushita, I., Nagai, H., Kurashima, A., Nakata, K., Toyota, E., Kobayashi, N., Kudo, K. & Keicho, N. (2007) 'Pulmonary Mycobacterium avium complex infection: association with NRAMP1 polymorphisms', *European Respiratory Journal,* **30**(1): 90-6.

Taype, C.A., Castroa, J.C., Accinellib, R.A., Herrera-Velita, P., Shaw, M.A. & Espinozaa, J.R. (2006) 'Association between SLC11A1 polymorphisms and susceptibility to different clinical forms of tuberculosis in the Peruvian population', *Infection, Genetics and Evolution* **6**(5): 361-7.

Telfer, J.F. & Brock, J.H. (2002) 'Expression of ferritin, transferrin receptor, and non-specific resistance associated macrophage proteins 1 and 2 (Nramp1 and Nramp2) in the human rheumatoid synovium', *Annals of the Rheumatic Diseases,* **61**(8): 741-4.

Terrin, N., Schmid, C.H. & Lau, J. (2005) 'In an empirical evaluation of the funnel plot, researchers could not visually identify publication bias', *Journal of Clinical Epidemiology,* **58**(9): 894-901.

Theurl, I., Fritsche, G., Ludwiczek, S., Garimorth, K., Bellmann-Weiler, R. & Weiss, G.N. (2005) 'The Macrophage: A Cellular Factory at the Interphase Between Iron and Immunity for the Control of Infections', *BioMetals,* **18**(4): 359-67.

Todd, J, A., Farrall & M (1996) 'Panning for gold: genome-wide scanning for linkage in type 1 diabetes', *Human Molecular Genetics,* **5 Spec No**:1443-8.

Trinklein, N.D., Aldred, S.F., Hartman, S.J., Schroeder, D.I., Otillar, R.P. & Myers, R.M. (2004) 'An Abundance of Bidirectional Promoters in the Human Genome', *Genome Research,* **14**(1): 62-6.

Tsuchiya, S., Kobayashi, Y., Goto, Y., Okumura, H., Nakae, S., Konno, T. & Tada, K. (1982) 'Induction of maturation in cultured human monocytic leukemia cells by a phorbol diester', *Cancer Research,* **42**(4): 1530-6.

Tsuchiya, S., Yamabe, M., Yamaguchi, Y., Kobayashi, Y., Konno, T. & Tada, K. (1980) 'Establishment and characterization of a human acute monocytic leukaemia cell line (THP-1)', *International Journal of Cancer,* **26**(2): 171-6.

Tsujimura, H., Nagamura-Inoue, T., Tamura, T. & Ozato, K. (2002) 'IFN consensus sequence binding protein/interferon regulatory factor-8 guides bone marrow progenitor cells toward the macrophage lineage', *The Journal of Immunology,* **169**(3): 1261-9.

Turcotte, K., Gauthier, S., Malo, D., Tam, M., Stevenson, M.M. & Gros, P. (2007) 'Icsbp1/IRF-8 Is Required for Innate and Adaptive Immune Responses against Intracellular Pathogens', *Journal of Immunology,* **179**(4): 2467-76.

Turcotte, K., Gauthier, S., Tuite, A., Mullick, A., Malo, D. & Gros, P. (2005) 'A mutation in the Icsbp1 gene causes susceptibility to infection and a chronic myeloid leukemia-like syndrome in BXH-2 mice', *The Journal of Experimental Medicine,* **201**(6): 881-90.

Usheva, A. & Shenk, T. (1996) 'YY1 transcriptional initiator: Protein interactions and association with a DNA site containing unpaired strands', *Proceedings of the National Academy of Sciences of the United States of America,* **93**(24): 13571-6.

Valberg, L.S., Flanagan, P.R., Kertesz, A. & Ebers, G.C. (1989) 'Abnormalities in iron metabolism in multiple sclerosis', *The Canadian Journal of Neurological Sciences,* **16**(2): 184-6.

Vaughn, C.P. & Elenitoba-Johnson, K.S.J. (2004) 'High-Resolution Melting Analysis for Detection of Internal Tandem Duplications', *The Journal of Molecular Diagnostics,* **6**(3): 211-6.

Vejbaesya, S., Chierakul, N., Luangtrakool, P. & Sermduangprateep, C. (2007a) 'NRAMP1 and TNF-alpha polymorphisms and susceptibility to tuberculosis in Thais', *Respirology,* **12**(2): 202-6.

Vejbaesya, S., Mahaisavariya, P., Luangtrakool, P. & Sermduangprateep, C. (2007b) 'TNF alpha and NRAMP1 polymorphisms in leprosy', *Journal of the Medical Association of Thailand,* **90**(6): 1188-92.

Velez, D.R., Hulme, W.F., Myers, J.L., Stryjewski, M.E., Abbate, E., Estevan, R., Patillo, S.G., Gilbert, J.R., Hamilton, C.D. & Scott, W.K. (2009) 'Association of SLC11A1 with tuberculosis and interactions with NOS2A and TLR2 in African-Americans and Caucasians', *The International Journal of Tuberculosis and Lung Disease,* **13**(9): 1068-76.

Vidal, S., Tremblay, M.L., Govoni, G., Gauthier, S., Sebastiani, G., Malo, D., Skamene, E., Olivier, M., Jothy, S. & Gros, P. (1995) 'The Ity/Lsh/Bcg locus: natural resistance to infection with intracellular parasites is abrogated by disruption of the Nramp1 gene', *The Journal of Experimental Medicine,* **182**(3): 655-66.

Vidal, S.M., Malo, D., Vogan, K., Skamene, E. & Gros, P. (1993) 'Natural resistance to infection with intracellular parasites: Isolation of a candidate for Bcg', *Cell,* **73**(3): 469-85.

Vidal, S.M., Pinner, E., Lepage, P., Gauthier, S. & Gros, P. (1996) 'Natural resistance to intracellular infections: Nramp1 encodes a membrane phosphoglycoprotein absent in macrophages from susceptible (Nramp1 D169) mouse strains', *Journal of Immunology,* **157**(8): 3559-68.

Vuyyuri, S.B., Ishaq, M., Kuppala, D., Grover, P. & Ahuja, Y.R. (2006) 'Evaluation of micronucleus frequencies and DNA damage in glass workers exposed to arsenic', *Environmental and Molecular Mutagenesis,* **47**(7): 562-70.

Wang, A.H., Quigley, G.J., Kolpak, F.J., Crawford, J.L., van Boom, J.H., van der Marel, G. & Rich, A. (1979) 'Molecular structure of a left-handed double helical DNA fragment at atomic resolution', *Nature,* **282**(5740): 680-6.

Weber, J., Werre, J.M., Julius, H.W. & Marx, J.J. (1988) 'Decreased iron absorption in patients with active rheumatoid arthritis, with and without iron deficiency', *Annals of the Rheumatic Diseases,* **47**(5): 404-9.

Wei, W., Pelechano, V., Järvelin, A.I. & Steinmetz, L.M. (2011) 'Functional consequences of bidirectional promoters', *Trends in Genetics,* **27**(7): 267-76.

White, H. & Potts, G. (2006) Mutation scanning by high resolution melt curve analysis. Evaluation of Rotor-Gene 6000 (Corbett Life Science), HR-1 and 384 well LightScanner (Idaho Technology). *National Genetics Reference Laboratory (Wessex).* http://www.ngrl.org.uk/wessex/downloads_reports.htm.

White, J.K., Shaw, M.A., Barton, C.H., Cerretti, D.P., Williams, H., Mock, B.A., Carter, N.P., Peacock, C.S. & Blackwell, J.M. (1994) 'Genetic and Physical Mapping of 2q35 in the Region of the NRAMP and IL8R Genes: Identification of a Polymorphic Repeat in Exon 2 of NRAMP', *Genomics,* **24**(2): 295-302.

White, J.K., Stewart, A., Popoff, J.-F., Wilson, S. & Blackwell, J.M. (2004) 'Incomplete glycosylation and defective intracellular targeting of mutant solute carrier family 11 member 1 (Slc11a1)', *Biochemical Journal,* **382**(3): 811-9.

Wicker, L.S., Chamberlain, G., Hunter, K., Rainbow, D., Howlett, S., Tiffen, P., Clark, J., Gonzalez-Munoz, A., Cumiskey, A.M., Rosa, R.L., Howson, J.M., Smink, L.J., Kingsnorth, A., Lyons, P.A., Gregory, S., Rogers, J., Todd, J.A. & Peterson, L.B. (2004) 'Fine mapping, gene content, comparative sequencing, and expression analyses support Ctla4 and Nramp1 as candidates for Idd5.1 and Idd5.2 in the nonobese diabetic mouse', *Journal of Immunology,* **173**(1): 164-73.

Wierstra, I. (2008) 'Sp1: Emerging roles--Beyond constitutive activation of TATA-less housekeeping genes', *Biochemical and Biophysical Research Communications,* **372**(1): 1-13.

Wittwer, C.T., Herrmann, M.G., Moss, A.A. & Rasmussen, R.P. (1997) 'Continuous fluorescence monitoring of rapid cycle DNA amplification', *Biotechniques,* **22**(1): 130-8.

Wittwer, C.T., Reed, G.H., Gundry, C.N., Vandersteen, J.G. & Pryor, R.J. (2003) 'High-resolution genotyping by amplicon melting analysis using LCGreen', *Clinical Chemistry,* **49**(6): 853-60.

Wojciechowski, W., Desanctis, J., Skamene, E. & Radzioch, D. (1999) 'Attenuation of MHC Class II Expression in Macrophages Infected with Mycobacterium bovis Bacillus Calmette-Guerin Involves Class II Transactivator and Depends on the Nramp1 Gene', *The Journal of Immunology,* **163**(5): 2688-96.

Wu, C., Orozco, C., Boyer, J., Leglise, M., Goodale, J., Batalov, S., Hodge, C., Haase, J., Janes, J., Huss, J. & Su, A. (2009) 'BioGPS: an extensible and customizable portal for querying and organizing gene annotation resources', *Genome Biology,* **10**(11): R130.

Wyllie, S., Seu, P. & Goss, J.A. (2002) 'The natural resistance-associated macrophage protein 1 Slc11a1 (formerly Nramp1) and iron metabolism in macrophages', *Microbes and Infection,* **4**(3): 351-9.

Xu, Y. & Uberbacher, E.C. (1997) 'Automated gene identification in large-scale genomic sequences', *Journal of Computational Biology,* **4**(3): 325-38.

Xu, Y.Z., Thuraisingam, T., Marino, R. & Radzioch, D. (2011) 'Recruitment of SWI/SNF complex is required for transcriptional activation of SLC11A1 gene during macrophage differentiation of HL-60 cells', *Journal of Biological Chemistry,* **286**(15): 12839-49.

Xu, Y.Z., Thuraisingam, T., Morais, D.A.D.L., Rola-Pleszczynski, M. & Radzioch, D. (2010) 'Nuclear translocation of β-actin is involved in transcriptional regulation during macrophage differentiation of HL-60 cells', *Molecular Biology of the Cell,* **21**(5): 811-20.

Xu, Z., Wei, W., Gagneur, J., Perocchi, F., Clauder-Munster, S., Camblong, J., Guffanti, E., Stutz, F., Huber, W. & Steinmetz, L.M. (2009) 'Bidirectional promoters generate pervasive transcription in yeast', *Nature,* **457**(7232): 1033-7.

Yang, C.H., Hsieh, L.L., Tsai, C.W., Chiou, F.S., Chou, S.L., Hsu, B.D. & Pai, C.Y. (2003) 'Evaluation of the DNA stability of forensic markers used in betel-quid chewers' oral swab samples and oral cancerous specimens: implications for forensic application', *Journal of Forensic Sciences,* **48**(1): 88-92.

Yang, J.H., Downes, K., Howson, J.M., Nutland, S., Stevens, H.E., Walker, N.M. & Todd, J.A. (unpublished) 'Evidence of association with type 1 diabetes in the SLC11A1 gene region', *BMC Medical Genetics*.

Yang, Y., Kim, S., Kim, J. & Koh, E. (2000a) 'NRAMP1 gene polymorphisms in patients with rheumatoid arthritis in Koreans', *Journal of Korean Medical Science,* **15**(1): 83-7.

Yang, Z., Wara-Aswapati, N., Chen, C., Tsukada, J. & Auron, P.E. (2000b) 'NF-IL6 (C/EBPβ) vigorously activates *il1b* gene expression via a Spi-1 (PU.1) protein-protein tether', *The Journal of Biological Chemistry,* **275**(28): 21272-7.

Yen, J.H., Lin, C.H., Tsai, W.C., Ou, T.T., Wu, C.C., Hu, C.J. & Liu, H.W. (2006) 'Natural resistance-associated macrophage protein 1 gene polymorphisms in rheumatoid arthritis', *Immunology Letters,* **102**(1): 91-7.

Yeung, Y., Phillips, E., Mann, D.A. & Barton, C.H. (2004) 'Oxidant regulation of the bivalent cation transporter Nramp1', *Biochemical Society Transactions,* **32**(6): 1008-10.

Yip, S.P., Leung, K.H. & Lin, C.K. (2003) 'Extent and distribution of linkage disequilibrium around the SLC11A1 locus', *Genes and Immunity,* **4**(3): 212-21.

Zaahl, M.G., Robson, K.J.H., Warnich, L. & Kotze, M.J. (2004) 'Expression of the SLC11A1 (*NRAMP1*) 5 '-(GT)(n) repeat: Opposite effect in the presence of-237C → T', *Blood Cells Molecules and Diseases,* **33**(1): 45-50.

Zaahl, M.G., Warnich, L., Victor, T.C. & Kotze, M.J. (2005) 'Association of functional polymorphisms of SLC11A1 with risk of esophageal cancer in the South African Colored population', *Cancer Genetics and Cytogenetics,* **159**(1): 48-52.

Zaahl, M.G., Winter, T.A., Warnich, L. & Kotze, M.J. (2006) 'The –237C–>T promoter polymorphism of the *SLC11A1* gene is associated with a protective effect in relation to inflammatory bowel disease in the South African population', *International Journal of Colorectal Disease,* **21**(5): 402-8.

Zenzie-Gregory, B., O'Shea-Greenfield, A. & Smale, S.T. (1992) 'Similar mechanisms for transcription initiation mediated through a TATA box or an initiator element', *The Journal of Biological Chemistry,* **267**(4): 2823-30.

Zhang, D.E., Hetherington, C.J., Tan, S., Dziennis, S.E., Gonzalex, D.A., Chen, H.M. & Tenen, D.G. (1994) 'Sp1 is a critical factor for the monocytic expression of human CD14', *The Journal of Biological Chemistry,* **269**(15): 11425-34.

Zhang, W., Shao, L., Weng, X., Hu, Z., Jin, A., Chen, S., Pang, M. & Chen, Z.W. (2005) 'Variants of the natural resistance-associated macrophage protein 1 gene (NRAMP1) are associated with severe forms of pulmonary tuberculosis', *Clinical Infectious Diseases,* **40**(9): 1232-6.

Zhao, Y., Wang, S., Aunan, K., Martin Seip, H. & Hao, J. (2006) 'Air pollution and lung cancer risks in China - a meta-analysis', *Science of The Total Environment,* **366**(2-3): 500-13.

Zhou, L., Wang, L., Palais, R., Pryor, R. & Wittwer, C.T. (2005) 'High-resolution DNA melting analysis for simultaneous mutation scanning and genotyping in solution', *Clinical Chemistry,* **51**(10): 1770-7.

Zlokarnik, G., Negulescu, P.A., Knapp, T.E., Mere, L., Burres, N., Feng, L., Whitney, M., Roemer, K. & Tsien, R.Y. (1998) 'Quantitation of Transcription and Clonal Selection of Single Living Cells with β-Lactamase as Reporter', *Science,* **279**(5347): 84-8.

Zwilling, B.S., Vespa, L. & Massie, M. (1987) 'Regulation of I-A expression by murine peritoneal macrophages: differences linked to the Bcg gene', *Journal of Immunology,* **138**(5): 1372-6.

Zwilling, S., Annweiler, A. & Wirth, T. (1994) 'The POU domains of the Oct1 and Oct2 transcription factors mediate specific interaction with TBP', *Nucleic Acids Research,* **22**(9): 1655-62.